Water Quality Monitoring in the Source Water Areas for New York City: An Integrative Watershed Approach

A Final Report on Monitoring Activities, 2000-2005

Submitted by:
Stroud Water Research Center
Contribution No. 2008006
970 Spencer Road
Avondale, PA 19311

October 2008

STROUD
WATER RESEARCH CENTER

Report Prepared by:

David B. Arscott, Ph.D.

Anthony K. Aufdenkampe, Ph.D.

Thomas L. Bott, Ph.D.

Charles L. Dow, Ph.D.

John K. Jackson, Ph.D.

Louis A. Kaplan, Ph.D.

J. Denis Newbold, Ph.D.

Bernard W. Sweeney, Ph.D.

Photo: Approaching the Cannonsville Reservoir, courtesy of James Blaine

Acknowledgments

The authors of this report represent only a few of the many Stroud employees who contributed their hard work to the project. Without the dedication of the following employees (with sincere apologizes to anyone inadvertently left off of this list) and many summer interns, this project would never have gotten off the ground:

Bernard Anderson
Melanie Arnold
Jessica Auman
Juliann Battle
Heather Brooks
Andrew Byler
Christopher Caine
Linda Carter
Arlene Casas
Amanda Christian
Chad Colburn
Buddy Kondikoff
William Crouch
Aaron deLong
Sarah Deonarine
Heather Eggleston
David Funk
Michael Gentile
Lara Hall
Susan Herbert
Jennifer Hindman
Brian Hughes
Michael Humprys
Karen Jansson
John Johansen
Erika Kratzer
Bryan Lees
David Lieb
Amy MacCausland
Jessie Mathiesen
William Milliken
Mark Monk
David Montgomery
John Nixon
Nancy Parsons
Sally Peirson
Nicholas Principe
Sherman Roberts
Krista Saladino
Rajiv Shah
Erin Shea
Robert Smith
Kevin Smith
Jan Surma
Philip Taylor
Thy Truong
Dave Van Horn
Roberta Weber

Paul Kiry at the Patrick Center for Environmental Research conducted most of the inorganic chemistry analysis for the project. A number of employees at the NYC Department of Environmental Protection helped us over the years with a number of project aspects including acquiring ancillary data for the project and gaining access to NYCDEP land. We thank the many private land owners within New York City's drinking watersheds who allowed us to access streams on their property. This project was funded by a grant under the Safe Drinking Water Act from the New York State Department of Environmental Conservation and the US Environmental Protection Agency.

Table of Contents

Table of common abbreviations used in this report.

Abbreviation	Definition
1k	reach-scale buffer extent for summary land cover statistics
1MP	1-methyl phenanthrene
2MP	2-methyl phenanthrene
aCOP	Cholestanol (5α-cholestan-3β-ol)
AFDM	ash free dry mass
AHTN	Galaxolide
ALK	Total alkalinity
AMW	Amawalk Reservoir
ANCOVA	Analysis of co-variance
ANOSIM	analysis of similarity
ANOVA	Analysis of variance
ANT	Anthracene
aONE	Cholestanone (5α-cholestan-3-one)
A_s	cross-sectional transient storage area
A_s/A	transient storage
b	riparian network-scale buffer extent for summary land cover statistics
BAA	Benz(a)anthracene
BAP	Benzo(a)pyrene
BBF	Benzo(b)fluoranthene
B-C	Bray-Curtis similarity
bCOP	Coprostanol (5β-cholestan-3β-ol)
BDOC	biodegradable dissolved organic carbon
BKF	Benzo(k)fluoranthene
BMP	Best management practice
BOD	biological oxygen demand
BOM	Benthic Organic Matter
bONE	Coprostanone (5β-cholestan-3-one)
C	Water-column nutrient concentration
CAF	Caffeine
CCA	Canonical correspondance analysis
Chl a	Chlorophyll *a*
CHOL	Cholesterol (cholest-5-en-3β-ol)
CHR	Chrysene
CIA	Coinertia Analysis
COMM	% commercial
COND	Specific Conductance (Tref = 25°C)
CONF	% conifer forest
CR_{24}	community respiration (24 h period)
CROP	% cropland
CRS	Cross River
CV	coefficient of variation
CWA	Clean Water Act (1972, amended in 1977)
DECD	% deciduous forest
DOC	Dissolved organic carbon
DOM	Dissolved organic matter
DON	Dissolved organic nitrogen
DRBC	Delaware River Basin Commission
EBC	East Branch of the Croton River
EBD	East Branch of the Delaware River
EOH	East of the Hudson River water supply region
EPA	United States Environmental Protection Agency
EPI	*Epi*-coprostanol (5 β -cholestan-3α-ol)
EPT	Ephemeroptera, Plecoptera, Trichoptera
ESP	Esopus Creek

Abbreviation	Definition
ETM+	Landsat Enhanced Thematic Mapper Plus
FLR	Fluoranthene
FLU	Fluorene
FM	Fragrance materials
FMST	% farmstead
FS	Fecal steroids
GC-MS	Gas chromatography-mass spectrometry
GIS	Geographic information system
GPP	gross primary production
GRAS	% grassland
HBI	Hilsenhoff Biotic Index
HHCB	Tonalide
HMW	High molecular weight
INDU	% industrial
I_s	saturation light intensity
ISD	Impact Source Determination
K_d, η	light extinction coefficient
KNC	Kensico Reservoir
K_S	half-saturation concentration
LCOD	Upstream lake category
LDNS	Upstream lake density (ha/km^2)
LMW	Low molecular weight
LRL	Laboratory reporting levels
LUPS	Area of 1st upstream lake (ha)
MBC	Middle Branch of the Croton River
MBRH	% mixed brush-grassland
MDL	Method detection limit
MFOR	% mixed forest
MLR	Multiple linear regression analysis
MOA	Memorandum of Understanding
MSC	Muscoot River
NCR	New Croton Reservoir
NDM	net daily metabolism
NMDS	non-metric multidimensional scaling
NOAA	National Oceanic and Atmospheric Administration
NRCS	Natural Resources Conservation Service (US federal agency)
NVK	Neversink River
NY DOT	New York Department of Transportation
NYC	New York City
NYC DEP	New York City Department of Environmental Protection
NYS DEC	New York State Department of Environmental Conservation
ORCH	% orchard
OURB	% other urban
PAH	Polycyclic aromatic hydrocarbons
PAR	photosynthetically active radiation
PCA	principal components analysis
PCBs	Polychorinated biphenyls
PDNS	population density
PHE	Phenanthrene
PI	photosynthesis-irradiation
PMA	Percent Model Affinity
POC	Particulate organic carbon
POM	Particulate organic matter
PN	Particulate nitrogen
PP	Particulate phosphorus

Abbreviation	Definition
PS_{max}	photosynthetic maximum
PYR	Pyrene
QA/QC	quality assurance/quality control
RA	relative abundances
RDA	Redundancy analysis - a multivariate method
RDNS	road density
RESD	% residential
RND	Rondout Creek
RPD	Relative percent differences
SCH	Schoharie Creek
SD	Standard Deviation
SDNS	Stream network density (m/km^2)
SDWA	Safe Drinking Water Act 1974
SHRB	% shrubland
SIM	Selective ion monitoring
SKN	Soluble Kjeldahl nitrogen
SNOL	Ethyl-cholestanol (24-ethyl-5α-cholestan-3β-ol)
sPAH	sum of soot PAH's
SPDE	mean annual watershed-area- normalized State Pollution Discharge Elimination System effluent volume (cm^3/cm^2)
SPDE#	Total number of point source dischargers in upstream watershed area
SRM	surface renewal model
SRP	Soluble reactive phosphorus
SS	Substation
S_w	uptake length
SWRC	Stroud Water Research Center
SWTR	Surface Water Treatment Rule
TDN	Total dissolved nitrogen
TDP	Total dissolved phosphorus
TEMP	Water temperature at time of chemical collection
TKN	Total Kjeldahl nitrogen
TMDL	Total maximum daily load
TN	Total nitrogen
TOC	Total organic carbon
TP	Total phosphorus
TRAN	% transportation
TSI	Trophic State Index
TSS	Total suspended solids
TTS	Titicus River
U	uptake flux of a nutrient or organic solute (mass per unit streambed area per unit time),
U_{max}	maximum uptake flux
USDA	U.S. Department of Agriculture
USGS	U.S. Geological Survey
V_f	uptake velocity
v_{hyd}	hydraulic exchange velocity
VIF	Variance inflation factor (related to MLR analyses)
vPAH	sum of volatile PAH's
v_w	water velocity
$v_w d$	specific discharge
W	watershed-scale extent for summary land cover statistics
WBC	West Branch of the Croton River
WBD	West Branch of the Delaware River
wbPCA	within and between PCA
WETL	% wetland
WOH	West of the Hudson River water supply region

Abbreviation	Definition
WOHcat	West of the Hudson River in the Catskill Mountains
WOHdel	West of the Hudson River in the Delaware River Watershed
WQS	NYS DEC macroinvertebrate water quality score
WTSH	Watershed area (km^2)
WWTP	waste water treatment plant

----------Intentionally Blank----------

Executive Summary

In this report, the Stroud Water Research Center (SWRC) presents results from the entire six years (2000 – 2005) of a water-quality monitoring project of the streams, rivers, and reservoirs that provide New York City's (NYC) drinking water. This project involved analyzing specific physical, chemical, and biological indicators to measure, quantify, and determine sources and impacts of selected contaminants throughout the watersheds that make up the NYC drinking water supply. The project was designed to enhance on-going monitoring within the watersheds and to provide an additional baseline of information useful in such aspects as measuring changes in water quality in response to changes in land use and the implementation of best management practices (BMP) for mitigating both point and non-point source pollution. The focus was on ecosystem impairment (e.g., differences in stream community structure and stream/reservoir productivity, levels of nutrient processing or sequestering) and contaminant sources (e.g., point sources such as wastewater treatment plants and non-point sources such as agricultural fields).

Principal objectives of the monitoring program

1. To provide dependent variables for statistical analyses relating aquatic ecosystem structure and function to land use, best management practice (BMP) implementation, and other watershed inputs or factors.

2. To provide chemical and biological indicators for evaluating the occurrence and source of selected aquatic contaminants.

3. To provide a baseline data set of population, community and ecosystem-level variables and molecular indicators of contaminants to assess changes in water quality and aquatic ecosystem structure and function in response to on-going and/or future shifts in land use/cover.

Project Design

This project was designed as a 6-y study divided into two distinct 3-y phases. In the first 3-y phase (Phase I; 2000-2002), 60 stream sampling stations were established that were distributed among major sub-basins of the principal source watersheds. The 60 sampling stations were designated either as "targeted" (n=50) or "integrative" (n=10) depending on their location in the watershed and type and intensity of variables being measured/monitored. Targeted stations occurred throughout the watersheds on streams of varying size. Integrative stations occurred sufficiently downstream to integrate effects of land use and other factors on a given project element or task under study over a large portion of the watershed. Site selection was primarily geared toward capturing the range in land uses/covers across the geologic and soil characteristics of all NYC source watersheds. Secondary site selection criteria included ongoing or future BMP implementation, presence of U.S. Geologic Survey (USGS) stream gauging stations, and the feasibility of studying the various study components. Sampling stations on eight reservoirs were also established in Phase I. For Phase II (2003-2005), 50 new (differing from Phase I) stream sites and four new reservoir sites were selected for study. It should be noted that winter sampling did take place in early 2006 at a subset of sites for a single project element. Monitoring

continued at twelve of the Phase I stream sites and three reservoir to maintain continuity between Phase I and II, to assess interannual variability, and to facilitate interpretations of Phase II data relative to Phase I. Phase II work built upon Phase I results by sampling other important tributaries to the reservoirs and conducting a more specified sampling effort in an attempt to refine any ambiguous results from the Phase I effort. The scientific strength of the program was in the number of elements being measured, the spatial scope of the study (110 stream /12 reservoir sites), and replicated sampling over 3 or 6 years at each site.

There were a total of seven primary project elements with an eighth element added in the Phase II to augment one of the original elements. Because a high degree of integration exists among elements, results from any one element built upon results from other elements. Some tasks involved targeted measures (i.e., "snapshots" in time and space), while others were integrated across space and time. Collectively, the project elements were designed to provide a holistic view of stream and reservoir water quality and the potential watershed factors governing or affecting their water quality. The project was designed as a broad synoptic survey repeated annually, rather than as a highly targeted, spatially narrow survey with a high degree of repetition in each year of study. Sampling was conducted primarily in late spring, summer, and early fall; however, winter sampling was conducted as part of one study task. Baseflow, or non-storm flow, conditions were the main focus of this project. Limited stormflow sampling did occur at 3 of the 110 sampling sites over the entire 6-y project period.

The project elements were:

(1) **Nutrients and Major Ions in Transport.** Major ions and nutrients were monitored in study streams under baseflow and stormflow conditions. Major ions included cations (i.e., sodium, magnesium, calcium, and potassium), and anions (i.e., sulfate, chloride). Nutrients included various forms of nitrogen and phosphorus; pH, alkalinity, and conductivity were also measured. Concentrations of nutrients and major ions transported in streams can be significant indicators of ecosystem impairment within the context of geochemical conditions, particularly when monitored through time and across landscapes of complex land use patterns. In addition, major ions and nutrients can be used to quantify and predict changes in water quality in response to changes in land use. Storms were sampled over the entire 6-y study period at three stream sites, each of which was selected to represent one of the three major land uses/cover types found within the study region: agriculture, urban/suburban, and forest.

(2) **Molecular Tracer Analysis.** Molecular tracers are a broad group of compounds present in the aquatic environment that are unique to various contaminant sources. The use of such tracers is an emerging technique that qualitatively links the presence of a particular contaminant in a stream or river to a specific source of that contamination within the upstream watershed (which would also include atmospherically deposited sources onto the watershed). Tracers used in this project included: (i) fragrances found in domestic products (e.g., detergents) and caffeine, which are used to indicate the presence of waste water treatment plant (WWTP) or septic effluent; (ii) fecal steroids, which track animal (farm or wildlife) and human contamination; and (iii) polycyclic aromatic hydrocarbons (PAH), which target urban/suburban sources of contamination. Tracers were measured primarily during summer baseflow (non-stormflow), however, a subset (49) of the 110 stream sites were also monitored during winter months.

Sampling of stormflow was performed during the spring, summer, and fall months at the three stormflow sampling sites described above under project element #1.

(3) **Molecular Tracer Source Signatures**. An important component to the compounds monitored as tracers of stream contamination (under project element #2, above), is the specificity between the tracer concentration measured in stream water and its source within the watershed. In Phase II of the project, an effort was made to better constrain signatures (i.e. ratios of certain tracers) of various potential contamination sources, especially fecal sources, to the NYC watershed water-supply area. Fecal samples were collected from various livestock, birds, other wildlife, and human sources (septic and waste-water treatment samples), all within the NYC watershed study area. These samples were analyzed for the suite of fecal steroid compounds included in the molecular tracer analysis of project element #2, and ultimately were incorporated in a statistical model that allowed for the prediction of the sampled contamination sources based on measured values of these fecal steroids.

(4) **Organic Matter Dynamics**. This project element actually covered two project tasks: organic particle dynamics and dissolved organic carbon (DOC) dynamics. Organic particle (suspended solids) and DOC, together as organic matter (OM), provide a linkage between the inputs from terrestrial environments and streams by connecting streams to their watershed. Within the context of drinking-water supply, OM provides precursors for disinfection by-products and the energy source (i.e. carbon) for bacterial growth. The objectives for this task were to characterize the concentration, size distribution (year 1 only), and transport of organic matter under baseflow conditions at the 110 stream sites, and to estimate response of organic matter transport to runoff events at the 3 stormflow sampling sites. DOC and the biodegradable portion of DOC (BDOC) were also monitored in the 12 study reservoirs.

(5) **Macroinvertebrate Community Structure and Function.** To provide a more integrated picture over time of water quality conditions in the NYC watersheds, benthic (i.e., bottom-dwelling) macroinvertebrates were monitored at the 110 stream sites. Benthic macroinvertebrates, such as insects, worms, and molluscs, provide an extended temporal perspective (relative to the molecular tracer, major ions, and nutrient sampling performed periodically) because they have limited mobility and relatively long life spans (e.g., a few months to a year or more for some insects and molluscs). Macroinvertebrates have measurable responses to a wide variety of environmental changes and stresses that can be easily analyzed, and they are an important link in the aquatic food web. Thus, the presence or conspicuous absence of certain macroinvertebrate species at a site is a meaningful record of environmental conditions during the recent past, including ephemeral events that might be missed by assessment programs which rely only on periodic sampling of water chemistry. Monitoring of macroinvertebrates at the 110 stream sites occurred during the first few weeks of May, when the species collected were near the end of their 6- to 9-month growth cycle, providing a strong "temporal perspective" during an important and significant portion of the year.

(6) **Nitrogen (N), Phosphorous (P), and Dissolved Organic Carbon (DOC) Spiraling.** In streams and rivers, nutrients, such as phosphorus, nitrogen, and carbohydrates undergo various transformations from a dissolved available form in the water column to uptake in the streambed with a complete ‘cycle’ occurring when nutrients return to the water column. Nutrients are also

moving downstream as they go through this cycle, and the combined processes are termed *spiraling*. The rates at which nutrients are used and cycled within streams and rivers is of practical interest both because nutrient cycling can be considered an ecosystem service - a process that directly or indirectly supplies human needs such as food production or water purification - and because such rates may provide a sensitive measure of human impact on an ecosystem, relative to what its condition or function would be in the absence of human activity. Thus spiraling represents a fundamental measure of stream ecosystem function. Spiraling of nitrogen, phosphorus and carbon (DOC) was measured in the 17 integrative stream sites during baseflow conditions.

(7) **Net Stream Metabolism**. Stream metabolism was assessed concurrently with the above spiraling work at the 17 integrative stream sites. Stream metabolism measurements provide data on two fundamental ecosystem functions – primary productivity and community respiration. Gross primary productivity (GPP) is a measure of the rate of synthesis of plant (primarily algal) biomass, and respiration is an index of the breakdown of reduced chemical energy, including the metabolic costs of photosynthesis. These functional attributes are expected to relate principally to biomass of algae, heterotrophic microorganisms, and, to a lesser extent, macroinvertebrates. Actual rates are also influenced by environmental variables of light, temperature, and dissolved and particulate nutrients. Changes in activity, or in the balance of activity, over time would be an important signal that watershed activities are affecting function in a stream entering a reservoir, and would indicate a need for follow-up work on upstream tributaries.

(8) **Reservoir Primary Productivity**. In reservoirs, phytoplankton productivity could be a significant source of particles, reflecting, in part, the input of nutrients from the source watershed. Along with affecting suspended particulate loads, algae can affect aesthetic aspects related to drinking water quality such as unpleasant tastes and odors as well as lead to significant health issues through the production of disinfection by-products. A primary goal for this project element was to assess reservoir condition on the basis of phytoplankton biomass and primary productivity. In addition, a working hypothesis for this element was that if the major tributary to a reservoir were the principal source of nutrients, gradients of productivity and algal biomass would occur within the reservoir. Primary productivity and algal biomass were measured during summer months at a total of 12 NYC drinking-water-supply reservoirs over the 6-y project period.

Highlights of project outcomes and results:

(1) **Nutrients and Major Ions in Transport.** Strong regional patterns in ion/nutrient chemistry were observed with West of Hudson River sites (WOH) differing significantly from East of Hudson River sites (EOH). Sub-regional differences among sites were also observed based on chemistry – all reflecting the obviously strong influence of geology on stream water quality. Superimposed on the geologic effects were the effects of human-specific land use. Relationships built between individual ion or nutrient values and land use/cover values that best predicted those concentrations revealed that urban or agricultural land uses were the best predictors of ion/nutrient concentrations. These relationships also suggested that land use defined over the entire watershed area, as

opposed to land use/cover defined at riparian or reach scales, was best at predicting in-stream ion/nutrient concentrations.

(2) **Molecular Tracer Analysis.** Improvements to the laboratory techniques for analyzing samples for molecular tracers resulted in laboratory reporting levels for this study that were approximately 3-5x lower then existing, widely used EPA methods. Certain PAH ratios and their positive relationship with riparian land uses, indicated that localized combustion byproducts predominated over other petroleum products (e.g. spills, asphalt) as the source of petroleum contamination in the study streams. Measurable concentrations of caffeine and fragrances, both tracers of human sewage, were found at all study sites. Tracer concentrations tended to vary concurrently, i.e. when one compound or a group of compounds was high, other compounds tended to be high, despite the very different sources of these tracers. Fecal steroid data indicated a wide mixture of fecal contamination sources across the study streams, from human sources, livestock, birds and other wildlife.

(3) **Molecular Tracer Source Signatures**. Fecal steroid, caffeine and fragrance tracer data, collected as part of the molecular tracer source signature work, demonstrated that substantial removal of these compounds can occur during wastewater treatment processes. Yet, these source data also showed a great deal of variability in the amount of removal within and between different treatment processes (i.e. septic v. wastewater treatment plants) of these source compounds. The fecal steroid source signatures (i.e. compound concentration ratios) allowed for a very strong separation between human and non-human sources, and to a lesser extent, separation among livestock, birds, and wildlife. A prediction model based on the fecal-steroid-source ratios suggested a dominance of non-human fecal sources in the stream-water samples.

(4) **Organic Matter Dynamics**. When examining regional averages of stream-water organic matter concentrations, the EOH regional values were generally twice those for the WOH region, regardless of the specific form (e.g. DOC, POM, BDOC, etc). Relative extent of wetlands and wastewater treatment plant effluent were the dominant predictors of OM concentrations regardless of the specific form of OM for EOH sites. A more diverse set of significant land use predictors of OM concentrations was found for WOH sites, where depending on the specific OM form, forested extent, wetlands extent or wastewater treatment plant effluent were the strongest predictors. Relatively strong relationships between caffeine and fragrances with DOC and BDOC among EOH sites support the connection between concentrations of these OM constituents and wastewater contamination in that region.

(5) **Macroinvertebrate Community Structure and Function.** Based on the Water Quality Score (WQS) metric developed by the NYS Department of Conservation, only one of the 110 sites was classified as ‘severely impacted’ based on 3-6 y mean values. The majority of sites were classified as ‘no’ or ‘slight’ impact. However, the macroinvertebrate assemblages associated with these WQS-based classification categories differed markedly. Interannual variation in macroinvertebrate assemblages was also significant and often lead to differing annual WQS-based classifications for a single site. A strong

geographic gradient was found in macroinvertebrate assemblages between EOH and WOH sites. Within regions, differences in assemblages were based on the predominate land use/cover gradient of the region: forest to urban for EOH sites versus forest to agriculture for WOH sites.

(6) **Nitrogen (N), Phosphorous (P), and Dissolved Organic Carbon (DOC) Spiraling.** The uptake velocity, or the mass-transfer coefficient, is a value calculated from the spiraling work that provides a relative measure of how well a stream ecosystem can process nutrients and is comparable among streams varying in size. The higher the value, the more uptake that is occurring, the healthier the stream. The uptake velocities for N (as NH_4^+) and P (as PO_4^{3-}) measured at the 17 integrative sites over the 6-y project period were correlated with land use/cover measures (positively with % forest cover, negatively with both population density and % agricultural land use), as well as with several measures of water quality that reflected human influences. These water-quality variables included nutrient concentrations, various molecular tracers, and macroinvertebrate-based indices of water quality (although the latter correlations were marginal). These results demonstrated that measures of ecosystem function (i.e. spiraling) can be related to human disturbance of aquatic environments. Further, these measures of ecosystem function provided direct information on how a stream is functioning as a whole rather than having to infer such information from other water-quality measurements.

(7) **Net Stream Metabolism**. As with most of the other project elements, stream metabolism measures differed significantly between the EOH and WOH regions. Both gross primary production (GPP - when not normalized for the amount of light or more specifically photosynthetically active radiation [PAR]) and community respiration were higher for WOH streams versus EOH streams. Unlike the other project elements, regional separation for metabolism measures was driven by differences in stream size and related differences in canopy cover – WOH study streams were larger and consequently had less canopy cover resulting in more light availability to the stream environment. Within this primary gradient defined by stream physical characteristics, increased stream metabolism was shown to be related to less human influence as reflected in certain land use measures (higher % forest, lower road density) and water quality measures (lower toxic PAH and caffeine concentrations).

(8) **Reservoir Primary Productivity**. Chlorophyll *a* concentrations, GPP - whether normalized for PAR or an areal basis, and community respiration tended to by higher in EOH reservoirs versus WOH reservoirs. A notable exception was the Cannonsville Reservoir (WOH) which was in fact more similar in terms of these measures to EOH reservoirs and also the Kensico Reservoir (EOH) which by virtue of being a terminal reservoir for WOH water was more similar to WOH reservoirs. Gradients of GPP/PAR and chlorophyll *a* did occur during certain sampling times within a few of the reservoirs with these gradients pointing to the primary reservoir tributary as controlling reservoir condition. Trophic status for the reservoirs, whether based on chlorophyll *a* or on area-normalized GPP, were reasonably similar to estimates reported by the NYC Department of Environmental Protection despite the limited temporal scope of reservoir sampling in this project.

In summary, this monitoring project provided several unique advantages. A spatial scope that had study sites distributed across the entire drinking-water-supply watershed. A temporal scope that included multiple years of data collected at each study site using consistently similar methods and personnel. The multiple study elements provided redundancy in supporting general relationships (e.g., the effects of urban-related watershed factors on in-stream biological and chemical constituents) while at the same time providing unique information (e.g., organic matter constituents pointing to the influence of wetlands on EOH streams). Inclusion of novel monitoring techniques such as molecular tracers (part of a growing 'emerging contaminants' subject area worldwide) and employing unique measures of ecosystem function (e.g., spiraling and stream metabolism) as monitoring tools helped to bridge the areas of basic research and applied monitoring - an important step in taking water quality monitoring to a more effective level. Taken together, the combination of well-established water-quality monitoring techniques with novel stream-monitoring tools applied across carefully selected spatial and temporal scales both captured and explained a great deal of environmental variation across the entire study area. This approach has provided a very effective baseline of information for assessing and placing in proper historical context, future water-quality conditions across the NYC drinking-water-supply watershed.

----------Intentionally Blank----------

Chapter 1 - Introduction

The drinking water industry in the United States and abroad now recognizes that protecting the sources of fresh water is a critical component of any long-term plan for a drinking water system. With this recognition has come a new understanding of the central role that watersheds play in the filtration/treatment process that is necessary to provide clean, safe drinking water to the public in the most cost-effective way. Providing safe drinking water has primarily encompassed chemical treatment or filtration for finished water and better regulation of point source discharges to improve surface water quality. Protection of source water areas and management of human activities in source water areas, however, are increasingly recognized as a very cost-effective means of providing high quality water for consumption. The natural ecosystem within source-water watersheds are increasingly viewed as financial assets (Davies and Masumder 2003), since having high quality water produced by protected or well-managed watersheds can greatly reduce treatment costs, even filtration costs (Ernst 2004). An integral part of source water protection is an understanding of the aquatic ecosystems within water supply watersheds. A successful management plan for New York City's (NYC) drinking water must therefore be based on a solid understanding of the streams and the watersheds they drain in order to make source watershed protection a reality.

Watersheds and their aquatic ecosystems have three critical, drinking-water related functions: (i) they are the ultimate sources of water; (ii) they are major sources of naturally occurring and anthropogenic constituents (physical, chemical, and biological; hereafter contaminants) in water; and (iii) they are primary natural processors of these water-borne constituents. Because past, present, and future land-use activities in source water areas affect each of these functions, successful source water protection requires an "Integrated Watershed Approach" to assess sources, impacts, and processes relevant to the streams and reservoirs of the source area.

An integrated watershed approach to contaminant dynamics in the NYC source area needs to recognize four basic elements: Source, Transport, Ecosystem Impairment, and Symptom. The existing monitoring programs, like most other source water programs, include strong elements of Transport (levels of contaminants in the source water and distribution system, consisting of streams, rivers, reservoirs, and distribution pipes) and Symptom (turbidity, oxygen deficits, taste and odor, disinfection byproduct formation potential, etc.). These elements are driven by local, state, and federal regulations and by operational needs (understanding ambient quality of water for treatment purposes). For instance, as part of NYC's Watershed Protection Plan, the NYC Department of Environmental Protection (NYC DEP) lists key potential sources of pollutants as waterfowl, wastewater treatment plants, failing septic systems, farms, and stormwater. To assess the impact of these sources, the NYC DEP uses regulatory benchmark comparisons, temporal trends, case studies, and modeling incorporating the following constituents: fecal coliforms, turbidity, total phosphorus, conductivity, and trophic status. (NYCDEP 2006). These measures of contaminant levels (i.e Transport) are being used to assess the water quality outcome of a given Source (i.e. Symptom) rather than being a direct measure of that Source or a direct assessment of any Ecosystem Impairment by that Source.

The monitoring program summarized here focused on elements of Ecosystem Impairment and Source and was intended to enhance on-going efforts by introducing both new study variables and a different scale (spatial and temporal) for certain study variables. To the extent possible, identifying sources of the principal contaminants in the various watersheds and sub-watersheds is critical to developing long-term plans for current remediation and future protection and development. This requires an intensive and coordinated spatial and temporal sampling program as well as sophisticated analytical techniques that can distinguish among the various possible sources of contaminants within each of the NYC source watersheds. Further, these principal contaminants have the potential for causing some impairment to streams, rivers, and reservoirs of the NYC water supply system. Such impairment can cause a change in the structural and/or functional properties of the ecosystem which renders it unable to effectively or efficiently utilize, process, metabolize, or otherwise sequester materials, including contaminants entering from the watershed.

(Shuhuai et al. 2001), in describing an economic assessment of a watershed management project within the drinking-water source area for Beijing, note a major shortcoming in the assessment. One of the stated benefits of Beijing source-area management project was improved water quality, yet the data necessary to assess such improvements were not available. By augmenting the existing monitoring effort in NYC's source-water watersheds through assessing contaminant sources and key structural and functional properties of streams, rivers, and reservoirs in the NYC distribution system, this project will provide: (i) a basis for measuring spatial variation in the source of contaminants and their impacts on ecosystem functioning and biological communities; (ii) a basis for measuring temporal/spatial change in both the source of contaminants and their impacts on stream, river, and reservoir functionality; and (iii) a stronger scientific basis for the overall management plan for the NYC source water area.

All three of the points above, describing what the data from the Source and Ecosystem Impairment monitoring will provide, can be summarized under a single, over-riding benefit of this project: a baseline of water-quality information. This baseline will put into perspective the present-day magnitude and complexity of contaminant/source issues throughout the NYC source water area as well as the current status of ecosystem health within the NYC source water system. Here, ecosystem health is whether the ability to process excess nutrients in watersheds is in good to excellent condition or where that ability has been compromised. Most importantly, these data in conjunction with data collected through the other monitoring efforts, will provide a well-rounded baseline for assessing water quality across the source-water areas well into the future. The necessary information will be in place to determine the success of on-going remediation efforts in NYC source-water areas and will be helpful in designing/implementing future remediation or conservation efforts (e.g., BMP, stream restoration, zoning) as part of an overall NYC management plan.

The principal objectives of this monitoring program have been:

1. To provide dependent variables for statistical analyses relating aquatic ecosystem structure and function to land use, best management practice (BMP) implementation, and other watershed inputs or factors.

2. To provide chemical and biological indicators for evaluating the occurrence and source of selected aquatic contaminants.

3. To provide a baseline data set of population, community and ecosystem-level variables and molecular indicators of contaminants to assess changes in water quality and aquatic ecosystem structure and function in response to on-going and/or future shifts in land use/cover. For example, (i) quantitative measures of stream ecosystem structure/function can be used in a before-after analytical framework; or (ii) measurements made across sites help define the true range of conditions throughout these watersheds. This range can then be compared to future changes to understand improvements or degradations at specific points in a watershed.

As has been established already, this monitoring program was designed to complement existing programs of the New York State Department of Environmental Conservation (NYS DEC), New York City Department of Environmental Protection, United States Environmental Protection Agency (US EPA), and the New York State Department of Health (NYS DOH), as well as programs under the direction of -- and/or in cooperation with -- the various counties in the study area. Several of the principal study elements in this program were not monitored by any of the above groups at the outset of this endeavor. While one or more groups were monitoring some elements (or parts of an element) they were doing so with lower spatial intensity and, in some cases, less accuracy or precision. Although the Stroud Center's program was designed to have some overlap of study site locations with NYS DEC and NYC DEP programs, to allow data generated from each program to supplement and add perspective to one another, this program is an independent effort designed to enhance overall monitoring in these source areas.

This final report of the monitoring program covers 6 years of study across the entire NYC drinking-water source areas. A technical overview of study design and study site descriptions (Chapter 2) is followed by separate chapters on the specific tasks of this program: Nutrients, Major Ions in transport (Chapter 3); Molecular Tracers in Streams (Chapter 4); Molecular Tracer Sources Tracking (Chapter 5); Organic Matter Dynamics (Chapter 6); Macroinvertebrate Community Structure and Function (Chapter 7); Nitrogen (N), Phosphorus (P), and DOC Spiraling (Chapter 8); Net Stream Metabolism (Chapter 9); and Reservoir Productivity (Chapter 10).

Each chapter contains an overview of field and laboratory methods along with a results and discussion of data from all six years of research/monitoring activities. Data discussion generally describes how data within each task characterized individual study sites, subwatersheds, and the two regions (East and West of the Hudson River) that comprise the NYC source water areas. Integration across monitoring tasks to the extent possible, are also discussed.

Literature cited

Davies, J.-M., and A. Masumder. 2003. Health and environmental policy issues in Canada: the role of watershed management in sustaining clean drinking water quality at surface sources. Journal of Environmental Management **68**:273-286.

Ernst, C. 2004. Protecting the source. Land conservation and the future of America's drinking water. Trust for Public Land and America Water Works Association.

NYCDEP. 2006. 2006 Watershed Protection Program Summary and Assessment. Department of Environmental Protection, New York City.

Shuhuai, D., G. Zhihui, H. M. Gregerson, K. N. Brooks, and P. F. Ffolliott. 2001. Protecting Beijing's municipal water supply through watershed management: An economic assessment. Journal of the American Water Resources Association **37**:585-594.

Chapter 2 – Technical Design

Overview

This chapter includes a description of the landscape template (including land cover, soils, geology, climate and hydrology) of the New York City (NYC) drinking-water-supply watersheds, located across 2 geographically distinct regions (see below). This information serves as important background material that provides the spatial context for understanding the results of this large-scale enhanced monitoring project conducted from 2000 to 2006. The landscape template variables presented in this chapter are tested extensively in subsequent chapters as explanatory variables for direct measures of stream and reservoir water quality or biological function. The primary objective for this chapter was to describe as well as compare and contrast watershed characteristics across the study area.

The overall project design was intended to: (i) expand understanding of sources of principal contaminants in "source water" watersheds of NYC; (ii) provide new information about present structure and function of the aquatic ecosystems comprising the "system"; and (iii) use that information as a measure of anthropogenic stress; an estimate of "functional capacity" of these ecosystems to absorb, sequester, or otherwise process natural inputs and contaminants; and a baseline to determine future improvement and/or deterioration in watershed conditions. The components of this monitoring program were intended to complement existing programs run by city, state, and federal entities (e.g., NYC Department of Environmental Protection), while also building on one another and adding novel information about water quality and stream health. Some project elements (e.g., grab samples of water chemistry) were instantaneous with regard to condition over time. Some elements (e.g., macroinvertebrates) contain information about water quality/habitat condition over time. Some (e.g., N, P, DOC spiraling, and stream metabolism) were integrative in a spatial sense. This programs strength lies in its breadth of study elements and its high degree of integration (same sites/timing/personnel).

This project is a spatially intense, broad synoptic survey repeated annually, rather than a highly targeted survey with limited spatial scope and high repetition within a site. All major watersheds throughout the study area were included in this monitoring regime, rather than one or two watersheds representing a small portion of the study area. This broad synoptic approach avoids two serious problems associated with a spatially limited, temporally intense approach: (1) pseudoreplication - where multiple samples taken from a given stream throughout the year still only represent one stream and one watershed; and (2) serial autocorrelation - where repeated measures of the same variable during the year tend to be correlated with one another or are non-independent (e.g., baseline chemistry, macroinvertebrates). This applies to both baseflow and stormflow sampling. This sampling scheme leads to a project focus on between-stream variability rather than between-storm variability for a given stream.

Study Regions

This study was conducted in 2 regions: 1) the west-of-Hudson River region (WOH) comprised of two sub-regions (the Catskills [1479 km^2] and the upper Delaware [2616 km^2]), and 2) the east-of-Hudson River region (EOH), also known as the Croton/Kensico system (971

km^2). The WOH includes 6 primary river basins and 6 reservoirs (Fig. 2.1) that drain either to the Hudson River (via Schoharie, Esopus, and Rondout Creeks) or to the Delaware River (via the Neversink River and the East and West Branches of the Delaware River). The EOH contains 12 reservoirs, 3 controlled lakes, and numerous tributaries that drain to the Hudson River (Fig 2.2). Water withdrawal for drinking water occurs from each WOH reservoir and from several EOH reservoirs.

The Delaware and Hudson River drainages were covered by dense mixed-hardwood or hardwood-conifer forests prior to European settlement (Jackson et al. 2005). Vast proportions of both watersheds were clear cut in the late 18th and 19th centuries and, today, forests in these watersheds are dominated by sugar and red maple, yellow birch, American beech, several species of oak, eastern hemlock, and white pine. Current land uses are described in subsequent sections.

Surficial geology

Surface geology in the 2 regions is the result of past glaciation by the Hudson–Champlain Lobe of the Laurentide Ice Sheet. In the Catskills, glacial history is complicated by the occurrences of both the Laurentide Ice Sheet and local mountain glaciers (Isachsen et al. 2000). The WOH generally can be separated into 2 distinct geologic regions: 1) the southeast (Neversink, Esopus, and upper Schoharie basins) is primarily bedrock outcrop mountain tops with till, kame (steep-sided mounds of sand and gravel deposited by meltwater from a glacier), and outwash sand and gravel deposits in narrow valleys; and 2) the northern and western areas that have more till and deeper soils on the ridges and side slopes and valleys with recent alluvium, outwash sand and gravel, and kame deposits. In the EOH, surficial geology is predominately glacial till riddled with kame deposits throughout with bedrock outcrops and swamp deposits more prevalent in the north.

Bedrock geology

Bedrock geology of the WOH (Isachsen et al. 2000) has roots in the Late Devonian Period (~375 million years before present [ybp]) and is mostly sedimentary (quartz-dominated shale, sandstone, siltstone, and conglomerates). Different formations occur from north to south and east to west (Oneonta, Lower Walton, and Upper Walton formations) within the WOH, but rock origin and composition remains relatively similar throughout the region. Geology in EOH watersheds is a mosaic of sedimentary, metamorphic, and igneous rock formations defining 2 distinct geologic regions (Isachsen et al. 2000), the Hudson Highlands (Middle Proterozoic ~1100 million ybp), and the Manhattan Prong (~500 million ybp). The Hudson Highlands region, which crosses the northwestern portion of the EOH, is composed of layered and unlayered metamorphic units, which are highly resistant to erosion and contain biotite, magnetite, mica, quartz, and feldspar gneiss. The Manhattan Prong dominates the southern portion of the EOH and also is found in the northeastern tip of the region. Its metamorphic rocks include Fordham, Yonkers, Pundridge, and Bedford gneiss, and Inwood (to the south) and Stockbridge (to the north) marble. A pocket of limestone, dolostone, and siltstone occurs near the northern tip of the EOH.

Soils

Soils in the 2 regions are primarily Udept Inceptisols (suborder/order) that are moderate to highly acidic (NRCS 1994). Inceptisols usually occur on relatively active landscapes, e.g., mountain slopes and river valleys, where the processes of erosion actively expose and deposit relatively unweathered material (Brady and Weil 1999). Udepts, which extend from southern New York through central and western Pennsylvania, West Virginia, and eastern Ohio, are freely drained Inceptisols and often have only thin, light-colored surface horizons. Some Udepts in southern New York and northern Pennsylvania are naturally unproductive because of low organic content and have been used for silviculture and pasture/grazing activities after earlier periods of crop production (Brady and Weil 1999). Aquepts (fluvially deposited wet Inceptisols) and Fluvents (fluvially deposited wet Entisols that are younger and less developed than Inceptisols) also are present in EOH and WOH valleys. These organically rich soils are too wet for crop production without artificial drainage. Saprists, wet Histosols of well-decomposed plant material usually associated with wetlands, are limited in extent in the WOH but occur throughout the EOH and account for up to ~5% of soil surface area in some subwatersheds.

Study Design

This 6-year study was split into two, 3-year phases: Phase I was from 2000 through 2002 while Phase II was from 2003 through 2005. Winter sampling at a subset of sites did occur during the winter of 2006. In Phase I, 60 stream and 8 reservoir sampling sites were established in the 2 regions (Tables 2.1, 2.2; and Figs 2.1, 2.2). The 60 stream sites were divided evenly between these regions (i.e., 30 sites EOH and 30 sites WOH) and site selection within each region was based on the following criteria: 1) a range of land covers (forested, agricultural, suburban, and urban), 2) a range of underlying geology/soils, 3) availability of US Geological Survey (USGS)-gauged stream-flow data (Tables 2.1, 2.2), 4) availability of background data (e.g., nearby historic or current New York City Department of Environmental Protection [NYC DEP] sites); and 5) feasibility of studying the various elements of the Project. Reservoir monitoring during Phase I occurred on all 6 WOH reservoirs and on 2 EOH reservoirs (Chapter 10, Table 10.2).

For Phase II, 50 new (differing from Phase I) stream stations were established (27 WOH and 23 EOH) and sampling continued at 12 Phase I sites, for an overall project total of 110 stream monitoring sites. Also for Phase II, 4 new EOH reservoirs were visited and sampling continued at 3 of the 6 WOH reservoirs monitored during Phase I (Chapter 10, Table 10.2). Selection of Phase II sites was based on a combination of (i) “areas of concern” revealed during Phase I, (ii) desire to broaden spatial coverage within source watersheds, and (iii) the need to extend the gradient of conditions captured during Phase I site selection (i.e., did we find the most degraded and least degraded conditions in each region?). In general, Phase II stream sites were located on other important tributaries to primary reservoirs in the system or further upstream in a given watershed from Phase I sites.

Stream monitoring sites were separated into two groups: "targeted" which encompassed all 110 sites and "integrative" covering 17 of the 110 sampling sites. Targeted sites were distributed throughout both regions on streams of varying in size. The locations of integrative sites were selected to be sufficiently downstream so that the stream chemical signal integrated effects of

land cover and other natural and anthropogenic factors in the watershed. In some instances our preference for a site located sufficiently downstream was constrained by the feasibility of 1 or more of the study elements of the Project (e.g., nutrient injections for determining nutrient spiraling length, see Chapter 8). Several of the monitoring tasks involved all 110 sites, while a few tasks (i.e., nutrient spiraling and ecosystem metabolism) were conducted only at integrative sites. Twenty eight (Tables 2.1 and 2.2) of the 60 Phase I stream sites were visited during winter baseflow (January through early March, 2001 to 2003) to collect water samples for molecular tracer analyses (see Chapter 4). Twenty eight sites were also sampled during Phase II (January through March, 2004 to 2006), 7 of which were continued from Phase I winter baseflow sampling. Autosamplers were deployed at 3 (Tables 2.1 and 2.2) of the 110 stream sites to collect water samples during storm events from which particulate and dissolved chemical components were analyzed. Autosamplers were maintained at the same 3 sites for the entire 6-year period (see Chapter 3). A total of 12 reservoirs were also studied for certain project elements (see Chapter 10). Stream and reservoir stations were located using a Trimble GPS Pathfinder ™ ProXR receiver unit (Tables 2.1, 2.2, and 10.1).

Study Site Characteristic Data

Landscape

Watershed, riparian, and reach delineations. Geographic data were manipulated using ArcMap™ (version 9.0, ESRI, Inc., Redlands, CA). Watershed boundaries provided by NYC DEP that did not precisely match our sample locations were modified by on-screen digitizing using USGS 1:24,000 topographic maps (6.1-m contours). Land cover, population density, road density, and known point sources were quantified and summarized at 3 spatial scales. Watershed boundaries defined the watershed scale (W). Thirty-meter buffers around each side of all streams or water bodies in the stream network upstream of each sampling site defined the riparian scale (b). These riparian-scale buffers were clipped at a distance of 1-km upstream from each sampling site to define the reach-scale (1k). The reach-scale delineation included tributaries (where present) but the main-stem stream received the greatest proportion of the 1-km length. Two sites (59 and 60) located on small streams with mapped channel lengths <1 km (0.71 and 0.95 km, respectively) were retained in all analyses. An in-depth analysis of the relationship between the 3 spatial scales across all 110 sites will not be presented in this report. We direct the reader to Arscott et al. (Arscott et al. 2006) for more information on how these 3 spatial scales relate to one another within the context of the Phase I sampling effort.

Land cover. Rasterized land-cover data (obtained from NYC DEP) were derived from 2001 Landsat Enhanced Thematic Mapper Plus (ETM+) satellite imagery (5 April, 8 June, 10 July, and 12 September 2001). A classification scheme based on Anderson Level 4 (1976) was developed by NYC DEP to classify ETM+ images after overlaying them with National Wetland Inventory polygon data (mid 1980s), NY State Office of Real Property Services Tax Parcel data, USDA Farm Security Agency and Watershed Agriculture programs, and other ancillary data sources (Adair et al. 2004). The spatial resolution of this composite land-cover data layer was 10-m grid-cell size.

Preliminary assessment of the success of classification indicated that the Anderson Level-2 classification was the most complete level. Nevertheless, many grid cells, particularly urban grid cells, were classified only at Anderson Level 1. Therefore, a computer routine was developed to classify several urban grid cells remaining at Anderson Level 1 to the appropriate Anderson Level-2 category (see Anderson et al. 1976). The reclassification scheme identified the majority value of all Anderson Level-2-categorized cells in a neighborhood surrounding the grid cell requiring reclassification and assigned that classification to the cell in question. This scheme was run iteratively, with the neighborhood of grid cells increasing by 1 grid-cell width in each run, until <5% of all cells requiring reclassification in the input raster remained unclassified. Some agriculture and brushland grid cells also were classified only to an Anderson Level-1 category, but those grid cells were either too few within a watershed or too isolated from other similarly categorized grid cells to achieve reclassification. Across the entire study area, approximately 0.15% of all grid cells were at the Anderson Level-1 urban, agriculture, or brushland classification, and over 90% of those cells were re-classified. In terms of Phase I study sites, 13 of 60 watersheds had >1% of cells classified to Anderson Level-1 urban, agriculture, or brushland categories, and only 2 of those 13 watersheds had >5% of cells classified to these same Anderson Level-1 categories. This analysis was not performed for Phase II sites. Following this reclassification scheme, land cover at Anderson Level-2 classification was summarized as % cover for watershed-, riparian-, and reach-scale areas. Principal Components Analysis (PCA) was used to illustrate primary land-cover variable(s) (after arcsine square root transformations) within each study region (WOH and EOH) that best defined land-cover gradients among sites. EOH and WOH results were compared to identify major regional differences in land-cover gradients. The following land use/cover and related categories were included in the PCA: Residential (RESD), Commercial (COMM), Industrial (INDU), Other Urban (OURB), Farmstead (FMST), Cropland (CROP), Orchard (ORCH), Grassland (GRAS), Brushland (SHRB), Mixed Brush/Herbaceous (MBRH), Deciduous Forest (DECD), Coniferous Forest (CONF), Mixed Deciduous/Coniferous Forest (MFOR), Wetlands (WETL), Open Water (WATR), Wastewater Treatment Plant effluent (SPDE), Road Density (RDNS), Population Density (PDNS).

Population and road density. Population density was compiled from the 2000 Census data using census blocks, the smallest population units available, within each county in the study area (Census 2000; http://www.census.gov/geo/www/census2k.html). Census data were retrieved as Census 2000 TIGER/Line data from Environmental Systems Research Institute, Inc. (ESRI) (http://www.esri.com/data/download/census2000_tigerline/index.html). Watershed-, riparian-, and reach-scale boundaries were used to determine the portion of each census block that fell within a given study watershed. The fraction of the census-block area falling within a given watershed, riparian, or reach delineation was multiplied by the total population count for that census block, summed for all census blocks within a delineated area, and then divided by that area to estimate scale-specific population densities. Census blocks were large relative to buffer delineations and, therefore, riparian and reach values were more likely than watershed values to have measurement error associated with cell size (i.e., buffers never contained an entire census block, whereas watersheds often did).

Road densities in EOH watersheds were quantified from digitized 1996 New York Department of Transportation (NY DOT) Planimetric Images provided by NYC DEP. WOH

roads were digitized in 1993 from USGS digital line graphs. Road data layers were intersected with watershed-, riparian-, and reach-scale delineations for all study 110 sites, and the lengths of roads in each area were summed and divided by watershed-, riparian-, or reach-scale area to derive road densities. Watershed-scale population and road densities were included in the PCA of landscape variables after log transformations (see *Land cover* above).

Point-source discharges. Point-source discharges were quantified as annual values and averaged over the individual years sampled for a given site (n=3 or 6) based on monthly mean daily discharge values supplied by the NYC DEP for all State Pollutant Discharge Elimination System monitored sites designated as having an 'active' operational status (SPDE; n = 109). Most of these sites were wastewater treatment facilities. A corresponding GIS point coverage of SPDE locations was used to determine the number of point sources in each study watershed. Each monthly mean daily discharge was multiplied by the number of days in the month, summed for all months and for all sites within a study watershed, and divided by basin area to derive an estimate of annual SPDE outflow across watersheds for each year. Point-source discharges were not quantified at the reach or riparian scales because all SPDE facilities release to a water body or waterway and selection of SPDE facilities within the buffer around the entire stream network would have provided a result identical to the watershed-scale result.

Landscape variable relationships. Landscape characteristics differed considerably between WOH and EOH regions (Tables 2.3 and 2.4, respectively). Agricultural land-cover categories included cropland, orchard, farmstead, and grassland. WOH 2000 real property tax parcel information indicated that ~80% of the actively farmed agricultural tax parcels were livestock operations, primarily dairy farms, and ~15% were field-crop operations. A head count of livestock has been estimated at 35,000 in the EBD and WBD subregions (National Research Council 2000). This count is greater than the number of humans (~25,000 based on the 2000 Census) in these subregions.

The proximity of EOH watersheds to NYC has resulted in clear influences from metropolitan infrastructure. Average population density (±1 SD) at the watershed scale in the EOH (207 ± 164 ind./km^2) was significantly greater (T-test, assumed unequal variance, $p < 0.0001$) than in WOH watersheds (8.5 ± 5.0 ind./km^2). Average road density was also significantly greater (T-test, assumed unequal variance, $p < 0.0001$) in EOH watersheds (mean = 3.6 ± 1.34 km/km^2) than for sites in WOH watersheds (mean = 0.8 ± 0.28 km/km^2). EOH watersheds had higher percentages of urban land covers (residential, commercial, industrial, and other urban land covers) and wetland and water cover than WOH watersheds. Water cover was high in EOH watersheds because several sites were downstream of reservoirs/controlled lakes. Twenty of the 57 WOH watersheds had forest cover (sum of deciduous, coniferous, and mixed forest) >90%, whereas only 2 EOH sites (48 [Crook Brook] and 125 [Quaker Brook]) approached that value (87%).

Watershed-scale variations in land cover within each region were explored using PCA (Figs. 2.3, 2.4). The first 2 factors accounted for 63% of the among-site variance in WOH watershed characteristics, with most of the variance represented on the 1st axis (factor 1 = 44%; Fig. 2.3). Grassland cover (GRAS = 8% absolute contribution to factor 1 definition), other urban (OURB, 8%) and road density (RDNS = 8%) contributed most to the definition of factor 1, followed closely by cropland (CROP = 7%), farmstead (FMST = 7%), and population density (PDNS =

7%). Factor 2 was defined primarily by mixed and coniferous forest (CONF and MFOR, respectively, both = 12%), commercial (COMM = 10%), and wastewater treatment plant effluent (SPDE = 9%). This multivariate, 2-dimensional space distinguished sites (Fig. 2.3) with highest deciduous forest cover (primarily Esopus Creek, Rondout Creek and Neversink River sites) from sites with more coniferous/mixed forest plus commercial cover (several Schoharie Creek sites) and from sites with predominantly agricultural and some urban cover (East and West Branch of the Delaware River).

For EOH sites, the first 2 factors accounted for 44% of the among-site variance in watershed characteristics, with loadings on each factor being nearly equal (Fig. 2.4). Population density (PDNS = 13% absolute contribution to factor 1 definition), road density (RDNS = 13%), and residential cover (RESD = 12%) contributed most to the definition of factor 1 (Fig. 2.4), but deciduous forest (DECD = 11%), wastewater treatment plant effluent (SPDE = 10%), and commercial cover (COMM = 9%), also were important along this dimension. Factor 2 was defined mostly by shrubland (SHRB = 10%), wetland (WETL = 10%), and cropland (CROP = 9%), followed closely by other urban (OURB = 8%), water (WATR = 8%), commercial cover (COMM = 8%) and farmstead (FMST = 7%). Sites within the same subregion did not always cluster close together in this 2-dimensional space (Fig. 2.4).

These results illustrated clear differences in gradients of land cover and other catchment variables between WOH and EOH. EOH sites were less forested, more urbanized, and had greater flow contributions from point-source discharges than WOH sites. EOH sites also had greater wetland and lake/reservoir area upstream from study sites than WOH sites. WOH sites were either more forested or had more agricultural land cover in their watersheds and always had lower population and road densities than EOH sites.

Hydrology

Precipitation. Daily precipitation data for the study region were compiled from the National Oceanic and Atmospheric Administration (NOAA), National Climatic Data Center (NCDC), Cooperative Summary of the Day (TD3200) CDROM containing period-of-record data through 2001. Additional 2002-2005 data were downloaded from http://cdo.ncdc.noaa.gov/pls/plclimprod/poemain.accessrouter?datasetabbv=SOD. NOAA sites were selected by importing the site coordinates in decimal degrees for NY climate divisions 2 and 5 and all sites in Connecticut into a geographical information system (GIS) layer using ArcMap™ (version 9.0, ERSI, Inc., Redlands, CA). All sites within a 10-km buffer around the entire study area were considered. Due to incomplete annual data within the precipitation dataset, final selection of sites depended upon the particular summary or analysis. For the regional average precipitation summary, a total of 12 sites (10 WOH, 2 EOH) were selected by keeping those sites with at least 4 y of data in the 2000 to 2005 period. For an analysis of the impact of topographic elevation on annual (Oct-Sep water year) precipitation by region and year, all sites within a given year were used. Daily precipitation data were summed by month and year for the study period for each NOAA site.

The period from 1964 to 1999 was the longest period of overlapping and continuous USGS streamflow monitoring data used to summarize hydrological trends across the study region (see below). Therefore, precipitation data for the period from 1964 to 1999 were collected from a

subset of the NOAA sites that had adequate historical data to provide a temporal perspective for the study period. For any given site, a single year's data record was omitted if it was incomplete. Thus, the number of years of data for the NOAA sites used for historical analysis ranged from 20 to 34.

Average annual precipitation over the study period was remarkably similar between the 2 regions (EOH: 120 cm, WOH: 125 cm). However, these values probably did not reflect the spatial distribution of precipitation across the study regions. Given uniform meteorological conditions, precipitation tends to increase with elevation (Dunne and Leopold 1978). Annual precipitation volume at WOH sites was significantly and positively related to elevation in 5 out of the 6 years of the study based on regression analysis of annual precipitation volumes versus latitude (no relationship was found with longitude) and elevation (range in slopes of 0.03 to 0.119 cm precip/m elevation, n = 9 to 34 depending upon year,$\alpha = 0.1$). For EOH sites, only 1 of the 6 years was found to have a significant, though negative, relationship between annual precipitation volume and elevation. The WOH precipitation-to-elevation relationships and the fact that only 4 of the 34 WOH NOAA sites used in the regression analyses were at elevations greater than the hypsometric mean elevation of 592 m (EOH hypsometric mean elevation = 162 m), suggested that the WOH average annual precipitation value was an underestimate of the actual mean value for this region.

Six NOAA sites had records sufficient for an historical evaluation of climatic conditions. Annual (October-to-September water year) precipitation totals for each of the 6 years (2000-2005) were assessed relative to the distribution of precipitation totals over the 1964 to 1999 period (Fig. 2.5). Years 2003 and 2004 were the wettest years in the 6-y study period for those sites having data for both years, and both years were wet years relative to the historical record of 1964 to 1999. Depending on the specific station used in the comparison, either 2001 or 2002 were among the driest years compared to the 1964 to 1999 period.

The wettest months of the year during the first phase of the study (2000-02) tended to be from March through June (Fig. 2.6), with the notable exception of April 2001, which had the lowest (WOH) or nearly the lowest (EOH) average monthly total. During the second phase (2003-05), however, the wettest months tended to be in the fall, most notably in the month of October in 2004 and 2005. The dry conditions noted for 2001 and 2002 began with low winter precipitation totals during 2001, especially at WOH sites. Low winter precipitation in early 2002 contributed to dry conditions in 2002.

Regional Patterns of Streamflow. Published streamflow data were available for 63 USGS sites located throughout the study regions (http://waterdata.usgs.gov/ny/nwis/sw). Ten of these sites were influenced either by reservoir/lake outlets or by interbasin transfers (based on USGS site information) and 2 sites did not have complete data for the October 1999-March 2006 period. Data for the entire period of record through March 2006 were obtained for the remaining 51 USGS sites. Daily mean discharges were converted from ft^3/s to $cm^3/cm^2/d$ (cm/d) by dividing discharge by watershed area to generate area-specific discharge rates, which facilitated comparisons of yield among watersheds. Streamflow was summarized across months and years (October-to-September water year) for the 2000 to 2006 (through April, 2006) study period and for time periods before our study. Data were available from 1964 to 1999 for WOH sites, but

none of the EOH sites had monitoring periods >8 y. Spatial summaries were computed on a subregion level (defined by 5 reservoir watersheds) for the WOH sites, but all EOH sites were summarized as a single region. The relationships between mean annual discharge, based on USGS sites, and other landscape variables were assessed using Pearson correlation.

Interannual patterns in flow reflected historic precipitation patterns (Fig 2.5). Total annual discharge for 2004 and 2005 was above the 75th percentile of total annual discharge for the defined historical period for all of the USGS sites, and in the case of 2004, at or above the maximum historic value for 4 of the USGS sites. Total annual discharge for 2001 and 2002 were below the 25th percentile for the historical period across all 8 USGS sites. Patterns of monthly discharge during the 6-y study period averaged across USGS sites for WOH and EOH were seasonal. In general, discharge was high in late winter/spring and low in late summer/autumn (Fig. 2.6). A rain-on-snow event in April 2001 led to high discharge in WOH streams. During 2003 and 2004, monthly discharge began to increase in September and October, which was contrary to the general pattern of low values well into the fall of each year.

Area-specific, USGS average annual discharge was significantly and positively correlated (r = 0.90, p=0.004) with % total forested area in the subregion (EOH and 6 WOH subregions), while significantly and negatively correlated (r = –0.82) with % total urban area. A significant and negative correlation (r=-0.86, p=0.01) also was found between total subregion area (as defined by the respective reservoirs; used the New Croton Reservoir for the EOH subregion) and the area-specific, average annual discharge values. Total subregion area was significantly and negatively correlated with % total forested area (r=-0.77, p=0.04) but not with % total urban area. Total number of USGS sites within each subregion ranged from 3 (Rondout) to 17 (EOH); Pearson correlation was used with no data transformations. Two plausible explanations exist for the inverse relationship between average annual discharge and % total urban area. First, high precipitation in the WOH region (see previous section) and steeper topography (and thinner soils) may result in higher specific yield per unit area in the WOH compared to the EOH region. Second, the EOH region is, in general, more likely to have higher hydrologic retention compared to the WOH due to greater % wetland area and greater number of lakes and reservoirs relative to the WOH region (Arscott et al. 2006).

Site-Specific Baseflow Hydrology. Discharge data for the USGS sites described in the previous section also were used to determine site- and sampling-date-specific flow conditions when sampling for other elements of the Project. Discharge, as mean daily flow, was estimated or extracted from existing USGS records for each study site (n = 110) on the dates of baseflow-specific sample collections. For sites without co-located USGS gauging stations (n = 79), discharge was estimated from discharge–watershed-area regression equations developed independently for each of the 6 subregions (EOH, West Br. Delaware - WBD, East Br. Delaware - EBD, Schoharie - SCH, Esopus - ESP, Neversink/Rondout - NVR) on each sampling date using data from the 51 USGS stations. Regression intercepts were not significantly different from 0 in all but 9 of the 282 initial equations. Therefore, a 2nd regression iteration was run for each date and study site with the intercept term set equal to 0. Outliers were determined visually from bivariate and residual plots of discharge versus watershed area and were removed prior to a 3rd regression iteration. The average daily sampling-date discharge values were also correlated

against land use/cover variables within each region as a comparison to results of annual average USGS site discharge versus land cover correlations.

Standard criteria were developed to ensure that a consistent definition of baseflow condition was met at the time of all summer baseflow sampling for water chemistry. Hydrologic conditions at anticipated sampling sites were checked on-line via the USGS real-time hydrological network (http://waterdata.usgs.gov/nwis/rt). A visual assessment was made of relevant hydrographs compared to the baseflow criterion that streamflow changed <10% over the 24 h preceding sampling (using provisional, 15-min discharge data available online). Hydrograph data were difficult to monitor during longer field excursions. Therefore, if a stream appeared unusually turbid or if the wetted perimeter displayed signs of high flow when samples were collected, the site was (re)sampled at a later date. The difference between mean daily discharge on the sampling date and the date prior to sampling was used as a post-sampling assessment of whether the baseflow criterion had been met for each sampling date. Both actual mean daily discharge values from co-located USGS sites and estimated discharge values for sites not co-located with USGS sties were used in this assessment. Only approximately 40% of all samples were within the 10% change-in-discharge criterion however >75% had changes in discharge from the previous day of <20%. Of the approximate 60% of samples that exceeded the 10% criterion, 85% of the samples occurred during decreasing flow conditions, usually days removed from any storms.

For those dates exceeding the 10% criterion, provisional 15-min instantaneous discharge hydrographs, for sites co-located with USGS gauging stations, were examined. This evaluation permitted a more precise determination of baseflow conditions than could be made from daily mean discharges, especially given the potential for short-duration summer storms common in this region. Sites not co-located with USGS sites were assessed based on conditions for the sampling date in question at the closest NY-project site that was co-located with a USGS site. For inorganic chemistry, DOC, and organic particles, 28 samples (out of 365 project samples) from 13 separate dates were potentially collected during minor runoff events (Table 2.5). For molecular tracers, 30 summer samples (out of 363) collected from 11 separate dates and 11 winter samples (out of 168) collected from 2 separate dates were potentially collected during minor runoff events. Note that provisional discharge data was not always available for the winter 2006 sampling effort and therefore not all of the sampling dates during this specific period could be evaluated.

A majority of the sites listed in Table 2.5 are associated with USGS sites that either drain a much larger area relative to the Project sampling sites (e.g., E. Br. Croton River nr Putnam Lake associated with sites 34, 125, 129, and 132) or are geographically distant from the associated sampling sites (e.g., Kisco R. below Mount Kisco and sampling sites 147, 148). Therefore, it is more than likely that the storm events identified using a particular USGS site did not impact sampling at the associated Project sampling site. For those sites co-located, or nearly so, with USGS sites, most of the dates listed in Table 2.5 are associated with storm events that had less than a doubling in discharge; i.e., minor storm events. Finally, field technicians did not notice any increased turbidity at the time of sampling at any of the sites for the dates in question. Therefore all baseflow-collected samples over the duration of this study were considered to be representative of baseflow conditions.

Area-specific baseflow discharge at each site in the WOH region, at the time of sample collection, was significantly and positively correlated with % forest cover ($r = 0.34$, p=0.008) and negatively correlated with % total urban cover ($r = –0.27$, p=0.04). Pearson correlation was used for this analysis with data transformations not necessary based on visual examination of scatter plots of discharge versus the given land cover variables. These patterns based on the significant WOH correlations were unexpected in the context of impervious surface influences on discharge. However, as noted in (Arscott et al. 2006), forested areas occurring on steeper slopes can lead to higher relative discharge compared to more urbanized areas. No significant correlations between land use/cover variables and baseflow discharge were found for the EOH region.

Stormflow Hydrology. Stormflow sampling occurred at 3 sites: W. Br. Delaware River at Hawleys (6); Neversink River near Claryville (29); and the Kisco River near Stanwood (55). USGS gauging stations were co-located at the Kisco River (USGS ID 01374987) and Neversink River (USGS ID 01435000) monitoring sites. Our monitoring site on the Neversink was ~1.5 km upstream from the USGS stage height recorder but there were no tributaries between our monitoring site and the USGS site. For the third monitoring site, the W. Br. Delaware River at Hawleys, a USGS gauging station was located several miles downstream in Walton (USGS ID 01423000). Storm hydrographs at that site (W. Br. Delaware R. at Hawleys) were estimated using the measured discharge at the USGS Walton gauge multiplied by the ratio of the watershed area at the monitoring site to the watershed area for the USGS gauging station at Walton. A MiniTroll stage recorder (pressure transducer), which records relative stage height, was located at the W.Br. Delaware R. monitoring site and was used to adjust the timing of the USGS-produced hydrograph for the peak stage at the monitoring site. These offsets in peak flow time (varied by storm event) were applied to all estimates of storm discharge. Because instantaneous flow data were collected at 15-minute intervals at each of the gauging stations, discharge taken at the interval closest to the actual sampling time was used as the corresponding sample discharge.

Six storms were sampled at each of the storm-sampling sites with both small and relative large events captured in the sampling effort (Fig. 2.7). The distribution of the storm sample flows, as well as the baseflow samples, relative to the frequency distribution of discharge (15-minute USGS provisional discharge data) over the entire 6-year sampling period is provided in Fig. 2.8. These flow frequency plots demonstrate that the combined baseflow/stormflow sampling effort captured the range of flow conditions within the study period at each of these sites. More specifically, sample flow percent exceedances (i.e., the percentage of discharge values that exceeded a given value) ranged from 3% to 93% for the W. Br. Delaware R. site; 0.1% to 90% for the Neversink R. site, and <0.1% to >99% for the Kisco River site.

Antecedent conditions, specifically, time to the previous storm, were consistent across a majority of the sampled storms. For 13 of the 18 sampled storms, time since the last storm ranged from 10 to 19 days. Three storms, site 6 on 17JUN01 and 07JUN02, and site 55 on 20SEP01, had times to the previous storm of 5, 7 and 6 days, respectively. Two storms had rather extended dry antecedent periods; site 55 on 16JUN05 and site 29 on 20SEP01, where days since the previous storm were 22 and 74 days, respectively.

Literature Cited

Adair, E. C., D. Binkley, and D. C. Andersen. 2004. Patterns of nitrogen accumulation and cycling in riparian floodplain ecosystems along the Green and Yampa rivers. Oecologia 139:108-116.

Anderson, J. R., E. E. Hardy, J. T. Roach, and R. E. Witmer. 1976. A land use and land cover classification system for use with remote sensor data. Professional paper 964, U.S. Geological Survey, Washington, D.C.

Arscott, D. B., C. L. Dow, and B. W. Sweeney. 2006. Landscape assessment of New York City's drinking water supply catchments. Journal of the North American Benthological Society. 25:867-886

Brady, N. C., and R. R. Weil. 1999. The nature and properties of soils, 12th edition. Prentice Hall, Upper Saddle River, NJ.

Dunne, T., and L. B. Leopold. 1978. Water in Environmental Planning, 16th edition. W.H. Freeman and Company.

Isachsen, Y. W., E. Landing, J. M. Lauber, L. V. Rickard, and W. B. Rogers, editors. 2000. Geology of New York. A simplified account, 2nd edition. The New York State Geological Survey, Albany, NY.

Jackson, J. K., A. D. Huryn, D. L. Strayer, D. L. Courtemanch, and B. W. Sweeney. 2005. Atlantic coast rivers of the northeastern United States. Pages 21-72 *in* A. C. Benke and C. E. Cushing, editors. Rivers of North America. Elsevier Academic Press, New York.

National Research Council. 2000. Watershed management for potable water supply: Assessing the New York City strategy. National Academy Press, Washington, D.C.

NRCS. 1994. State soil geographic (STATSGO) data base. Data use information. Miscellaneous Publication 1492, USDA Natural Resources Conservation Service, Fort Worth, TX.

Table 2.1. Location information for West of Hudson stream sites. Each site was located using a Trimble GPS Pathfinder TM ProXR receiver unit, with real-time correction (Datum = WGS 84). Phase I (P1) and Phase II (P2) Type columns define sites as Targeted (T) or Integrative (I) and as winter baseflow (WB) and/or stormflow (S) sites (see text for definition of site types). See Table 2.3 for site names and other descriptive information.

Site	P1 – Type	P2 – Type	Co-located USGS Site ID	Latitude	Longitude
				Decimal Degrees	
1	T WB			42.42772334	-74.61744145
2	T WB			42.36879344	-74.67698677
3	T	I WB		42.34367436	-74.71979975
4	T			42.25943847	-74.92804414
5	I			42.26017240	-74.92766609
6	T WB S	T WB S		42.17548414	-75.01828999
7	T			42.19867690	-75.12118309
8	T WB			42.15065084	-75.16552055
9	T	I WB	1424001030	42.17376864	-75.27943302
10	T WB	I WB		42.16987985	-74.61151354
11	I WB		0141339800	42.15072089	-74.60162743
12	T WB		0141340800	42.14439909	-74.61928462
13	T WB			42.12377199	-74.67493757
14	T		0141400000	42.13256027	-74.69542765
15	T	I WB	0141500000	42.12610104	-74.81170240
16	T WB		0134970000	42.24246695	-74.31036639
17	T WB			42.22823947	-74.28426781
18	I WB		0134970500	42.23850629	-74.33987649
19	T		0134981000	42.23183665	-74.39324622
20	T WB			42.30365750	-74.41848748
21	T			42.30934333	-74.42320999
22	T WB			42.09767742	-74.44927928
23	I WB	T WB	0136220000	42.11731029	-74.37679339
24	T WB			42.08329019	-74.31573473
25	T			42.04674796	-74.27654312
26	T	T WB	0136250000	42.03961869	-74.28169149
27	T WB		0143449800	41.92040232	-74.57448625
28	T			41.91759972	-74.57345882
29	I WB S	I WB S	0143500000	41.90174954	-74.58072348
30	I WB		0136500000	41.86688935	-74.48668300
101		T		42.33553867	-74.73917211
102		T WB		42.25703301	-74.77161393
103		T WB		42.29949546	-74.89223927
104		T		42.24288046	-74.96426207
105		T WB	0142274700	42.18096091	-75.10621802
106		T		42.11789180	-75.24962674
107		T WB	0141308800	42.29375686	-74.55917861

Table 2.1. Continued.

Site	P1 – Type	P2 – Type	Co-located USGS Site ID	Latitude	Longitude
				Decimal Degrees	
108		T WB		42.23393721	-74.59036309
109		T		42.18139839	-74.59126882
110		T		42.17068580	-74.51546992
111		T		42.10767973	-74.56120015
112		T	0141450000	42.10617040	-74.73026838
113		T		42.12910492	-74.89832297
114		T		42.06546841	-74.87722641
115		T		42.17198754	-74.14987465
116		T		42.24242108	-74.17846641
117		T WB		42.29337212	-74.30532935
118		T	0135003500	42.33792438	-74.45102525
119		T WB	0136219550	42.10938420	-74.45181128
120		T		42.12109310	-74.39868066
121		T		42.10009907	-74.29540223
122		T		41.99047876	-74.49263600
123		T WB		41.91630759	-74.43564844
151		T		42.34512936	-74.73337798
153		T		42.15946134	-75.27729896
159		T		42.14392778	-74.48091667
160		T		42.15120278	-74.51986944

Table 2.2. Location information for the East of Hudson stream sites. Each site (except 150; from map) was located using a Trimble GPS Pathfinder TM ProXR receiver unit, with real-time correction (Datum = WGS 84). Phase I (P1) and Phase II (P2) Type columns define sites as Targeted (T) or Integrative (I) and a winter baseflow (WB) and/or stormflow (S) site (see text for definition of site types). See Table 2.4 for site names and descriptive information.

Site	P1 - Type	P2 - Type	Co-located USGS Site ID	Latitude	Longitude
				Decimal Degrees	
31	T			41.51192020	-73.62245192
32	T WB			41.53699463	-73.57880320
33	T WB			41.50200353	-73.74451453
34	T	I WB		41.49438077	-73.54641599
35	T			41.47062908	-73.65523955
36	T		0137455900	41.47173317	-73.76077430
37	T		0137459800	41.47251000	-73.69147481
38	T			41.44961309	-73.73434766
39	T			41.40645621	-73.59321777
40	I WB		0137465400	41.43476191	-73.65427494
41	T		0137462010	41.38842945	-73.68323767
42	T			41.37637348	-73.63146001
43	T WB			41.37015736	-73.78453355
44	T		0137453100	41.35571736	-73.65809238
45	T		0137470100	41.35221469	-73.67104106
46	I WB	I WB	0137493000	41.33265904	-73.76496965
47	T		0137482100	41.32701362	-73.65540697
48	T			41.31807254	-73.58746553
49	T WB			41.28583097	-73.76606514
50	T		0137497600	41.28246754	-73.72512418
51	T			41.27889870	-73.83525209
52	I WB	I WB	0137489000	41.26028843	-73.60198649
53	T			41.24594902	-73.66911572
54	T			41.24858170	-73.82106251
55	I WB S	T WB S	0137498700	41.22898049	-73.74356273
56	T			41.22616065	-73.79458926
57	T			41.20828791	-73.74064652
58	T WB			41.32619926	-73.69326132
59	T			41.09521797	-73.77215219
60	T WB			41.06916880	-73.71789007
124		T		41.54005559	-73.61557599
125		T WB		41.49874968	-73.53383643
126		T		41.50820788	-73.68247079
127		T		41.48360034	-73.76890208
129		T		41.42346001	-73.55755546
130		I WB		41.32768298	-73.58078559
131		T		41.33487622	-73.55814227

Table 2.2. Continued.

Site	P1 - Type	P2 - Type	Co-located USGS Site ID	Latitude	Longitude
				Decimal Degrees	
132		T		41.42927864	-73.58463644
133		T WB		41.37483505	-73.76203475
134		T		41.33612911	-73.73477869
137		T		41.28965343	-73.65908981
138		T	0137490100	41.26682982	-73.66836286
139		I WB		41.27257487	-73.74575572
140		T		41.29094958	-73.83465386
141		T		41.24316019	-73.81795596
142		T WB		41.19248383	-73.72695417
143		T		41.27460174	-73.61832933
145		T WB		41.24776891	-73.67044354
146		T		41.21572580	-73.63194603
147		T		41.12490180	-73.74346656
148		T WB		41.10273616	-73.75709573
149		T		41.25844110	-73.56610994
150		T WB	0137450500	41.40277778	-73.59305556

Table 2.3. Phase I and II percent land cover categories for stream sampling sites in the West of Hudson region. Urban/suburban did not include % transportation land cover.

Site	Site Name	Wtsd Area (km^2)	Population Density ($ind./km^2$)	SPDES Annual Flow (cm^3/cm^2)	Road Density (m/km^2)	Urban And Suburban	Agricultural	Brush	Forest	Water	Wetland
1	W. Br. Delaware R. nr Stamford	5.9	10.0	0	820	10.0	13.5	6.6	66.8	0.5	1.1
2	Town Brook nr Hobart	41.4	9.5	0	1046	4.4	25.6	7.8	60.4	0.1	0.5
3	W. Br. Delaware River at South Kortright	122.6	22.5	0.536	1277	5.7	26.4	5.8	58.8	0.4	1.3
4	Little Delaware R. nr Delhi	135.4	7.0	0	1094	5.2	12.2	7.3	72.7	0.4	0.7
5	W. Br. Delaware R. nr Delhi	372.3	21.4	0.171	1135	5.7	21.6	6.8	62.7	0.2	1.3
6	W. Br. Delaware R. at Hawleys.	663.9	16.2	0.393	1127	5.6	19.4	6.3	65.6	0.3	1.2
7	West Brook nr Walton	34.8	9.1	0	984	4.6	23.7	3.0	65.8	0.2	1.3
8	W. Br. Delaware R. nr Walton	878.6	18.3	0.455	1147	5.8	19.4	5.8	65.8	0.2	1.2
9	Trout Creek nr Trout Creek	53.3	10.9	0.009	1171	8.5	16.7	4.3	67.4	0.3	1.2
10	E. Br. Delaware R. nr Arkville	181.6	11.9	0.008	1113	5.9	5.7	7.9	79.5	0.2	0.7
11	Bush Kill nr Arkville	121.1	10.4	0.004	1019	5.5	3.3	4.5	85.8	0.1	0.6
12	Dry Brook nr Arkville	211.9	7.7	0.002	806	3.8	2.9	3.1	89.4	0.1	0.6
13	E. Br. Delaware R. nr Dunraven	448.2	12.1	0.056	983	5.1	4.1	5.4	84.4	0.1	0.7
14	Platt Kill at Dunraven	90.7	8.8	0	909	4.7	7.3	7.2	80.2	0.0	0.5
15	Tremper Kill nr Andes	77.8	8.4	0.028	1204	4.8	11.0	7.5	75.0	0.3	1.3
16	East Kill nr Jewett Center	93.1	8.1	0.016	865	2.9	1.8	2.9	89.7	0.4	1.5
17	Schoharie Creek nr Jewett Center	133.2	14.2	0.328	1001	4.0	1.4	2.2	89.3	0.3	1.9
18	Schoharie Creek nr Lexington	250.1	10.7	0.181	936	3.6	1.7	2.6	89.0	0.4	1.7
19	West Kill nr Lexington	74.4	3.6	0	332	1.9	0.7	1.9	94.5	0.0	0.6
20	Batavia Kill nr Prattsville	189.4	13.3	0.025	888	4.9	4.0	3.4	84.8	0.2	1.7
21	Schoharie Creek nr Prattsville	589.0	10.5	0.085	831	3.8	2.7	3.1	87.6	0.3	1.5
22	Esopus Creek nr Big Indian	76.7	3.2	0	364	0.7	0.2	0.3	98.0	0.0	0.6
23	Esopus Creek nr Allaben	163.4	6.3	0.11	571	1.6	0.6	0.6	95.9	0.0	0.6
24	Stony Creek at Phoenicia	83.5	8.0	0	631	1.0	0.2	0.3	97.5	0.1	0.6
25	Beaver Kill at Mount Tremper	64.5	11.0	0	637	1.8	0.6	0.9	95.4	0.0	0.9
26	Esopus Creek nr Mount Tremper.	438.8	8.6	0.046	539	1.5	0.5	0.5	96.2	0.1	0.8
27	W. Br. Neversink nr Claryville	87.1	1.4	0	361	1.1	0.3	0.5	97.4	0.2	0.5
28	E. Br. Neversink nr Claryville	71.1	2.9	0	509	1.0	0.4	0.7	97.1	0.0	0.5
29	Neversink River nr Claryville	165.9	2.3	0	453	1.1	0.3	0.6	97.0	0.1	0.7
30	Rondout Creek nr Lowes Corner	100.3	4.0	0	584	0.9	0.4	0.9	97.2	0.0	0.4
101	Rose Brook nr South Kortright	38.1	3.9	0	604	3.4	12.4	7.6	75.3	0.0	0.4
102	Coulter Brook nr Bovina Center	12.5	3.9	0	644	2.7	5.1	5.4	85.9	0.0	0.2
103	Elk Creek at East Delhi	39.7	10.7	0	1026	5.1	24.3	6.2	61.8	0.2	1.1
104	Planter Brook at Fraser	36.5	7.9	0	1074	5.7	25.9	6.2	59.4	0.1	1.5

Table 2.3. Continued.

Site	Site Name	Wtsd Area (km^2)	Population Density ($ind./km^2$)	SPDES Annual Flow (cm^3/cm^2)	Road Density (m/km^2)	Urban And Suburban	Agricultural	Brush	Forest	Water	Wetland
105	East Brook nr Walton	61.5	7.0	0	1041	5.2	22.2	7.2	63.4	0.2	0.8
106	Dryden Brook nr Beerston	24.8	6.0	0	803	4.7	3.1	4.9	85.6	0.1	0.6
107	E. Br. Delaware at Roxbury	34.2	6.8	0	738	3.1	6.9	4.1	84.0	0.2	1.5
108	Scudders Run nr Roxbury Run	2.4	16.9	0.716	1159	4.1	2.2	3.6	89.1	0.1	0.4
109	Batavia Kill nr Kellys Corner	49.6	9.5	0	1079	6.3	5.9	7.3	79.8	0.0	0.6
110	Vly Creek nr Fleischmanns	55.1	3.9	0	763	3.9	3.5	3.6	88.0	0.0	0.6
111	Dry Brook nr Mapledale	44.0	1.0	0	494	0.8	2.0	0.8	95.7	0.1	0.4
112	Mill Brook nr Grant Mills	64.5	2.0	0	516	1.0	2.4	4.3	91.9	0.0	0.4
113	Coles Clove nr Downsville	35.9	3.4	0	700	3.8	13.0	4.3	77.9	0.1	0.8
114	Holiday Brook nr Downsville	12.1	2.0	0	751	3.8	1.6	4.8	89.1	0.1	0.5
115	Schoharie Creek near Elka Park	35.5	4.6	0	563	2.0	0.7	1.6	93.1	0.1	2.0
116	East Kill near East Jewett	39.0	4.3	0	567	1.4	0.6	1.3	94.7	0.7	1.0
117	Batavia Kill near Windham	132.4	14.1	0.045	884	5.0	3.2	3.9	84.7	0.3	1.9
118	Bear Kill nr Grand Gorge	66.9	14.8	0.283	1023	5.2	14.9	4.6	73.1	0.3	1.5
119	Birch Creek at Big Indian	32.2	13.6	0.639	1143	4.0	1.8	1.6	91.1	0.0	0.2
120	Bushnellsville Creek at Shandaken	28.8	5.4	0	381	1.4	0.3	0.5	97.3	0.0	0.1
121	Warner Creek nr Chichester	23.4	5.3	0	546	0.3	0.3	0.1	98.3	0.0	0.7
122	W. Br. Neversink River above Frost Valley	22.1	2.1	0	328	0.6	0.1	0.1	98.9	0.0	0.2
123	Rondout Creek near Peekamoose	45.6	1.7	0	520	0.1	0.1	0.1	99.5	0.0	0.1
151	Betty Brook nr South Kortright	23.6	9.4	0	1045	4.8	15.9	7.0	67.6	0.7	2.5
153	Loomis Brook nr Trout Creek.	31.7	11.4	0	1046	6.8	12.4	8.1	69.9	0.1	0.8
159	Birch Creek above Pine Hill	11.6	10.2	0	1478	4.3	1.5	1.7	91.2	0.0	0.1
160	Emory Brook at Fleischmanns	16.5	11.8	0	1102	5.9	1.4	5.5	86.5	0.0	0.4

Table 2.4. Phase I and II percent land cover categories for stream sampling sites in the East of Hudson region. Urban/suburban did include % transportation land cover.

Site	Site Name	Wtsd Area (km^2)	Population Density ($ind./km^2$)	SPDES Annual Flow (cm^3/cm^2)	Road Density (m/km^2)	Urban And Suburban	Agricultural	Brush	Forest	Water	Wetland
31	W. Patterson Creek nr Patterson	11.0	85.5	0	2132	12.0	4.2	0.7	76.8	0.7	5.1
32	Brady Brook nr Pawling	17.7	22.4	0	1971	7.9	32.9	1.9	54.8	0.1	1.9
33	Leetown Stream nr Farmers Mills	8.4	123.9	0	2262	15.1	1.6	4.5	70.0	0.9	7.5
34	Haviland Hollow Br. at Haviland Hollow	25.1	56.4	0	1515	5.4	5.3	0.8	83.4	0.3	4.5
35	Trib to Middle Br. Croton R.	26.9	104.7	0.1	3077	16.3	2.3	1.9	70.8	1.0	7.3
36	W. Br. Croton R. nr Allen Corners	28.4	35.1	0	1720	5.4	2.6	1.7	75.2	3.2	11.6
37	Horse Pound Brook nr Lake Carmel	10.3	108.8	0	2240	13.2	1.5	2.2	76.0	1.2	5.4
38	W. Br. Croton R. nr Kent Cliffs	58.2	63.8	0	2066	8.6	1.8	1.9	73.9	4.6	8.9
39	Trib to E. Br. Croton R. nr Brewster	1.5	646.0	0	6134	40.6	2.4	3.0	53.1	0.0	0.6
40	Middle Br. Croton R. nr Carmel	35.5	259.6	0.1	4482	22.4	2.4	2.0	63.6	2.8	6.4
41	West Br. Croton R. nr Crafts	117.1	96.9	0.003	2192	10.9	1.8	1.8	71.0	7.1	7.1
42	Holly Stream nr Deans Corner	11.9	87.2	0.077	2864	16.9	8.5	3.2	62.7	0.2	6.8
43	Secor Brook at West Mahopac	6.8	462.7	3.075	4854	33.7	4.1	1.5	45.0	2.1	11.7
44	E. Br. Croton River nr Croton Falls	238.3	147.3	0.277	2680	15.2	9.3	2.1	61.6	2.8	8.6
45	W. Br. Croton River nr Butterville	209.1	163.1	0.612	2931	16.1	2.6	1.8	65.3	7.2	6.4
46	Muscoot River nr Baldwin Place	35.1	391.9	0.734	4288	29.3	4.6	1.2	45.3	8.3	9.7
47	Titicus River nr Purdys Station	63.9	137.0	0	3020	17.2	8.3	3.4	56.7	4.6	8.4
48	Crook Brook nr Grant Corner	5.3	33.0	0	2822	4.2	0.9	1.4	87.2	2.0	3.6
49	Hallocks Mill Brook nr Amawalk	29.5	516.0	6.94	5339	33.1	13.2	0.3	42.6	1.7	8.0
50	Angle Fly Brook nr Whitehall Corners	7.7	163.2	0	2564	15.8	14.4	0.5	61.9	0.1	6.3
51	Hunter Brook nr Mohansic State Park	15.6	444.4	0.06	5131	27.8	8.1	1.3	58.5	0.1	3.9
52	Cross River in Ward Pound Ridge Resv.	44.5	130.6	0.004	3545	13.7	3.9	2.0	65.8	3.4	9.8
53	Stone Hill River nr Bedford Hills	34.6	90.6	0	3431	17.2	3.2	3.2	65.5	0.6	9.4
54	Unnamed Tributary of the Croton River	3.6	60.7	0	2116	20.6	9.5	0.0	67.9	0.0	1.8
55	Kisco River nr Stanwood	45.5	380.4	0.073	4901	26.7	4.5	2.1	60.4	0.2	5.9
56	Gedney Brook nr Kitchawan	3.1	101.6	0	5123	22.2	12.1	1.6	57.4	2.3	4.1
57	Kisco River at Mount Kisco	38.9	371.1	0	4678	26.4	4.2	2.3	59.9	0.2	6.6
58	Trib of Croton R. nr Lake Purdy	5.4	465.0	6.103	5273	27.4	10.9	0.9	54.1	0.1	5.1
59	Trib of Kensico Resv nr Hawthorn	0.2	465.9	0	5826	57.1	6.4	0.6	32.8	0.0	3.0
60	Trib of Kensico Resv nr WCA	0.4	86.5	0	3751	54.4	16.0	0.5	26.2	0.0	2.7
124	Unnamed trib of the E. Br. Croton River nr Pawling	4.0	68.5	0	2740	12.5	6.6	1.7	73.6	1.3	3.7
125	Quaker Brook at W.G. Merrit County Park	17.9	28.6	0	1511	3.8	4.0	0.6	86.8	0.4	4.0
126	Stump Pond Stream nr Pawling	12.9	92.2	0.01	3066	16.6	2.5	2.2	69.6	0.7	8.2
127	Black Pond Brook at Meads Corner	9.5	45.1	0	1641	6.6	3.4	2.2	69.3	5.9	12.3
129	Unnamed tributary of the E. Br. Croton River	6.0	110.2	0	2164	14.8	6.2	0.1	75.9	0.1	2.9

Table 2.4. Continued.

Site	Site Name	Wtsd Area (km^2)	Population Density ($ind./km^2$)	SPDES Annual Flow (cm^3/cm^2)	Road Density (m/km^2)	Urban And Suburban	Agricultural	Brush	Forest	Water	Wetland
130	Titicus River near Salem Center	31.2	206.1	0	3420	21.4	10.9	3.3	51.8	1.5	9.5
131	Titicus River near North Salem	24.0	245.4	0	3565	20.9	10.5	0.9	53.3	2.0	11.0
132	Bog Brook nr Sears Corner	5.6	125.8	2.556	2995	20.6	5.0	3.5	62.2	0.0	8.3
133	Unnamed trib of the Muscoot River at Mahopac Falls	16.1	332.0	0.099	4068	25.8	2.6	0.8	46.2	16.6	6.9
134	Plum Brook at Shenorock	5.9	563.1	1.09	5073	34.3	2.5	1.5	55.9	1.1	2.7
137	Unnamed trib of the Muscoot Resv nr Goldens Bridge	5.4	211.9	0.03	4423	25.3	2.5	0.6	62.9	1.4	6.0
138	Cross River nr Katonah	116.7	107.9	0.12	3295	14.1	3.7	2.2	64.4	5.3	8.9
139	Muscoot River nr Whitehall Corners	96.9	344.1	0.367	4265	28.6	6.5	1.1	45.3	8.3	8.7
140	Hunter Brook nr Yorktown	7.1	528.8	0	5670	32.9	10.8	0.4	53.3	0.0	2.4
141	Unnamed trib of the Croton Resv nr Croton Heights	3.2	200.1	0	3865	16.1	5.5	0.3	76.8	0.0	0.9
142	Kisco River nr Bedford	15.0	95.5	0	3289	16.2	5.0	4.2	67.1	0.5	6.7
143	Unnamed tributary to Cross River nr Cross River	5.7	130.9	0.086	2186	18.0	4.4	4.0	60.5	0.0	11.6
145	Broad Brook nr Bedford Hills	13.4	204.0	3.438	5370	33.2	6.9	2.0	52.4	0.2	4.1
146	Stone Hill River nr Bedford	19.4	98.1	0	3148	12.0	1.1	1.9	71.9	1.0	11.0
147	Unnamed trib of the Kensico Reservoir at Mt Pleasant.	4.0	228.9	0	5329	17.1	5.9	0.3	71.2	0.9	4.2
148	Unnamed trib of the Kensico Reservoir nr Thornwood	1.0	439.4	0	6776	53.7	10.0	0.0	35.9	0.0	0.4
149	Waccabuc River at Boutonville	27.8	158.9	0.009	3972	16.5	4.7	2.1	61.1	4.3	9.6
150	E. Br. Croton River at Brewster	248.2	123.8	0.102	2433	12.0	11.1	1.8	64.9	1.9	7.9

Table 2.5. Sampling sites/dates, along with the associated project task, where samples were collected under potentially non-baseflow conditions. The USGS gauging sites paired with each site, or group of sites are provided; those USGS sites co-located or closely associated with sampling sites are also indicated. Provisional 15-minute discharge data collected at the USGS sites were used to provide the various summary values. Project task abbreviations: T=Molecular tracers; I=Ions/Nutrients; D=DOC/BDOC; S=Seston (organic particles).

Project Task	Sampling Date	Sampling site(s)	USGS gauging station (source of discharge data)	USGS station co-located with site [1]	Time between sample & start of storm event (d)	Time between sample & storm peak (d)	Sample time relative to time of peak flow	% increase in storm flow
T	07-Aug-00	27	WEST BRANCH NEVERSINK R AT CLARYVILLE	*	1.00	0.34	After	82
I/D/S/T	07-Aug-00	28	EAST BR NEVERSINK RIVER NR CLARYVILLE NY	*	0.95	0.30	After	94
I/D/S/T	07-Aug-00	29	NEVERSINK RIVER NEAR CLARYVILLE NY	*	0.86	0.17	After	72
I/D/S/T	13-Sep-00	51,54	MUSCOOT RIVER AT BALDWIN PLACE NY		0.48	0.21	Before	16
I/D/S/T	13-Sep-00	56	KISCO RIVER BELOW MOUNT KISCO NY		0.64	0.05	Before	377
I/D/S	11-Jul-01	26	ESOPUS CREEK AT COLDBROOK NY	*	0.18	0.49	Before	62
T	13-Jul-01	26	ESOPUS CREEK AT COLDBROOK NY	*	0.10	0.63	Before	54
I/D/S	21-Aug-01	34	EAST BRANCH CROTON RIVER NEAR PUTNAM LAKE NY		1.01	0.82	After	235
T	22-Aug-01	34	EAST BRANCH CROTON RIVER NEAR PUTNAM LAKE NY		2.39	2.20	After	235
T	13-Feb-02	20	BATAVIA KILL AT RED FALLS NEAR PRATTSVILLE NY	*	1.23	0.86	After	50
T	21-Feb-02	32	HORSE POUND BROOK NEAR LAKE CARMEL NY		0.71	0.32	After	125
T	21-Feb-02	33	WEST BRANCH CROTON RIVER AT RICHARDSVILLE NY		0.93	0.59	Before	27
T	21-Feb-02	40	MIDDLE BRANCH CROTON RIVER NEAR CARMEL NY	*	0.89	0.51	After	78
T	21-Feb-02	43,46,49	MUSCOOT RIVER AT BALDWIN PLACE NY	* (site 46)	0.66	0.19	After	129
T	21-Feb-02	52	CROSS RIVER NEAR CROSS RIVER NY	*	0.55	0.05	After	181
T	21-Feb-02	55,60	KISCO RIVER BELOW MOUNT KISCO NY	* (site 55)	0.66	0.18	After	169
T	21-Feb-02	58	ANGLE FLY BROOK AT WHITEHALL CORNERS NY		0.89	0.55	After	477
T	24-Jun-02	27	WEST BRANCH NEVERSINK R AT CLARYVILLE	*	0.80	0.59	After	101
T	24-Jun-02	28	EAST BR NEVERSINK RIVER NR CLARYVILLE NY	*	0.79	0.56	After	80
T	24-Jun-02	29	NEVERSINK RIVER NEAR CLARYVILLE NY	*	0.76	0.47	After	71
I/D/S	27-Jun-02	8	WEST BRANCH DELAWARE RIVER AT WALTON NY	*	0.33	0.10	Before	65
I/D/S	30-Jul-02	52	CROSS RIVER NEAR CROSS RIVER NY	*	1.49	1.13	After	96
I/D/S/T	19-Aug-03	115	SUGARLOAF BROOK SOUTH OF TANNERSVILLE NY		1.89	1.76	After	666
I/D/S/T	01-Oct-03	127	WEST BRANCH CROTON RIVER AT RICHARDSVILLE NY		1.00	0.83	After	49
I/D/S/T	01-Oct-03	129,132	EAST BRANCH CROTON RIVER NEAR PUTNAM LAKE NY		3.00	0.93	After	78
I/D/S/T	01-Oct-03	150	EAST BRANCH CROTON RIVER AT BREWSTER NY		0.47	0.98	Before	85
I/D/S/T	03-Jun-04	138	CROSS RIVER AT KATONAH NY	*	2.70	0.78	After	61
I/D/S/T	03-Jun-04	147,148	KISCO RIVER BELOW MOUNT KISCO NY		2.95	1.54	After	133
I/D/S/T	03-Jun-04	34,125,129,132	EAST BRANCH CROTON RIVER NEAR PUTNAM LAKE NY		2.51	0.31	After	31
I/D/S/T	02-Aug-04	10	EAST BR DELAWARE R AT MARGARETVILLE NY		1.96	1.18	After	68
I/D/S/T	17-Aug-04	103	W BR DELAWARE RIVER UPSTREAM FROM DELHI NY		1.81	1.31	After	304
I/D/S/T	17-Aug-04	6	WEST BRANCH DELAWARE RIVER AT WALTON NY		1.96	0.71	After	134
I/D/S/T	28-Jun-05	112,114	MILL BROOK NEAR DUNRAVEN NY		0.36	0.00	Before	80
I/D/S/T	02-Aug-05	109	BUSH KILL NEAR ARKVILLE NY		1.78	1.34	After	132
I/D/S/T	02-Aug-05	111	DRY BROOK AT ARKVILLE		2.03	1.61	After	103

[1] A few of the 'co-located' sites are within 1 or 2 km of one another along the same reach, without any major tributaries in between.

Figure 2.1: Location of stream sampling sites in the West of Hudson watersheds. Sites are identified as Targeted or Integrative and whether they were sampled in Phase I, 2, or both. Study sites names and descriptive information is found in Tables 2.1 and 2.3, by site number.

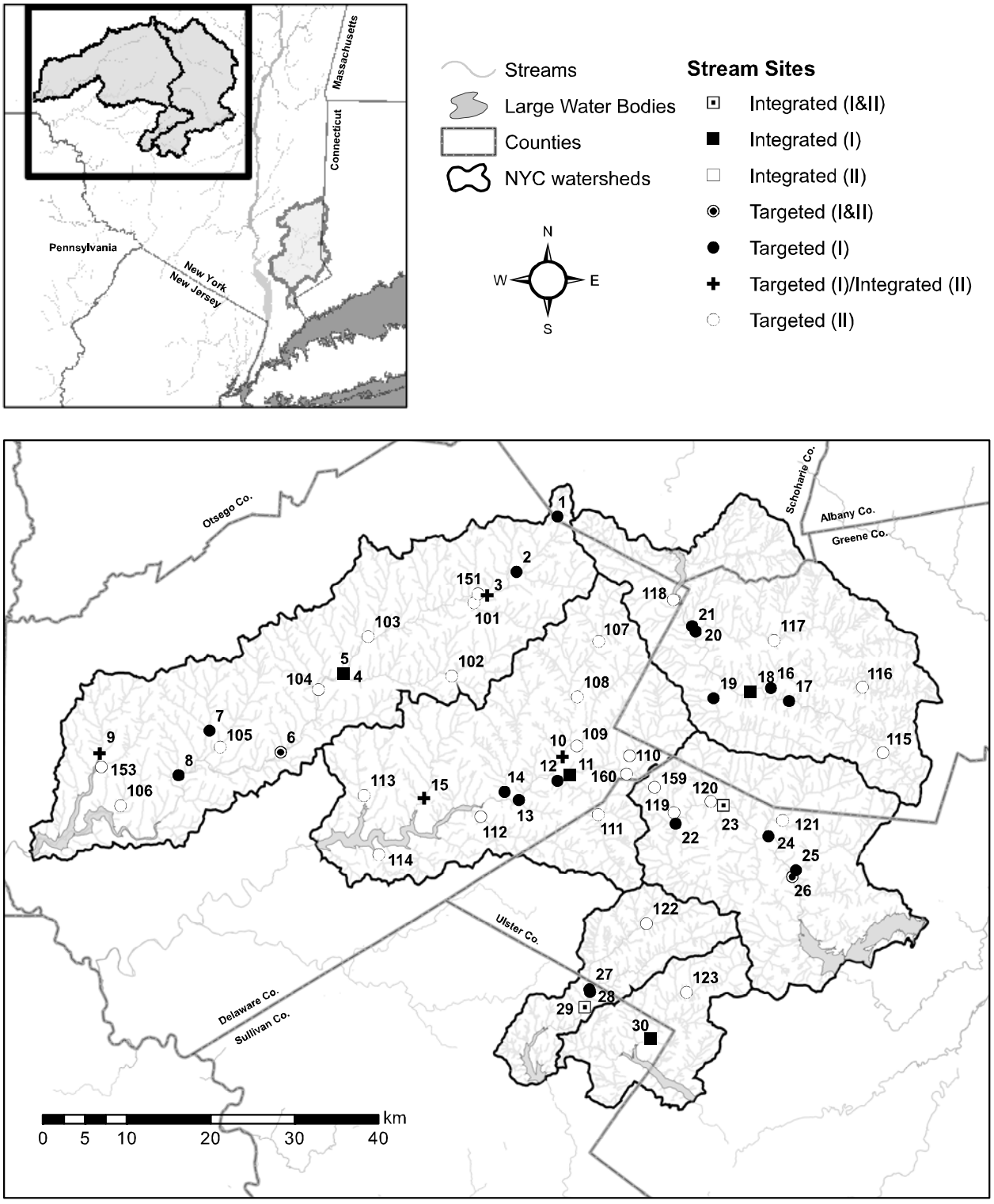

Figure 2.2**.** Location of stream sampling sites in the East of Hudson watersheds (a.k.a., Croton/Kensico System). Study sites names and descriptive information is found in Tables 2.1 and 2.3, by site number.

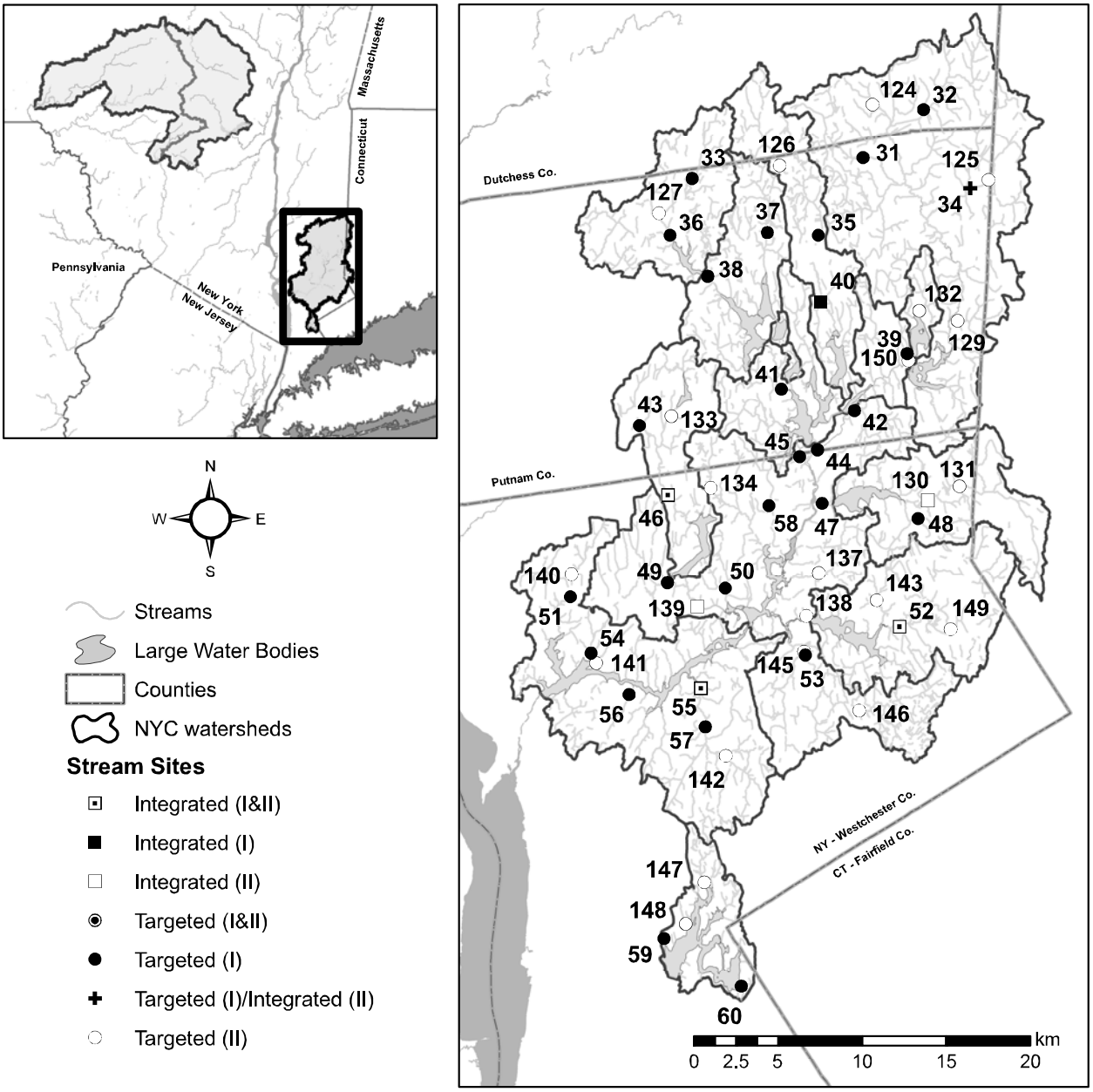

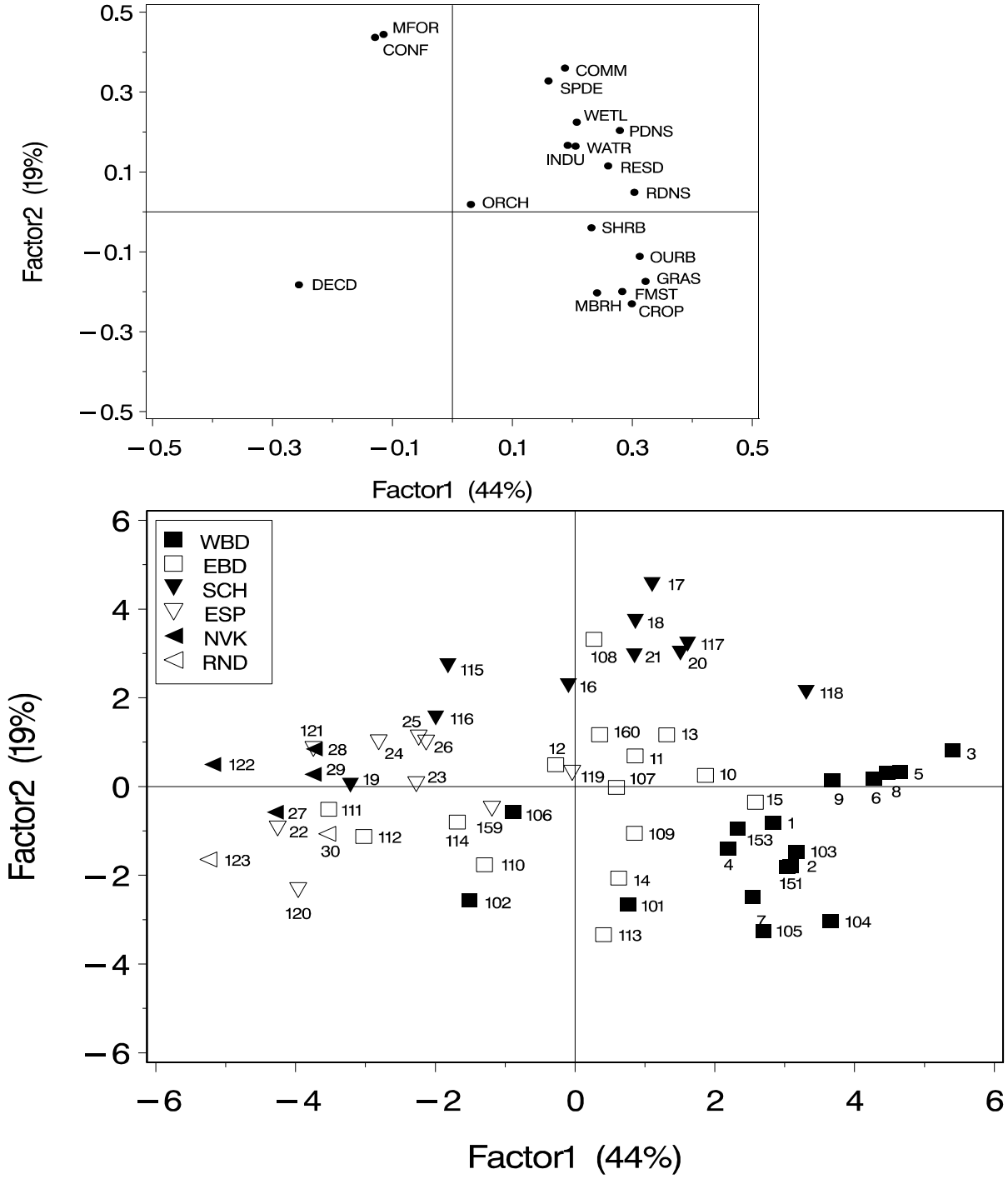

Figure 2.3. Principal Components Analysis (PCA) of land cover, population, road density, and wastewater treatment plant effluent volumes for WOH watersheds. Factor loadings are provided in the top plot with scores shown in the bottom plot; percentage of variation explained by each PCA axis is provided in the axes labels. See Table 2.3 for site names corresponding to site numbers provided in the bottom plot; see text for land use abbreviations. Subwatershed designations are as follows: WBD = W. Br. Delaware R.; EBD = E. Br. Delaware R., SCH = Schoharie Cr., ESP = Esopus Cr., NVK = Neversink R., RND = Rondout Cr.

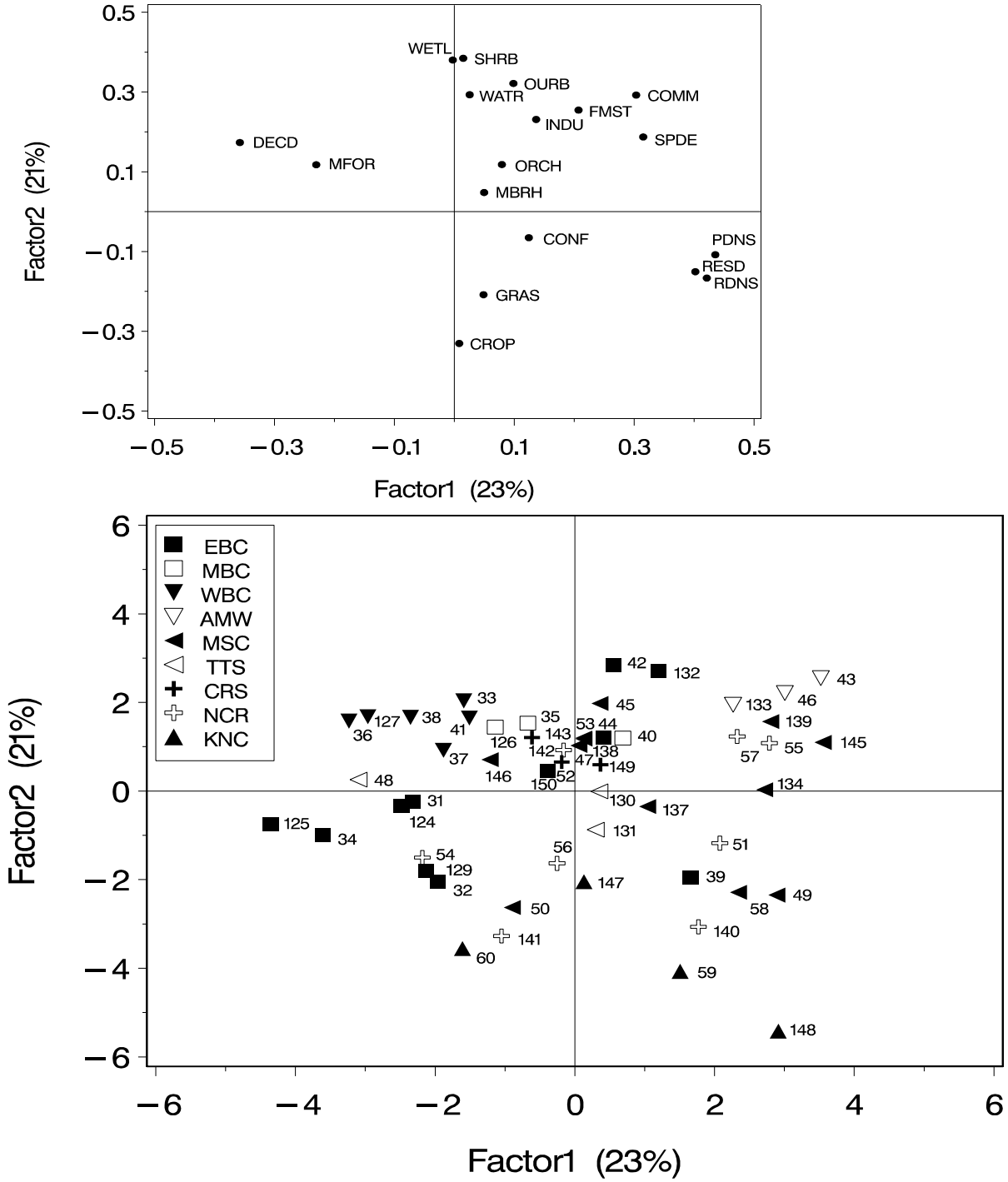

Figure 2.4. PCA of land use, population, road density, and wastewater treatment plant effluent volumes for EOH watersheds. Factor loadings are provided in the top plot with scores shown in the bottom plot; percentage of variation explained by each PCA axis is provided in the axes labels. See Table 2.4 for site names corresponding to site numbers provided in the bottom plot; see text for land use abbreviations. Subwatershed designations are as follows: EBC = E. Br. Croton R., MBC = Middle Br. Croton R., WBC = W. Br. Croton R., AMW = Amawalk Reservoir, MSC – Muscoot R., TTS = Titicus R., CRS = Cross R., NCR = New Croton Reservoir. KNC = Kensico Reservoir.

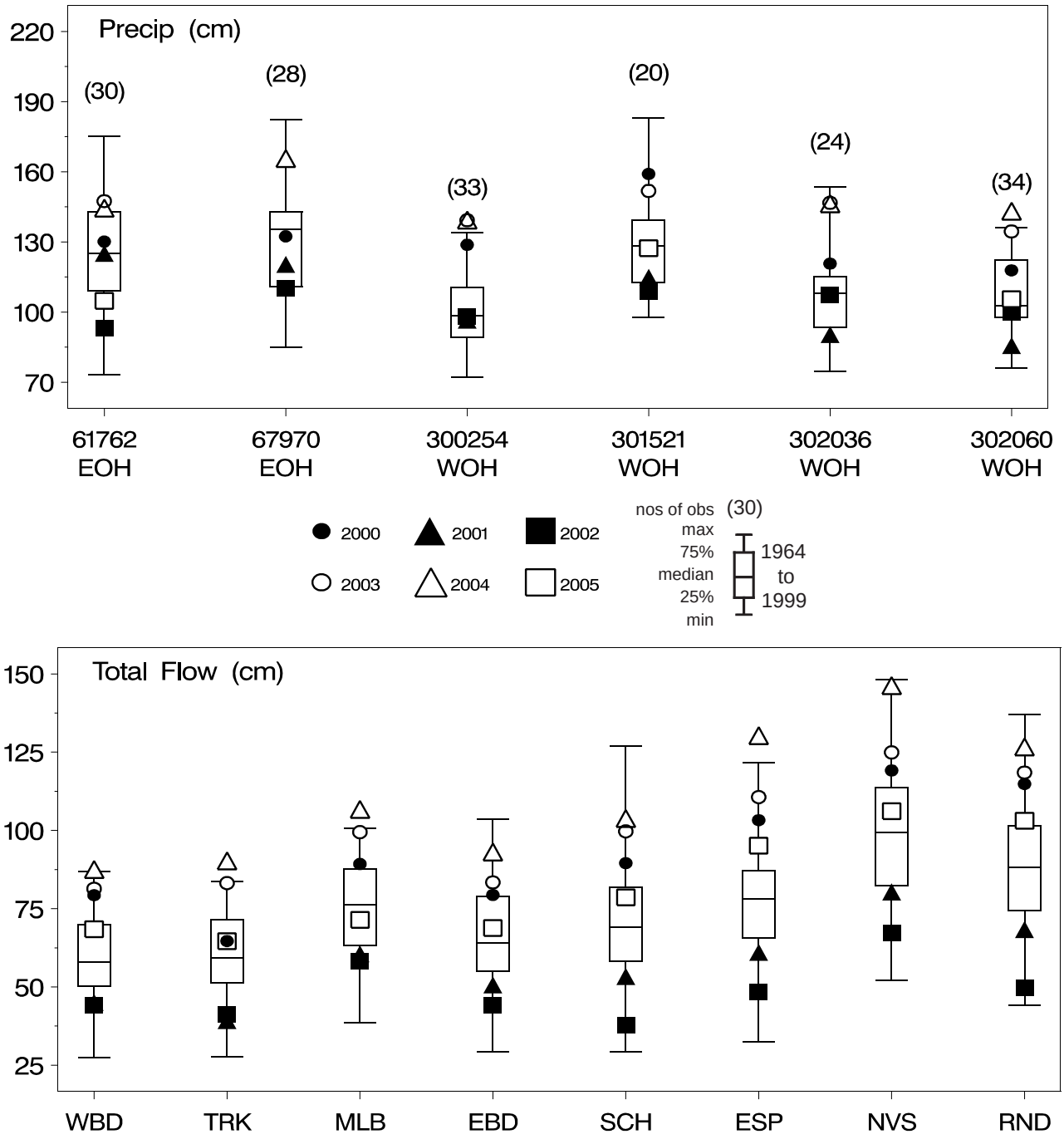

Figure 2.5. Box plots of total annual precipitation at long-term precipitation monitoring sites (1964–1999 – variable number of years with complete precipitation records, depending upon site, as indicated by the numbers in parentheses in the top plot) in either East of Hudson (EOH) or West of Hudson (WOH) regions (numbers are NOAA site identifiers) (top). The bottom plot shows watershed-area-normalized total annual discharge from 1964 to 1999 for stream gauging sites unaffected by water withdrawals or reservoir operations where historic data existed (only WOH sites). Subregion identifiers: WBD = West Branch of the Delaware River, EBD = East Branch of the Delaware River watershed, TRK = Tremper Kill (in the EBD watershed), MLB = Mill Brook (in the EBD watershed), SCH = Schoharie Creek, ESP = Esopus Creek, NVS = Neversink River, RND = Rondout Creek. In both panels years 2000 to 2005 are identified individually.

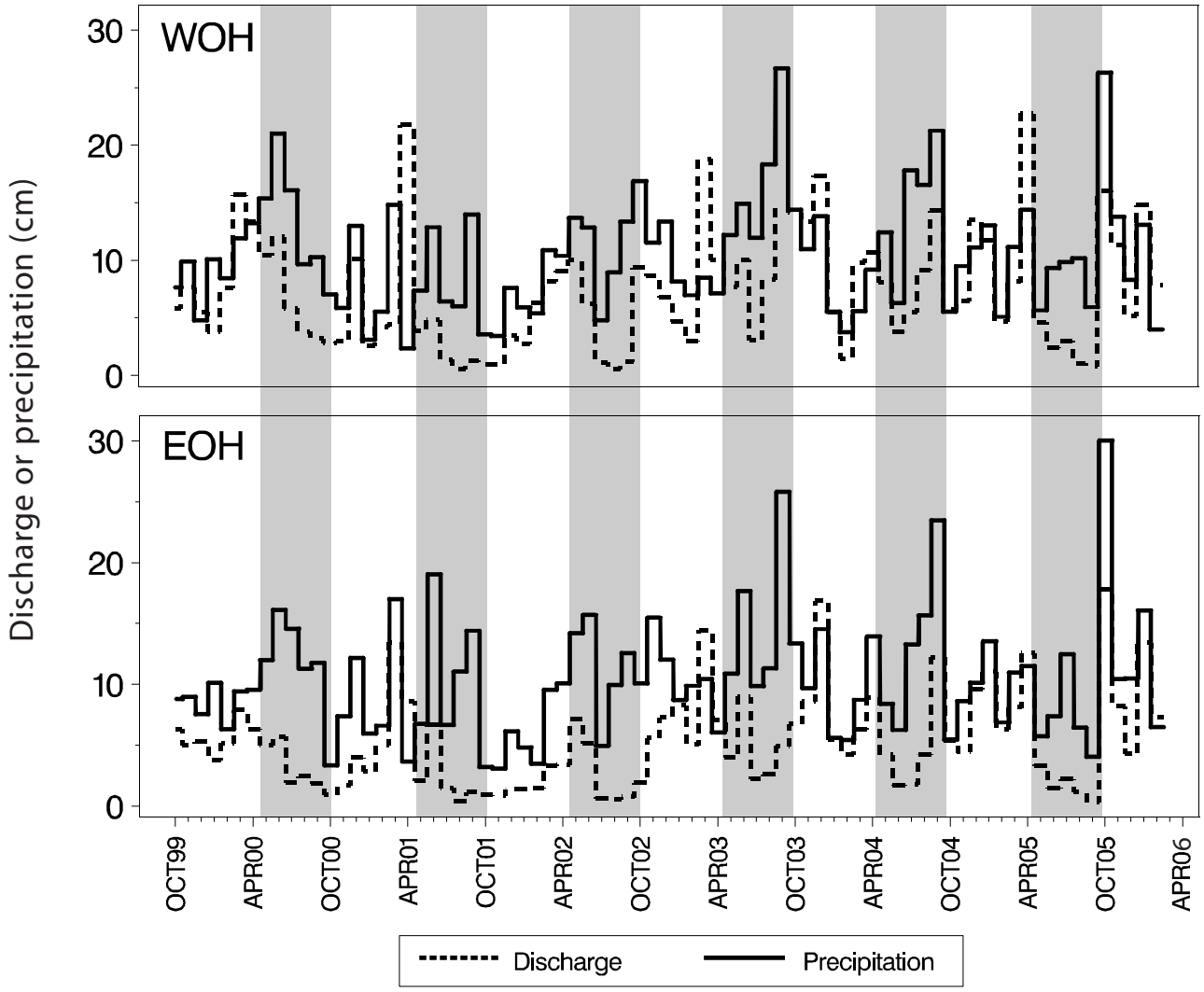

Figure 2.6. Mean monthly precipitation and area-specific discharge within West of Hudson (WOH) and East of Hudson (EOH) regions over the 6-y study period. The spring through summer (May–October) sampling windows are indicated by shaded areas. EOH discharge sites: $n = 8$, precipitation sites: $n = 2$ to 6 depending on month, WOH discharge sites: $n = 44$, precipitation sites: $n = 7$ to 12 depending on month. The October 2005 monthly precipitation value on the EOH plot was truncated at 30 cm; actual value was 38 cm.

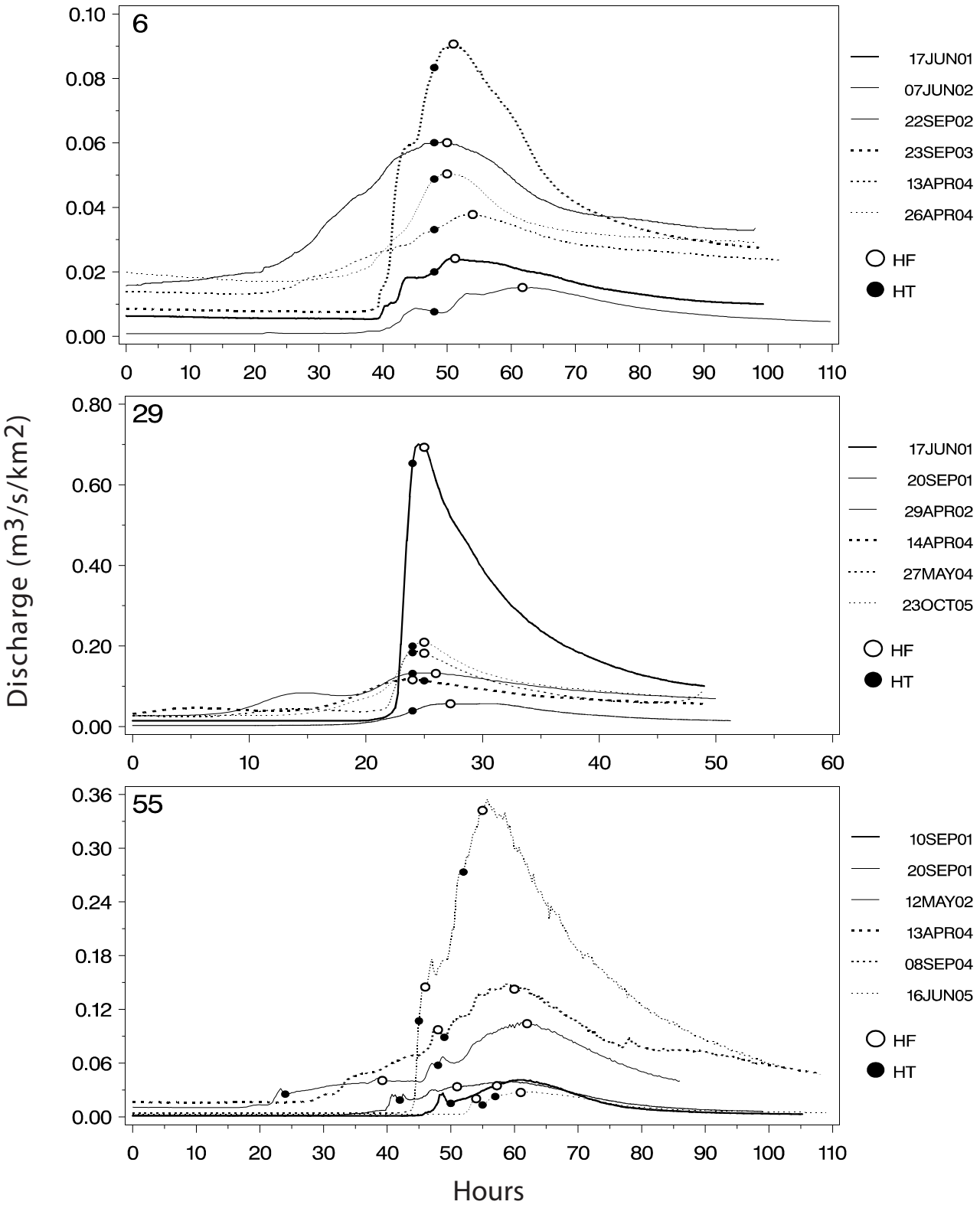

Figure 2.7. Storm hydrographs and corresponding samples for the 6 storms collected at each of the 3 storm-sampling sites: W. Br. Delaware R. at Hawleys (6), Neversink R. at Claryville (29), and Kisco River near Stanwood (55). The time scale represents hours since an arbitrary starting point, generally within 1 or 2 days of a given storm. Samples were collected at, or near, high turbidity (HT) or high flow (HF) conditions.

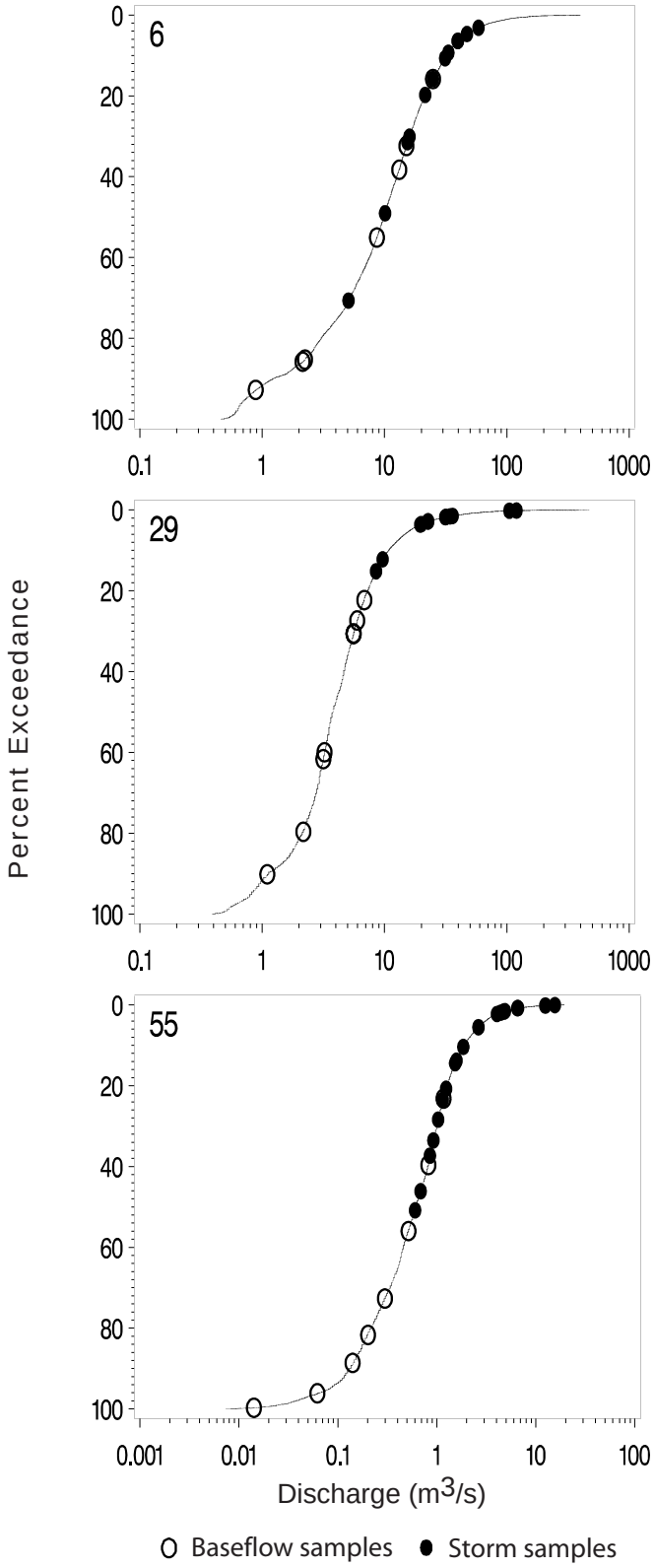

Figure 2.8. Flow-frequency curves for the 3 storm-sampling sites (see Fig. 2.7 for stream names) for the 6-year study period using USGS provisional 15-minute discharge data. Open and closed circles, representing baseflow and storm flow samples, respectively, are plotted based on the discharge at the time of sampling and show the range in flows sampled at each of the 3 storm sampling sites.

----------Intentionally Blank----------

Chapter 3 – Nutrients and Major Ions in transport

Research Task

Concentrations of nutrients and major ions transported in streams can be sensitive indicators of ecosystem impairment, particularly when monitored over a several year period of time and across landscapes of complex land-use patterns. They also provide important supplementary data for the other aspects of this monitoring project. These stream constituents provide an assessment of inorganic and nutrient water quality relative to differences in existing watershed characteristics and can be used to quantify and predict changes in water quality in response to changes in land use. We monitored nutrients and major ions, as well as suspended particles, over a 6-year period (2000-05) under baseflow conditions at 110 sites located throughout the NYC drinking-water source watersheds. Sampling was also carried out during 6 separate storms, occurring over the 6-year study period, at three of the 110 baseflow sites.

Methods

Baseflow Sampling

Samples analyzed for nutrients and major ions for each of the 110 study sites east and west of the Hudson River (EOH and WOH, respectively) were collected primarily between June and September with a few samples collected on May 31st of 2005, and a few samples collected on the first few days of October in 2000 and 2003. The majority of the 110 sites were sampled once per year over either the 2000-02 period (i.e. Phase I of the project) or over the 2003-05 (i.e. Phase II of the project). Three sites were only sampled in 2 years and 12 sites were sampled all 6 years of the project. Nutrient and major ion baseflow sampling was coordinated with the molecular tracer and organic matter tasks when possible. Baseflow conditions were defined as relatively constant stream flow, changing <10% over the 24 h preceding sampling, based on either colocated or nearby real-time USGS gauging stations. Please see the 'Site specific baseflow hydrology' subsection in the Technical Design chapter (chapter 2) for more specific information regarding baseflow conditions. Inorganic chemical analyses included cations (Ca^{2+}, Mg^{2+}, Na^{+}, K^{+}) and anions (Cl^{-}, SO_4^{2-}), pH, specific conductance, and alkalinity. Nutrient chemistry analyses included NO_3-N, NH_4-N, soluble and total Kjeldahl N (SKN and TKN, respectively), soluble reactive P (SRP), total dissolved P (TDP), and total P (TP). Analyzed nutrient values were used to calculate the following derived nutrient values: total N (TN = TKN + NO_3-N), total dissolved N (TDN = SKN + NO_3-N), organic N (DON = SKN – NH_4-N), particulate N (PN = TN – TDN), and particulate P (PP = TP – TDP).

A stream grab sample (500–1000 mL) for nutrients and major ions was taken from the thalweg of each stream using acid-washed 1-L Nalgene® bottles. Samples were chilled to ~4°C in coolers until they could be processed. An Orion® field pH meter, and a YSI® conductivity/temperature meter were used to measure pH, specific conductance (T_{ref} = 25°C), and temperature in situ. Immediately upon return from the field, the grab sample from each site was divided among 5 to 6 split samples for subsequent analysis of nutrients and major ions. One split was frozen for analysis of TKN (semi-automated phenate block digester method) and TP (EPA methods 365.1 and 365.5). A 2nd split was refrigerated at 4°C for subsequent alkalinity

analysis (EPA method 310.1). An additional split sample for alkalinity analysis was collected for WOH sites because low alkalinities, which required a modified titration analysis using an increased sample volume, were expected (APHA Standard Method 2320). The remaining water was then filtered through a cellulose–nitrate membrane 0.45-µm filter, divided among three 125-mL polyethylene bottles, and stored for later analysis of dissolved nutrients, anions, and cations. One filtered split was frozen for subsequent analysis of SKN (semiautomated phenate block digester method), NO_3-N and NO_2-N (EPA method 353.2), NH_4-N (EPA method 350.1), SRP (EPA method 365.1), and TDP (EPA method 365.5). A 2nd filtered split was refrigerated at 4°C for analysis of Cl^- (EPA method 325.3) and SO_4^{2-} (EPA method 375.4). The last filtered split was acid-fixed with 0.2 µL HNO_3/mL for later analysis of Ca^{2+}, K^+, Na^+, and Mg^{2+} (EPA method 200.7 for all cations; switched to EPA methods 215.1 for Ca^{2+}, 258.1 for K^+, 273.1 for Na^+, and 242.1 for Mg^{2+} by 2002). All nutrient and major ion analyses were done by the Patrick Center for Environmental Research at the Academy of Natural Sciences of Philadelphia.

Stormflow Sampling

The concentrations of nutrients and major ions along with suspended solids, molecular tracers, and DOC, were quantified for a total of six storms at each of three baseflow sampling sites (Neversink River – 29, W. Br. Delaware River – 6, Kisco River – 55). These three sampling sites were selected to represent the 3 major land uses found across the study region: forested (site 29), agriculture (site 6) and urban/suburban (site 55). Fig. 2.7 in the Technical Design chapter (chapter 2) provides sampling dates along with where on each storm hydrograph sampling occurred. To coincide with some of the sampled storms, additional baseflow sampling, as described above, was conducted at these sites in order to have representative baseflow chemistry near the time of the separate storm events. These additional baseflow samples were only used in conjunction with analysis of the storm samples and were not used in any baseflow-specific analyses.

Each sampling site was instrumented with at least two ISCO automated samplers, the first of which was set to trigger following a 10-15-cm rise in stage height. The second ISCO was triggered by the completion of sampling by the first ISCO. Once triggered, the ISCOs sampled hourly in duplicate for a total of 6 h. If a third or fourth ISCO was used at a particular site, the triggering sequence was established in a similar fashion but with a greater delay after onset of sampling to capture later portions of the storm hydrograph. When a run-off event was imminent, changes in stream discharge and stage height at or near each site were monitored using real-time updates of stream-specific gauging stations on the USGS website. There was no USGS gauging station in close proximity to the storm sampling site at the W. Branch of the Delaware River, so we equipped this site with a single water-level recorder (pressure transducer) to record actual changes in stage height. Storm hydrology is specifically covered in the Technical Design chapter (chapter 2).

The first sample from each duplicate pair of hourly samples was used for the analyses in this task, and the second in each pair was used for molecular tracer analyses. Two sets of duplicate samples were analyzed for each storm; one sample corresponded to peak flow (±1 h), as determined by provisional hydrograph data provided by the U.S. Geological Survey (or pressure transducer data) and the other corresponded to peak TSS transport (±1 h) selected by visual

comparison of sample turbidity among collected sample jars. Each sample was filtered, with ~50 mL of the filtrate from each sample used for DOC analysis. After thorough shaking of the original sample, the unfiltered nutrient and alkalinity sample splits were collected, as described above. The remaining unfiltered sample volume was processed for total and volatile suspended solids also as described above (following thorough shaking at each step). The filtrate from the DOC processing was subsequently re-filtered through a cellulose nitrate membrane (0.45µm) filter and split among (3) 125-mL HDPE bottles for dissolved nutrients and major ions, as described above. The resulting (5-6) 100-mL sample splits were filtered, fixed, and stored as necessary for subsequent analysis of whole and dissolved nutrients (SKN, TKN, TP, NO_3-N, NH_4-N, SRP, TDP), anions (Cl, SO_4), cations (Ca, K, Na, Mg), and alkalinity. Samples were collected and stored on ice within 6-12 hours of sample collection by the ISCO automated sampler.

Nitrogen and phosphorus nutrient fluxes, as 'instantaneous' flux values, were calculated for the three separate flow conditions sampled at the three stormflow sampling sites: baseflow, high-turbidity flow, and peak flow. Specifics regarding these separate flow conditions can be found in the Technical Design chapter (chapter 2). Fluxes are the product of concentration and USGS-measured (or estimated in the case of the W. Br. Delaware R. site, site 6) instantaneous flow, normalized for watershed area.

Data Analysis

Inter-relationships among major ions and nutrients. Principal Components Analysis (PCA) was used to examine how the inorganic chemistry data collected under baseflow conditions at the 110 stream sites varied at 3 different regional scales. The correlation matrix, based on log-transformed variables where appropriate with constants added to PN and PP values to avoid taking the log of zero values, was used in each of the PCAs. An initial PCA was run using all 110 sites in order to examine relationships across the entire study area. A second PCA was run for just the EOH sites, and third PCA was run for just the WOH sites. Regarding the first two PCAs, sites 43, 49 and 58 were excluded because of anomalously high NH_4-N (site 49) or NO_3-N (sites 43, 58) relative to the other study sites. This and all subsequent analyses were run using SAS version 9 (SAS Institute, Cary, North Carolina).

Ion and nutrient relationships with watershed characteristics. The 6-y mean ion and nutrient chemistry values were related separately to landuse variables (% land use, road density, and point-source discharge) compiled at three separate spatial scales (whole watershed, riparian, and reach) using multiple linear regression (MLR). This analysis is an updated version of a similar analysis using the 3-y mean values of the 60 Phase I sites presented in Dow et al. 2006. The 6-y mean values of all water-chemistry variables (except pH, PN, and PP) were log10(x) transformed; PN values were log10(x + 0.002) transformed; PP values were log10(x + 0.0003) transformed, and pH was not transformed. All scaled landuse variables listed in Table 3.1 (except % transportation, % water, and population density) were used in the MLR analyses; the only other variable included was point-source discharge. All % landuse variables were arcsine square-root(x) transformed, road density was log10(x +1) transformed, and point-source discharge was log10(x + 0.001) transformed. Stepwise variable selection with a variable significance cutoff of 0.05 was used in selecting independent variables in the MLR models (SAS/STAT, version 9, SAS Institute, Cary, North Carolina).

Additional effects of scale on the chemistry–landuse variable relationships were analyzed by running the MLR analyses using data from sites grouped into regions/subregions. These regions/subregions were: 1) all WOH sites, 2) West and East Branch of the Delaware River sites (WOHdel), 3) Schoharie, Esopus, Neversink, and Rondout sites (WOHcat), and 4) all EOH sites. These regional groupings follow what was done in the original MLR analysis in Dow et al. 2006.

The best model for each variable from the scale comparison was the model with the highest overall adjusted R^2 value and no significant multicollinearity. Multicollinearity was assessed using the variance inflation factor (VIF). VIF values >10 for any independent variables suggest problems associated with multicollinearity in the regression model (Myers 1990). The best model was considered unique relative to the models from the remaining scales if: 1) the adjusted R^2 of the best model was 10% or greater than the adjusted R^2 for models for at the other scales, and 2) if no strong relationship (e.g., $R^2 > 0.50$) could be found for a regression between the strongest predictor from the best model using either group of significant predictors from the models for the other scales.

Another update to an analysis presented in (Dow et al. 2006) is a plot of the mean base cation sum ($Ca^{2+} + Mg^{2+} + Na^{+} + K^{+}$) against mean alkalinity by region (i.e. WOH, EOH) using all 110 baseflow-monitored sites. This analysis, originally from (Rhodes et al. 2001), provided a perspective regarding landuse vs geological influences on stream chemistry. A 1:1 line in these plots indicates that stream chemistry is controlled solely by mineral weathering (Rhodes et al. 2001). A watershed baseline also was defined for each region by regressing the mean base cation sum against mean alkalinity for the sites with the least-disturbed watersheds in each region. In the WOH region, these watersheds had >97% forested area with no known point-source discharges: sites 22, 24, and 121 from the Esopus Creek watershed, sites 27, 28, 29, and 122 from the Neversink River watershed, and sites 30 and 123 from the Rondout Creek watershed. In the EOH region, these watersheds had >75% forested area with no known point-source discharges: sites 31, 34, 36, 37, 48, 125, and 129 from the northern and eastern portion of the EOH region

Flow and Time Trends of ions and nutrients during baseflow. Twelve of the 110 stream sites were sampled for all baseflow-specific task parameters each of the six project years (2000-05); 8 WOH (site #: 3, 6, 9, 10, 15, 23, 26, and 29)) and 4 EOH (site #: 34, 46, 52, and 55). See chapter 2 for further information regarding these sites, including stream names, watershed characteristics, etc.. Sampling was performed across all 6 years at these 12 sites in order to provide a consistent temporal perspective over the duration of the project. These 12 sites were selected from the original 60 sites monitored in Phase I of the project primarily to represent the spectrum of watershed conditions from forested to highly urbanized within both EOH and WOH regions. With one sample per year, most of the sites had an n=6, however, 3 of the sites (6, 29, 55) were also stormflow monitoring sites and therefore had additional baseflow samples in some years. The additional baseflow sampling was intended to provide baseflow-specific water quality conditions at or near the time of a sampled storm. Data from these 12 sites were used to examine flow relationships with analyte concentrations and to allow for a trend analysis in analyte data across the six years of the Project.

Discharge-concentration relationships were assessed for all ions and nutrients. Of the 12 sites with 6 years of data, 8 were co-located with USGS streamflow monitoring sites, with discharge estimated from watershed-specific discharge versus watershed area relationships (see appendix of Arscott et al. 2006 for details) at the remaining 4 sites. Actual or estimated mean-daily discharge values were selected for each sampling date. Linear regression was used to define the relationship between concentration and discharge. Significance of the regression relationships was assess at an α=0.05. All concentration values were $\log_{10}$ transformed, with constants added to certain analytes to avoid taking the log of zero. Discharge values, normalized for watershed area (i.e. units of $m^3/s/km^2$), were also $\log_{10}$ transformed.

Temporal trends in the concentration data were assessed using either the residuals from the discharge-concentration regressions, if a regression was significant, or the original concentration data. Using regression residuals (as the observed – predicted value) follows the recommendation found in (Helsel and Hirsch 2002) to account for relationships in exogenous variables (i.e. discharge) first, before conducting trend analyses. The nonparametric Mann-Kendall test (i.e. the Kendall's tau correlation) was used to determine whether the residuals/concentrations tended to increase or decrease with year (Helsel and Hirsch 2002). As with the discharge-concentration relationships, trend significance was assessed at an α=0.05.

Nutrient flux differences for baseflow and stormflow samples. An analysis of variance (ANOVA) was used to look at differences in the instantaneous flux values between the 3 storm-sampling sites. Separate analyses were run for baseflow flux values and stormflow flux values. Flux values were log10-transformed adding 0.01 to the PN, PP, and NH_4-N fluxes to avoid taking the log of zero values. A 1-way ANOVA was run for the baseflow samples where site was the single factor. For the stormflow analysis, a 2-way ANOVA was run with site and sample type (i.e. HF or HT samples) as the factors with an interaction term (i.e. site*sample type) also included in the model. Post-hoc tests to look at differences between factor mean values were conducted using the Tukey's studentized range test.

Ion and nutrient relationships with baseflow and stormflow. Concentration versus streamflow relationships were examined at the 3 storm-sampling sites using both baseflow and stormflow-collected samples. Three separate linear regressions were used to relate concentration to discharge with each regression allowing a comparison of results between 2 of the 3 storm-sampling sites. These three comparisons were between: [1] the agricultural site (6) and the forested site (29), [2] the urban site (55) and the forested site, and lastly [3] the agricultural site and the urban site. Mean-daily discharge was used for baseflow-associated samples and 15-minute instantaneous discharge was used for storm-associated samples. Discharge, in units of $cm^3/s/km^2$, was $\log_{10}$-transformed with these specific units leading to all positive values after transformation, allowing for easier interpretation of results. Concentration values were also $\log_{10}$-transformed with constants added to some analytes to avoid taking the log of negative values. Due to an anomalous event captured at the Kisco River on 08SEP04, concentration values collected during this storm for pH, conductivity, alkalinity, Ca, Mg, Na, and Cl were not included in these analyses. These specific analytes were obvious outliers relative to the other storm values collected at this site. See the Results and Discussion section for further information on this particular storm event.

Two additional terms were included in the linear regression analysis to allow for a comparison in the resulting concentration v. discharge relationships among the 3 storm-sampling sites. The first term is commonly referred to as an indicator or 'dummy' variable (Neter et al. 1990) which allows categorical variables to be included in a linear regression framework. Here, the indicator variable was assigned 1 for a selected station and 0 for one of the other stations. Including this indicator term allows for a statistical comparison of whether the intercept term would differ between 2 separate concentration v. discharge relationships, one for each of the 2 sites being compared. The third term, allowing for similar comparison of slopes as just described for regression equation intercepts, is an interaction term where the indicator variable is multiplied by the discharge variable. The use of the indicator variable as described here provides a means of assessing whether concentration v. discharge relationship for 2 separate sites are statistical similar or not. Ultimately, this comparison will provide some idea of whether concentration v. disharge relationships, over a range of discharge conditions from baseflow to stormflow, are affected by the predominant land-use conditions found across these 3 storm-sampling sites.

Results and Discussion

Baseflow Sampling

Inter-relationships among major ions and nutrients. The general patterns in cation and anion sums observed throughout this project (Dow et al. 2006) was very much evident when examining mean data for covering the entire project period (Figs. 3.1, 3.2). In general, the ionic composition, which indicates the amount of dissolved solids in stream water, was two to four times greater for EOH sites relative to WOH sites. Nutrient concentration differences between the two regions were not as striking, but as has been previously noted (Dow et al. 2006), 3 sites in the EOH region had extremely high concentrations of N species (Fig. 2). These 3 sites were affected greatly by point-source discharges (see Table 2.4 in chapter 2 for watershed-area-normalized effluent discharge across all sites), with well documented history of capacity exceedance by a WWTP at one site (49). The West Branch Delaware River sub-watershed (WBD) sites were the only study sites to exhibit any noticeable patterns in ion and nutrient concentrations with increasing watershed area of all subwatersheds (Figs. 3.1, 3.2). The observed pattern of increasing concentration with increasing watershed area for WBD sites is most evident with cations (Fig. 3.1) and phosphorus (Fig. 3.2) concentrations.

The PCA, where all sites where included (Fig. 3.3), provided another view of the clear differences in stream chemistry between the two regions, WOH v. EOH. The first axes of this PCA using all sites explained 66% of the variability in the stream ion and nutrient concentrations and defined an overall gradient of low to high ion and nutrient concentrations going from WOH to EOH sites. The second axis, explaining 11% of the dataset variability, separated sites having overall higher nutrient concentrations from sites having overall higher cation (Ca^{2+}, Mg^{2+}, Na^{+}, K^{+}) concentrations. The regional PCAs essentially mirrored the PCA using all sites in that the first axes of each regional PCA explained a large portion of the overall variability in concentration data and each showed a gradient in sites of low to high ion and nutrient concentrations. The second axis in each regional PCA also tended to separate sites based on higher nutrient concentrations versus higher ion concentrations. A certain amount of separation between subregions within the WOH PCA was evident, however, not to the extent found when

using the initial 60, Phase I sites (Dow et al. 2006) Along the first axis of the WOH PCA, Neversink and Rondout sites grouped separately from W and E. Br. Delaware sites. Most Schohaire sites grouped separately from the remaining WOH sites along the second axis of the WOH PCA.

Ion and nutrient relationships with watershed characteristics. The individual MLR model results using data from all 6 years of the project at all 110 sites were in general terms quite similar to results using only the 60 Phase I sites (Dow et al. 2006). Significant MLR models were generated for every analyte in all 4 regions/subregions (WOHdel, WOHcat, WOH, EOH) at ≥2 of the 3 spatial scales, as was the case with the MLR models developed using only Phase I data. The single exception was that NH_4-N only generated a single significant model at the riparian scale in the WOHcat subregion (Table 3.2). Similarly, each of the landuse variables (Table 3.1) was included in at least 1 model, and 13 of the 16 landuse variables were the most significant predictors (i.e., highest partial R^2) in at least 1 model (14 of the 16 using only Phase I data). For the WOH models, ~37% (7 of 19) of the most significant predictors could be classified as urban, ~53% (10 of 19) as agricultural, and ~10% (2 of 19) as undisturbed. In the WOHdel subregion, ~47% (9 of 19) of the most significant predictors could be classified as urban, ~32% (6 of 19) as agricultural, and ~21% (4 of 19) as undisturbed. In the WOHcat subregion, ~58% (11 of 19) of the most significant predictors could be classified as urban, ~37% (7 of 19) as agricultural, and ~5% (1 of 19) as undisturbed. In the EOH region, all 19 of the most significant predictors could be classified as urban. While these values are different from the percentages reported in (Dow et al. 2006) using only Phase I data, there were no radical shifts in the breakdown of the most significant predictors between the three land use groups within any given region. The largest shift occurred within the WOHcat subregion between the agriculture and undisturbed groupings, where the previous breakdown was 11% of the most significant predictors classified as agricultural and 22% as undisturbed.

The best predictor variable in 66 of the 76 significant models contributed ≥50% to the variance explained by the model (i.e., partial R^2 of the best predictor relative to the overall unadjusted model R^2; R^2 values in Table 3 are the adjusted model R^2). Six of the 10 models in which the partial R^2 of the best predictor was ≤50% occurred in the WOHdel subregion; 6 of these 10 models were for some form of phosphorus. As was found using just Phase I data, these results imply that the most important predictor variable in any given model had most of the power to explain variability in ion and nutrient concentrations across the region/subregion, regardless of the number of significant predictors in the model.

The watershed-, riparian-, and reach-scale MLR models were compared for each analyte in each region/subregion (76 comparisons), and the best (highest adjusted R^2, no multicollinearity) of the 3 models in each comparison was identified (Table 3.2). The best MLR models generally came from the watershed and riparian spatial scales within each region/subregion; only 2 models across all 4 regions/subregions were at the reach-scale (Table 3.2). A majority of the best models were based on landuse variables quantified at the watershed scale in the EOH and WOH regions and the WOHdel subregions. Only the WOHcat subregion had a greater number of riparian-scale models versus watershed-scale. These results are in contrast to those found using only Phase I data where riparian-scale, and to a lesser extent reach-scale models, were selected more often as the best relative to the results using all 6 years of project data. The EOH region was the only

region/subregion where a majority of the best models were considered unique; <½ of the best models in the WOHdel and WOHcat subregions and <¼ of the best models in the WOH region were considered unique.

The plots of the sum of base cations vs alkalinity for both WOH and EOH regions (Fig. 3.4) reflect the general patterns among sites shown using only Phase I data (Dow et al. 2006). Following (Rhodes et al. 2001), sites that plot above the defined watershed baseline probably have anthropogenic contributions to base cation concentrations within a watershed. The WOH watershed baseline regression had a slope of 1.02 and an x-intercept of –178 µeq/L (Fig. 3.4). This x-intercept value can be interpreted as a loss of alkalinity caused by regional acid inputs and is somewhat consistent with the ~100 µeq/L loss in acid-neutralizing capacity from acid inputs reported by (Rhodes et al. 2001) for minimally disturbed watersheds in western Massachusetts. In addition, the effects of acid deposition in the Neversink watershed have been well documented (Lawrence et al. 2001). The EOH watershed baseline regression had a slope of 1.5 with an x-intercept of –351 µeq/L. The inferred loss of alkalinity caused by regional acid inputs is greater for EOH watersheds than for WOH watersheds, but this result may actually indicate that the least-disturbed sites selected from the EOH region were not 'minimally disturbed.' The fact that some EOH sites are below the defined watershed baseline and that the % forested area is much lower for EOH least-disturbed sites relative to WOH least-disturbed sites suggest that the true watershed baseline for the EOH region may be much lower than defined here.

As brought out in (Dow et al. 2006), the plots of the sum of base cations vs alkalinity indicate that geology is one of the driving factors behind differences in stream chemistry between the WOH and EOH regions. Only 2 of the EOH sites (sites 41 and 125) overlapped with WOH sites in these plots (Fig. 3.4). EOH sites have higher base cation sums and higher alkalinities than WOH sites, and both variables reflect underlying differences between the 2 regions in the geological influences on stream chemistry. Within the WOH region, the subtle differences in stream chemistry attributable to geology when using just Phase I data (Dow et al. 2006) were still observed when using all 6 years of data. Gradients of high-to-low base cations and alkalinity exist from west to east (from the West Branch Delaware sites to the Esopus sites) and from north to south (from the Schoharie sites to the Neversink sites).

Flow and Time Trends of ions and nutrients during baseflow. Significant ion relationships with flow were all negative; i.e. as baseflow increased, ion concentration decreased (Table 3.3). The vast majority of the significant relationships were within the base cations and alkalinity. Impacted sites, whether urbanized or agricultural, had a greater number of significant ion versus flow relationships than the relatively non-impacted sites. Site 26, Esopus Creek below the portal outflow from the Schoharie Reservoir, did not have any significant ion versus flow relationships. Only 2 sites had significant negative flow relationships for chloride, with only 1 site having a similar flow relationship with sulfate. All 3 of these significant chloride/sulfate versus flow relationships occurred for sites that are relatively urbanized or agricultural watersheds. Only ten significant trends, all positive, were found across all ions and sites. Four of these significant trends were found for sodium, at more impacted sites, suggesting a possible increasing influence from road salt over the study period. However, only 1 of these 4 sites also had a significant chloride trend.

Few significant flow relationships or trends were found across the nitrogen and phosphorus analytes (Table 3.4). Five sites had significant flow relationships with total N (TN) with one positive and the remaining four negative. Site 55 (Kisco River) had six significant nutrient versus flow relationships, all negative, with 3 for nitrogen (NO_3-N, TDN, and TN) and 3 for phosphorus (SRP, TDP, and TP). Site 55 was also the only site with any significant flow relationships within the phosphorus group of analytes. Only 9 significant trends, all but one positive, were found with no real definable patterns in terms of a given anaylte or site.

Site 26 experiences strong flow modification from the Shandanken Tunnel inflow upstream of the sampling site which is likely the driving force in the stream chemistry signal observed at this sampling site. For the other 11 sites though, similar source-area contributions to baseflow may be occurring where lower baseflow chemistry reflects a greater contribution from deeper groundwater sources containing higher ionic concentrations and higher baseflow constituting a dilution of this groundwater signal by shallower groundwater/soil water contributions to stream flow. Nine of the 12 sites do have some type of contribution from WWTP effluent. Therefore, these relationships between conductivity and discharge at these sites may simply reflect a dilution of WWTP effluent during wetter periods (i.e., greater baseflow discharge). Changes in watershed-level compiled WWTP effluent volumes seem to have been negligible over time (Fig. 3.5) and were therefore unlikely to be behind any temporal trends (observed or not) in ion or nutrient concentrations at these 12 sites.

Stormflow Sampling

General patterns and observations. Storm-specific concentrations of ions and nutrients (Fig. 3.6) tended to follow the geographic patterns observed with baseflow concentrations: the EOH site (55) had ion concentrations that were 2 to 4 times that of the two WOH sites (6 and 29). Similarly, nutrient concentrations at the EOH site were generally no more than twice that at the 2 WOH sites. A notable exception was the nutrient concentrations that occurred during the 17JUN01 event sampled at the Neversink R. site, which were among the highest sampled for any of the storms at any of the three sites. Within each site, baseflow ion concentrations, as reflected in the average values over the entire project period, tended to be greater than stormflow concentrations while baseflow-specific nutrient concentrations tended to be less than stormflow concentrations.

A unusual chemical response occurred at the Kisco River (55) site during a storm event on 08SEP04 (Fig. 3.7). While only 2 to 4 storm samples were collected from this site for chemical analyses, the automated sampler used in the sampling process collected many more additional samples, generally from the start of an event to peak flow. Because the 2 to 4 samples to be analyzed were not selected until later (i.e. not in the field), pH and conductivity measurements were usually taken for each filled sample bottle. The pH and conductivity values for this particular storm showed a very dramatic, but short-lived, change in chemistry that occurred at the beginning of the storm hydrograph. Conductivity values went from < 200 μS/cm to nearly 700 μS/cm over a 3 hr period, and then dropped back down to approximately 100 μS/cm. pH meanwhile, went from approximately 5 down to < 3 and then back up to 7 over the same time period. No reason was found for this abrupt and dramatic change in chemistry during this particular storm (NYC DEP personnel were informed at the time).

Nutrient flux relationships at baseflow and stormflow. The mean instantaneous nutrient fluxes at baseflow were generally an order to several orders of magnitude less than the corresponding stormflow fluxes (Figs. 3.8, 3.9). The largest differences between baseflow and stormflow fluxes occurred for the forested site (Neversink, site 29). Mean stormflow fluxes for the Neversink were also always greater than the other two storm-sampling sites. Both of these differences are in large part due to a single storm event that occurred on 17JUN01. This storm event had a peak discharge that was approximately 2.5 times that of the next largest storm sampled at the Neversink site (Fig. 2.7, Chapter 2) along with nutrient concentrations that were much greater than any other storm-sampled concentrations at the this site. The magnitude of the 17JUN01 storm event along with the corresponding concentrations and fluxes demonstrates the importance a single storm event can have on nutrient loads and transport in a watershed (Macrae et al. 2007) even for a primarily forested watershed. Beyond this single storm event, nutrient fluxes at the Neversink would also tend to be larger relative to the other two storm-sampling sites due to greater discharge per watershed area for the Neversink as shown in (Arscott et al. 2006).

For the baseflow fluxes, the only significant site effect was found for PP, where site 29 PP fluxes were significant less than the fluxes measured at sites 6 and 55. No significant sample effects or interaction between site and sample were found for the stormflow fluxes. The lack of any significant sample effects suggests that no real difference, at least in terms of fluxes, existed between the high flow (HF) and high turbidity (HT) samples across all nutrients. When all storms were included in the analysis, significant differences between sites were found for NO_3-N and TDN where site 29 was significant greater than 6 but not site 55, and for PN, PP, and TP where site 55 was significantly greater than site 6 but not site 29. Somewhat different results were found when the 17JUN01 storm at the Neversink was excluded. Here, significant site effects were found for PN, PP, and TP where site 55 was significantly greater than both site 6 and site 29; for TDP where site 55 was significantly greater than site 29 but not site 6 and for TN where site 55 was significantly greater than site 6 but not site 29. It is interesting to note that in no case did site 6, the W. Br. Delaware, have nutrient fluxes, dissolved or particulate, N or P, that were significantly greater than the other 2 sites. The W. Br. Delaware watershed (Cannonsville Reservoir) was under phosphorus restrictions for a number of years which was lifted in 2002 (NYCDEP 2006).

Ion and nutrient relationships with baseflow and stormflow. The concentration versus discharge relationships across all sampled flow regimes (Table 3.5) lead to a number of comparisons that could be made including: 1. another view of the geologic differences among sites between the 2 study regions; 2. variation in land use/cover impacts on stream chemistry; and 3. effects of different flow regimes (i.e. baseflow v. stormflow) on stream chemistry both within and between sites. Of the 27 regression analyses for all ions (including conductivity and pH) across all 3 storm sampling sites, only 5 were not significant: pH, Na^+,K^+ and Alkalinity at the Neversink R. site (29) and K^+ at the Delaware R. site (6) (Table 3.5). A very different set of results were found across the nutrient relationships, where of the 30 regression analyses, only half were significant. Of the 15 significant relationships, 8 were for the Neversink R. site (29), the forested site, while only 2 significant nutrient versus flow relationships were found for the Delaware R. site (6), the agriculture site.

The intercept of these regression equations is operationally defined as the concentration (log10-transformed in all cases) at 0 discharge. Since this definition does not have any physical basis, a more useable definition for these intercepts is to consider them as the concentration under unchanging, low-flow conditions. As such, the intercepts then provide some indication of concentrations that are primarily influenced by geology. A comparison of the intercepts for a particular analyte provides a means of assessing whether the unchanging, low-flow stream chemistry signatures are different, in a relative sense, between sites. In nearly all cases, the intercepts from the agricultural and urban site regressions were significantly different, and higher, then corresponding regression intercepts from the forested site regressions (Table 3.5). This result was expected given the differences in baseflow chemistry observed between these sites as reflected in the alkalinity versus base cation plots shown in Fig. 3.4 where the Neversink site (forested) is part of the 'NVK' group designation; the W. Br. Delaware site (agriculture) is part of the 'WBD' group, and the Kisco R. site (urban) is part of the 'NCR' group. Somewhat surprising is that the intercepts from only 4 of the urban-site regressions were significantly different from the agricultural-site regressions. Given that the urban site is in the EOH region and the agricultural site is in the WOH region, with the well-defined geologic differences between the 2 regions, having so few statistically significant differences in the intercepts was unexpected.

Few statistically significant differences in slopes were found among the ion regression results, either between the forested site and the two impacted sites, or between the two impacted sites (Table 3.5). Ignoring statistical significance, in nearly all cases, the direction (positive v. negative rate of change) was the same. A notable exception is the SO_4 results, where the forested site had a significant and positive slope (i.e SO_4 concentration increased with discharge), while both the agricultural and urban sites had significant, negative slopes. The Neversink R. result for SO_4 concentration versus discharge is in contrast to decreases in SO_4 concentration observed during high-flow events for tributaries within the Neversink watershed in at least one past study (Wigington et al. 1996).

In contrast to the ion-versus-discharge slopes, the comparison among the nutrient-versus-discharge slopes showed many more statistical differences between the forested site slopes with those of either the agricultural or urban sites. The statistical differences in slopes, coupled with the fact that the forested site had many more statistically significant results over either of the other 2 sites may simply be a function of the very low nutrient concentrations at the forested sites. Such low concentrations, especially under baseflow conditions, may simply be broadening the range in concentration, and hence increasing the potential difference in concentrations over the range in discharge. Further, the largest high-flow event sampled, on 17JUN01, was sampled at the forested site, which may be leading to skewed results in the other direction, i.e. much higher concentrations than for any of the other storms sampled at the forested site.

The concentration v. discharge relationships using both baseflow and stormflow values were compared to the corresponding relationships using only baseflow values (Tables 3.3, 3.4) to assess the consistency in ion and nutrient concentration variation across differing flow regimes. Consistency was defined as having statistically significant concentration v. discharge relationships with similar slope direction, whether positive or negative, for both flow regimes (e.g. baseflow + stormflow; baseflow only). In general, consistent relationships for both flow

regimes were found across ions and nutrients for the agricultural and urban sites, but not for the forested site. The general pattern for the inconsistent results found for the forested site was that the baseflow+stormflow results were significant while the baseflow-only results were not. A notable exception to the consistent results found for the urban site, occurred within all of the P-specific relationships where none were consistent across the two flow regimes.

At a certain level, the storm-sampling effort of this project was meant to provide some perspective for the baseflow-centered sampling effort that defined the primary emphasis of the project. An obvious comparison between samples taken at baseflow and those taken under stormflow are differences in concentration. These differences in concentration then lead to looking at differences in load or the product of concentration and discharge. Examining load, especially for nutrients, is an important aspect of determining how much is leaving a watershed, or in the specific case of this study area, how much is being delivered to receiving reservoirs. The storm-sampling effort undertaken for this project does certainly provide a perspective on concentration differences, under differing land use/cover landscapes. However, the storm-sampling effort was not specifically design to answer questions regarding loads or fluxes.

Literature Cited

American Public Health Association (APHA). 1992. Standard methods for the examination of water and wastewater. 18th edition. American Water Works Association, Water Environment Federation, Washington, DC. pp. 2-44.

Arscott, D. B., C. L. Dow, and B. W. Sweeney. 2006. The landscape template of New York city's drinking-water-supply watersheds. Journal of the North American Benthological Society **25**:867-886.

Dow, C. L., D. B. Arscott, and J. D. Newbold. 2006. Relating major ions and nutrients to watershed conditions across a mixed-use, water-supply watershed. Journal of the North American Benthological Society **25**:887-911.

Helsel, D. R., and R. M. Hirsch. 2002. Statistical Methods in Water Resources. Techniques of Water-Resources Investigations of the USGS:510.

Lawrence, G. B., D. A. Burns, B. P. Baldigo, P. S. Murdoch, and G. M. Lovett. 2001. Controls of stream chemistry and fish populations in the Neversink watershed, Catskill Mountains, New York. WRIR 00-4040, U.S. Geological Survey, Troy, NY.

Macrae, M. L., M. C. English, S. L. Schiff, and M. Stone. 2007. Capturing temporal variability for estimates of annual hydrochemical export from a first-order agricultural catchment in southern Ontario, Canada. Hydrological Processes **21**:1651-1663.

Myers, R. H. 1990. Classical and modern regression with applications. 2nd edition. PWS-Kent Publishing Company, Boston, Massachusetts.

Neter, J., W. Wasserman, and M. H. Kutner. 1990. Applied Linear Statistical Models, 3rd edition edition. IRWIN / McGraw-Hill Professional Publishing.

NYCDEP. 2006. 2006 Watershed Protection Program Summary and Assessment. Department of Environmental Protection, New York City.

Rhodes, A. L., R. M. Newton, and A. Pufall. 2001. Influences of land use on water quality of a diverse New England watershed. Environmental Science and Technology **35**:3640-3645.

Wigington, P. J., D. R. DeWalle, P. S. Murdoch, W. A. Kretser, H. A. Simonin, J. Van Sickle, and J. P. Baker. 1996. Episodic acidification of small streams in the northeastern United States: Ionic controls of episodes. Ecological Applications **6**:389-407.

Table 3.1. Landuse variables derived from Geographical Information System data layers and quantified at the watershed (W), riparian (b), and reach (1k) scales. Variables were used in the individual major ion and nutrient multiple linear regressions (see Table 3.2 for those results).

Landuse variables	Abbreviation	Scale	General classification
Scale-defined variables			
% residential	RESD	W, b, 1k	Urban
% commercial	COMM	W, b, 1k	Urban
% industrial	INDU	W, b	Urban
% other urban	OURB	W, b, 1k	Urban
% cropland (and pasture)	CROP	W, b, 1k	Agriculture
% orchard	ORCH	W, b, 1k	Agriculture
% farmstead	FMST	W, b, 1k	Agriculture
% grassland	GRAS	W, b, 1k	Agriculture
% shrubland	SHRB	W, b, 1k	Undisturbed
% mixed brush-grassland	MBRH	W, b, 1k	Undisturbed
% deciduous forest	DECD	W, b, 1k	Undisturbed
% conifer forest	CONF	W, b, 1k	Undisturbed
% mixed forest	MFOR	W, b, 1k	Undisturbed
% wetland	WETL	W, b, 1k	Undisturbed
Road density (m/km^2)	RDNS	W, b, 1k	Urban
Unscaled variable			
Point-source discharge (mean annual watershed-area-normalized State Pollution Discharge Elimination System effluent volume) (cm^3/cm^2)	SPDE	NA	Urban

Table 3.2. Stepwise multiple linear regression (MLR) results of mean analyte concentration against watershed landscape variables at each of the 3 watershed scales. The 'best' MLR (highest adjusted R^2, no multi-collinearity) is in bold and marked with an asterisk. See text for definition of a unique model (UNQ = 'Y').

ION/ NUT	Model Adj. R^2 W		b		1k		UNQ	Significant Predictors, 'Best' Model (Partial R^2, slope direction)
WOH Delaware								
COND	**0.79**	*	0.75		0.53		N	RDNS(0.64,+) COMM(0.12,+) WETL(0.06,+)
PH	0.10		**0.13**	*	.		N	SHRB(0.16,+)
ALKL	**0.79**	*	0.69		0.37		N	COMM(0.39,+) GRAS(0.24,+) SHRB(0.13,+) ORCH(0.06,+)
CL	**0.80**	*	0.26		0.42		Y	RESD(0.42,+) COMM(0.22,+) FMST(0.13,+) OURB(0.05,-)
SO_4	**0.27**	*	0.25		0.09		Y	RESD(0.16,-) RDNS(0.15,+)
CA	**0.76**	*	0.69		0.42		N	COMM(0.48,+) GRAS(0.18,+) SHRB(0.10,+) WETL(0.04,+)
MG	0.83		**0.86**	*	0.48		N	DECD(0.82,-) SPDE(0.04,+)
NA	**0.76**	*	0.69		0.59		Y	RDNS(0.63,+) ORCH(0.09,+) COMM(0.06,+)
K	0.79		**0.84**	*	0.43		N	DECD(0.67,-) CONF(0.09,-) OURB(0.05,-) INDU(0.04,+) MBRH(0.02,-)
NH_4N	0.53		0.58		**0.58**	*	Y	COMM(0.28,+) CROP(0.14,+) WETL(0.09,+) GRAS(0.08,+) SHRB(0.06,+)
NO_3N	**0.68**	*	0.51		0.36		Y	FMST(0.54,+) MFOR(0.12,+) WETL(0.05,+)
ORGN	0.62		**0.69**	*	0.39		N	CROP(0.41,+) RDNS(0.17,-) ORCH(0.14,+)
TDN	**0.72**	*	0.64		0.39		N	FMST(0.62,+) WETL(0.07,+) MFOR(0.06,+)
PN	0.37		**0.59**	*	0.44		Y	COMM(0.29,+) MFOR(0.17,-) RDNS(0.12,-) SHRB(0.06,+)
TN	**0.74**	*	0.70		0.42		N	FMST(0.63,+) SPDE(0.10,+) WETL(0.04,+)
SRP	**0.55**	*	0.41		0.19		Y	GRAS(0.34,+) SHRB(0.18,+) ORCH(0.08,+)
TDP	**0.73**	*	0.52		0.25		Y	GRAS(0.34,+) ORCH(0.15,+) MBRH(0.12,-) CONF(0.10,-) COMM(0.08,+)
PP	0.64		**0.73**	*	0.59		Y	COMM(0.30,+) MFOR(0.21,-) RDNS(0.15,-) OURB(0.06,+) ORCH(0.06,+)
TP	**0.77**	*	0.71		0.43		Y	CONF(0.29,-) COMM(0.26,+) ORCH(0.11,+) MBRH(0.09,-) DECD(0.06,-)
WOH Catskills								
COND	**0.92**	*	0.92		0.75		N	RESD(0.78,+) INDU(0.10,+) MFOR(0.04,-) RDNS(0.02,-)
PH	**0.65**	*	0.60		0.49		N	RESD(0.55,+) INDU(0.13,+)
ALKL	0.72		**0.83**	*	0.57		Y	RESD(0.66,+) CONF(0.08,-) WETL(0.06,+) RDNS(0.05,+)
CL	0.79		**0.86**	*	0.62		N	RESD(0.60,+) INDU(0.20,+) DECD(0.05,-) WETL(0.04,-)
SO_4	**0.75**	*	0.69		0.15		N	MBRH(0.39,+) GRAS(0.26,+) WETL(0.13,-)
CA	**0.79**	*	0.72		0.55		N	RESD(0.67,+) INDU(0.08,+) MFOR(0.07,-)
MG	0.92		**0.94**	*	0.63		N	RESD(0.62,+) FMST(0.13,+) RDNS(0.13,+) SHRB(0.05,+) INDU(0.02,+) DECD(0.01,+)
NA	0.92		**0.94**	*	0.75		N	RESD(0.73,+) INDU(0.18,+) CROP(0.02,+) WETL(0.02,-)
K	0.65		**0.77**	*	0.38		Y	FMST(0.48,+) WETL(0.13,-) INDU(0.12,+) MFOR(0.07,-)
NH_4N	.		**0.35**	*	.		Y	CROP(0.21,-) SPDE(0.19,+)
NO_3N	0.15		**0.17**	*	0.13		Y	RDNS(0.21,+)
ORGN	**0.61**	*	0.56		0.49		N	GRAS(0.51,+) CONF(0.12,+)
TDN	**0.14**	*	0.13		.		Y	RDNS(0.17,+)
PN	0.22		**0.22**	*	.		N	FMST(0.25,+)
TN	0.19		**0.19**	*	0.13		N	CROP(0.22,+)
SRP	0.90		**0.90**	*	0.14		Y	RDNS(0.48,+) MFOR(0.23,-) CROP(0.10,+) ORCH(0.05,-) GRAS(0.03,+) COMM(0.03,-)
TDP	0.89		**0.82**	*	.		N	GRAS(0.47,+) CONF(0.19,-) SHRB(0.08,-) CROP(0.08,+) ORCH(0.04,-)
PP	**0.49**	*	0.48		0.39		N	INDU(0.51,+)
TP	**0.82**	*	0.81		0.19		N	GRAS(0.39,+) MFOR(0.31,-) SHRB(0.07,-) CROP(0.04,+) RESD(0.04,+)

Table 3.2. Continued.

ION/ NUT	Model Adj. R^2 W		b		1k		UNQ	Significant Predictors, 'Best' Model (Partial R^2, slope direction)
WOH								
COND	**0.82**	*	0.72		0.57		Y	RESD(0.59,+) SPDE(0.13,+) FMST(0.10,+) ORCH(0.01,+)
PH	0.20		**0.25**	*	0.14		Y	SPDE(0.15,+) SHRB(0.13,+)
ALKL	**0.64**	*	0.60		0.40		N	RESD(0.48,+) FMST(0.11,+) DECD(0.04,+) COMM(0.04,+)
CL	**0.65**	*	0.63		0.48		N	RESD(0.51,+) SPDE(0.16,+)
SO4	0.44		**0.45**	*	0.24		Y	CROP(0.26,+) ORCH(0.08,+) SPDE(0.06,+) COMM(0.06,-) OURB(0.05,+)
CA	**0.70**	*	0.63		0.41		N	RESD(0.47,+) GRAS(0.11,+) COMM(0.08,+) MFOR(0.04,-) MBRH(0.03,-)
MG	**0.85**	*	0.82		0.43		N	CROP(0.60,+) RESD(0.20,+) SPDE(0.04,+) DECD(0.03,+)
NA	**0.81**	*	0.69		0.57		Y	RESD(0.58,+) SPDE(0.15,+) OURB(0.04,-) FMST(0.03,+) ORCH(0.02,+)
K	**0.81**	*	0.75		0.49		N	GRAS(0.73,+) MBRH(0.04,-) RDNS(0.03,+) MFOR(0.02,-)
NH_4N	0.50		**0.50**	*	0.47		N	FMST(0.35,+) ORCH(0.17,+)
NO_3N	**0.39**	*	0.34		0.29		N	FMST(0.40,+)
ORGN	0.61		0.63	*	0.33		N	DECD(0.50,-) RDNS(0.06,-) CONF(0.05,-) COMM(0.05,+)
TDN	**0.60**	*	0.56		0.47		N	FMST(0.60,+)
PN	**0.34**	*	0.31		0.22		N	FMST(0.25,+) COMM(0.12,+)
TN	**0.67**	*	0.62		0.46		N	FMST(0.65,+) SPDE(0.03,+)
SRP	**0.77**	*	0.74		0.31		N	CONF(0.61,-) RDNS(0.15,+) CROP(0.02,+)
TDP	**0.81**	*	0.78		0.35		N	GRAS(0.58,+) CONF(0.16,-) MBRH(0.06,-) ORCH(0.02,+)
PP	0.59		**0.60**	*	0.50		N	COMM(0.30,+) CROP(0.15,+) RDNS(0.10,-) ORCH(0.08,+)
TP	**0.81**	*	0.78		0.38		N	GRAS(0.59,+) CONF(0.09,-) COMM(0.08,+) MBRH(0.04,-) ORCH(0.03,+)
EOH								
COND	**0.60**	*	0.52		0.25		N	RDNS(0.53,+) CONF(0.09,-)
PH	0.11		**0.26**	*	0.26		Y	OURB(0.15,+) WETL(0.14,-)
ALKL	**0.54**	*	0.39		.		Y	RDNS(0.21,+) CROP(0.16,+) CONF(0.13,-) SHRB(0.09,+)
CL	**0.67**	*	0.61		0.42		N	RDNS(0.50,+) SPDE(0.09,+) DECD(0.08,+) RESD(0.03,+)
SO_4	**0.55**	*	0.49		0.42		N	RDNS(0.45,+) SHRB(0.07,-) SPDE(0.05,+)
CA	**0.65**	*	0.44		0.07		Y	RDNS(0.45,+) CONF(0.09,-) CROP(0.08,+) SHRB(0.05,+)
MG	**0.58**	*	0.39		0.06		Y	RDNS(0.36,+) CONF(0.12,-) CROP(0.10,+) INDU(0.04,+)
NA	**0.66**	*	0.61		0.29		N	RDNS(0.44,+) SPDE(0.12,+) DECD(0.09,+) MFOR(0.04,+)
K	**0.61**	*	0.52		0.28		N	RDNS(0.42,+) SPDE(0.12,+) CROP(0.09,+)
NH_4N	0.35		**0.35**	*	0.32		N	SPDE(0.25,+) CROP(0.08,+) WETL(0.06,+)
NO_3N	**0.49**	*	0.33		0.31		Y	RESD(0.41,+) WETL(0.06,-) FMST(0.05,+)
ORGN	**0.63**	*	0.61		0.47		N	SPDE(0.48,+) WETL(0.08,+) RESD(0.08,+)
TDN	**0.58**	*	0.45		0.35		Y	RESD(0.41,+) SPDE(0.15,+) CROP(0.05,+)
PN	**0.61**	*	0.58		0.54		N	SPDE(0.40,+) WETL(0.13,+) OURB(0.07,-) RDNS(0.05,+)
TN	**0.62**	*	0.49		0.44		Y	RESD(0.42,+) SPDE(0.18,+) CROP(0.05,+)
SRP	**0.48**	*	0.15		0.27		Y	RESD(0.32,+) OURB(0.07,+) DECD(0.07,+) GRAS(0.06,+)
TDP	**0.56**	*	0.22		0.30		Y	RESD(0.35,+) OURB(0.08,+) GRAS(0.07,+) DECD(0.06,+) RDNS(0.04,+)
PP	0.62		0.57		**0.75**	*	Y	SPDE(0.32,+) WETL(0.10,+) FMST(0.09,+) COMM(0.09,+) CONF(0.07,+) SHRB(0.07,-) ORCH(0.04,-)
TP	**0.60**	*	0.36		0.53		Y	SPDE(0.33,+) RESD(0.16,+) WETL(0.06,+) OURB(0.05,+) GRAS(0.04,+)

Table 3.3. Conductivity, pH, cation, and anion results (α=0.05) for regressions of concentration versus discharge (Q), showing R^2 and slope direction in parentheses (+ = positive, - = negative) and for trend analysis (T) showing trend direction, using either regression residuals, if the concentration-v.-discharge regression was significant, or raw concentrations.

	COND		pH		Ca		K		Mg		Na		Alkl		Cl		SO_4	
Site	Q	T	Q	T	Q	T	Q	T	Q	T	Q	T	Q	T	Q	T	Q	T
3	0.75(-)	+			0.84(-)				0.92(-)		0.69(-)	+	0.83(-)					
6	0.83(-)				0.84(-)		0.61(-)		0.93(-)		0.82(-)	+	0.73(-)		0.83(-)	+		
9									0.81(-)									
10	0.97(-)				0.70(-)				0.88(-)		0.91(-)		0.82(-)					
15							0.77(-)		0.69(-)									
23								+										
26																		
29											0.70(-)							
34					0.84(-)				0.78(-)				0.86(-)					
46	0.75(-)	+	0.78(-)		0.75(-)	+	0.83(-)		0.79(-)	+			0.83(-)				0.91(-)	
52									0.68(-)			+	0.78(-)					
55	0.83(-)				0.90(-)		0.71(-)		0.83(-)		0.56(-)	+	0.76(-)		0.66(-)			

Table 3.4. Nitrogen and Phosphorus results (α=0.05) for regressions of concentration versus discharge (Q), showing R^2 and slope direction in parentheses (+ = positive, - = negative) and for trend analysis (T) showing trend direction, using either regression residuals, if the concentration-v.-discharge regression was significant, or raw concentrations. No significant flow relationships or trends were found for PN or PP.

	NH_4N		NO_3N		ORGN		TDN		TN		SRP		TDP		TP	
Site	Q	T	Q	T	Q	T	Q	T	Q	T	Q	T	Q	T	Q	T
3			0.78(-)				0.78(-)		0.82(-)							
6																
9			0.67(-)			+								+		
10						+		+	0.85(+)	-						
15																
23																
26									0.69(-)							
29					0.66(+)			+								
34		+				-										
46			0.74(-)	+			0.75(-)	+	0.76(-)	+						
52																
55			0.81(-)				0.77(-)		0.73(-)		0.68(-)		0.81(-)		0.74(-)	

Table 3.5. Concentration versus discharge relationships based on linear regression analysis for the 3 storm-sampling sites (site numbers are provided in parentheses in the top header row). Model: $\log_{10}$(analyte concentration) = β_o + β_1 *$\log_{10}$(discharge), where β_o= Intercept and β_1= slope. Non-significant ' α= 0.05 values were set to '---'. See text for further details on the comparison of regression results between sites. All baseflow and stormflow data collected at a site were used in the analyses unless otherwise noted in the text.

	Forested site (29)			Agricultural site (6)			Urban/Suburban site (55)		
Analyte	**R^2**	**β_o**	**β_1**	**R^2**	**β_o**	**β_1**	**R^2**	**β_o**	**β_1**
Insitu measurements									
COND	0.26	1.9	-0.097	0.78	2.8 *	-0.18	0.56	3.1 *	-0.15
pH	---	7.6	---	0.42	11 *	-0.74	0.41	8.9	-0.31 †
Cations									
Ca	0.66	0.95	-0.12	0.83	1.7 *	-0.17	0.71	2.2 * †	-0.18
Mg	0.72	0.39	-0.14	0.92	1.1 *	-0.19 *	0.70	1.7 * †	-0.18
K	---	-0.9	---	---	--- *	---	0.30	0.85 * †	-0.08 *
Na	---	0.47	---	0.76	1.8 *	-0.23 *	0.50	1.9 *	-0.13 †
Anions									
ALKL	---	1.1	---	0.74	2.2 *	-0.19	0.61	2.5 *	-0.16
Cl	0.28	0.96	-0.13	0.62	2.0 *	-0.23	0.49	2.4 *	-0.16
SO_4	0.25	0.38	0.078	0.21	1.3 *	-0.087 *	0.19	1.4 *	-0.063 *
Nutrients (N/P)									
NH_4N	---	-2.2	---	---	-1.2	---	---	-1.9	---
NO_3N	---	-1.2	---	---	--- *	---	0.33	0.40 *	-0.15 *
ORGN	0.75	-4.2	0.62	0.48	-1.7 *	0.22 *	---	-0.44 * †	--- * †
TDN	0.35	-1.6	0.23	---	--- *	--- *	0.25	0.39 *	-0.097 *
PN	0.54	-6.1	1.0	---	-2.9	---	0.39	-3.6	0.7
TN	0.55	-3.0	0.55	---	--- *	--- *	---	--- *	--- *
SRP	0.34	-3.7	0.23	---	-1.7 *	---	---	-1.5 *	---
PP	0.61	-7.7	1.1	0.35	-3.7 *	0.48 *	0.45	-3.4 *	0.53 *
TDP	0.34	-3.6	0.25	---	-1.5 *	---	---	-1.3 *	--- *
TP	0.63	-6.4	0.93	---	-2.3 *	--- *	0.25	-2.1 *	0.28 *

* - Intercept or slope of the agricultural or urban/suburban site regression significantly (α= 0.05) different from the corresponding forested site coefficient.

† - Intercept or slope of the urban/suburban site regression significantly (α= 0.05) different from the corresponding agricultural site coefficient.

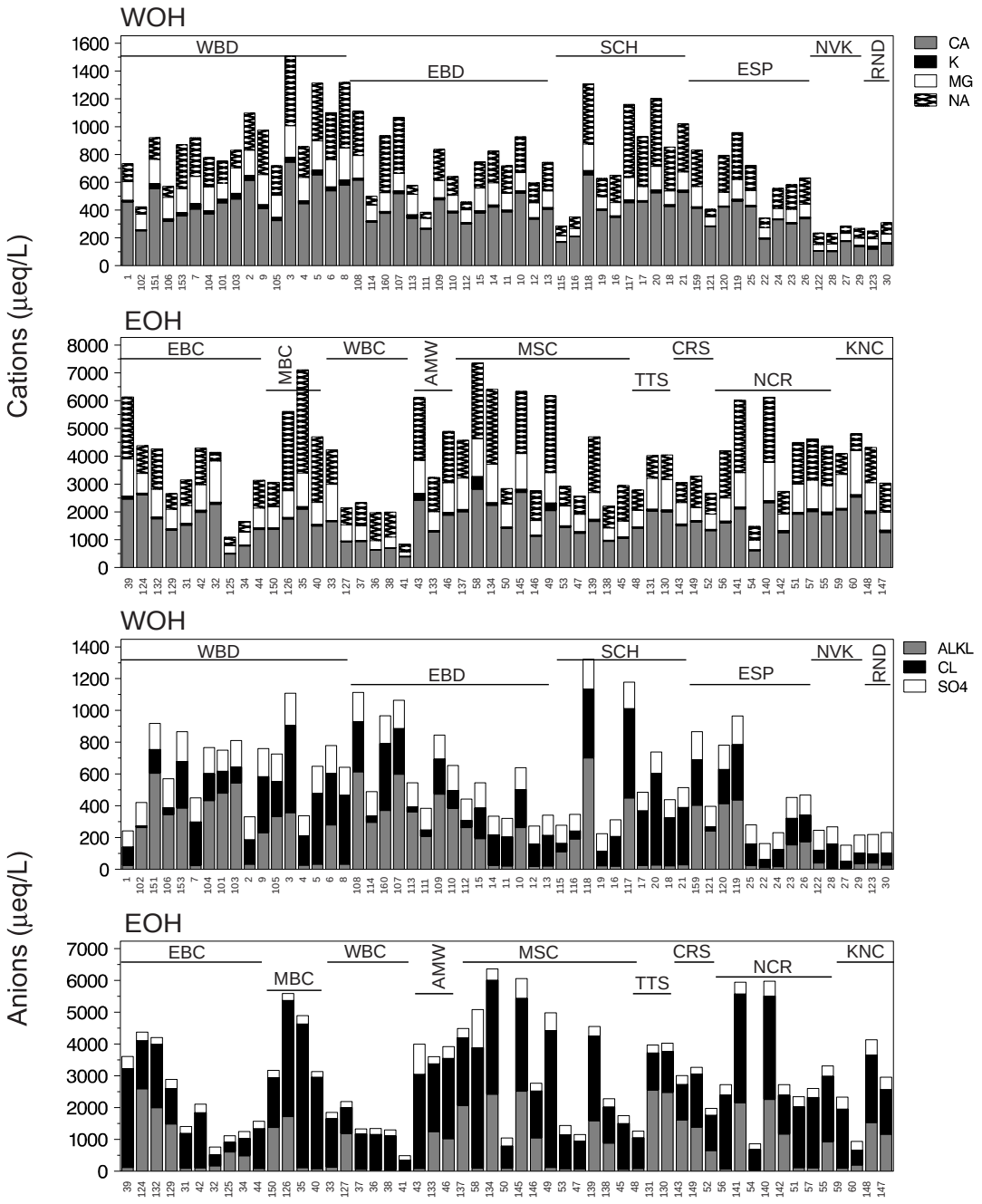

Figure 3.1 Six-year mean concentrations (n=2 to 6) for major cations and anions/alkalinity (Alk) in stream water collected during summer baseflow from 57 west of Hudson River (WOH) and 53 east of Hudson River (EOH) study sites on streams contributing to New York City's drinking-water-supply reservoirs (see Chapter 2 for site names and locations). Sites in each panel are arranged by geographical subregion and are sorted from smallest to largest watershed area within each subregion. Subregion abbreviations are: WBD = West Branch Delaware River, EBD = East Branch Delaware River, SCH = Schoharie Creek, ESP = Esopus Creek, NVK = Neversink River; RND = Rondout Creek, EBC = East Br. Croton River; MBC = Middle Branch Croton River, WBC = West Branch Croton River, AMW = Amawalk Reservoir Streams; MSC = Muscoot River, TTS = Titicus River; CRS = Cross River, NCR = New Croton Reservoir sites; KNC = Kensico Reservoir sites.

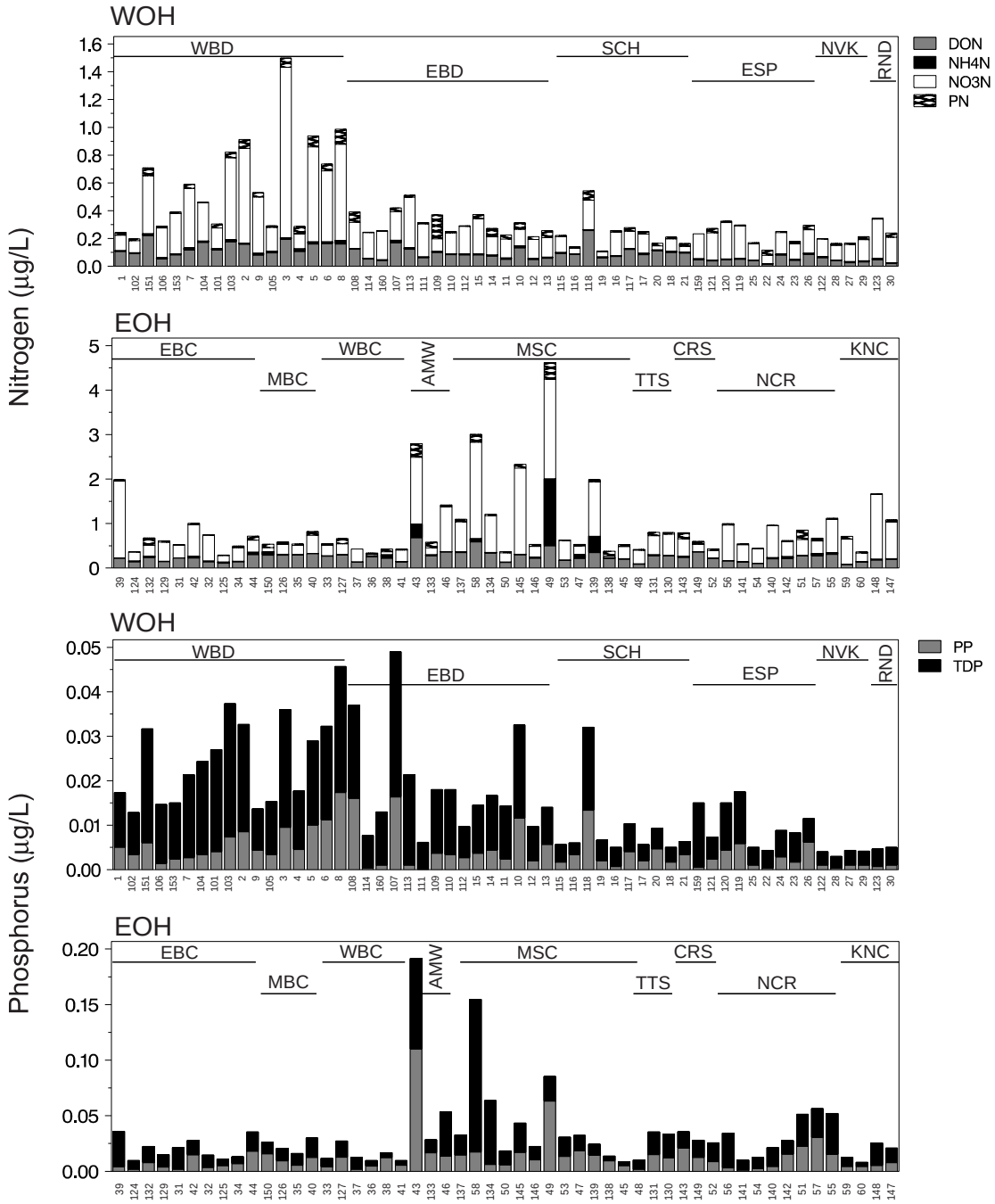

Figure 3.2. Six-year mean concentrations (n=2 to 6) of N and P species in stream water collected during summer baseflow from 57 west of Hudson River (WOH) and 53 east of Hudson River (EOH) study sites on streams contributing to New York City's drinking-water-supply reservoirs (see Chapter 2 for site names and locations). Sites in each panel are arranged by geographical subregion and are sorted from smallest-to-largest watershed area within each subregion. See Fig. 3.1 legend for subregion abbreviations. The following concentration values were truncated: NO_3-N concentrations at sites 43, 49, and 58 (actual mean values of 6.87, 2.24, and 5.67 mg/L, respectively); NH_4-N concentrations at sites 43 and 49(actual mean values of 6.87 and 17.8 mg/L, respectively) and DON concentration at site 49 (actual mean value of 1.10 mg/L).

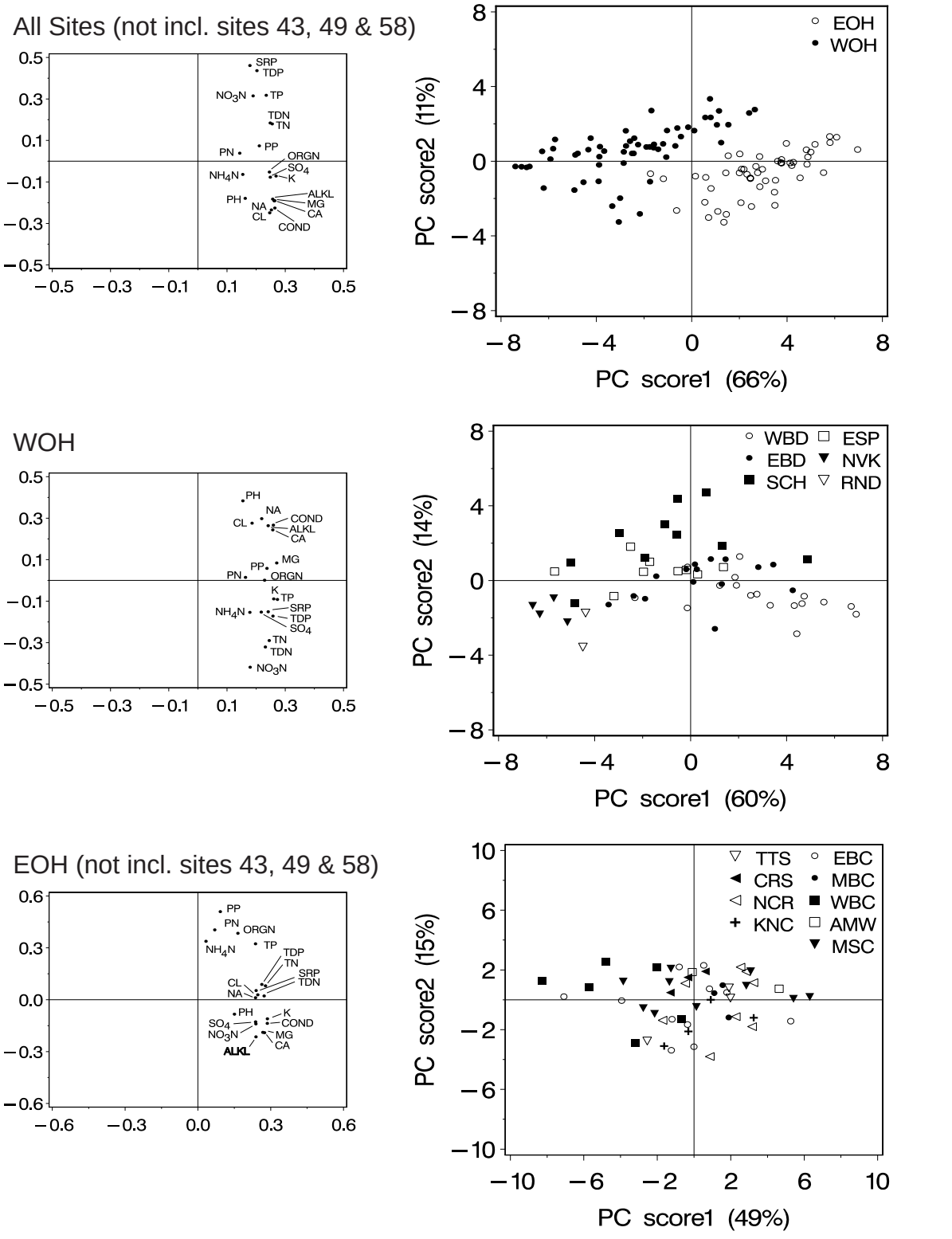

Figure 3.3. PCA results (input variable loadings on the left, site scores on the right) for 3 separate analyses of inter-relationships among ion/nutrient chemistry for all sites (top), WOH sites (middle) and EOH sites (bottom). Sites 43, 49, and 58 were excluded because of extremely high nutrient values (see Fig 3.2 for more details). Variance explained by each axis included in the axis labels (score plots). See Fig. 3.1 legend for subregion abbreviations.

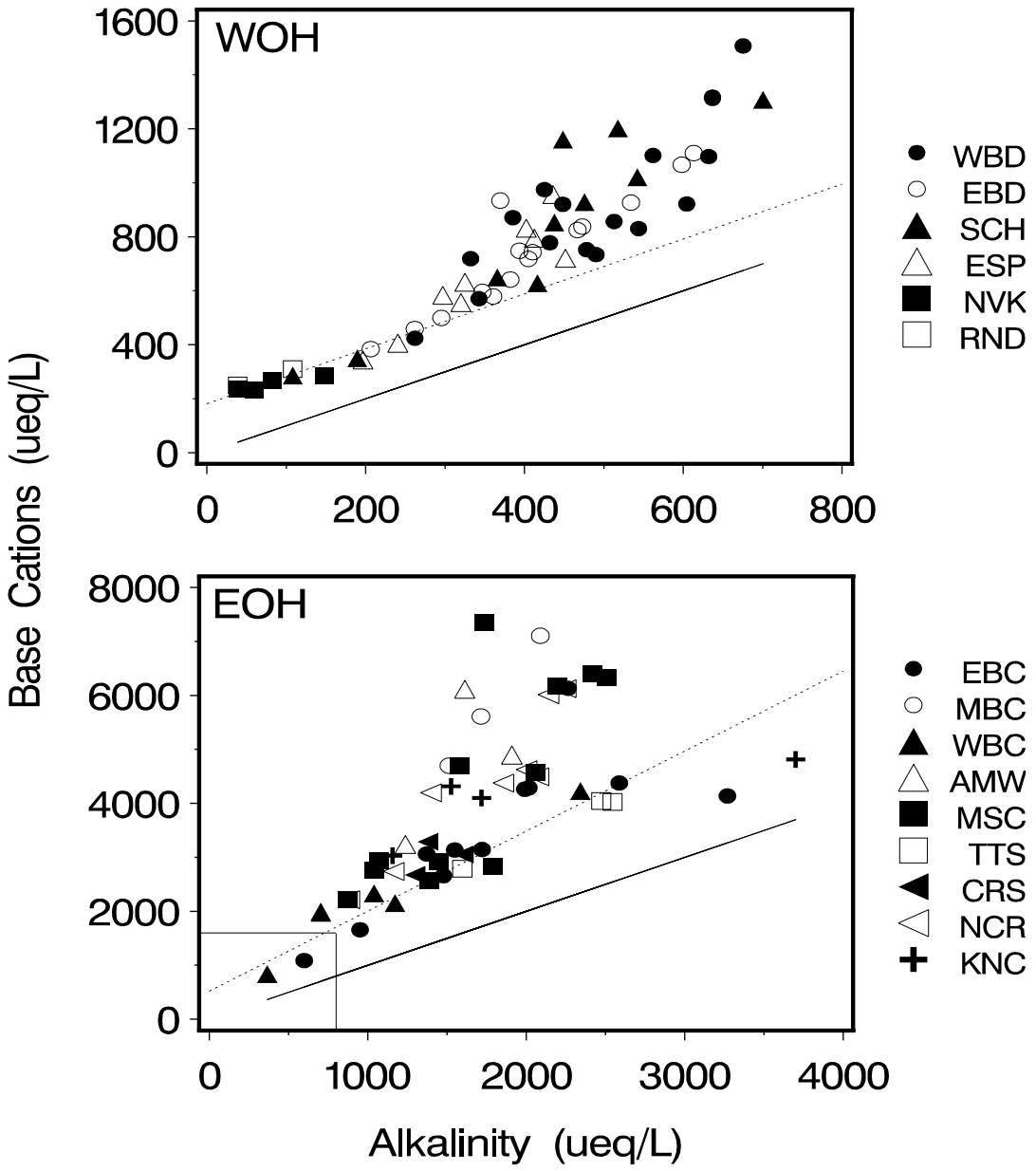

Figure 3.4. Sum of base cations (Ca^{2+}, Mg^{2+}, Na^{+}, K^{+}) versus alkalinity for the 57 WOH sites (top) and 53 EOH sites (bottom) sampled over the 6-year period of 2000-05. Concentration values are means of 2 to 6 samples per site. The solid line represents the 1:1 line while the dotted line represents the watershed baseline from a regression using the least-disturbed sites within each region based on %forested area in a watershed (see text for details). The box in the lower-left portion of the EOH plot panel indicates the range of values for WOH sites. See Fig. 3.1 legend for subregion abbreviations.

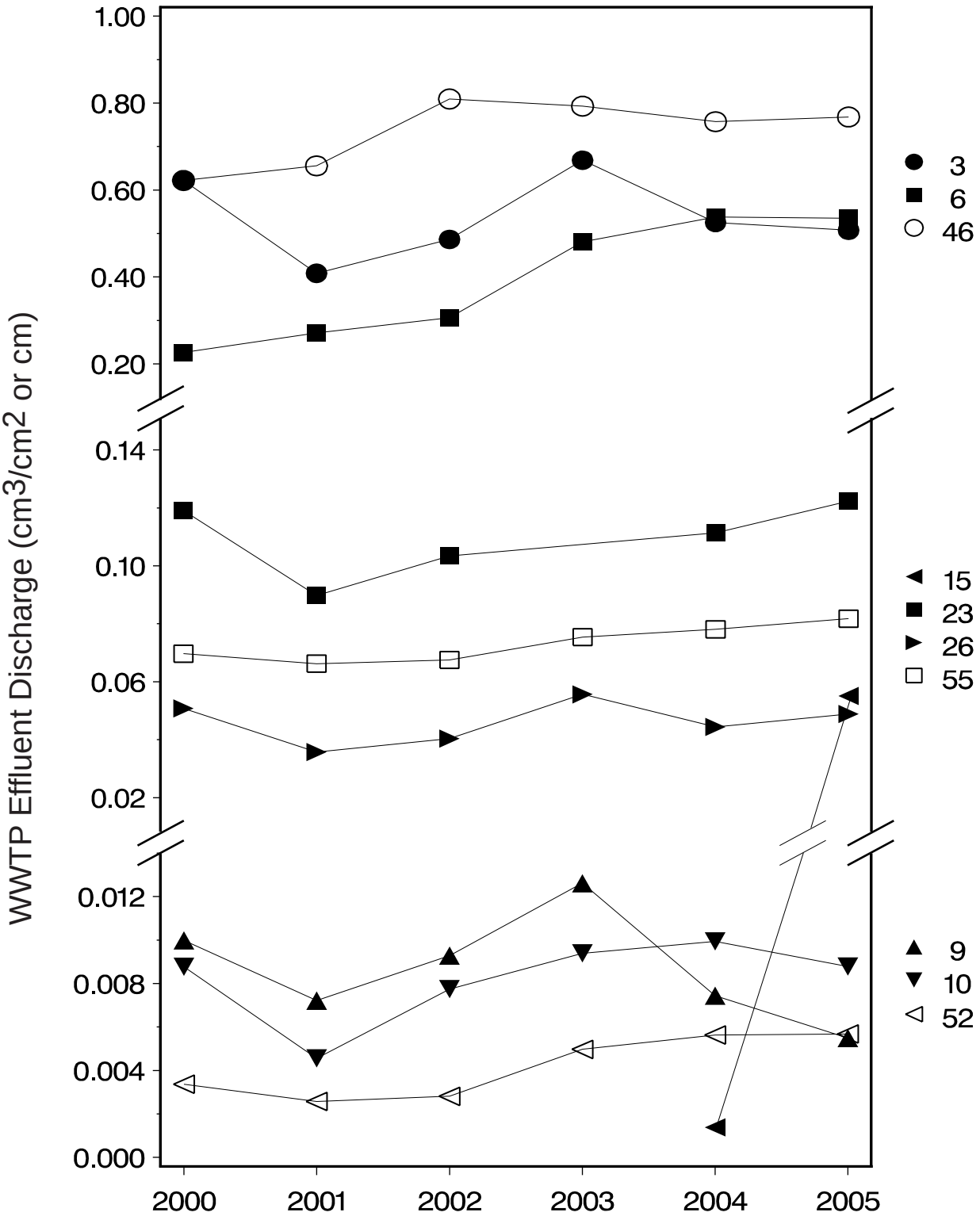

Figure 3.5. WWTP annual effluent volumes normalized for watershed area for those sites sampled all 6 years of the project study period. Sites 29 and 34, also sampled all 6 years of the study, did not have any WWTPs within their respective watersheds. Site names corresponding to the site numbers provided can be found in tables 2.3 and 2.4 in chapter 2.

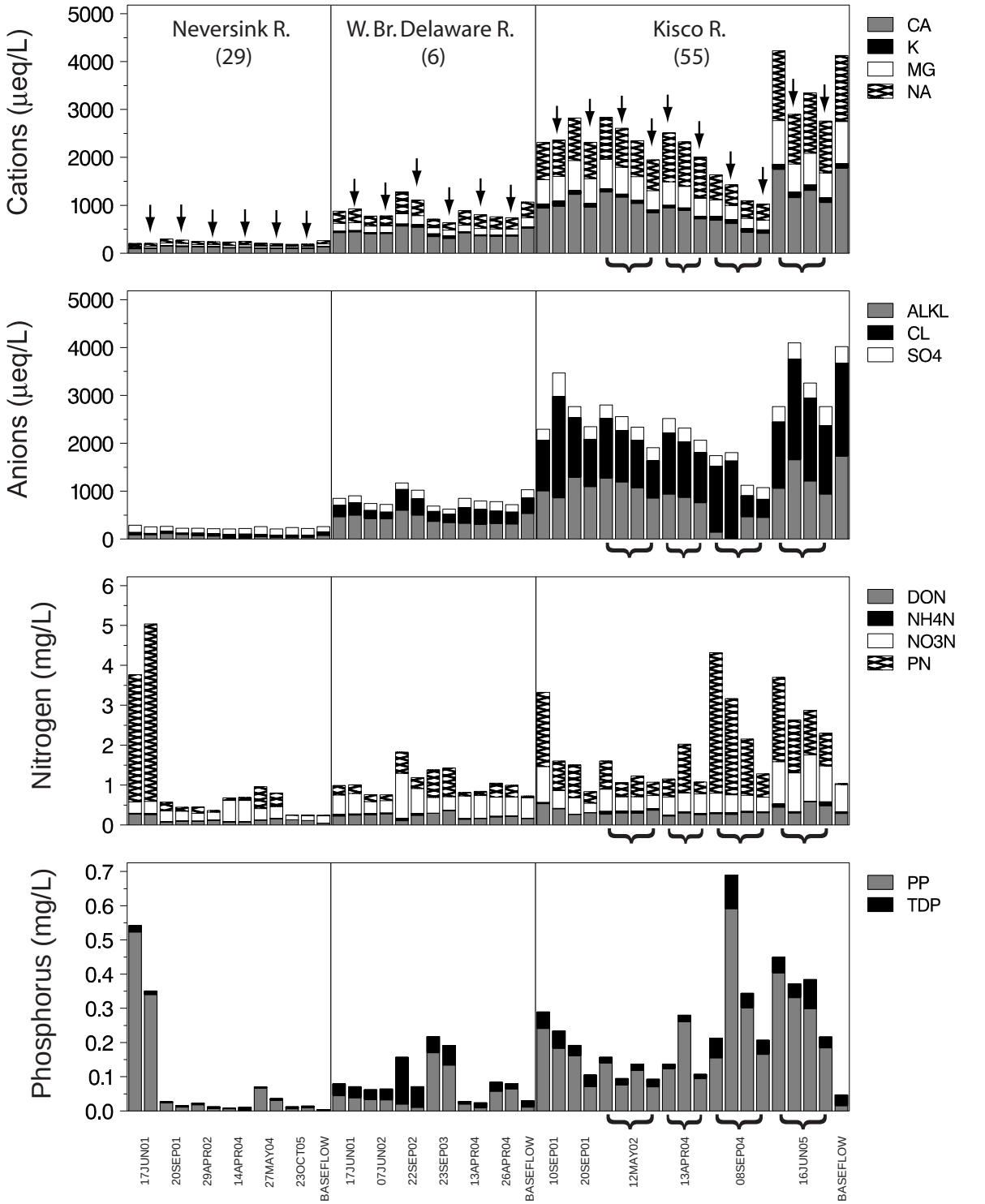

Figure 3.6. Ion and nutrient concentrations for each storm sampled over the 6-year project period at the three storm-sampling sites. Site names and numbers are provided in the top panel. Each date along the x-axis represents a sampled event where a peak flow (indicated by the arrows in the upper plot) and a high turbidity (unmarked) sample were collected. For the Kisco R. (55) site, more than one peak or high turbidity flow sample could have been collected per storm; dates on which this occurred are indicated by the brackets. Average baseflow values for each site are also provided with each site's set of storm samples.

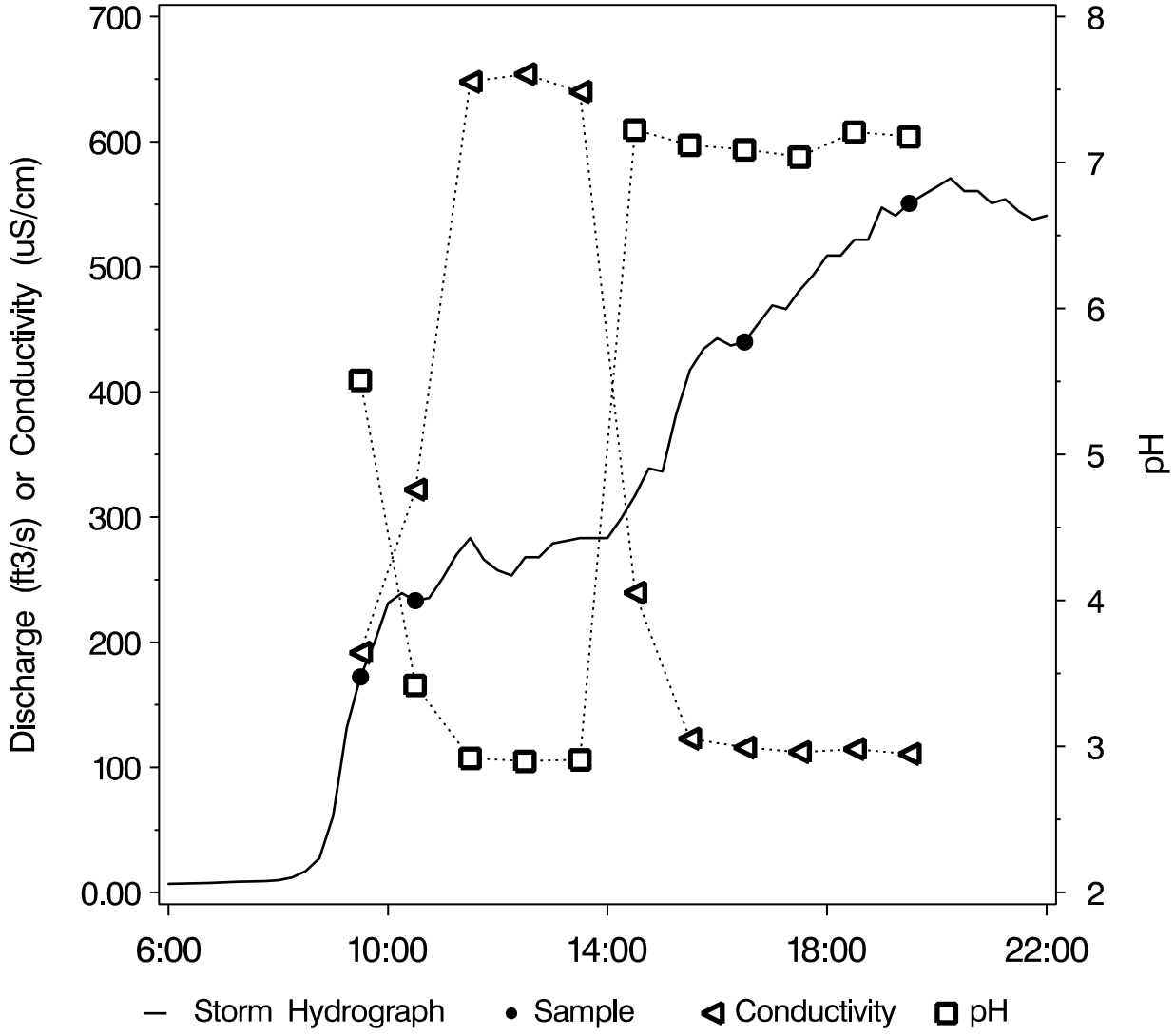

Figure 3.7. Storm event occurring 08SEP04 on the Kisco River (site 55), having a dramatic, and likely unnatural drop in pH, coinciding with a spike in conductivity.

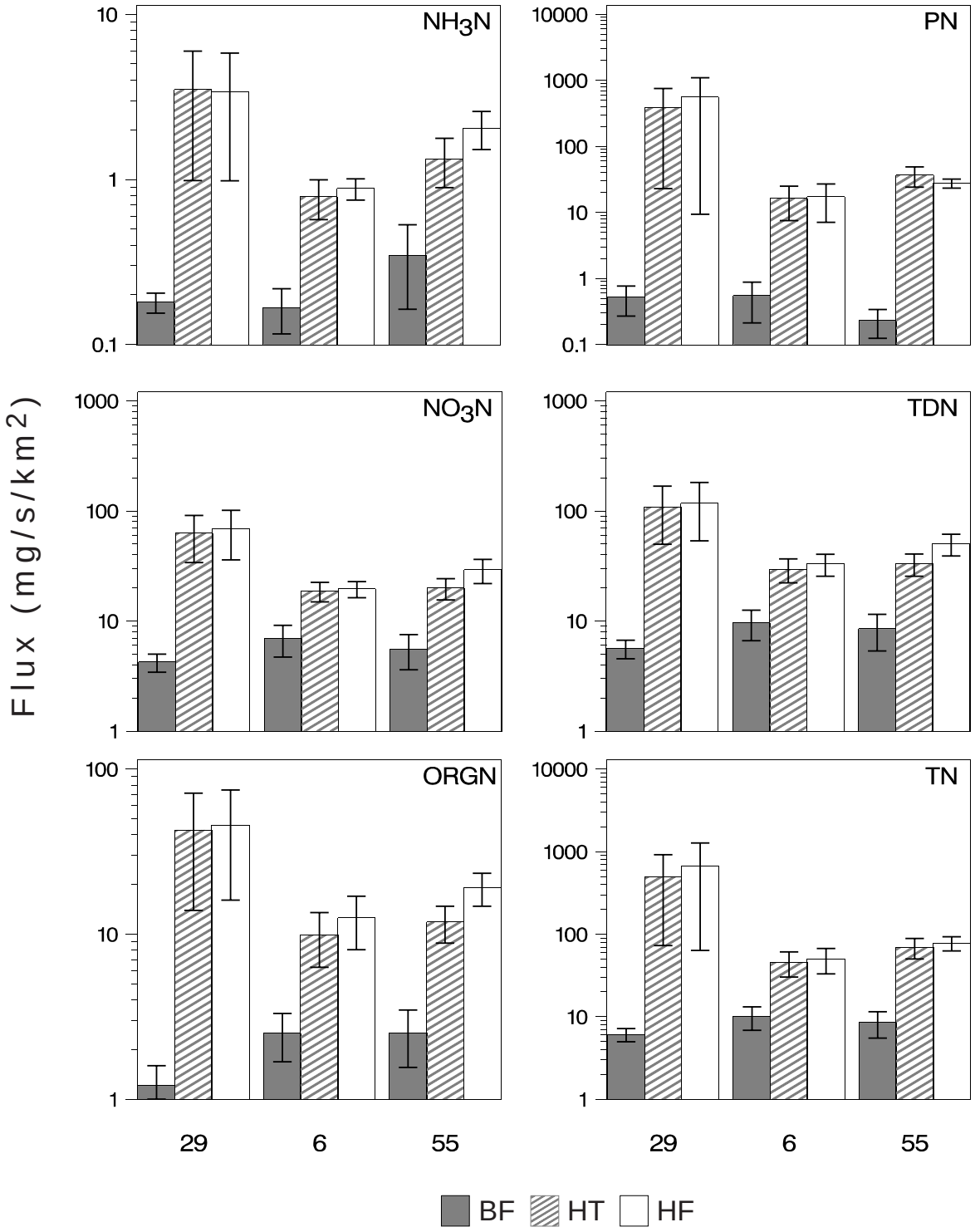

Figure 3.8. Mean instantaneous nitrogen fluxes at baseflow (BF), high turbidity stormflow (HT) and peak stormflow (HF) at the 3 stormflow-monitoring sites over the 2000-2005 period. Error bars represent one standard error; number of observations was between 6 and 8.

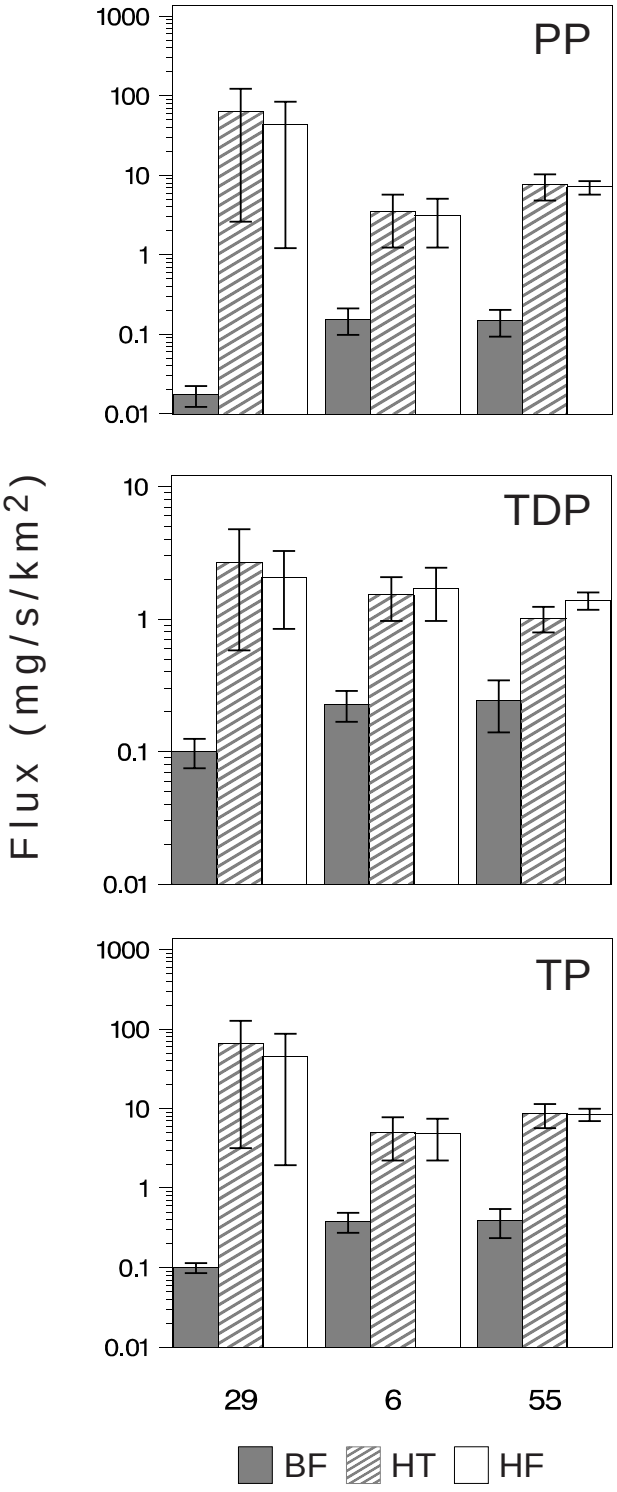

Figure 3.9. Mean instantaneous phosphorus fluxes at baseflow (BF), high turbidity stormflow (HT) and peak stormflow (HF) at the 3 stormflow-monitoring sites over the 2000-2005 period. Error bars represent one standard error; number of observations was between 6 and 8.

----------Intentionally Blank----------

Chapter 4. Molecular Tracers of Contamination in Streams and Rivers

Introduction

Degradation of water quality can occur from a variety of point and non-point sources originating from both anthropogenic and natural factors, such as industrial effluent, sewage from waste water treatment plants (WWTP) or septic leakage, road and agricultural runoff, atmospheric deposition, and even wildlife. The range of contaminants includes excessive nutrient loading, heavy metals, pesticides, other toxic organic compounds, and pathogens. In order to best maintain the quality of drinking water resources, targeted efforts to reduce or eliminate primary contamination sources first require the accurate identification and quantification of all contaminant sources that contribute to the degradation of water quality.

The use of molecular tracers to identify sources of contaminants is an emerging technique that qualitatively links chemical fingerprints unique to these sources with contaminants of concern (Leeming et al. 1996, Standley et al. 2000, Kolpin et al. 2002, Yunker et al. 2002, Buerge et al. 2003, Glassmeyer et al. 2005). These tracer compounds do not themselves need to be toxic or directly contribute to water quality degradation, but rather they only need to enable discrimination between different sources and therefore act as proxies for contaminants originating from those same sources. For example, a recent and increasingly used proxy to detect potential sewage contamination is caffeine. While not considered toxic to humans or aquatic life at any measured environmental concentration, in temperate latitudes the only source of caffeine to surface waters is from the urine of consumers of caffeinated beverages and pharmaceuticals (Buerge et al. 2003). Therefore, high aquatic concentrations of caffeine are a strong indicator of sewage and or septic contamination (Standley et al. 2000, Buerge et al. 2003, Vogel et al. 2005).

The practice of using source-specific organic compounds, or biomarkers, to estimate source contributions has been well developed by the field of organic geochemistry originally to identify natural organic matter (NOM) sources to petroleum formation and more recently to elucidate a wide range of processes in the cycling of natural organic carbon (Eglington 1969, Hedges and Prahl 1993). Organic geochemists have long recognized that a compound must meet a certain set of criteria to be useful as a biomarker, or as a tracer of sources (Hedges and Prahl 1993). The ability for quantitative interpretation of tracer data increases as each of the following criteria are met: (1) the tracer must be detectable at a concentration well below that of interest; (2) ambient concentrations of the tracer molecule must be accurately quantified; (3) all sources of the tracer are known and relatively unique; and (4) environmental diagenesis or degradation of the tracer compound is either (a) minimal, (b) well understood, and/or (c) proportional to other tracer compounds to which it might be compared (e.g., ratios do not change with degradation).

Enhanced monitoring projects of ambient water quality could substantially benefit by adopting the biomarker approach of organic geochemistry. However, most organic contaminant monitoring efforts, even in watersheds with many unknown sources, focus on regulated compounds and pay little attention to proxies for source identification. Furthermore, the most widely used EPA methods (i.e., 625 or 8270) have method detection limits (generally 1-100 µg/L) that are often orders of magnitude higher than EPA water quality criteria for those same

compounds (USEPA 2002b). Last, most recent studies using more sensitive methods do not quantify ambient concentrations by correcting for known analytical biases, such as extraction recovery (Kolpin et al. 2002, Glassmeyer et al. 2005). Because extraction recovery and many other analytical biases vary by sample, failure to quantify and apply sample-specific recovery corrections introduces unnecessary analytical imprecision and inaccuracy.

The contaminant monitoring study presented here was designed using the biomarker approach of organic geochemistry. We present a modified method that quantifies 12 polycyclic aromatic hydrocarbons (PAH), 2 fragrance materials (FM), caffeine (CAF) and 10 fecal steroids (FS) to laboratory reporting levels (LRL) ranging from 0.00018 to 0.092 µg/L (Table 4.1, Fig. 4.1). For most of these compounds, this method was the most sensitive published method that we were aware of. In addition, ambient stream water concentrations were more accurately quantified by correcting for analytical biases for each sample using a suite of internal surrogate recovery standards. We then describe concentration distributions of these compounds measured at 110 stream and river sites for 6 consecutive years (2000-2006) as part of a multi-disciplinary enhanced monitoring project in New York City (NYC) drinking water supply watersheds (Blaine et al. 2006). From patterns in tracer compounds we infer potential contamination sources to waters upstream of study sites. Last, we relate mean tracer concentrations measured at these sites to watershed landscape properties.

Research Task

Our investigation of molecular tracers of soot and sewage contamination targets two of the overall projects primary objectives, as listed in the Quality Assurance Project Plan (QAPP). First, molecular tracers are designed to act as indicators for evaluating the occurrence and source of selected aquatic chemical contaminants. Second, the six-year data sets will be utilized as a baseline for assessing changes in water quality in response to changes in land use and best management practice (BMP) implementations.

Given these objectives, molecular tracer concentrations were analyzed from 3 to 12 different times at each of 110 stream sampling sites within New York City drinking water source watersheds (see Chapt. 2 and Tables 2.1-2.4 and Figs. 2.1-2.2) during baseflow conditions to determine the relative influence of contaminant sources on water quality. In Phase I, 60 sites were visited each year at summer baseflow and 28 of those sites were also visited during winter baseflow conditions. In Phase II, we continued sampling 12 Phase I sites and 50 additional sites during summer baseflow, with 28 (7 continued from Phase I) of those also sampled during winter baseflow. Winter baseflow sampling was designed to target background levels (no overland flow), winter recreation area influences, and the effect of low temperatures on sewage treatment efficiency. Storm flow samples were also collected at three of the 110 sampling stations in each of six years to determine changes in source composition with storm runoff.

We have chosen a suite of 25 organic compounds that act as robust proxies for a variety of contamination sources (Table 4.1). These compounds include twelve polycyclic aromatic hydrocarbons (PAH), two fragrance materials (FM), caffeine (CAF) and ten fecal steroids (FS).

Polycyclic aromatic hydrocarbons are found in raw and refined petroleum and coal products and are also formed during the combustion of vegetation, wood, waste, coal and petroleum.

Thus PAHs have both natural and anthropogenic sources. The compounds that we quantify here are fluorene (FLU), phenanthrene (PHE), anthracene (ANT), 2-methyl phenanthrene (2MP), 1-methyl phenanthrene (1MP), fluoranthene (FLR), pyrene (PYR), benzo(a)anthracene (BAA), chrysene (CHR), benzo(b)fluoranthene (BBF), benzo(k)fluoranthene (BKF), and benzo(a)pyrene (BAP).

Fragrance materials are anthropogenic compounds used in a variety of consumer products such as soaps, detergents and lotions. Thus, FMs enter the environment primarily through greywater sewage (Simonich *et al.* 2000). The compounds that we quantify here are tonalide (7-acetyl-1,1,3,4,4,6,-hexamethyl-1,2,3,4-tetrahydronaphthalene, AHTN) and galaxolide (1,3,4,6,7,8-hexahydro-4,6,6,7,8,8-hexamethylcyclopenta[γ]-2-benzopyran, HHCB). Both AHTN and HHCB are non-biodegradable, making them particularly suited for tracers studies (Simonich *et al.* 2002).

Caffeine is a natural compound that occurs in certain tropical plants, including tea and coffee, and is added to numerous food products and pharmaceuticals. In temperate climates, the primary source of caffeine to watersheds is via the urine of those who consume caffeine-containing products (Buerge *et al.* 2003).

Fecal steroids are natural compounds that are produced in the intestines of birds and mammals. Ratios of certain steroids to others allow for the discrimination between human fecal material and that of other animals (Leeming *et al.* 1996). The steroids we quantify for this study are coprostanol (5β-cholestan-3β-ol, bCOP), *epi*coprostanol (5β-cholestan-3α-ol, EPI), cholesterol (cholest-5-en-3β-ol, CHOL), cholestanol (5α-cholestan-3β-ol, aCOP),), coprostanone (5β-cholestan-3-one, bONE), cholestanone (5α-cholestan-3-one, aONE), 24-ethyl-coprostanol (24-ethyl-5β-cholestan-3β-ol, eCOP), 24-ethyl-*epi*coprostanol (24-ethyl-5β-cholestan-3α-ol, eEPI), 24-ethyl-cholesterol (24-ethyl-cholest-5-en-3β-ol, eCHO), and 24-ethylcholestanol (24-ethyl-5α-cholestan-3β-ol, SNOL).

Methods

Detailed descriptions of our field and laboratory methods are provided in the Quality Assurance Project Plan (QAPP) for each Project Year and the Standard Operating Procedures attached therein. In 2003 at the beginning of Phase II, we modified our protocol slightly over that used previously in order to increase reproducibility, recovery and sensitivity, as was described in an addendum to our Year 4 QAPP. What follows is a brief description of methods, noting where differences occurred between Phase I & II.

Field

During summer and winter baseflow collections, 8 L water samples (4 L in Phase I) were collected for tracer analysis in pre-cleaned glass jars. At the same time, samples were collected for all other baseflow analyses (i.e. nutrients, major ions, TSS, DOC, etc. see Chapt. 3 & 6). Storm flow samples were collected using ISCO samplers fitted with pre-cleaned glass receiving bottles. The ISCO samplers were set to begin sampling with a small rise (approximately 10 to 15 cm) of stream water and took two 1-liter samples every hour for up to 12 hours. A subset of two paired 1-L samples for each stream – representing high flow (HF) and high turbidity (HT) – were

chosen for analysis. Selection of the two samples were based on examining the storm hydrograph available from a nearby USGS gauging station collecting near real-time data or from a co-located stage recorder (In-Situ, Inc., Mini-Troll). Peak particulate concentrations were determined visually. High flow samples were removed from the ISCO apparatus within 12 hours of collection and then handled in the same manner as baseflow water samples. Water samples were stored in a cool and dark place and extracted within 7 days.

All glass sampling equipment and sample jugs were washed with detergent, rinsed with nanopure water and finally combusted in a kiln at 480°C for 4 h to remove all remaining organic compounds. Metal and Teflon sampling equipment (including jug cap liners), which could not be kilned, were cleaned with detergent and nanopure water, dried and finally by rinsed with hexane/acetone (1:1) followed by dichloromethane, as was any field equipment that needed to be reused between sites. The probe and collection tubing on ISCO samplers were cleaned weekly with 0.1 N HCl, 0.1 N NaOH, and deionized water.

Field blanks and duplicates were each collected at three sites during summer baseflow sampling (5% of sites) and two sites during winter baseflow sampling. One set of field blanks and duplicates was collected through the ISCO sampler during stormflow collections.

Laboratory

Molecular tracers were extracted from all samples by liquid-solid extraction onto an Empore™ disk, using protocols similar to EPA approved alternate test method 608 ATM 3M0222 or to EPA Method 3535. As a whole, our complete set of SOPs for extraction and GC-MS analysis describe a method very similar to EPA method 8270.

In brief, sample water was filtered through a glass fiber filter stacked on top of an Empore™ C-18 disk. Particulate tracer compounds were extracted from the filter by sonic extraction and dissolved tracers were eluted from the Empore disk with solvents. Surrogate recovery standards – perdeuterated phenanthrene (PHE-D10), perdeuterated chrysene (CHR-D12), perdeuterated perylene (PER-D12), perdeuterated caffeine (CAF-D9) and perdeuterated cholesterol (CHO-D6) – were added to the surface of both the filter and the disk, after they were separated but prior to extraction. (In Phase I, no CAF-D9 was added and CHO-^{13}C2 was used instead of CHO-D6). Dissolved and particulate extracts were then back-extracted in a separatory funnel with an aqueous salt solution to remove impurities, mixed with anhydrous sodium sulfate to remove moisture, rotoevaporated, and transferred to auto-injector vials. Samples were gently dried under a stream of nitrogen, redissolved in 15 µL pyridine, and derivatized (in order to analyze fecal sterols, which contain alcohol groups) by purging sealed vials with N_2, adding 15 µL of BSTFA (N,*O*-bis(trimethylsilyl)trifluoroacetamide) with 1% TMCS (Trimethylchlorosilane), and heating to 70°C for 30 minutes in an aluminum heating block. In Phase I, dried extracts were redissolved and derivitized in 50 µL MSTFA (N-methyl-N-(trimethylsilyl)trifluoroacetamide) with 1% TMCS (Trimethylchlorosilane). Derivitized sample extracts were then spiked with 5 µL internal standard solution (25-ng/µL in each of p-terphenyl-d14 and 5α-cholestane in pyridine; in Phase I with 2.5 µL of 2-methylnaphthalene (2MN)) and were analyzed for each of the molecular tracers compounds by capillary gas chromatography – mass spectrometry (GC/MS) in selective ion monitoring (SIM) mode, using a J&W DB1701 column (30 m, 0.25 mm i.d., 250 µm coating) on an Agilent 6890 series GC interfaced with a 5973n series MSD.

Laboratory blanks and duplicates, and matrix spike samples, were prepared in conjunction with all sites having field blanks and duplicates (3 sites during summer baseflow sampling and two sites during winter baseflow sampling).

Quantification

Each batch of 12-15 samples was analyzed by GC-MS along with 7-8 analytical standard mixes at 5-6 levels of 0.04 (Phase II only), 0.2, 1.0, 4.0, 20 and 50 ng/μL nominal concentration (exact concentrations for each compound were slightly different, but known to 3 significant figures) and 2-3 check standards at 4.0 ng/ μL nominal concentration. To enable the greatest consistency, we quantified tracer concentrations from all 6 years using an automated data quantification system (Dow and Aufdenkampe 2006). In brief, after confirmation by the analyst, for each compound the peak areas of 1 quantitation and 1-2 confirmation ions were exported for all standards and samples from the Agilent GC-MS "ChemStation" chromatography software directly into our central server. We then manipulated these raw data with SAS-based scripts (SAS/Base v.9.1; SAS Institute, Inc., Cary NC) to produce final concentration data. Thus, decisions regarding how to fit the calibration curve, when to drop outlying standards, whether or not peak identity was adequately confirmed, etc. were all made uniformly for the entire 6-y dataset using the same objective criteria. Additional benefits of this quantitation system included documentation of all calibration decisions, which could be easily reviewed or revised at any time, less potential for error, and better quality control. If a compound concentration was above the highest calibration standard, the sample extract was diluted and reanalyzed. If a compound concentration was below the lowest calibration standard, the compound was flagged as "estimated" but nevertheless quantified using a linear fit from the origin to the lowest standard. If any compound in a check standard did not give a concentration within 20% of the known value, all samples analyzed after that check standard were reanalyzed for that compound.

All data presented here were corrected for extraction recoveries and other analytical biases measured for each sample using internal surrogate standards, which were added to each sample prior to filtration and extraction. Surrogate standard recoveries were assigned to tracer compounds, based on recovery data from lab-spiked matrix samples for all compounds, as follows (see Table 1 for analyte abbreviations): perdeuterated phenanthrene (FLU, PHE, ANT), perdeuterated chrysene (FLR, PYR, BAA, CHR, HHCB, AHTN), perdeuterated perylene (BBF, BKF, BAP), perdeuterated caffeine (CAF, Phase II only) and perdeuterated cholesterol (fecal steroids, ^{13}C2-cholesterol for Phase I). 2MP and 1MP were corrected using the average recovery of perdeuterated phenanthrene and perdeuterated chrysene. In Phase I, CAF was corrected with the average recovery of perdeuterated phenanthrene (most similar molecular weight) and ^{13}C2-cholesterol (most polar surrogate). These assignments were confirmed with lab-spiked test samples (i.e. known amounts of compounds added to clean water), by matching measured recoveries of each tracer with the surrogate having the most consistently similar recovery.

Laboratory reporting levels (LRL) were assigned to each analyte using the definitions and methods of USGS Open File Report 99-193 (USGS 1999). In brief, the LRL is defined as the concentration above which there is 99% confidence that reporting a false negative will be avoided. In other words, if the ambient concentration is above the LRL, the laboratory is 99% confident to detect a concentration. The LRL is equivalent to 2 times the method detection limit

(MDL) as defined by EPA in CFR Title 40 Part 136 Appendix B (USGS 1999). In brief, CFR 40-136-B states that the MDL is 3 times the standard deviation (99% confidence interval of the mean) of greater than 7 replicates of an analytical standard spiked at the lowest reliably detectable and quantifiable concentration in a clean sample matrix. For our method, where contamination of blanks and MDL study samples did occur occasionally, we removed outlier high concentration MDL sample data using Chauvenet's criterion (Taylor 1997) prior to calculating our LRL. This insured that our calculated LRL remained true to the intended definition as the 99% confidence limit for no false negatives.

Data were not censored below estimated MDL or LRL values *a priori* for most of our statistical analyses, with the exception of values for ratios of two or more compounds. A number of studies and reports have examined the numerous negative effects of censoring data (Gilliom et al. 1984, Porter et al. 1988, Helsel 1990, USGS 1999). In the Discussion, we examine in detail these rational for minimizing data censorship. Ratios of two tracer compounds were censored, or eliminated from consideration, if one compound had a concentration below its censorship limit, which was either the LRL or the 75% percentile of measured blanks, whichever was greater. For the ratio of high to low molecular weight PAHs, the value was eliminated if the sum of measured concentrations in the either the numerator or denominator was less than the sum of the censorship limits for the same compounds.

Fecal Coliform Densities

Fecal coliforms were sample at 28 stream sites (14 WOH, 14 EOH) during the summer baseflow sampling of 2005. These data were collected in order to assess relationships between fecal steroid data and the more typical fecal contamination monitoring of sampling for fecal coliforms. Samples were collected in pre-sterilized, 125 mL glass containers and stored for no more than 6-8 hours at 4^{o}C prior to filtration and incubation. Three separate aliquots, 1mL, 10 mL and 100mL, were filtered through a 0.45 µm presterilized membrane with the goal of having one of the aliquots yield counts of 20 to 60 colonies. Filters were saturated with m-FC fecal coliform broth and incubated at 44.5° ± 0.2° C for 24 ± 2 hr. Immediately following incubation, colonies were hand counted from the filter that most closely approximated the desired 20 to 60 colonies per filter.

Statistical analyses

Prior to all statistical analyses, concentration data for all 25 tracer compounds were log transformed (after adding 0.00003 µg/L to all values, a value just below the minimum detected concentration). Log-normal distributions were confirmed with a Shapiro-Wilk test, where normality was rejected at level of $p < 0.01$, which corresponded to a Shapiro-Wilk statistic (W) > 0.94 for $n = 57$ (pearson correlation, regression and analysis of variance do not require strict conformation to normality) (SAS/STAT; SAS Institute, Inc., Cary NC). For the EOH dataset, 18 of 25 compounds showed log-normal distributions, with the exceptions being 2 fragrances and 5 steroids. Removal of 3 obvious outlier sites, all with large sewage treatment plants upstream (sites 43, 49 and 58), improved the number of log-normal distributions to 20 of 25, with the exceptions being 1 fragrance and 4 steroids. This reduced EOH dataset was commonly used for a number of statistical analyes. For the WOH dataset, 17 of 25 tracers were log-normal, with the exceptions being 2 fragrances, 2 steroids, and 4 PAH.

Redundancy analysis

Three RDA's were built using subsets of the 110-site summer-collected database. Subsets of sites were defined by geographic region for each RDA (i.e. all EOH and WOH sites, EOH sites only, and WOH sites only). As many as 99 possible watershed-characteristic variables (Table 4.2) could have been included in the selection procedure (see forward selection procedure below), and these were described by 4 general categories: watershed scale (all watershed area upstream of the site –"W"), riparian scale (30-m riparian buffer on both sides of the stream network upstream of the site – "b"), reach scale (30-m riparian buffer on both sides of the stream network upstream of the site, truncated 1- km above the site – "1k"), and scale independent. All watershed-characteristic variables were derived using a geographic information system (GIS). The first 3 categories contained land use variables presented in Chapter 2 as well as in Arscott et al. (2006) and Dow et al. (2006). In addition surficial geology, soil characteristics (% Clay, % organic matter, pH, and erodability (Kf)), and lake density and channel network variables were quantified at the watershed-scale. The scale independent category included watershed area, number of permitted point-source discharges, distance from the nearest point-source, and the mean annual watershed-area-normalized effluent volumes (point-source discharge; Chapter 2). All landuse percentages were arcsine-square-root transformed to minimize bimodality, and density data were $\log_{10}(x)$ transformed to reduce magnitude effects. CANOCO version 4.02 (Microcomputer Power, Ithaca, New York; ter Braak and S. Milauer 1998) was used to build all models, and the manual forward selection procedure was used to select watershed-characteristic variables that significantly contributed to a model explaining molecular tracer concentrations. The manual forward selection procedure used a partial Monte Carlo permutation test (permuted 1000 times) to assess the usefulness of explanatory variables ($p = 0.05$) in the ordination.

Multiple Linear Regression analysis

The 6-y geometric means for individual tracer concentrations and sums, as previously described, as well as arithmetic means for ratios were related separately to land use variables (% land use, road density, and point-source discharge) compiled at three separate spatial scales (whole watershed, riparian, and reach) using multiple linear regression (MLR). All scaled land use variables listed in Table 3.1 in Chapter 3 (except % transportation, % water) plus point-source discharge were used in the MLR analyses. All % land use variables were arcsine square-root(x) transformed, population density was $\log_{10}(x)$ transformed, road density was $\log_{10}(x+1)$ transformed, and point-source discharge was $\log_{10}(x + 0.001)$ transformed. Stepwise variable selection with a variable significance cutoff of 0.05 was used in selecting independent variables in the MLR models (SAS/STAT, version 9, SAS Institute, Cary, North Carolina). Separate MLR analyses were run for WOH, EOH, and EOH minus sites 43, 49, and 58 regions.

The best model for each variable from the scale comparison was the model with the highest overall adjusted R^2 value and no significant multicollinearity. Multicollinearity was assessed using the variance inflation factor (VIF). VIF values >10 for any independent variables suggest problems associated with multicollinearity in the regression model (Myers 1990). The best model was considered unique relative to the models from the remaining scales if: 1) the adjusted R^2 of the best model was 10% or greater than the adjusted R^2 for models for at the other scales, and 2) if no strong relationship (e.g., $R^2 > 0.50$) could be found for a regression between the

strongest predictor from the best model using either group of significant predictors from the models for the other scales.

Results

Analytical method

Relatively modest modifications to widely used EPA methods for semi-volatile organic compounds (i.e., 625 or 8270) resulted in laboratory reporting levels (and therefore method detection limits) that were 3-5 orders of magnitude lower than the given MDL for those methods (Table 4.1, Fig. 4.1). These large increases in sensitivity were achieved by: (1) increasing sample volumes from 1 to 8 L (4 L in Phase I) by the use of solid-phase extraction rather than liquid-liquid extraction (4-8 x sensitivity); (2) decreasing final extract volumes from 1 mL to 35 µL (52.5 µL in Phase I) (20-30 x sensitivity); (3) setting the Mass Selective Detector to Selective Ion Monitoring (SIM) mode rather than full scan (~10 x sensitivity); (4) using calibration standards with a lower minimum concentration and employing a separate, quadratic calibration curve when analyte concentrations were in the range of 0.0.4 - 4.0 ng/µL in the injected extract (5 x sensitivity); and (5) correcting for differences in sample-to-sample analytical recovery with internal surrogate standards (~2 x sensitivity as observed by a halving of standard deviations in our MDL study). Cumulatively, these modifications resulted in a theoretical 8000+ x (= 4 x 20 x 10 x 5 x 2) improvement in sensitivity of our method over EPA 625 or EPA 8270, which closely matched the observed improvements in our LRL over given MDL values for these methods. LRL values were generally a factor of 5 to 10 greater than instrument detection concentrations.

A consequence of having a sensitive method is that analytical blanks are much more likely to contain detectable concentrations. Of the 89 blanks analyzed with our 527 baseflow samples, the percentage of these blanks exceeding our LRL values ranged from 11% for HHCB to 87% for PHE (because only 6 of the 25 compounds showed a significant difference between between lab and field blanks [$p < 0.05$ for paired t-test with pairing by extraction week], the two datasets are pooled for subsequent discussion). For 9 of our 23 (eCOP and eEPI do not have defined LRL values) tracer compounds, <30% of analyzed blanks exceeded LRLs. For 11 compounds, 30%-50% of blanks exceed LRLs, and for 4 compounds 50% to 88% of blanks exceeded LRLs. Contamination was highly variable between blanks, exhibiting a 50 to 1000-fold range in magnitude. Based on Phase I data only, contamination was also random; concentrations of tracers in blanks were generally not correlated with the minimum, mean, maximum or coefficient of variance of concentrations of tracers in samples from the same extraction batch (exceptions were the minimums and means of 1MP and PHE, where p-values ranged from 0.02 to 0.0012). Therefore, blanks were not useful in determining whether or not a specific sample might be contaminated let alone the magnitude of that contamination. On the other hand, concentration distributions measured in blanks did allow estimation of probabilities of contamination to a given concentration level.

From our blank data we calculated the 75 and 95 percentile concentrations for each analyte, which we used as the levels above which we have a 75% and 95% confidence respectively of not reporting a false positive (Table 4.1, Fig. 4.1), (using a 99% confidence interval was equivalent to using the highest blank observed during the study). The 95% confidence levels ranged from

0.0024 to 0.040 µg/L, still well below the given MDL for EPA methods and below or comparable to detection limits from more recent methods (Kolpin et al. 2002, Glassmeyer et al. 2005). The 75% confidence levels for no false positives were below the median sample concentrations for 21 of 25 analytes. As mentioned in the methods, data were not censored *a priori* below any of these levels prior to statistical analyses, following the recommendations of numerous studies (Gilliom et al. 1984, Porter et al. 1988, Helsel 1990, USGS 1999). The rationale for not censoring data is presented at length in the Discussion section.

Recoveries of internal surrogate standards added to each sample typically ranged from 14% TO 128% for CAF-D9, 63% to 97% for PHE-D10, 63% to 96% for CHR-D12, 50% to 88% for PER-D12 and 45% to 81% for CHO-D6 (or CHO-^{13}C2) (given values are for the 25th and 75th percentile of measured recoveries). Recoveries deviated below (-) or above (+) 100% possibly due to incomplete extraction from the sample water or particle matrix (-), volatilization during evaporation (-), adsorption to glassware (-), incomplete transfers from one vessel to another (-), incomplete dissolution by final solvents (-), inaccurate volumes of final solvents (- or +), unintended evaporation of final extract solvents (+), or contamination from other samples or standards (+). Recoveries, for Phase I data, were typically lower for higher molecular weight compounds, with analysis of variance (ANOVA) confirming that PHEd10 recoveries were significantly higher than all other surrogates, and CHRd12 recoveries were significantly higher than recoveries of PERd12. These observations suggest that evaporative losses of tracers were less important than hydrophobic interactions with stream particles, glassware, etc.

Based on Phase I analyses, internal surrogate standard recoveries appear to adequately track variability due to real differences in sample to sample handling. Relative percent differences (RPD) between sample duplicates almost always decreased by correcting for surrogate recoveries (with the exception of duplicates of samples with low concentrations near the LRL, which on average showed no improvement in precision after surrogate recovery corrections). Correcting for average recoveries were not adequate; despite utmost care in uniform treatment, recoveries varied as much between samples within an extraction batch as between batches (ANOVA showed significant differences for only 2 of 15 batches in Phase I). These results together support the practice of using internal surrogate standard recoveries measured for each sample to correct for sample-specific analytical biases in order to more accurately estimate ambient concentrations in the environment.

Summer Baseflow

Measured concentrations of molecular tracers ranged over 6 orders of magnitude, from below instrument detection to values of around 0.00003 to 10+ µg/L, depending on the compound (Figs. 4.1). Detection frequencies for each compound ranged from 86-98% of the 180 samples collected at 60 sites over the 3-y project (Fig. 4.1). However, generally only 50-80% of measurements for a given compound were above the respective LRLs (with the exceptions of bCOP, aCOP and CHO, which showed 94-98% above LRLs).

Total concentrations of PAHs in summer base flow samples varied by up to three orders of magnitude between sites (Fig 4.2), whereas interannual variability within a site was generally less than one order of magnitude (applicable only to Phase I data). We thus consider means from the two Phases to be comparable. In general, total PAH concentrations were higher at east of

Hudson (EOH) sites relative to west of Hudson (WOH) sites, such that 41 of the 53 EOH sites were in top 50% of most contaminated sites (Fig. 4.1).

Molecular tracers do not necessarily need to be toxic compounds. However, ten of the twelve PAHs analyzed for this project are listed by the EPA as Priority Toxic Pollutants and five of these are known human carcinogens (EPA 2002a, EPA 2002b). These five most toxic PAHs (BAA, CHR, BAP, BBF, BKF) have been given exceptionally low "National Recommended Water Quality Criteria for Human Health" of 0.0038 µg/L for the consumption of the water or 0.018 µg/L for the consumption of organisms living in the water (EPA 2002b). Similarly, NY State Department of Environmental Conservation (NYSDEC) has set water quality guidance values of 0.002 µg/L for these same compounds (BAA, CHR, BAP, BBF, BKF) for ambient waters directly feeding water supplies, 0.0012 µg/L for BAP in waters used for fish consumption, and 0.03 µg/L for BAA as a flag of chronic toxicity to aquatic life (NYSDEC 1998). Although these are non-regulatory guidance values that are not enforceable, and none of the sites are near water supply intakes, these guidance values are useful to place measured PAH concentrations in the context of potential human and ecosystem toxicity. Measured concentrations of one or more of these five compounds exceeded the strictest NYS guidance values limit of 0.002 µg/L in 111 summer baseflow samples out of the total of 365 collected, whereas only 16 out of 365 samples exceeded the least strict EPA guidance limit of 0.018 µg/L. On average across the five PAHs, 26 of 110 sites in the summer and 13 of 49 sampled in the winter had geometric mean concentrations that exceeded the lower guidance limit of 0.002 µg/L. Figs. 4.3 and 4.4 show data for BAA and BAP; concentrations of the other three compounds show similar trends. For example, the average number of compounds to exceed a limit in a sample was 3.2 out of 5 (i.e. if one compound exceeded a limit, so did a majority of the other five).

The ratios of certain PAH compounds to others have been used to identify both petroleum sources, such as spills of kerosene, diesel oil, lubricating oil and crude oil (Yunker et al. 2002, Zakaria et al. 2002), and combustion sources, such as automotive exhaust, smelter emissions, coal burning emissions and wood smoke (Dickhut et al. 2000, Yunker et al. 2002). Two of the most useful of these ratios are that of ANT/(ANT+PHE) and FLR/(FLR+PYR), where low values suggest petroleum sources and high values combustion sources (Fig. 4.5, 4.6). The petroleum/combustion transition point for ANT/(ANT+PHE) is considered to be 0.1. For FLR/(FLR+PYR) the transition is less clear, and values between 0.4 and 0.5 are considered to indicate mixed sources (Yunker *et al.* 2002). Another useful source indicator is the ratio of high molecular weight (HMW) PAH compounds to low molecular weight (LMW) PAH compounds (H/L_{PAH})(Fig. 4.7). In general, LMW volatile PAHs strongly predominate over HMW PAHs in crude oil and most refined petroleum products (with the exception of asphalt) (Zakaria *et al.* 2002), whereas HMW PAHs are the primary constituents of soot (Countway *et al.* 2003). Ratios above approximately 0.5 appear to indicate combustion sources. In general, PAH source indicator ratios were high at studied sites.

Caffeine concentrations spanned almost four orders of magnitude between sites (Fig. 4.8). Fragrance materials showed generally uniform concentrations between sites, with the exception of some sites with notably high concentrations, and interannual variability within a site was minimal (Fig. 4.9).

Total fecal steroid (FS) concentrations in summer baseflow were in a similar range between Phase I and Phase II, (Fig. 4.10). Coprostanol concentrations showed a similar pattern to that of total fecal steroids (Fig. 4.11). The primary exception is that concentrations of bCOP ranged over five orders of magnitude, whereas total fecal steroids only ranged two orders of magnitude. Because bCOP is the dominant FS found for humans and is a relatively minor FS component for most other animals (Leeming *et al.* 1996), concentrations of bCOP in surface waters tend to directly correlate with human sewage inputs (Leeming and Nichols 1996). Thus, linear relationships between bCOP and bacterial indicators of human sewage (fecal streptococci and thermotolerant coliforms), allow for the translation of bCOP concentrations into fecal bacterial counts. Using the relationships in Leeming and Nichols (1996), four EOH sites (139, 143, 138 and 55) exceeded 0.1 µg/L of bCOP corresponding to 35 enterococci (a subset of fecal streptococci) and 300 thermotolerant coliforms per 100 mL of water.

Similar to PAHs, ratios of fecal steroids can help distinguish potential sources (Fig. 4.12). The ratio bCOP/(bCOP+aCOP) has been used to identify sites where fecal material from humans relative to that from livestock and wildlife dominates (Grimalt et al. 1990, O'Leary et al. 1999). O'Leary et al. (1999) suggested that values of this ratio >0.3 were a clear indication of human fecal material in greater relative abundance compared to non-human fecal material and values between 0.2 and 0.3 suggest mixed sources. The ratio bCOP/(bCOP+EPI) has also been used to distinguish human sewage from other fecal sources, with values > 0.5 attributed only to humans (Leeming *et al.* 1998). Last, because cholesterol is widely found in all organisms, bCOP/CHO has also been used to trace human sewage (Mudge and Seguel 1999).

Values of bCOP/(bCOP+aCOP) in particular (Fig. 4.12) show that some sites exhibited substantial interannual variability while others exhibited very stable ratios from year to year. Twenty eight sites have mean bCOP/(bCOP+aCOP) ratios over 0.2. Ratios of bCOP/(bCOP+CHO) mirror these patterns (Fig. 4.13).

Winter Baseflow

The concentrations and ratios of PAHs measured during winter baseflow exhibit similar levels of interannual variability at each site as was seen for summer baseflow (Fig. 4.14-4.15). As observed in Phase I, no general seasonal trend was observed for all sites – the majority of sites show no difference between winter and summer baseflow. There are however, a few notable exceptions in either direction. Sites 2, 20, 58 and 46 tended to have higher total PAH concentrations in winter whereas sites 3, 10 and 117 had higher PAHs during the summer.

Caffeine and fragrance materials also appeared to show no seasonal trend within observed interannual variability (Fig. 4.16), with the notable exceptions of sites 58, 43 and 49 which all had higher summer concentrations of fragrances.

Fecal steroids and their source indicator ratios, on the other hand, did show distinct seasonal trends (Fig. 4.17). In general, the total fecal steroids were less concentrated in winter months, especially WOH (Fig. 4.17). The ratio bCOP/(bCOP+aCOP), an indicator of human fecal material, tended to be higher during the winter than summer, again predominantly at WOH sites (Fig. 4.17).

Stormflow

Concentrations of PAHs increased with increasing discharge during storm events at all three sites where storms were sampled (Fig. 4.18). Also, PAH concentration tended to be higher during the peak in turbidity during each storm, rather than during the maximum discharge. Ratios of Anthracene to Anthracene plus Fluoranthene tended to decrease with increasing storm discharge (Fig. 4.19), whereas the ratio of high to low molecular weight PAHs showed the opposite trend of increasing with increasing storm discharge (Fig. 4.20).

Caffeine and fragrance material concentrations generally increased substantially during high storm flows, but only site 29 showed a consistent relationship between discharge and concentration when the data from all years are pooled (Fig. 4.21 and 4.22).

The sum of fecal steroids increase with increasing storm flow at all sites (Fig. 4.23), but the ratio of coprostanol to coprostanol plus cholestanol, bCOP/(bCOP+aCOP), shows different patterns at each site (Fig. 4.23). At site 6, the West Branch of the Delaware, bCOP/(bCOP+aCOP) tends to increase during a storm, whereas tend to decrease with storm flow at site 55, the Kisco (Fig. 4.23). The Neversink, site 29, generally shows little change in bCOP/(bCOP+aCOP) during storms.

Statistical analyses-RDA

Results from the three Redundancy Analyses (RDA) performed using various subsets of the 110 site data matrix (110 summer sites) and 27 molecular tracer variables (22 compound concentrations and 5 summary concentrations) are reported in Tables 4.3 and Figs. 4.25-4.27. Table 4.2 documents all independent variables available for each model.

Common to all analyses was that most of the constrained variance loaded on factor 1 (F1) with tracer-land use correlations for F1 and F2 $r \geq 0.74$ (Table 4.3). Typically, PAHs and fecal steroids (along with caffeine and fragrances) loaded on the opposite ends of the F2 axis (see Figs. 4.25-4.27). Variables that were positively correlated with molecular tracers loading on the F1 axis typically included land uses that replaced forest cover (i.e. industry, grass), other human impacts (i.e. road density, septic), or surficial geology (soil organic matter, average lake area).

For the RDA of all 110 sites (EOH and WOH), the first two factors of the RDA accounted for 44.3% of the among-site variability in tracer concentrations and 90.1% of the explainable tracer-environment relationship (Table 4.3, Fig. 4.25). Tracer-environment correlations were $r = 0.820$ and 0.773 for factors 1 and 2, respectively. Monte Carlo test of significance of the first and all canonical axes were both significant ($p < 0.001$; 1000 iterations). Environmental factors positively associated with increasing tracer concentrations (positive F1) included SPDE discharge, population density both at the watershed scale, plus average lake area, and % of soil organic matter. Environmental factors associated with low tracer concentrations (negative F1) included %decidous and %coniferous forest (at watershed scale), and % of soil as clay. SPDE discharge was primarily associated with sites with elevated concentrations of fecal steroids and fragrances whereas, population density was better related to higher PAH concentrations. Several environmental variables included in the final ordination best described differences between WOH and EOH sites. For example, WOH streams were generally larger (greater length of

channel network compared to EOH) and were in watersheds with less productive soils (lower OM content compared to EOH sites) and the EOH region has more lakes and reservoirs upstream of our study sites (greater # of lakes upstream and average lake area compared to WOH sites). Finally, the among-site variance in tracer concentrations that was extracted by this suite of environmental variables resulted in WOH sites being distinctly separate from EOH sites in the site ordination. WOH sites had lower tracer concentrations and were characterized by having a greater proportion of their watersheds with forest cover, lower population densities, and fewer WWTPs contributing to river discharge.

For the WOH RDA model (57 sites), the first two factors accounted for 28.8% of the among-site variability in tracer concentrations and 92% of the explainable tracer-environment relationship (Table 4.3, Fig. 4.26). Tracer-environment correlations were r = 0.738 and 0.501 for factors 1 and 2, respectively. Monte Carlo test of significance of the first and all canonical axes were both significant ($p < 0.001$; 1000 iterations). Environmental factors positively associated with increasing tracer concentrations (positive F1) included (in order of loading): % industry, %septic, %grassland, and road density, all at the watershed scale. Environmental factors associated with low tracer concentrations (negative F1) included %farmstead at the reach scale.

For the EOH RDA model (53 sites), the first two factors accounted for 44.1% of the among-site variability in tracer concentrations and 87.5% of the explainable tracer-environment relationship (Table 4.3, Fig. 4.27). Tracer-environment correlations were r = 0.815 and 0.785 for factors 1 and 2, respectively. Monte Carlo test of significance of the first and all canonical axes were both significant ($p < 0.001$; 1000 iterations). Environmental factors positively associated with increasing tracer concentrations (positive F1) included (in order of loading): SPDE discharge (watershed scale), outwash sand and gravel, soil organic matter, road density at both the riparian and reach scales, other urban land use at the reach scale, and watershed area. Environmental factors associated with low tracer concentrations (negative F1) included distance to waste water treatment plant, %deciduous forest at the watershed scale, and soil clay.

Statistical analyses-MLR

Multiple linear regression analyses of tracer concentrations, sums, and ratios were used as an initial step towards tracking sources of individual molecular tracers (Table 4.4). MLR is particularly suited to the task of examining how several independently varying landscape properties are together related to 1 dependent variable such as the concentration of a tracer. Stepwise MLR systematically determines which subset of independent variables combine linearly to best explain variability of the chosen dependent variable, taking into account covariance within the independent set (Neter et al. 1996). However, in datasets exhibiting substantial covariance between independent variables, it is typical that 2 MLR models using different sets of variables might yield very similar results. For example, if A and B are strongly correlated they most likely will not both be significant variables in a single MLR model for predicting Y, but an MLR model using variables A, C, and D might predict Y almost equally well to a MLR using B, C, and D, and the standardized slopes and significance of A and B in their respective models will likely be similar. However, if A and B are moderately correlated, they might both be included in the model, but with reduced significance and potentially very different slopes relative to the inclusion of A or B alone. These were the issues we faced with this dataset. Therefore although the "best" models in Table 4.4 were selected using the variance

inflation factor criteria to minimize unstable slopes, the best MLR models in Table 4.4 were not the only significant models showing interesting trends. Only selected models were shown in Table 4.4 as examples.

For WOH sites, generally 30-50% of the variance in PAH concentrations could be predicted from 2 or 4 landscape properties (Table 4.4). Variables related to human development – such as industrial (INDU), commercial (COMM) and other urban (OURB) land uses – exhibited positive partial correlations to PAHs. Landscape properties related to natural vegetation – such as mixed forest (MFOR) and farmstead (FMST) – were inverse predictors of PAH concentrations. These land use groupings (such as INDU, COMM, and OURB, or forest variables) showed high internal covariance (Fig. 8 in Dow et al. 2006), and thus these variables were largely interchangeable within these MLR models. Agricultural vegetation, such as crops (CROP), grassland (GRAS) and orchard (ORCH), showed positive partial correlations with PAHs in these MLR models, and simple bivariate correlations between these variables and PAHs also showed positive correlations (data not shown).

WOH PAH ratios generally showed weaker relationships to landscape variables (R^2 = 0.10 to 0.21, Table 4.4), largely due to the reduction of the dataset from censoring data prior to calculating ratios. ANT/(ANT+PHE), an indicator of combustion soot over petroleum sources (Dickhut et al. 2000, Yunker et al. 2002, Zakaria et al. 2002), was positively correlated to local industry.

At WOH sites the fragrance HHCB was positively related to SPDE (R^2 = 0.25), whereas CAF showed a weak positive relationship with watershed-scale grasslands (R^2 = 0.16) (Table 4.4). Conversely, total fecal steroids (FS), bCOP and aCOP could be more strongly explained (R^2 = 0.47 to 0.54) by watershed-scale agricultural land uses FMST and GRAS and by COMM. As with PAH ratios, reductions in data due to censoring only allowed a few fecal steroid ratios to be adequately tested. However, bCOP/(bCOP+EPI) showed a strong relationship (R^2 = 0.52) to shrub lands (+) and residential (+) land uses.

At EOH sites, 7-31% of the variability in PAH concentrations could be predicted from geographic variables (Table 4.4). Population density (PDNS) was the most important predictor. Caffeine, fragrances, and fecal steroids at EOH sites were strongly related to point source discharge (SPDE, mostly sewage treatment plants). However, 3 sites (43, 49, 58) with exceptionally high sewage discharge had substantial potential to skew regressions. Therefore, MLR analyses were rerun for EOH excluding these sites (Table 4.4). Despite these changes, 36-45% of variability in CAF, HHCB, bCOP and FS was explained by land use, with SPDE a significant predictor to every model.

Discussion

Need for more sensitive analytical methods

A comparison of recommended ambient water criteria for priority organic pollutants (NYSDEC 1998, USEPA 2002b, a) versus method detection limits using the most common analytical methods (USEPA 1998) indicated that typical laboratories can not detect these compounds at concentrations that were orders of magnitude higher than levels of concern.

Furthermore, ambient water criteria have been continually revised downward, despite the fact that EPA's Guidelines for Deriving Numerical Criteria for the Protection of Aquatic Life (USEPA 1985) have not been officially revised since 1985 (although a draft revision is in review http://www.epa.gov/waterscience/criteria/alcg_sab_draft.pdf). Clearly, monitoring programs need to employ much more sensitive analytical methods to obtain useful data on organic pollutants, in order to: (1) assess whether current criteria are being met; (2) provide data relevant to potential future decreases in water quality criteria; (3) assess whether concentrations below criteria levels are increasing over time; (4) interpret patterns of pollutant concentrations to identify potential sources before water quality criteria are exceeded (more below).

Although USGS laboratories and monitoring programs have taken strong steps to increase analytical sensitivity for organic contaminants (Kolpin et al. 2002, Phillips and Bode 2002, Glassmeyer et al. 2005), most federal and state monitoring programs still use methods with grossly inadequate sensitivity for monitoring contamination of ambient and drinking water. Evidence for this comes from Proficiency Testing (PT) programs in use by the 13 states participating in the National Environmental Laboratory Accreditation Conference (NELAC). All laboratories providing monitoring data in these states must regularly analyze a blind PT sample and provide the correct concentrations of all compounds for which they are certified. The concentration ranges in the blind test samples for non-potable water accreditation (http://www.epa.gov/nelac/pttables/npw_fopt_final111004.pdf) have minimum values of 0.5-20 µg/L for pesticides, 7-25 µg/L for volalite aromatics and halocarbons, 10-200 µg/L for semi-volatile base/neutrals (which include PAHs), and 30-200 µg/L for acid organics (phenols) – values which all closely match the method detection limits published in EPA method 8270 (USEPA 1998). In mid-2007, the NYS Environmental Laboratory Accreditation Program (ELAP) began offering low-level PAH PT samples and accreditation, but the 0.1-8 µg/L concentration range is still orders of magnitude higher than ambient water guidance values. Thus, most commercial laboratories have little incentive to enhance the sensitivity of their measurements to levels that are necessary for meaningful monitoring of environmental contaminants. At the same time, most monitoring projects maintain a purely regulatory mindset, where they only analyze regulated pollutants and require that laboratories adhere to published EPA methods. This mindset, at its worst, may even discourage more sensitive analyses because they would increase the detection frequency of pollutants and "alarm the public". Fueling this mindset is the practice of focusing on detection frequency as the primary result of a monitoring study (e.g. Kolpin et al. 2002), rather than distributions of quantified concentrations relative to water quality criteria or other reference levels (Fig 4.3-4.4).

Results from our method (Table 4.1, Fig. 4.1) demonstrate that relatively modest modifications to EPA method 8270D – that use equipment that all analytical chemistry laboratories possess – can improve sensitivity by 4-5 orders of magnitude. Although for this study we only quantified 25 compounds (with only 10 listed as priority pollutants), our modified method should provide similar increases in sensitivity to all 245 analytes listed in EPA method 8270D. These improvements were generally sufficient to quantify compounds below any current recommended water quality criteria (USEPA 2004) and also below any probable future criteria. We believe that all monitoring programs should demand similar sensitivity levels from all contracted laboratories. Because the required modifications to EPA method 8270D were minor (and often listed as options in the method itself) and because NELAC certification is largely

based on performance with blind test samples, laboratories have substantial freedom make the necessary modifications and still conform to EPA analytical guidelines. Our laboratory was a case in point; we have maintained NELAC certification for PAHs through the NY State Environmental Laboratory Approval Program (ELAP, http://www.wadsworth.org/labcert/elap/elap.html).

The Delaware River Basin Commission's (DRBC) work with polychlorinated biphenyls (PCB) provides an example of a local monitoring agency working with commercial laboratories to reduce detection levels to those appropriate to monitor Total Maximum Daily Load (TMDL) concentrations. Existing human health water quality criteria for different zones of the Delaware estuary range from 7.9 to 64 picograms per liter (pg/L) total PCBs, and the proposed Stage II TMDL for the entire estuary is a uniform 16 pg/L total PCBs (0.000016 µg/L) for all zones (DRBC resolution No. 2005-19). The most common EPA methods for PCBs (methods 608 and 8082) listed method detection limits in water ranging from 0.054 to 0.90 µg/L for individual PCBs. Even the more recent EPA method 1668, which utilizes high resolution GC/MS instrumentation that is unavailable to many commercial laboratories, has listed MDLs of 4-455 pg/L for individual PCBs. Given these analytical inadequacies, the DRBC worked with several local laboratories to slightly modify EPA 1668 to yield quantitation levels around 5 pg/L for each of 209 PCBs (http://www.state.nj.us/drbc/PCB_info.htm). These minor modifications were to increase to 2 L sample volumes, decrease to 20 µL extract volumes, and add lower calibration standards to give a 5 level curve down to 0.5 ng/mL. As with our modified method 8270, analytical blanks were a big issue with this modified method 1668, but quantifying blanks by a more sensitive method was the first step to reducing blanks. Monitoring agencies could substantially maximize the value of data obtained with limited monitoring funds by following the DRBC example of demanding improvements in analytical sensitivity and thereby avoid empty datasets of "non-detects".

Minimizing data censorship

Although it is relatively common for laboratories to censor concentration data if they fall below reporting levels set relative their measured MDLs or blanks, there are a number of reasons for minimizing or even eliminating this practice in water quality studies. These reasons have been substantiated at length in the literature. Gilliom et al. (1984) demonstrated that censoring data at any level tends to eliminate valuable information, and that even when low-level data were substantially degraded by random noise, trends were more effectively detected in the uncensored data. Porter et al. (1988) and Helsel (1990) independently echo these findings in their explorations of statistical treatments of "non-detects" in water quality data and describe these "less than" values as a serious interpretation problem for data analysts.

As a result of these and many other studies, the USGS National Water Quality Laboratory has adopted the convention of not censoring any data from "information-rich" methods such as GC-MS, but rather simply flagging data as "estimated" if they are below the quantified 99% confidence limits for no false positives or the 99% confidence limits for no false negatives (USGS 1999). This reporting convention allows the data analyst to choose the approach best suited for the given analysis. For instance, for statistical analyses concentration data should be left completely uncensored, because analysis of the full data distribution, even if it contains large errors at low concentrations, is always preferable over the alternative of assuming a data

distribution for the censored data (Helsel 1990). On the other hand, evaluation of data at a specific site relative to water quality criteria for the purposes of regulatory action clearly requires consideration of reporting levels based on confidence limits. In this case, censorship is appropriate. Censorship of derived variables, such as concentration ratios, may be appropriate prior to statistical analyses, because the reliability of the ratio is independent from its magnitude and the purpose of a ratio is primarily to distinguish sources where concentrations are high. For these examples, the convention of reporting all data requires that every reported concentration is linked to an associated confidence level for no false positives and no false negatives. The commonly used MDL approach quantifies neither of these limits (USGS 1999).

The situation with our dataset, where false positives (contamination) can occur to levels substantially greater than reliable quantitation levels (the LRL), is not described elsewhere to our knowledge. However, for all trace-level water quality analyses, the frequencies of analyte detections in blanks will increase as analytical sensitivities are improved. Regardless, the general approach to reporting 99% (or 95%) confidence limits for no false positives or no false negatives provides a means for honestly evaluating data quality while maximizing data information.

Temporal variability – Phase I assessment

Baseflow stream water concentrations of tracers showed relatively substantial temporal variability, generally ranging about 1 order of magnitude for individual compounds at each site over the 3-6 years of study. Although spatial variability dominated over temporal variability (Fig. 6 in, Aufdenkampe et al. 2006), the latter needs to be considered by monitoring programs that infrequently revisit sites, not only because site rankings are subject to temporal variability, but also because a once-every-5-year sampling program, for example, will be unable to discern all but the grossest temporal trends.

The observed temporal variability in our dataset does not appear to be entirely random. Within and between PCA analyses of Phase I data (Aufdenkampe et al. 2006) showed that sample year explained 12.4% and 14.2% of our data matrix variance for WOH (29 sites) and EOH (27) datasets respectively. As a whole, concentrations of molecular tracers could be partially explained by hydrology. Most tracers (log transformed) showed a negative correlation to basin-area-normalized discharge (log transformed) (data not shown), with correlation coefficients ranging from -0.11 for caffeine ($p = 0.05$) to -0.28 for total PAHs ($p < 0.001$) to -0.38 for cholesterol ($p < 0.001$). Similarly, most tracers (with the exception of caffeine) showed a positive correlation to concentrations of total suspended solids (TSS), with correlation coefficients ranging from 0.16 for total PAHs ($p = 0.005$) to 0.34 for the sum of seven fecal steroids ($p < 0.001$). When combined using multiple linear regression (MLR), discharge and TSS together explain 5% to 21% of the variability in tracer concentrations.

In general, tracer concentrations were greater at most sites in 2002 compared to 2000 or 2001 (Fig. 6 in, Aufdenkampe et al. 2006), corresponding to generally lower total annual flow in 2002 that was below historic means (1964-1999) (Arscott et al. 2006). However, to frame the temporal variability in our dataset as "inter-annual" variability ignores short term variability in hydrologic and atmospheric conditions. For example, although 2000 appeared to be the wettest of the 3 sample years in general and below historic means (Fig 4A in Arscott et al. 2006), site

specific discharge (normalized by watershed area) on the day that tracer samples were collected at all East and West Branch of the Delaware (EBD & WBD) sites were by far highest in 2002 (Fig 6A in Arscott et al. 2006).

A closer look at patterns in temporal variability reveals that tracer concentrations might respond differently to hydrological variations in different watersheds. In the EOH region, Phase I tracer concentrations were highest during the lower baseflow discharge in 2002 (Aufdenkampe et al. 2006). At these sites, point-source discharges – which generally have relatively stable discharge rates – were more important and may have been less diluted during low stream flow conditions. On the other hand, in the WOH region, elevated tracer concentrations in 2002 were related to increased precipitation and stream baseflow discharge, which may have increased run-off from agricultural lands and sub-surface flushing of septic systems, which in turn increased loading to streams of fecal steroids, fragrances, and caffeine. It is likely that temporal variability also depends on a variety of other natural and anthropogenic factors, such as the spatial configuration of different land covers and land uses, with different effects on each tracer compound. Although these hypotheses remain untested, our continued effort at many of these sites should allow more rigorous examination of inter-annual variability in the future.

Sources of contamination to streams

To improve water quality or to mitigate future degradation, it is evident that watershed managers would value knowing the contributions of each potential contamination source to their specific catchment. There are 2 ways to categorize sources – by land use or by input process. Relating contaminant concentrations or loads as a function of land use/cover can aid in planning by enabling the watershed manager to consider land use-specific impacts on water quality. However, a land use is not itself a source, but rather a proxy for processes that mobilize contaminants into the aquatic system. For instance, the concentrations of a particular PAH may be positively related to residential land use in a watershed, yet it is the sum of characteristics of residential land use – such as automobile exhaust, runoff from paved areas, leaking fuel tanks, or improper disposal of petroleum products – that ultimately is the source of the PAH measured in the stream. Molecular tracers offer the potential to fingerprint these input processes, through the use of ratios, factor analysis or other statistical techniques. Understanding the relative importance of these input processes is necessary for managing water quality in existing land uses. Thus the geographic and mechanistic perspectives complement one another, and our dataset can evaluate sources from both perspectives.

Geographically, the most dominant pattern was that the concentrations of all tracer compounds generally varied concurrently (F1 axes in Figs. 4.25-4.27) – where 1 tracer or a group of tracers was high, the others also tended to be high. This result was not necessarily expected because of the very different input mechanisms of PAHs versus caffeine, fragrances and fecal steroids. However, there was minor separation between PAHs and the tracers of wastewater contamination (F2 axes in Figs. 4.25-4.27, Table 4.4). Also, there was no one master landscape variable that consistently explained inter-site differences in both RDA and MLR analyses, except that sites with a higher percentage of their catchment in forest (MFOR, CONF, DECD or MCON) generally had lower concentrations of all tracers.

Patterns of tracer concentrations as a function of land use were distinctly different between EOH and WOH sites (Figs. 4.25-4.27). EOH sites tended to have higher proportion of PAH's relative to fecal steroids, caffeine, and fragrances, and the most pristine sites were all located WOH. Within the WOH region, sites with elevated concentrations of molecular tracers were associated with nearby rural community infrastructure (i.e., commercial or other urban categories), riparian railroad infrastructure, and farmstead and row crop components of agricultural land uses. These sites were also typically on larger streams (lower WBD) where larger communities were located. In the EOH region, sites with high concentrations of molecular tracers were either associated with point source discharges or urban infrastructure, whereas sites with lower concentrations of molecular tracers were either more forested or had more agriculture in their catchments. However, agriculture in general was a very small component of any sub-catchment in the EOH region.

PAHs were generally related to riparian urban land uses (COMM, INDU, OURB, PDNS, SPDE) (Figs. 4.25-4.27, Table 4.4). Three groups of mechanistic source pathways can be distinguished based on PAH ratios. These are: 1) petroleum products – such as kerosene, diesel oil, lubricating oil and crude oil – which are characterized by lower ratios of less stable to more stable isomers (i.e., ANT/(ANT+PHE) or FLR/(FLR+PYR)) and by generally lower ratios of high to low molecular weight PAHs (Yunker et al. 2002, Zakaria et al. 2002); 2) combustion byproducts – such as automotive exhaust, smelter emissions, coal burning emissions and wood smoke – which are characterized by higher ratios of less stable to more stable isomers and by generally higher H/L_{PAH} ratios (Dickhut et al. 2000, Yunker et al. 2002); and 3) asphalt, which is characterized by low ratios of less stable to more stable isomers (similar to petroleum products) and by higher H/L_{PAH} ratios (similar to combustion byproducts) (Yunker et al. 2002). In our study, high ratios of ANT/(ANT+PHE), FLR/(FLR+PYR) and H/L_{PAH} all suggested that combustion emissions generally appeared to dominate over petroleum spills as the primary source of PAHs to most stream sites (Figs. 4.5-4.7). High H/L_{PAH} ratios alone would be inconclusive evidence for pyrogenic sources, because high molecular weight PAHs are relatively abundant in asphalt (Yunker et al. 2002), because diesel soot has relatively low H/L_{PAH} ratios (Miguel et al. 1998), and because high and low molecular weight PAHs have different fate and transport characteristics in the environment due to different volatility and particle affinity. However, these are not issues with the other two ratios (for ANT vs. PHE and FLR vs. PYR the molecular weight is identical and volatililty and particle affinity are very similar). Furthermore, because all 3 ratios suggest pyrogenic sources, and because mean site PAH concentrations were related to urban landuses, we have reasonable confidence in our conclusion.

Although combustion soot has the potential to travel long distances (i.e., from mid-western coal burning), our relatively strong relationships with riparian urban land use suggested that local sources may dominate. Relatively high methlyphenathrene (1MP+2MP) to phenanthrene ratios (generally > 0.5, data not shown) support this conclusion, as low ratios (< 0.2) have been associated with aging of soot aerosols (Nielsen 1996, Simó et al. 1997, Stein et al. 2006). Last, the observation that EOH sites tended to exhibit slightly higher PAH ratios than WOH sites (Figs. 4.5-4.7) despite further transport distance from mid-western coal burning, was further evidence for the importance of local sources of combustion derived PAHs.

Variability in fecal steroid concentrations showed the strongest relationships to point-source discharge (SPDE) at 3 EOH sites (43, 49 and 58)(Figs. 4.25-4.27, Tables 4.4). The remaining EOH sites showed relationships between most fecal steroids and industrial and other urban land use and also to point source discharges (Table 4.4, not all data shown). However aCOP and EPI, two steroids that are relatively abundant in birds and wildlife (Leeming et al. 1996) were most related to wetland and coniferous forest landcovers respectively (Table 4.4, not all data shown). WOH fecal steroid concentrations were positively associated with residential and agricultural land uses and negatively related to forest cover (Table 4.4). These data suggest a wide mixture of point and non-point sources of fecal contamination to streams.

Previous studies have used steroid ratios to distinguish whether fecal sources were primarily human. Ratios of coprostanol – a steroid that predominates in human feces but is relatively less abundant in feces of other animals (Leeming et al. 1996) – to other steroids such as bCOP/(bCOP+aCOP) or bCOP/(bCOP+EPI) responded strongly to known inputs of human sewage (i.e. sites 43, 49 and 58, Fig. 4.12 and Table 4.4). However, the previous suggested delimitation of bCOP/(bCOP+aCOP) = 0.2 to distinguish between human fecal sources (>0.2) and other animals (<0.2) may only apply to catchments with limited livestock (Grimalt et al. 1990, O'Leary et al. 1999). In the northeastern USA, raw livestock feces appear to have relative bCOP concentrations nearly as high as waste water treatment plant effluent and septic leachate (Standley et al. 2000, and Chapter 5). A more robust fecal steroid index of human contamination for North America will require multivariate analyses of the full suite of fecal steroid compounds (Chapter 5), similar to that performed by Leeming et al. (Leeming et al. 1996, Leeming et al. 1998) for Australia. With simple ratios alone, it is impossible to determine whether human or livestock inputs were most responsible for the high fecal steroid levels at the high agriculture WOH sites in the WBD and EBD basins (Fig. 4.12-4.13).

Fragrance materials, HHCB and AHTN, and caffeine were more related to land use, and specifically to point source and urban/commercial land use, than any of the other tracers. They are introduced to streams and rivers from relatively unambiguous sources. Fragrance materials are anthropogenic compounds introduced to the environment primarily in domestic greywater sewage (Simonich et al. 2000). Because of the low biodegradability of these polycyclic compounds, they are transported relatively conservatively though sewage treatment (Simonich et al. 2002, Artola-Garicano et al. 2003, Phillips et al. 2005). The primary source of caffeine to streams and rivers in temperate climates is the urine of humans (and sometimes domestic animals) (Buerge et al. 2003). Although removed more effectively than HHCB and AHTN by waste water treatment processes (Phillips et al. 2005), caffeine still displays relatively low rates of biodegradation in the environment, is non-volatile and has low particle affinity, all resulting in relatively efficient transport through waterways (Buerge et al. 2003, Glassmeyer et al. 2005). As a result of these properties, concentrations of fragrance materials and caffeine appear to be robust indicators of sewage, septic and greywater sources, with the distinction that caffeine primarily indicates poorly treated sources including septic systems. These distinctions are supported by our MLR analyses of geographic sources.

Analysis of different distance scales between upstream land use and tracer concentrations, using variance partitioning, showed that the best predictor scale depended on the specific landscape variable (Table 4.4, Figs. 4.25-4.27). Kratzer et al. (2006) illustrated that catchment-

and riparian-scale variables explained most of the variance in macroinvertebrates collected from these exact same sites. Results from analyses herein suggest that accounting for local-scale factors in addition to catchment and riparian scale was important for predicting molecular tracer concentrations. Arscott et al. (2006) and Dow et al. (2006) demonstrated that catchment- and riparian-scale variables were closely related and probably did not describe any different phenomenon aside from absolute values in each category. Since RDA standardizes all variables, the analysis primarily highlights differences in variance structure. Therefore, attributing any meaningful differences between catchment and riparian in these analyses may not be appropriate.

Literature Cited

Arscott, D. B., C. L. Dow, and B. W. Sweeney. 2006. The landscape template of New York City's drinking-water-supply watersheds. Journal of the North American Benthological Society **25**:867-886.

Artola-Garicano, E., I. Borkent, J. L. M. Hermens, and W. H. J. Vaes. 2003. Removal of two polycyclic musks in sewage treatment plants: freely dissolved and total concentrations. Environmental Science and Technology **37**:3111 -3116.

Aufdenkampe, A. K., D. B. Arscott, C. L. Dow, and L. J. Standley. 2006. Molecular tracers of soot and sewage contamination in streams supplying New York City drinking water. Journal of the North American Benthological Society **25**:928–953.

Blaine, J. G., B. W. Sweeney, and D. B. Arscott. 2006. Enhanced source water monitoring for New York City: historical framework, political context, and project design. Journal of the North American Benthological Society **25**:851-866.

Buerge, I. J., T. Poiger, M. D. Müller, and H.-R. Buser. 2003. Caffeine, an anthropogenic marker for wastewater contamination of surface waters. Environmental Science and Technology **37**:691 -700.

Countway, R. E., R. M. Dickhut, and E. A. Canuel. 2003. Polycyclic aromatic hydrocarbon (PAH) distributions and associations with organic matter in surface waters of the York River, VA Estuary. Organic Geochemistry **34**:209-224.

Dickhut, R. M., E. A. Canuel, K. E. Gustafson, K. Liu, K. M. Arzayus, S. E. Walker, G. Edgecombe, M. O. Gaylor, and E. H. MacDonald. 2000. Automotive sources of carcinogenic polycyclic aromatic hydrocarbons associated with particulate matter in the Chesapeake Bay Region. Environmental Science and Technology **34**:4635 -4640.

Dow, C. L., D. B. Arscott, and J. D. Newbold. 2006. Relating major ions and nutrients to watershed conditions across a mixed-use, water-supply watershed. Journal of the North American Benthological Society **25**:887-911.

Dow, C. L., and A. K. Aufdenkampe. 2006. Using SAS to improve the quantification of environmental chemistry samples. *in* Proceedings of the Northeast SAS Users Group Conference, Philadelphia, PA, September 20-22, 2006. (Available at http://www.nesug.org/html/Proceedings/nesug06.pdf).

Eglington, G. 1969. Organic chemistry: the organic chemist's approach. Pages 20-71 *in* G. Eglington and M. T. J. Murphy, editors. Organic Geochemsitry. Springer-Verlag, New York.

Gilliom, R. J., R. M. Hirsch, and E. J. Gilroy. 1984. Effect of censoring trace-level water-quality data on trend-detection capability. Environmental Science and Technology **18**:530-535.

Glassmeyer, S. T., E. T. Furlong, D. W. Kolpin, J. D. Cahill, S. D. Zaugg , S. L. Werner, and M. T. Meyer. 2005. Transport of chemical and microbial compounds from known wastewater discharges: potential for use as indicators of human fecal contamination. Environmental Science and Technology **39**:5157-5169.

Grimalt, J. O., P. Fernandez, J. M. Bayona, and J. Albaiges. 1990. Assessment of fecal sterols and ketones as indicators of urban sewage inputs to coastal waters. Environmental Science and Technology **24**:357 - 363.

Hedges, J. I., and F. G. Prahl. 1993. Early diagenisis: Consequences for applications of molecular biomarkers. Pages 237-253 *in* M. H. Engel and S. A. Macko, editors. Organic Geochemistry. Plenum Press, New York.

Helsel, D. R. 1990. Less than obvious. Environmental Science and Technology **24**:1767-1774.

Kolpin, D. W., E. T. Furlong, M. T. Meyer, E. M. Thurman, S. D. Zaugg, L. B. Barber, and H. T. Buxton. 2002. Pharmaceuticals, hormones, and other organic wastewater contaminants in U.S. streams, 1999-2000: A National Reconnaissance. Environmental Science and Technology **36**:1202 -1211.

Kratzer, E. B., J. K. Jackson, D. B. Arscott, A. K. Aufdenkampe, C. L. Dow, L. A. Kaplan, J. D. Newbold, and B. W. Sweeney. 2006. Macroinvertebrate distribution in relation to land use and water chemistry in New York City drinking-water-supply watersheds. Journal of the North American Benthological Society **25**:954-976.

Leeming, R., A. Ball, N. Ashbolt, and P. Nichols. 1996. Using faecal sterols from humans and animals to distinguish faecal pollution in receiving waters. Water Research **30**:2893-2900.

Leeming, R., and P. Nichols. 1996. Concentrations of coprostanol that correspond to existing bacterial indicator guideline limits. Water Research **30**:2997-3006.

Leeming, R., P. D. Nichols, and N. J. Ashbolt. 1998. Distinguishing sources of faecal pollution in Australian inland and coastal waters using sterol biomarkers and microbial faecal indicators. Research Report No 204., Water Services Association of Australia.

Miguel, A. H., T. W. Kirchstetter, R. A. Harley, and S. V. Hering. 1998. On-road emissions of particulate polycyclic aromatic hydrocarbons and black carbon from gasoline and diesel vehicles. Environmental Science and Technology **32**:450-455.

Mudge, S. M., and C. G. Seguel. 1999. Organic contamination of San Vicente Bay, Chile. Marine Pollution Bulletin **38**:1011-1021.

Neter, J., M. H. Kutner, C. J. Nachtsheim, and W. Wasserman. 1996. Applied linear regression models, 3rd edition. IRWIN / McGraw-Hill Professional Publishing, Chicago.

Nielsen, T. 1996. Traffic contribution of polycyclic aromatic hydrocarbons in the center of a large city. Atmospheric Environment **30**:3481-3490.

NYSDEC. 1998. Division of Water Technical and Operational Guidance Series (1.1.1) - Ambient water quality standards and guidance values and groundwater effluent limitations. NY State Department of Environmental Conservation, NY.

O'Leary, T., R. Leeming, P. D. Nichols, and J. K. Volkman. 1999. Assessment of the sources, transport and fate of sewage-derived organic matter in Port Phillip Bay, Australia, using the signature lipid coprostanol. Marine and Freshwater Research **50**:547-556.

Phillips, P. J., and R. W. Bode. 2002. Concentrations of pesticides and pesticide degradates in the Croton River watershed in southeastern New York, July-September 2000. WRIR 02-4063, USGS, Denver, CO.

Phillips, P. J., B. Stinson, S. D. Zaugg, E. T. Fulong, D. W. Kolpin, K. M. Esposito, B. Bodniewicz, R. Pape, and J. Anderson. 2005. A multi-disciplinary approach to the removal of emerging contaminants in municipal wastewater treatment plants in New York State, 2003-2004. Pages 5095-5124 *in* Water Environment Federation WEFTEC 78th Annual Technical Exhibition and Conference, Washington DC.

Porter, P. S., R. C. Ward, and H. F. Bell. 1988. The detection limit. Environmental Science and Technology **22**:856-861.

Simó, R., J. O. Grimalt, and J. Albaigés. 1997. Loss of Unburned-Fuel Hydrocarbons from Combustion Aerosols during Atmospheric Transport. Environmental Science and Technology **31**:2697-2700.

Simonich, S. L., W. M. Begley, G. Debaere, and W. S. Eckhoff. 2000. Trace Analysis of Fragrance Materials in Wastewater and Treated Wastewater. Environmental Science and Technology **34**:959 -965.

Simonich, S. L., T. W. Federle, W. S. Eckhoff, A. Rottiers, S. Webb, D. Sabaliunas, and W. de Wolf. 2002. Removal of Fragrance Materials during U.S. and European Wastewater Treatment. Environmental Science and Technology **36**:2839 -2847.

Standley, L. J., L. A. Kaplan, and D. Smith. 2000. Molecular tracers of organic matter sources to surface water resources. Environmental Science and Technology **34**:3124-3130.

Stein, E. D., L. L. Tiefenthaler, and K. Schiff. 2006. Watershed-based sources of polycyclic aromatic hydrocarbons in urban storm water. Environmental Toxicology and Chemistry **24**:373-385.

Taylor, J. R. 1997. An Introduction to Error Analysis: The Study of Uncertainties in Physical Measurements, Second Edition edition. University Science Books, Saulsalito, CA.

USEPA. 1985. Guidelines for deriving numerical criteria for the protection of aquatic life.

USEPA. 1998. Method 8270d: Semivolatile organic compounds by gas chromatography/mass spectrometry (GC/MS). EPA Method 8270D, US EPA.

USEPA. 2002a. 2002 Edition of the Drinking Water Standards and Health Advisories. EPA 822-R-02-038, US EPA Office of Water, Office of Science and Technology.

USEPA. 2002b. National Recommended Water Quality Criteria: 2002. EPA-822-R-02-047, US EPA Office of Water, Office of Science and Technology.

USEPA. 2004. Current National Recommended Water Quality Criteria. *in*.

USGS. 1999. New Reporting Procedures Based on Long-Term Method Detection Levels and Some Considerations for Interpretations of Water-Quality Data Provided by the U.S. Geological Survey National Water Quality Laboratory. Open-File Report 99–193, U.S. Geological Survey, Reston, Virginia.

Vogel, J. R., L. B. Barber, E. T. Furlong, T. B. Coplen, I. M. Verstraeten, and M. T. Meyer. 2005. Occurrence of selected pharmaceutical and non-pharmaceutical compounds, and stable hydrogen and oxygen isotope ratios in a riverbank filtration study, Platte River, Nebraska, 2002 to 2005, Volume 2. Data Series 141, USGS.

Yunker, M. B., R. W. Macdonald, R. Vingarzan, R. H. Mitchell, D. Goyette, and S. Sylvestre. 2002. PAHs in the Fraser River basin: a critical appraisal of PAH ratios as indicators of PAH source and composition. Organic Geochemistry **33**:489-515.

Zakaria, M. P., H. Takada, S. Tsutsumi, K. Ohno, J. Yamada, E. Kouno, and H. Kumata. 2002. Distribution of Polycyclic Aromatic Hydrocarbons (PAHs) in Rivers and Estuaries in Malaysia: A Widespread Input of Petrogenic PAHs. Environmental Science and Technology **36**:1907 -1918.

Table 4.1: Compounds chosen as molecular tracers of contamination, abbreviations used in text and figures, their Laboratory Reporting Levels (LRL), which are equivalent to 99% confidence levels for no false negatives, and their 75% and 95% confidence levels for no false positives, which is derived from distributions of measured blanks. Ambient water quality criteria are listed for reference.

Analyte	Abbreviation	Laboratory Reporting Level (µg/L)	75% Confidence No False Positives (µg/L)	95% Confidence No False Positives (µg/L)	NY ambient water quality guidance values (ug/L)[a]				EPA: Human health for consumption of (ug/L)[b]	
					H(WS)[c]	H(FC)[c]	A(C)[c]	A(A)[c]	Water + Organism	Organism Only
PAH										
fluorene	FLU	0.00059	0.0007	0.0035	50		1	5	1100	5300
phenanthrene	PHE	0.00054	0.0024	0.0135	50		5	45		
anthracene	ANT	0.00066	0.0008	0.0038	50		3.8	35	8300	40000
2-methyl phenanthrene	2MP	0.0012	0.0011	0.0105						
1-methyl phenanthrene	1MP	0.00074	0.0007	0.0055						
fluoranthene	FLR	0.00036	0.0015	0.0044	50				130	140
pyrene	PYR	0.00033	0.00081	0.0078	50		5	42	830	4000
benz(a)anthracene	BAA	0.00035	0.00062	0.0025	0.002		0.03	0.23	0.0038	0.018
chrysene	CHR	0.00018	0.00053	0.0042	0.002				0.0038	0.018
benzo(b)fluoranthene	BBF	0.00031	0.00058	0.012	0.002				0.0038	0.018
benzo(k)fluoranthene	BKF	0.00065	0.00049	0.0108	0.002				0.0038	0.018
benzo(a)pyrene	BAP	0.00031	0.00048	0.0091	0.002	0.0012			0.0038	0.018
Fragrances & Caffeine										
tonalide	HHCB	0.0068	0.0040	0.013						
galaxolide	AHTN	0.0032	0.0058	0.016						
caffeine	CAF	0.0039	0.0023	0.011						
Steroids										
coprostanol (5β-cholestan-3β-ol)	bCOP	0.00059	0.0013	0.016	0.3[d]	0.3[d]	0.3[d]	0.3[d]		
epi-coprostanol (5β -cholestan-3α-ol)	EPI	0.0026	0.0016	0.017						
cholesterol (cholest-5-en-3β-ol)	CHO	0.013	0.024	0.038						
cholestanol (5α-cholestan-3β-ol)	aCOP	0.0015	0.0022	0.040						
cholestanone (5α-cholestan-3-one)	aONE	0.0021	0.0014	0.015						
coprostanone (5β-cholestan-3-one)	bONE	0.0052	0.0025	0.028						
24-ethyl-coprostanol (24-ethyl-5β-cholestan-3β-ol)	eCOP	N/A	0.	0.						
24-ethyl-*epi* coprostanol (24-ethyl-5β-cholestan-3α-ol)	eEPI	N/A	0.	0.00054						
24-ethyl-cholesterol (24-ethyl-cholest-5-en-3β-ol)	eCHO	0.0923	0.1899	0.447						
ethyl-cholestanol (24-ethyl-5α-cholestan-3β-ol)	SNOL	0.0050	0.0080	0.023						

a - NYSDEC. 1998. Division of Water Technical and Operational Guidance Series (1.1.1) - Ambient water quality standards and guidance values and groundwater effluent limitations. NY State Department of Environmental Conservation, NY.

b - USEPA. 2002. National recommended water quality criteria: 2002. EPA-822-R-02-047, United States Environmental Protection Agency, Washington, DC.

c - H(WS) = source of drinking water (water supply); H(FC) = human consumption of fish; A(C) = fish propagation - aquatic life (chronic); A(A) = fish survival - aquatic life (acute).

d - Based on a limit of 200 fecal coliforms per 100 mL and the upper 95% confidence limit for the relationship between fecal coliforms and coprostanol as given by Leeming and Nichols (1996)

Table 4.2. Land use and other catchment characteristic variables (n = 99) used to explain molecular tracer concentrations in EOH and WOH stream sites using Redundancy Analysis (see Figs. 4.25-4.26). Landuse/landscape variables were quantified at 3 scales: within the entire watershed (W), riparian (b), and reach (1k). Other variables included those related to density, point source, surficial geology, and soils. For further discussion of land use categories and scale quantification see Chapter 2 and Arscott et al. (2006).

Scaled watershed characteristic variables	Abbreviation	Scale
Landuse/cover variables		
% residential	RESD	W, b, 1k
% commercial	COMM	W, b, 1k
% industrial	INDU	W, b, 1k
% other urban	OURB	W, b, 1k
% commercial & industrial	CMIN	W, b, 1k
% cropland (and pasture)	CROP	W, b, 1k
% orchard	ORCH	W, b, 1k
% farmstead	FMST	W, b, 1k
% farmstead & cropland	FMCR	W, b, 1k
% grassland	GRAS	W, b, 1k
% shrubland	SHRB	W, b, 1k
% mixed brush-grassland	MBRH	W, b, 1k
% grassland & mixed brush-grassland	GMBR	W, b, 1k
% deciduous forest	DECD	W, b, 1k
% conifer forest	CONF	W, b, 1k
% mixed forest	MFOR	W, b, 1k
% conifer & mixed forest	MCON	W, b, 1k
% wetland	WETL	W, b, 1k
% water	WATR	W
Density variables		
Popn density (people/km^2)	PDNS	W, b, 1k
Road density (m/km^2)	RDNS	W, b, 1k
Total # of septic systems	NOSE [1]	W, b, 1k
Septic system density	SEPT	W, b, 1k
Railroad density (m/km^2)	RAIL	W, b, 1k

Non-scaled watershed characteristic variables	Abbreviation
Point-source variables	
Point-source discharge	SPDE [2]
Total # of SPDEs	SPDTO
Distance to WWTP (m)	SPDDT
Water-body variables	
# of Lakes upstream	LNOS
Sum of Lake Area (ha)	LAREA
Average Lake Area (ha)	LxAREA
Largest Lake (ha)	LLARG
Upstrm Dist. to 1st Resv/Lake (m)	LUPD
Area of 1st Upstrm Resv/ Lake (ha)	LUPS
Lake Density (ha/km2)	LDNS
Upstream Channel Length (km)	SUPL
Channel length (km) per / km2	SDNS
Soil variables	
Soil %Clay	SClay
Soil %OM	Som
Soil pH	SpH
Soil Kfactor	SKf
Surficial Geology	
Alluvial fan	AlluvF
Bedrock	BEDR
Kame deposits	KameD
Kame moraine	KameM
Lacustrine sand	LacS
Lacustrine silt and clay	LacSC
Outwash sand and gravel	OUTW
Recent alluvium	RAlluv
Swamp deposits	SwampD
Till	Till
Till moraine	TillM
Other	
Watershed area (km^2)	WTSD
Study site elevation (m)	ELEV

[1] WOH sites only.
[2] mean annual watershed-area-normalized State Pollution Discharge Elimination System effluent volume (cm^3/cm^2).

Table 4.3. Results from Redundancy Analyses (RDA) using subsets of the 110 site (summer) database for 27 molecular tracer variables. Both the 1st and all canonical axes were significant at $p<0.001$ (Monte Carlo Permutations = 1000). See Table 4.2 for abbreviations and variables included in all models, and Figs. 4.25-4.27 for loading and site scores.

	E & WOH	WOH	EOH
No. of sites	110	57	53
Canonical eigenvalues (total variance explained)			
All Axes	0.474	0.309	0.478
F1	0.383	0.264	0.339
F2	0.060	0.024	0.101
Tracer-land use correlations			
F1	0.820	0.738	0.815
F2	0.773	0.501	0.785
# of variables	12	5	10
# of catchment	5	4	3
# of riparian			1
# of local	2	1	2
# of no-scale	1		1
# of geology	4		3

Table 4.4: Selected multiple linear regression (MLR) results of mean analyte concentration as a function of watershed landscape variables at each of the 3 watershed scales. The 'best' MLR (highest adjusted R^2, no multi-collinearity) is in bold and marked with an asterisk. See text for definition of a unique model (UNQ = 'Y') and for definitions of tracer ratio abbreviations. See Table 2 for land-use/cover abbreviations. Scale abbreviations: W = whole upstream catchment; b = whole upstream riparian buffer (30-m); 1k = 1-km upstream riparian buffer (30-m).

		Scale-model Adj. R^2							
Tracer Compound	n	W		b		1k		UNQ	Significant Predictors, 'Best' Model (Partial R^2, slope direction)
WOH									
FLU	57	**0.14**	*	**0.14**		0.10		N	PDNS(0.16,+)
PHE	57	0.21		**0.40**	*	0.26		Y	MFOR(0.19,-) RDNS(0.13,-) INDU(0.12,+)
FLR	57	0.31		**0.43**	*	0.39		N	COMM(0.31,+) INDU(0.06,+) OURB(0.05,-) MFOR(0.05,-)
PYR	57	0.32		**0.42**	*	0.35		Y	INDU(0.19,+) MFOR(0.16,-) SPDE(0.10,+)
BAA	57	0.33		0.42		**0.51**	*	Y	OURB(0.20,+) SPDE(0.15,+) FMST(0.06,-) CROP(0.06,+)
CHR	57	0.28		**0.31**	*	0.21		N	INDU(0.13,+) CROP(0.12,+) ORCH(0.06,+) WETL(0.05,-)
BAP	57	0.38		0.45		**0.50**	*	Y	CROP(0.19,+) COMM(0.15,+) FMST(0.13,-) GRAS(0.06,+)
ANT/(ANT+PHE)	29	0.13		0.15		**0.21**	*	Y	INDU(0.24,+)
$(HMW/LMW)_{PAH}$									
CAF	57	**0.16**	*	0.14		0.10		N	GRAS(0.17,+)
HHCB	57	**0.25**	*	**0.25**	*	**0.25**	*	Y	SPDE(0.26,+)
Total Fecal Steroids	57	0.40		**0.54**	*	0.45		Y	COMM(0.44,+) CROP(0.12,+)
bCOP	57	**0.47**	*	0.45		0.37		N	FMST(0.37,+) WETL(0.09,+) SHRB(0.04,+)
aCOP	57	0.39		**0.49**	*	0.48		N	COMM(0.34,+) MFOR(0.16,-)
bCOP/(bCOP+aCOP)	56	0.13		**0.16**	*	0.15		N	SHRB(0.10,+) RDNS(0.09,-)
bCOP/(bCOP+EPI)	48	**0.52**	*	0.41		0.15		Y	SHRB(0.42,+) RESD(0.12,+)
EOH									
FLU	53	**0.31**		**0.31**	*	0.25		Y	PDNS(0.23,+) GRAS(0.06,+) WETL(0.06,+)
PHE	53	0.12		**0.19**	*	0.09		N	PDNS(0.15,+) RESD(0.07,-)
FLR	53	0.24		**0.25**	*	.		N	PDNS(0.26,+)
PYR	53	**0.22**		**0.22**	*	0.07		N	PDNS(0.24,+)
BAA	53	0.18		**0.21**	*	0.06		N	PDNS(0.16,+) CONF(0.07,+)
CHR	53	0.22		**0.23**	*	.		N	PDNS(0.24,+)
BAP	53	**0.07**		**0.07**	*	**0.07**		N	PDNS(0.09,+)
FLR/(FLR+PYR)	50	**0.24**	*	0.12		0.12		Y	SPDE(0.14,+) INDU(0.13,-)
$(HMW/LMW)_{PAH}$	53	0.06		**0.08**	*	.		N	SHRB(0.10,-)
CAF	53	0.38		0.36		**0.51**	*	Y	SPDE(0.33,+) ORCH(0.08,-) COMM(0.08,+) CONF(0.06,+)
HHCB	53	**0.49**	*	**0.49**		0.43		N	SPDE(0.44,+) RESD(0.07,+)
Total Fecal Steroids	53	0.36		0.35		**0.40**	*	N	SPDE(0.27,+) CONF(0.11,+) SHRB(0.05,+)
bCOP	53	0.50		**0.51**	*	0.44		N	SPDE(0.35,+) WETL(0.07,+) CONF(0.07,+) CROP(0.06,+)
aCOP	53	0.30		0.22		**0.38**	*	N	SPDE(0.23,+) SHRB(0.08,+) CONF(0.06,+) WETL(0.05,+)
bCOP/(bCOP+aCOP)	53	0.23		**0.29**	*	0.23		N	SPDE(0.25,+) OURB(0.07,-)
bCOP/(bCOP+EPI)	48	0.16		0.10		**0.19**	*	Y	SPDE(0.12,+) CONF(0.11,+)
EOH [minus sites 43, 49, 58]									
CAF	50	0.32		0.23		**0.37**	*	Y	SPDE(0.19,+) ORCH(0.10,-) CONF(0.07,+) COMM(0.06,+)
HHCB	50	**0.45**	*	0.39		0.29		N	COMM(0.35,+) CONF(0.08,+) SPDE(0.05,+)
Total Fecal Steroids	50	0.30		0.19		**0.42**	*	Y	CONF(0.14,+) SPDE(0.14,+) SHRB(0.10,+) CROP(0.08,-)
bCOP	50	0.33		**0.36**	*	**0.36**		N	WETL(0.21,+) SPDE(0.10,+) CONF(0.09,+)
aCOP	50	0.22		0.21		**0.34**	*	Y	CROP(0.12,-) CONF(0.10,+) SPDE(0.08,+) SHRB(0.08,+)
bCOP/(bCOP+aCOP)	50	**0.10**	*	.		.		Y	FMST(0.12,+)
bCOP/(bCOP+EPI)	45	0.07		**0.08**		**0.08**	*	Y	CONF(0.11,+)

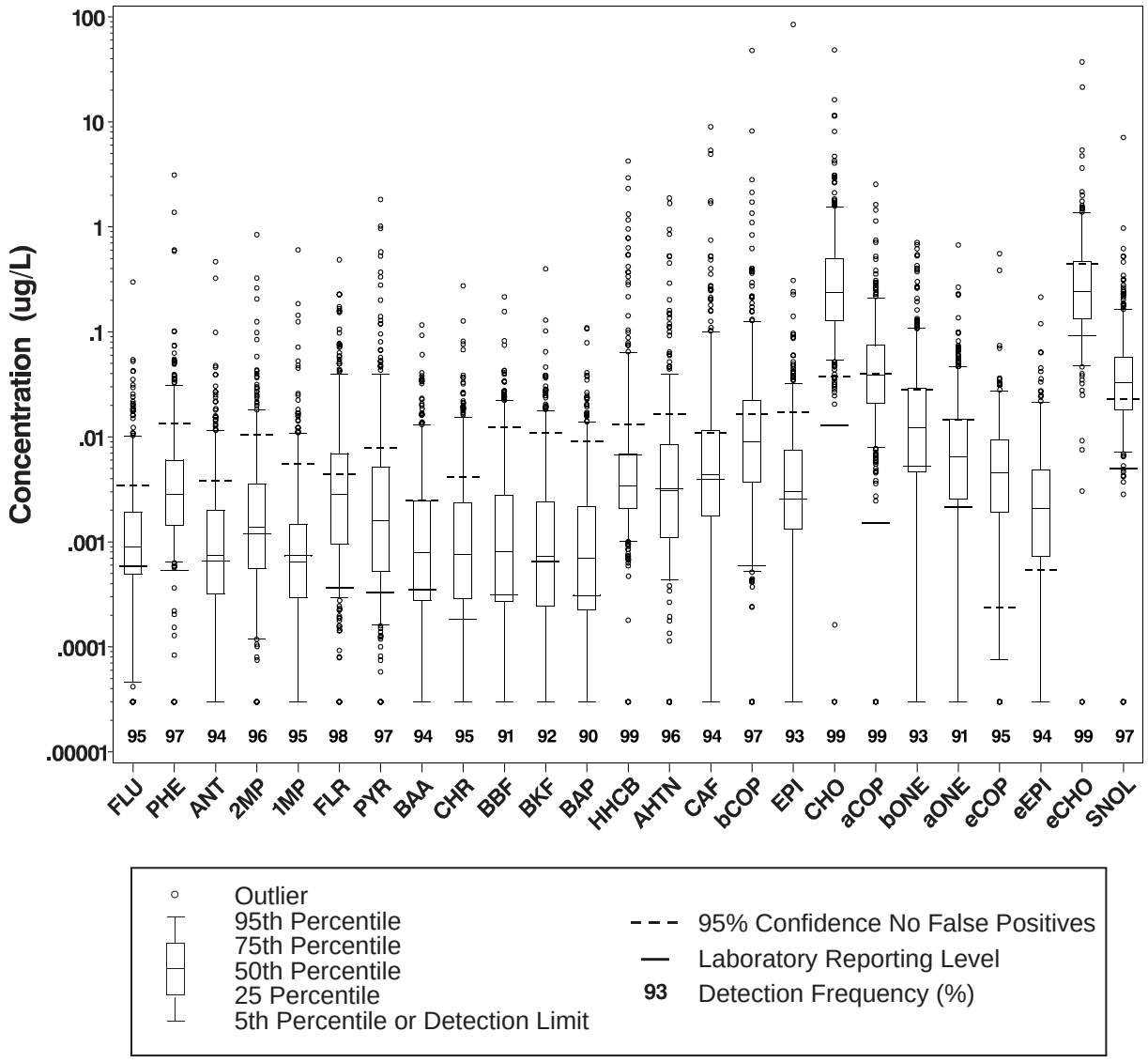

Figure 4.1: Distribution of measured baseflow concentrations for each of 25 tracer compounds for 2000-2005 (n = 527, 269 for eCHO, eCOP, and eEPI), relative to measured Laboratory Reporting Levels (LRL), which are equivalent to the 99% confidence level for no false negatives, and the 95% confidence level for no false positives (see methods). Detection frequency values, as a percentage of total samples, are given in bold. 0.00003 was added to all values in order to plot all on a log scale. LRL values for eCOP and eEPI can not be measured, because no laboratory standards exist for these compounds.

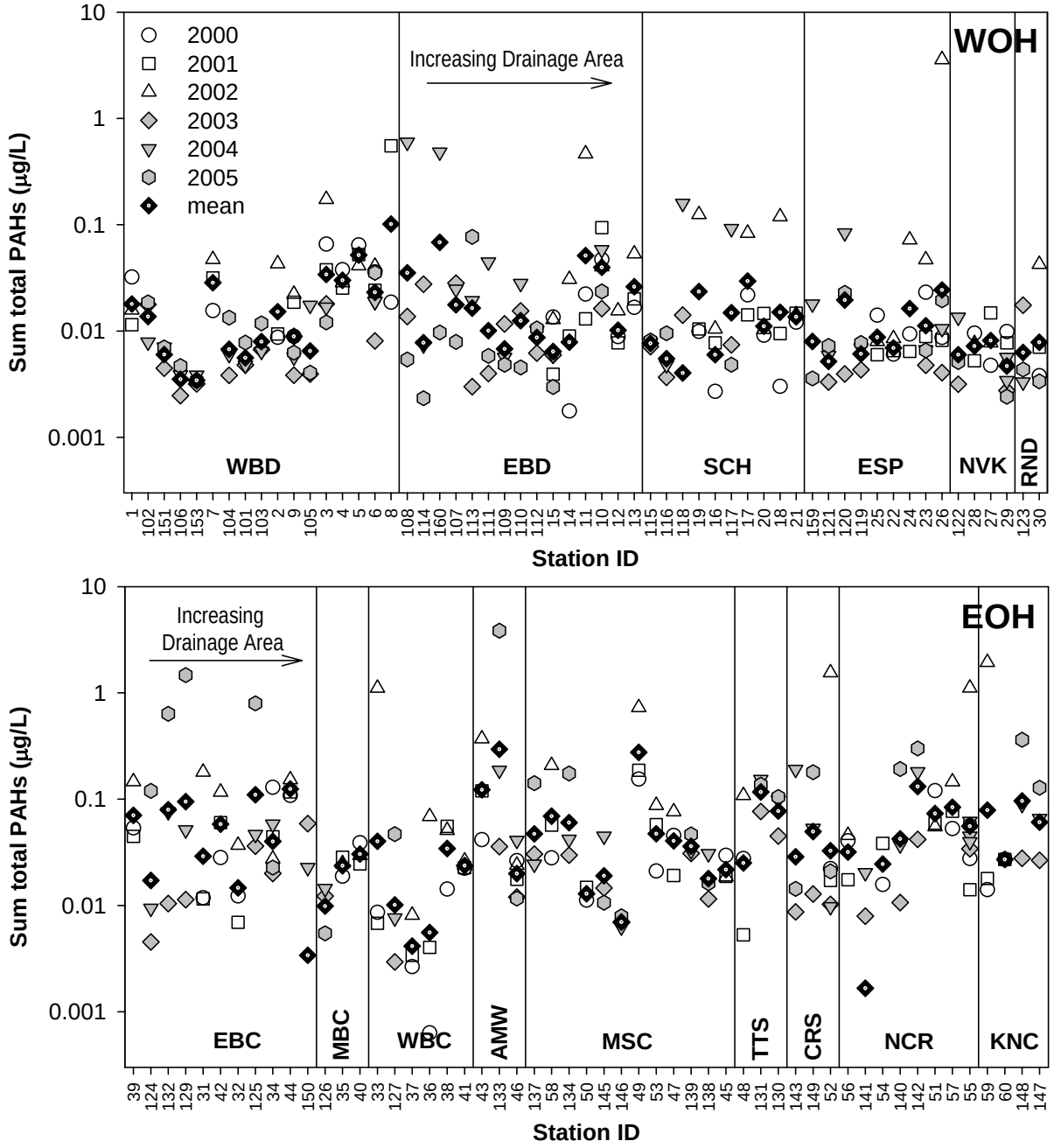

Figure 4.2: Summer baseflow stream water concentrations of the sum of all measured PAH compounds (1MP, 2MP, ANT, BAA, BAP, BBF, BKF, CHR, FLR, FLU, PHE, PYR) for all Phase I and Phase II sites both (A) West of Hudson and (B) East of Hudson. Geomentric means of all measured values at each site are given by solid black diamonds. Sites are arranged by subwatershed in order of increasing basin area. Subwatershed designations are as follows: WBD = W. Br. Delaware R.; EBD = E. Br. Delaware R., SCH = Schoharie Cr., ESP = Esopus Cr., NVK = Neversink R., RND = Rondout Cr., EBC = E. Br. Croton R., MBC = Middle Br. Croton R., WBC = W. Br. Croton R., AMW = Amawalk Reservoir, MSC – Muscoot R., TTS = Titicus R., CRS = Cross R., NCR = New Croton Reservoir. KNC = Kensico Reservoir.

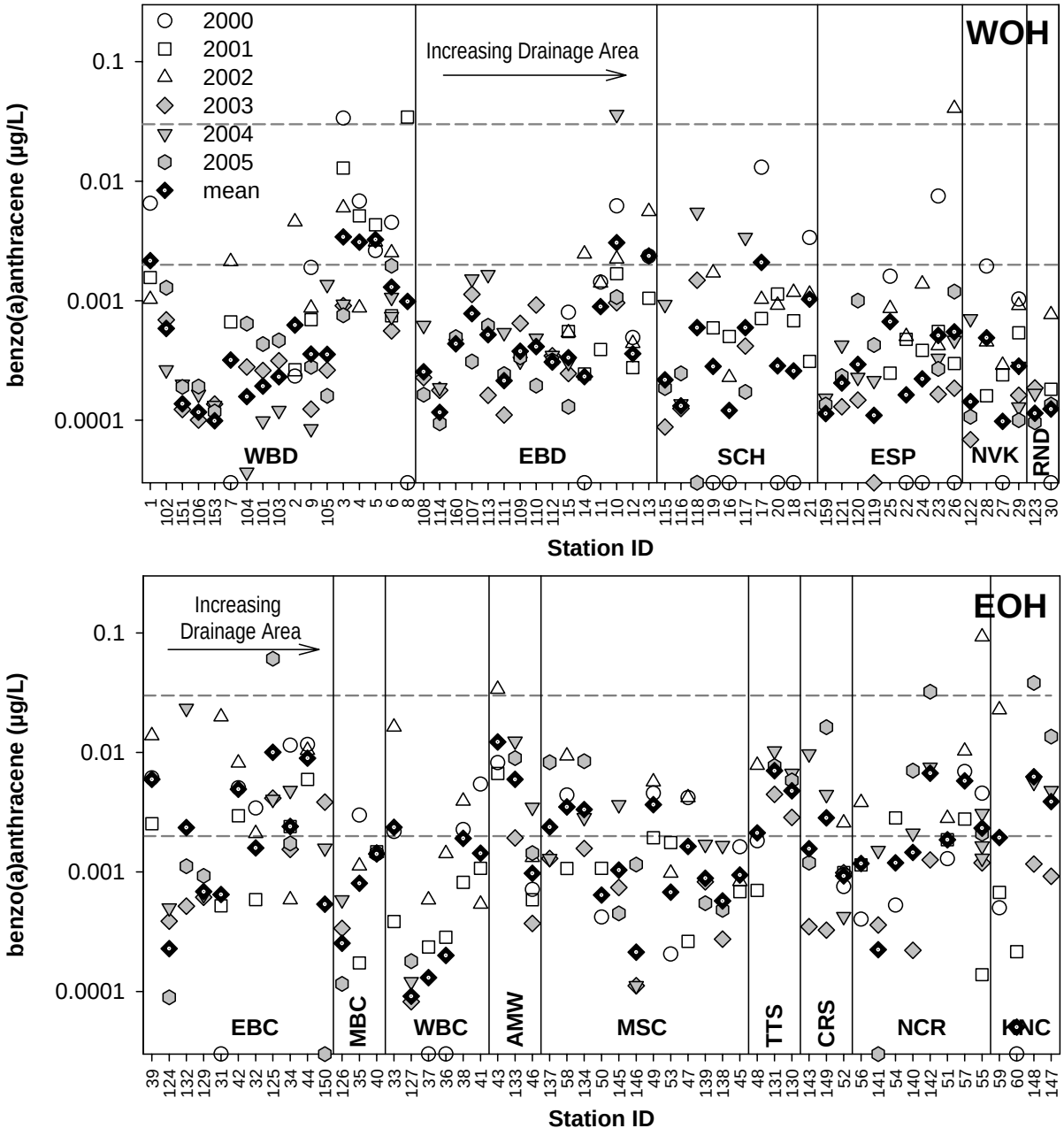

Figure 4.3: Summer baseflow stream water concentrations of benzo(a)anthracene for all Phase I and Phase II sites sites both (A) West of Hudson and (B) East of Hudson. Geomentric means of all measured values at each site are given by solid black diamonds. Short-dashed lines show NY State ambient water quality guidance values for human health risks associated with water supply (lower line, H(WS) in Table 4.1) and for aquatic life chronic toxicity (upper line, A(C) in Table 4.1) (NYSDEC 1998). Sites are arranged in order of increasing basin area by subwatershed, as designated in Chapter 2 and in Fig. 4.2.

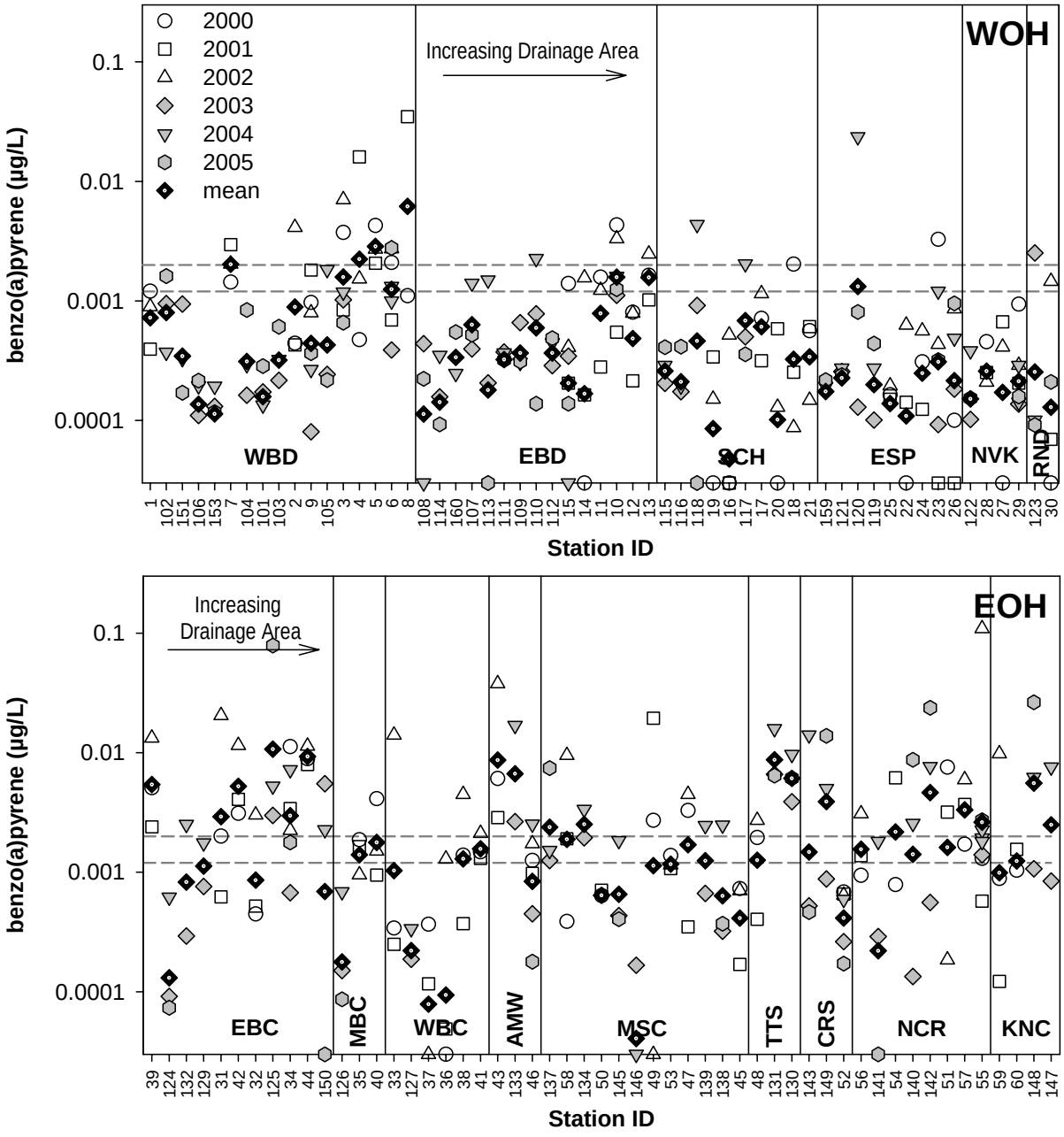

Figure 4.4: Summer baseflow stream water concentrations of benzo(a)pyrene for all Phase I and Phase II sites sites both (A) West of Hudson and (B) East of Hudson. Geomentric means of all measured values at each site are given by solid black diamonds. Short-dashed lines show NY State ambient water quality guidance values for human health risks associated with fish consumption (lower line, H(WS) in Table 4.1) and for human health risks associated with water supply (upper line, A(C) in Table 4.1) (NYSDEC 1998). Sites are arranged in order of increasing basin area by subwatershed, as designated in Chapter 2 and in Fig. 4.2.

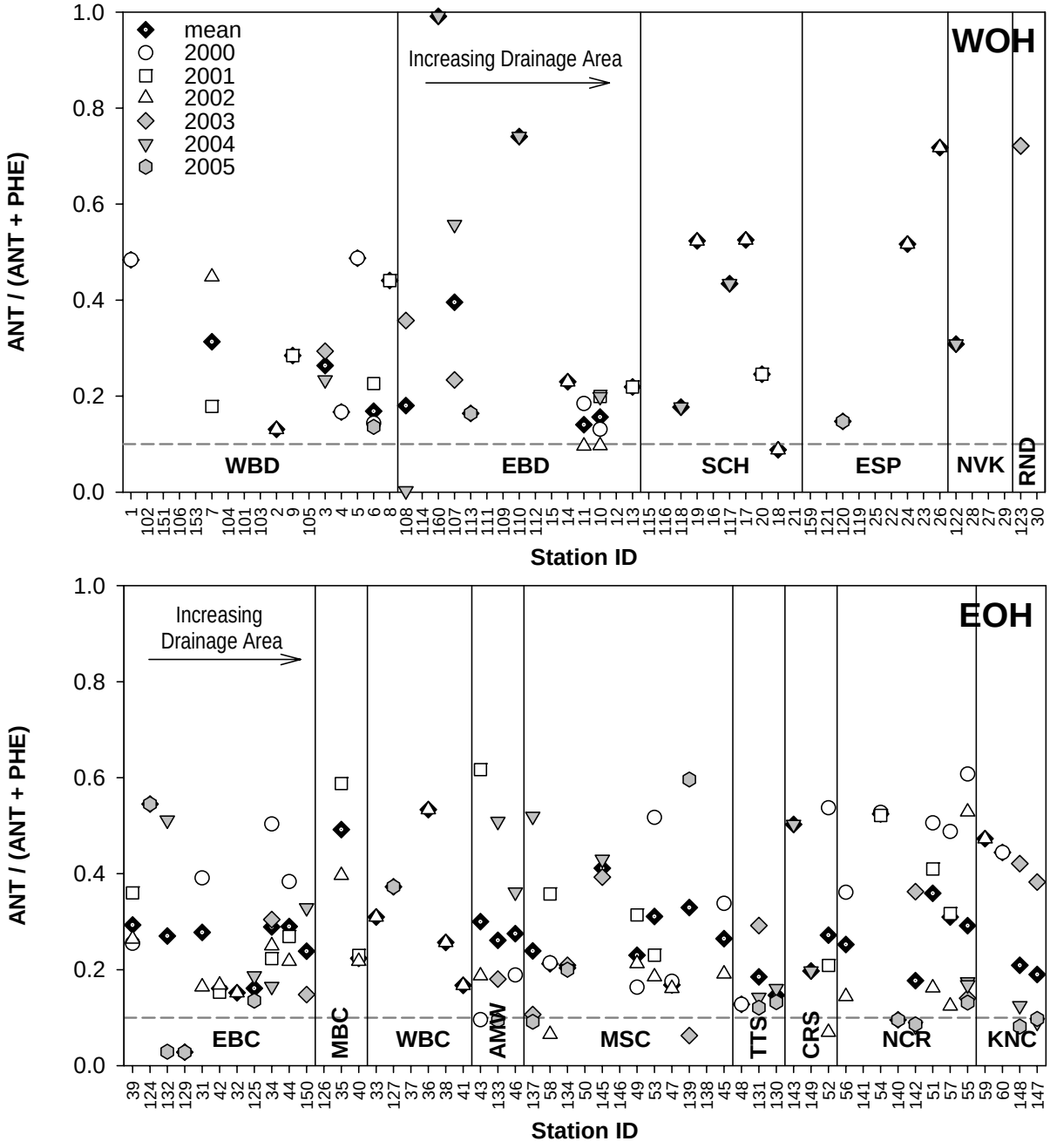

Figure 4.5: Summer baseflow ratios of anthracene/(anthracene+phenanthrene), a PAH source indicator, for all Phase I and Phase II sites both (A) West of Hudson and (B) East of Hudson. Arithmetic means of all measured values at each site are given by solid black diamonds. Short-dahsed lines show a suggested delimitation between combustion sources (ANT/(ANT+PHE) > 0.1) and petroleum sources (ANT/(ANT+PHE) < 0.1) (Yunker et al. 2002).

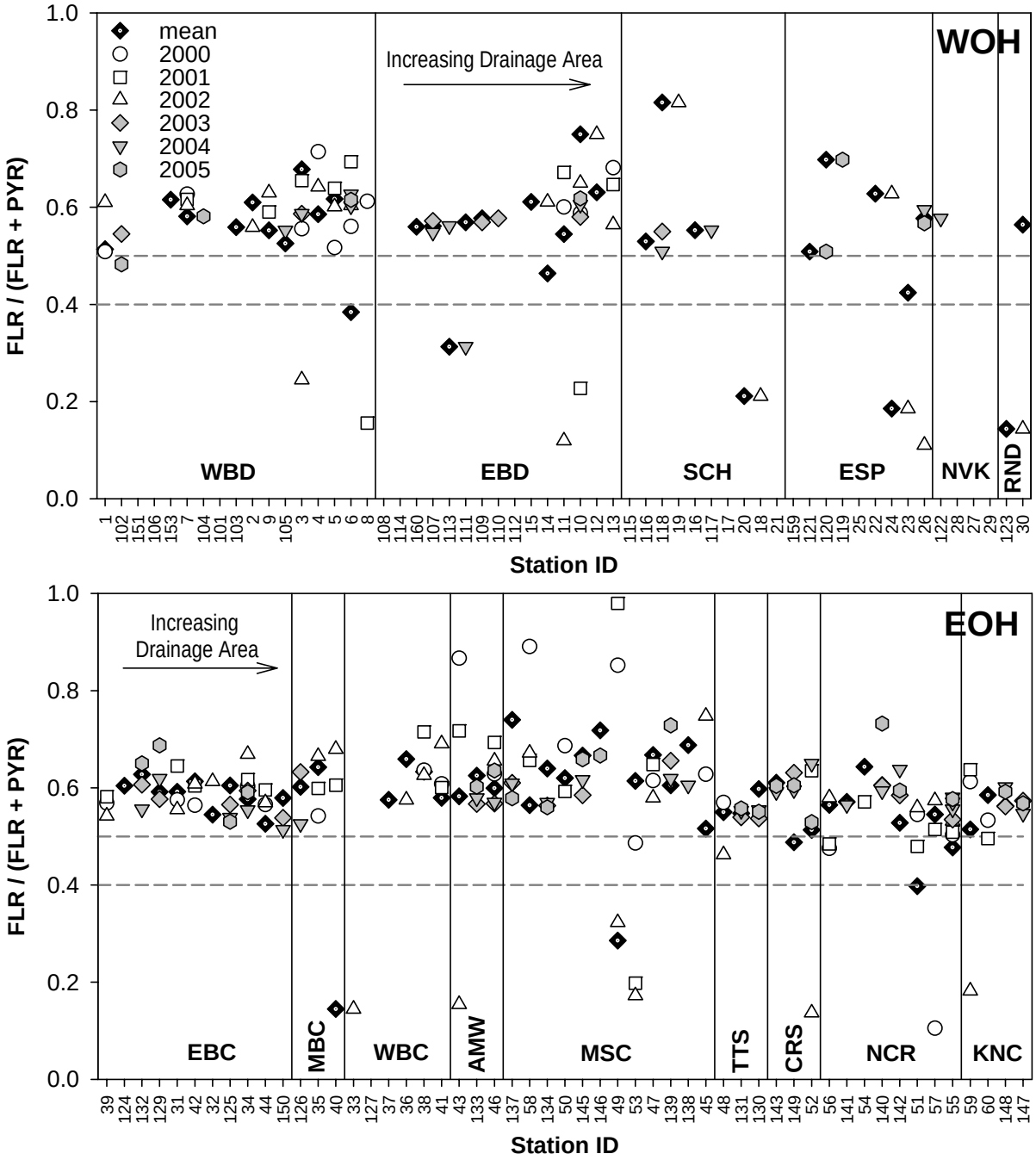

Figure 4.6: Summer baseflow ratios of fluoranthene/(fluoranthene+pyrene), a PAH source indicator, for all Phase I and Phase II sites both (A) West of Hudson and (B) East of Hudson. Arithmetic means of all measured values at each site are given by solid black diamonds. Short-dashed lines show a suggested delimitation between combustion sources (FLR/(FLR+PYR) > 0.5) and petroleum sources (FLR/(FLR+PYR) < 0.4) (Yunker et al. 2002).

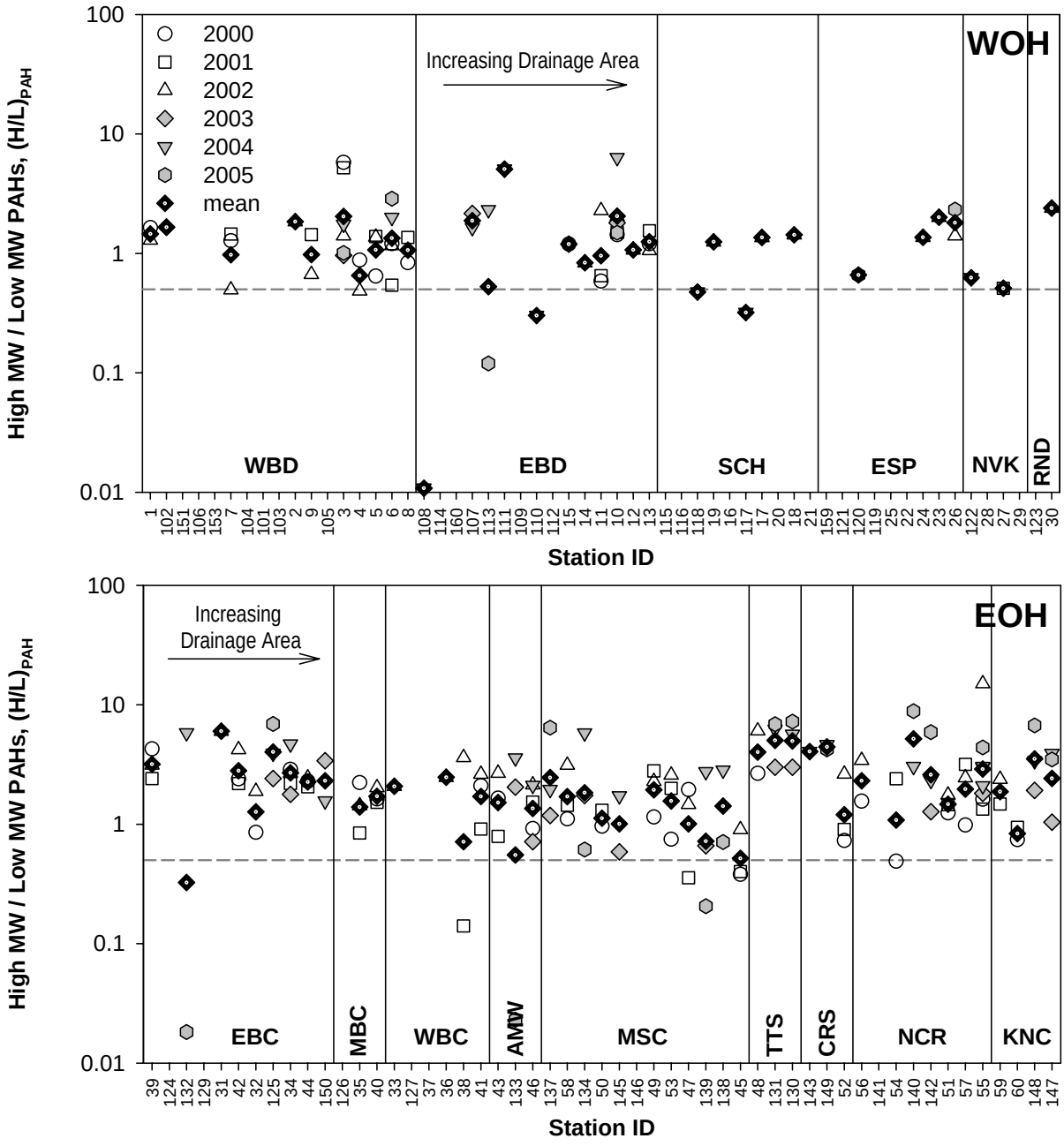

Figure 4.7: Summer baseflow ratios of high versus low molecular weight PAHs, a PAH source indicator, for all Phase I and Phase II sites both (A) West of Hudson and (B) East of Hudson. H/L_{PAH} is defined as sum(FLR, PYR, BAA, CHR, BBF, BKF, BAP) / sum(FLU, PHE, ANT, 2MP, 1MP)). Geomentric means of all measured values at each site are given by solid black diamonds. The short-dashed line shows a suggested delimitation between combustion or asphalt sources ($(H/L)_{PAH} > 0.5$) versus petroleum sources ($(H/L)_{PAH} < 0.5$) (Zakaria et al. 2002).

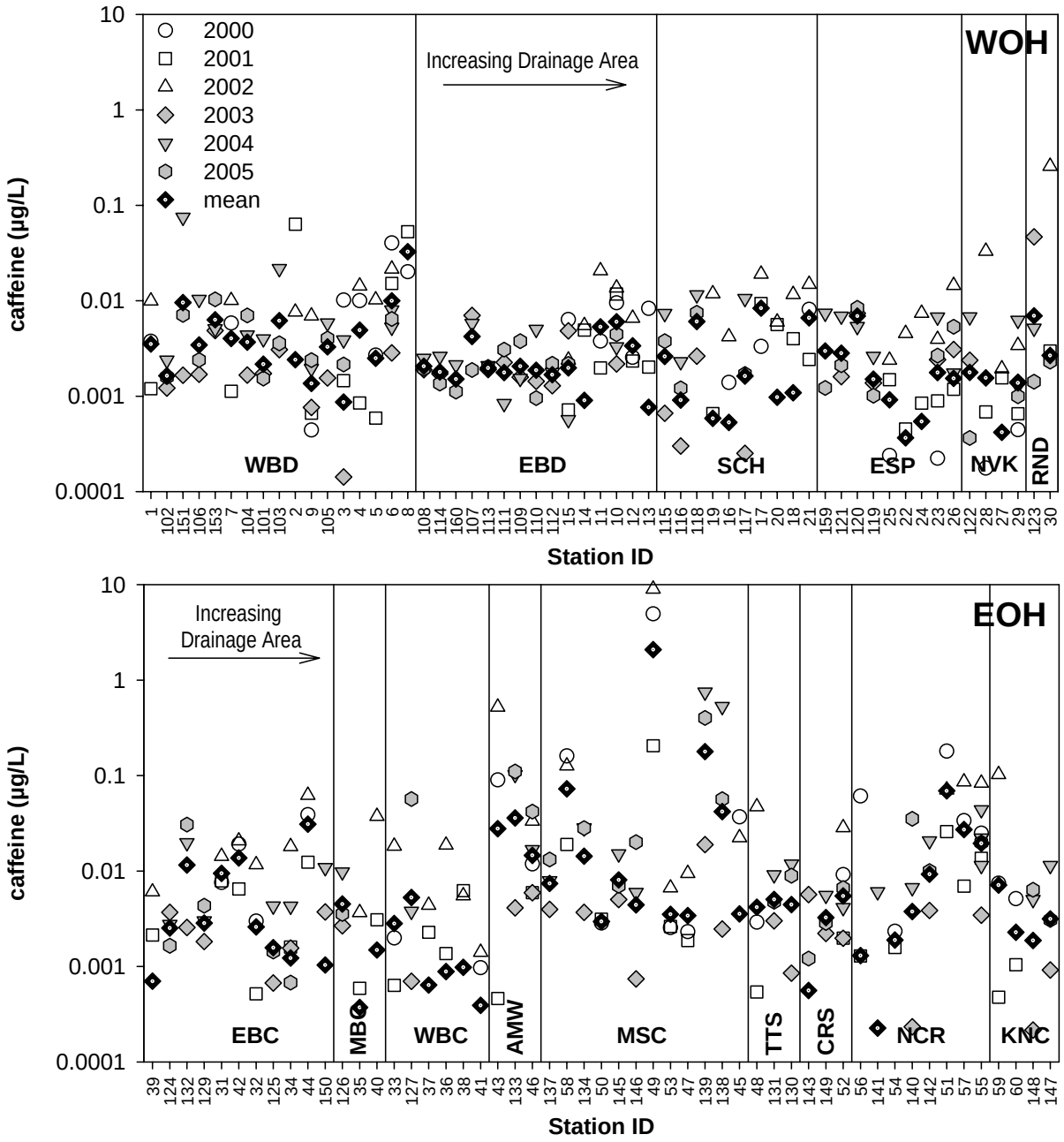

Figure 4.8: Summer baseflow stream water concentrations of caffeine (CAF) for all Phase I and Phase II sites sites both (A) West of Hudson and (B) East of Hudson. Geomentric means of all measured values at each site are given by solid black diamonds.

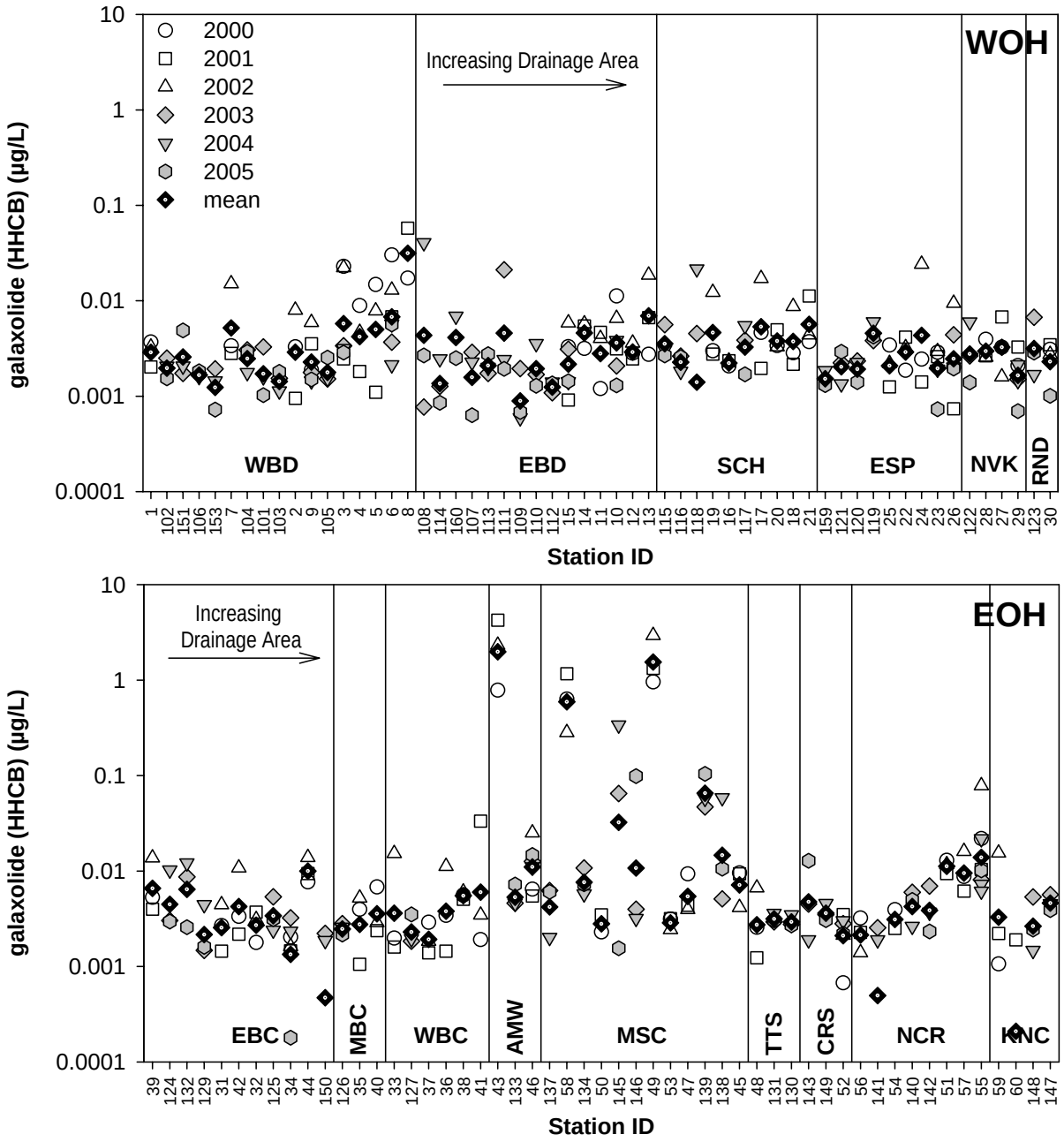

Figure 4.9: Summer baseflow stream water concentrations of the fragrance material galaxolide (HHCB) for all Phase I and Phase II sites sites both (A) West of Hudson and (B) East of Hudson. Geomentric means of all measured values at each site are given by solid black diamonds.

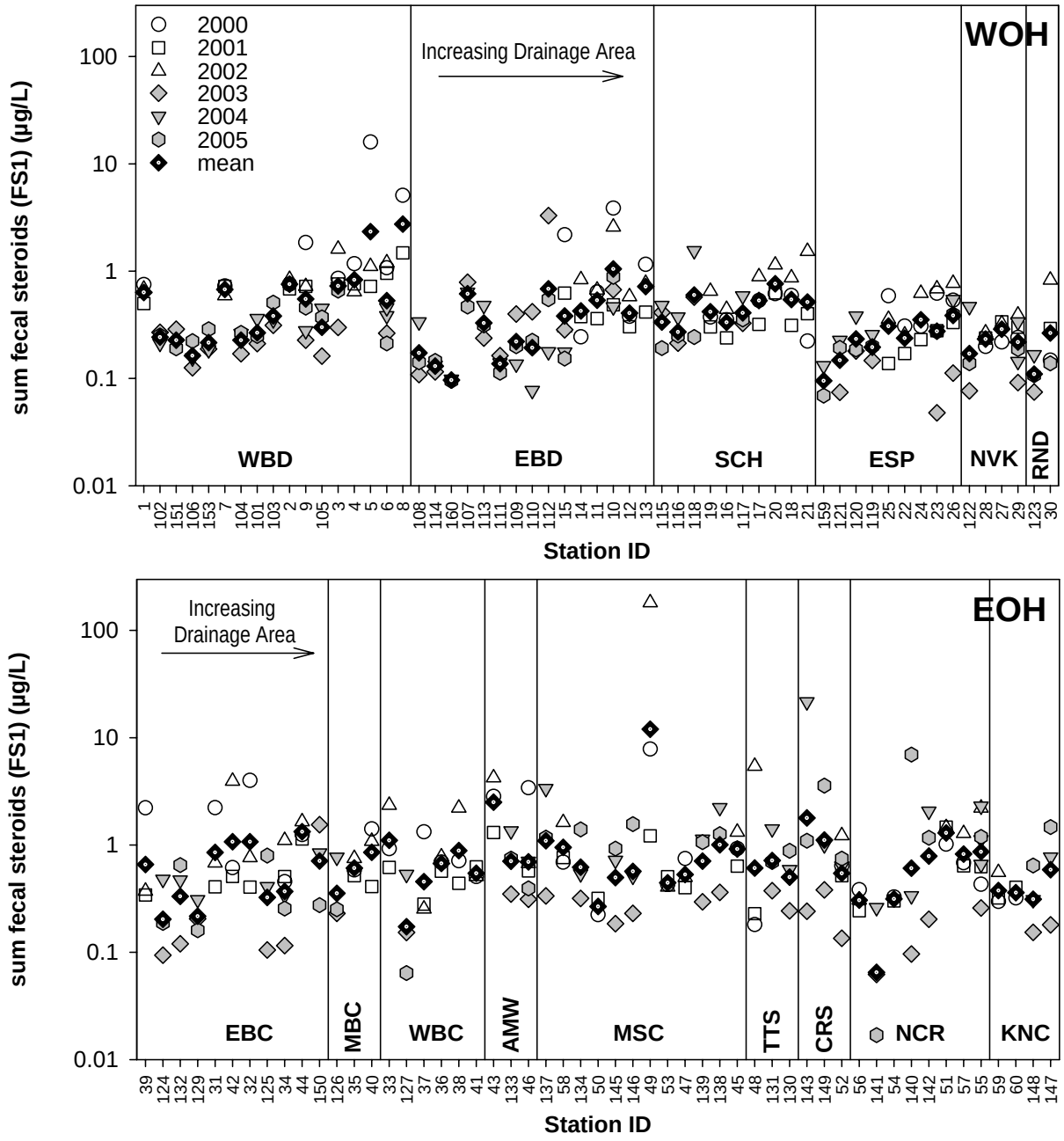

Figure 4.10: Summer baseflow stream water concentrations of the sum of the seven fecal steroids measured in both Phase I and Phase II (FS1) – aCOP, aONE, bCOP, bONE, CHO, EPI and SNOL (see table 4.1) – for all Phase I and Phase II sites sites both (A) West of Hudson and (B) East of Hudson. Geomentric means of all measured values at each site are given by the solid grey line.

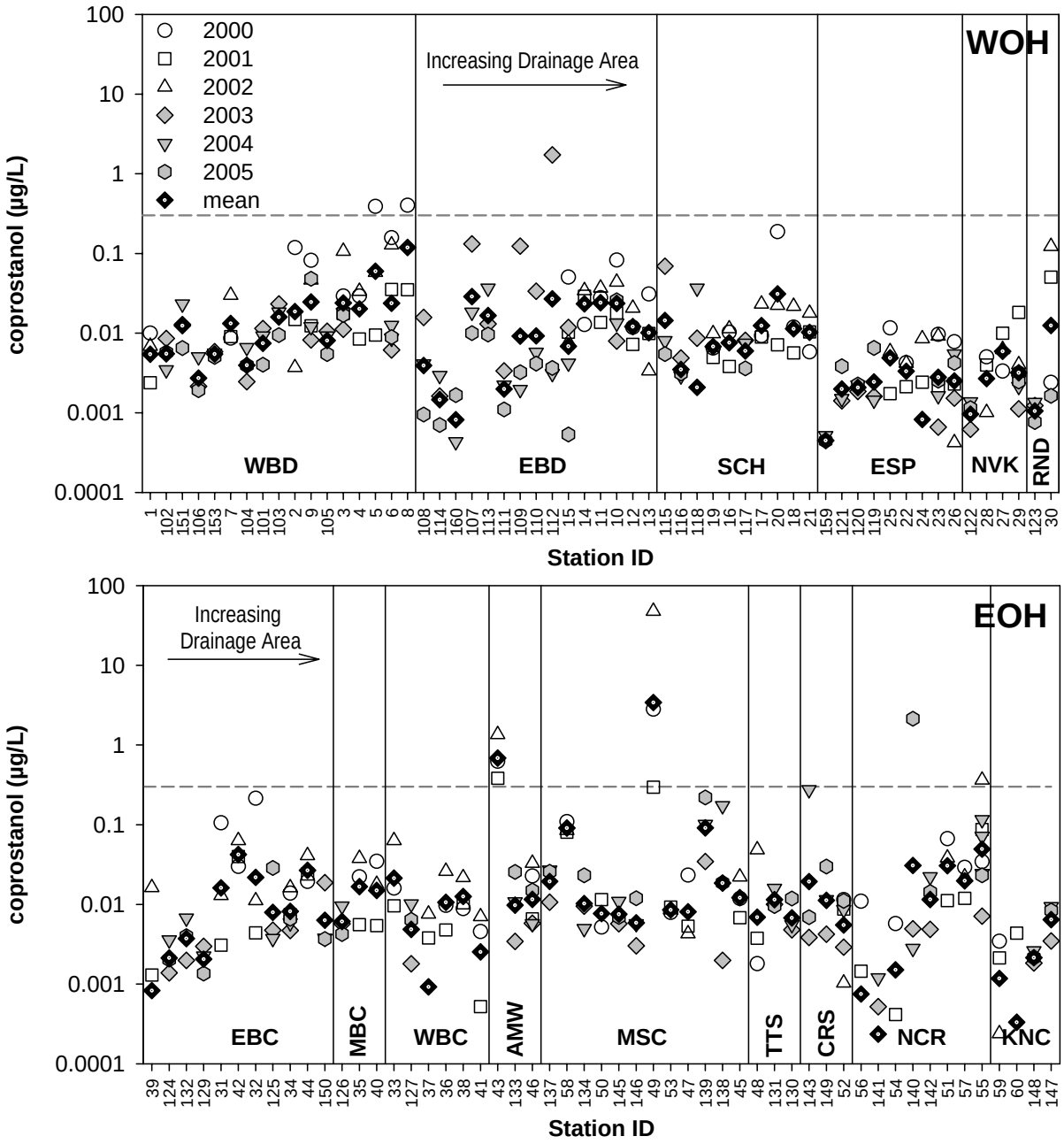

Figure 4.11: Summer baseflow stream water concentrations of coprostanol (bCOP) for all Phase I and Phase II sites sites both (A) West of Hudson and (B) East of Hudson. Geomentric means of all measured values at each site are given by solid black diamonds. The short-dashed line shows the concentration of coprostanol corresponding to 200 fecal coliforms per 100 mL, using the upper 95% confidence limit of the relationship between the two given by Leeming and Nichols (Leeming and Nichols 1996).

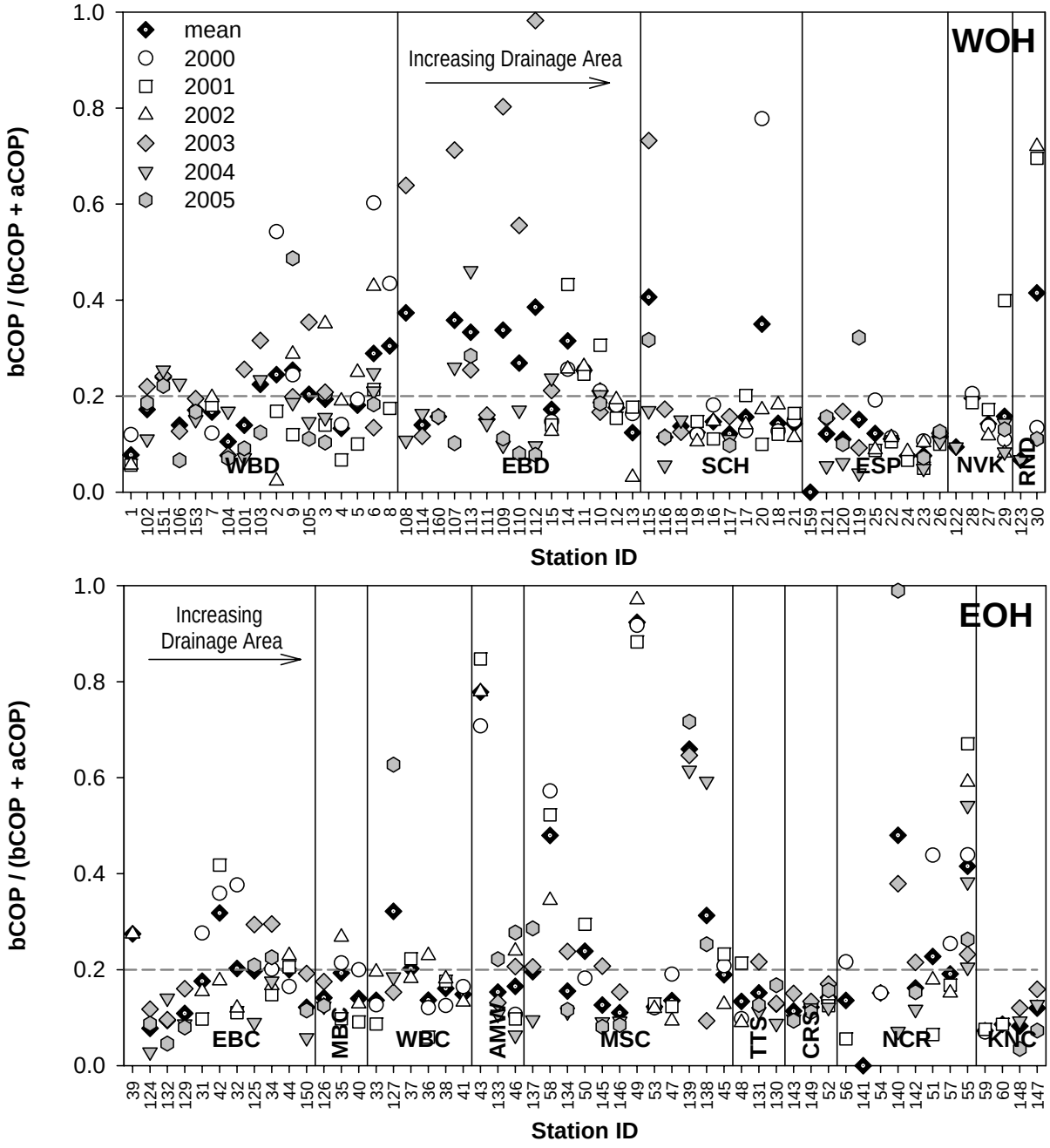

Figure 4.12: Summer baseflow ratios of coprostanol/(coprostanol+cholestanol) (bCOP/(bCOP+aCOP)), a fecal steroid source indicator, for all Phase I and Phase II sites both (A) West of Hudson and (B) East of Hudson. Arithmetic means of all measured values at each site are given by solid black diamonds. The short-dashed line in (B) shows a suggested delimitation between human fecal sources (bCOP/(bCOP+aCOP) > 0.2) and wildlife sources (bCOP/(bCOP+aCOP) > 0.2) in watersheds with minimal livestock (Grimalt et al. 1990, O'Leary et al. 1999).

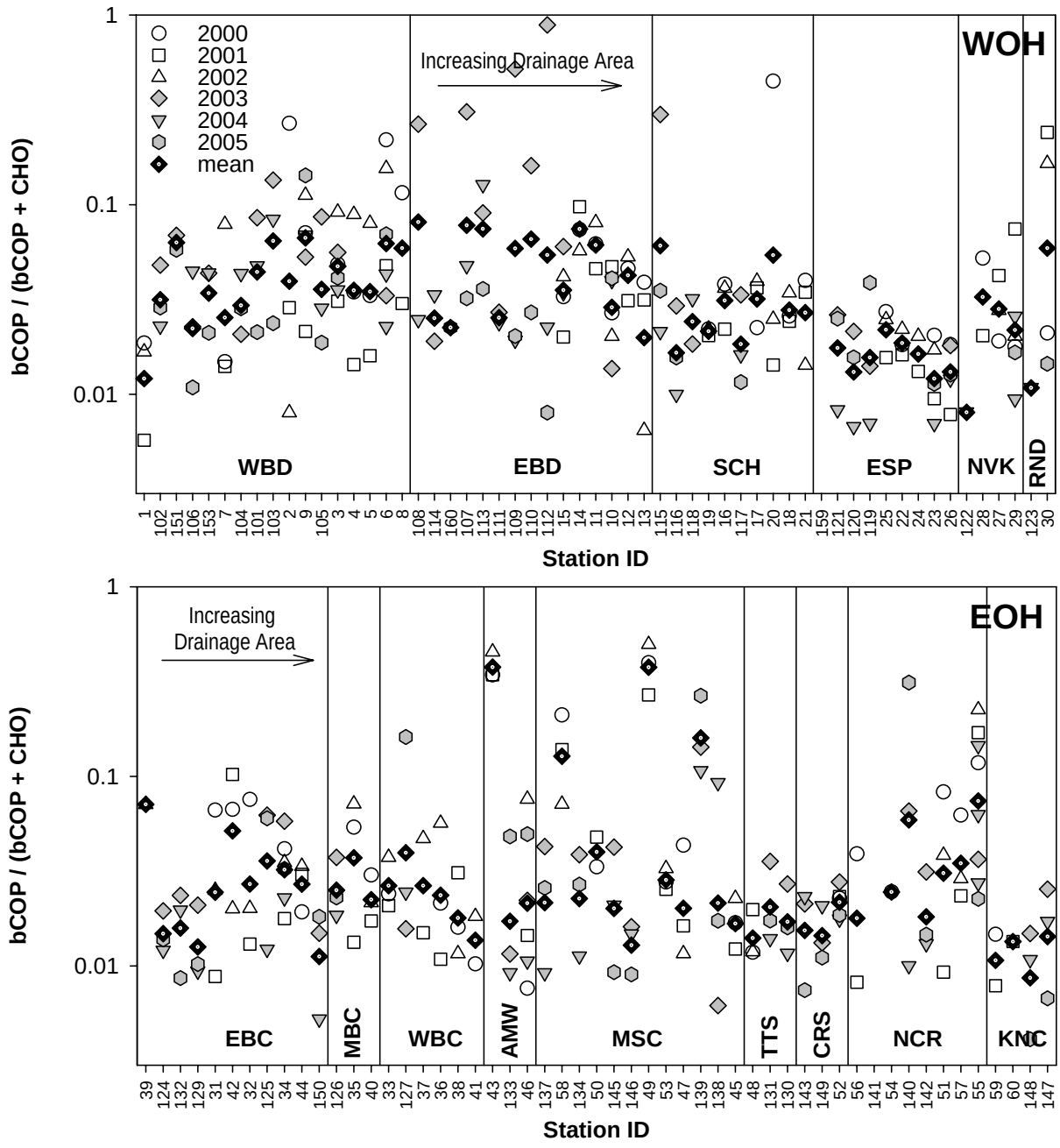

Figure 4.13: Summer baseflow ratios of coprostanol/cholesterol (bCOP/(bCOP+CHO)), a fecal steroid source indicator, for all Phase I and Phase II sites both (A) West of Hudson and (B) East of Hudson. Arithmetic means of all measured values at each site are given by solid black diamonds. High values of bCOP/(bCOP+CHO) indicate human fecal sources dominate over livestock and wildlife sources [Mudge, 1999 #4878]. .

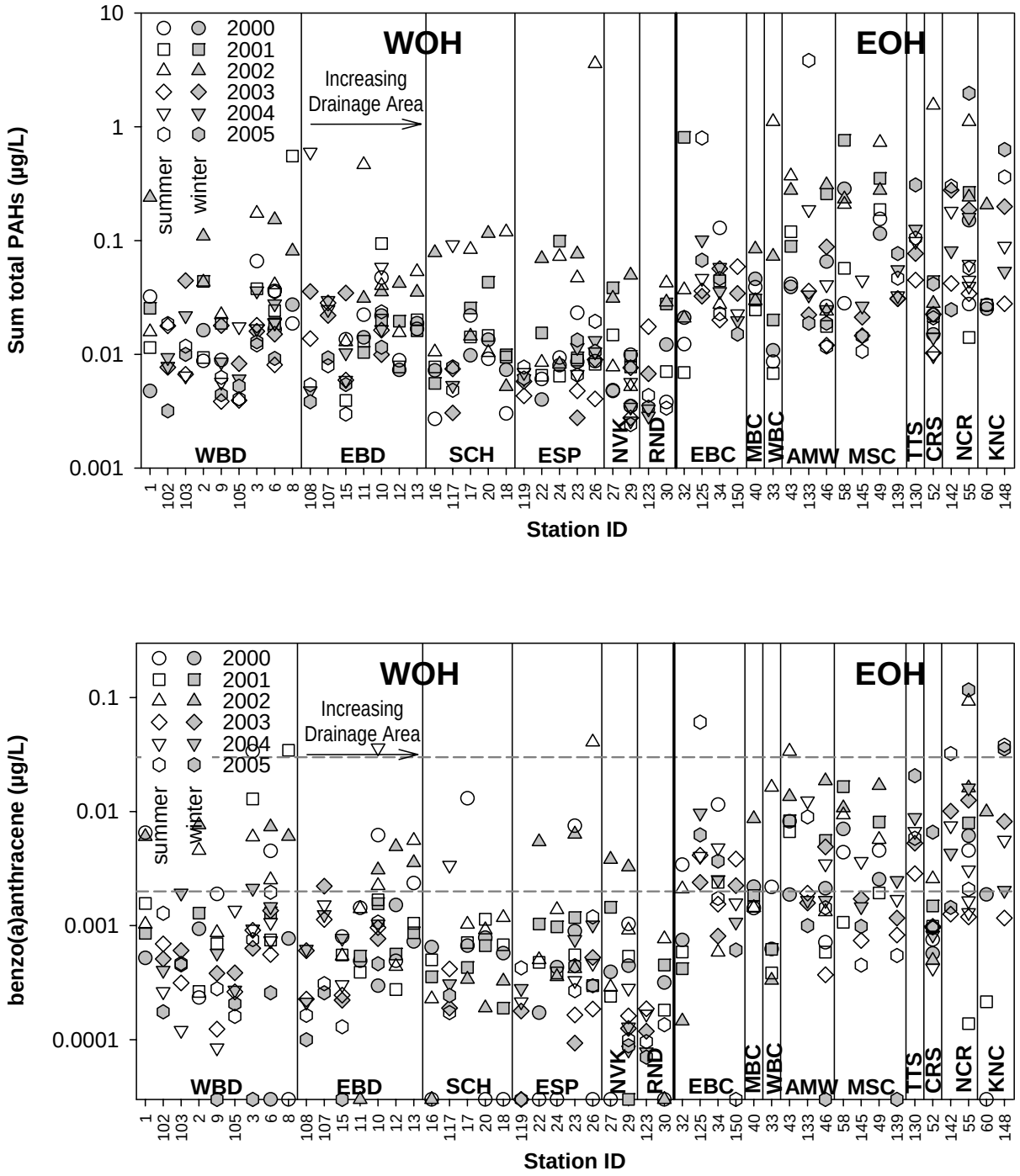

Figure 4.14: A comparison of winter baseflow with summer baseflow concentrations of (A) the sum of all PAH compounds (as in Fig. 4.2), and (B) benzo(a)anthracene, for Phase I and Phase II sites having winterbaseflow data. Sites are arranged in order of increasing basin area by subwatershed within both West of Hudson (WOH) and East of Hudson (EOH) regions. Winter baseflow data are shown as grey symbols, and summer data as unfilled symbols. Lines for ambient water guidance values are as in Fig. 4.3.

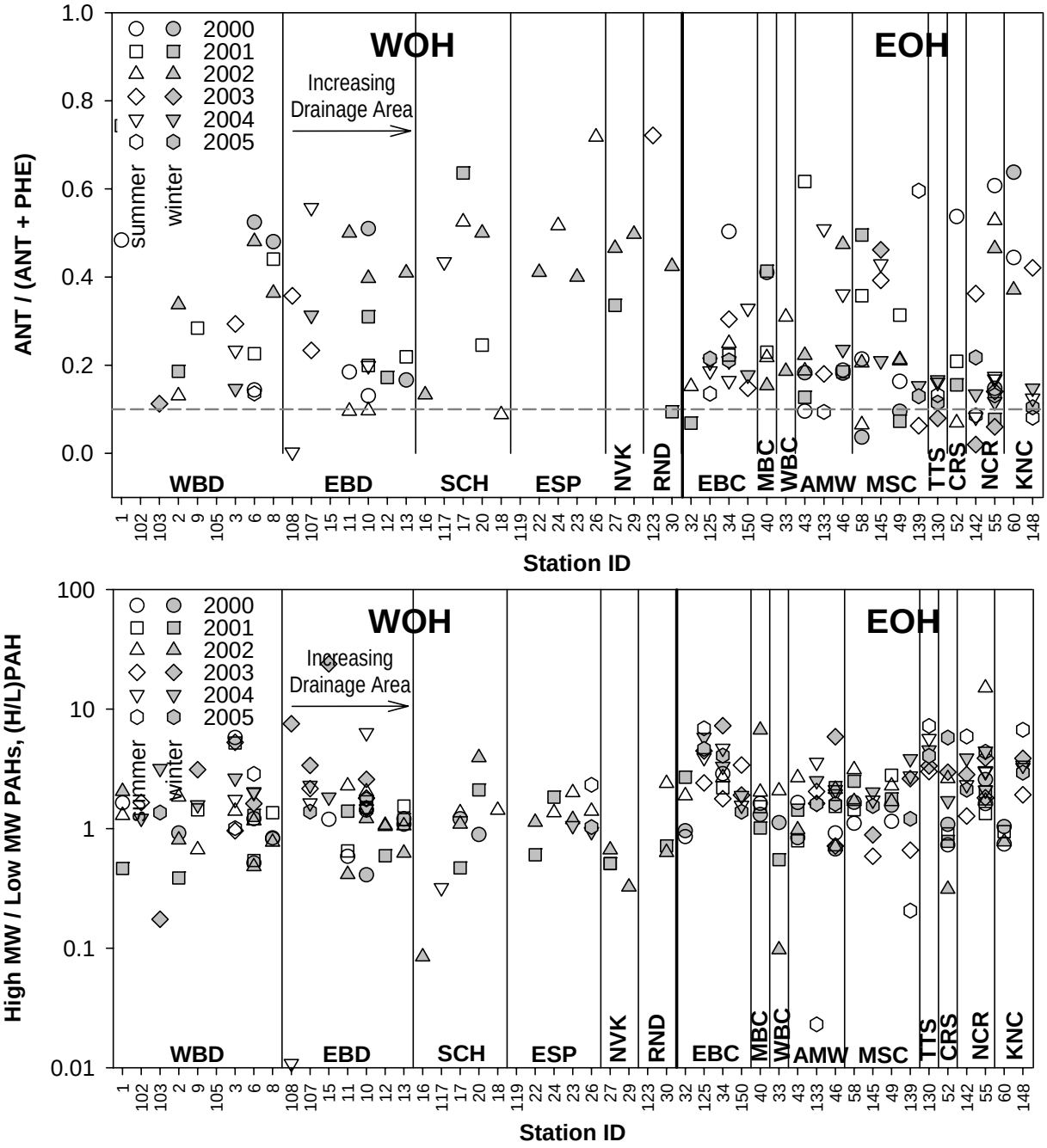

Figure 4.15: A comparison of winter baseflow with summer baseflow values of the (A) the anthracene/(anthracene+phenanthrene) ratio, and (B) the high-to-low molecular weight PAH ratio (H/L_{PAH}), for Phase I and Phase II sites having winterbaseflow data. Sites are arranged in order of increasing basin area by subwatershed within both West of Hudson (WOH) and East of Hudson (EOH) regions. Winter baseflow data are shown as grey symbols, and summer data as unfilled symbols. Lines for ambient water guidance values are as in Fig. 4.7.

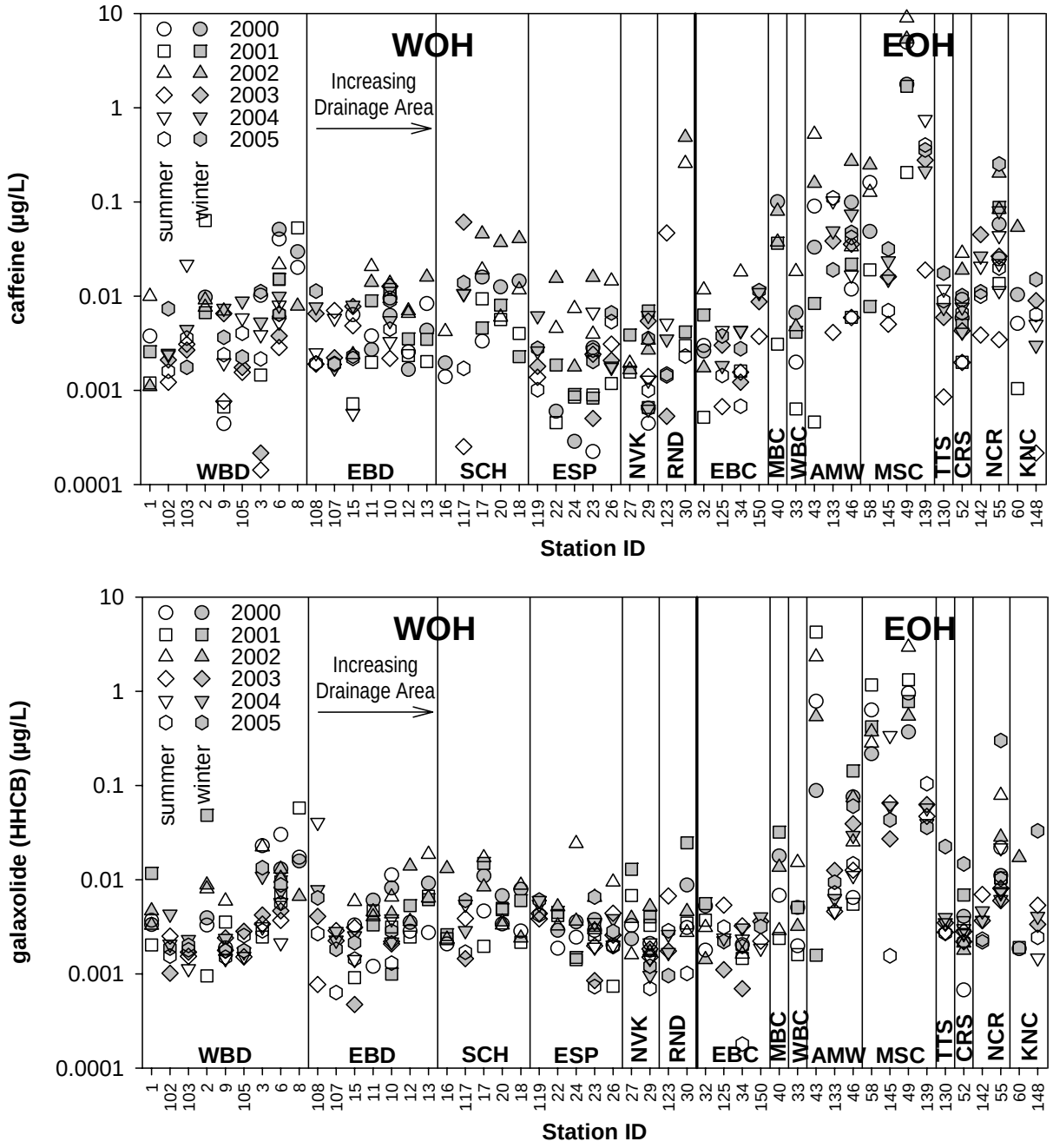

Figure 4.16: A comparison of winter baseflow with summer baseflow concentrations of (A) caffeine, and (B) the fragrance material galaxolide (HHCB), for Phase I and Phase II sites having winterbaseflow data. Sites are arranged in order of increasing basin area by subwatershed within both West of Hudson (WOH) and East of Hudson (EOH) regions. Winter baseflow data are shown as grey symbols, and summer data as unfilled symbols.

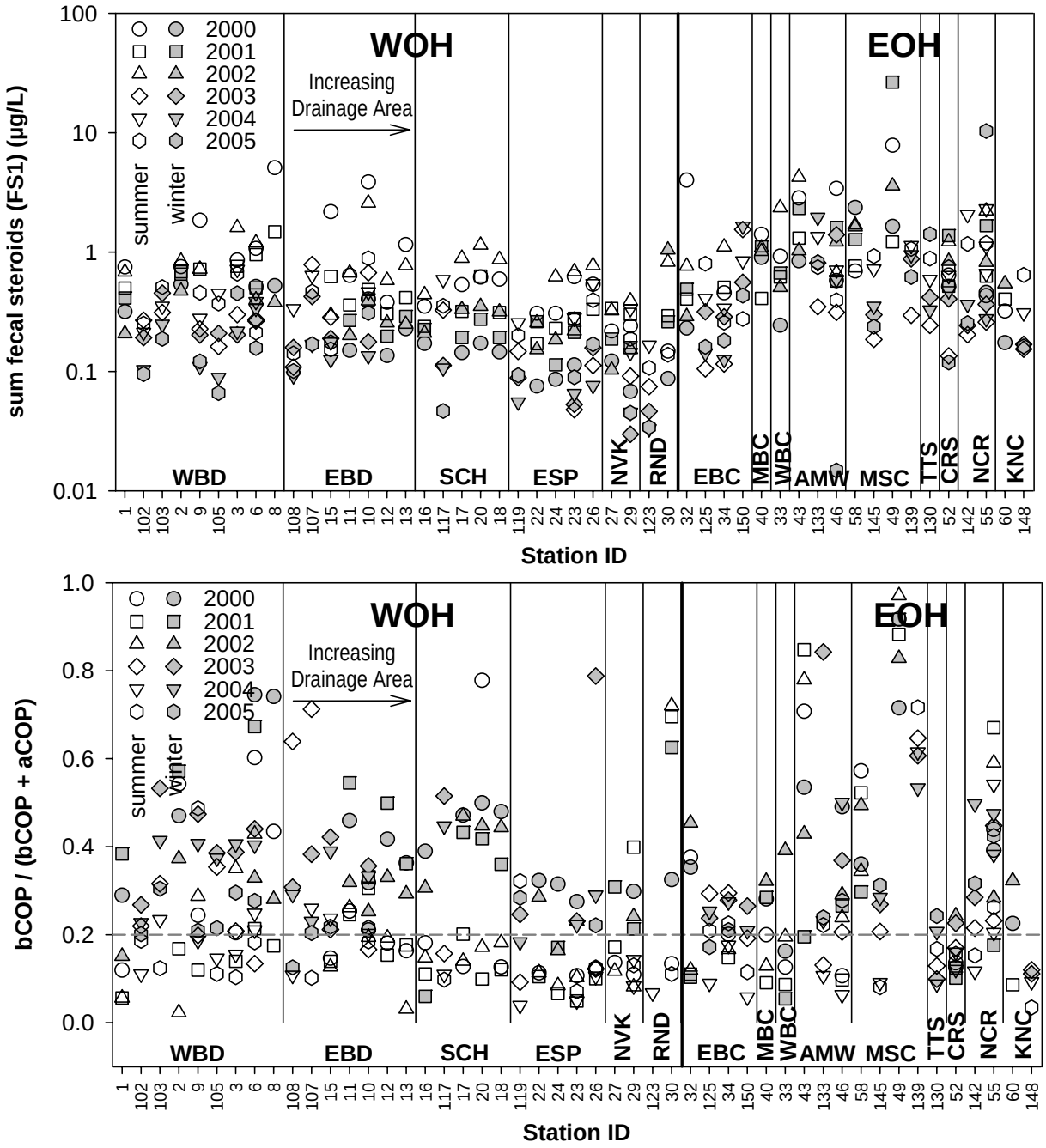

Figure 4.17: A comparison of winter baseflow with summer baseflow concentrations of (top plot) the sum of seven fecal steroids (FS) – aCOP, aONE, bCOP, bONE, CHO, EPI and SNOL, and (bottom plot) the coprostanol/(coprostanol+cholestanol) ratio (bCOP/(bCOP+aCOP)), for Phase I and Phase II sites having winterbaseflow data. Sites are arranged in order of increasing basin area by subwatershed within both West of Hudson (WOH) and East of Hudson (EOH) regions. Winter baseflow data are shown as grey symbols, and summer data as unfilled symbols. Lines for ambient water guidance values are as in Fig. 4.12.

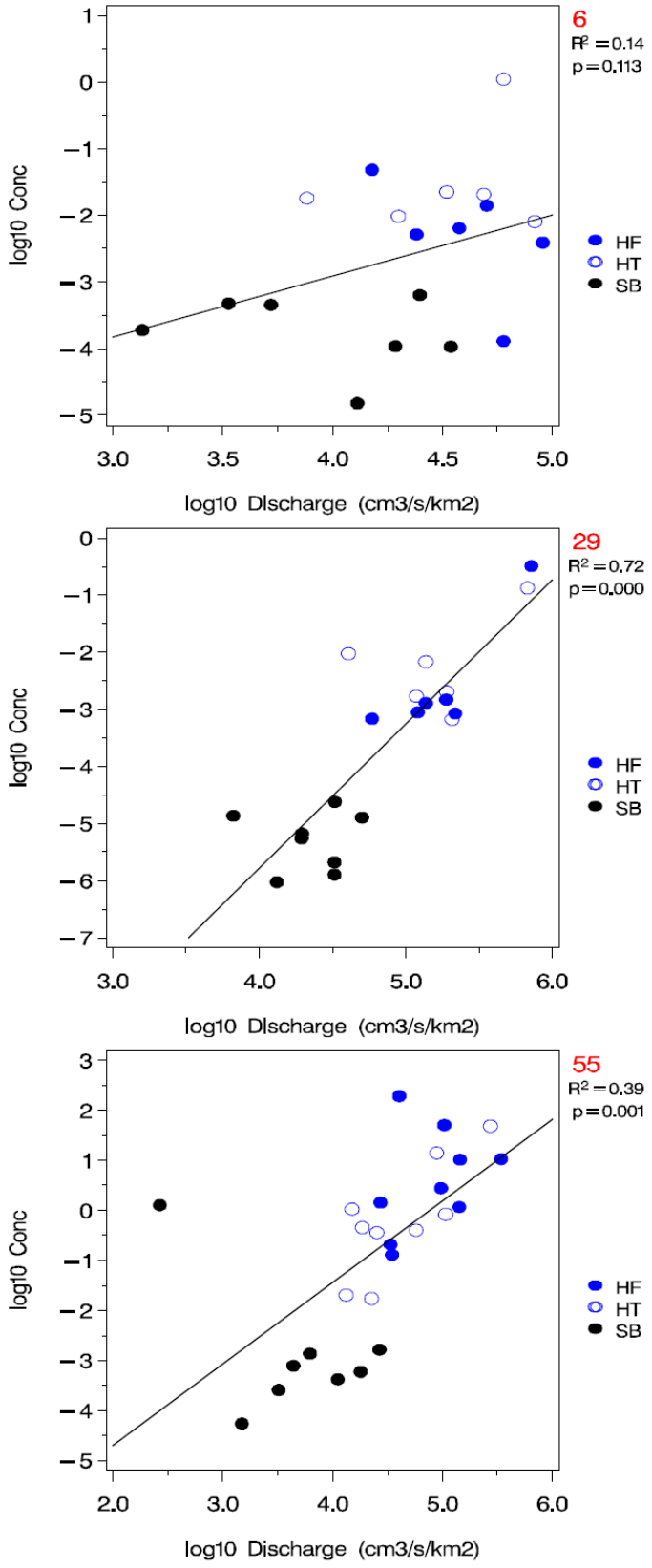

Figure 4.18: Comparison of the sum of PAH concentrations versus discharge in high-tubidity (HT) and high-flow (HF) storm samples and summer baseflow (BF) samples at each of the three storm sites.

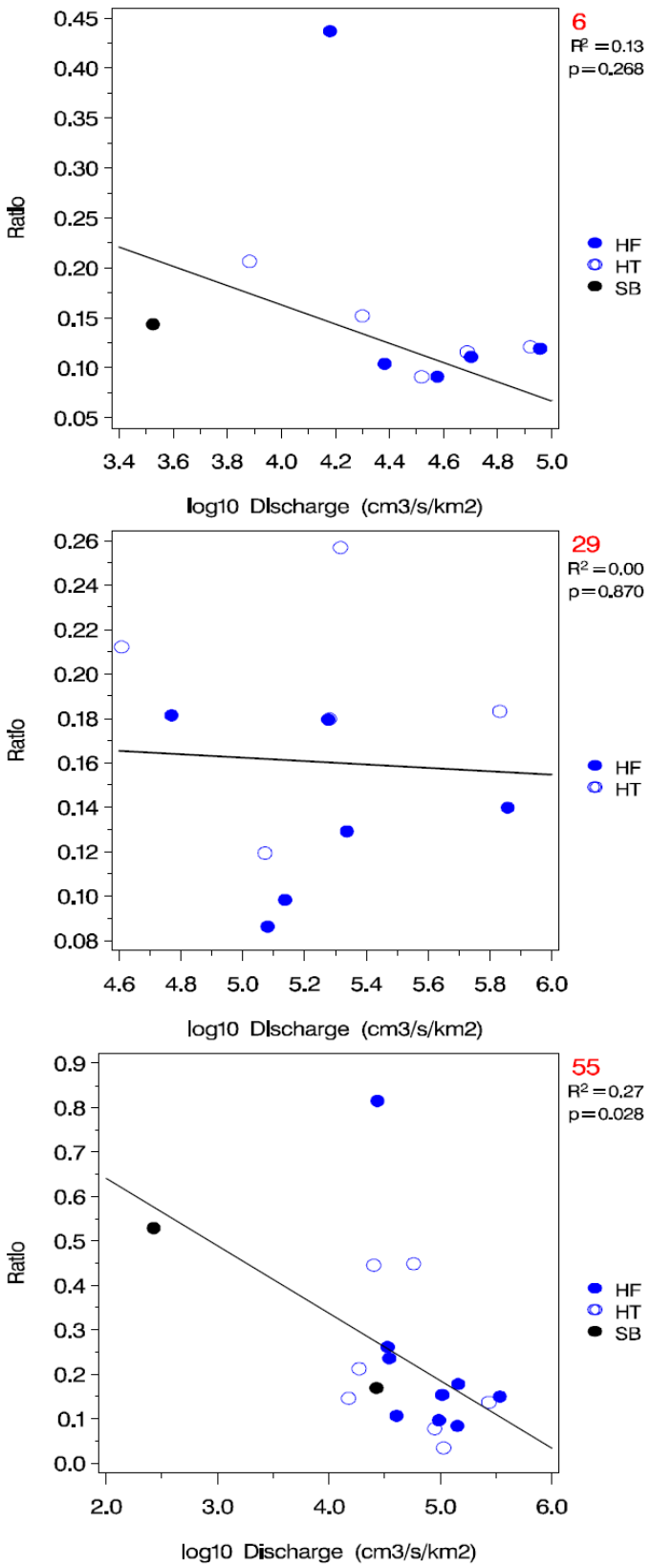

Figure 4.19: Comparison of ANT/(ANT+PHE) ratios versus discharge in high-tubidity (HT) and high-flow (HF) storm samples and summer baseflow (BF) samples at each of the three storm sites.

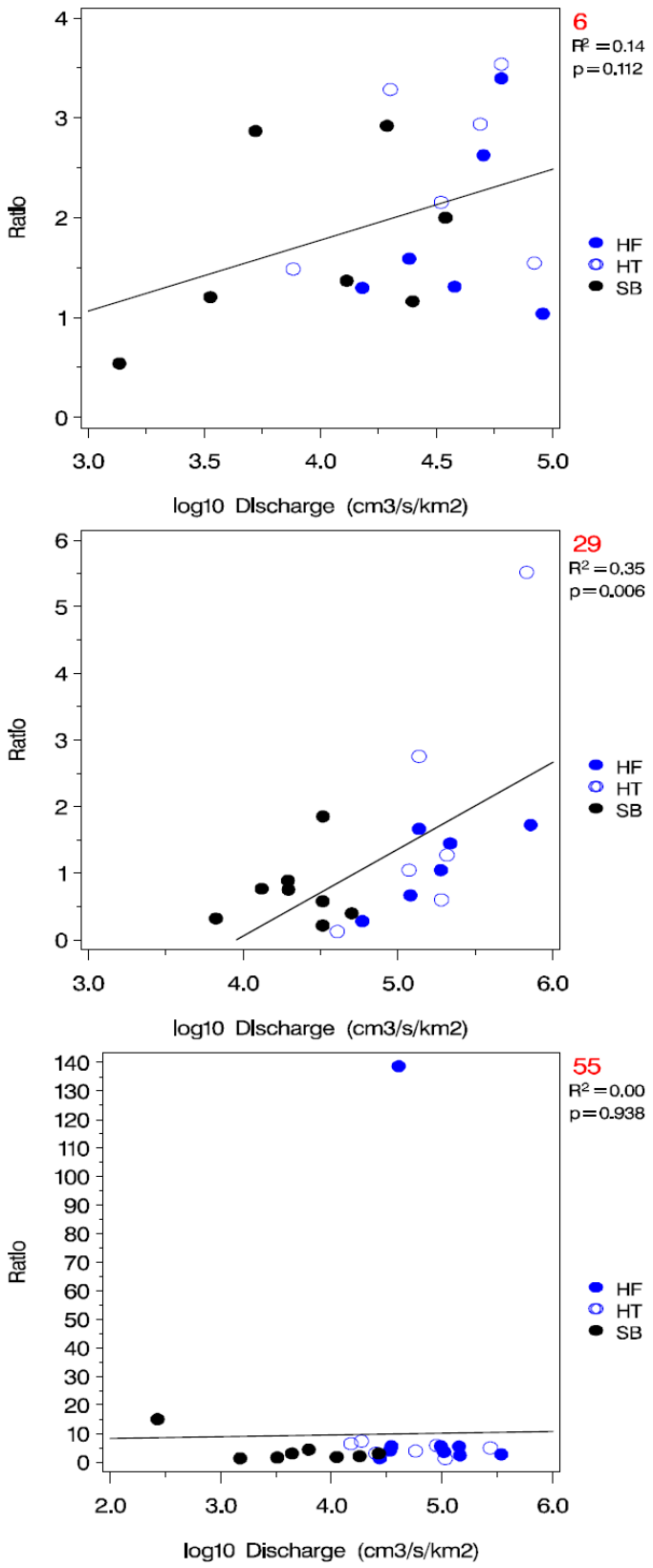

Figure 4.20: Comparison of $(H/L)_{PAH}$ ratios versus discharge in high-tubidity (HT) and high-flow (HF) storm samples and summer baseflow (BF) samples at each of the three storm sites.

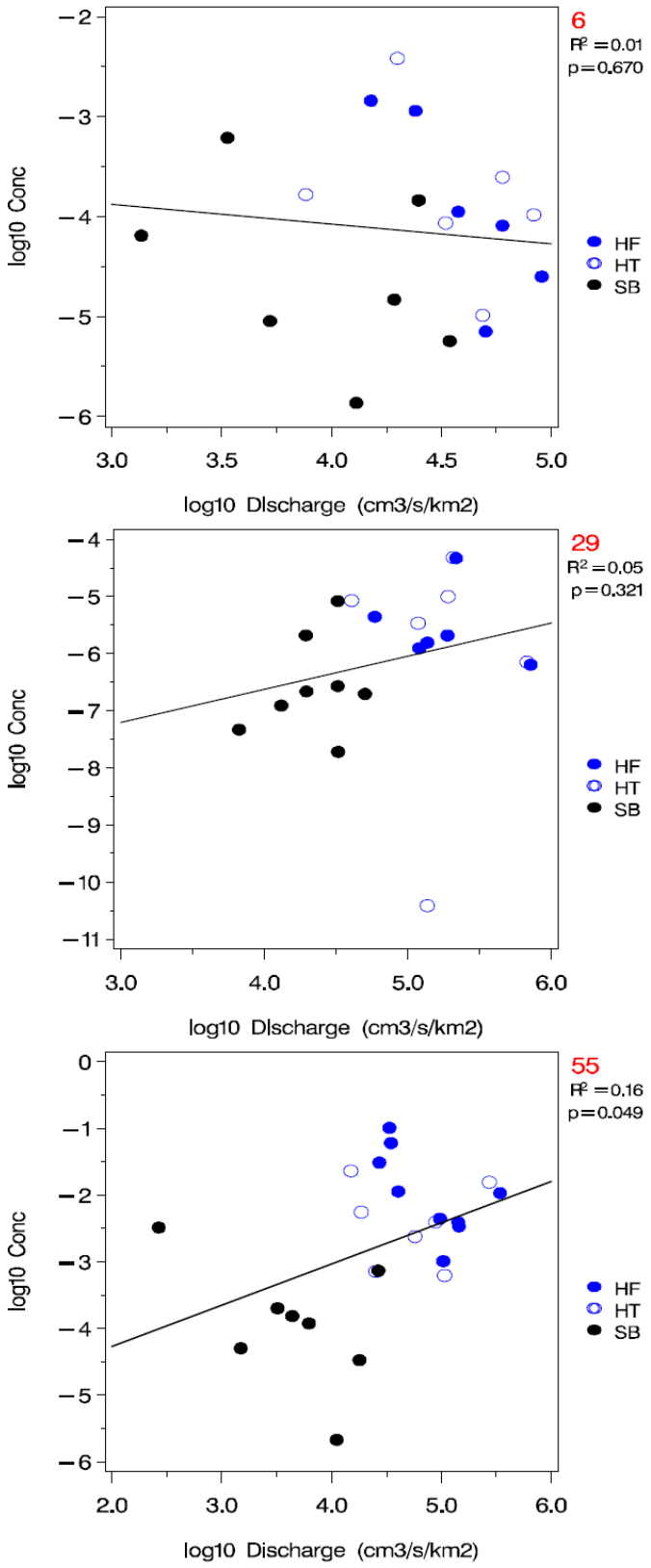

Figure 4.21: Comparison of caffeine concentrations versus discharge in high-tubidity (HT) and high-flow (HF) storm samples and summer baseflow (BF) samples at each of the three storm sites.

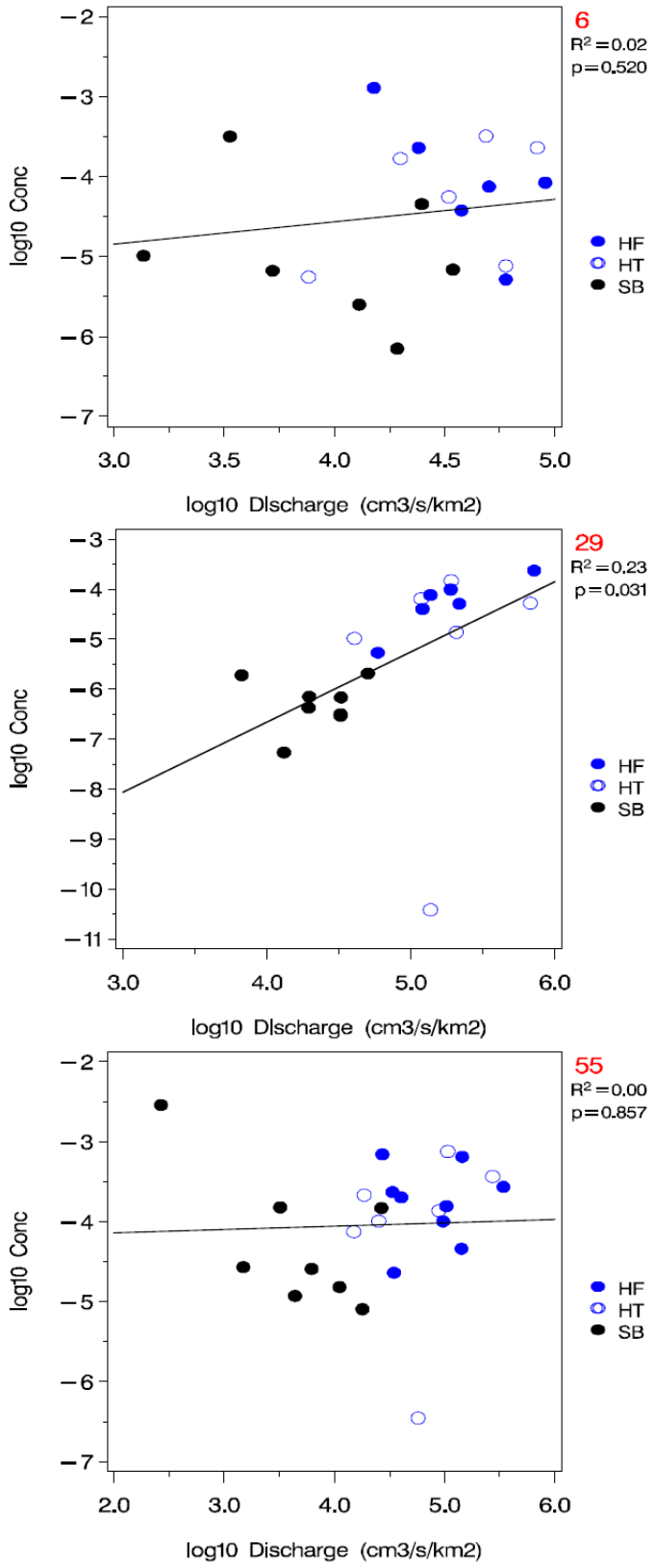

Figure 4.22: Comparison of fragrance material tonalide (HHCB) concentrations versus discharge in high-tubidity (HT) and high-flow (HF) storm samples and summer baseflow (BF) samples at each of the three storm sites.

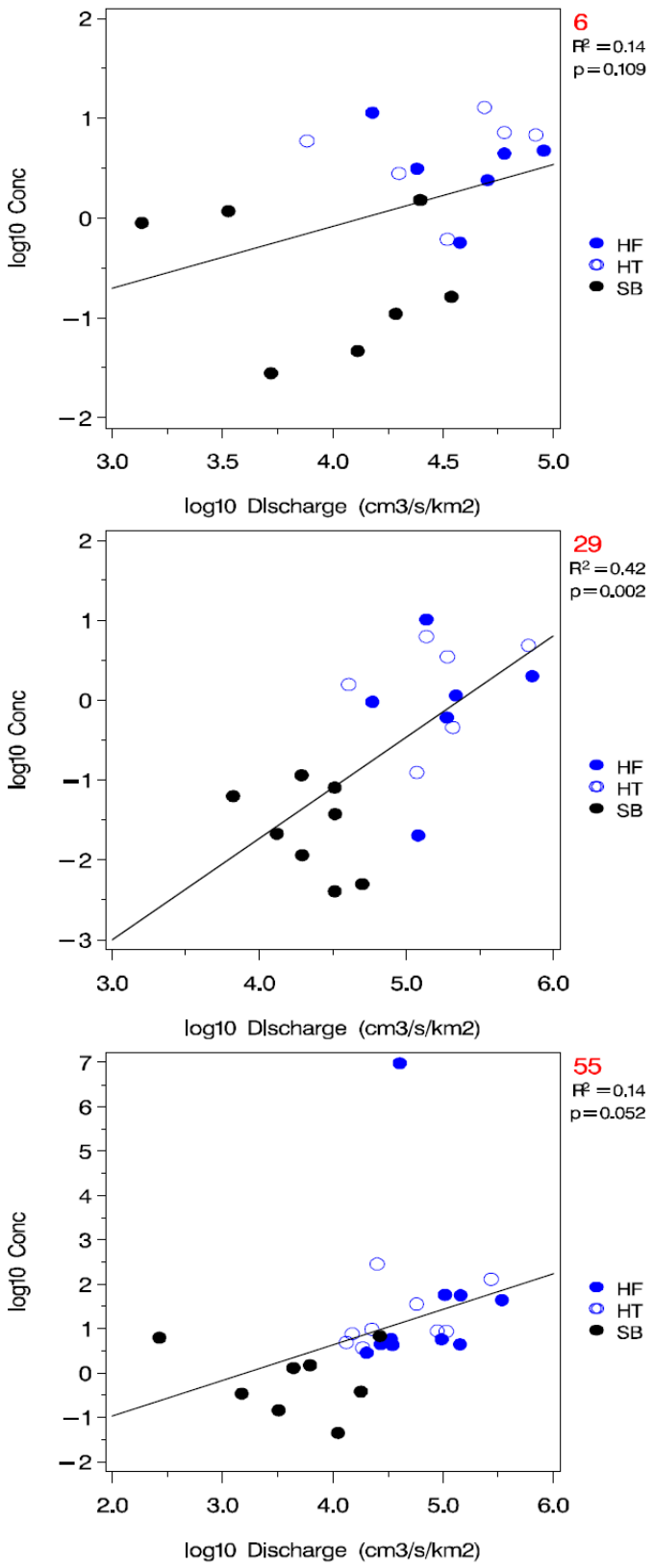

Figure 4.23: Comparison of the sum of seven fecal steroids (see Fig. 4.10) versus discharge in high-tubidity (HT) & high-flow (HF) storm samples and summer baseflow (BF) samples at each of the three storm sites.

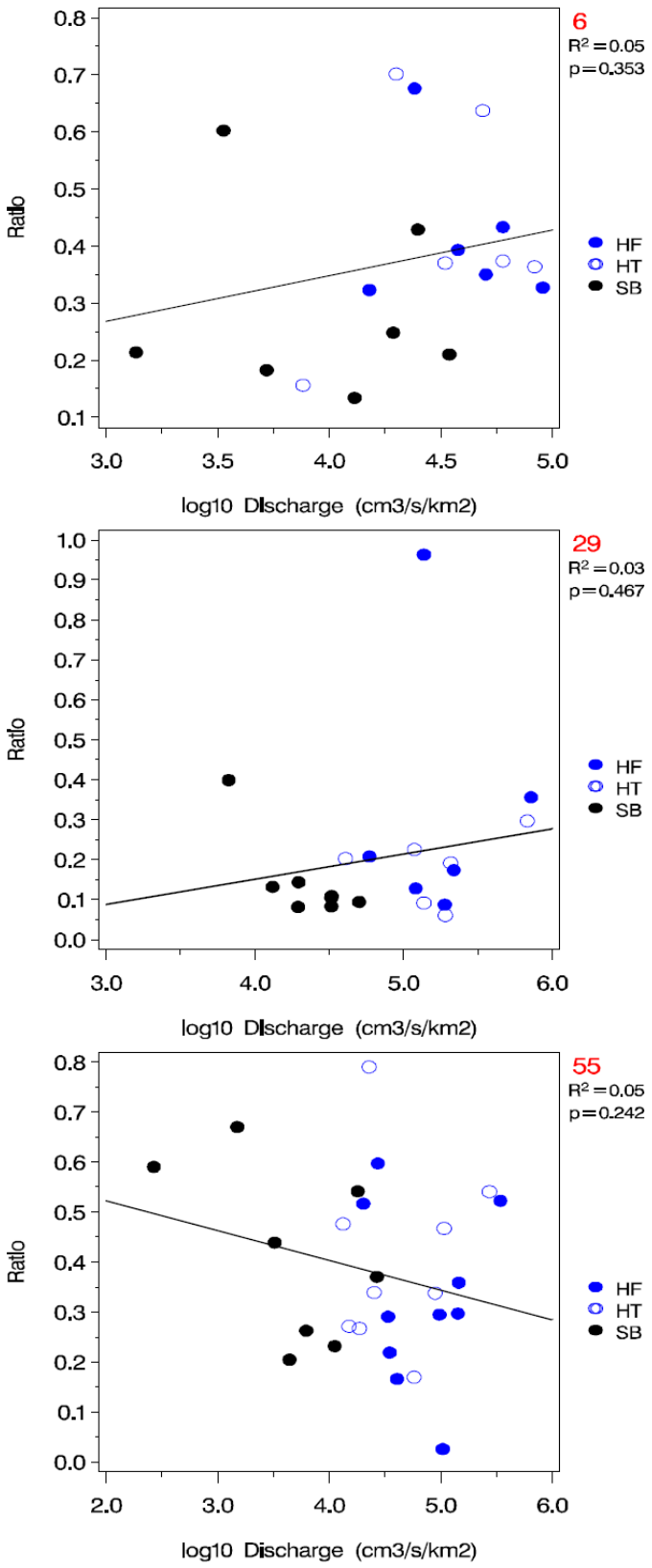

Figure 4.24: Comparison of bCOP/(bCOP+aCOP) ratios versus discharge in high-tubidity (HT) and high-flow (HF) storm samples and summer baseflow (BF) samples at each of the three storm sites.

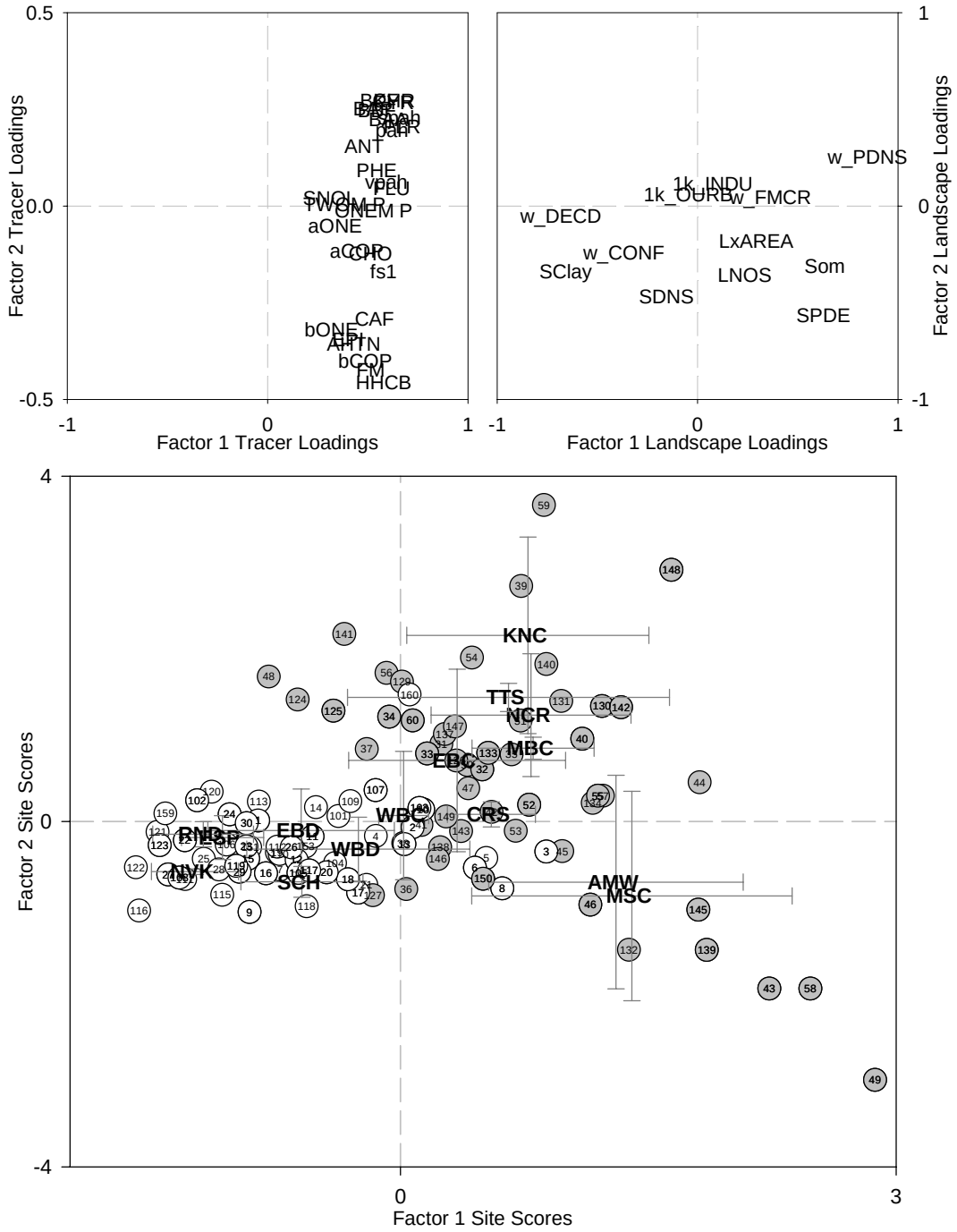

Figure 4.25: Redundancy Analysis explaining (A) molecular tracer compound concentrations via (B) land use/cover and catchment characteristics for (C) all 110 sites visited during the summer in this study. WOH sites are designated by white circles and EOH by grey circles, with site numbers within each circle, as defined in Tables 2.3 & 2.4, Chapter 2. Molecular tracer compound abbreviations are defined in Table 4.1, and land use/cover abbreviations are in Table 4.2.

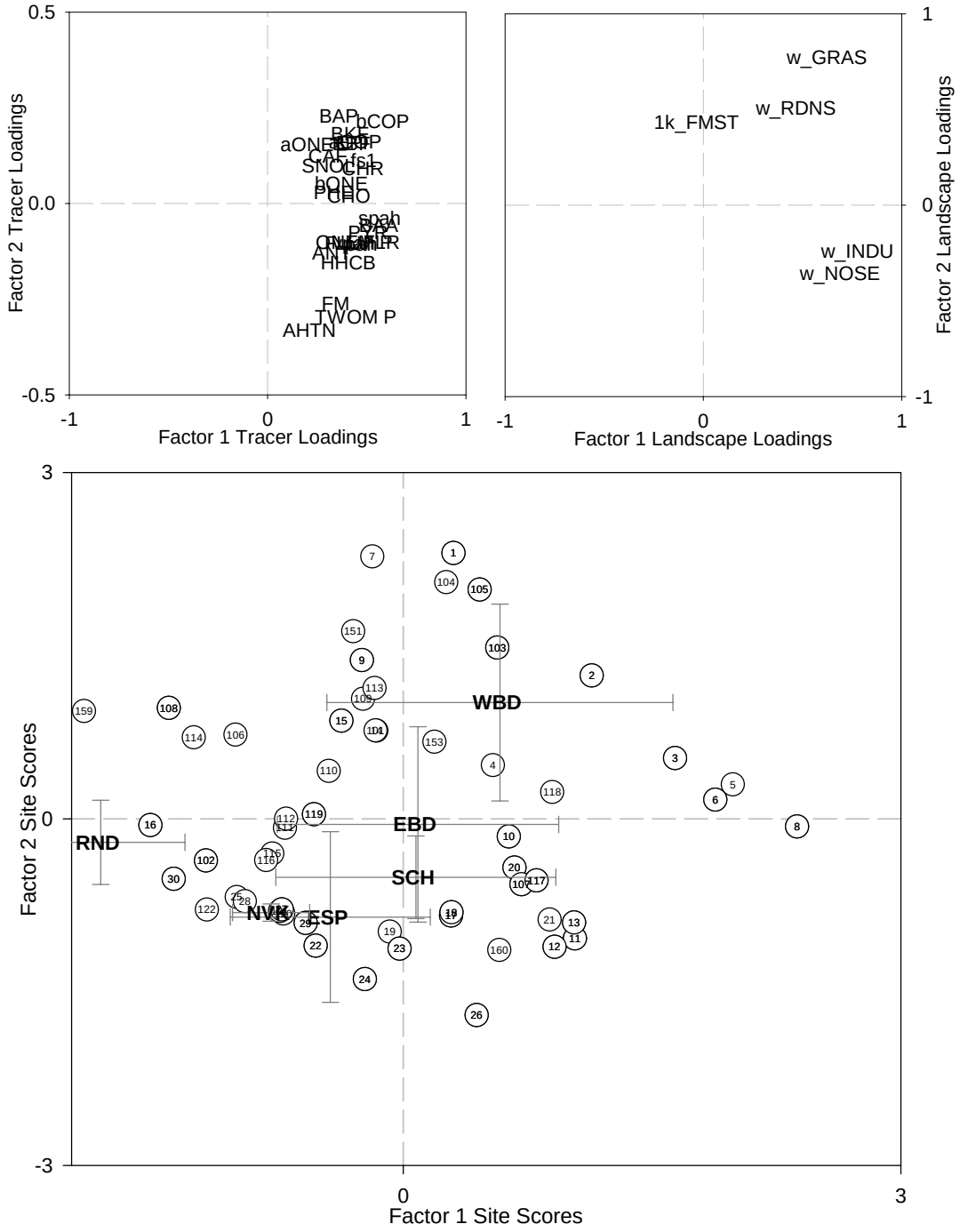

Figure 4.26: Redundancy Analysis explaining (A) molecular tracer compound concentrations via (B) land use/cover and catchment characteristics for (C) all 57 WOH sites visited during the summer in this study. Site numbers are given within each circle, as defined in Table 2.3, Chapter 2. Molecular tracer compound abbreviations are defined in Table 4.1, and land use/cover abbreviations are in Table 4.2.

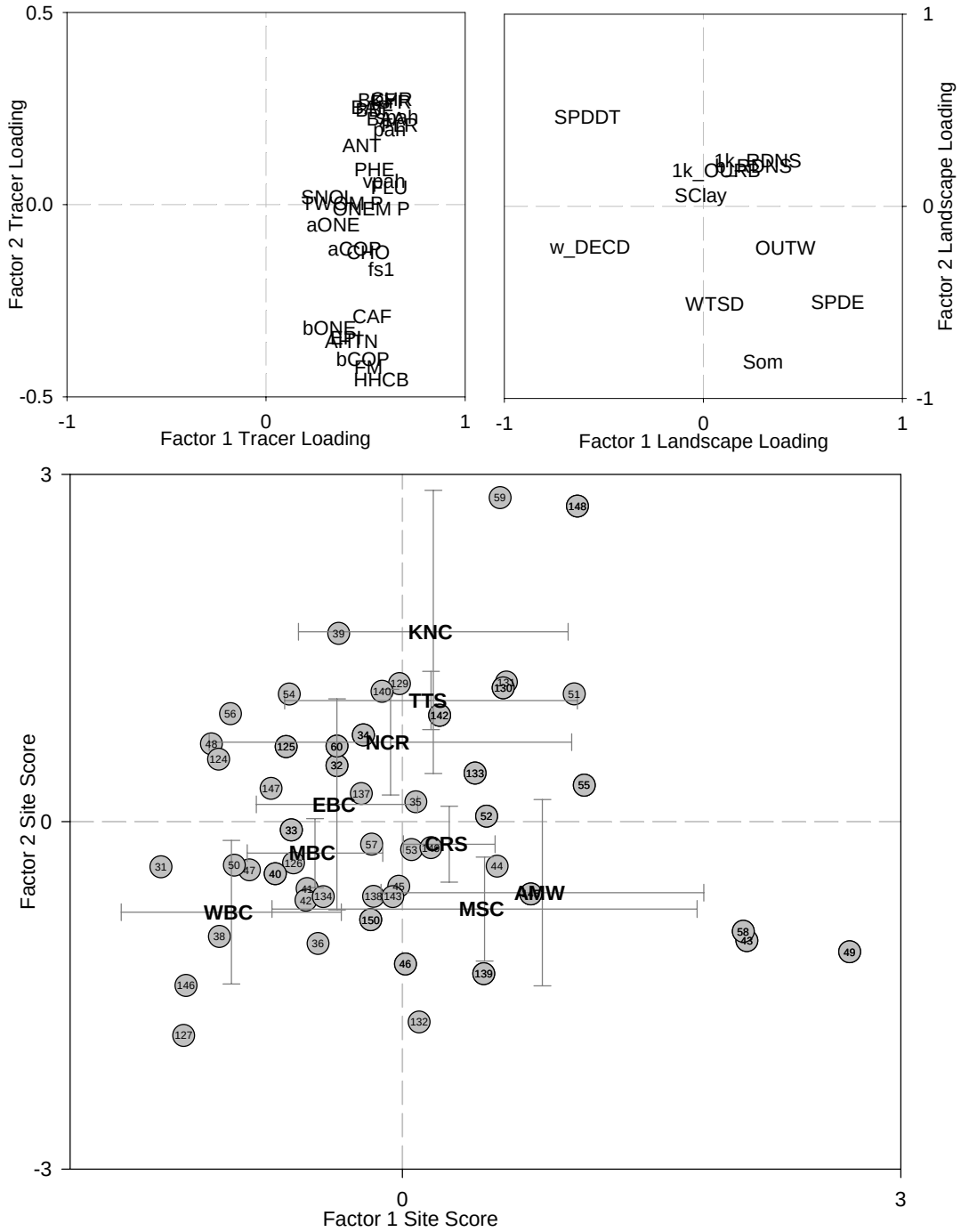

Figure 4.27: Redundancy Analysis explaining (A) molecular tracer compound concentrations via (B) land use/cover and catchment characteristics for (C) all 53 EOH sites visited during the summer in this study. Site numbers are given within each circle, as defined in Table 2.4, Chapter 2. Molecular tracer compound abbreviations are defined in Table 4.1, and land use/cover abbreviations are in Table 4.2.

Chapter 5. Molecular Tracer Source Signatures

Research Task

The interpretation of source-specific organic compounds, or biomarkers, to estimate source contributions (Eglington 1969, Hedges and Prahl 1993) is most powerful when the following conditions are met: (1) the tracer must be detectable at a concentration well below that of interest; (2) ambient concentrations of the tracer molecule must be accurately quantified; (3) all sources of the tracer are known and relatively unique; and (4) environmental diagenesis or degradation of the tracer compound is either (a) minimal, (b) well understood, and/or (c) proportional to other tracer compounds to which it might be compared (e.g., ratios do not change with degradation) (Hedges and Prahl 1993). Most research efforts approach the tasks sequentially in the order above, and for most organic tracers, environmental diagenesis is not well understood for many years, if not decades.

In Chapter 4 of this report, we describe research results that confirm the first two conditions above (i.e. detection and quantitation of tracers at ambient stream concentrations). In this chapter, we describe the results from a research effort in Phase II of this project to better constrain the concentrations and signatures (ratios) of various potential contamination sources to NY source watersheds (condition #3 above).

A large number of studies have quantified souce signatures of PAHs (Nielsen 1996, Simó et al. 1997, Miguel et al. 1998, Dickhut et al. 2000, Yunker et al. 2002, Zakaria et al. 2002, Stein et al. 2006). Concentrations of caffeine and fragrances have been measured in the effluent and influent of sewage treatment plants (Simonich et al. 2002, Artola-Garicano et al. 2003, Phillips et al. 2005) and during diagenesis within Swiss lakes (Buerge et al. 2003). Much less data exists on signatures of the full suite of fecal steroids from potential sources, including livestock and wildlife, and the only detailed studies were all conducted in Australia (Leeming et al. 1996, Leeming et al. 1998). For these reasons, we have focused our efforts on better defining the signatures of our 10 fecal steroid compounds from four different waste water treatment plants (WWTP) and three different household septic systems within the NY watersheds and from fecal materials from cows (n=3), horses (n = 3), deer (n = 3), beaver (n = 1), opossum (n = 1), raccoon (n = 1), geese (n = 2) and gull (n = 1).

Methods

Sample collection and extraction

Water samples from WWTP and septic influents and effluents (Table 5.1) were collected in precombusted (480° C) glass bottles directly from the water source. WWTP influent and effluent samples were collected inside WWTP facilities with the assistance of WWTP managers. Septic samples were collected in collaboration with Dr. James Hassett (SUNY-ESF) from an array of septic systems that have been extensively studied. Septic influent was collected from the "box" just prior to the holding tank, and septic effluent collected from shallow wells just below the leaching field. The samples were stored on ice and placed in a refrigerator (4° C) upon return to the laboratory. Field blanks and duplicates were collected at 2 sampling sites.

In the laboratory, WWTP and septic water samples were processed using methods very similar to those used for stream water samples (see Chapter 4 methods). In brief, water samples were spiked with surrogate recovery standards, then extracted by solid-liquid extraction using an Empore™ C-18 disk with two glass fiber filters (GF/F and GF/D) stacked on top of the disk. Extract volume was assessed gravimetrically prior to filtration. The glass fiber filters with particulate matter were separated from the C-18 disk. The particulate matter underwent sonic extraction three times using DCM/MeOH (1:1 v/v), and organics were extracted from the C-18 disk using the sequential solvent series of acetone, DCM (2 times), DCM/hexane (1:1, v/v), and hexane. Dissolved and particulate organic extracts were combined prior to cleaup and GC-MS analysis.

Fecal material from a variety of animal species (Table 5.1) was collected in ziploc bags or plastic containers at the site of collection and immediately frozen when the sample was returned to the lab. Fecal material was freeze dried and underwent a solid-liquid extraction, i.e. sonication and centrifugation using a 2:1 (v/v) mixture of dichloromethane (DCM)/Methanol (MeOH).

In the laboratory, fecal materials required a slightly modified extraction and clean-up processs relative to stream or waste water samples. In brief, freeze-dried samples were weighed into a vial, spiked with surrogate recovery standards, and sonic extracted once using DCM/MeOH (1:1 v/v) and repeated two times using DCM. After each extract step, supernatant was pipetted into another container.

Sample extract clean-up and analysis

The organic extracts from fecal and water samples were back extracted in a separatory funnel with a pre-extracted 5% aqueous salt solution to remove ionic and highly polar impurities. The organic phase was removed from the separatory funnel. The 5% salt solution was extracted two times with DCM. The extracts were combined and mixed with anhydrous sodium sulfate to remove moisture. The extracts from water samples were rotoevaporated to 1 mL, and transferred to an auto sample vial. Samples were gently dried under a stream of nitrogen. An aliquot of pyridine was added, along with BSTFA derivatizing agent (N,O-bis(trimethylsilyl)trifuoroacetamide with 1% trimethylchlorosilane). The samples were heated at 70^{o} C for 30 minutes. An internal standard (p-terphenyl-D12, and 5α-chloestane) was added. [2.2.5] These derivatized sample extracts were analyzed for each of the molecular tracer compounds by GC-MS in selective ion monitoring (SIM) mode, using a DB1701 column (J&W Scientific, 30 m, 0.25 mm i.d., 0.025 μm film thickness) on an Agilent 6890 series GC interfaced with a 5973n series MSD using electron impact ionization.

The feces extracts were concentrated to 250 μL and subjected to treatment with 5% deactivated silica gel chromatography. The column was eluted sequentially with hexane, 10% DCM in Hexane, 15% MeOH in DCM. More polar compounds remained on the silica gel column. The eluents were combined and reduced to 1 mL by rotoevaporation. They were then prepared for GC-MS like the extracts from the water samples.

All source sample extracts were analyzed by GC-MS using the same protocols described in Chapter 4 for stream water samples.

Fecal steroid end-member model

Principal component analysis (PCA) was used to develop an end-member model using selected fecal steroid ratios with potential to predict sources of human and animal waste contamination in streams across the NYC watershed. Fecal steroid ratios, for all sources listed in Table 5.1 were included in PCAs without any data transformation. An intial exploratory PCA was run using the 13 steroid ratios listed in Table 5.2. Most of these ratios have been used by previously published studies to distinguish fecal sources or were were structural analogues to previously used ratios (See Discussion below). Because the goal was to develop as simple a PCA as possible that could be used to separate sources, ratios that appeared to have minimal independent explanatory power were excluded iteratively. Subsquent PCAs were run until it was determined that the maximum amount of source separation was achieved, while also explaining a majority of the variance of the input values. Ratios were excluded in these subsequent analyses based on a minimum overall contribution to explained variance for the first and second axes and a subjective assessment of the redundancy of one ratio versus another in separating sources. The PCA was run using the correlation matrix and confined to using the first two factors for ease in both interpretation and prediction.

Prediction using the PCA model involves the factor scoring coefficients along with the mean and standard deviation of the input data to the PCA. Because the PCA is based on standardized variables, i.e subtracting the mean from each input value and dividing by the standard deviation, the input data for prediction must also be standardized. An important assumption is that the values used for prediction are derived from the same population (i.e. same mean and variance) as the original input values. After standardization, the prediction data are multiplied by the factor scoring coefficients, both the first and second factors, and then plotted along with the original input data. Source inferences for the predicted values can then be made based on the relative position of the plotted predicted values relative to the original input values.

The fecal contamination source predictive model was only applied to stream molecular tracer data collected during Phase II of the project (2003-05). This was due to having three fecal steroid compounds (eCOP, eCHO, and eEPI), important to determining sources of fecal contaimation, only analyzed during the second phase of the project. Site mean ratios were used as predictive values, without any ratio censoring applied (see Methods/Quantification section of Chapter 4 for ratio censoring description). The predictive model was also applied to a validation dataset of fecal steroid signatures of known sources similar to the sources sampled in this study. This validation dataset was derived from fecal steroid source tracking work conducted in Australia (Leeming et al. 1996, Leeming et al. 1998). The predicted factor scores for the stream sites were correlated (Pearson) against selected watershed characteristics to assess correspondence between predicted source signatures and watershed-level measures of human influence

Results and Discussion

Source sample composition.

Total fecal steroid concentrations in the Septic and WWTP influent samples were roughly comparable at approximately 1000 ug/L (Fig. 5.1A). In contrast, effluent samples from septic systems were 1 to 2 orders of magnitude greater than WWTP effluent samples. One of the three

septic effluent samples had a total fecal steroid concentration that was among the highest of any of the influent or effluent waste samples. Among the WWTP effluent samples there was also a high degree of variablility where one sample had a concentration > 10 ug/L with the other 3 samples < 1 ug/L. Mean stream water total fecal steroid concentrations were within the range of WWTP effluent concentrations. The more urban region, EOH, had a mean stream water concentration (1.3 ug/L) that was more than twice the corresponding WOH mean value (0.6 ug/L).

The fecal steroid compostion of the wastewater samples were generally dominated by two compounds: bCOP and CHO (Fig. 5.2A). Cholesterol (CHO) tends to be found in the feces of many warm-blooded animals. Coprostanol (bCOP) has been found to be a major component of human feces in previous work (Leeming et al. 1996), which follows from the fact that bCOP is a product of the bacterial degradation of CHO occuring in humans (Björkhem et al. 1973, Walker et al. 1982). A notable exception to the fecal steroid composition of wastewater samples in this study was the composition for one of the WWTP effluent samples (label 'S' in Fig. 5.2A) where eCHO was the dominate compound. The fecal steroid composition of the WWTP influent samples, and to a lesser extent, the septic influent samples, were rather similar. The effluent sample for both effluent types, however, were much less similar as compared to corresponding influent samples and also across samples of a given wastewater effluent type.

The range in total fecal steroid concentrations found in waste water effluent samples collected in this study coupled with the differences in fecal steroid composition of these samples has potential implications for the fate of other related emerging contaminants. The term, 'emerging contamintants', has been coined to cover a host of trace compounds, from fecal steroids to caffeine to pharmaceuticals, that occur in the environment (Petrovic et al. 2003, Phillips et al. 2005). As noted by (Phillips et al. 2005), relatively little is known regarding the effectiveness of WWTP and septic systems at removing such emerging contaminants. The data presented here do suggest that for fecal steroids, substantial removal of these compounds can and does occur during the wastewater treatement process despite the fact that these compounds are not directly targeted in the treatment process. Yet, there is also a great deal of variability in the amount of removal, certainly between septic and treatment plants, but also within each of these treatment types.

Animal feces showed a wide range in total steroid concentrations (Fig. 5.1B) as well as in the relative composition of the measured fecal steroids (Fig. 5.2B). Omnivores, including the opossum, raccoon, and seagull, had the highest total fecal concentrations at > 1000 ug/g. The herbivores (cow, horse, deer, beaver, and goose) had a range in total concentrations of approximately 200 to 1000 ug/g. The more dramatic differences between the animal feces occurred when examining the relative composition of the fecal steroids. The large herbivores (excluding the goose samples) all tended to have very similar and somewhat evenly distributed relative amounts among the 10 steroid compounds. Dramatic differences were observed within the omnivore group, especially between the opossum versus the raccoon and gull samples. Both the raccoon and gull samples were dominated by CHO while both goose samples were dominated by eCHO. These differences in steroid composition among the various animal species and between animal species and humans demonstrate the utility in using these compounds in specific tracers of fecal contamination.

The focus of this source signature effort has been on fecal steroids. However, the other molecular tracers (PAHs, fragrances, caffeine) were also measured in the source samples. PAHs were only found in WWTP influent and effluent samples with a total PAH concentration range for WWTP influent samples of 2.0 to 4.4 μg/L compared to the range for effluent samples of 0.06 to 0.14 μg/L. A slightly higher range in caffeine concentrations was found among the influent samples: 10.3 – 64.8 μg/L for septic sytems versus 43.3 – 57.9 μg/L for WWTP (Fig. 5.3A). As was shown for fecal steroids, effluent samples showed considerable decreases in caffeine concentrations relative to influent values: 0.09 – 2.7 μg/L for septic systems and 0.03 – 2.3 μg/L for WWTPs. Caffeine was not found in any of the animal feces samples. A wide range in total fragrance concentrations were found for the influent and effluent samples of both septic systems and WWTPs (Fig. 5.3B,C). Septic influent samples had the most dramatic range in total fragrance concentrations of 0.8 to 47.8 μg/L compared to a range of 4.7 to 21.5 μg/L for WWTP influent samples. Once again, as was shown with fecal steroids and caffeine, effluent fragrance concentrations were much lower relative to influent values: 1.1 to 5.9 μg/L for septic and 0.05 to 2.9 μg/L for WWTPs.

Fecal steroid end-member model

Human fecal material has higher relative concentrations of coprostanol (bCOP) to other steroids compared to all other animals (Walker et al. 1982, Leeming et al. 1996). As a result, previous studies have used ratios of coprostanol to other steroids as a tracer for human fecal contamination. For example, Grimalt et al. (1990) and Elhmmali et al. (2000) both used the ratio bCOP/(bCOP+aCOP) to distinguish between sites with high urban sewage loads and pristine sites. Grimalt et al. (1990) also found the ratio of cholestanone isomers bONE/(bONE+aONE) to similarily distinguish urban versus pristine sites, and they suggest that values of either ratio >0.2 suggests human-dominated fecal sources. However, their study sites did not have any appreciable livestock, and Standley et al. (2000) show both of these ratios can exceed 0.85 for cattle, horses and deer.

The work of Leeming et al. (1996, 1998) are the most extensive studies of fecal steroid signatures for a variety of animal species. Their data show that no single simple ratio clearly separates humans from other sources. However, a PCA analysis of the steroid data did an excellent job of separating sources (Leeming et al. 1996). Their PCA shows for instance that human fecal materials tended to have higher proportions of 5β stanols (bCOP, EPI, eCOP, eEPI) over other sterols and higher proportions of C_{27} sterols (bCOP, EPI, CHO, aCOP) over C_{29} steroids (eCOP, eEPI, eCHO, SNOL). Given these findings, we explored principal components analyses of fecal steroid ratios in our dataset from NY that might reflect these differences (Table 5.2).

The PCA for defining fecal contamination sources in the NYC watershed (Fig. 5.4) was determined based on using 7 of the 13 fecal source ratios listed in Table 5.2. Combined, the first 2 factors of the PCA explained 87% of the variability in the input data, with the majority of that explained variability (67%) found in the first PC factor. Strong separation between non-human and human sources occurred along the first principal component (PC) factor (i.e. x-axis in Fig 5.4B and C) while birds vs. herbivores and septic vs. WWTP sources were separated by the second PC factor (i.e y-axes in Fig. 5.4B and C). A noteworthy exception to the human signal

gradient along the first PC factor is a single WWTP effluent signature that plotted to the left of the first PC factor; i.e. among non-human signatures and specifically among the group of herbivore signatures. This particular WWTP may be operating under more stringent treatment requirements compared to the other sampled WWTP, however, no quantitative data have been compiled to date to support this observation.

The predicted source signatures based on the validation dataset from Leeming et al. (1996, 1998) (Fig. 5.4B) demonstrate that the derived multivariate model for separating fecal contamination sources was robust in terms of separating human from nonhuman sources. The 3 human fecal signatures from the validation dataset plotted to the right along the first PC factor that defined increasing human signal. Only one animal species from the validation dataset, a seagull, also plotted among the cluster of input data points defining human source signatures. Given the omnivorious nature of seagulls and their apparent fondness for human food, this is not necessarily a surprising result. It should be noted though, that the input data also contained a source signature for a gull that did not plot near the cluster of human source signature data. The multivariate model was less successful in separating among the non-human source validation data. The only non-human source validation data to plot among similarily defined input data were the herbivore species (6 total). Despite the differences between the predicted versus actual sources for the validation data, the multivariate model did demonstrate applicability in defining source signatures beyond the input data used to develop the model. That the defined model was at all applicable beyond the geographic scope of the study region is encouraging given that the validation dataset was compiled by different researchers in another country and hemisphere.

The predicted source signatures based on Phase II stream samples (Fig. 5.4C) suggest 2 possible scenarios for fecal contamination source signatures as defined by the multivariate model: (1) dominance of non-human source signatures over human in stream water, or (2) that human fecal signatures are altered during steroid degradation within streams. There was no strong separation among stream sites receiving WWTP effluent (small, open squares in Fig. 5.4C) versus sites not receiving any WWTP effluent (small, filled circles in Fig. 5.4C). However, forested sites (green circles/squares) tended to plot farther away from the defined human fecal signature along the first PC factor, relative to both agriculturally-defined and urban sites.

Regardless of whether human fecal sources dominate or not, sites scores along Factor 1 were positively correlated with watershed-normalized WWTP effluent, % total urban area, and % total agriculture (Fig 5.5A,D, and E). The first factor site scores were also positively correlated with fecal coliform counts (Fig 5.5F) taken at selected stream sites during the last year of the project (2005). Factor 1 site scores were negatively correlated with % forested area (Fig. 5.5C; the strongest relationship among the 6 shown in Fig. 5.5). Lastly, sites scores based on Factor 2 were negatively correlated with watershed normalized WWTP effluent (Fig. 5.5B). These statistically significant relationships provide further evidence of the appropriateness of the multivariate model to separate human from nonhuman contaminant source signatures

Literature Cited

Artola-Garicano, E., I. Borkent, J. L. M. Hermens, and W. H. J. Vaes. 2003. Removal of Two Polycyclic Musks in Sewage Treatment Plants: Freely Dissolved and Total Concentrations. Environmental Science and Technology **37**:3111 -3116.

Björkhem, I., Ö. Wrange, and J.-Å. Gustafsson. 1973. Microbial Transformation of Cholesterol into Coprostanol. Properties of a 3-Oxo-□^{4}-Steroid-5□-Reductase. European Journal of Biochemistry **37**:143-147.

Buerge, I. J., T. Poiger, M. D. Müller, and H.-R. Buser. 2003. Caffeine, an Anthropogenic Marker for Wastewater Contamination of Surface Waters. Environmental Science and Technology **37**:691 -700.

Dickhut, R. M., E. A. Canuel, K. E. Gustafson, K. Liu, K. M. Arzayus, S. E. Walker, G. Edgecombe, M. O. Gaylor, and E. H. MacDonald. 2000. Automotive Sources of Carcinogenic Polycyclic Aromatic Hydrocarbons Associated with Particulate Matter in the Chesapeake Bay Region. Environmental Science and Technology **34**:4635 -4640.

Eglington, G. 1969. Organic chemistry: the organic chemist's approach. Pages 20-71 *in* G. Eglington and M. T. J. Murphy, editors. Organic Geochemsitry. Springer-Verlag, New York.

Elhmmali, M. M., D. J. Roberts, and R. P. Evershed. 2000. Combined analysis of bile acids and sterols/stanols from riverine particulates to assess sewage discharges and fecal sources. Environmental Science and Technology **34**:39-46.

Grimalt, J. O., P. Fernandez, J. M. Bayona, and J. Albaiges. 1990. Assessment of fecal sterols and ketones as indicators of urban sewage inputs to coastal waters. Environmental Science and Technology **24**:357 - 363.

Hedges, J. I., and F. G. Prahl. 1993. Early diagenisis: Consequences for applications of molecular biomarkers. Pages 237-253 *in* M. H. Engel and S. A. Macko, editors. Organic Geochemistry. Plenum Press, New York.

Leeming, R., A. Ball, N. Ashbolt, and P. Nichols. 1996. Using faecal sterols from humans and animals to distinguish faecal pollution in receiving waters. Water Research **30**:2893-2900.

Leeming, R., P. D. Nichols, and N. J. Ashbolt. 1998. Distinguishing sources of faecal pollution in Australian inland and coastal waters using sterol biomarkers and microbial faecal indicators. Research Report No 204., Water Services Association of Australia.

Miguel, A. H., T. W. Kirchstetter, R. A. Harley, and S. V. Hering. 1998. On-Road Emissions of Particulate Polycyclic Aromatic Hydrocarbons and Black Carbon from Gasoline and Diesel Vehicles. Environmental Science and Technology **32**:450-455.

Nielsen, T. 1996. Traffic contribution of polycyclic aromatic hydrocarbons in the center of a large city. Atmospheric Environment **30**:3481-3490.

Petrovic, M., S. Gonzalez, and D. Barcelo. 2003. Analysis and removal of emerging contaminants in wastewater and drinking water. TrAC Trends in Analytical Chemistry **22**:685-696.

Phillips, P. J., B. Stinson, S. D. Zaugg, E. T. Fulong, D. W. Kolpin, K. M. Esposito, B. Bodniewicz, R. Pape, and J. Anderson. 2005. A multi-disciplinary approach to the removal of emerging contaminants in municipal wastewater treatment plants in New York State, 2003-2004. Pages 5095-5124 *in* Water Environment Federation WEFTEC 78th Annual Technical Exhibition and Conference, Washington DC.

Simó, R., J. O. Grimalt, and J. Albaigés. 1997. Loss of Unburned-Fuel Hydrocarbons from Combustion Aerosols during Atmospheric Transport. Environmental Science and Technology **31**:2697-2700.

Simonich, S. L., T. W. Federle, W. S. Eckhoff, A. Rottiers, S. Webb, D. Sabaliunas, and W. de Wolf. 2002. Removal of Fragrance Materials during U.S. and European Wastewater Treatment. Environmental Science and Technology **36**:2839 -2847.

Standley, L. J., L. A. Kaplan, and D. Smith. 2000. Molecular tracers of organic matter sources to surface water resources. Environmental Science and Technology **34**:3124-3130.

Stein, E. D., L. L. Tiefenthaler, and K. Schiff. 2006. Watershed-based sources of polycyclic aromatic hydrocarbons in urban storm water. Environmental Toxicology and Chemistry **24**:373-385.

Walker, R. W., C. K. Wun, and W. Litsky. 1982. Coprostanol as an indicator of fecal pollution. CRC Critical Reviews in Environmental Control **12**:91-112.

Yunker, M. B., R. W. Macdonald, R. Vingarzan, R. H. Mitchell, D. Goyette, and S. Sylvestre. 2002. PAHs in the Fraser River basin: a critical appraisal of PAH ratios as indicators of PAH source and composition. Organic Geochemistry **33**:489-515.

Zakaria, M. P., H. Takada, S. Tsutsumi, K. Ohno, J. Yamada, E. Kouno, and H. Kumata. 2002. Distribution of Polycyclic Aromatic Hydrocarbons (PAHs) in Rivers and Estuaries in Malaysia: A Widespread Input of Petrogenic PAHs. Environmental Science and Technology **36**:1907 -1918.

Table 5.1. Source sample types and desciptions.

Sample	Abbrev.	Description
Cow 1	CW-1	Site 1, Holstein dairy cows, fed silage and haylage, some pasture grazing, ruminant (composite)
Cow 2	CW-2	Site 2, Holstein dairy cows, fed silage and haylage, some pasture grazing, ruminant, (composite)
Cow 3	CW-3	Site 3, Holstein dairy cows, more pasture grazing, fed silage and haylage, ruminant, (composite)
Horse 1	HR-1	Site 1, grain fed, grass & hay free choice, supplements and wormer, individual animal
Horse 2	HR-2	Site 2, grain fed, grass & hay free choice, wormer, individual animal
Horse 3	HR-3	Site 2, grain fed, grass & hay free choice, wormer, individual animal
Deer 1	DR-1	Site 1, white tail deer, random sampling in one area of grazing forest
Deer 2	DR-2	Site 2, white tail deer, random sampling in different area of grazing forest
Deer 3	DR-3	Site 3, white tail deer, random sampling in different area of grazing forest
Beaver	BV	Eats predominantly tree bark. Specialized digestive system for bark
Opossum	OP	Marsupial, habitat deciduous forest or farmland. Prefer wet areas
Raccoon	RC	Lives near water, adaptable to suburbs and cities, nocturnal
Goose 1	GS-1	Site 1, Canada goose, eats grasses, leaves, roots and grains, random sampling
Goose 2	GS-2	Site 1, Canada goose, eats grasses, leaves, roots and grains, random sampling in different area of site
Gull	GL	Omnivore, composite of 7 samples. Ring Billed gull, fresh water in summer, frequents parking lots, migratory
Septic Influent 1	Sep-I1	Remediated. Raised bed (soil added) leaching field. Sampled at septic tank outlet (grab).
Septic Influent 2	Sep-I2	Remediated. Non raised soil bed leaching field. Sampled at septic tank outlet (grab).
Septic Influent 3	Sep-I3	Remediated. Leaching field up hill. Pump septage. Sampled at septic tank outlet (grab).
Septic Effluent 1	Sep-E1	Sampled at end of leaching field from lysimeter 54 inches below ground level (grab).
Septic Effluent 2	Sep-E2	Sampled at end of leaching field from lysimeter 41 inches below ground level (grab).
Septic Effluent 3	Sep-E3	Sampled at end of leaching field from lysimeter 38 inches below ground level (grab)
WWTP Influent 1	WTP-I1	Upgraded. Sampled before grey water entered WWTP (grab). Source- rural residential and small industry.
WWTP Influent 2	WTP-I2	Upgraded. Sampled before grey water entered WWTP (grab).. Source- rural residential and small industry.
WWTP Influent 3	WTP-I3	Upgraded. Sampled before grey water entered WWTP (grab). Source- rural residential, industry, agriculture.
WWTP Influent 4	WTP-I4	WWTP not upgraded. Sampled before grey water entered WWTP (grab). Source- residential
WWTP Effluent 1	WTP-E1	Sampled as water left WWTP (grab). Treatment Process: coarse bar track, primary settling tank, rotating biological contracter, secondary settling tank, sand filter, membrane filtration chlorination, dechlorination, discharge.
WWTP Effluent 2	WTP-E2	Sampled as water left WWTP (grab). Treatment process: grit chamber, aeration and settling tank, chlorination, sand filtration, dechlorination, discharge.
WWTP Effluent 3	WTP-E3	Sampled as water left WWTP (grab). Treatment process: grid channel, equilization tank, aeration basin, secondary clarifier, chlorination, sand filtration, dechlorination, discharge.
WWTP Effluent 4	WTP-E4	Sampled as water left WWTP (grab sample). Treatment Process: bar screens, grit separator, primary clarifier, trickling filter, rapid mix tank, secondary clarifier, sand filtration, chlorination, dechlorination, discharge.

Table 5.2. Fecal steroid signatures (ratios) used in the fecal matter end-member model development.

Signature (ratio)	Abbrev.	End-member model [1]	Source/Rational
bONE / (bONE + aONE)	bone/baone		Grimalt et al. 1990; Standley et al. 2000
bCOP / (bCOP + EPI)	bcop/bepicop	*	
bCOP / (bCOP + CHO)	bcop/bcopcho		
bCOP / (bCOP + eCOP)	bcop/becop		
bCOP / (bCOP + aCOP)	bcop/bacop	*	Grimalt et al. 1990; Standley et al. 2000
aCOP / (aCOP + SNOL)	acop/snolacop	*	
CHO / (CHO + eCHO)	cho/choecho	*	
EPI / (EPI + eEPI)	epi/eepi		
eCOP / (eCOP + eEPI)	ecop/ecopeepi	*	
eCOP / (eCOP + eCHO)	ecop/ecopecho		
eCOP / (eCOP + SNOL)	ecop/ecopsnol	*	
(bCOP + eCOP + EPI + eEPI) / (bCOP + eCOP + EPI + eEPI + aCOP + CHO + eCHO + SNOL)	beta/c27c29		
(bCOP + aCOP + EPI + CHO) / (bCOP + eCOP + EPI + eEPI + aCOP + CHO + eCHO + SNOL)	c27/c27c29	*	

[1] Indicates whether a ratio was included in the final end-member model; see Fig. 5.4.

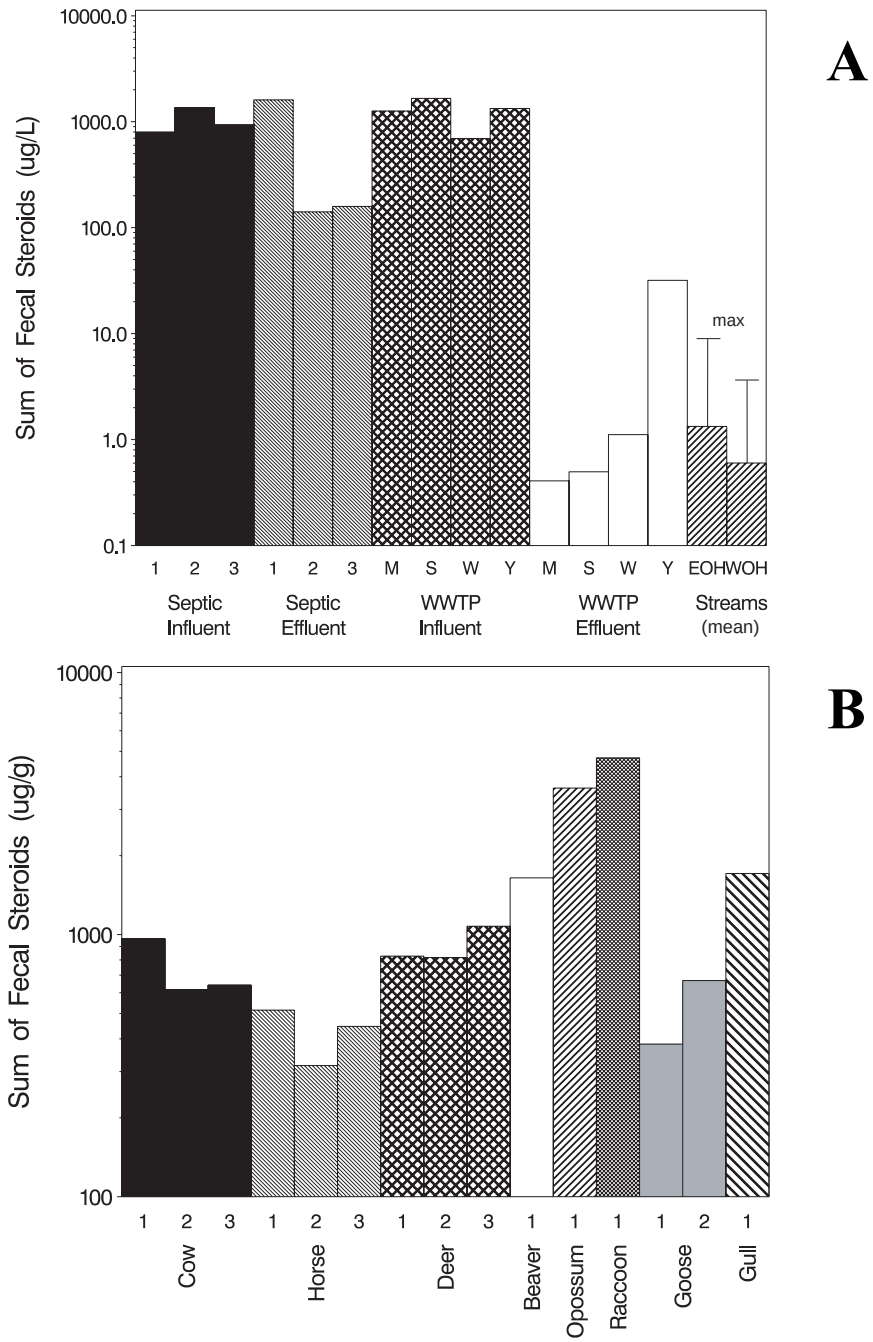

Figure 5.1. Concentrations of the sum of the ten fecal steroids measured in Phase II (FS2) – aCOP, aONE, bCOP, bONE, CHO, EPI, eCOP, eEPI, eCHO and SNOL (see table 4.1) – for all collected samples from (A) waste waters and from (B) animal feces. The mean and maximum stream water concentrations for EOH and WOH sites is also given in panel A.

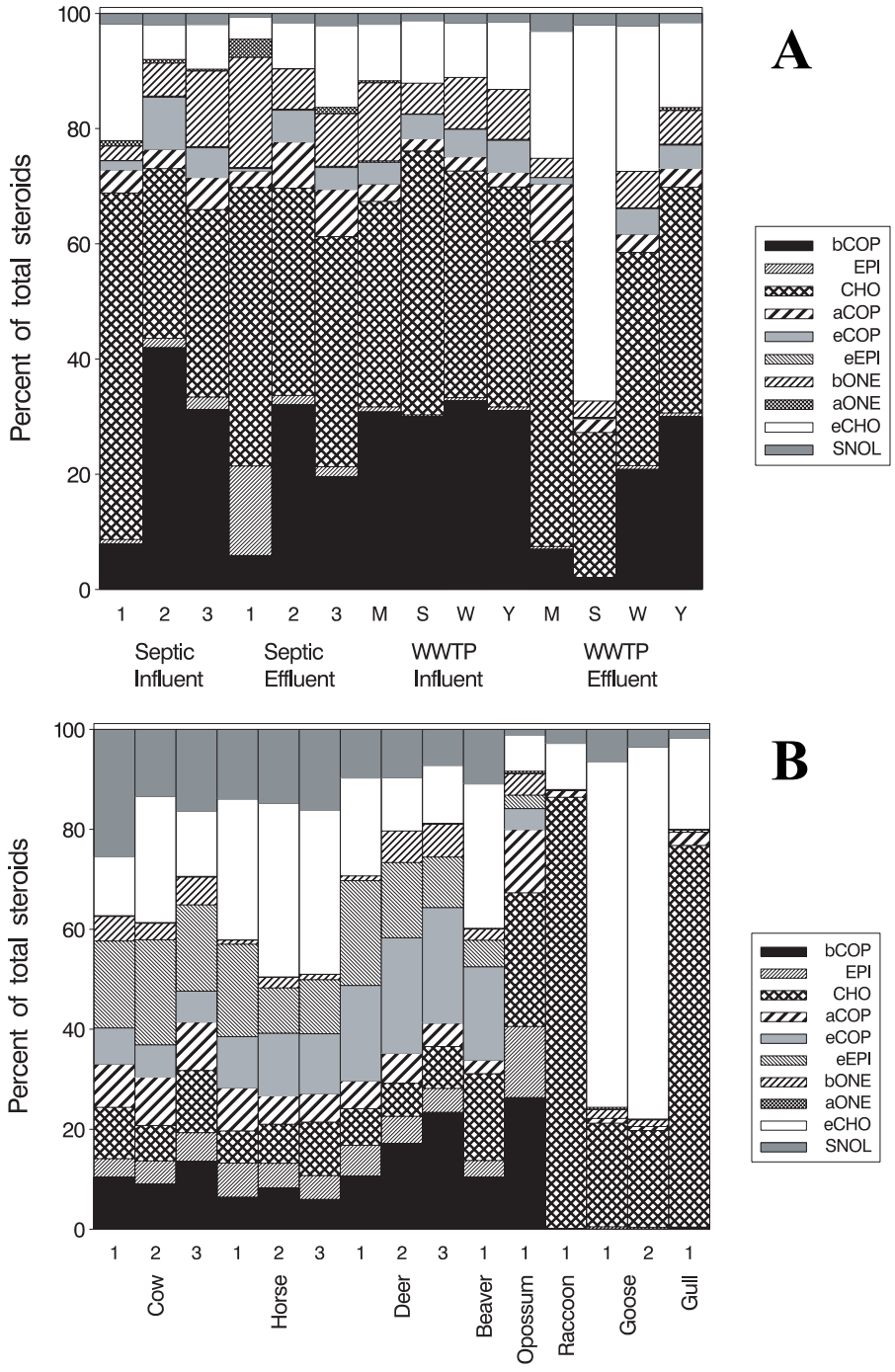

Figure 5.2. The proportion of each of ten fecal steroids to their sum for all collected samples from (A) waste waters and from (B) animal feces.

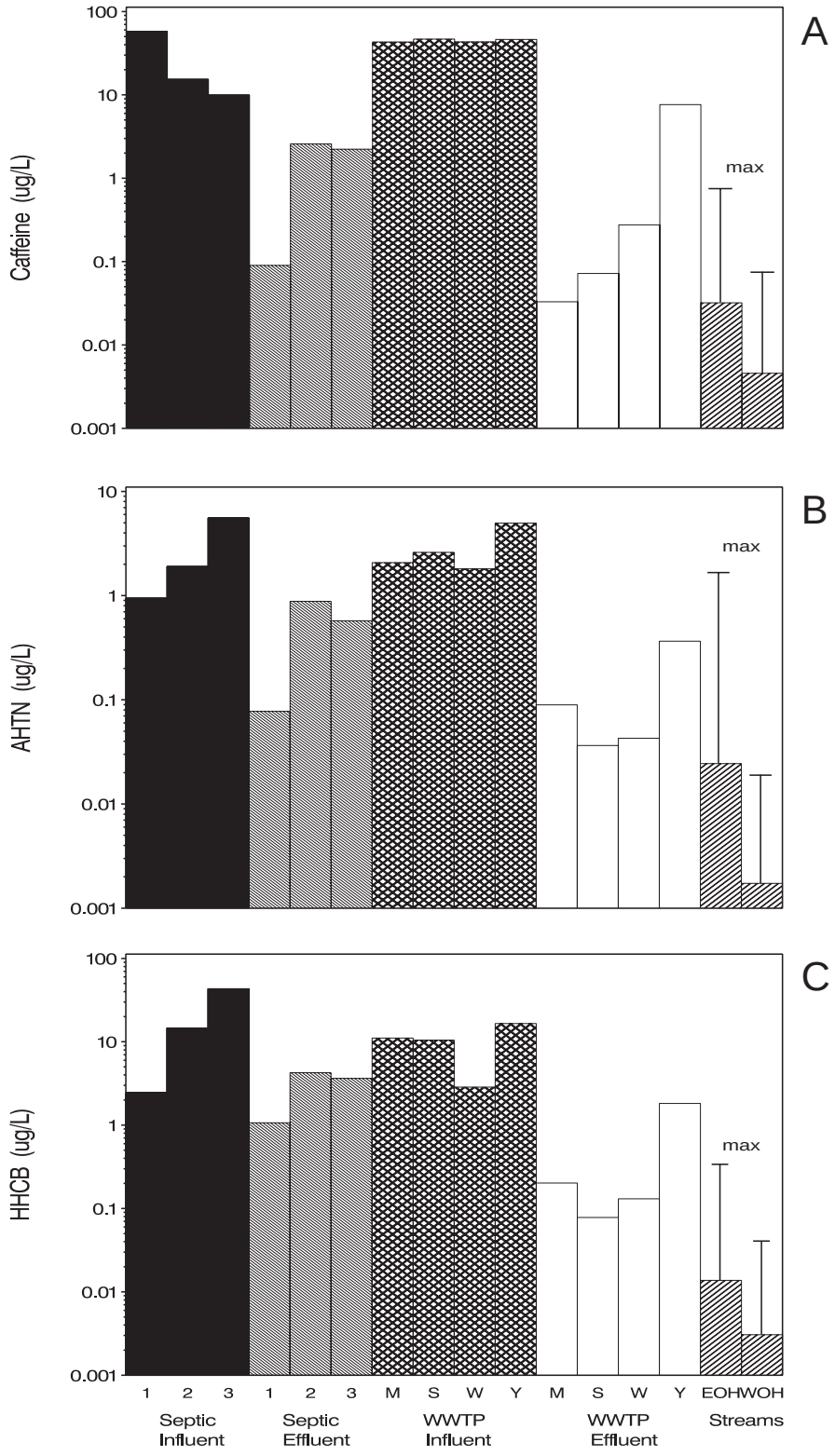

Figure 5.3. Concentrations of caffeine (A), and the fragrances AHTN (B) and HHCB (C) measured in Phase II for samples collected from waste waters. The mean and maximum stream water concentrations for EOH and WOH sites is also given in each panel.

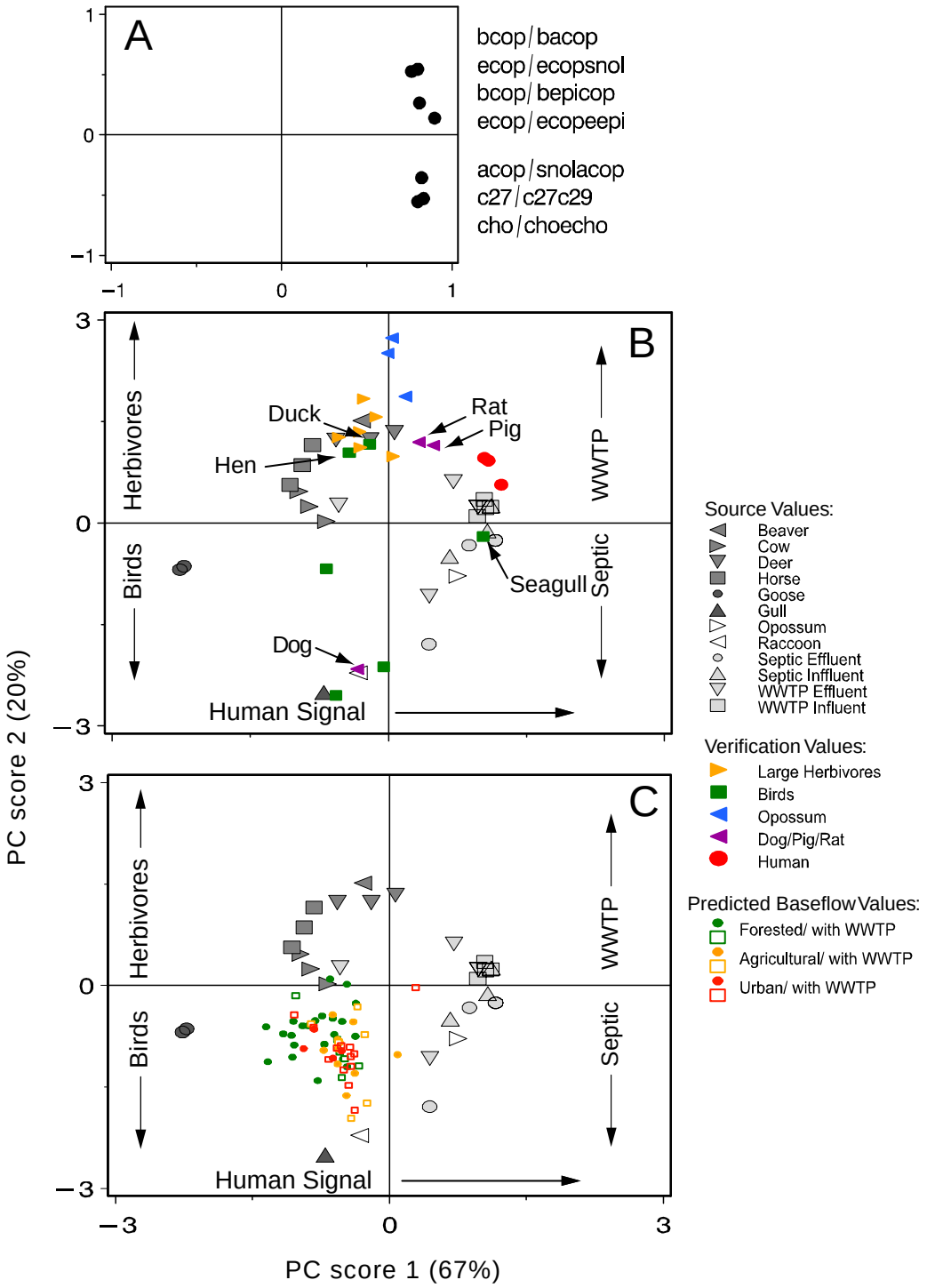

Figure 5.4. Principal Component Analysis (PCA) results for fecal steroid ratios of source samples, with ratio loadings along Factor 1 and Factor 2 shown in (A), and sample scores shown in (B) and (C). Ratio loadings were used to calculate'verification' scores for Australian fecal samples analyzed by Leeming et al. (1996 and 1998) (B), and for NY stream samples analyzed for this project (Chapter 4) (C). Forested stream sites defined as having >75% forested area with < 10% agriculture and < 10% urban; agriculture sites defined as having > 10% agriculture and < 10% urban; urban sites defined as having >10% urban area.

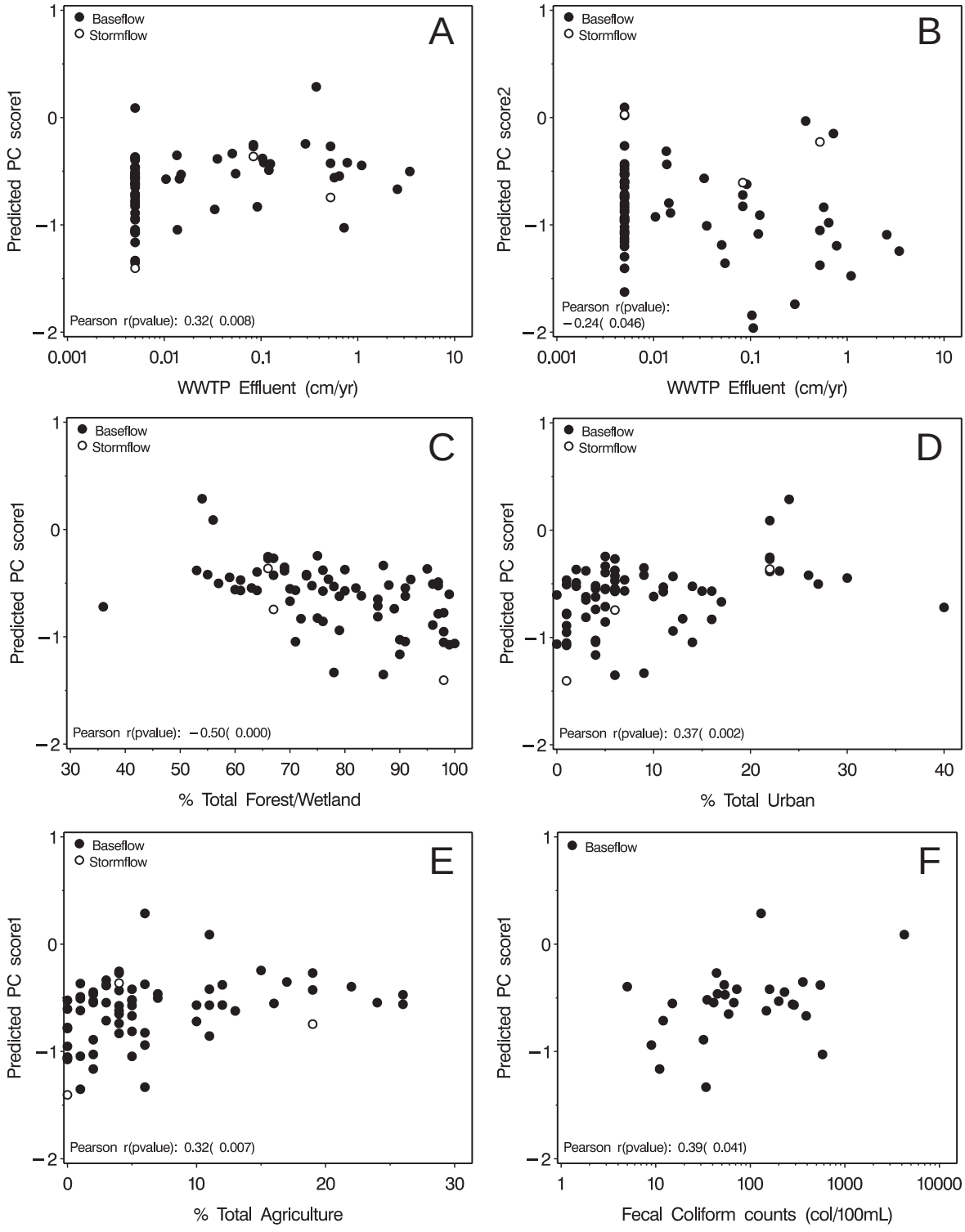

Figure 5.5. Mean sample scores for NY streams calculated from Factor 1 loadings of the PCA of fecal steroid ratios of fecal sources in NY State (see Fig. 5.4 and methods). Plotted is score 1 vs. WWTP discharge (A), score 2 vs. WWTP discharge (B), score 1 vs. % of watershed area in forest and wetland (C), score 1 vs. % of watershed in urban landuse (D), score 1 vs. % of watershed in agriculture (E) and score 1 vs. fecal coliform counts measured in stream samples collected along with tracers sampes during 2005 summer baseflow.

----------Intentionally Blank----------

Chapter 6. Organic Matter Transport

Research Task

The rivers of the world export ~1 Pg of organic matter (OM) to the oceans annually (Spitzy and Ittekkot 1991), and that OM is primarily composed of dissolved organic molecules and dead particulate matter (Wetzel 1995). This detritus provides an important source of organic energy for heterotrophic microorganisms and macroinvertebrates, sustaining stream ecosystem metabolism and contributing to the aquatic food web through the microbial loop (Pomeroy 1974, Hall et al. 2000). The concentrations of OM that are either dissolved or suspended in streams result from terrestrial inputs and in-stream production of OM followed by transformations of the OM within stream ecosystems. Inputs of OM from terrestrial environments to streams connect streams with their watersheds (Hynes 1975), and the transport within the stream can provide a longitudinal linkage between upstream production and downstream processing (Vannote et al. 1980).

With particular reference to drinking water supplies, OM provides precursors for disinfection by-products (DBP) and the carbon (C) and energy sources for bacterial regrowth. DBPs include carcinogens and mutagens resulting from reactions of OM with chemical oxidants, including trihalomethanes and haloacetic acids following chlorination (Chow et al. 2003) and ketones following ozonation (Matsuda et al. 1992). The growth of heterotrophic bacteria in water distribution systems can be promoted by the presence of biodegradable constituents within the OM pool, leading to the deterioration of water quality (Escobar et al. 2001, Laurent et al. 2005).

The U.S. EPA National Primary Drinking Water Regulations establish maximum contaminant levels for DBP concentrations and densities of bacteria. Modifications to disinfectant dosing can lead to conflicts, as high disinfectant levels increase chemical risks but lower microbial risks, and vice versa. While the OM that supports bacteria growth is not necessarily composed of the same molecules that react to form DBPs, nevertheless, a reduction in OM is an approach that could help reduce both risks simultaneously.

Land use affects stream water concentrations of dissolved and particulate OM. Here land use implies both land use and land cover. Wetlands are sources of dissolved organic C (DOC) (Gergel et al. 1999, Elder et al. 2000, Hillman et al. 2004), and forests are more retentive than agricultural lands of suspended solids (Jones et al. 2001, Dodds and Whiles 2004), particulate organic C (POC) (Neill et al. 2001, Thomas et al. 2004), and DOC (Quinn and Stroud 2002). The effects of urbanization are more equivocal leading to increases (Duncan 1999), decreases (Dodds and Whiles 2004), or no impact (Jones et al. 2001) on suspended solids. A tentative link has been found between increased DOC concentrations and urban density and drainage infrastructure (Hatt et al. 2004).

This chapter draws directly from and extends a previously published account of a 3-year data set of OM concentrations in streams from the New York City drinking water supply watersheds, the Phase I study (Kaplan et al. 2006). With the completion of Phase II, there is now a 6-year data set that provides more extensive and intensive data that support the main results and conclusions that have been published. The structure of the presentation and content of this

chapter closely follow that of the published work. In all, OM was sampled at 110 sites throughout the New York City drinking water supply watersheds and concentration patterns were analyzed to: (1) establish regional baseflow concentrations of OM, (2) estimate the magnitudes of temporal and spatial variability in those concentrations, and (3) identify which factors associated with anthropogenic modification of land use at the watershed scale affect OM concentrations. The baseline, once established, can be used in the future to assess the efficacy of best management practices designed to improve source-water quality. In addition, the concentrations of various OM constituents were related to instream processes and land use.

Methods

Samples for DOC, biodegradable DOC (BDOC), total suspended solids (TSS), and particulate organic matter (POM) were measured annually at each site during summer baseflow. Baseflow conditions were defined operationally as relatively constant stream flow, changing <10% over the 24 h preceding sampling, based on either co-located or nearby real-time USGS gauging stations. If gauges did not co-occur with a site, discharge was estimated from discharge-watershed-area regression equations developed independently for groups of watersheds within each region. During the 6-year study period, 60 sites were sampled in the first 3 years, 50 new sites were sampled in the last 3 years, and 12 sites of the original 60 sites were sampled for all 6 years.

Single samples for DOC and BDOC were collected in glassware that was rendered organic C free by combustion at 500°C for six hours. Samples were protected from the atmosphere by sealing the collection vessels with persulfate-cleaned Teflon-backed silicone-septa (Kaplan 1994). In phase I, baseflow stream samples were collected in 500-ml borosilicate bottles that were rinsed twice with site water, filled, capped, and placed on ice in the dark. Within 48 h, the samples were filtered into three 40-mL borosilicate vials for DOC and ten 40-mL borosilicate vials for BDOC analysis. Five of the vials for BDOC analyses were fixed with azide to stop any microbial activity, and the DOC concentrations in the water were measured within 1 wk. The other 5 vials were incubated for 28 d at room temperature in the dark to allow the bacterial inoculum in the filtered water to grow and metabolize the BDOC. Azide blanks were determined for DOC contributions before taking the azide solution into the field, with an acceptance criterion of <0.1 mg C/L. On average, DOC contributions from the azide were 0.023 ± 0.022 mg C/L (mean ± SD, n = 19). BDOC was calculated as the difference in DOC of water samples before and after incubation and was not corrected for azide blanks. In Phase II, 1 L borosilicate bottles were used for sampling and the water was kept on ice in a cooler prior to filtration. Filtration to remove particles was performed with precombusted glass fiber filters (Whatman GF/F), an acetal-resin syringe type filter holder, and a peristaltic pump. After incubation, the water in the vials was refiltered and DOC concentrations were measured (Kaplan 1994). DOC analyses were done in Phase I by the Pt-catalyzed persulfate oxidation method with either an OI 700 or an OI 1010 analyzer (Kaplan 1992), and during Phase II uv-promoted persulfate oxidation with a Sievers 800 analyzer was used. Direct comparisons of the OI 1010 and the Sievers 800 with stream water samples showed that results for these analyzers were equivalent (Aiken et al. 2002).

Samples for suspended particle analyses during phase I of this project were collected with a gasoline-powered pump, filling ten 5-L polyethylene bottles from the thalweg. One 5-L bottle

was reserved for subsequent analysis of TSS. The remaining water, approximately 45 L, was separated in the field into 3 fractions: <10 µm, 10 to 20 µm, and >20 µm, by filtering a known volume through a stacked series of 20 µm and 10 µm mesh Nytex® sieves. The material collected on the 20 µm and 10 µm Nytex® sieves was transferred to 250 mL polyethylene bottles by spraying the mesh with deionized water and collecting the transfer water with a funnel. Approximately 5 L of the filtrate that passed through the stacked sieves were saved for further processing. Samples were chilled at 4 °C in coolers and processed within 7 d from the time of collection.

In Phase II, 5-L samples of water for suspended particle analyses were collected in triplicate at 60% depth from the thalweg, capped and returned to the laboratory in a cooler. Samples were chilled to ~4ºC until they could be processed (within 7 days from the time of collection). In the laboratory, each sample was measured in a graduated cylinder, and as much water as would go through a GF/F filter was filtered with an ashed, tared, GF/F filter for TSS. Filters were analyzed for TSS by drying at 60ºC for ~48 hours to obtain dry weight and volatile suspended solids (VSS) by muffling at 500ºC for ~2 hours for ash weight. The dry weight per L is the TSS fraction (mg/L), while the difference between the dry weight and the ash weight per L, the ash-free dry mass (AFDM) per L, is the POM fraction (mg/L). Size fractionation was not performed during Phase II. The AFDM concentrations were converted to particulate OC (POC) concentrations, assuming that AFDM was 45% C (POC = 0.45(AFDM) (Gjessing 1976, Hedges et al. 1986). POC and DOC concentrations were added to obtain estimates of TOC.

Supplemental data generated by other scientists involved in this project were used in the analysis of DOC, BDOC, and POM patterns. These included site characterizations, including land use/cover, population density, and point source discharges (Chapter 2), concentrations of Chl *a* attached to the streambed determined as part of the macroinvertebrate studies (Chapter 7), and concentrations of fragrances associated with detergents, fecal steroids, and caffeine analyzed as part of a larger study of molecular tracers (Chapter 4).

Data Analyses

The use of single samples made it possible to achieve a broad spatial coverage of the water-supply watersheds, while field duplicates, collected as part of the quality-assurance plan, provided estimates of precision, expressed as relative % difference (DOC: 1.8 ± 2.2%, $n = 28$; BDOC: 29 ± 36%, $n = 24$; TSS: 17 ± 26%, $n = 15$; POM: 20 ± 27%, $n = 15$). Data were managed and analyzed with SAS (SAS version 9.1; SAS Institute, Cary, North Carolina). Statistical significance of all tests was set at $p < 0.05$. Concentration and point-source discharge data were $\log_{10}$ transformed, % land use/cover data were arcsine square-root transformed, and geometric means were calculated for the molecular tracer data prior to analyses. OM constituent (DOC, BDOC, POM, and TOC,) concentrations were compared between regions and among subregions within regions using analysis of variance (ANOVA). When means differed significantly, Tukey's Studentized Range test was used to determine which means differed.

Paired *t*-tests were used to examine upstream–downstream trends in concentrations of OM constituents over all six years for samples collected within a few days of each other at all sites aligned along the main stems of rivers associated with terminal reservoirs. As the comparisons made were between adjacent sites along the main stems and not multiple comparisons over the

entire watershed, *p*-values were not Bonferroni adjusted. The coefficient of variation (CV) associated with the 6-y mean summer baseflow concentration was used to examine interannual variability of each OM constituent at each site. The influence of baseflow discharge on interannual variability of concentrations of OM constituents was examined using analysis of covariance (ANCOVA).

Spearman Rank Correlation was used to relate mean concentrations of OM constituents to % forested area while simple linear regression was used to determine whether mean concentrations of OM constituents were related to all other land use/cover variables or to other water-chemistry variables (from the supplemental data sets, see above). Stepwise multiple linear regression (MLR) with a significance cutoff of $p < 0.05$ for including independent variables was used to determine the influence of land use/cover (from the supplemental data sets, see above) on mean concentrations of organic C constituents. R^2 values, adjusted for the number of explanatory variables included in final models, were used as a measure of the variance explained by each MLR.

Results

Spatial patterns

Regions. The 6-y mean baseflow concentrations of TOC in the East of Hudson (EOH) exceeded those in the West of Hudson (WOH) by 2.2x (ANOVA: $p < 0.01$; Table 6.1). DOC concentrations exceeded POC concentrations (DOC:POC > 1) at every site. The range of ratios was considerably broader in the EOH region (1.7 [Secor Brook at West Mahopac, site 43] to 32.7 [Cross River in Ward Pound Ridge Resv., site 52]) than the WOH region (2.8 [Schoharie Creek near Prattsville, site 21] to 10.5 [W. Br. Neversink River above Frost Valley, site 122]), and the mean ratio was significantly higher in the EOH than in the WOH region (EOH: 9.5 ± 6.1, WOH: 6.3 ± 2.0; ANOVA: $p < 0.01$).

Despite considerable overlap among some subregions, DOC concentrations differed significantly between regions (ANOVA, $p < 0.01$; Table 6.1, Fig. 6.1A, B). The 5 sites with the highest DOC concentrations, all ≥ 5 mg C/L, were from the EOH region (sites 36 and 127 in the West Branch Croton River [WBC] subregion, 44 in the East Branch Croton River [EBC] subregion, 49 in the Muscoot River [MSC] subregion, and 149 in the Cross River [CRS] subregion; Fig. 1A), whereas the 5 sites with the lowest DOC concentrations, all < 1 mg C/L, were from the WOH region (sites 19 in the Schoharie Creek [SCH] subregion, 22, 120, and 159 in the Esopus Creek [ESP] subregion, and 30 in the Rondout Creek [RND] subregion; Fig. 6.1B).

BDOC concentrations were higher in the EOH region than in the WOH (ANOVA : $p < 0.01$; Table 6.1). BDOC concentrations <0.35 mg/L were observed for ~50% of the EOH sites (Fig. 6.2A) and ~75% of the WOH sites (Fig. 6.2B). However, BDOC as a % of DOC was significantly higher in the WOH region than in the EOH region (ANOVA: $p < 0.01$; Table 1).

Most of the TSS particles were in the 0.5- to 10-µm size range (EOH: 67 ± 17%, range = 28–91%; WOH: 73 ± 12%, range = 50–96%), as was most POM (EOH: 71 ± 15%, range = 36–92%; WOH: 77 ± 11%, range = 48–94%). The % of TSS consisting of POM did not differ between regions, but POM concentrations were significantly higher in the EOH region than in the WOH

region (ANOVA: $p < 0.03$; Table 6.1). POM concentrations <1 mg/L were observed at 19 of 53 (36%) EOH sites (Fig. 6.3A) and at 46 of 57 (81%) WOH sites (Fig. 6.3B). Three of the 5 sites with the lowest POM concentrations (all < 0.4 mg/L) were in the EOH region, but in the EOH region POM concentrations were >2 mg/L at 13 sites and > 3 mg/L at 9 sites.

Among subregions. Concentrations of OM constituents were more similar among subregions in the EOH region than in the WOH region. While TOC, DOC, BDOC, and POM concentrations and the % of DOC consisting of BDOC was highest in the Amawalk Reservoir and DOC, BDOC, and POM concentrations in the Cross River subregion were the next highest within the EOH, none of these differences were statistically significant. The 5 EOH sites (59, 32, 48, 141, and 50) with the lowest mean DOC concentrations were distributed among all different EOH subregions (Fig. 6.1A). These sites also had low concentrations of BDOC (≤0.2 mg/L; Fig. 6.2A) and POM (<1.5 mg/L; Fig. 6.3A). The 5 sites were further characterized by small- to mid-sized watershed areas (0.2–17.7 km^2), and broad ranges of population density (22.4–466 ind./km^2) and % wetland land cover (0.9–6.3%) (see Technical Design Chapter, Chapter 2). Another common element for all 5 sites with low OM concentrations was the absence of known point-source discharges under the State Pollution Discharge Elimination System (SPDE), typically wastewater treatment plant effluents (see Technical Design Chapter, Chapter 2).

Concentrations of OM constituents in the WOH subregions generally declined along the sequence: West Branch Delaware (WBD) > Schoharie Creek (SCH) > East Branch Delaware (EBD) > Neversink River (NVK) > Esopus Creek (ESP) > Rondout Creek (RND) (Table 6.1). TOC, DOC (Fig. 6.1B), and BDOC (Fig. 6.2B) concentrations were significantly higher in WBD than in NVK, ESP, or RND (ANOVA, Tukey's test: $p < 0.05$; Table 1). POM concentrations did not differ among subregions (ANOVA, Tukey's test: $p > 0.05$; Table 6.1, Fig. 6.3B). The sequence of declining OM constituent concentrations among the WOH subregions corresponded closely to increases in % forested land cover (Spearman Rank Correlation: $r = –0.94$, $p < 0.005$), which increased along the sequence of subregions: 65.1% (WBD) < 82.4% (EBD) < 89.1% (SCH) <96.6% (ESP) < 97.1% (NVR) < 97.2% (RND).

Within-watershed spatial patterns. Upstream–downstream changes in organic C concentrations were examined for longitudinal (upstream to downstream) trends in concentrations. Study watersheds in the WOH region were associated with terminal reservoirs, and a subset of sites in each watershed was aligned along the main stem of the river. In addition to concentration trends, fluxes (concentration × discharge) of OM moving toward the reservoirs where examined when baseflow samples from the main stem were collected on the same day or within a few days of each other. Despite consistent upstream–downstream differences at some sites over 3-y periods, or in one case, a 6-y period, few upstream–downstream comparisons were significant.

In the WOH region, DOC increased in the downstream direction in all 3 y during Phase I in the WBD subregion between sites 1 and 3 (paired *t*-test: $p = 0.22$) and in the ESP subregion between sites 22 and 23 (paired *t*-test: $p = 0.14$) and in all 6 years between sites 23 and 26 (paired *t*-test: $p < 0.01$). The Schoharie Aqueduct, transporting water from the Schoharie Reservoir to the Ashokan Reservoir, is between sites 23 and 26 and strongly affects water quality measured at site 26. Concentration changes within Birch Creek from upstream (site

119), measured during Phase II, were not consistent. Two other upstream–downstream DOC concentration patterns seen in Phase I sampling involved mixing of tributary inputs. In the EBD subregion, DOC concentrations decreased between sites 10 and 13 (paired *t*-test: $p < 0.03$), a pattern that probably reflected dilution of DOC at site 13 caused by the entry of water with low DOC concentrations from the Dry Brook tributary (site 12) and from groundwater. When an upstream site in the EBD subregion was included in Phase II (site 107), the upstream-downstream changes in DOC concentrations were not consistent. In the Neversink River, DOC concentrations were always higher in the East Branch Neversink River (site 28) than in the West Branch Neversink River (site 27) yielding intermediate DOC concentrations in the Neversink River below the confluence (site 29; paired *t*-tests: $p = 0.25$). DOC flux increased in the downstream direction for all pairs of mainstem sites in all watersheds in the WOH region, including those sites without consistent increases in downstream concentration. No consistent longitudinal concentration patterns were observed for BDOC, but BDOC flux increased downstream in the EBD subregion based on data from the 2 y when samples were collected on the same dates.

POM increased in the downstream direction in all 3 y of Phase I sampling in Schoharie Creek between site 18 and site 21 (paired *t*-test: $p = 0.18$). POM concentration and watershed area were significantly positively correlated ($r = 0.39$, $p < 0.02$) when all watersheds in the WOH region with >78% forest land cover were considered. POM flux increased in the downstream direction in all watersheds except the WBD. DOC dominated the TOC concentration pool at all sites, and the TOC flux pattern reflected the DOC flux pattern, even when POM flux did not increase downstream.

One upstream–downstream mainstem comparison was made in the EOH region during Phase I and two new comparisons in Phase II. In the Kisco River DOC, BDOC, and POM increased between the upstream site (57) and the downstream site (55) (paired *t*-tests: $p < 0.02$, $p = 0.06$, $p < 0.03$, respectively) during Phase I. Further upstream on the Kisco River during Phase II, there were consistent increases between sites 142 and 55 in both DOC ($p = 0.06$) and POM ($p = 0.11$), but neither of these changes were statistically significant. In the Titicus River, there were consistent decreases in downstream concentrations of DOC ($p = 0.06$) and POM ($p = 0.02$), but not BDOC between sites 131 and 130, and only the POM changes were significant.

Interannual variability in organic C concentrations. The coefficient of variation (cv) for analyte concentrations at a site over the course of the study can be used as a measure of interannual variability. Mean cv's for all sites in the EOH region were 20% for DOC (range: 1–62%), 44% for BDOC (range: 1–119%), and 57% for POM (range: 1–145%), and in the WOH region, 18% for DOC (range: 2–64%), 33% for BDOC (range: 4–102%), and 44% for POM (range: 5–135%) in the WOH region. During Phase I, DOC concentrations decreased between years 1 and 2 and increased between years 2 and 3 at several sites, and these variations were directly related to changes in baseflow discharge (ANCOVA: $p < 0.01$). Extending this analysis to all data from Phases I and II, the relationships between baseflow discharge and DOC concentration were positive and significant in both the EOH and WOH regions (ANCOVA: $p < 0.02$, EOH; $p < 0.001$, WOH). There were significant site effects for both regions (ANCOVA: $p < 0.025$, EOH; $p < 0.008$, WOH). Considering individual sites, based on 3-year data sets, discharge and DOC concentrations were strongly positively correlated ($r > 0.94$) at 13 sites in the

EOH and at 32 sites in the WOH. When considering the 12 sites for which there are 6 years of data, the correlations of baseflow discharge and DOC concentration were positive and significant in 4 WOH sites and 1 EOH site ($p < 0.05$).

Relationships among OM constituents and land use/cover and supplemental variables

EOH. Watershed-area-normalized point-source discharges (SPDE effluents) were 3.5× to 9.5× greater at sites 43, 49, 58, 132, and 145 than at the site receiving the next highest discharge, and 29 of the EOH sites received no SPDE discharges. These large disparities in SPDE discharges across the EOH region strongly influenced the relationships between OM constituents and molecular tracers specific to human wastewater (fragrances and caffeine) and fecal matter (total fecal steroids). When data from all EOH sites were considered, DOC and BDOC were positively correlated with fragrances (DOC: $r = 0.40$, $p < 0.01$; BDOC: $r = 0.53$, $p < 0.01$), caffeine (DOC: $r = 0.50$, $p < 0.01$; BDOC: $r = 0.65$, $p < 0.01$), and total fecal steroids (DOC: $r = 0.52$, $p < 0.01$; BDOC: $r = 0.63$, $p < 0.01$), and POM was positively correlated with fecal steroids ($r = 0.52$, $p < 0.01$). When the values for sites 43, 49, 58, 132, and 145 were omitted the correlations of caffeine and fecal steroids (Fig. 6.4A,B) with DOC, BDOC, or POM were still significant, but the correlations of DOC and BDOC with fragrances were not. Percent wetlands was positively correlated with DOC ($r = 0.61$, $p < 0.01$) and BDOC ($r = 0.63$, $p < 0.01$), and these correlations improved when the high SPDE sites were omitted (Fig. 6.4C) but correlations between OM constituents and benthic chlorophyll *a* were not significant.

The % wetlands and SPDE discharges explained most of the variance in DOC and BDOC concentrations in MLR models using all sites and % wetlands, road density and % residential explained most of the variance in POM concentrations (Table 6.2). However, the models were sensitive to the effects of SPDE discharges at sites 43, 49, 58, 132 and 145 and when these sites were removed from the analysis, % wetlands explained 36% of the variance in DOC concentrations, % wetlands and % industry explained 61% of the variance in BDOC concentrations, and % mixed forest and % orchard explained 46% of the variance in POM concentrations.

WOH. The 6-y mean concentrations of DOC, BDOC, and POM were positively related to the molecular tracer caffeine (DOC: $r = 0.40$, $p < 0.01$; BDOC: $r = 0.64$, $p < 0.01$; POM: $r = 0.28$, $p < 0.04$) and fecal steroids (DOC: $r = 0.52$, $p < 0.01$; BDOC: $r = 0.84$, $p < 0.01$; POM: $r = 0.56$, $p < 0.01$; Fig. 6.5A,B). Only BDOC was related to concentrations of fragrances ($r = 0.37$, $p < 0.01$). DOC, BDOC, and POM were positively related to % agriculture (a combination of farmstead, cropland, and grassland) (DOC: $r = 0.67$, $p < 0.01$; BDOC: $r = 0.62$, $p < 0.01$; POM: $r = 0.36$, $p < 0.01$, Fig. 6.5C) and negatively related to % deciduous forest (DOC: $r = -0.67$, $p < 0.01$; BDOC: $r = -0.52$, $p < 0.01$; Fig. 6.5D). The 9 sites with the highest % agriculture were located in the WBD. DOC and BDOC also were related to the density of benthic chlorophyll *a* (DOC: $r = 0.35$, $p < 0.01$; BDOC: $r = 0.44$, $p < 0.01$). Chlorophyll *a*, in turn, was related to nutrient concentrations (total P: $r = 0.61$, $p < 0.01$; free + organically bound NH_3-N: $r = 0.48$, $p < 0.01$).

A MLR analysis showed that % deciduous forest (–) and % coniferous forest (–) explained most of the variance the DOC concentrations, while % wetlands (+), mixed forest (–), and

industry (–) explained most of the variance in BDOC concentrations. A MLR with SPDE (+) and % mixed forest (–) explained most of the variance in POM concentrations (Table 6.2).

Discussion

Baseflow sampling

The broad spatial coverage and 6-y time frame of our monitoring efforts within a large, yet constrained geographic region combined with landuse/land-cover data provided an in-depth perspective on the quantity and character of OM transported by these streams under baseflow conditions. Our study was not intended to generate annual export budgets of OM for the watersheds. In fact, such an objective would have required focusing on fluxes that occurred during storms (Hinton et al. 1997, Buffam et al. 2001). Instead, our study was done under baseflow conditions to provide a baseline of OM concentrations measured under conditions that were easier to replicate than stormflow conditions. Thus, our study was designed to facilitate comparisons with surveys done in the future.

Baseflow can account for as much as 67% of the total runoff in upland watersheds in the Mid-Atlantic region (Olmsted and Hely 1962). The application of a hydrograph separation technique to 50 USGS-gauged streams draining the major watersheds in the EOH and WOH regions revealed that average annual baseflow accounted for 41% to 67% of the total discharge during the 2000 to 2005 study period (C. L. Dow, Stroud Water Research Center, personal communication). OM fluxes are influenced by increases in TOC concentrations and changes in TOC quality during storm flows. However, the contribution of baseflow to total discharge and the fact that weather patterns in the region keep streams under baseflow conditions more often than stormflow conditions suggest that samples collected under baseflow conditions provide an appropriate reflection of landuse and land-cover impacts on OM components of water quality.

Composition of OM

Our findings that TOC concentrations at baseflow were dominated by DOC and that POM in seston was dominated by fine particles across both regions were consistent with observations from watersheds across a wide area of temperate North America, including the Cascade Mountains of Oregon (Naiman and Sedell 1979), the Boreal biome of eastern Canada (Naiman 1982), the southern Appalachian Mountains (Wallace et al. 1982), sections of Pennsylvania, Michigan, Idaho, and Oregon (Minshall et al. 1983), and southwestern British Columbia (Kiffney and Bull 2000). Streams in which POC dominates the TOC pool have been studied, but these studies included measurements made during storms when POC may increase proportionately more than DOC (Golladay 1997, Kaiser et al. 2004), streams in the headwaters of protected forested watersheds that are influenced by low-DOC ground waters and receive large inputs of forest litter (Comiskey 1978), or large turbid rivers, such as the Brazos or Missouri Rivers in North America (Malcolm and Durum 1976), or the Amazon (Aufdenkampe et al. 2007) that consistently transport high concentrations of suspended sediments.

POM size classes in our study included a 0.5- to 10-μm size class, which falls within the range of ultrafine particulate OM (Minshall et al. 1983). Our observation that >70% of POM in both regions was in this size class emphasizes the quantitative importance of the smallest organic

particles in the seston of low- to mid-order streams. The consistent importance of this size class across the wide variety of streams and land uses suggests that similar instream physical transport and retention processes, rather than variations in sources, controlled the size distributions of organic particles in suspension.

The 0.5- to 10-µm size class overlaps with the size of protozoan pathogens such as *Cryptosporidium*, which has been identified in storm samples from the WOH and EOH regions (Jiang et al. 2005) and is a particular concern in drinking water. However, *Cryptosporidium* is a specialized form of POM, and without data specific to the transport behavior of these spores relative to the bulk POM, our POM data should not be considered representative of *Cryptosporidium* transport behavior.

Spatial and temporal patterns in DOC composition

Increases in DOC concentrations with distance downstream, as observed for some sites in the WBD and ESP watersheds, have been reported previously for small headwater streams dominated by low DOC concentrations from groundwater sources (Kaplan et al. 1980, Wallace et al. 1982, Tate and Meyer 1983). Increases in POM concentrations with stream size also have been reported (Whiles and Dodds 2002). A more general finding for DOC, based on data for 31 streams, was that DOM concentrations and DOM flux increased as a function of watershed area or stream order. This pattern suggests that DOM is sufficiently refractory to accumulate in larger streams (Mulholland 1997), and it further suggests that the DOM is derived primarily from the terrestrial environment (allochthonous C) because much of the autochthonous DOM in streams is biologically labile (Kaplan and Bott 1982). However, DOC concentrations did not change systematically with distance downstream in the Tagliamento River system, where much of the DOC was recalcitrant soil-derived C (Kaiser et al. 2004). The concentrations of BDOC in our study indicated that most DOC was refractory, despite the fact that a significant fraction of the DOC was biodegradable.

Rates of ecosystem metabolism indicate that massive microbial degradation of DOC occurs in streams and rivers (Cole and Caraco 2001, Mayorga et al. 2005, Cole et al. 2007, Battin et al. 2008), including metabolism within the hyporheic zone (Sobczak and Findlay 2002). The slow metabolism of a large recalcitrant DOC pool is considered instrumental in providing metabolic stability within stream ecosystems (Wetzel 2003). However, the processes that continually produce, transform, and consume DOC molecules in transport complicate attempts to understand the dynamics of DOC concentrations in streams and rivers without direct measurements of uptake rates (Kaplan et al. 2007).

Allochthonous sources of OM dominate the pool of OM transported in most streams in the Eastern Deciduous Forest biome (Webster and Meyer 1997). However, autochthonous sources of DOC certainly can contribute significantly to TOC in forest streams during seasons when the forest canopy is open (Kaplan and Bott 1982), in desert streams where adequate sunlight and infrequent storms allow algal biomass to accumulate (Jones et al. 1996), and in forest streams when logging opens the forest canopy and facilitates chlorophyll *a* accrual (Kiffney et al. 2000). In our study, the positive correlations between benthic chlorophyll *a* and DOC and BDOC concentrations suggest a significant role for autochthonous DOC in the WOH watersheds.

Nutrient concentrations at agriculturally impacted sites in the WOH region probably contributed to the higher benthic chlorophyll *a* density there than in the EOH region.

Increased DOC concentrations with increased stream discharge during storms or snowmelt is a common phenomenon and is assumed to result from the alteration of flow paths for water entering streams (McDowell and Likens 1988). A negative correlation of DOC concentration and discharge reported for headwater streams in British Columbia appears to have been heavily influenced by dry-season benthic algal biomass accumulations and high levels of DOC concentrations from exudates (Kiffney et al. 2000). Our data, which reveal a positive correlation between DOC concentrations and rates of baseflow discharge, suggest that even changes from high to low baseflow conditions were accompanied by shifts in flow paths along hydrologic gradients. A long-term trend of increasing DOC concentration has been observed in the Hudson River (Findlay 2005, Burns et al. 2005) and elsewhere (Worrall and Burt 2007), but was not observed over our 6-year study period. We did document interannual variations in precipitation and discharge during our study, and the years 2003 and 2004 were the wettest (see Technical Design Chapter, Chapter 2, Fig. 2.5). These differences in hydrology and the relationship we have documented between baseflow discharge and DOC concentration may have been sufficient to overcome any contravening effects of a long-term DOC concentration trend. For those sites that were sampled over the 6-year period from 2000 through 2005, when the relationships between DOC concentration and discharge were significant, a plot of the residual versus year showed no consistent influence of position along the 6-y timeline on DOC concentrations. However, to the extent that the phenomenon observed in the Hudson River is representative of phenomena occurring within the watersheds of the WOH and EOH regions, this trend could adversely impact the quality of the NYC water supply.

Landuse effects on OM

Forest cover in the WOH region and point-source discharge and wetlands in the EOH region were the primary landuse/land-cover characteristics that influenced concentrations of OM in the study streams. In the WOH, the positive relationships between OM concentrations and agriculture, benthic chlorophyll *a*, fragrances, caffeine, and fecal steroids support the idea that conversion of forests to other landuses adversely impacts organic matter dynamics. Densities of algal biomass are influenced by levels of light and nutrients, both of which may be higher when a watershed is used for agriculture rather than covered by forest. Fragrances and caffeine are clear signals of sources related to human activities, although the fecal steroids could be from humans, domesticated animals, or wildlife.

In the EOH region, the particularly strong relationships between DOC and BDOC and caffeine, fragrances, and fecal steroids identify organically enriched point-source discharge as a contributor to the organic loading (Westerhoff and Anning 2000, Kolpin et al. 2002, Glassmeyer et al. 2005). These anthropogenic inputs of organic C supplemented the natural background concentrations of organic C from wetlands, even when sites with high point-source discharges were removed from the data set. The strong contribution of wetlands to BDOC concentrations in the EOH region is particularly interesting because organic C accumulates in wetlands, whereas BDOC usually is consumed and not exported. This apparent disparity (i.e., the suggestion that wetlands are a source of BDOC) could mean that partial photochemical oxidation of DOC (Mopper and Kieber 2002, Latch and McNeill 2006) may transform some recalcitrant DOC

molecules into biologically labile DOC (BDOC) once it leaves the wetlands and is transported downstream. Support for this phenomenon comes from the observation that photolysis products of recalcitrant DOC from *Typha latifolia* and *Juncus effusus* stimulated production of bacteria from the Talladega Wetland Ecosystem (Wetzel et al. 1995), but this area of inquiry would benefit from direct experimentation.

DOC from point sources (Sirivedhin and Gray 2005) and peat soils (Fleck et al. 2004) have been identified as potential disinfection by-product (DBP) precursors, as have biologically labile algal exudates (Nguyen et al. 2005). The literature on the relative importance of DOC sources to DBP formation is equivocal. For example, an analysis of 17 different Alaskan water supplies found that phenolic compounds in DOC were the primary contributors to DBPs (White et al. 2003), whereas a study of wastewater effluents and surface waters found that DBP formation potential was negatively correlated to the phenolic signature of the DOC (Sirivedhin and Gray 2005). Thus, whether the wetland influence (EOH) or the algal influence (WOH) on stream DOC have any particular significance to DBP formation potential is unclear, but these factors probably do contribute to the higher % of DOC consisting of BDOC in the WOH than in the EOH.

DOC in drinking water

A survey of DOC and BDOC in US drinking-water sources revealed median concentrations of DOC (2.27 mg/L) and BDOC (296 μg/L) in 53 surface-water supplies (Kaplan et al. 1994). The median concentrations of DOC (1.50 mg/L) and BDOC (241 μg/L) in the WOH were below the concentrations reported in the US drinking water survey, whereas median concentrations for DOC (3.26 mg/L) and BDOC (312 μg/L) in the EOH region were higher than ~76% (DOC) and ~64% (BDOC) of the concentrations reported in the survey (Kaplan et al. 1994). Sobczak and Findlay (2002) reported DOC concentrations from streams in forested sites in the Catskill region and the Hudson River valley that were comparable to the concentrations in the EOH and WOH regions. Sobczak and Findlay (2002) also measured BDOC in batch cultures. They reported a lower % of DOC consisting of BDOC but a higher % of DOC lost along hyporheic flow paths than in streams in our study (except for the Neversink, which showed no uptake of DOC – see the N, P, and DOC Spiraling chapter, Chapter 8).

From a drinking-water treatment perspective, low organic C concentrations are desirable because of the influence of organic C on DBP concentrations and bacterial regrowth. Moreover, organic C can influence other aspects of drinking-water quality, including the aesthetics of taste and pollutant transport. For example, microorganisms such as Cyanobacteria and *Streptomyces* can produce geosmin and 2-methylisoborneol, organic compounds known to impart undesirable taste and odor to water supplies (Suffet et al. 1999, Hockelmann and Juttner 2005). DOC alters the availability of hydrophobic pollutants (Caron and Suffet 1989) and heavy metals such as Cd, Cu, Cr (Guggenberger et al. 1994), and Hg (Wallschlager et al. 1996), and facilitates movement of these metals from watershed soils into streams and reservoirs (Shafer et al. 1997). OM associated with particles can adsorb nutrients and contribute to eutrophication of downstream reservoirs, and particulate matter in streams increases turbidity, which can limit instream primary production and reduce habitat quality for stream invertebrates (Wood and Armitage 1997) and spawning fishes (Waters 1995). However, organic C also is a natural and important component of stream ecosystem function. Our data from watersheds in the WOH region with high % forest land cover (ESP: 96.6% forested, NVR: 97.0% forested, RND: 97.2% forested) and from sites in

the EOH that are in small to moderately sized watersheds with no SPDE discharges (e.g., sites 32 and 59) probably provide lower limits for OM levels that be achieved through best management practices in the 2 regions.

In conclusion, our spatially extensive study of OM concentrations under baseflow conditions revealed distinct regional differences that were related to differences in land use and land cover. In the absence of human activities, differences between the regions in DOC concentrations would have been expected because % wetlands is higher in the EOH than in the WOH region and, indeed, wetlands influenced DOC and BDOC concentrations in the EOH region. Reduction in forest cover appeared to increase concentrations of DOC and BDOC in the WBD watershed and clearly distinguished the WBD subregion from other subregions in the WOH region where forest cover was high. High levels of SPDE effluents at 6 sites spread among the MNC, AMW, and EBC subregions strongly influenced DOC, BDOC, and POM in the EOH, but human activity was a predictor of BDOC even with these sites removed from the data set. BDOC is a source of energy and organic C building blocks for heterotrophic microbial metabolism and is the organic analog to the inorganic nutrients (N and P) that are most commonly associated with water-quality assessments (Carpenter et al. 1998, Neill et al. 2001). In both the WOH and EOH regions, OM concentrations were related to the human activities in the watersheds, and this relationship suggests that continuing efforts to improve water quality by addressing human impacts at the watershed scale are appropriate.

Literature Cited

Aiken, G., L. A. Kaplan, and J. Weishaar. 2002. Assessment of relative accuracy in the determination of organic matter concentrations in aquatic systems. Journal of Environmental Monitoring. 4:70-74.

Aufdenkampe, A. K., E. Mayorga, J. I. Hedges, C. Llerena, P. D. Quay, J. Gudeman, A. V. Krusche and J. E. Richey. 2007. Organic matter in the Peruvian headwaters of the Amazon: Compositional evolution from the Andes to the lowland Amazon mainstem. Organic Geochemistry 38: 337-364.

Aufdenkampe, A. K., L. J. Standley, C. L. Dow, and D. B. Arscott. 2006. Molecular tracers of soot and sewage contamination in streams supplying New York City drinking water. Journal of the North American Benthological Society 25:928-953.

Battin, T. J., L. A. Kaplan, S. Findlay, C. S. Hopkinson, E. Marti, A. I. Packman, J. D. Newbold, and F. Sabater. 2008. Biophysical controls on dissolved organic carbon in fluvial networks. Nature Geosciences 1: 95-100.

Buffam, I., J. N. Galloway, L. K. Blum, and K. J. McGlathery. 2001. A storm/baseflow comparison of dissolved organic matter concentrations and bioavailability in an Appalachian stream. Biogeochemistry 53:269–306.

Burns, D., T. Vitvar, J. McDonnell, J. Hassett, J. Duncan, and C. Kendall. 2005. Effects of suburban development on runoff generation in the Croton River basin, New York, USA. Journal of Hydrology 311:266–281.

Caron, G., and I. H. Suffet. 1989. Binding of nonpolar pollutants to dissolved organic carbon: environmental fate modeling. Pages 117–130 *in* I. H. Suffet and P. MacCarthy (editors). Aquatic humic substances influence on fate and treatment of pollutants. American Chemical Society, Washington, DC.

Carpenter, S. R., N. F. Caraco, D. L. Correll, R. W. Howarth, A. N. Sharpley, and V. H. Smith. 1998. Nonpoint pollution of surface waters with phosphorus and nitrogen. Ecological Applications 8:559–568.

Chow, A. T., K. K. Tanji, and S. Gao. 2003. Production of dissolved organic carbon (DOC) and trihalomethane (THM) precursor from peat soils. Water Research 37:4475–4485.

Cole, J. J., and N. F. Caraco. 2001. Carbon in catchments: connecting terrestrial carbon losses with aquatic metabolism. Marine and Freshwater Research 52:101–110.

Cole. J.J., Y. T. Prairie, N. F. Caraco, W. H. McDowell, L. J. Tranvik, R. G. Striegl, C. M. Duarte, P. Kortelainen, J. A. Downing,J. J. Middelburg, and J. Melack. 2007. Plumbing the global carbon cycle: Integrating inland waters into the terrestrial carbon budget. Ecosystems DOI:10.1007/s10021-00609013-8.

Comiskey, C. E. 1978. Aspects of the organic carbon cycle on Walker Branch watershed: a study of land/water interaction. Ph.D. Dissertation, University of Tennessee, Knoxville, Tennessee.

Dodds, W. K., and M. R. Whiles. 2004. Quality and quantity of suspended particles in rivers: continent-scale patterns in the United States. Environmental Management 33:355–367.

Duncan, H. P. 1999. Urban stormwater quality: a statistical overview. Report 99/3. Cooperative Research Center for Catchment Hydrology, Melbourne, Australia. (Available from:http://www.catchment.crc.org.au/archive/pubs/prog12.html)

Elder, J. F., N. B. Rybicki, V. Carter, and V. Weintraub. 2000. Sources and yields of dissolved carbon in Northern Wisconsin stream catchments with differing amounts of peatland. Wetlands 20:113–125.

Escobar, I. C., A. A. Randall, and J. S. Taylor. 2001. Bacterial growth in distribution systems: effect of assimilable organic carbon and biodegradable dissolved organic carbon. Environmental Science and Technology 35:3442–3447.

Findlay, S. E. G. 2005. Increased carbon transport in the Hudson River: unexpected consequence of nitrogen deposition? Frontiers in Ecology and the Environment 3:133–137.

Fleck, J. A., D. A. Bossio, and R. Fujii. 2004. Dissolved organic carbon and disinfection by-product precursor release from managed peat soils. Journal of Environmental Quality 33:465–475.

Gergel, S. E., M. G. Turner, and T. K. Kratz. 1999. Dissolved organic carbon as an indicator of the scale of watershed influence on lakes and rivers. Ecological Applications 9:1377–1390.

Gjessing, E. T. 1976. Physical and chemical characteristics of aquatic humus. Ann Arbor Science, Ann Arbor, Michigan.

Glassmeyer, S. T., E. T. Furlong, D. W. Kolpin, J. D. Cahill, S. D. Zaugg, S. L. Werner, and M. T. Meyer. 2005. Transport of chemical and microbial compounds from known wastewater discharges: potential for use as indicators of human fecal contamination. Environmental Science and Technology 39:5157–5169.

Golladay, S. W. 1997. Suspended particulate organic matter concentration and export in streams. Journal of the North American Benthological Society 16:122–131.

Guggenberger, G., B. Glaser, and W. Zech. 1994. Heavy metal binding by hydrophobic and hydrophilic dissolved organic carbon fractions in a spodosol A and B horizons. Water, Air, and Soil Pollution 72:111–127.

Hall, R. O., J. B. Wallace, and S. L. Eggert. 2000. Organic matter flow in stream food webs with reduced detrital resource base. Ecology 81:3445–3463.

Hatt, B. E., T. D. Flectcher, C. J. Walsh, and S. L. Taylor. 2004. The influence of urban density and drainage infrastructure on the concentrations and loads of pollutants in small streams. Environmental Management 34:112–124.

Hedges, J. I., W. A. Clark, P. D. Quay, J. E. Richey, A. H. Devol, and U. de M. Santos. 1986. Compositions and fluxes for particulate organic material in the Amazon River. Limnology and Oceanography 31:717–738.

Hillman, G. R., J. C. Feng, C. C. Feng, and Y. Wang. 2004. Effects of catchment characteristics and disturbances on storage and export of dissolved organic carbon in a boreal headwater stream. Canadian Journal of Fisheries and Aquatic Sciences 61:1447–1460.

Hinton, M. J., S. L. Schiff, and M. C. English. 1997. The significance of runoff events on the concentrations and export of dissolved organic carbon from two Precambrian Shield watersheds. Biogeochemistry 36:67–88.

Hockelmann, C., and F. Juttner. 2005. Off-flavours in water: hydroxyketones and beta-ionone derivatives as new odour compounds of freshwater cyanobacteria. Flavour and Fragrance Journal 20:387–394.

Hynes, H. B. N. 1975. Eldgardo Baldi Memorial Lecture: The stream and its valley. Verhandlungen der Internationalen Vereinigung für theoretische und angewandte Limnologie 19:1–15.

Jiang, J., K. A. Alderisio, and L. Xiao. 2005. Distribution of *Cryptosporidium* genotypes in storm event water samples from three watersheds in New York. Applied and Environmental Microbiology 71:4446–4454.

Jones, J. B., S. G. Fisher, and N. B. Grimm. 1996. A long-term perspective of dissolved organic carbon transport in Sycamore Creek, Arizona. Hydrobiologia 317:183–188.

Jones, K. B., A. C. Neale, M. S. Nash, R. D. V. Remortel, J. D. Wickham, K. H. Riitters, and R. V. O'Neill. 2001. Predicting nutrient and sediment loadings to streams from landscape metrics: a multiple watershed study from the United States Mid-Atlantic Region. Landscape Ecology 16:301–312.

Kaiser, E., D. B. Arscott, K. Tockner, and B. Sulzberger. 2004. Sources and distribution of organic carbon and nitrogen in the Tagliamento River, Italy. Aquatic Sciences – Research Across Boundaries 66:103–116.

Kaplan, L. A. 1992. Comparison of high-temperature and persulfate oxidation methods for determination of dissolved organic carbon in freshwaters. Limnology and Oceanography 37:1119–1125.

Kaplan, L. A. 1994. A field and laboratory procedure to collect, process, and preserve freshwater samples for dissolved organic carbon analysis. Limnology and Oceanography 39:1470–1476.

Kaplan, L. A., and T. L. Bott. 1982. Diel fluctuations of DOC generated by algae in a piedmont stream. Limnology and Oceanography 27:1091–1100.

Kaplan, L. A., R. A. Larson, and T. L. Bott. 1980. Patterns of dissolved organic carbon in transport. Limnology and Oceanography 25:1034–1043.

Kaplan, L. A., J. D. Newbold, D. J. Van Horn, C. L. Dow, A. K. Aufdenkampe, and J. K. Jackson. 2006. Organic matter transport in New York City drinking-water-supply watersheds. Journal North American Benthological Society 25:912-927.

Kaplan, L. A., D. J. Reasoner, and E. W. Rice. 1994. A survey of BOM in US drinking waters. Journal of the American Water Works Association 86:121–132.

Kaplan, L. A., T. N. Wiegner, J. D. Newbold, P. H. Ostrom, and H. Gandhi. 2008. Untangling the complex issue of dissolved organic carbon uptake: a stable isotope approach. Freshwater Biology 53:855-864 doi:101111/j.1365-2427.2007.01941x.

Kiffney, P. M., and J. P. Bull. 2000. Factors controlling periphyton accrual during summer in headwater streams of southwestern British Columbia, Canada. Journal of Freshwater Ecology 15:339–351.

Kiffney, P. M., J. S. Richardson, and M. C. Feller. 2000. Fluvial and epilithic organic matter dynamics in headwater streams of southwestern British Columbia, Canada. Archiv für Hydrobiologie 149:109–129.

Kolpin, D. W., E. T. Furlong, M. T. Meyer, E. M. Thurman, S. D. Zaugg, L. B. Barber, and H. T. Buxton. 2002. Pharmaceuticals, hormones, and other organic wastewater contaminants in U.S. streams, 1999-2000: a national reconnaissance. Environmental Science and Technology 36:1202–1211.

Laurent, P., P. Servais, V. Gauthier, M. Prevost, J.-C. Joret, and J.-C. Block. 2005. Biodegradable organic matter and bacteria in drinking water distribution systems. Pages 147–204 *in* M. Prevost, P. Laurent, P. Servais, and J.-C. Joret (editors). Biogdegradable organic matter in drinking water treatment and distribution. American Water Works Association, Denver, Colorado.

Latch, D. E. and K. McNeill. 2006. Microheterogeneity of singlet oxygen distributions in irradiated humic acid solutions. Science 311:1743–1747.

Malcolm, R. L., and W. H. Durum. 1976. Organic carbon and nitrogen concentrations and annual organic carbon load of six selected rivers of the United States. Geological Survey Water-Supply Paper 1817-F:1–21. **(**Available from: Superintendent of Documents, Government Publishing Office, Washington, DC 20402 USA.)

Matsuda, H., Y. Ose, T. Sato, H. Nagase, H. Kito, and K. Sumida. 1992. Mutagenicity from ozonation of humic substances. Science of the Total Environment 117/118:521–529.

Mayorga, E., A. K. Aufdenkampe, C. A. Masiello, A. V. Krusche, J. I. Hedges, P. D. Quay, and J. E. Richey. 2005. Young organic matter as a source of carbon dioxide outgassing from Amazonian rivers. Nature 436:538–541.

McDowell, W. H., and G. E. Likens. 1988. Origin, composition, and flux of dissolved organic carbon in the Hubbard Brook Valley. Ecological Monographs 58:177–195.

Minshall, G. W., R. C. Petersen, K. W. Cummins, T. L. Bott, J. R. Sedell, C. E. Cushing, and R. L. Vannote. 1983. Interbiome comparison of stream ecosystem dynamics. Ecological Monographs 53:1–25.

Mopper, K., and D. J. Kieber. 2002. Photochemistry and the cycling of carbon, sulfur, nitrogen and phosphorus. Pages 455–489 *in* D. Hansell and C. Carlson (editors). Biogeochemistry of marine dissolved organic matter. Academic Press, San Diego, California.

Mulholland, P. J. 1997. Dissolved organic matter concentration and flux in streams. Journal of the North American Benthological Society 16:131–141.

Naiman, R. J. 1982. Characteristics of sediment and organic carbon export from pristine boreal forest watersheds. Canadian Journal of Fisheries and Aquatic Sciences 39:1699–1718.

Naiman, R. J., and J. R. Sedell. 1979. Characterization of particulate organic matter transported by some Cascade Mountain streams. Journal Fisheries Research Board Canada 36:17–31.

Neill, C., L. A. Deegan, S. M. Thomas, and C. C. Cerrib. 2001. Deforestation for pasture alters nitrogen and phosphorus in small Amazonian streams. Ecological Applications 11:1817–1828.

Nguyen, M. L., P. Westerhoff, L. Baker, Q. Hu, M. Esparza-Soto, and M. Sommerfeld. 2005. Characteristics and reactivity of algae-produced dissolved organic carbon. Journal of Environmental Engineering 131:1574–1582.

Olmsted, F. H., and A. G. Hely. 1962. Relationship between ground water and surface water in Brandywine Creek basin Pennsylvania. U.S. Geological Survey Professional Paper 417-A. Government Printing Office, Washington, DC.

Pomeroy, L. R. 1974. The ocean's food web, a changing paradigm. BioScience 24:499–504.

Quinn, J. M., and M. J. Stroud. 2002. Water quality and sediment and nutrient export from New Zealand hill-land catchments of contrasting land use. New Zealand Journal of Marine and Freshwater Research 36:409–429.

Shafer, M. M., J. T. Overdier, J. P. Hurley, D. Armstrong, and D. Webb. 1997. The influence of dissolved organic carbon, suspended particulates, and hydrology on the concentration, partitioning and variability of trace metals in two contrasting Wisconsin watersheds (U.S.A.). Chemical Geology 136:71–97.

Sirivedhin, T., and K. A. Gray. 2005. Comparison of the disinfection by-product formation potentials between a wastewater effluent and surface waters. Water Research 39:1025–1036.

Sobczak, W. V., and S. Findlay. 2002. Variation in bioavailability of dissolved organic carbon among stream hyporheic flowpaths. Ecology 83:3194–3209.

Spitzy, A., and V. Ittekkot. 1991. Dissolved and particulate organic matter in rivers. Pages 5–17 *in* R. F. C. Mantoura, J.-M. Martin, and R. Wollast (editors). Ocean margin processes in global change. John Wiley and Sons, Berlin, Germany.

Suffet, I. H., D. Khiari, and A. Bruchet. 1999. The drinking water taste and odor wheel for the millennium: beyond geosmin and 2-methylisoborneol. Water Science and Technology 40:1–13.

Tate, C. M., and J. L. Meyer. 1983. The influence of hydrologic conditions and successional state on dissolved organic carbon export from forested watersheds. Ecology 64:25–32.

Thomas, S. M., C. Neill, L. A. Deegan, A. V. Krusche, V. M. Ballester, and R. L. Victoria. 2004. Influences of land use and stream size on particulate and dissolved materials in a small Amazonian stream network. Biogeochemistry 68:135–151.

Vannote, R. L., G. W. Minshall, K. W. Cummins, J. R. Sedell, and C. E. Cushing. 1980. The river continuum concept. Canadian Journal of Fisheries and Aquatic Sciences 32:130–137.

Wallace, J. B., D. H. Ross, and J. L. Meyer. 1982. Seston and dissolved organic carbon dynamics in a southern Appalachian stream. Ecology 63:824–838.

Wallschlager, D. M., V. M. Desai, and R. D. Wilken. 1996. The role of humic substances in the aqueous mobilization of mercury from contaminated floodplain soils. Water, Air and Soil Pollution 90:507–520.

Waters, T. F. 1995. Sediments in streams, sources, biological effects and controls. American Fisheries Society, Bethesda, Maryland.

Webster, J. R., and J. L. Meyer. 1997. Organic matter budgets for streams: a synthesis. Journal of the North American Benthological Society 16:141–161.

Westerhoff, P., and D. Anning. 2000. Concentrations and characteristics of organic carbon in surface water in Arizona: influence of urbanization. Journal of Hydrology 236:202–222.

Wetzel, R. G. 1995. Death, detritus, and energy flow in aquatic ecosystems. Freshwater Biology 33:83–89.

Wetzel, R. G. 2003. Dissolved organic carbon: detrital energetics, metabolic regulators, and drivers of ecosystem stability of aquatic ecosystems. Pages 455–477 *in* S. E. G. Findlay and R. L. Sinsabaugh (editors). Aquatic ecosystems: interactivity of dissolved organic matter. Academic Press, New York.

Wetzel. R. G., P. G. Hatcher, and T. S. Biachi. 1995. Natural photolysis by ultraviolet irradiance of recalcitrant dissolved organic matter to simple substrates for rapid bacterial metabolism. Limnology and Oceanography 40:1369–1380.

Whiles, M. R., and W. K. Dodds. 2002. Relationships between stream size, suspended particles, and filter-feeding macroinvertebrates in a Great Plains drainage network. Journal of Environmental Quality 31:1589–1600.

White, D. M., D. S. Garland, J. Narr, and C. R. Woolard. 2003. Natural organic matter and DBP formation potential in Alaskan water supplies. Water Research 37:939–947.

Wood, P. J., and P. D. Armitage. 1997. Biological effects of fine sediment in the lotic environment. Environmental Management 21:203–217.

Worrall, F., and T. P. Burt. 2007. Trends in DOC concentration in Great Britain. Journal of Hydrology 346:81-92.

Table 6.1. Mean (± 1SD) dissolved organic C (DOC), bioavailable DOC (BDOC), particulate organic matter (POM) and total organic C (TOC=DOC + 0.45[POM]) sampled annually between 2000 and 2005 during summer baseflow in watersheds in the east of the Hudson River (EOH) and west of the Hudson River (WOH) regions. Significant differences between regions are indicated in bold font. Among watersheds within regions, means with different letters within columns are significantly different ($p < 0.05$).

Region / Watershed (number of watersheds)	DOC	BDOC		POM		TOC
	mg/L	mg/L	% DOC	mg/L	% TSS	mg/L
EOH (55)	**3.56 ± 1.53**	**0.43 ± 0.40**	**11.1 ± 4.1**	**1.79 ± 1.66**	38.2 ± 10.0	**4.36 ± 1.94**
WOH (55)	**1.63 ± 0.62**	**0.21 ± 0.10**	**12.3 ± 3.7**	**0.74 ± 0.32**	35.5 ± 12.2	**1.97 ± 0.71**
EOH						
AMW (3)	4.76 ± 1.03	0.66 ± 0.30	13.1 ± 3.9	4.33 ± 3.66	44.1 ± 4.3	6.71 ± 2.53
CRS (3)	4.33 ± 1.11	0.51 ± 0.17	12.2 ± 1.2	3.76 ± 3.37	43.2 ± 4.9	6.02 ± 1.82
MBC (3)	4.09 ± 0.40	0.43 ± 0.19	9.8 ± 3.9	1.30 ± 0.61	41.0 ± 14.5	4.68 ± 0.46
WBC (6)	4.02 ± 2.05	0.43 ± 0.21	10.8 ± 4.8	2.50 ± 1.58	35.9 ± 12.4	5.15 ± 2.26
MSC (12)	4.01 ± 2.03	0.61 ± 0.76	12.8 ± 5.9	1.48 ± 1.04	43.7 ± 12.4	4.67 ± 2.21
TTS (3)	3.22 ± 1.37	0.36 ± 0.20	10.3 ± 3.4	1.13 ± 0.71	29.9 ± 3.3	3.73 ± 1.68
EBC (11)	3.08 ± 1.28	0.33 ± 0.18	10.4 ± 3.0	1.75 ± 1.35	37.9 ± 9.0	3.87 ± 1.71
NCR (3)	3.02 ± 0.83	0.32 ± 0.15	9.6 ± 3.4	0.86 ± 0.43	36.0 ± 6.6	3.41 ± 0.97
KNC (4)	2.22 ± 0.86	0.24 ± 0.10	10.7 ± 3.9	1.13 ± 0.81	28.7 ± 1.8	2.73 ± 0.97
WOH						
WBD (17)	2.07± 0.60 ^{A}	0.32 ± 0.12 ^{A}	16.2 ± 5.0	0.82 ± 0.28	32.8 ± 6.3 ^{A}	2.44 ± 0.68 ^{A}
SCH (10)	1.82 ± 0.72 ^{A,B}	0.26 ± 0.07 ^{A,B}	14.8 ± 3.6	0.73 ± 0.38	35.9 ± 5.6 ^{A}	2.14 ± 0.83 ^{A,B}
EBD (15)	1.54 ± 0.42 ^{A,B}	0.23 ± 0.11 ^{A,B}	14.8 ± 5.0	0.74 ± 0.37	36.7 ± 9.6 ^{A}	1.87 ± 0.57 ^{A,B,C}
NVK (4)	1.28 ± 0.18 ^{A,B,C}	0.15 ± 0.04 ^{B}	12.1 ± 4.4	0.56 ± 0.19	55.7 ± 14.1 ^{B}	1.54 ± 0.14 ^{A,B,C}
ESP (9)	1.06 ± 0.28 ^{C}	0.16 ± 0.05 ^{B}	14.7 ± 4.3	0.76 ± 0.30	22.6 ± 8.1 ^{C}	1.40 ± 0.38 ^{C}
RND (2)	1.03 ± 0.16 ^{B,C}	0.12 ± 0.04 ^{B}	11.6 ± 5,8	0.37 ± 0.00	64.3 ± 9.9 ^{B}	1.20 ± 0.16 ^{B}

EBC = E. Br. Croton R., MBC = Middle Br. Croton R., WBC = W. Br. Croton R., AMW = Amawalk Reservoir, MSC = Muscoot R., TTS = Titicus R., CRS = Cross R., NCR = New Croton Reservoir, KNC = Kensico Reservoir, WBD = W. Br. Delaware R., EBD = E. Br. Delaware R., SCH = Schoharie Cr., ESP = Esopus Cr., NVK = Neversink R., RND = Rondout Cr.

Table 6.2. Partial R^2 values and direction of slopes (+/-) for significant predictive watershed landuse variables ($p<0.05$) from stepwise multiple linear regression models explaining concentrations of dissolved organic C (DOC), biodegradable DOC (BDOC), and particulate organic matter (POM) among east of Hudson River (EOH) and west of Hudson river (WOH) sites in New York City drinking-water-supply watersheds. Total R^2 values reported are the adjusted R^2 values to compensate for the number of predictors used. SPDE = mean annual watershed-area-normalized State Pollution Discharge Elimination System effluent volume = point-source discharge. Blanks indicate that the landscape characteristic was not a significant predictor in the model.

		Dependent Variable		
	Landscape Characteristic	DOC	BDOC	POM
EOH	% wetland	0.45 (+)	0.40 (+)	0.15 (+)
	SPDE	0.14 (+)	0.16 (+)	0.07(+)
	% mixed brushland	0.04 (-)	0.05 (-)	
	% cropland		0.04 (+)	
	% coniferous forest		0.03 (+)	
	road density			
	% residential			0.08 (+)
	% mixed forest			0.08 (+)
	Total R^2	0.62	0.65	0.26
WOH	% wetlands	0.05 (+)	0.37 (+)	
	% mixed forest		0.15 (-)	0.09 (-)
	% industry		0.10 (+)	
	% deciduous forest	0.46 (-)		
	% coniferous forest	0.11 (-)		
	% residential	0.05 (-)		
	% commercial	0.04 (+)		
	SPDE			0.29 (+)
	% orchard			0.07 (+)
	% shrubland	0.02 (+)		
	Total R^2	0.70	0.60	0.42

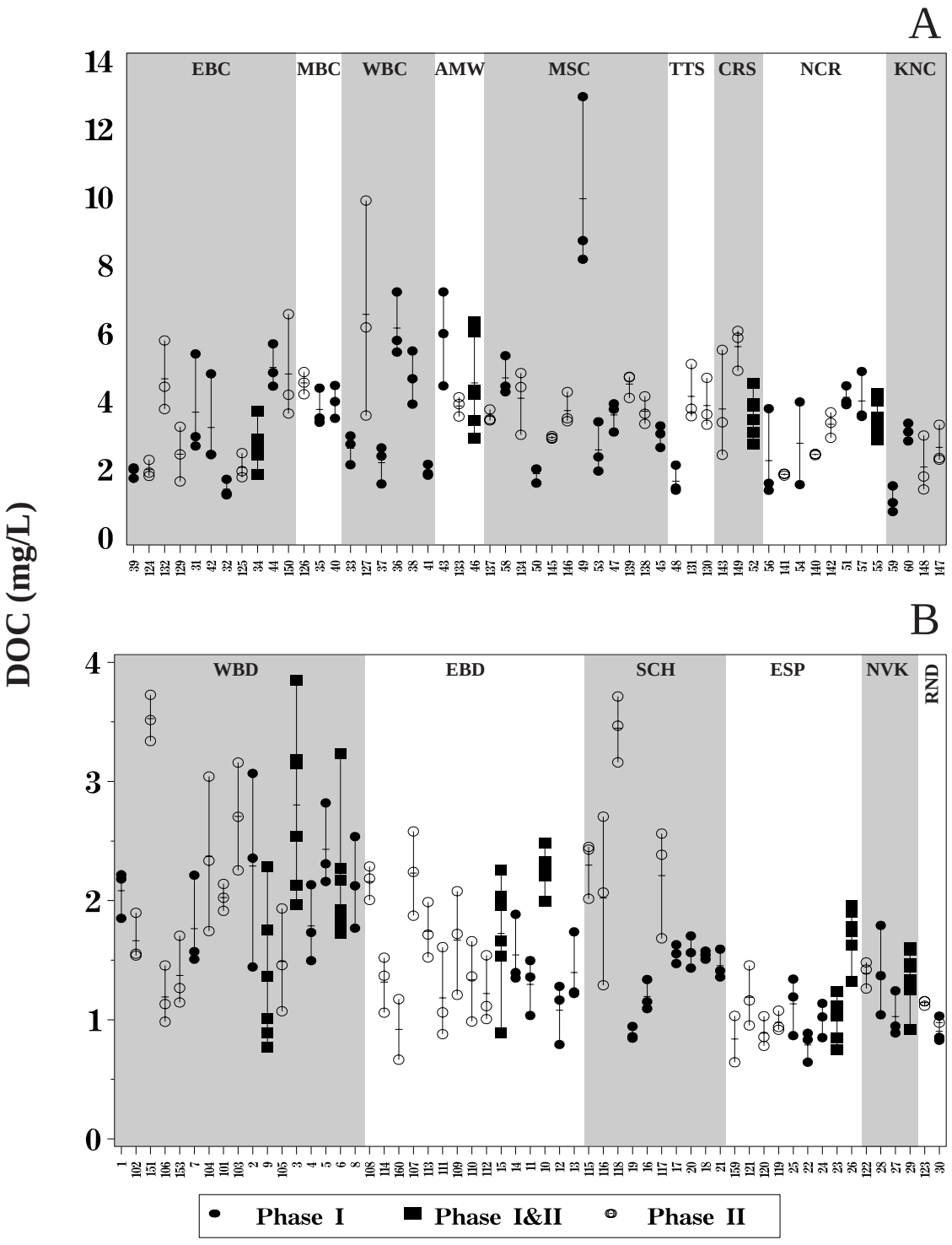

Figure 6.1. Baseflow concentrations and the mean of dissolved organic C (DOC) in watersheds of the east of Hudson River (EOH; A) and west of Hudson River (WOH; B) regions of the New York City drinking-water supply for the years 2000-2005. See Table 6.1 for watershed abbreviations. Sites are ordered by increasing watershed area from left to right.

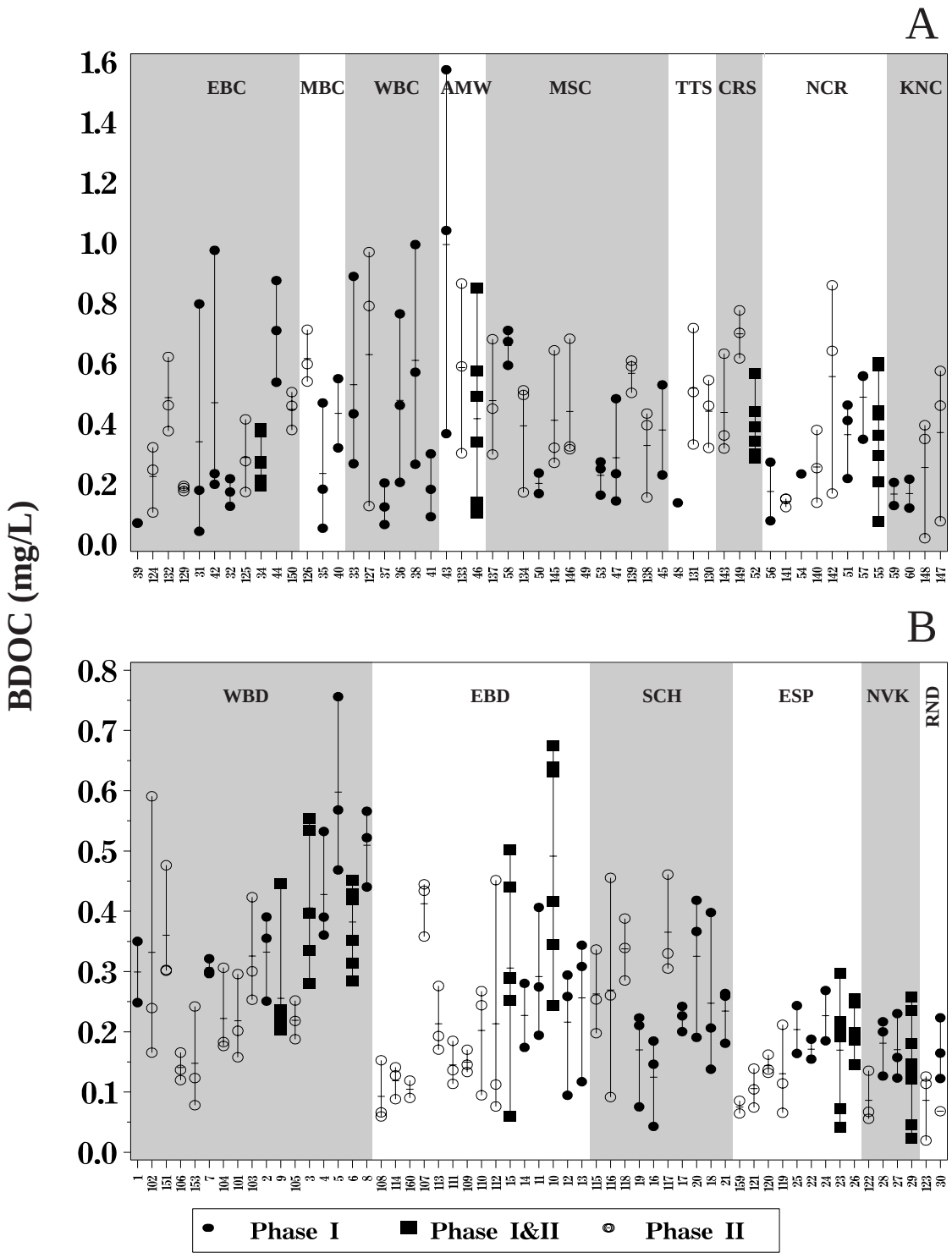

Figure 6.2 Baseflow concentrations and the mean of biodegradable dissolved organic C (BDOC) in watersheds of the east of Hudson River (EOH; A) and west of Hudson River (WOH; B) regions of the New York City drinking-water supply for the years 2000-2005. See Table 6.1 for watershed abbreviations. Sites are ordered by increasing watershed area from left to right.

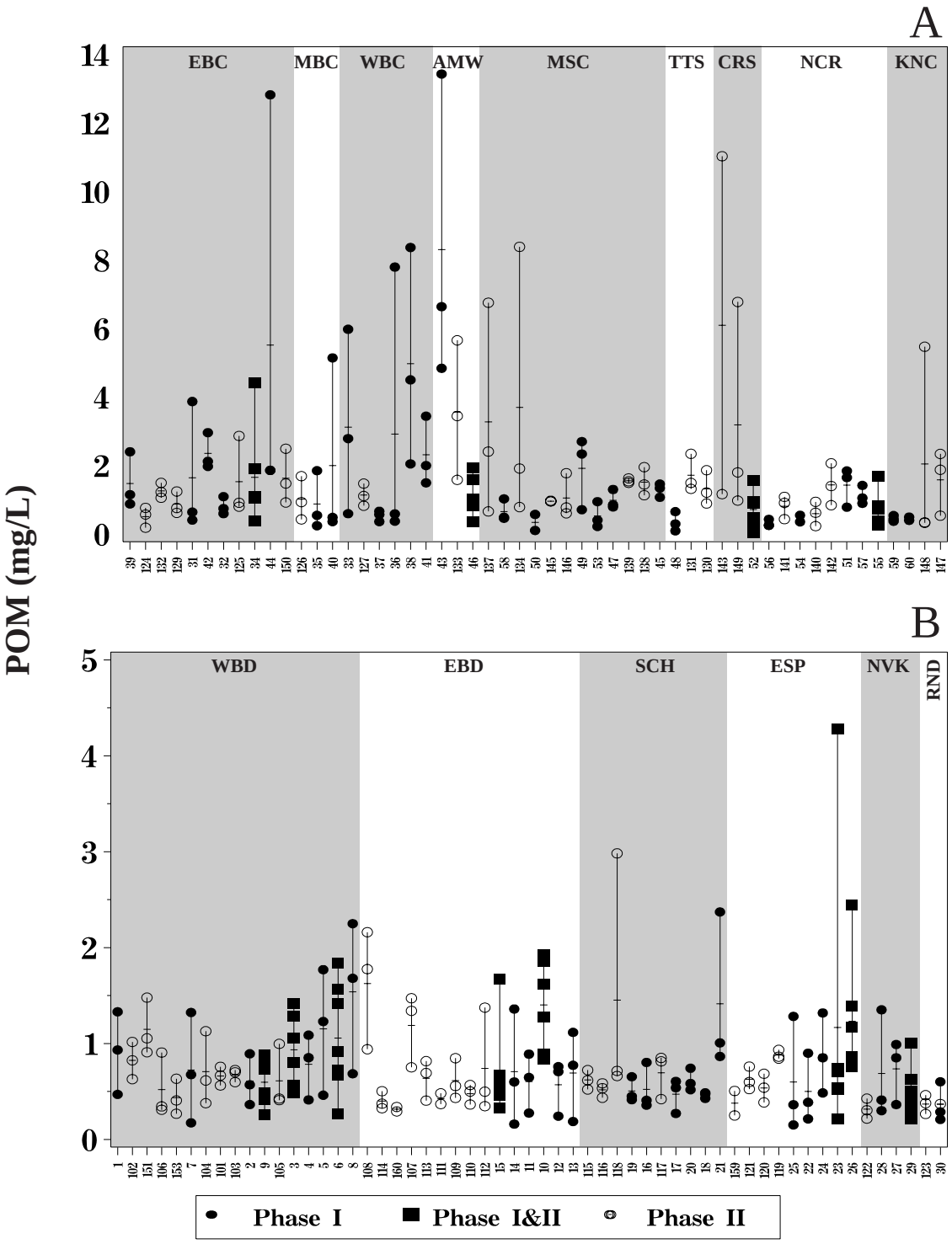

Figure 6.3. Baseflow concentrations and the mean of particulate organic matter (POM) in watersheds of the east of Hudson River (EOH; A) and west of Hudson River (WOH; B) regions of the New York City drinking-water supply for the years 2000-2005. See Table 6.1 for watershed abbreviations. Sites are ordered by increasing watershed area from left to right.

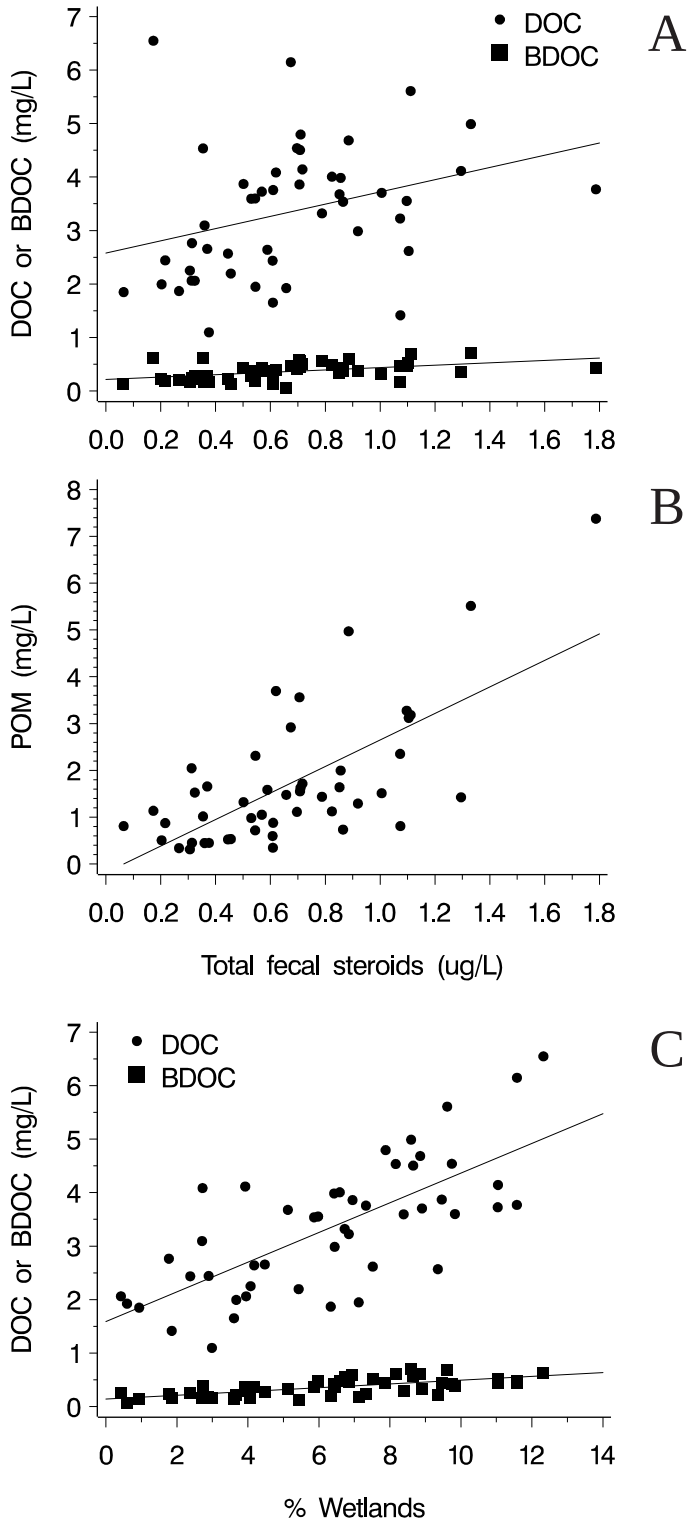

Figure 6.4. Relationship between dissolved organic C (DOC) and biodegradable DOC (BDOC) concentrations and fecal steroid concentrations (A), between particulate organic matter (POM) and total fecal steroid concentrations (B), and between DOC and BDOC and % wetland land cover (C) at sites in the east of Hudson (EOH) region of the New York City drinking-water supply. Sites 43, 49, 58, 132, and 145 were excluded.

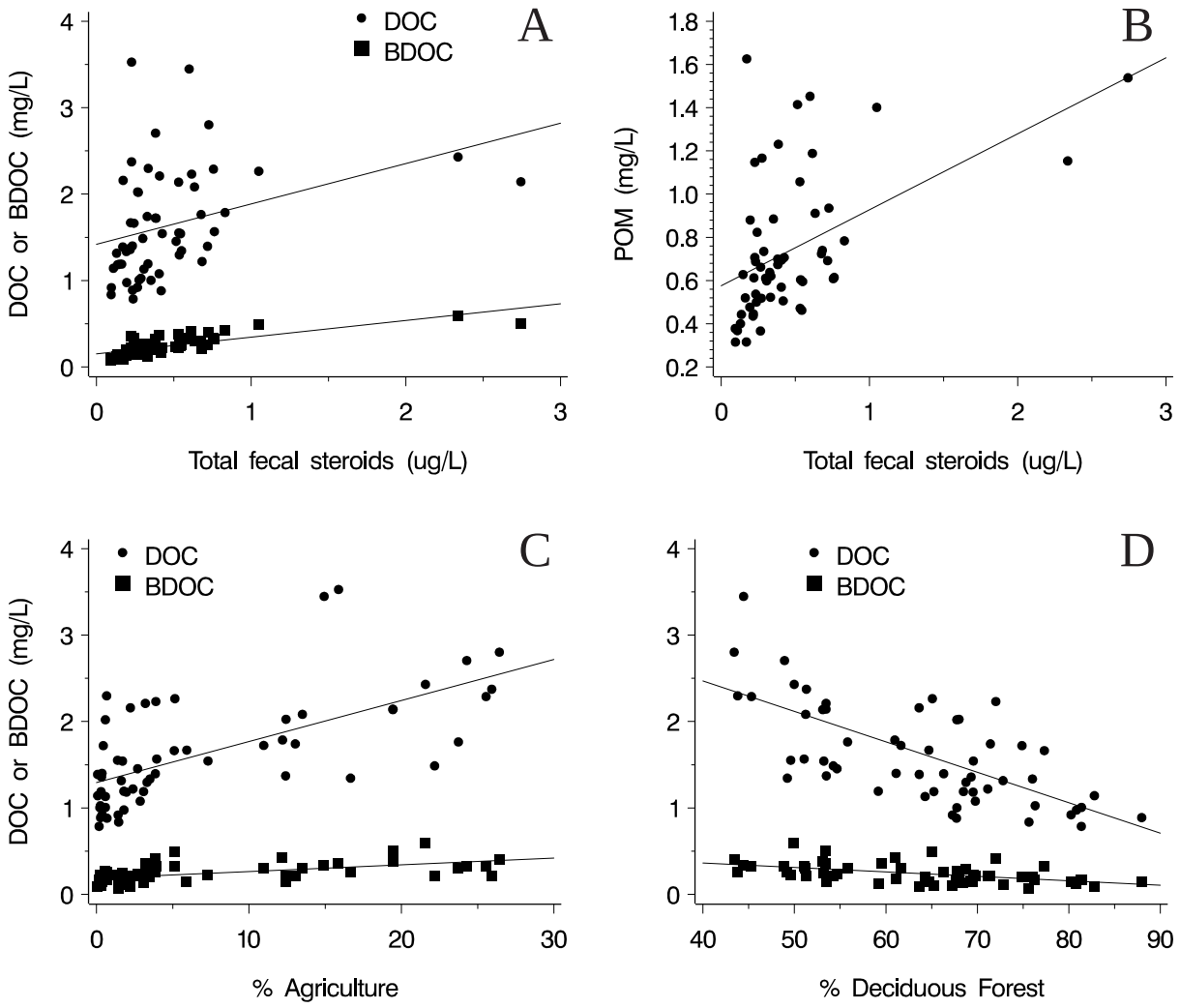

Figure 6.5. Relationship between dissolved organic C (DOC) and biodegradable DOC (BDOC) concentrations and total fecal steroid concentrations (A), % agriculture land use (C), % deciduous forest land cover (D), and particulate organic matter (POM) and total fecal steroid concentrations (B) in sites in the west of Hudson (WOH) region of the New York City drinking-water supply.

Chapter 7 - Macroinvertebrate Community Structure and Function

Research Task

This portion of the NY Watersheds study uses naturally occurring benthic (i.e., bottom-dwelling) macroinvertebrate populations in the streams and rivers of the NY Watersheds to assess whether statistically significant and ecologically meaningful differences in environmental quality occur. Benthic macroinvertebrates such as insects, worms, and molluscs are the preferred group of aquatic organisms monitored in water quality assessment programs (Hellawell 1986) because: (1) they provide an extended temporal perspective (relative to traditional water samples that are collected periodically) because they have limited mobility and relatively long life spans (e.g., a few months for some chironomid midges to a year or more for some insects and molluscs); (2) the group has measurable responses to a wide variety of environmental changes and stresses; (3) they are an important link in the aquatic food web, converting plant and microbial matter into animal tissue that is then available to fish; and (4) they are abundant and their responses can be easily analyzed statistically (Weber 1973). Thus, the presence or conspicuous absence of certain macroinvertebrate species at a site is a meaningful record of environmental conditions during the recent past, including ephemeral events that might be missed by assessment programs that rely only on periodic sampling of water chemistry. Most stream ecosystems have relatively diverse macroinvertebrate assemblages with species from a number of different orders [e.g., mayflies (Ephemeroptera), caddisflies (Trichoptera), stoneflies (Plecoptera), beetles (Coleoptera), true flies (Diptera)]. Likewise, the common trophic groups (i.e., herbivores, detritivores, predators) are represented by a number of different species. Various abiotic factors (e.g., hydrology, substrate, temperature, oxygen, pH) and biotic factors (e.g., food quality and quantity, interactions with competitors or predators) have molded, through natural selection, a unique set of optimum environmental requirements for each species. These environmental requirements contribute significantly to the distribution and abundance of these organisms within and among natural stream ecosystems, and influence their response to environmental perturbation.

Aquatic macroinvertebrate species characteristic of the streams and rivers of New York can be typically divided into two subsets based on their period of major growth and activity: (1) species with their principal larval growth during fall - winter - spring and whose adults (in the case of aquatic insects) emerge during spring or early summer; and (2) species with their principal larval growth and adult emerge during summer. Sampling in this program focuses on collecting the fall-winter-spring species near the end of their growth cycle (i.e., when individuals are largest). These larger individuals are often easier to identify. In addition, because they have been actively growing and developing in the streams since at least the previous September, the presence/absence, absolute abundance, physiological state, etc. of larvae collected in spring integrates both habitat and water quality conditions in a given stream or river over the previous 6-9 months. Thus, the macroinvertebrates collected in spring provide a strong "temporal perspective" during an important and significant portion of the year.

Methods

Field Collection of Macroinvertebrate Samples

Macroinvertebrates were collected at 110 locations distributed throughout the watersheds (see Chapter 2, Figs. 2.1 and 2.2, Tables 2.3 and 2.4) that were sampled in two phases (Table 7.1). There were 12 locations that were sampled in both Phases 1 and 2. The sampling protocol was designed to characterize riffle-inhabiting macroinvertebrates in a reach that included several riffles (i.e., for additional habitat and biotic diversity) rather than the approach of characterizing macroinvertebrates from a single riffle or part of a riffle. Reach length varied among streams and rivers, but generally included 20-50 m of riffle. Random sampling locations were chosen based on their longitudinal (e.g., along the length of the study reach) and lateral positions. For example, a sampling location in a stream might be designated as 17-25, which would represent 17 m upstream and 25% across the stream from the bank. The sampling protocol called for collecting a total of four composite samples representing 16 samples at each site. The sampling design was modified for several sites each year in response to limited riffle habitat availability. In most cases this resulted in eight samples being collected and/or samples being collected where possible (i.e., partially-random) rather than at random locations. Only four samples could be collected at a few sites.

Benthic macroinvertebrates were collected in riffle habitats with a Surber sampler (1 ft^2 or 0.093 m^2; 0.250-mm mesh) using a quantitative composite sampling regime. Sampling started at the downstream end of the sampling area and proceeded in an upstream direction. The operator identified the location of each sampling location based on the longitudinal and lateral position. If boulders or large woody debris interfered with sampling at the designated sampling location, the location was moved slightly until there was no obstruction. If it was impossible to obtain a good sample from this location, an alternative sampling site that was also randomly chosen was used for this sample.

To collect the macroinvertebrate sample, the back edge of the Surber sampler is set on the stream bottom so that there is a tight seal across the substrate to prevent animals from migrating under the sampler. The square bottom frame is then laid out on the stream bottom to delimit the 1 ft^2 sample area. Rocks that were under the frame were included in the sample if more than half of the rock was inside the frame; if more than half of the rock was outside of the frame it was not included in the sample. Larger rocks (> 65 mm in longest dimension) are removed individually, and scrubbed with a soft bristled brush under the water in front of the net. Scrubbing removes most attached organisms while the water current moving through the sampler carries these dislodged organisms into the sample net. Each scrubbed rock was placed in a plastic bucket (held by a second person) for subsequent counting. The minimum rock counted and/or measured is > 65 mm on the longest axis. Large rocks that could not be moved were scrubbed in place. After all rocks were scrubbed and removed, the enclosed benthic area was rapidly stirred and agitated for at least 20 seconds to suspend any residual organisms in the water column and subsequently into the sample net. The sampler was then removed from the bottom and stream water splashed onto the outside of the net in order to wash clinging animals into the bottom of the net. Each sample was randomly assigned to one of four composite samples so the net for a sample was inverted and the contents washed into a plastic bucket designated for that composite sample.

Composite samples resulted from combining four 1 ft^2 samples (if possible) into one composite sample (i.e., containing macroinvertebrates from 4 ft^2) and then subsampling the combined samples in the field such that a subsample equaled one Surber sample (i.e., macroinvertebrates representative of 1 ft^2). After all samples (usually 16) had been collected and combined into four composite samples, each composite sample was split into subsamples (each representing 1 ft^2), with one of the subsamples being preserved and brought back to the laboratory for analysis. Each composite sample was washed into a large sample splitter that was placed in a large plastic trash can half filled with water. The mixture of macroinvertebrates, detritus, and sediments was homogenized and resuspended by stirring, agitating, and pushing water into the subsampler. The material then resettled across the bottom of the subsampler while slowly drawing the subsampler out of the barrel. If the material did not appear evenly distributed, the resuspension and settling process was repeated. The net-covered bottom (0.250-mm mesh) was separated from the rest of the subsampler, and the + shaped plastic separator was pushed into the sample material, dividing the material into four equal parts. A spatula and scissors was used to separate subsamples and transfer a subsample to a labeled sample jar filled with 5% buffered formalin, which was then transported to the laboratory. If the composite sample contained four samples, then 1/4th of the composite material represented macroinvertebrates from 1 ft^2. If only eight samples were collected, then each composite sample contained the contents of two samples (i.e., macroinvertebrates from 2 ft^2), and the composite sample was split into two subsamples (each representing 1 ft^2).

Sample compositing has advantages over standard (non-compositing) macroinvertebrate sampling. For example, compositing increases the accuracy of the desired description by increasing the number of samples collected and therefore the area sampled in these riffles without increasing the number of samples processed. At the same time, compositing homogenizes spatial variation when these samples are combined, which reduces variance among samples in statistical analyses.

Associated with each sample, water depth was measured to the nearest cm and current velocity was estimated with a current meter set at a point 0.6 of the distance from the bottom to the water surface. The number of large rocks (> 65 mm in longest dimension) that had been in that sample was also recorded. Periphyton biomass (as chlorophyll *a* and ash free dry mass) was measured for each composite sample by collecting a small algae-covered stone (3-5 cm in diameter) near where each sample were collected and placed in labeled plastic Tupperware containers associated with each composite sample (i.e., 2 or 4 rocks per composite sample). The plastic Tupperware containers were stored on dry ice (in field) or in a freezer (in laboratory) until chlorophyll *a* and ash free dry mass analyses were completed in the laboratory (< 28 d for chlorophyll *a*).

Laboratory Processing of Macroinvertebrate Samples

Benthic materials (i.e., macroinvertebrates and detritus) were transferred from the sample jar into a 250-µm mesh sieve and rinsed thoroughly with water to remove fine particles. Because macroinvertebrates were abundant (hundreds to thousands per sample), each sample was split into four subsamples, and then one of those subsamples was split into four subsamples (i.e., $1/16^{th}$ of a sample). Actual subsample size processed varied among samples (e.g., $1/16^{th}$, $1/8^{th}$,

3/16th, 1/4th) and reflected the number of macroinvertebrate per sample. Our target was to identify 100-300 macroinvertebrates per subsample. Macroinvertebrates were separated from detritus by taking a small portion from the subsample and placing it in a plastic sorting tray partially filled with 80% ethanol. This material was then carefully examined with the aid of a dissecting microscope (12 X magnification). All macroinvertebrates were removed from the detrital material collected in the subsample, and the detrital material was transferred to an aluminum weigh boat (see Benthic Organic Matter below).

All macroinvertebrates were identified to the lowest taxonomic level possible. For aquatic insects, this was generally genus or species; other macroinvertebrates (e.g., crustaceans, mites, flatworms, oligochaetes, and nematodes) were commonly left at higher taxonomic levels (e.g., order, family). Specimens that were damaged or extremely small were identified to the lowest taxonomic level possible, but these were higher than species and even genus. Chironomids were subsampled before identification, and the number examined represented the percentage of chironomids in that sample. For example, if a sample contained 300 macroinvertebrates and 40% of them were chironomids, then 40 chironomids were identified to genus/species and these identifications were applied proportionally to the remaining 80 chironomids. Identified macroinvertebrates were placed in vials containing 80% ethanol and a permanent label. Macroinvertebrate specimens (sorted and unsorted material) are being archived by the Stroud Center for at least 10 years after the collection date. After verification, selected voucher specimens may be incorporated into the permanent macroinvertebrate collection at the Stroud Center.

Periphyton chlorophyll *a* and biomass were estimated for rocks collected in association with each composite sample. For chlorophyll *a* analyses, rocks were extracted overnight in alkaline acetone and optical densities determined at 665 nm and 750 nm (for turbidity) before and after acidification with a drop of 1 N HCL. Optical densities were used to determine chlorophyll *a* concentrations with correction for phaeophytin (Lorenzen 1967). These rocks were then scrubbed with small brushes to remove attached organic material (i.e., the biofilm of algae, fungi, and bacteria). This organic material was captured on a pre-ashed GF/F filter, dried at 60°C for > 48 h, weighed (dry mass of organic and inorganic matter on rock surfaces), ashed at 550°C for 5 hours, and then weighed again (dry mass of inorganic materials). Weight loss during ashing represents the organic content of the periphyton expressed as mg or g AFDM/m^2. Periphyton chlorophyll *a* and biomass are measures of the biofilm that represents macroinvertebrate food attached to rocks.

Benthic Organic Matter (BOM) is also a measure of macroinvertebrate food, but in the form of medium and coarse organic particles (i.e., captured by a 0.250-mm mesh sieve) intermixed among rocks and finer substrates in the streambed. BOM was estimated as the detrital material associated with each processed subsample. After the macroinvertebrates were removed, the wet detritus (organic and inorganic material) was transferred to an aluminum weigh boat and dried at 60°C for > 48 h. The sample was weighed (dry mass of organic and inorganic materials), ashed at 550°C for 5 hours, and then weighed again (dry mass of inorganic materials). Weight loss during ashing represents BOM expressed as mg or g AFDM/m^2.

Data Analysis

Stream ecologists have not been able to identify a single descriptor of aquatic macroinvertebrate assemblages that is generally accepted as better than all others (i.e., most accurate and sensitive) (Resh and Jackson 1993, Barbour et al. 1999). Thus, the macroinvertebrate data were summarized as estimates of density for individual species or groups of species, and with community structure metrics that are commonly used in water quality monitoring programs (including those used to calculate the NY Water Quality Score; Bode et al. 2002b). Each of the variables described below is calculated with information from the same data set, which results in a certain degree of redundancy among the descriptors. Thus, when meaningful changes in aquatic macroinvertebrate assemblages occur, it would be expected that those changes would be apparent in changes for more than one descriptor. Not all macroinvertebrates were identified to the species level because of specimen size, damage, or taxonomic/time limitations. Thus, our estimates of richness may slightly underestimate actual richness.

Density Measures	Densities of selected groups of species were examined. This included pollution-intolerant taxa [e.g., many Ephemeroptera (mayflies), Plecoptera (stoneflies), Trichoptera (caddisflies)] and pollution-tolerant taxa [e.g., many Diptera (true flies), Odonata (dragonflies, damselflies), Coleoptera (beetles)]. In response to moderate exposure to pollution, a decrease in density of pollution-intolerant taxa accompanied by an increase in density of pollution-tolerant species would be predicted. Total Macroinvertebrate Density includes both pollution-intolerant and pollution-tolerant species, and it often increases in response to pollution as a result of dramatic increases in the density of selected pollution-tolerant species. In contrast, Ephemeroptera, Plecoptera, and Trichoptera together form a special group that is commonly used to assess changes in water/habitat quality in streams and rivers the group includes numerous pollution-intolerant species; thus, low EPT density would be predicted in response to low water/habitat quality. All density data were ln transformed, a standard procedure to correct for the clumped spatial dispersion of invertebrate populations in streams and rivers (Elliott 1977).
Total Richness	Total Richness summarizes species responses (as presence/absence but not abundance) of all taxa, including pollution-sensitive and pollution-tolerant taxa. It is reported as the mean number of aquatic macroinvertebrate species found in each subsample. Total Richness generally decreases in response to moderate to severe pollution.
EPT Richness	EPT Richness is often calculated in addition to Total Richness and reported as the mean number of Ephemeroptera, Plecoptera, and Trichoptera species found in each subsample. These three insect orders contain many pollution-sensitive taxa; thus, this metric

	summarizes responses of mostly pollution-sensitive taxa. EPT Richness generally decreases in response to moderate to severe pollution.
HBI	Hillsenhoff Biotic Index - Analyses involving abundance (i.e., density) or presence/absence (richness) incorporate pollution tolerance information indirectly, through the interpretation of results for individual taxa or groups of taxa. Biotic indexes combine relative abundance data and pollution tolerance values for each taxon to form a weighted average for the aquatic macroinvertebrates at that site. A biotic index is estimated with data from each sample, and summarized as a mean per sample. Tolerance values (values range from 0 to 10, with 10 being most tolerant and 0 being least tolerant of pollution) for the Hillsenhoff Biotic Index were obtained from two sources: Bode et al. (2002b) and unpublished data obtained from US EPA.
PMA	Percent Model Affinity - PMA compares the observed distribution of individuals among seven orders with a hypothetical macroinvertebrate community representing an unimpacted macroinvertebrate assemblage. The model community consists of Ephemeroptera (40%), Plecoptera (5%), Trichoptera (10%), Coleoptera (10%), Chironomidae (20%), Oligochaeta (5%), Other (10%). The PMA is calculated by comparing values for each taxonomic group from the model and observed communities, and taking the sum of the smaller of the two values from each taxonomic group.
WQS	Water Quality Score - The values for each of the four metrics (Total Richness, EPT Richness, HBI, and PMA are converted to a WQS (range = 0-10) using the Biological Assessment Profile in Bode et al. (2002b). The WQS for the site is the mean of the WQSs for the four individual indexes. Based on data collected with a kick sampler (0.8 x 0.9-mm mesh) between July and September, a WQS of 7.5-10 indicates no impact, 5.0-7.5 indicates slight impact, 2.5-5.0 indicates moderate impact, and 0.0-2.5 indicates severe impact. The applicability of this system to other sampling designs (e.g., different sampling efforts or different seasons) remains unknown.

Total Richness, EPT Richness, and HBI all have a long history in water quality monitoring. PMA is less commonly used. While numerous multimetric indexes have been developed for stream macroinvertebrate assemblages and are widely used in water quality monitoring, the Biological Assessment Profile used to calculate a Water Quality Score and to assess water quality impact has been developed specifically for New York streams by NYSDEC (Bode et al. 2002b).

Differences among stations for the period 2000-2005 were examined using a two-way analysis of variance (ANOVA; station by year, no interaction), with a Tukey's multiple range test to determine the significance of specific station differences. Annual means (n = 3-6 per site) were entered as the observations, rather than the individual samples. The null hypothesis was that the aquatic macroinvertebrate assemblages did not differ significantly among sites, especially relative to the designated reference stations for either WQS or Best Available Conditions (BAC) reference sites. BAC reference sites were determined using 7 land use/cover conditions and 16 water chemistry variables. Every attempt was made to select BAC sites independent of biological information, although they were determined *a posteriori* and therefore biases may have either benefited or hindered the attempt at an objective selection process. WQS and BAC reference sites were defined as the macroinvertebrate assemblages observed at the five WOH and five EOH sites over six years with the highest Water Quality Scores (i.e., the top 10% of sites in each region, Table 7.2) or BAC, respectively. Statistically significant degradation was defined *a priori* as a WQS that was significantly lower than the WQS or BAC reference sites. Sites differed significantly when the statistical analysis indicated there was a < 5% risk of classifying stations as different when they were not. All analyses employed the General Linear Models procedure (SAS/STAT, version 9, SAS Institute, Cary, North Carolina).

Non-metric Multidimensional Scaling (NMS) ordination technique was used to examine how genus-level taxa differed among all sites, EOH sites, and WOH sites (PC-ORD Version 4.37, MjM Software, Gleneden Beach, OR). Analyses were done using three-year averages (Phase I, 2000-2002 and Phase II, 2003-2005) where density for common taxa (taxa present at ≥ 7 sites) was $\log_{10}(x + 1)$ transformed. All NMS ordinations used Sorenson (Bray-Curtis) distance and step length was 0.2. Number of axes was determined based on results of a Monte Carlo test (50 runs, $p = 0.0196$) and a plot of stress versus iteration number was used to determine solution was stable. The NMS using macroinvertebrates from all sites required 84 iterations, the final stress was 16.3, and the final instability was 0.00001. The NMS on WOH sites required 78 iterations, the final stress was 12.5, and the final instability was 0.00001. The NMS on EOH sites required 84 iterations, the final stress was 16.9, and the final instability was 0.00001. To improve interpretation of EOH and WOH ordinations, a second matrix was included with either land use/cover and chemistry variables (r^2 cutoff set at 0.20) or metrics (WQS, total richness, EPT richness, HBI, PMA, total density; r^2 cutoff set at 0.15). To reduce redundancy in the land use/cover and water chemistry variables for the second matrix, we used Canonical Correspondence Analysis and the automatic forward selection procedure to identify significant variables ($p < 0.05$) (CANOCO Version 4.5, Microcomputer Power, Ithaca, NY) (see Kratzer et al. 2006).

Results and Discussion

Range of Conditions Observed at WOH and EOH Sites in 2000-2005

The 110 sampling sites in the NYC watersheds were classified as exhibiting no impact, slight impact, moderate impact, or severe impact based on the aquatic macroinvertebrates collected at those sites averaged over three or six years (Fig. 7.1). The majority (79%) of sites were classified as exhibiting no impact (38%) or slight impact (41%); 20% of the sites were classified as exhibiting moderate impact; and one site (Hallocks Mill Brook near Amawalk) was classified as exhibiting severe impact (Fig. 7.2). All WOH sites were classified as either no impact (60%) or

slight impact (40%) (Figs. 7.2-7.8). All sites classified as exhibiting either moderate or severe impact were EOH sites (Figs. 7.2 and 7.9-7.17). Thus, the difference in WQSs between the highest and lowest quality WOH sites was much smaller than the difference in WQSs between the highest and lowest quality EOH sites (Table 7.2, Figs. 7.3-7.17). Based on WQS, the 17 integrated sites were representative of many of the sites that were classified as no impact (9), slight impact (6), or moderate impact (2) (Fig. 7.18). Conditions characteristic of severe impact were not represented among the 17 integrated sites, although Site 55 (Kisco River near Stanwood) and Site 130 (Titicus River near Salem Center) were classified as moderately impacted (Figs. 7.12, 7.16, and 7.18).

The macroinvertebrate assemblages associated with the classification categories (i.e., no impact, slight impact, and moderate impact) differed markedly. For example, total species richness averaged about 33 species per 100 individuals while EPT richness averaged about 13 species per 100 individuals at an unimpacted site (i.e., WQS = 8.75). In contrast, total species richness averaged about 25 species at a slightly impacted site (i.e., WQS = 6.25) and 17 species at a moderately impacted site (i.e., WQS = 3.75). EPT richness averaged about seven species at a slightly impacted site and two species at a moderately impacted site. This change from an unimpacted site to a moderately impacted site represents a 48% reduction in total species richness, and an 85% reduction in EPT richness (Fig. 7.19). Data for mayfly density are more variable (note the log scale on Fig. 7.20), but paralleled these differences. Mayfly density ranged from 1000-10,000 individuals/m^2 at unimpacted sites versus 0-3000 individuals/m^2 at moderately impacted sites (Table 7.3). Mayflies, often considered the most sensitive macroinvertebrate group, were frequently at very low densities or absent at moderately impacted sites.

Annual variation in macroinvertebrate assemblages resulted in annual differences in WQSs for most sites (Figs. 7.21 and 7.22). For example, WQSs in 2001 were higher at most sites relative to all other years. In some cases, annual variation in WQS did not affect site classification based on the three or six year average. For example for the ten sites with the highest average WQS in the WOH or EOH, nine sites in the WOH and three sites in the EOH were classified as unimpacted in all three or six years sampled (Figs. 7.21 and 7.22). Similarly, all 10 sites in the EOH with the lowest average WQS were classified as severe impact (1 site) or moderately impacted (9 sites) in all three years sampled. In other cases, one of the years did not agree with the three-year or six-year mean site classifications (Fig. 7.23). Overall, 61% of the annual classifications did not agree with classifications based on average WQS. For the 97 sites with three years of data the three annual classifications agreed with the average classification at 41% of the sites, two of three annual classifications agreed with the average classification at 43% of the sites, one of three annual classifications agreed with the average classification at 14% of the sites, and only one site (Site 120 - Bushnellsville Creek) had none of three annual classifications agreed with the average classification (Fig. 7.23). For the 12 sites with six years of data the six annual classifications agreed with the average classification at 17% of the sites, five of six annual classifications agreed with the average classification at 33% of the sites, four of six annual classifications agreed with the average classification at 17% of the sites, and three of six annual classifications agreed with the average classification at 33% of the sites (Fig. 7.23). In some cases, annual classifications might be higher than average; in other cases, annual classifications might be lower than average (Figs. 7.21 and 7.22). Only two sites span three classifications: Sites 32 and 120. Site 32, Brady Brook near Pawling, was classified as

moderately impacted in 2000, unimpacted in 2001, and slightly impacted in 2002. Site 120, Bushnellsville Creek near Shandaken was non-impacted in 2003 and 2004 and moderately impacted in 2005 (Appendix B.6.5). Agreement between annual classifications and the classification based on average WQS was lowest when average WQS was near a line separating two classification categories (e.g., no versus slight impact or slight versus moderate impact). For these conditions, annual variation in macroinvertebrate assemblages inevitably resulted in variation in site classification. This illustrates the importance of having more than one year of data before labeling a site with a classification category. Caution should be exercised when using site classifications based on an average WQS near a classification line. The agreement for these sites would be expected to be about 50%.

Reference Sites, Site Classifications, and Evaluation of Differences (2000-2005)

WOH and EOH sites had consistently different faunas based on results from Non-metric Multidimensional Scaling that examined genus-level densities using 3-yr averages (Fig. 7.24). This presumably reflects a number of biogeographic, ecological, and anthropogenic differences between the regions (Kratzer et al. 2006). These results suggest that more conservative (i.e., reducing Type I errors) site evaluations would result if reference sites were designated for the WOH and EOH watersheds separately. In stream bioassessment, reference conditions represent a regional state that is natural or the least disturbed and are often designated to make comparisons and gage impairment. In this study, sites were statistically compared to references sites that were determined in two ways: 1) using WQS scores and 2) Best Available Conditions (BAC).

The WQS reference sites for WOH were Site 121 - Warner Creek near Chichester, Site 9 - Trout Creek near Trout Creek, Site 109 - Batavia Kill near Kellys Corner, Site 25 - Beaver Kill at Mount Tremper, and Site 153 - Loomis Brook near Trout Creek (Table 7.2). The EOH WQS reference sites were Site 125 - Quaker Brook at W.G. Merrit County Park, Site 52 - Cross River in Ward Pound Ridge Resv., Site 34 - Haviland Hollow Brook, Site 33 - Leetown Stream near Farmers Mills, and Site 127 - Black Pond Brook at Meads Corner (Table 7.2). Site comparisons, excluding those used as WQS reference sites are presented for 52 WOH sites and 48 EOH sites (Fig. 7.25), and for the sites within the respective watersheds (Fig. 7.26).

The BAC reference sites for WOH were Site 22 - Esopus Creek near Big Indian, Site 111 - Dry Brook near Mapledale, Site 112 - Mill Brook near Grant Mills, Site 121 - Warner Creek near Chichester, and Site 114 - Holiday Brook near Downsville. The EOH BAC reference sites were Site 125 - Quaker Brook at W.G. Merrit County Park, Site 37 - Horse Pound Brook near Lake Carmel, Site 34 - Haviland Hollow Brook, Site 124 - Unnamed tributary of the East Branch Croton River near Pawling, and Site 127 - Black Pond Brook at Meads Corner.

As already noted, the majority of WOH and EOH sites were classified as exhibiting no impact (38%) or slight impact (41%). Only 20% of the sites were classified as exhibiting moderate impact, and one site was classified as exhibiting severe impact (Fig. 7.2). Overall, site classifications indicated that 62% of the sites exhibited some degradation. When the data from 2000 to 2005 were analyzed in a 2-way ANOVA (station by year), many of the sites classified as exhibiting some degradation could not be differentiated statistically from the WQS or BAC reference sites (Fig. 7.25). For example, of the 23 WOH sites classified as exhibiting slight impact, six had a WQS that was statistically different from the WQS reference sites and none

had a WQS that differed from the BAC reference sites. Thus, 13% of the sites differed from the WQS reference sites and none could be distinguished with confidence from reference conditions at BAC reference sites defined using land use and water chemistry. In the EOH, there were 29 sites having the lowest WQSs that could be distinguished from both the WQS and BAC reference conditions. These results suggest that, with three years of data, a WQS difference of >1.60 points is required to distinguish between WOH sites using WQS reference conditions and >1.78 points are required in the EOH using either WQS or BAC reference conditions. This difference is smaller than the 2.5 points between water quality categories (non, slight, moderate and severe) therefore some of the sites that were statistically different from the reference sites were only slightly impacted. The fact that BAC reference sites did not have the highest WQSs (especially in WOH) demonstrates the disconnect that can occur between such metrics and the characteristics of land use/cover and water chemistry that relate to water quality.

Comparison with Recent NYSDEC and NYCDEP Data

The WQS protocol developed by NYSDEC summarizes data from 100 macroinvertebrates collected from riffles in July-September with a kick net (0.8 x 0.9-mm mesh) into a single water quality score, and then classifies the site primarily based on that score (Bode et al. 2002b). Various forms of this is a standard semi-quantitative method have been incorporated into numerous state and federal monitoring programs, especially since USEPA's rapid bioassessment manual was first published in 1989 (Barbour et al. 1999, Carter and Resh 2001). The NYSDEC program predates the rapid bioassessment manual and has a much longer history than most of these other monitoring programs. The applicability of the NYSDEC summarization and classification protocol to other sampling designs remains unknown. WQSs calculated in our study based on approximately 200 macroinvertebrates from each of four quantitative composite samples collected from riffles in April/May with a Surber sampler (0.250-mm mesh). This is a standard quantitative approach to sampling stream macroinvertebrates that has a long history in stream ecology (Surber 1937). One could expect that WQSs calculated using the two methods would differ because of the different collecting devices, sampling areas, numbers of individuals identified, and seasons. Data (i.e., 1994-1997 for NYCDEP and 1998-2004 for NYSDEC) from 19 WOH sites and 26 EOH sites show that the two techniques rarely resulted in large differences in WQS (Fig. 7.27). In other words, the NYSDEC and NYCDEP scores were either within or close to the range in our scores. However, as average WQS decreased, some EOH sites deviated from this general pattern (i.e., Sites 134, 130, 140, and 142) and showed a greater range in WQSs and further suggest that WQSs resulting with our methodology were lower than the NYSDEC and NYCDEP methods. Many sites had WQSs that straddled two water quality categories, though at Site 46 WQSs spanned three water quality categories from moderately impacted in 2002 (SWRC data) to non-impacted in 1999 (NYSDEC data). The WQS comparisons may be misleading in that data are not available for each site in each year, and furthermore, within year comparisons were not always possible at a site. Nevertheless, SWRC and NYSDEC score comparisons for all 45 sites (Fig. 7.27) and for 21 sites with intra annual comparisons (Fig. 7.28) illustrate that our scores tended to be lower than NYSDEC WQSs.

NYSDEC have developed a method that uses macroinvertebrate community structure to identify point and nonpoint sources that are contributing to site degradation (Bode et al. 2002b, Riva-Murray et al. 2002). The impact source determination (ISD) procedure compares the relative abundances of key taxa from a site with relative abundances of those taxa in natural

communities as well as in communities significantly impaired by nonpoint nutrients and pesticides, municipal/industrial effluents, toxins, sewage effluent/animal wastes, siltation, and impoundments. Our initial results suggest that the ISD methods are not able to consistently identify the non-impacted sites, and 3-4 sources are often identified for impaired sites. This may reflect the different collecting devices, sampling areas, numbers of individuals identified, and seasons. At this point, it appears that significant changes in the ISD procedures may be required before they can be used with the SWRC data.

Ecosystem Implications of Degradation

At the 17 integrated sites, measures of ecosystem function such as gross primary production, net ecosystem metabolism, or nutrient (nitrogen and phosphorus) uptake velocities were measured in addition to samples of aquatic macroinvertebrates, base flow organic and inorganic chemistry, tracers, and seston. These 17 sites represent a range of conditions (Fig. 7.18), from unimpaired (i.e., Site 9 - Trout Creek near Trout Creek) to moderate impacted (Site 55 - Kisco River near Stanwood and Site 130 - Titicus River near Salem Center). The analyses of these measures of ecosystem function indicate that gross primary production, community respiration, P/R, and nutrient uptake velocities were depressed at Sites 55 and 130 relative to the other integrated sites. Details of these analyses can be found in Chapters 8 and 9 of this report. The implications are that the observed differences in macroinvertebrate community structure are not just a matter of changes in macroinvertebrate abundances. Rather, these differences are associated with measurable changes in the ability of the ecosystem to produce and break down organic matter, and to process available nutrients. This relationship extrapolated across all sites suggests that the 45 EOH sites and 23 WOH sites where macroinvertebrates exhibit evidence of slight to severe impact also have experienced some degradation of ecosystem function.

Factors Related to Macroinvertebrate Distribution and Abundance

Non-metric Multidimensional Scaling was used to examine spatial variability across macroinvertebrate taxa using three year averages for all sites, EOH sites, and WOH sites. The NMS using data from all the sites indicated the first two axes accounted for 87.2% of the variance in the ordination (Fig. 7.24). Spatial differences among community assemblages were evident in the NMS ordination as sites clustered based on geographic regions, EOH and WOH. There was more variability in macroinvertebrate communities among EOH sites than WOH sites (Kratzer et al. 2006). Based on the initial NMS on all sites, associations between regional (e.g., watershed land use) and local (e.g., baseflow water chemistry) environmental factors were examined separately for EOH and WOH sites.

WOH sites grouped by sub-region with similar assemblages in the West and East Branches of the Delaware Watersheds and similar assemblages in the Schoharie and Esopus Watersheds (Fig. 7.29). Among the WOH sites there was an important relationship between macroinvertebrate assemblages and land use and environmental conditions. This relationship was strong along Axis 2 (40.3% of total variance explained), which was primarily a forest - farmland gradient. Sites in the Neversink (primarily forested sites) and the West and East Branches of the Delaware (many farmland influenced sites) played an important role along this gradient. The farmland influence was characterized by high alkalinity and DOC, which is indicative of rich organic soils, and was correlated to many land use variables (% farmland, % grassland, and %

cropland) and higher population density. Axis 3 (28.0% of total variance explained) corresponded to total dissolved phosphorus (TDP) and variables related to large rivers (high velocity and depth, and large watershed area). Most sites in the Schoharie and Esopus Watersheds were relatively large rivers that had limited riparian buffers and low phosphorus levels. The changes in the macroinvertebrate assemblages were rather subtle relative to the differences observed among EOH sites. For example, the most agricultural sites were not dominated by chironomids. Rather, these sites supported a number mayfly, stonefly, and caddisfly species as well as numerous chironomid species. In fact these sites tended to have higher richness than forested sites but higher HBI suggesting that despite the presence of EPT taxa, pollution tolerant taxa were more abundant (Fig. 7.29). Even though macroinvertebrate assemblages appeared to be responding to environmental conditions in the WOH streams, no relationship was observed between WQS and the forest-to-agriculture gradient.

Among the EOH sites, there was a strong relationship between macroinvertebrate assemblages (as described by WQS or by macroinvertebrate densities) and environmental conditions (Fig. 7.30). This relationship was strongest (accounted for 70.5% of total variance) along Axis 1, which was primarily a forest-to-urban gradient. The urban influence was characterized by land use (% urban) and by high levels of chlorophyll *a* on instream rocks, which infers an open canopy or fewer trees in the riparian zone. Urban influenced sites also had higher densities of roads and people, and larger residential areas in the watershed. A diverse assemblage of macroinvertebrates characterized more forested sites (e.g., sites in the East, West and Middle Branches of the Croton) while various chironomid midges predominated at the sites with more impervious surface in the watershed (e.g., sites in Croton and Kensico Reservoirs and their tributaries). WQS correlated strongly with this forest-to-urban gradient. Macroinvertebrates also appeared to respond to point source discharge (i.e., SPDES) that correlated to Axis 2 (accounted for 15.7% of total variance) and characterized some stream sites in the Cross and Muscoot Reservoir areas.

Thus, the analyses of macroinvertebrate data from the WOH and EOH sites in Phase I (2000-2002) and Phase II (2003-2005) indicate that assemblages differ among many of these sites, and that environmental conditions may be contributing to the intersite differences (Figs. 7.29 and 7.30). In the case of the EOH sites, the macroinvertebrates appear to respond strongly to land use and water chemistry. A diverse assemblage of macroinvertebrates characterized more forested sites while various chironomid midges predominated at the sites with more impervious surfaces and higher populations in the watershed. Assuming that reference conditions at these sites consists of an abundant and diverse macroinvertebrate assemblage, the predominance of chironomids at these sites reflects a significant loss of species richness, a change in relative abundance, and an increase in pollution tolerance. Differences in land use (e.g., forest versus agriculture) and water chemistry (e.g., phosphorus) were also associated with differences among macroinvertebrate assemblages at WOH sites. However, the responses to environmental conditions at WOH sites suggest greater species richness (e.g., chironomids and EPT taxa) but poorer water quality (i.e., high HBI) with an increase in agriculture, yet no change in relative abundance or WQS based on land use. Instead, WQS distinguished large rivers from small streams in the WOH.

Temporal Coherence Among the 12 Long-term Sites

Temporal coherence is defined as the synchronous fluctuations in parameter(s) among locations within a geographic region and is a way to examine if populations are influenced more by site-specific or regional-specific factors (Magnuson et al. 1990). Synchronous patterns among macroinvertebrate taxa groups or species suggest year specific factors (e.g., climate) are influencing biota. In contrast, absence of temporal coherence suggest site-specific or local-scale factors are most important (Rusak et al. 1999). Pearson product-moment correlation was used to assess the synchrony of hydrology (see Table 7.4, Richter et al. 1996) and macroinvertebrates (Tables 7.5 and 7.6) for 12 streams (WOH-Sites 3, 6, 9, 10, 15, 23, 26, 29 & EOH-Sites 34, 46, 52, 55) over a 6-yr period. Correlation coefficients were calculated for metrics, taxa (i.e., order, family, and sub-tribes of Chironomidae), and hydrologic parameters for all possible site pairs (Magnuson et al. 1990). For the macroinvertebrate analyses there were 66 site pairs (e.g., Sites 3 & 6, 3 & 9, 3 & 10, etc.) for the 12 sites, 28 site pairs for WOH, and 6 site pairs for EOH. For the hydrologic parameters there were only 45 site pairs because no hydrology data was available for Sites 6 and 26 in WOH. Correlation coefficients were averaged by site pairs and variables, and significant pairwise comparisons (i.e., $r \geq +0.67$) were expressed as a percentage (Table 7.5).

Temporal coherence among streams was more pronounced when examining WOH and EOH assemblages separately (Table 7.6). This was not unexpected because it has already been established that there are distinct regional assemblages (Fig. 7.24) and greater temporal coherence is more likely among sites with more similar communities. EOH site pairs had lower mean correlation values for taxa and metrics compared to WOH (Table 7.6). This may be due to the greater range of degradation in the east or a function of a smaller sample size. It was expected that not all the taxa would indicate temporal coherence and those taxa that did have synchrony might have different coherence patterns from other taxa because of taxa differences in generation time. In the WOH, Baetidae ($r = 0.50$, % = 50), Capniidae/Leutridae ($r = 0.63$; % = 61), Coleoptera ($r = 0.56$; % = 39), Ephemerellidae ($r = 0.57$; % = 43), and taxa richness ($r = 0.41$; % = 36) had many site pair correlations. In the EOH, Oligochaeta ($r = 0.91$) and Diamesinae ($r = 0.85$) had 100% correlation among the six site pairs (Table 7.5).

Of the 16 hydrological parameters, three (e.g., sumq365, minq30 and minq90) had 100% strong correlations and many others (e.g., sumq60, sumq90, maxq30, npulse_high, minq7, and xpulse_low_duration) had high ($r \geq 66$) mean correlations (Table 7.4). Regressions (of r values) indicated many relationships between taxa and hydrologic parameters with strong correlations. For example in the WOH, Coleoptera ($r^2 = 0.57$) related positively to low flow (minq7), and Baetidae ($r^2 = 0.48$) and Capniidae/Leuctridae ($r^2 = 0.59$) were positively related to the number of high pulse events (npulse_high). In addition, Baetidae ($r^2 = 0.44$) had a positive association to annual peak discharge (peakq365). In the EOH, Oligochaeta positively correlated to annual peak discharge (peakq365) and total annual discharge (sumq365), but Diamesinae was negatively related to total annual discharge (Fig. 7.31). Theses results imply certain taxa are controlled by factors beyond the individual stream or watershed and are responding to regional factors (e.g., annual flow, flood or drought events). Because taxa have differences in life history (e.g., habitat or food requirements), they may have different responses to the same hydrologic events.

Not surprisingly, sites that were closer to one another tended to have stronger correlations among taxa ($r^2 = 0.45$, df = 65, $p < 0.05$; Fig. 7.32), although strongly correlated sites were not

always within the same watershed. This suggests taxa and hydrological conditions are spatial related, but not necessarily determined by watershed features (e.g., watershed area, land cover, regional geology). Site pairs for taxa with strong correlations ($r \geq 33$, % ≥ 30) were only seen in the WOH: Sites 3 & 10, 3 & 23, 6 & 9, 6 & 23, 10 & 15, 15 & 29, 23 & 26, and 23 & 29. Although EOH sites were spatial close to one another (< 33 km) they had low mean correlations ($r < 0.27$), implying degraded sites are less likely to show temporal coherence (Fig. 7.32).

Literature Cited

Barbour, M. T., J. Gerritsen, B. D. Snyder, and J. B. Stribling. 1999. Rapid Bioassessment Protocols for use in streams and wadeable rivers: Periphyton, benthic macroinvertebrates and fish. Second Edition. EPA 841-F-99-002. U.S. Environmental Protection Agency; Office of Water; Washington, D.C.

Bode, R. W., M. A. Novak, L. E. Abele, and D. L. Heitzman. 2000a. Assessment of water quality of streams in the New York City watershed based on analysis of invertebrate tissues and invertebrate communities. New York Department of Environmental Conservation Report, Albany, New York.

Bode, R. W., M. A. Novak, L. E. Abele, D. L. Heitzman, and S. Passy. 2000b. Assessment of water quality of streams in the New York City watershed based on analysis of invertebrate tissues and invertebrate communities. Part II: 1999 sampling results. New York Department of Environmental Conservation Report, Albany, New York

Bode, R. W., M. A. Novak, L. E. Abele, D. L. Heitzman, and A. J. Smith. 2002a. Pesticides in streams of the Croton system, and their biological impacts. Part I. Targeted land uses. New York Department of Environmental Conservation Report, Albany, New York

Bode, R. W., M. A. Novak. L. E. Abele, D. L. Heitzman, and A. J. Smith. 2002b. Quality assurance work plan for biological stream monitoring in New York State. New York State Department of Environmental Conservation Report, Albany, New York.

Bode, R. W., M. A. Novak. L. E. Abele, D. L. Heitzman, and A. J. Smith. 2003. Pesticides in streams of the Croton system, and their biological impacts. Part II. Longitudinal trends. New York State Department of Environmental Conservation Report, Albany, New York.

Bode, R. W., M. A. Novak. L. E. Abele, D. L. Heitzman, and A. J. Smith. 2005. Pesticides in streams of the Croton system, and their biological impacts. Part III. Seasonal trends. New York State Department of Environmental Conservation Report, Albany, New York.

Bode, R. W., M. A. Novak. L. E. Abele, D. L. Heitzman, and A. J. Smith. 2006. Pesticides in streams of the Croton system, and their biological impacts. Part IV. Seasonal and longitudinal trend studies. New York State Department of Environmental Conservation Report, Albany, New York.

Bode, R. W., M. A. Novak. L. E. Abele, D. L. Heitzman, and A. J. Smith. 2007. Pesticides in streams of the Croton system, and their biological impacts. Part V. Long-term trends. New York State Department of Environmental Conservation Report, Albany, New York.

Carter, J. L. and V. H. Resh. 2001. After site selection and before data analysis: sampling, sorting, and laboratory procedures used in stream benthic macroinvertebrate monitoring programs by USA state agencies. Journal of the North American Benthological Society 20: 658-682

Cutietta-Olson, C. R. and M. Rosenfeld. 2000. Report on stream macroinvertebrate biomonitoring: conducted within the watersheds of the New York City water supply system during 1994-1998. New York City Department of Environmental Protection, Bureau of Water Supply Quality and Protection, New York

Elliott, J. M. 1977. Some methods for the statistical analysis of samples of benthic invertebrates. 2nd ed. Freshwater Biological Association Scientific Publication No. 25. 156 pp.

Hellawell, J. M. 1986. Biological Indicators of Freshwater Pollution and Environmental Management. Elsevier Applied Science, London, England.

Kratzer, E. B., J. K. Jackson, D. B. Arscott, A. K. Aufdenkampe, C. L. Dow, L. A. Kaplan, J. D. Newbold, and B. W. Sweeney. 2006. Macroinvertebrate distribution in relation to land use and water chemistry in New York City drinking-water-supply watershed. Journal of the North American Benthological Society 25:954-976.

Lorenzen, C. J. 1967. Determinations of chlorophyll and phaeo-pigments: spectrophotometric equations. Limnology and Oceanography 12:343-346.

Magnuson, J. J., B. J. Benson, and T. K. Kratz. 1990. Temporal coherence in the limnology of a suite of lakes in Wisconsin, USA. Freshwater Biology 23:145-159.

Resh, V. H. and J. K. Jackson. 1993. Rapid assessment approaches to biomonitoring using benthic macroinvertebrates. Pages 195-233 *in*: Freshwater Biomonitoring and Benthic Macroinvertebrates (D. M. Rosenberg and V. H. Resh, eds.). Chapman and Hall, New York.

Richter, B. D., J. V. Baumgartner, J. Powell, and D. P. Braun. 1996. A method for assessing hydrologic alteration within ecosystems. Conservation Biology 10:1163-1174.

Riva-Murray, K., R. W. Bode, P. J. Phillips, and G. L. Wall. 2002. Impact source determination with biomonitoring data in New York State: concordance with environmental data. Northeastern Naturalist 9:127-162.

Rusak, J. A., N. D. Yan, K. M. Somers, and D. J. McQueen. 1999. The temporal coherence of zooplankton populations abundances in neighboring north-temperate lakes. American Naturalist 153:46-58.

Smith, A. J., R. W. Bode, M. A. Novak. L. E. Abele, and D. L. Heitzman. 2006. A Nutrient Biotic Index (NBI) for use with benthic macroinvertebrate communities and its relationship with surface water nutrient concentrations in flowing waters. New York State Department of Environmental Conservation Report, Albany, New York.

Surber, E. W. 1937. Rainbow trout and bottom fauna production in one mile of stream. Transactions of the American Fisheries Society 66:193-202.

Weber, C. I. 1973. Biological field and laboratory methods for measuring the quality of surface waters and effluents. EPA-670/4-73-001.

Table 7.1. Number of sites and timing of when macroinvertebrate samples were collected for Phase I and 2 of this project.

Phase	Year	No. Sites	Collection dates
1	2000	60	1-18 May
	2001	60	30 April - 10 May
	2002	60	5-16 May
2	2003	60	5-16 May
	2004	62	3-13 May
	2005	63	2-12 May

Table 7.2. Ten West of the Hudson River (WOH) and East of the Hudson River (EOH) sites where macroinvertebrates indicated the highest and lowest stream quality based on the Water Quality Score (WQS).

Site number	Site Description	WQS	Site number	Site Description	WQS
Highest Quality (descending order)			Lowest Quality (ascending order)		
West of the Hudson River					
121	Warner Creek nr Chichester	9.0	117	Batavia Kill nr Windham	6.4
9	Trout Creek nr Trout Creek	8.6	26	Esopus Creek nr Mount Tremper	6.5
109	Batavia Kill nr Kellys Corner	8.6	30	Rondout Creek nr Lowes Corner	6.5
25	Beaver Kill at Mount Tremper	8.5	120	Bushnellsville Creek at Shandaken	6.6
153	Loomis Brook nr Trout Creek	8.5	20	Batavia Kill nr Prattsville	6.7
11	Bush Kill nr Arkville	8.4	118	Bear Kill nr Grand Gorge	6.7
102	Coulter Brook nr Bovina Center	8.4	123	Rondout Creek nr Peekamoose	6.8
27	W. Br. Neversink R. nr Claryville	8.4	21	Schoharie Creek nr Prattsville	6.9
13	E. Br. Delaware R. nr Dunraven	8.4	17	Schoharie Creek nr Jewett Center	7.0
7	West Brook nr Walton	8.3	3	W. Br. Delaware R. at South Kortright	7.0
East of the Hudson River					
125	Quaker Brook at Merrit Cnty Park	8.5	49	Hallocks Mill Brook nr Amawalk	1.8
52	Cross River in WPR Resv	8.1	59	Trib of Kensico Resv nr Hawthorn	3.2
34	Haviland Hollow Brook	8.1	60	Trib of Kensico Resv nr WCA	3.5
33	Leetown Stm nr Farmers Mills	7.8	58	Trib of Croton R. nr Lake Purdy	3.6
127	Black Pond Brook at Meads Corner	7.7	43	Secor Brook at West Mahopac	3.7
124	Trib of E. Br. Croton R. nr Pawling	7.7	138	Cross River nr Katonah	3.8
146	Stone Hill River nr Bedford	7.6	140	Hunter Brook nr Yorktown	3.8
36	W. Br. Croton R. nr Allen Corners	7.6	57	Kisco River at Mount Kisco	3.9
129	Trib of E. Br. Croton R.	7.5	148	Trib of Kensico Res. nr Thornwood	4.0
149	Waccabuc R. at Boutonville	7.5	133	Trib of Muscoot R. at Mahopac Falls	4.3

Table 7.3. Mean Density (individuals/m^2) ± 1 SE of selected groups of aquatic macroinvertebrates from 110 sites (WOH followed by EOH) in the NYC drinking water watersheds. Column labels are underlined: Total Macroinvertebrate density, Total Insect density, EPT density, Ephemeroptera density, Plecoptera density, Trichoptera density, Diptera density, Coleoptera density, Total Noninsect density, Oligochaeta density.

Site	Total	Insects	EPT	E	P	T	D	C	Noninsects	O
1	9048±875	8732±795	3965±1248	2398±951	871±211	696±156	4287±1742	466±103	315±91	110±61
2	15732±5151	13600±3863	3795±494	2443±435	560±47	792±186	8959±3255	839±529	2132±1400	644±327
3	28773±3160	25233±2750	4758±462	2591±291	346±110	1821±225	19706±2980	761±169	3540±826	2282±682
4	32664±15286	30634±14356	13474±8878	10886±7568	738±359	1849±968	15957±4824	1211±665	2022±935	681±183
5	17366±4395	13780±3050	5246±2832	4170±2268	388±188	688±533	7576±1180	951±751	3585±1351	1828±422
6	35694±8451	28747±7591	9145±2475	5625±1718	849±195	2670±672	13993±4719	5595±1359	6947±1372	3029±900
7	18872±4224	16558±3256	6771±2167	4449±1618	1137±459	1184±235	9272±1013	496±101	2314±1006	601±180
8	16125±1015	13474±638	3889±429	2625±102	465±303	799±231	9094±839	491±175	2650±665	1589±855
9	28100±6599	24715±5991	10909±2917	7746±2255	1228±386	1936±356	12484±3182	1277±399	3385±738	619±238
10	26511±2848	21440±2011	8014±959	5472±787	662±117	1880±315	12000±2099	1419±439	5071±993	2600±691
11	34628±8369	30983±8159	14217±4059	8860±1691	1520±394	3838±2208	16458±6228	308±32	3645±266	1099±516
12	24848±5439	21522±4322	6984±2050	4930±1019	194±121	1861±969	14461±4155	76±49	3326±1118	1842±818
13	16727±2277	13930±1713	6510±1009	4473±1056	245±78	1791±251	7174±1818	246±130	2797±708	991±487
14	19939±3457	15306±3264	7333±1548	5357±1640	530±86	1446±532	7654±2450	312±141	4633±610	1565±758
15	36227±7255	29329±6089	9562±2688	6196±1557	559±211	2807±993	18918±3881	831±260	6898±1778	1681±573
16	6826±1056	5846±945	2020±377	1395±333	408±108	216±130	3663±679	155±70	980±135	266±129
17	16149±6992	12594±4797	3041±565	1969±180	584±547	488±157	9499±4252	47±32	3555±2229	2049±1511
18	12071±4020	10619±3693	3326±1014	2261±675	194±79	871±404	7271±2835	14±4	1452±540	780±375
19	13917±3854	12706±3580	3589±627	2515±584	542±333	532±183	9025±2992	77±69	1211±301	675±151
20	10372±3407	7170±2055	1778±165	614±125	540±304	624±349	5213±1856	168±53	3201±1425	705±298
21	15232±4548	11349±3688	2585±59	1816±196	286±165	484±197	8483±3811	280±164	3883±1233	1729±818
22	33649±2446	29649±2151	10222±1478	7842±1869	530±52	1849±456	19384±3619	29±14	4000±311	2165±696
23	17849±4382	16014±3998	6421±1482	5348±1232	228±53	845±302	9516±2911	73±42	1835±585	958±494
24	15963±9186	14694±8589	3558±859	2789±519	216±59	553±390	11119±7749	3±3	1269±607	508±413
25	9870±1441	8415±852	4506±247	3177±259	450±66	879±214	3812±1060	83±40	1455±618	914±582
26	15999±5498	11796±3495	2473±316	1962±272	90±18	421±171	9302±3376	14±7	4203±2017	2297±1411
27	19440±4469	17076±3903	6961±1273	4747±867	591±133	1623±289	10028±2765	85±55	2364±1409	897±659
28	13194±4447	11237±4505	3692±1026	1339±582	1179±413	1174±300	6911±3809	627±266	1958±224	728±286

Table 7.3. Continued with WOH sites.

Site	Total	Insects	EPT	E	P	T	D	C	Noninsects	O
29	18505±3856	16482±3620	4714±907	2782±551	834±221	1098±246	11673±2907	95±34	2023±390	557±178
30	19595±4542	17523±4250	3951±914	2667±665	324±65	960±436	13520±3738	53±21	2072±920	817±366
101	21658±3985	18974±3516	6541±1521	5432±1418	741±86	368±87	11611±3864	823±87	2684±726	718±487
102	15679±496	14772±332	7409±853	5994±748	590±97	824±181	7180±806	168±31	907±165	129±15
103	41508±8594	36769±8950	15216±2761	9845±1423	2595±553	2777±863	19826±6996	1699±421	4738±367	1479±379
104	15492±3777	13808±3550	7148±3058	5176±2430	949±408	1024±259	6427±1265	226±73	1685±702	878±574
105	20920±8259	16550±5412	7808±3362	5289±1898	818±567	1702±964	7875±2813	821±622	4370±3419	1482±1354
106	10976±3776	10165±3370	5331±2391	3863±1666	926±585	542±243	4574±1023	251±89	810±413	198±174
107	37047±2087	25403±3415	9180±2399	4796±1108	1302±883	3082±963	12853±2762	3348±1025	11644±1592	6053±1466
108	5196±650	4980±562	2569±357	906±231	1364±112	299±36	2101±82	299±129	216±92	78±44
109	17630±3904	15699±2992	8689±3390	6252±2774	977±247	1460±374	6736±534	266±27	1931±1010	521±367
110	12216±4339	11251±3579	5445±2800	4077±2147	596±358	773±305	5697±1341	107±34	965±799	155±127
111	16096±3019	15008±2517	6437±2278	4502±1432	216±46	1719±1111	8547±909	24±13	1088±565	200±103
112	12937±2847	10724±1678	3951±1300	2630±1033	352±25	969±445	6689±353	77±31	2213±1449	731±555
113	16912±3775	15713±3247	5391±1602	3436±846	644±250	1311±628	10177±1608	135±74	1198±671	516±410
114	10771±2284	9195±1576	4214±1664	3245±1271	435±187	535±221	4665±422	316±111	1576±712	1022±505
115	7311±2729	6028±2194	2259±520	1231±219	405±131	623±226	3684±1696	78±35	1283±539	390±213
116	7191±2172	6357±2129	2012±304	1539±290	138±17	335±73	4324±1834	18±6	834±199	22±5
117	7823±2151	7213±1926	2179±1083	1887±1091	160±58	132±21	5006±1639	25±19	609±249	79±23
118	12710±3587	11778±3025	3076±436	2440±279	308±150	328±61	8406±2533	278±126	933±640	724±546
119	18647±5312	16129±4232	7448±3559	5897±2769	721±438	830±381	8404±2161	277±163	2518±1114	433±233
120	13972±4438	12857±3952	4882±2209	3782±1771	166±52	933±442	7947±2881	22±22	1114±523	541±273
121	5832±1914	5064±1686	3415±1254	2505±1000	438±123	472±166	1574±570	71±24	768±229	322±127
122	11283±2165	10214±1778	2705±640	923±174	949±48	834±427	6858±970	648±213	1068±392	44±28
123	27843±13552	24755±12199	5563±2463	2955±1228	1404±585	1205±768	14997±6804	4195±3056	3088±1478	777±591
151	26313±4739	24035±4608	5827±613	3300±438	744±228	1783±382	17612±4102	575±247	2278±291	1259±66
153	17774±2959	16287±2720	10085±1928	8128±1450	663±57	1294±497	6060±1670	111±41	1487±246	568±137
159	11148±3256	10389±2721	5926±3215	4397±2151	1049±675	480±389	4328±609	135±115	759±535	462±407
160	27036±15437	22376±11151	8996±6487	5735±3728	1545±1100	1717±1659	12996±4380	384±283	4659±4287	1961±1932

Table 7.3. Continued with EOH sites.

Site	Total	Insects	EPT	E	P	T	D	C	Noninsects	O
31	21090±4594	15606±3440	6165±2788	2824±1144	2358±1148	982±551	7885±94	1513±749	5484±1282	2301±950
32	42439±7343	34724±6984	7125±1809	3986±1278	2495±935	645±273	26222±9216	1376±647	7715±361	4459±1677
33	17130±5414	14934±4749	7947±3436	3037±1889	3890±1451	1020±627	5613±2262	1188±523	2196±665	583±113
34	13581±2687	10971±2115	4696±796	2398±471	1255±239	1043±212	4820±1126	1428±407	2610±661	799±202
35	22677±6559	18836±6575	9578±3347	7288±3056	1393±545	897±678	8265±3070	947±443	3841±1966	2289±1393
36	37476±15015	27143±1241	7912±2632	3351±1832	3846±768	716±158	15204±8259	3907±1586	10332±4048	3302±1846
37	18699±3445	15778±4404	9937±2876	4859±3348	4351±722	727±128	4713±1432	975±378	2920±1232	2072±1560
38	19882&2187	15422±2580	4364±1468	2476±1198	55±31	1834±306	10964±1483	29±19	4460±756	1339±79
39	29789±9935	25008±8944	5114±3599	134±50	4217±3311	762±292	19746±1007	143±103	4781±2850	4294±2668
40	14583±2042	10557±2216	3997±649	2266±169	1383±713	348±136	6527±2786	29±19	4025±419	1788±1296
41	20292±3192	16755±3094	8203±1070	2827±443	3680±972	1697±506	3828±989	4717±1039	3536±122	1931±514
42	32401±2093	28796±1431	5419±410	2086±419	2552±467	781±354	20315±1094	3004±1097	3606±768	2014±130
43	81907±24172	56573±1599	2681±1412	186±127	1047±548	1448±946	50323±1358	3570±1634	25333±9876	23025±8859
44	25238±1858	21720±499	4086±651	1276±117	29±14	2781±662	17520±444	115±117	3517±1394	1725±729
45	14374±2682	10512±2642	4408±1073	3020±971	153±153	1235±522	4720±1288	1370±516	3861±261	754±562
46	57570±19491	30907±4185	18269±3630	5928±2935	8029±1991	4312±1569	12215±3083	409±138	26663±1708	25022±1708
47	27210±9724	23667±8390	1716±1061	997±655	94±64	625±469	21880±8343	43±22	3543±1338	1720±533
48	14812±1092	12275±1219	5532±351	1675±661	3558±736	299±151	6074±1516	631±266	2538±130	1278±459
49	164319±22227	69154±1706	22±22	0±0	11±11	11±11	69036±1712	97±59	95165±3848	90029±3765
50	13944±4988	12756±4825	5983±1384	2678±565	2831±709	474±236	5891±4426	875±338	1188±171	719±96
51	41787±7323	33845±7240	1957±872	86±50	650±196	1221±659	30320±6187	1568±382	7943±3995	6389±4612
52	15540±4014	12299±2834	5599±741	2142±321	2047±634	1410±182	5476±2272	1193±182	3241±1237	1697±825
53	25544±10047	20870±8276	5937±2329	1219±617	3167±1497	1551±221	14067±5859	852±245	4674 ±1908	4166±1721
54	10848±2610	10041±2517	5648±962	1524±459	3513±371	612±215	3956±1637	434±170	807±109	592±41
55	54611±9109	35191±3907	5295±1067	1692±839	2229±627	1374±328	28815±3672	1081±225	19419±5409	16816±4909
56	33639±6257	26858±3272	15030±1684	5668±1850	8569±1976	793±574	10867±3857	961±279	6781±3629	6007±3470
57	79111±22781	57376±1754	2910±1371	416±394	1935±761	559±269	53534±1656	932±316	21735±6943	18466±8363
58	82996±21759	51154±1203	989±712	29±29	115±57	846±782	48602±1192	1548±771	31842±1065	28043±9858
59	42178±11438	36145±9983	414±73	37±20	72±72	305±138	35416±1002	300±1113	6033±2165	4345±2671
60	15070±1942	9762±1672	196±32	0±0	41±25	156±47	9486±1625	58±14	5308±625	1418±291

Table 7.3. Continued with EOH sites.

Site	Total	Insects	EPT	E	P	T	D	C	Noninsects	O
124	14760±4928	13137±4174	6635±1248	2893±214	2934±1030	808±232	3910±2260	2561±837	1623±776	409±259
125	9292±1836	8386±1760	4178±680	2031±399	1588±296	559±137	3712±1314	467±111	906±79	242±58
126	8727±1887	7600±1410	3284±1093	1773±639	935±287	576±176	1666±395	2581±602	1128±508	601±300
127	28595±4782	22746±3262	14803±2172	7147±1669	6659±1169	996±192	5706±1174	2043±435	5849±1524	1233±286
129	16237±5455	14347±5256	7593±1770	5014±1183	2184±623	395±83	5306±2820	1447±705	1890±216	1385±217
130	40956±19359	35044±1745	4124±1916	1360±499	2413±1454	351±39	30495±1546	418±149	5912±1988	4129±1625
131	23630±6799	18191±4019	2246±1079	913±317	755±423	578±356	15658±3309	282±31	5438±3355	4803±3296
132	22881±1961	20492±1889	11104±2991	8665±3118	1739±336	700±54	6753±1755	2606±1191	2388±411	1039±100
133	19996±5171	15373±3843	1170±530	180±73	13±8	977±472	13958±3491	238±93	4622±1953	4062±1861
134	45419±6275	36401±4239	12464±3391	2659±972	9381±2519	423±83	23582±991	327±139	9018±4692	8131±4759
137	54452±8689	37477±8009	9262±4310	2136±1090	5778±3499	1348±718	28057±6134	115±76	16975±1967	16287±2226
138	58149±25374	53592±2526	1436±674	213±174	46±25	1177±496	52156±2461	0±0	4557±165	1697±318
139	9758±3971	7036±2756	2814±611	2049±436	28±8	737±304	4209±2147	13±11	2723±1240	1628±1021
140	21252±8705	13400±4751	631±148	258±61	93±27	280±129	12430±4506	308±126	7852±3964	7161±3618
141	16103±745	14483±226	4910±1255	1003±184	3051±1064	856±291	9094±1069	479±57	1620±917	1398±844
142	10953±851	8556±549	615±205	358±159	113±68	144±12	7800±459	140±55	2398±457	2077±438
143	23557±2736	15765±3562	3119±1038	333±35	1421±558	1365±489	11599±2356	1018±552	7791±1734	2275±1063
145	24052±1878	20205±1945	1407±175	356±87	358±111	693±228	17987±1644	796±401	3847±243	3043±57
146	18443±4040	14068±2818	7832±1205	2572±983	3094±132	2165±268	5656±1700	526±50	4375±1222	1478±713
147	12183±322	8391±685	2754±678	290±24	1922±821	542±293	4459±329	1166±311	3792±630	3164±637
148	21799±1604	19374±1880	1553±601	127±79	265±148	1161±574	17809±2004	12±6	2425±350	2205±423
149	9163±1753	7985±1605	3528±1091	830±120	1183±454	1514±518	3127±465	1274±508	1178±170	540±129
150	39744±2384	35124±1467	6270±1143	2656±1161	11±11	3602±148	28840±1887	14±14	4619±959	2144±498

Table 7.4. Pearson product-moment correlation was used to assess the synchrony of hydrologic parameters of 45 site pairs (4 EOH and 6 WOH sites). Correlation coefficients (r) were averaged for each variable and significant pairwise comparisons (i.e., $r \geq +0.67$) were expressed as a percentage.

Hydrologic Parameters	Mean correlation (*r*)	Strong correlations (%)
General		
Cumulative discharge 30 d prior to sampling (sumq30)	0.21	22
Cumulative discharge 60 d prior to sampling (sumq60)	0.78	78
Cumulative discharge 90 d prior to sampling (sumq90)	0.68	51
Cumulative discharge 1 yr prior to sampling (sumq365)	0.94	100
Measure of storms/floods		
Peak discharge (cfs) during 30 d prior to sampling (peakq30)	0.29	31
Peak discharge (cfs) during 90 d prior to sampling (peakq120)	0.61	44
Peak discharge (cfs) during 5 mo prior to sampling (peakq150)	0.59	49
Peak discharge (cfs) during 6 mo prior to sampling (peakq180)	0.61	51
Peak discharge (cfs) during 1 yr prior to sampling (peakq365)	0.47	38
Largest change in discharge in a 48 hr period 30 d prior to sampling (maxq30)	0.71	60
Largest change in discharge in a 48 hr period 90 d prior to sampling (maxq90)	0.82	84
Measure of flashiness		
No. high pulses during 1 yr prior to sample date (npulse_high)	0.80	82
Measure of low flow/drought		
Annual minimum flow 7-day mean (minq7)	0.84	89
Annual minimum flow 30-day mean (minq30)	0.90	100
Annual minimum flow 90-day mean (minq90)	0.94	100
No. days with low pulse for the 1 yr prior to sampling (xpulse_low_duration)	0.66	62

Table 7.5. Matrix for EOH site pairs showing correlation coefficients for taxa. Correlations were averaged to determine mean correlation (*r*) and strong correlations (%), which were defined as percentage of $r \geq +0.67$.

	Taxa (n = 29)				Coherence of site pairs across rows	
EOH Site Pairs	Chironomidae	Oligochaeta	Tanytarsini	Other taxa	Mean correlation (*r*)	Strong correlations (%)
Sites 34 & 46	0.06	0.93	0.09		0.12	21
Sites 34 & 52	0.09	0.84	0.59		0.27	21
Sites 34 & 55	-0.24	0.86	-0.28	Etc.	0.22	14
Sites 46 & 52	0.75	0.92	-0.08		0.11	21
Sites 46 & 55	0.45	0.92	0.49		0.23	24
Sites 52 & 55	0.61	0.98	0.40		0.16	24
	Coherence of variables across site pairs					
Mean correlation (*r*)	0.29	0.91	0.20		0.19	
Strong correlations (%)	17	100	0			21

Table 7.6. Temporal coherence results for 31 common taxa (e.g., order, families, sub-tribes of chironomids) and 6 metrics using site pairs from all 12 sites, 8 WOH sites, and 6 EOH sites.

Variable	Sites	Mean correlation (*r*)	Strong correlations (%)
Taxa	All	0.20	20
	WOH	0.32	26
	EOH	0.19	21
Metrics	All	0.23	16
	WOH	0.29	18
	EOH	0.09	6

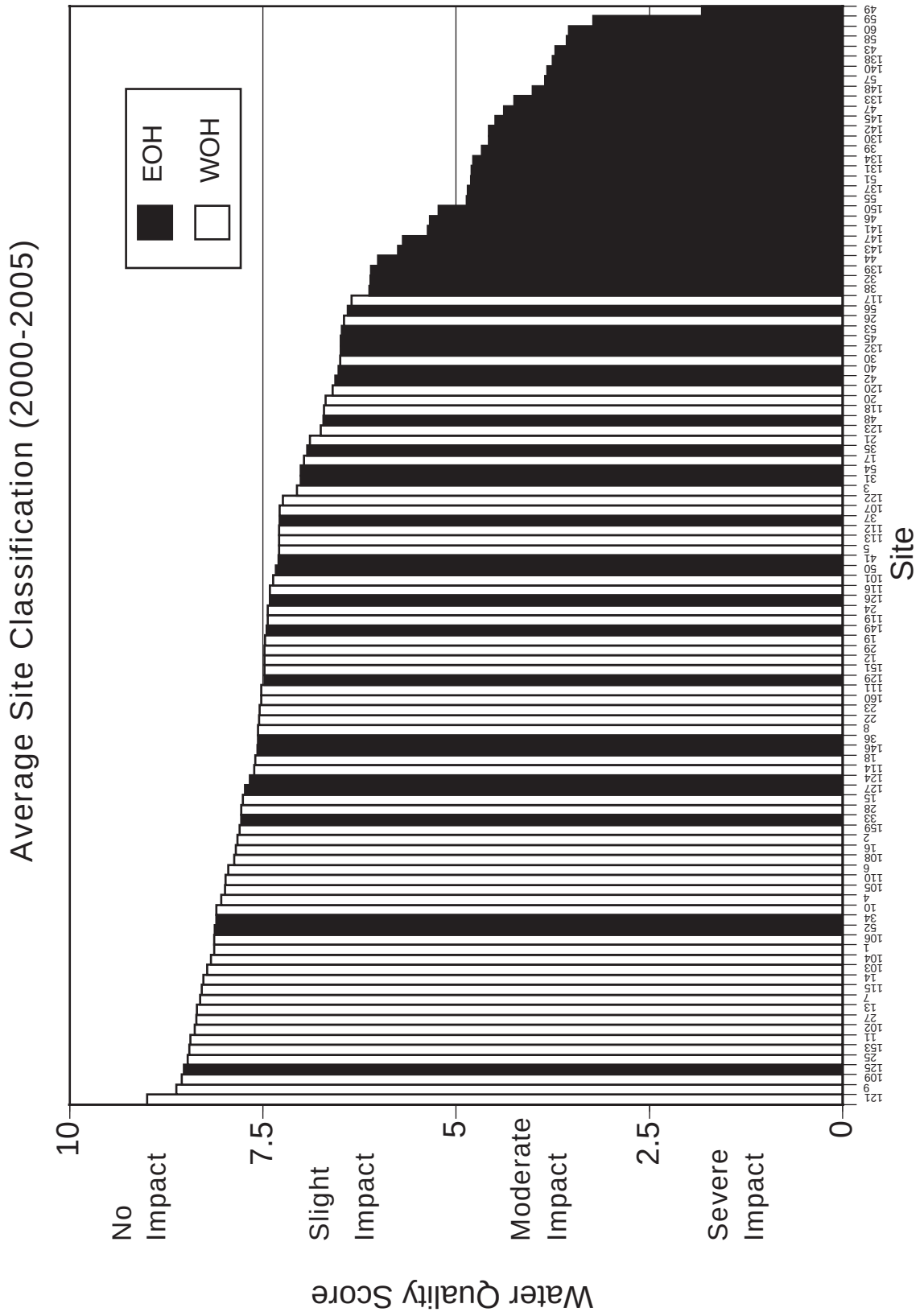

Figure 7.1. Water Quality Score (WQS; mean per 100 individuals) at each site West (WOH) and East (EOH) of the Hudson River.

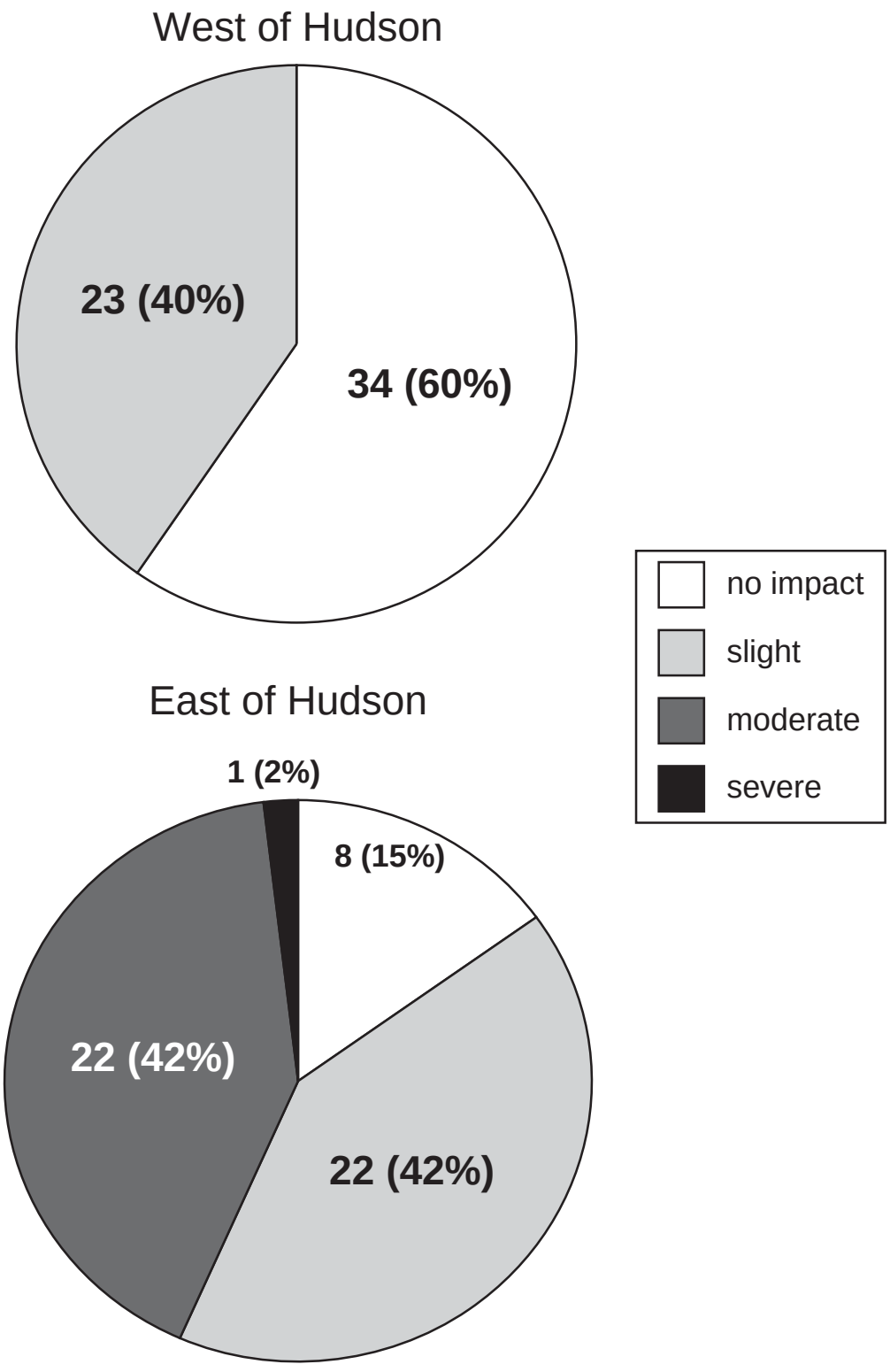

Figure 7.2. Number (and %) of sites classified as exhibiting no impact, slight impact, moderate impact, or severe impact among the 57 West and 53 East of Hudson River sites.

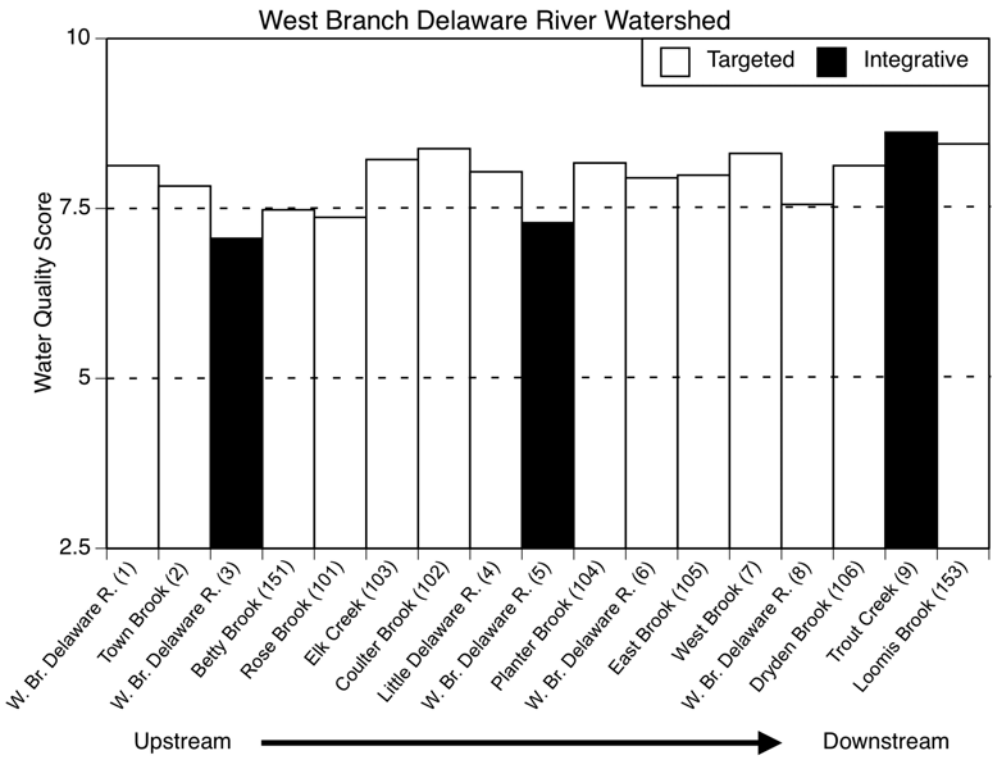

Figure 7.3. Mean Water Quality Score for sites located in the West Branch of the Delaware River Watershed in the WOH.

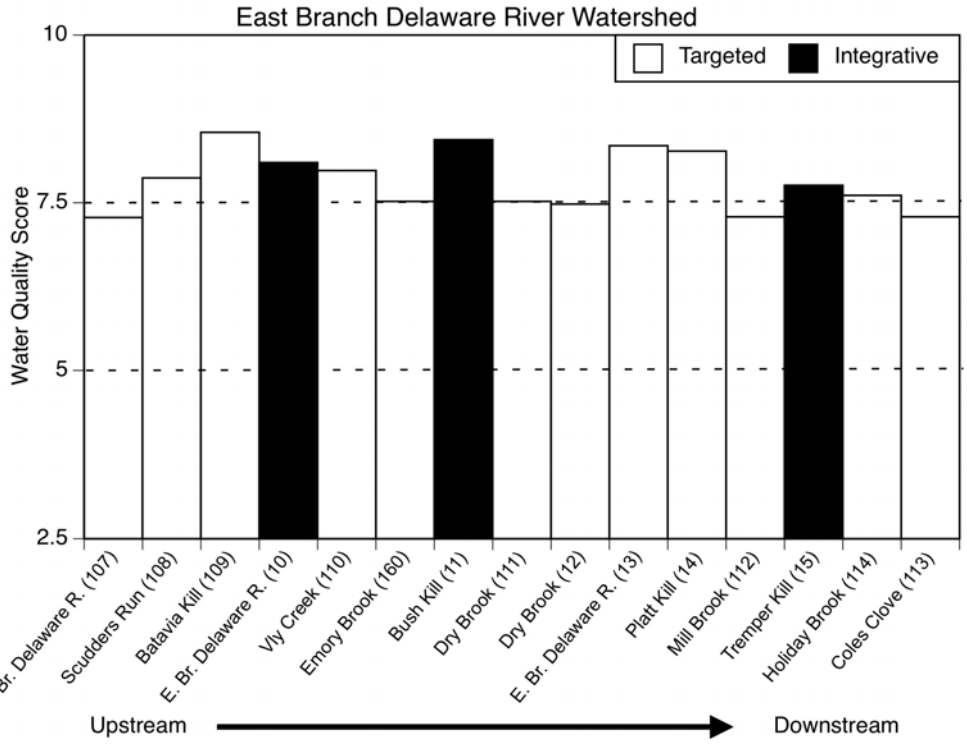

Figure 7.4. Mean Water Quality Score for sites located in the East Branch of the Delaware River Watershed in the WOH.

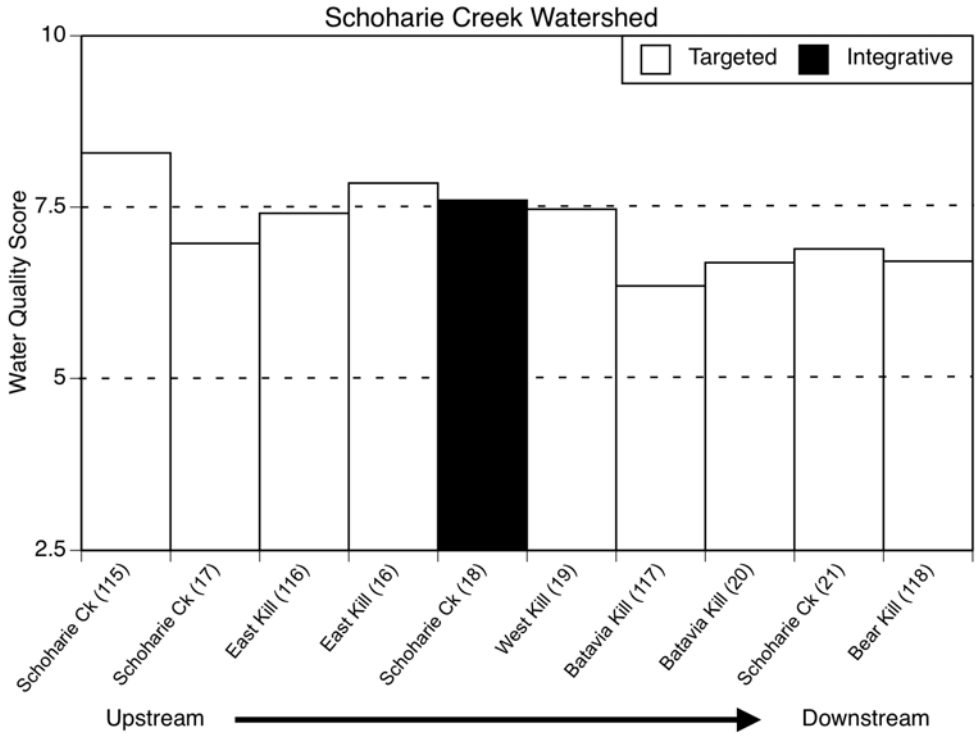

Figure 7.5. Mean Water Quality Score for sites located in the Schoharie Creek Watershed in the WOH.

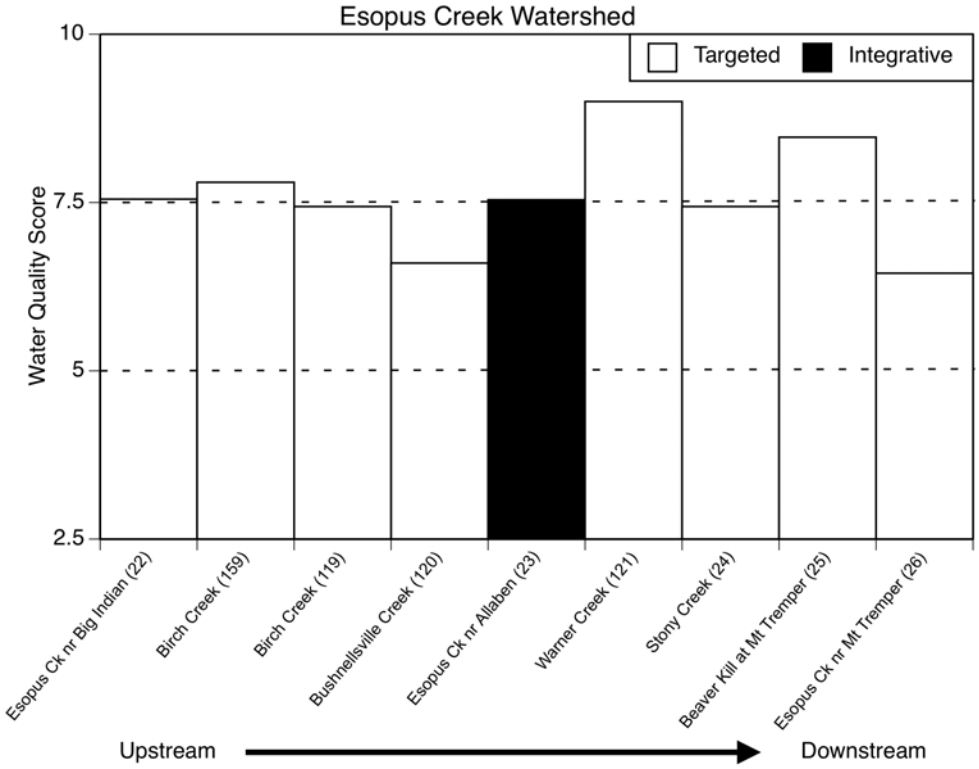

Figure 7.6. Mean Water Quality Score for sites located in the Esopus Creek Watershed in the WOH.

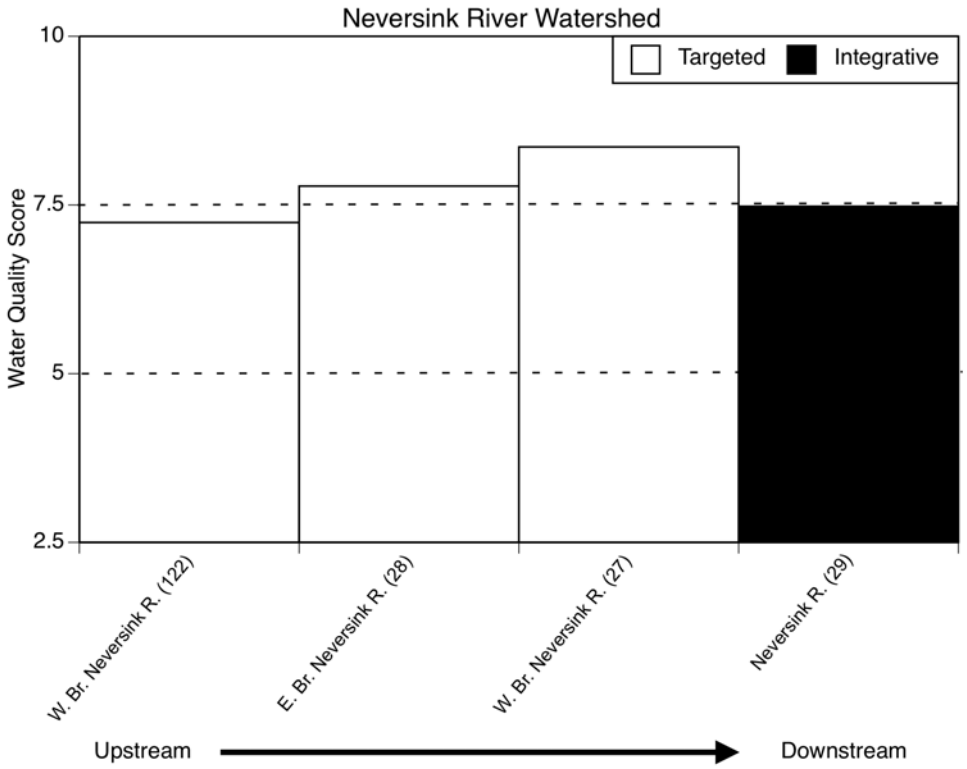

Figure 7.7. Mean Water Quality Score for sites located in the Neversink River Watershed in the WOH.

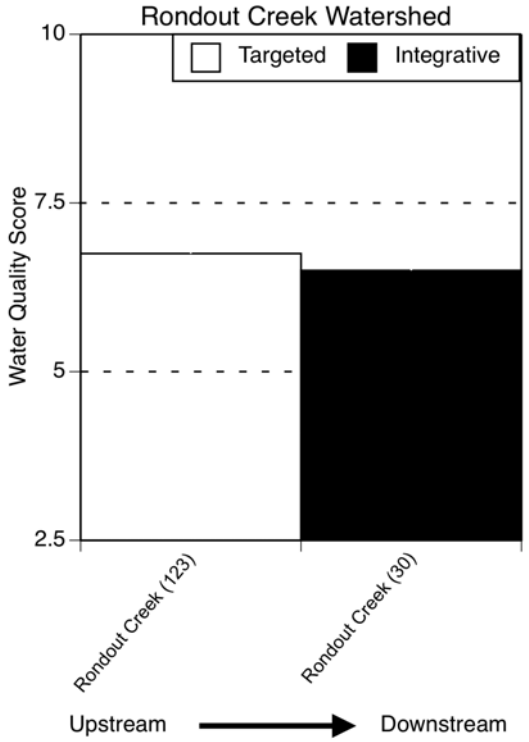

Figure 7.8. Mean Water Quality Score for sites located in the Rondout Creek Watershed in the WOH.

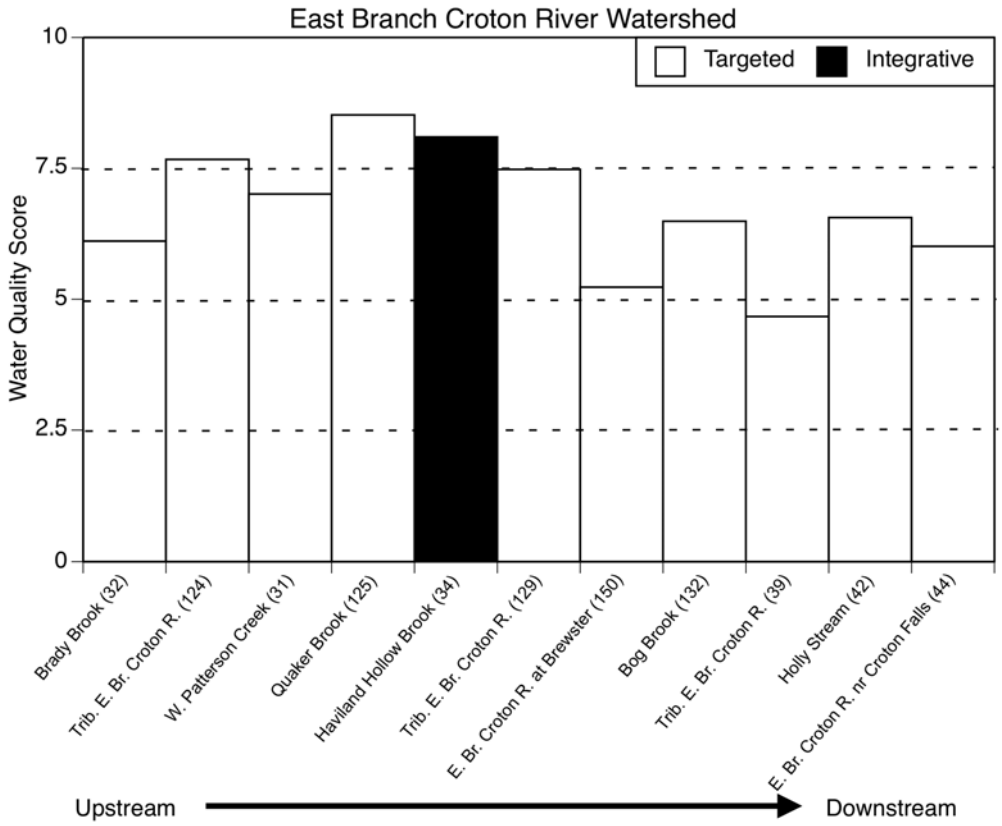

Figure 7.9. Mean Water Quality Score for sites located in the East Branch Croton River Watershed in the EOH.

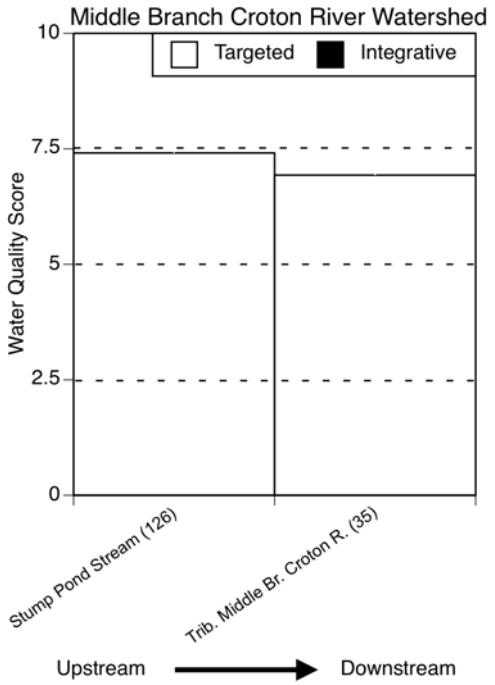

Figure 7.10. Mean Water Quality Score for sites located in the Middle Branch Croton River Watershed in the EOH.

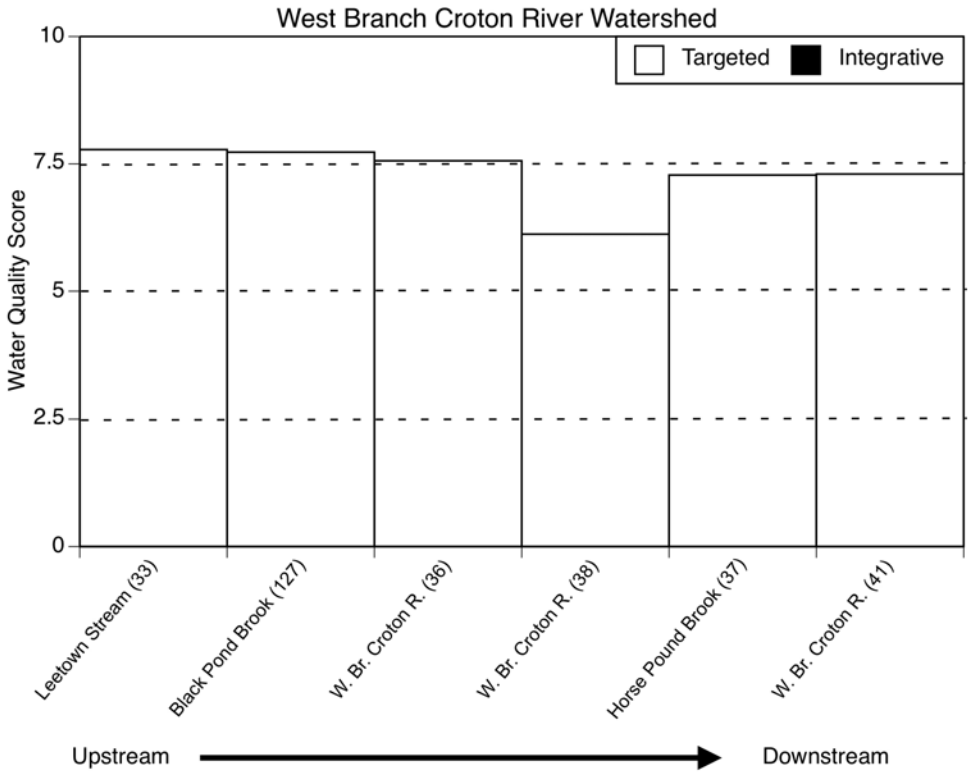

Figure 7.11. Mean Water Quality Score for sites located in the West Branch Croton River Watershed in the EOH.

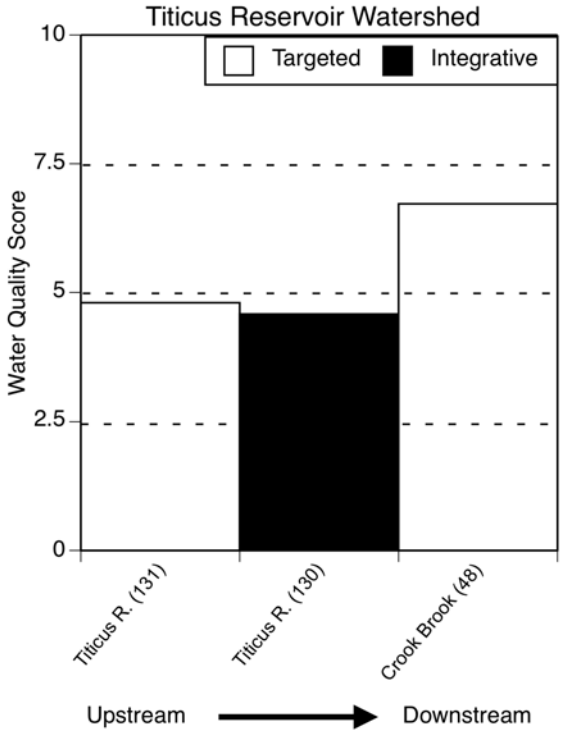

Figure 7.12. Mean Water Quality Score for sites located in the Titicus Reservoir Watershed in the EOH.

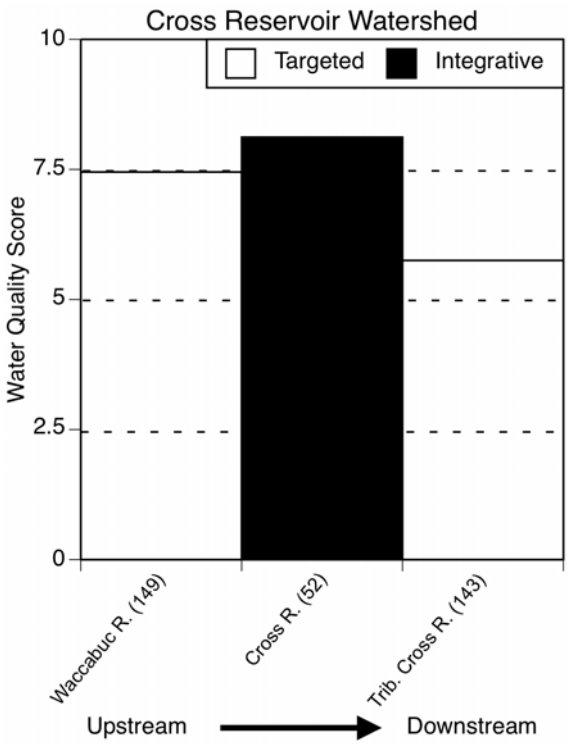

Figure 7.13. Mean Water Quality Score for sites located in the Cross Reservoir Watershed in the EOH.

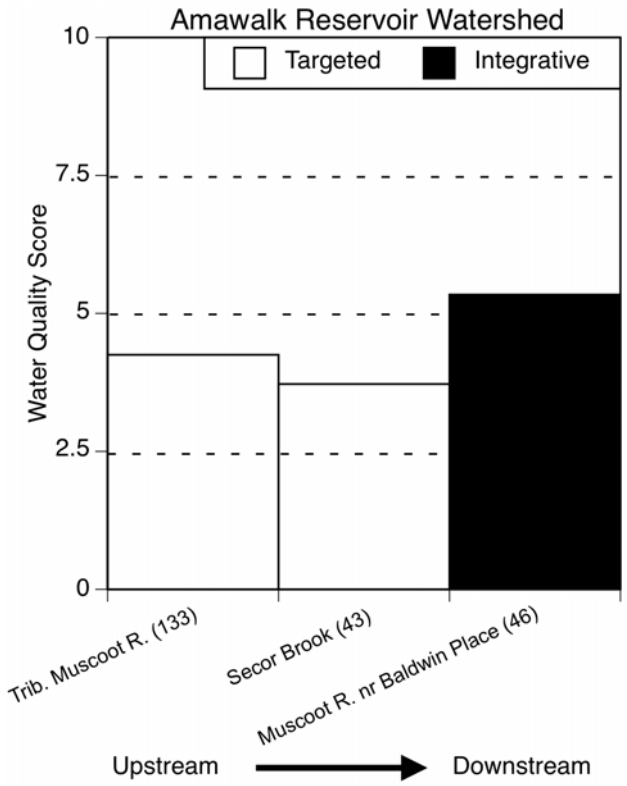

Figure 7.14. Mean Water Quality Score for sites located in the Amawalk Reservoir Watershed in the EOH.

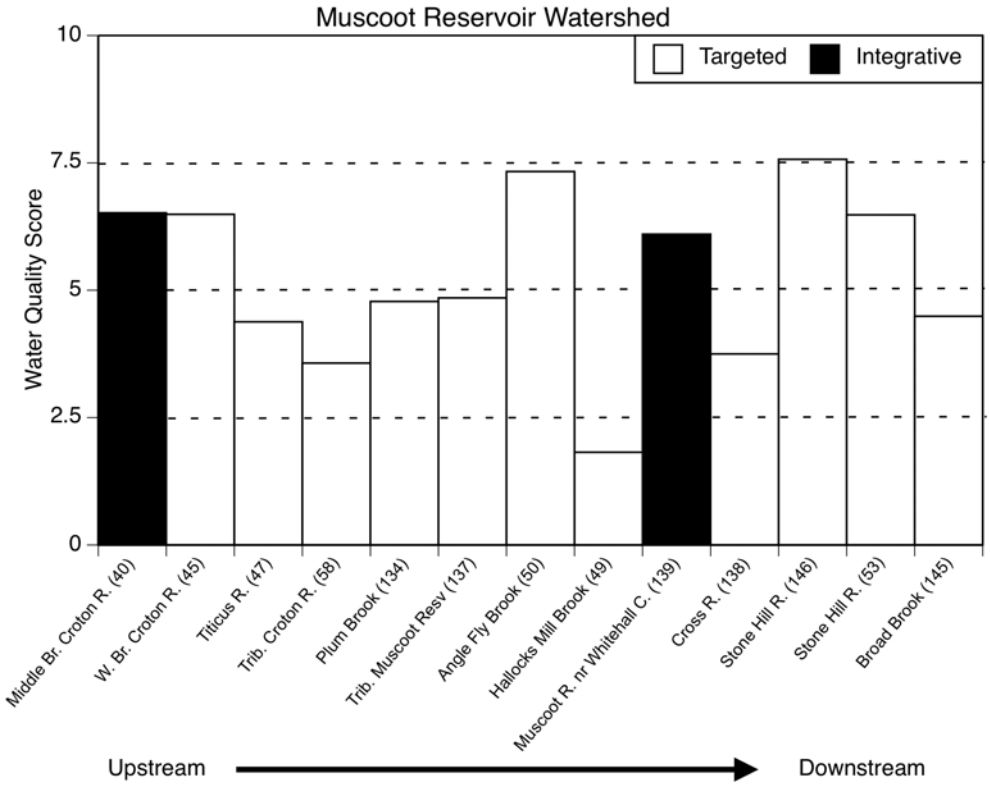

Figure 7.15. Mean Water Quality Score for sites located in the Muscoot Reservoir Watershed in the EOH.

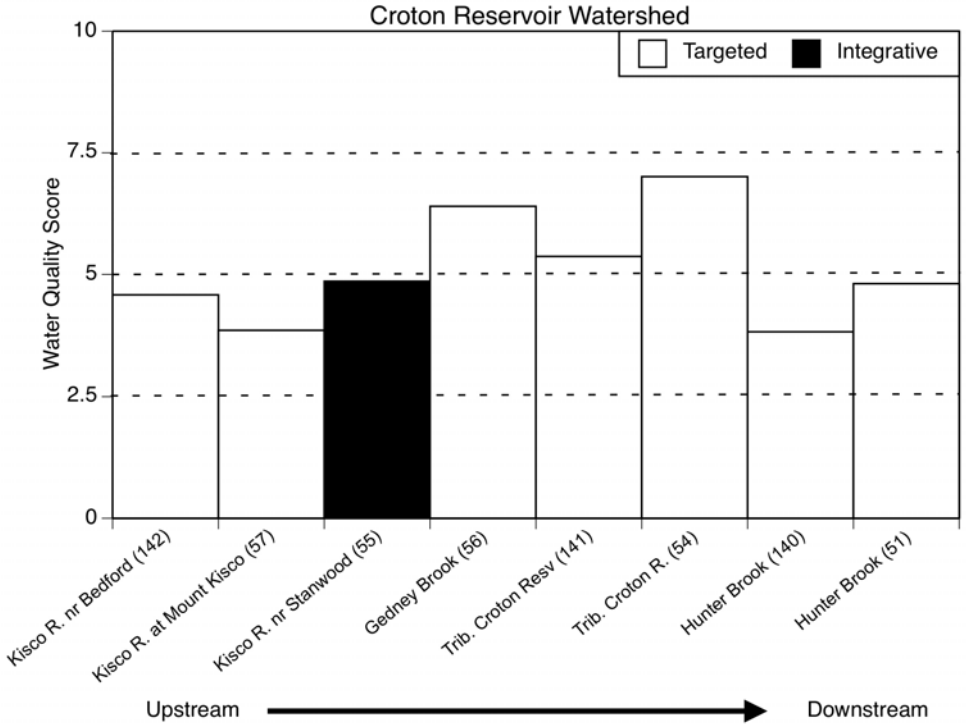

Figure 7.16. Mean Water Quality Score for sites located in the Croton Reservoir Watershed in the EOH.

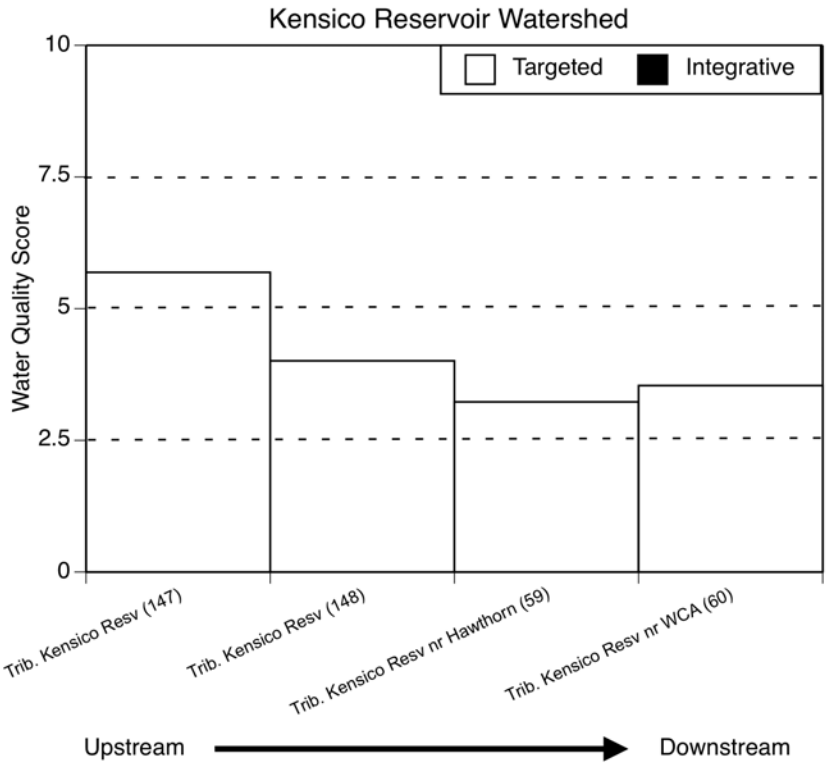

Figure 7.17. Mean Water Quality Score for sites located in the Kensico Reservoir Watershed in the EOH.

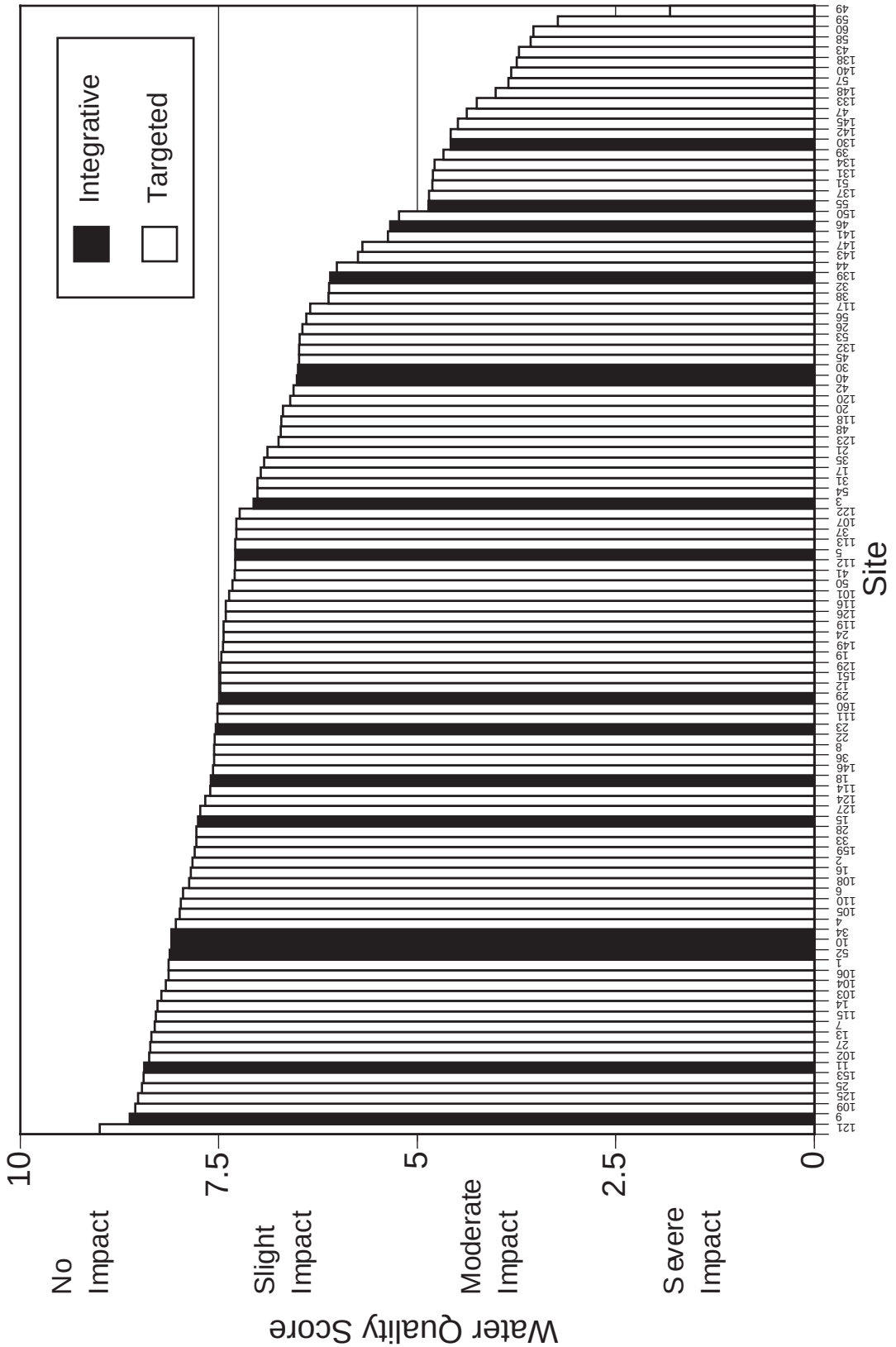

Figure 7.18. Water Quality Score (WQS; mean per 100 individuals) at each integrative and targeted study site.

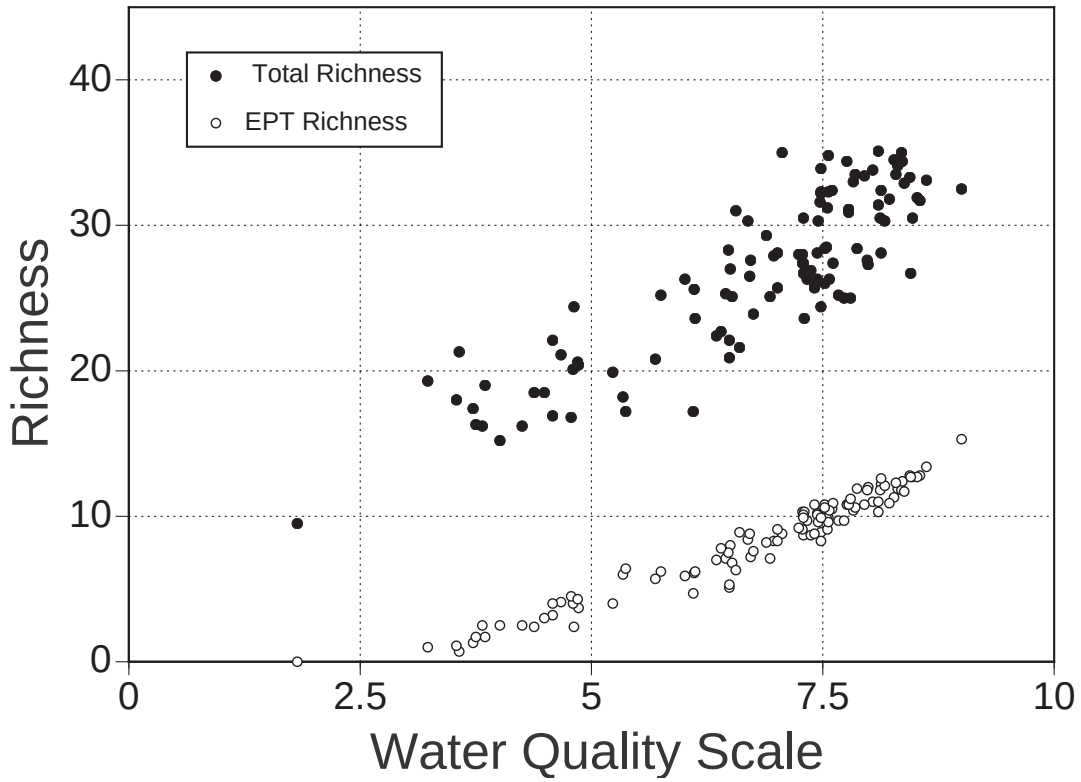

Figure 7.19. Total and EPT Richness (species or taxa mean per 100 individuals) versus Water Quality Score (WQS; mean per 100 individuals) at each site using 3 or 6 yr means.

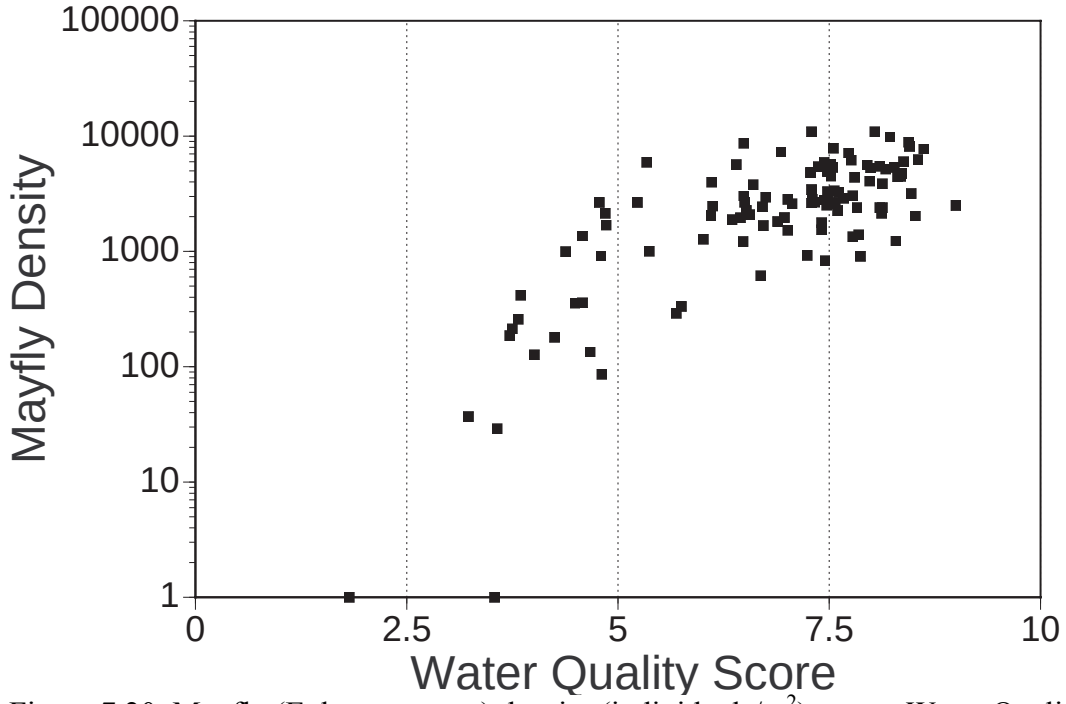

Figure 7.20. Mayfly (Ephemeroptera) density (individuals/m^2) versus Water Quality Score (WQS; mean per 100 individuals) at each site using 3 or 6 yr means. Zero densities converted to one in order to appear on the figure.

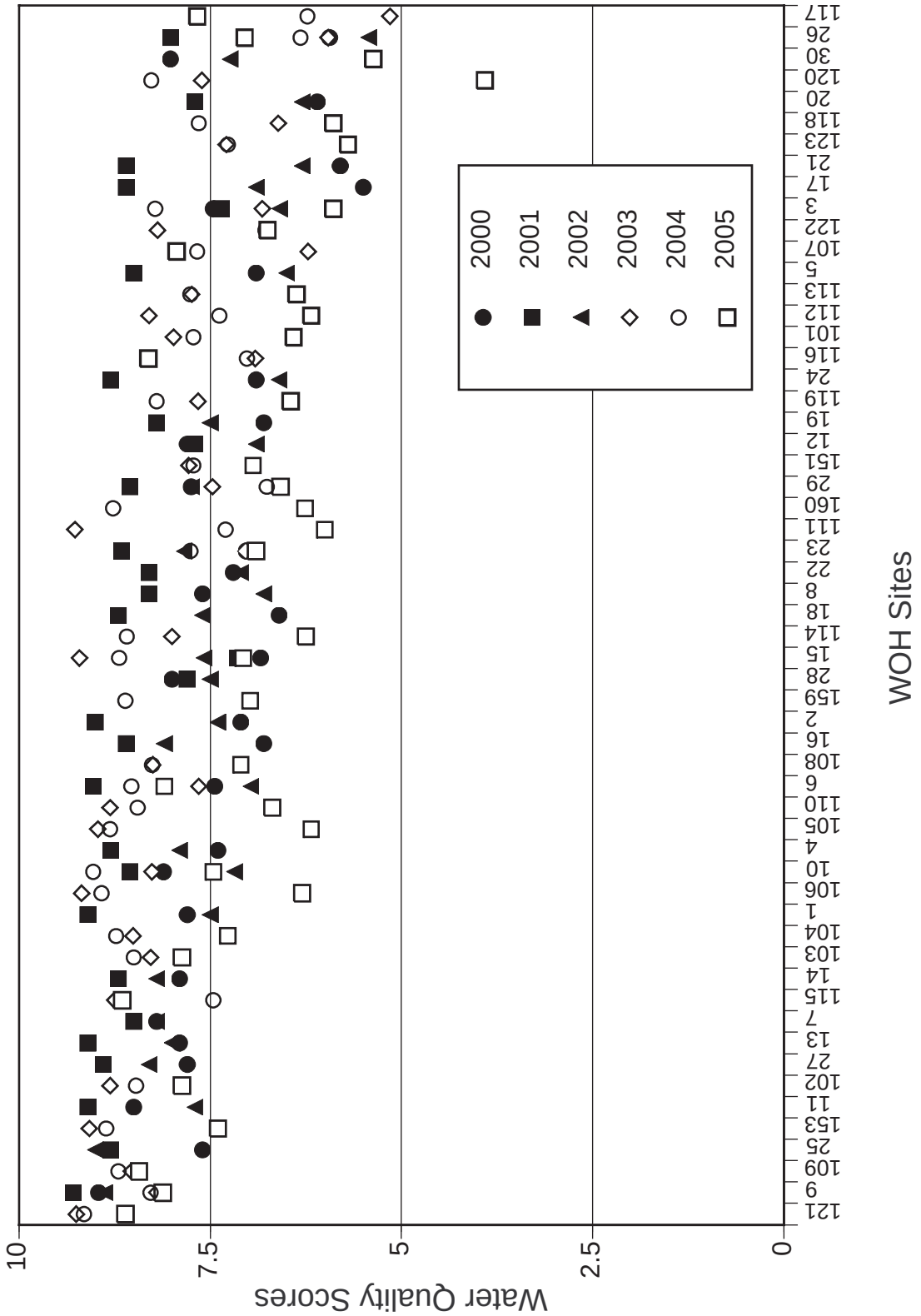

Figure 7.21. Water Quality Score (WQS; mean per 100 individuals) at each site in the WOH from 2000 to 2005.

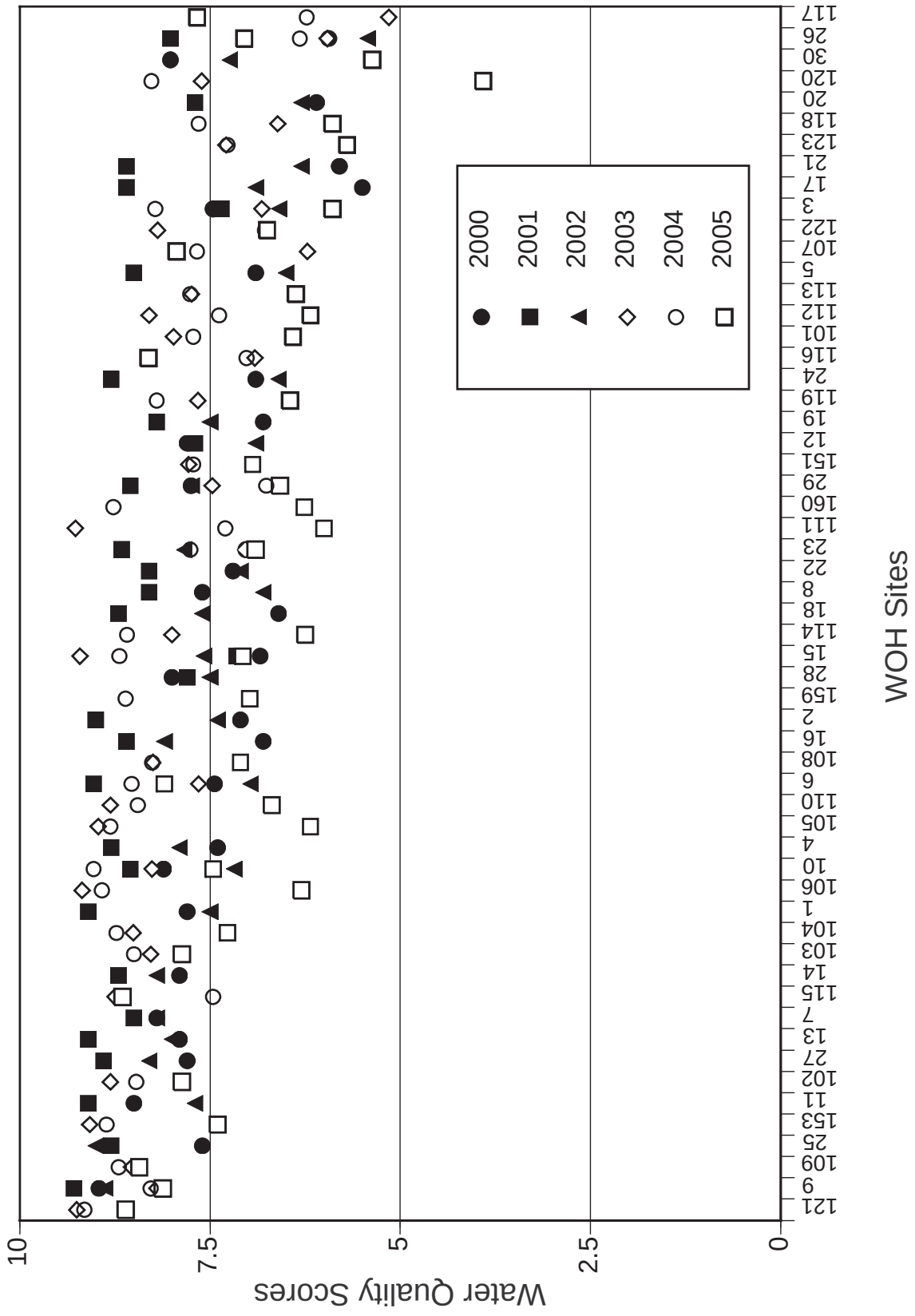

Figure 7.22. Water Quality Score (WQS; mean per 100 individuals) at each site in the EOH from 2000 to 2005.

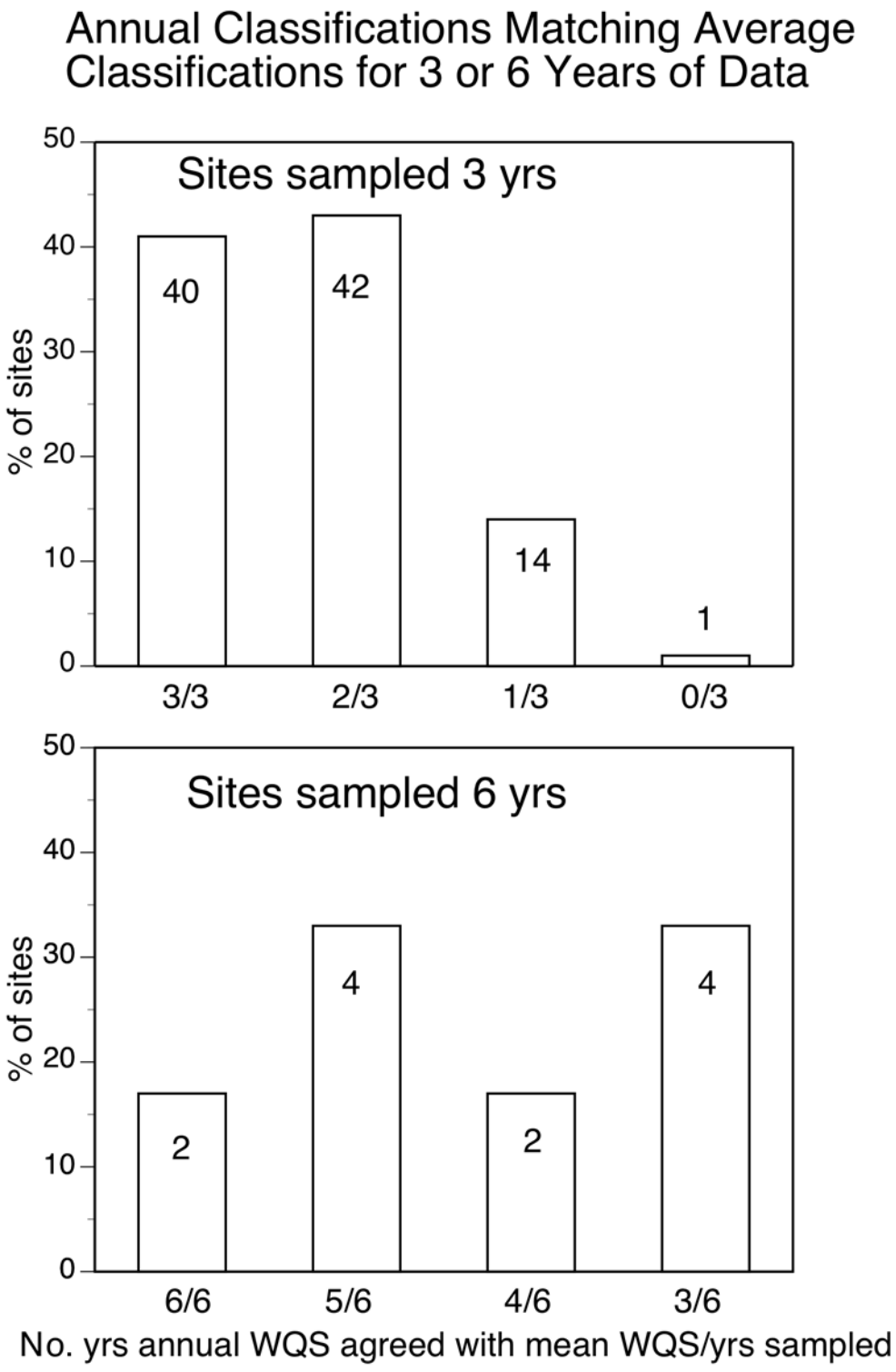

Figure 7.23. Number of annual site classifications matching average site classifications. Number in column indicates number of sites whose annual WQS agreed with the average WQS.

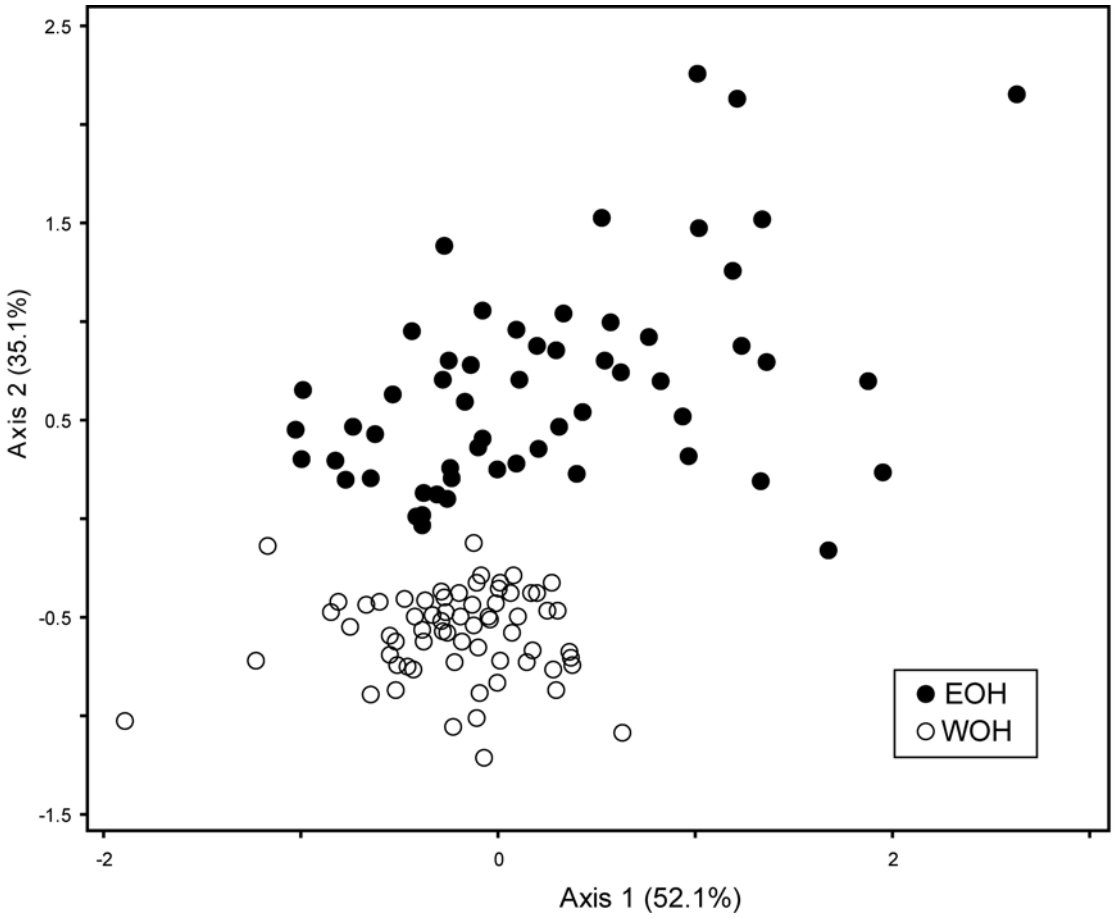

Figure 7.24**.** Non-metric Multidimensional Scaling ordination of macroinvertebrate assemblages in WOH and EOH sites using mean densities from Phase I (2000-2002) and Phase II (2003-2005).

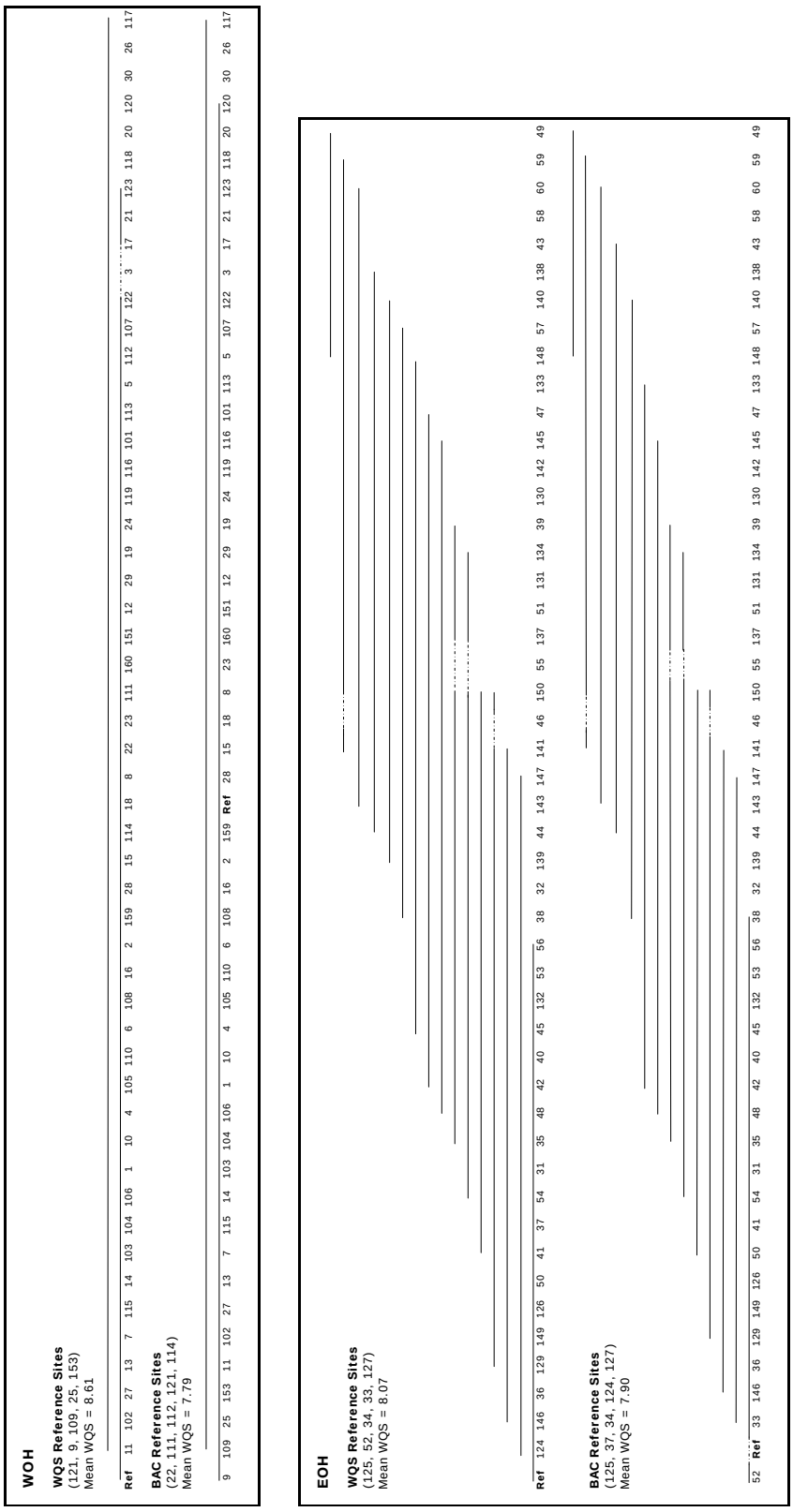

Figure 7.25. Results of Tukey's test for WOH and EOH comparing WQS and BAC reference sites to other sites in the region using data from 2000 to 2005. Sites under the same line were not significantly different ($p > 0.05$).

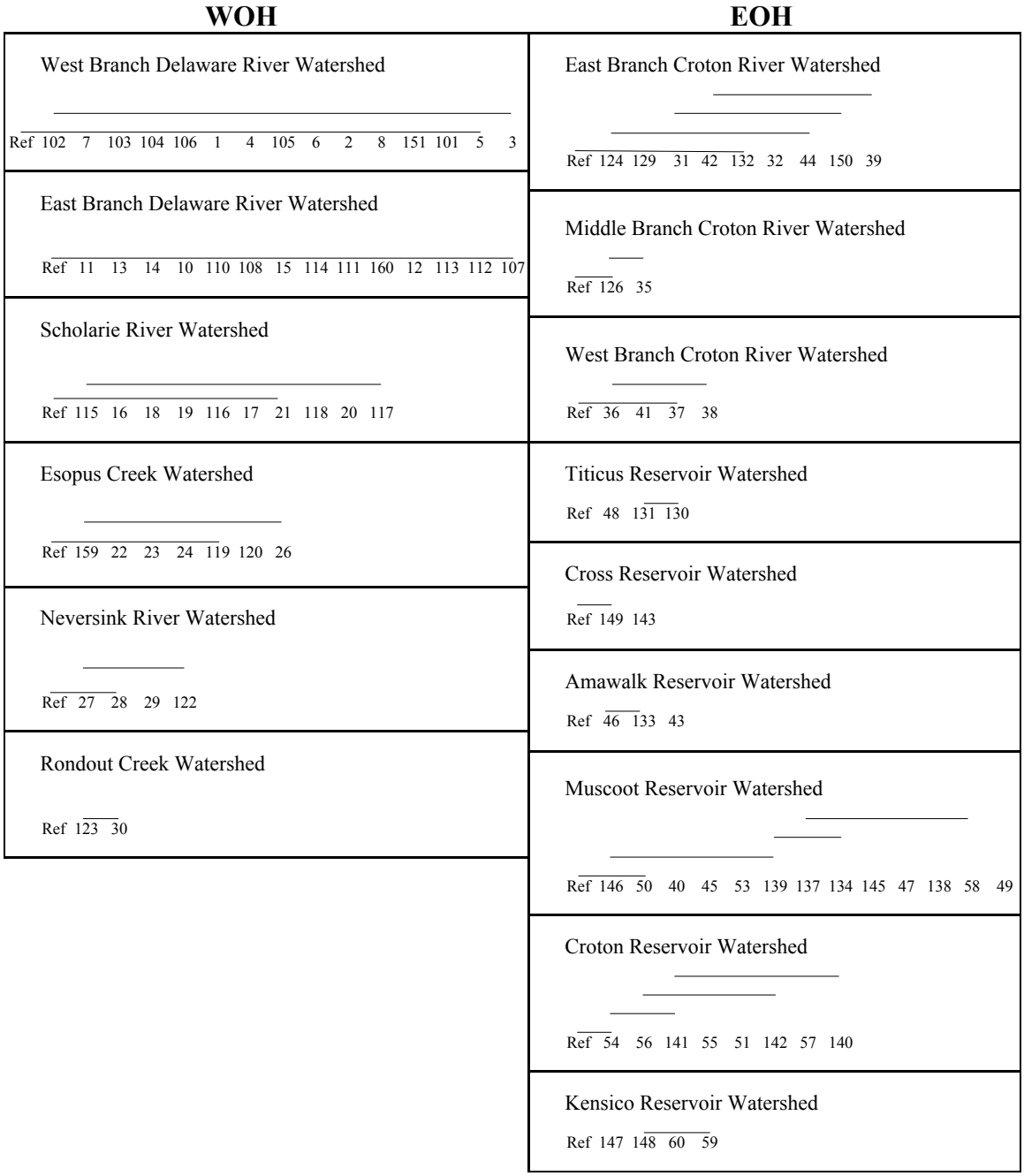

Figure 7.26. Results of Tukey's test comparing WQS reference sites to sites within the respective watershed for 2000 to 2005. Sites under the same line were not significantly different ($p > 0.05$).

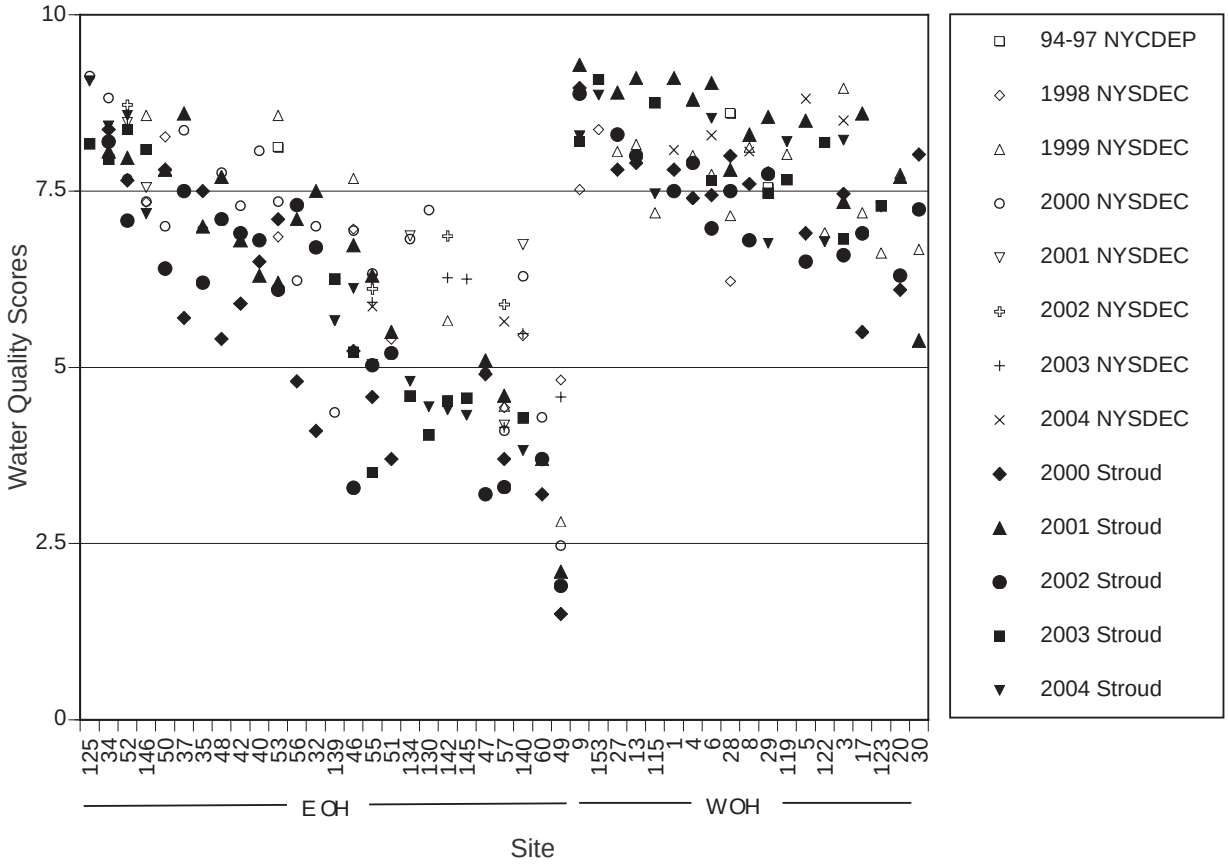

Figure 7.27. Water Quality Scores determined by NYCDEP (1994-1997; Cutietta-Olson and Rosenfeld 2000), NYSDEC (1998-2004; Bode et al. 2000a, 2000b, 2002a, 2003, 2005, 2006, 2007, Smith et al. 2006) and Stroud (2000-2005; this study).

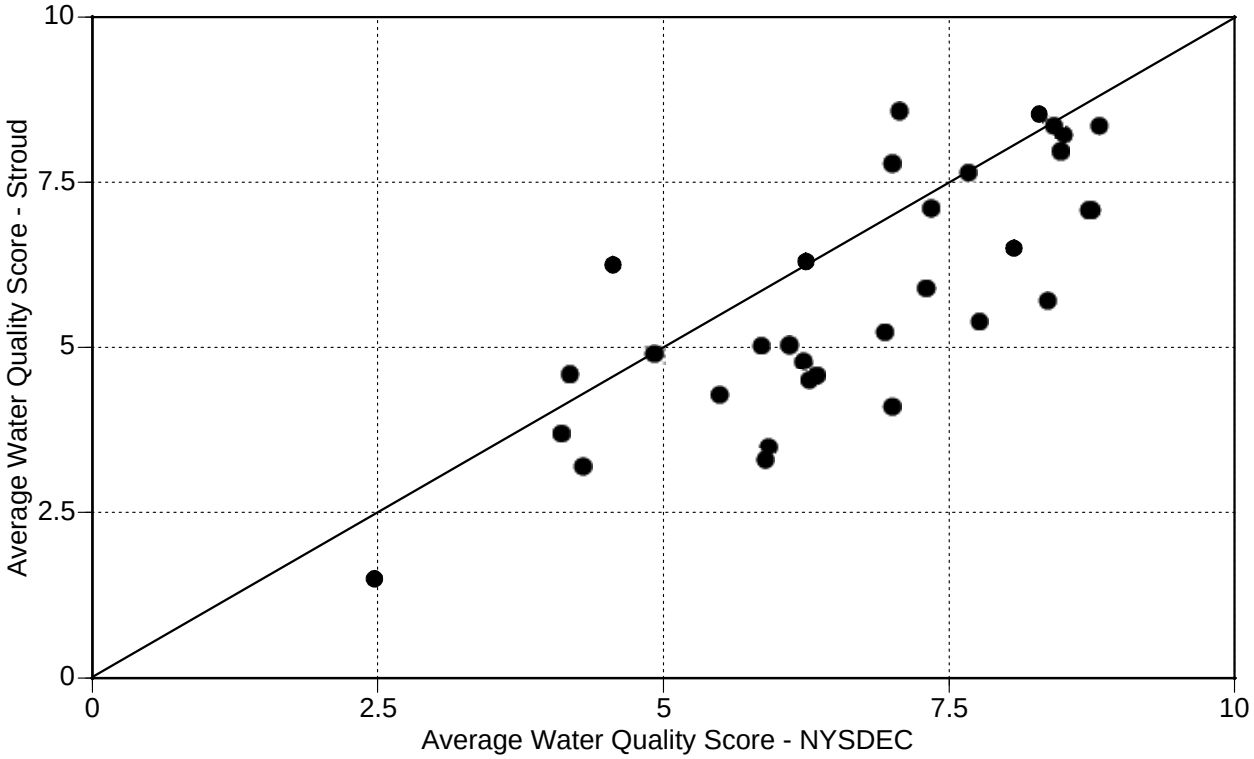

Figure 7.28. Mean Water Quality Score reported by NYSDEC (Bode et al. 2002a, 2005, 2006, 2007, Smith et al. 2006) and Stroud (2000-2005; this study). Site pairs are based on sampling done in the same year and location.

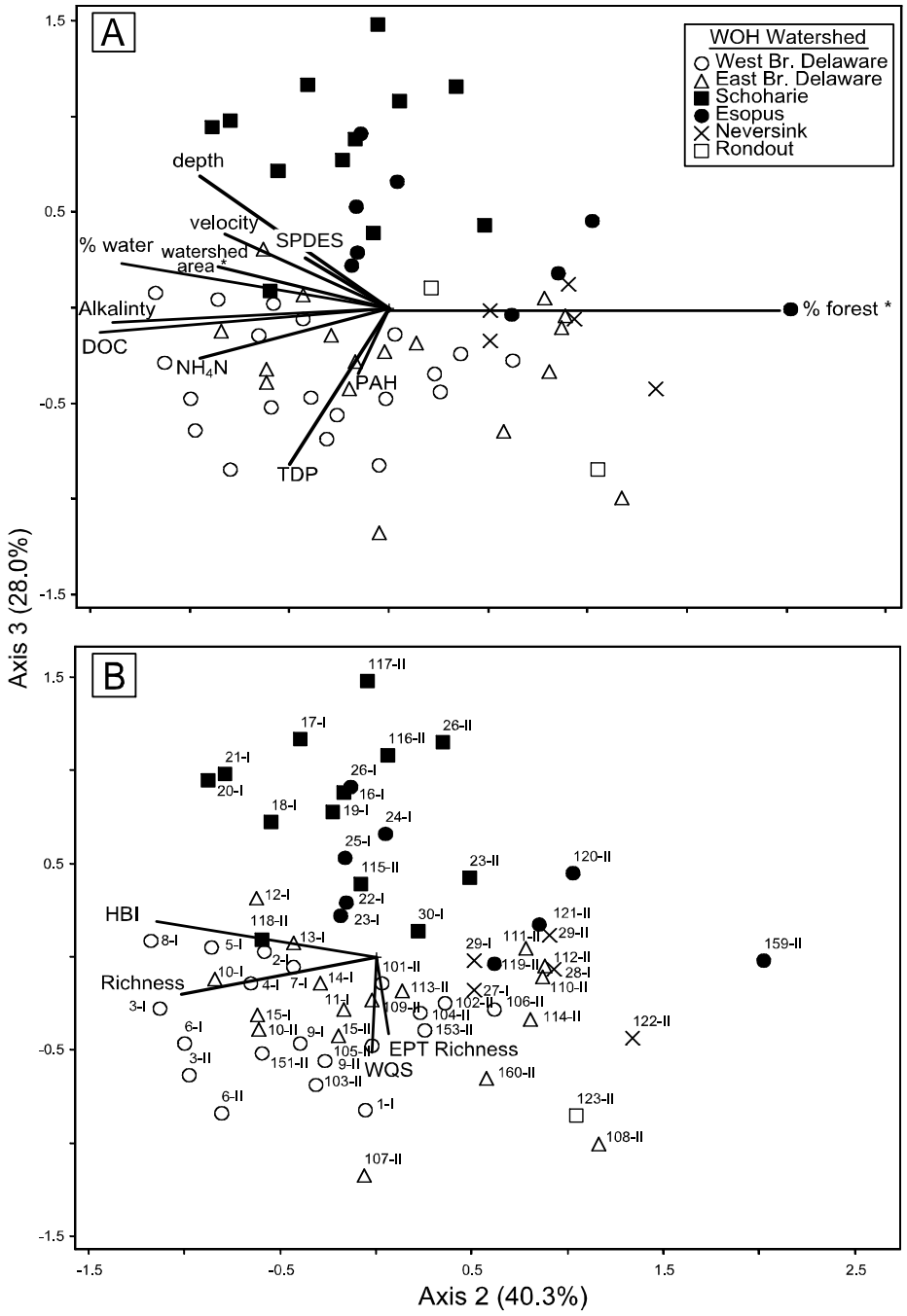

Figure 7.29. Non-metric Multidimensional Scaling ordination of macroinvertebrate assemblages in WOH sites using mean densities from Phase I (2000-2002) and Phase II (2003-2005). A) Symbols indicate sites within the same watershed and vectors indicate land use and water chemistry variables. B) Same ordination but sites are labeled (site no. followed by Phase I or 2) and vectors are for biometrics. Key: Land use variables indicates the amount of area [e.g., % (deciduous) forest, % water] in the watershed or *riparian zone (30 m corridor for entire stream length) above sampling point; depth and velocity measured where macroinvertebrate samples were taken; SPDES = point source discharge; DOC = dissolved organic carbon, TDP = total dissolved phosphorus; PAH = polycyclic aromatic hydrocarbons.

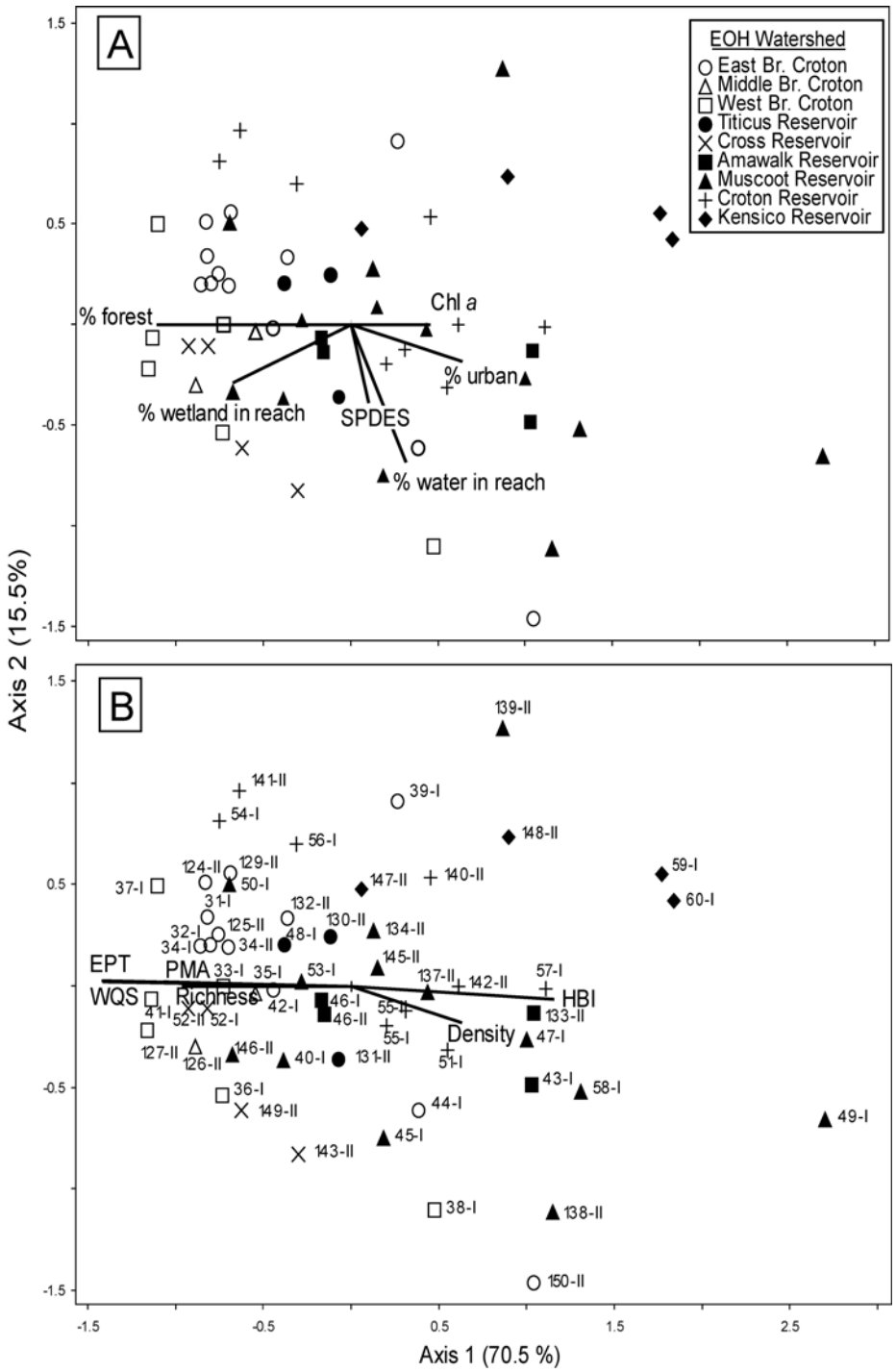

Figure 7.30. Non-metric Multidimensional Scaling ordination of macroinvertebrate assemblages in EOH sites using mean densities from Phase I (2000-2002) and Phase II (2003-2005). A) Symbols indicate sites within the same watershed and vectors indicate land use and water chemistry variables. B) Same ordination but sites are labeled (site no. followed by Phase I or 2) and vectors are for biometrics. Key: Land use variables indicates the amount of area [e.g., % (deciduous) forest, % urban, % wetland] in the watershed or reach (1 km upstream in 30 m riparian corridor) above sampling point; SPDES = point source discharge; Chl *a* = chlorophyll *a*.

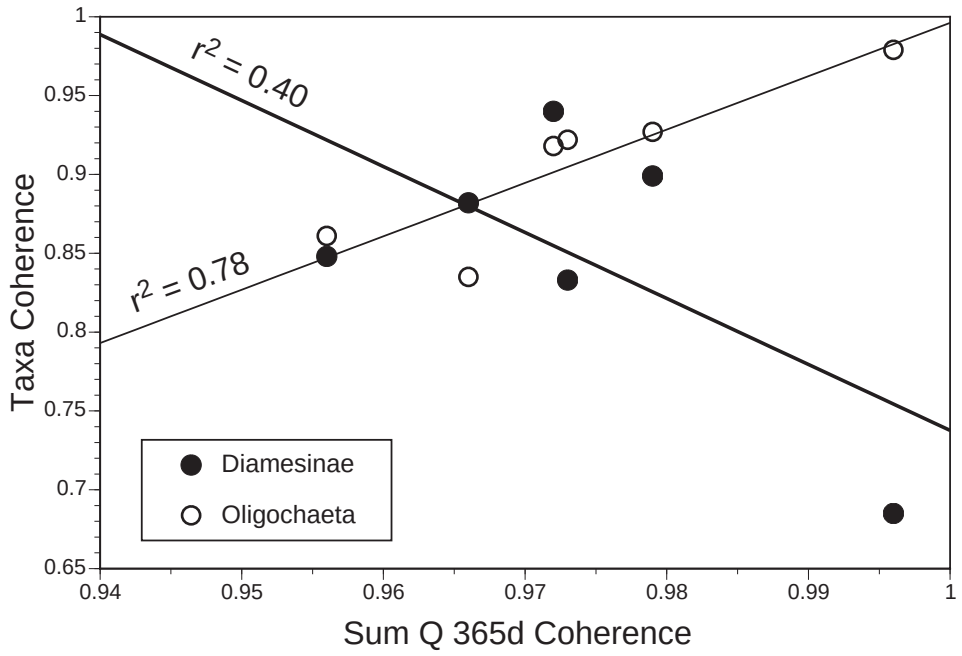

Figure 7.31. Temporal coherence results of correlations (*r*) for two taxa and a hydrologic parameter (i.e., cumulative discharge 1 yr prior to sampling) for six EOH site pairs sampled six years. Oligochaetes were positively related to high annual flows and Diamesinae negatively related.

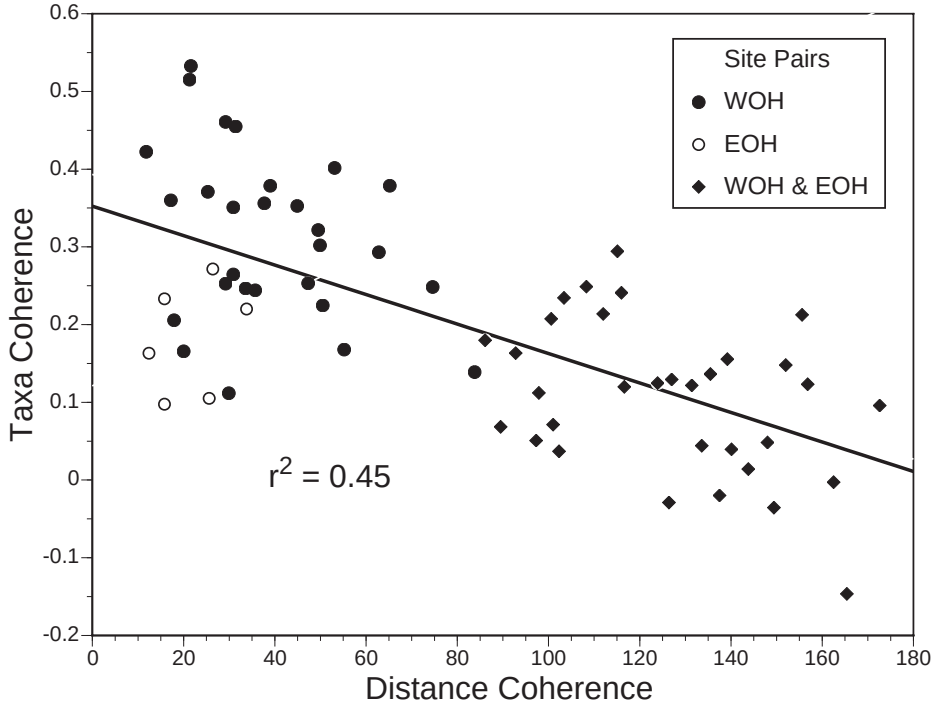

Figure 7.32. Mean correlations (*r*) for 31 common macroinvertebrate taxa (i.e., orders, families, and sub-tribes of chironomids) versus coherence for distance (km) between 66 site pairs.

----------Intentionally Blank----------

Chapter 8 – Nitrogen (N), Phosphorus (P), and Dissolved Organic Carbon (DOC) Spiraling

Research Task

The rates at which nutrients are used and cycled by ecosystem processes may be of practical interest both because nutrient cycling can be considered an ecosystem service (Palmer et al. 2004)—a process that directly or indirectly supplies human needs such as food production or water purification—and because such rates may provide a sensitive measure of human impact on an ecosystem, relative to what its condition or function would be in the absence of human activity (Odum 1985). In streams and rivers, nutrients move downstream as they cycle, and the combined processes are termed *spiraling* (Webster and Patten 1979). As a nutrient atom undergoes various transformations usually involving transfer from a dissolved available form in the water column to the streambed it completes a cycle by returning to the water column. It moves some distance downstream, the average or expected distance an atom moves is termed the spiraling length (Newbold et al. 1981). Early considerations of the spiraling concept (Wallace et al. 1977, Webster and Patten 1979, Newbold et al. 1982) suggested that evolutionary adaptations of stream-dwelling organisms can be expected to retain nutrients in place and cycle the nutrient supply efficiently, so that an intact or undisturbed stream ecosystem should cycle nutrients over relatively short distances or spiraling lengths. It follows that disturbance or stress should produce longer spiraling lengths and, thus, that spiraling length might prove a sensitive indicator of human impact on ecosystem function. Human inputs or alterations to streams might increase spiraling length in several ways. First, a direct toxic depression of metabolic activity could reduce nutrient use, allowing nutrients to be transported farther downstream before uptake or transformation. Second, an alteration of ecosystem structure (e.g., the loss or substitution of species or functional groups) might reduce the efficiency of nutrient processing or retention. Third, pollution to streams and rivers in the form of surplus nutrients might saturate the uptake capacity, again allowing nutrients to travel farther between cycles. Last, physical alteration, such as the removal of streambed heterogeneity, might interfere with the ability of the stream to retain nutrients. Of course, other disturbances can be envisioned that could shorten spiraling length. Removal of forest canopy, for example, might be expected to increase primary production and attendant nutrient uptake, or an impoundment might slow downstream transport, thereby allowing shorter spirals.

Tests of the responses of spiraling to disturbance have been accomplished through field measurements of nutrient uptake length. Uptake length is the portion of the spiraling length involving transfer from a dissolved available form in the water column to a sequestered form on the stream bed and is the parameter of choice because its measurement is straightforward and because uptake length makes up the major portion of the total spiraling length (Newbold et al. 1982). Disturbances reported to increase uptake length include logging (Butturini and Sabater 1998) and urbanization (Grimm et al. 2005, Meyer et al. 2005). PO_4^{3-} uptake lengths were longer in second-growth forests compared to old-growth forests, a phenomenon attributed to the greater storage of fine-grained sediments in streams within the latter (Valett et al. 2002a). Opening the forest canopy also increased NH_4^+ uptake length because stream channels flowing through meadows were narrower than channels in woodlands, thereby reducing habitat per unit length (Sweeney et al. 2004).

These studies tend to support the underlying hypothesis that disturbance increases spiraling length, but they cannot yet be regarded as conclusive. Moreover, many questions remain regarding the specific mechanisms by which disturbance may affect spiraling. This chapter reports the uptake lengths of NH_4^+, PO_4^{3-}, glucose, and arabinose measured in streams that were identified as key freshwater sources to the New York City (NYC) drinking-water-supply. PO_4^{3-} and NH_4^+ represent easily assimilable forms of P and N, both of which potentially limit algal and microbial processes in streams and downstream reservoirs. Glucose and arabinose represent 2 monomeric carbohydrates that differ in bioavailability (Kaplan and Newbold 2003) and, thus, partially represent the range of bioavailability characteristic of natural dissolved organic C (Frazier et al. 2005). Carbohydrates were used in addition to the nutrients N and P because of their potential to reflect impacts on heterotrophic metabolism. NO_3^- uptake length was not measured, primarily because of logistical constraints. Uptake lengths of NO_3^- are typically several times longer (i.e., uptake rates several times smaller) than those of NH_4^+ (Webster et al. 2003, Hall and Tank 2003), particularly where ambient NO_3^- concentrations are elevated (Davis and Minshall 1999, Hall and Tank 2003). Thus, long reach lengths would have been necessary and, in many cases, the feasible length was constrained by tributary junctions and reservoirs. In addition, simultaneous addition of NO_3^- and NH_4^+ can confound estimates of NO_3^- uptake (Bernhardt et al. 2002).

The streams monitored in this study reflected a range of sizes, ambient solute concentrations, and watershed land covers and were the subject of a comprehensive analysis of water quality, biological condition, and ecosystem function (Blaine et al. 2006). Thus, they provided the opportunity for a relatively robust test of the hypothesis that human impacts increase spiraling length and for an examination of the proximate factors governing spiraling length. Results from the first three years of this study were reported by Newbold et al. (2006). This chapter reports measurements from the entire six years of the Project (2000 through 2005), thus augmenting the results reported by Newbold et al. (2006) and reanalyzing the results in the context of the entire dataset.

Methods

Study sites

Seventeen study sites were established along streams flowing into NYC drinking-water reservoirs (integrated sites in Figs. 2.1 and 2.2, Chapter 2). Ten of these streams were located in the Catskill and Delaware regions west of the Hudson River (WOH) and seven were located in the Croton/Kensico region east of the Hudson River (EOH). Low population density, high forest cover, and agriculture characterized the WOH region, whereas the EOH region was more influenced by urban and suburban development (Arscott et al. 2006). Watershed areas of the WOH sites ranged from 100 to 272 km^2, whereas those EOH were considerably smaller (35–46 km^2). The stream reaches used in our study also were used for concurrent measurements of stream ecosystem metabolism (Bott et al. 2006).

Stream solute additions

Solute uptake length (S_w) for NH_4^+, PO_4^{3-}, glucose, and arabinose were measured once annually in seven streams for three years from 2000 and 2002, in another seven streams for three years from 2003 to 2005, and in another three streams for six years from 2000 to 2005. Solute additions were made under baseflow conditions between June and October using the Stream Solute Workshop (1990) approach. Each addition involved simultaneous injections of a conservative tracer (sodium bromide), PO_4^{3-}, NH_4^+, glucose, and arabinose, for 75 to 155 min at rates designed to achieve concentration elevations in the stream of 30 µg/L PO_4^{3-}-P, 30 µg/L NH_4^+-N, 14 µg/L glucose-C, and 12 µg/L arabinose-C. One day before additions, time-of-travel was estimated with rhodamine WT and channel width and depth were measured at 20 transects throughout the reach. The time-of-travel and depth measurements were used to finalize the reach length (300–5400 m), chosen to achieve an expected uptake of 35 to 70% of each added solute.

Immediately before solute addition, water samples for ambient concentrations were taken at each of 5 downstream sampling stations. Five subsequent water samples were taken from each station within the period of plateau concentration, or in the period of maximal concentrations for an assay of NH_4^+, soluble reactive P (SRP), glucose, and arabinose, in addition to the conservative tracer. Supplementary samples for total dissolved P (TDP), total dissolved N (TDN), and NO_3^-, in addition to NH_4^+ and SRP, were taken from just upstream of the injection site before and after the injection, and at the lowermost station before, during, and after each addition. Samples for N and P assays were field-filtered (0.45-µm Whatman® cellulose nitrate membrane) and frozen within 24 h of collection for analysis within 60 d. Samples for glucose and arabinose assays were sterile-filtered (0.2-µm HT Tuffryn Acrodisc®) and frozen within 24 h for analysis within 2 mo.

S_w for a given solute was estimated from the concentration elevations, $\Delta C(x,t)=C(x,t) - C(x,t_0)$, where $C(x,t)$ and $C(x,t_0)$ are the concentrations of the solute measured at a distance x (m) downstream of the injection point at time t after the beginning of the injection, and time t_0 (immediately before the injection), respectively. The ratio, r_c, is the concentration elevation relative to that of the Br^- (the conservative tracer), $r_c = \Delta C/\Delta [Br^-]$, and was calculated to adjust for longitudinal dilution and dispersion. The longitudinal loss rate, k_l, of the solute was estimated by nonlinear regression from the relationship $r_c(x) = r_0 \exp(-k_l x)$, where r_0 is the concentration ratio elevation at $x = 0$. S_w for the respective solute was calculated as $S_w = 1/k_l$ (Newbold et al. 1981). At one site (site 139, Muscoot River near Whitehall Corners), the background concentration of NH_4^+, in each of the three years of measurement, greatly exceeded and therefore overwhelmed the concentration elevation due to the nutrient addition. For this site, the uptake length was estimated from longitudinal decline in total (background + added) NH_4^+. This approach has been employed in other studies (e.g., Martí et al. 1997, Doyle et al 2003), although it measures net rather than total uptake (Martí et al. 1997, Payne et al. 2005).

S_w is strongly scale dependent (Butturini and Sabater 1998), i.e., for a given nutrient concentration and uptake flux (U) of nutrient from the water column to the streambed, S_w varies in proportion to the product of the water depth, d, and water velocity, v_w (Stream Solute Workshop 1990). Therefore, S_w was converted to a mass-transfer coefficient, or uptake velocity (V_f), calculated as $V_f = k_l v_w d = v_w d/S_w$ to facilitate comparisons of spiraling among streams of

varying size. The scaling factor, $v_w d$, is equivalent to the specific discharge (i.e., stream flow [Q] divided by stream width [w]), because $Q = v_w w d$.

Conservative tracer (Br^-) data were analyzed with a 1-dimensional advection–dispersion model that includes a transient storage component (OTIS-P, Runkel et al. 1998) to describe stream flow characteristics, including: Q, cross-sectional area ([A], from which $v_w = Q/A$, and $d = A/w$), cross-sectional transient storage area (A_s), longitudinal dispersion coefficient, and transient storage exchange coefficient (α). The transient storage represents short-term detention of the stream water in lateral zones such as backwaters or eddies, or within the sediments where the downstream velocity is negligible (Bencala and Walters 1983). In our study, the size of the transient storage zone is reported as the ratio A_s/A, and the rate of transfer into the transient storage zone is reported as a hydraulic exchange velocity ($v_{hyd} = \alpha d$) for dimensional consistency with V_f.

Our study was not designed to assess nitrification of the added NH_4^+, but an approximate mass-transfer coefficient was calculated for nitrification using the supplementary samples for NO_3^- taken before and during the injections. Our approach was that of Mulholland et al. (2000), simplified by assuming that re-uptake of nitrification-produced NO_3^- within our relatively short reaches was negligible. The estimation required quantification of increases in NO_3^--N that were within the range of 0 to 30 µg/L above ambient concentration (because we added ~30 µg/L as NH_4^+-N). This quantification proved feasible only in streams where ambient NO_3^--N was ≤175 µg/L; at higher concentrations, our estimates were highly variable and often negative.

The results from 2 of 30 additions (i.e., site 40 in 2000, and site 5 in 2002) were not used in the analysis because they were affected by unusually high concentrations of suspended solids associated with minor flow fluctuations. In addition, the S_w for NH_4^+ at site 30 in 2000 could not be calculated because the variance in the sampled NH_4^+ concentrations was excessive.

Analytical methods

The carbohydrates, glucose and arabinose, were analyzed by high performance liquid chromatography (HPLC) with pulsed amperometric detection (Dionex 500) (Cheng and Kaplan 2001). Br^- was analyzed by ion chromatography with conductivity detection (Dionex 500). SRP was determined by the ascorbic acid method (EPA method 365.1). TDP was determined as SRP after ammonium persulfate digestion (EPA method 365.5). NH_4^+ was determined by the phenate procedure (EPA method 350.1), and NO_3^- (including NO_2^-) by Cd reduction (EPA method 353.2). Total dissolved N (TDN) was determined as the sum of NO_3^--N plus soluble Kjeldahl N (SKN, semiautomated phenate block digestion followed by NH_4^+ assay).

Covariates

Data from other components of the Project were used in the analyses of spiraling patterns. Site characterizations, including land cover and population density are summarized in Chapter 2. Ambient dissolved organic C (DOC) and biodegradeable DOC (BDOC) were sampled annually from each of the reaches (Chapter 6), but on different dates from the solute additions. Measured ecosystem metabolism, as daily community respiration (CR_{24}), daily gross primary production (GPP), water temperature, and light (photosynthetically active radiation [PAR]) over 3-d periods

that included the solute additions are presented in Chapter 9. Benthic stocks of chlorophyll *a* and periphyton-associated organic matter (BOM) are also presented in Chapter 9. Macroinvertebrate sampling was conducted in the spring of each year (Chapter 7). Two variables derived from the macroinvertebrate data, the Hilsenhoff Biotic Index (HBI; Hilsenhoff 1988) and species richness/100 individuals, were used in our analyses. Concentrations of molecular tracers were sampled during baseflow in the summer of each year (Chapter 4), but not concurrently with the additions. Relationships were analyzed between V_f s and 5 groups of tracers: 1) total PAHs, 2) toxic PAHs [the sum of benzo(b)fluoranthene, chrysene, benzo(a)pyrene, benzo(b)fluoranthene, and benzo(k)fluoranthene], 3) caffeine, 4) fragrance materials (FM; the sum of tonalide and galaxolide, both used in perfumes and soaps), and 5) fecal steroids (the sum of 7 steroid compounds). Molecular tracer concentrations were log-transformed before calculation of 3-6 y means from each site.

Analysis of uptake kinetics

V_fs were compared among streams using a kinetic model based on the Michaelis-Menten equation, which describes enzyme kinetics, but has been used to describe the rate of nutrient uptake by natural streambed communities (e.g., McIntire and Colby 1978, Mulholland et al. 2002, Payn et al. 2005):

$$U = U_{max}C/(K_s + C) \quad [1]$$

in which U represents the uptake flux of a nutrient or organic solute (mass per unit streambed area per unit time), U_{max} is the maximum uptake flux that would occur under high (saturating) water-column nutrient concentration, C, and K_s is the half-saturation concentration, i.e., the concentration at which $U = U_{max}/2$. The V_f reported here is related to the flux by $V_f = U/C$ (Stream Solute Workshop 1990) which, substituting for U in equation 1, yields:

$$V_f = U_{max}/(K_s + C) \quad [2]$$

In equation 2, V_f reaches a maximum as C approaches 0; hence, $V_{fmax} = U_{max}/K_s$ and equation 2 becomes:

$$V_f = V_{fmax}K_s/(K_s + C), \quad [3]$$

which we will refer to as the concentration-specific Michaelis-Menten curve.

V_{fmax} and K_s were estimated by nonlinear least squares (Proc NLIN, version 9.1, SAS Institute, Cary, North Carolina) using equation 3, the measured values for V_f and the ambient (pre-addition) concentrations (C) of the corresponding solute. Equation 3 was used rather than the more-familiar equation 1 because U, the dependent variable in equation 1, is the product of $V_f \times C$, making it dependent on the independent variable, C. Equation 3 was fitted using not only SRP and NH_4^+ (the added nutrients), but also TDP and TDN, to represent C. Our rationale for using TDP and TDN was that the availability of alternative forms of either P or N may influence the demand for the added form.

Hypotheses and statistical analysis

Our primary hypothesis was that human impacts increase spiraling length or, equivalently, (because streams of different sizes were compared) that human impacts decrease nutrient V_f. Possible mechanisms through which the effect of human impacts might have occurred were considered as secondary hypotheses. The relative influences considered were: 1) a saturating effect of human-induced nutrient enrichment, which would decrease V_f, 2) a stimulatory effect of nutrient enrichment, which would increase V_f, and 3) other unspecified impacts, such as the presence of toxins that would decrease V_f. Correlation coefficients and standardized regression coefficients in the framework of a path analysis were used to test these hypotheses (Fig. 8.1) (Wright 1934).

The 27 or 28 measurements from the individual solute additions were used for the regressions and many of the correlations. We were cognizant that the multiple (usually 3) observations from each site cannot be regarded as truly independent samples. However, substantial within-site interannual variability in ambient concentrations, stream flow, and ecosystem metabolism introduced some degree of independence between the measures and, more important, should contribute explanatory power to the analysis. Since the lack of independence could produce spurious results, correlations also were computed using the (n = 10) values for each variable averaged across the 3-6 y at each site. Results of the latter correlations are noted when they contradicted a major result obtained from the correlation of individual (n = 27 or 28) values. In cases of disagreement between the individual and 3-6 y-mean correlations, analysis of covariance (ANCOVA), with site as a main effect, was used to identify possible within-site (year-to-year) relationships that might have been masked by the 3-6 y averaging. For correlations and regressions involving variables that were not measured concurrently with the solute additions (invertebrates, molecular tracers, and land cover), only the 3-6 y means (n = 10) were used.

Results

Physical and chemical characteristics of streams

The experiments were conducted under baseflow conditions at stream flows ranging from 0.02 to 7.67 m^3/s, with correspondingly wide ranges in velocity, width, and depth (Table 8.1). A_s/A ranged from 0.01 to 0.65, and v_{hyd} ranged from undetectable to 0.310 mm/s. Ambient solute concentrations and conductivity are given in Table 8.2. The three assayed forms of nitrogen (TDN, NO_3^-, and NH_4^+) correlated among each other ($r=0.59$, $p<0.05$), as did the two forms of phosphorus (SRP and TDP, $r=0.98$). However, none of the nitrogen forms correlated with either form of phosphorus ($r=0.41$, $p>0.05$). At one site (Site 139, Muscoot River near Whitehall Corners), NH_4^+ was exceptionally high (0.277-0.401 mg/L relative to a range of 0.001-0.028 mg/L from all other sites), and other forms of nitrogen (NO_3^- and TDN) exceeded those of the other sites as well. When Site 139 was excluded from the correlation analysis, both SRP and TDP from among the remaining sites correlated with NH_4^+, NO_3^-, and TDN ($r=0.48$, $p<0.05$). TDN, SRP, and TDP all correlated with conductivity ($r=0.63$) and DOC ($r=0.68$). Glucose correlated with TDP and conductivity ($r=0.52$), whereas arabinose correlated only with NH_4^+ ($r=0.61$). Molar N:P ratios (based on TDN and TDP) varied by more than a factor of 10, from 36

(Site 11, Bush Kill) to 470 (Site 139, Muscoot River near Whitehall Corners), with a median of 89.

In addition, there were correlations of physical characteristics with chemical properties that were related to a regional interaction between watershed size and stream chemistry, but have bearing on subsequent data interpretation. TDP, SRP, DOC, and conductivity were negatively correlated with velocity, depth, width, and flow ($r = –0.48$, $p < 0.05$), reflecting a general pattern of higher nutrient and major ion concentrations in EOH streams (where sites occupied smaller watersheds) than in WOH streams (Dow et al. 2006, Chapter 3 of this report). TDN and NO_3^- were positively correlated with hydraulic exchange velocity (r=0.54).

S_w *and scaling with stream size*

As expected from scaling considerations, S_w for all solutes varied with specific discharge (i.e., the scaling factor, $v_w d$; Fig. 8.2A–D) and converting S_w to V_f (Table 8.3) removed most of the influence of scale (Fig. 8.2E–H, Table 8.4). Of the 4 solutes, only the NH_4^+-V_f was correlated with $v_w d$ (Fig. 8.2F, Table 8.4). This correlation may have represented stimulation by current velocity of nutrient uptake (Whitford and Schumacher 1961, Borchardt et al. 1994, Larned et al. 2004), but it appears at least as likely that it was an artifact of the higher TDN in the more populated EOH sites where the study watersheds were smaller. V_fs were not related to v_{hyd}, A_s/A, PAR, or water temperature, except that glucose-V_f was negatively correlated with A_s/A (r=-0.52).

V_f *and ambient solute concentration*

PO_4^{3-}-V_f varied inversely with ambient SRP concentration in a manner consistent with Michaelis–Menten kinetics. The nonlinear regression of the concentration specific Michaelis–Menten curve (eq. 3) explained 72% of the variance in V_f, as compared to 62% (r^2) explained by correlation (Table 8.4), and yielded parameter estimates (mean ± standard deviation) of $V_{f\max}$ = 0.032 ± 0.067 mm/s and K_s = 12 ± 35 µg/L (Fig. 8.3A).

NH_4^+-V_f varied inversely with ambient NH_4^+, except that the correlation was significant only when site 139 (Muscoot River near Whitehall Corners) was excluded from the analysis (Table 8.4). NH_4^+-N concentration at site 139, as noted previously, was far higher than at any other site. This site was also excluded from the estimation of the Michaelis-Menten parameters, both because it would have exerted a disproportionate influence on the parameter values and because we suspected that uptake at this site was dominated by nitrification. The non-linear regression yielded parameter estimates of V_{fmax} = 0.1143 ± 0. 058 mm/s and Ks = 9.27 ± 6.43 µg/L. The nonlinear regression (Fig. 8.3B) explained 37% of the variance, which was actually somewhat less than that explained by simple correlation (40%; Table 8.4). Thus, while the data were consistent with the Michaelis-Menten model, they did not provide evidence for its superiority over an empirical, linear relation.

V_f s of arabinose and glucose were not correlated with concentrations of any solutes, including ambient concentrations of arabinose, glucose, DOC, and BDOC (Table 8.4). In contrast, both PO_4^{3-}-V_f and NH_4^+-V_f were negatively correlated with DOC and with BDOC. However, DOC was correlated with both SRP (r = 0.68, p < 0.01) and TDN (r = 0.75, p < 0.01),

and BDOC was weakly correlated with TDN (r = 0.70, p = <0.01), so these associations probably reflect the influences of TDP and TDN, respectively.

Comparisons among V_f*s*

Similarities and differences among the V_fs of the various solutes are potentially useful in interpreting human impacts. V_fs of PO_4^{3-} and NH_4^+ were correlated (Fig. 8.4A) [r=0.51 p=0.035]. V_fs of glucose and arabinose, were strongly correlated with each other (Fig. 8.4B) (r=0.82 p<0.01). Arabinose-V_f was correlated with NH_4^+-V_f (r=0.51, $p < 0.05$) and glucose-V_f. showed a marginal correlation with NH_4^+-V_f as well (r=0.47, p=0.06). Neither carbohydrate-V_f was correlated with PO_4^{3-}-V_f (r =0.15, $p > 0.50$).

NH_4^+-V_f averaged ~2.7× higher than PO_4^{3-}-V_f and exceeded the respective PO_4^{3-}-V_f in all but one (at site 139) of the 57 individual measurements (Table 8.3). The mean glucose-V_f was similar to the mean NH_4^+-V_f (0.058 and 0.052 mm/s, respectively) whereas the mean arabinose-V_f (0.022 mm/s) was comparable to the mean PO_4^{3-}-V_f (0.019 mm/s).

The residuals (i.e., the difference between observed and predicted values) from equation 3, as fitted using SRP and TDN for PO_4^{3-}-V_f and NH_4^+-V_f, respectively, were examined to investigate the possibility that high concentrations of one nutrient had a stimulating effect on the uptake of another. Neither set of residuals were correlated with any of the measured nutrient forms ($|r| < 0.3$, $p > 0.27$).

Nitrification

Among the 17 injections for which ambient NO_3-N ≤ 175 µg/L, nitrification could be estimated for 14. Three sites were excluded because background NO_3-N varied excessively during the injection. For the 14 sites, nitrification-V_f (that part of the total NH_4^+ uptake that was nitrified rather than assimilated) ranged from 0 to 0.025 mm/s with a mean of 0.007 mm/s. Nitrification-V_f varied between 0 and 32% of NH_4^+-V_f with a mean of 10%. This proportion was correlated with ambient NO_3^- concentration (r = 0.87, $p < 0.01$). Nitrification-V_f also was correlated with ambient NO_3^-concentration (r = 0.56, $p < 0.01$), but not with ambient NH_4^+ concentration (r=0.42, p>0.05).

Ecosystem metabolism, benthic chlorophyll, and BOM

Both PO_4^{3-}-V_f and NH_4^+-V_f were correlated with CR_{24}, (Table 8.4, Fig. 8.5A–D, E–H, respectively). NH_4^+-V_f was correlated with GPP, but PO_4^{3-}-V_f was not (Table 8.4, Fig. 8.5E-F). Neither of the carbohydrate V_f s correlated with either of the measures of ecosystem metabolism. Because these correlations involved 3- or 6-year averages, they would not have reflected any influence year-to-year, within-site variations, in CR_{24} or GPP on nutrient uptake. To investigate such within site variations, we used ANCOVA, with V_f as the dependent variable, site as a main effect, and CR_{24} or GPP as a continuous covariate. The year-to-year within-site variations in CR_{24} explained 21% ($p < 0.01$) of the residual variance (i.e., the variance unexplained by site effect) in PO_4^{3-}-V_f. Also, year-to-year within-site variations in GPP explained 19% of the residual variance in PO_4^{3-}-V_f ($p< 0.01$). Neither CR_{24} nor GPP explained a significant fraction of the residual within-site variance in NH_4^+-V_f . However, CR_{24} explained 20% ($p < 0.01$) and 19%

($p < 0.01$) of the residual within-site variance in glucose-V_f and arabinose-V_f, respectively, and GPP explained 11% (p=0.02) and 13% ($p = 0.02$), respectively.

None of the V_fs were correlated with benthic chlorophyll *a* (Table 8.4), whereas BOM was negatively correlated with NH_4^+-V_f but with none of the other V_f s. The negative correlation with BOM was opposite to the result expected from a nutrient demand exerted by heterotrophic microbes.

Nutrient uptake flux, U

U expresses the transfer of nutrient to a unit area of streambed because mass per unit time is related to V_f by $U = V_f C$. NH_4^+-*U* at site 139 (Muscoot River near Whitehall Corners) was 8.2 $\mu g\ m^{-2}\ s^{-1}$, far greater than at all other sites (0.30 - 0.88 $\mu g\ m^{-2}\ s^{-1}$). Thus site 139 was excluded from correlations with other sites. For the other 16 sites, no significant correlations were found among the Us of individual solutes ($|r| \leq 0.31$, $p > 0.25$, e.g., Fig. 8.6A). None of the four *U*s correlated with either CR_{24} or GPP ($|r| \leq 0.39$, $p > 0.12$), except for a positive correlation of arabinose-*U* with CR_{24} ($r = 0.51$, $p < 0.05$, Fig. 8.6 B).

Benthic macroinvertebrates

PO_4^{3-}-V_f was marginally correlated with HBI (Table 8.4, Fig. 8.7A r=-0.47, $p = 0.056$), The HBI, reported in this study by Kratzer et al. 2006 and in Chapter 7, is an inverse index of water quality (Hilsenhoff 1988), so the negative correlation represents a positive association between PO_4^{3-}-V_f and conditions favorable to the macroinvertebrate community. PO_4^{3-}-V_f was also marginally correlated with species richness (r=0.45, p=0.07). NH_4^+-V_f was marginally correlated with species richness (r=0.48, p=0.051, Fig. 8.7B), but not with HBI (Table 8.4). Benthic macroinvertebrates variables were not correlated with carbohydrate V_fs.

Molecular tracers

PO_4^{3-}-V_f was negatively correlated with log-transformed concentrations of total PAHs, toxic PAHs (Fig. 8.7C), fecal steroids, and fragrance materials, but not with caffeine (Table 8.4). NH_4^+-V_f did not correlate with any of the molecular tracers except for a marginal negative correlation with caffeine (Fig. 8.7D r=-0.47, p=0.057). No correlations were found between carbohydrate V_fs and molecular tracers.

Land cover

Both PO_4^{3-}-V_f and NH_4^+-V_f were positively correlated with % forest cover within the watershed (Figs. 8.8A and C), and negatively correlated with watershed population density (Figs. 8.8B and D) and % agricultural land use in the watershed (Table 8.4), except that the correlation between NH_4^+-V_f and % agricultural land use was marginal (r=-0.46, p=0.06). Neither of the carbohydrate V_fs were correlated with any descriptors of land cover/use.

Spiraling and human impact

PO_4^{3-}-V_f path analysis. Fig. 8.9A represents relationships among the measured variables in the form of a path analysis relating land use to PO_4^{3-}-V_f. To simplify the analysis, only one variable each was used among groups of variables representing land use (% forest), nutrients (SRP), and metabolism (CR_{24}). Not all of the path coefficients and correlations were significant (those that were significant at $p < 0.05$ are shown in bold face). Nonetheless, we report all the path coefficients (standardized regression coefficients) to provide estimates of the relative importance of the variables. Given this caveat, the analysis suggests that land use (as % forest) influenced P uptake through 3 main pathways. First, % forest negatively influenced SRP, which (through saturation mechanisms) inversely influenced PO_4^{3-}-V_f (path effect = the product of the path coefficients = 0.27). Second, % forest had a positive influence on CR_{24}, which in turn positively influenced phosphate-V_f, yielding a relatively weak path effect of 0.06. Third, % forest positively and directly influenced PO_4^{3-}-V_f, with a path effect of 0.45. A 4th possible pathway, involving an influence of SRP on CR_{24} was considered but rejected because the apparent influence of SRP on CR_{24} was not significant (p=0.22) and negative (i.e., the inverse of an expected influence). The analysis suggests that nutrient saturation (the first path), while important, accounted for <½ of the overall influence of land-use on nutrient uptake, i.e., that there were other mechanisms through which human activity impacted spiraling. If there was an effect of land use independent of the saturating effect of SRP, then we might identify one or more water quality parameters that would reflect this independent effect. Such a parameter would correlate with some measure of land use but not with SRP, and it would explain additional variation in PO_4^{3-}-V_f beyond that accounted for by SRP. In a previous analysis of a subset of the data presented here (years 2000-2002 from ten sites), Newbold et al. 2006 found that toxic PAHs met these criteria. Among the data from years 2000 to 2005 from 17 sites analyzed here, toxic PAHs were correlated with both % forest and PO_4^{3-}-V_f as in the previous analysis. However, unlike the previous analysis, toxic PAHs also correlated with SRP and, in a regression of toxic PAHs together with SRP on PO_4^{3-}-V_f, the standardized regression coefficient for toxic PAHs (-0.32) was not significant (p=0.11). Thus toxic PAHs did not provide confirmatory evidence of an effect of land use (human activity) that was independent of the nutrient saturation effect. Another molecular tracer that correlated with PO_4^{3-}-V_f, fecal steroids, did not correlate significantly with SRP (r=0.42, p=0.09) and, when regressed on PO_4^{3-}-V_f along with SRP, yielded a standardized regression coefficient (-0.37) that was significant (p=0.03). However, fecal steroids was not significantly correlated with % forest (-0.44, p=0.08) or other measures of land use, perhaps reflecting influence by other factors such as wildlife populations. Invertebrate species richness correlated with both % forest, and marginally (p=0.07) with PO_4^{3-}-V_f (Fig. 8.9A). But species richness, like toxic PAHS, covaried with SRP ($r = -0.61$, $p = 0.01$), so that species richness provided no additional evidence of an independent (non-nutrient-related) mechanism.

NH_4^+-V_f path analysis. TDN was used to represent the primary nutrient in the path analysis for NH_4^+-V_f (Fig. 8.9B). Referring to the 3 pathways described for the PO_4^{3-} analysis, the path effect of % forest on NH_4^+-V_f via the TDN pathway was 0.22, the path effect of % forest on NH_4^+-V_f via the CR_{24} pathway was 0.14, and the direct path effect of % forest on NH_4^+-V_f was 0.36. This analysis, like that of PO_4^{3-} uptake, pointed to a role for mechanisms other than nutrient saturation. Although the coefficient for the direct (%forest-to- NH_4^+-V_f) path was not significant (p=0.2) in the full model presented in Fig. 8.9B, the simplified multiple regression of

TDN and % forest on NH_4^+-V_f confirmed a significant ($p = 0.04$) direct effect of % forest on NH_4^+-V_f. Invertebrate species richness correlated with both % forest, and marginally (p=0.051) with NH_4^+-V_f (Fig. 8.9B). However, because species richness covaried with TDN ($r = –0.64$, $p < 0.01$), species richness provided no additional evidence of an independent (non-nutrient-related) mechanism.

Discussion

Stream channel and flow characteristics

The scaling of S_w with stream size has been widely observed (Butturini and Sabater 1998, Peterson et al. 2001, Hall et al. 2002) and is expected if V_fs are relatively independent of stream-scaling influences (Wollheim et al. 2001). We saw no relationship between V_fs and either v_{hyd} or A_s of the streams except for a negative correlation of glucose-V_f with A_s/A. A negative relationship, however, is inconsistent with any hypothesized role for transient storage in solute uptake, and we suspect it was an artifact of the regionally based covariation between TDN and A_s/A. Transient storage can influence solute uptake (Valett et al. 1996, Hall et al. 2002, Gücker and Boëchat 2004), particularly when the range of A_s/A is large, but several studies have reported no statistical relationship between solute uptake and transient storage parameters (e.g., Webster et al. 2003, Niyogi et al. 2004, Meyer et al. 2005), or that additional factors produce a relationship opposite to that expected (Hall et al. 2002, Valett et al. 2002b).

V_f *and ambient solute concentration*

Nutrient V_fs in streams respond to short-term variations in nutrient concentration in a manner consistent with the Michaelis–Menten model of saturation kinetics (Mullholland et al. 1990, 2002, Dodds et al. 2002a, Payn et al. 2005). The saturation concept has also been used to explain differences in V_f observed among streams of differing nutrient concentration (Davis and Minshall 1999, Niyogi et al. 2004), and several other interstream comparisons have observed inverse relationships between nutrient concentration and V_f (Webster et al. 2003, Dodds et al. 2002a, Bernhardt et al. 2002, Hall et al. 2002, Haggard et al. 2005). However, to our knowledge, our study is the first to apply the Michaelis–Menten model quantitatively to such interstream comparisons.

The ability of the Michaelis–Menten model to explain significant variation in the V_fs of PO_4^{3-} and NH_4^+ among different streams has implications that are substantially different from application to a single stream. When the nutrient concentration is varied experimentally in a single stream, other factors that might govern nutrient demand, such as the biomass of nutrient-assimilating autotrophs and heterotrophs, light, temperature, and current, remain approximately constant. The response that is observed is clearly a response in the uptake kinetics. When different streams are compared, however, the uptake kinetics become only one of the many influences on nutrient demand. In the context of equation 3, these other influences would produce variability in V_{fmax} among streams, reducing the explanatory power of the model. Given these considerations, it is not surprising that equation 3 did not explain a higher proportion of the variance in V_f (66% for PO_4^{3-} and 36% for NH_4^+). Rather, our results suggest that stream-to-stream variability in V_{fmax} is less than might be expected.

Our estimates of V_f for N and P were probably lower than the true V_f that would be measured at ambient concentrations using isotopic tracers (Mulholland et al. 1990, Mulholland et al. 2002). However, we believe that the utility of our results for comparisons among streams was not compromised because our nutrient additions were relatively low (~30 µg/L) and consistent among all injections. Limited data comparing ^{33}P additions to P enrichments suggest that our estimated V_fs may be 50 to 75% of the true V_f s (Mulholland et al. 1990). A more extensive paired comparison of ^{15}N-tracer with NH_4^+ enrichments in 10 streams suggests that the additions we used (30 µg/L) were likely to yield V_f estimates that were ~35% of their true value (Mulholland et al. 2002). Mulholland et al. (2002) reported a median NH_4^+-V_f , based on ^{15}N-tracer additions, of 0.20 mm/s for 9 sites where DIN concentrations were <62 µg/L. In our study, the median NH_4^+-V_f among 5 measurements, where DIN was <73 µg/L, was 0.07 mm/s, which is 35% of the ^{15}N-based estimates of Mulholland et al. (2002) and consistent with their prediction.

Our estimated half-saturation constants (K_s) for SRP of 12 µg/L was higher than those reported by Bothwell (1985, 1988) (<1–4 µg/L), and very near those of Rosemond et al. (2002) (7–13 µg/L), but well below the concentrations (up to ~50 µg/L) sometimes observed to stimulate periphyton biomass accumulation in rivers (Borchardt 1996, Dodds et al. 2002). Our estimate for K_s also was well below our additions of ~30 µg/L. The latter result implies that the short-term K_s governing uptake during our additions exceeded the long-term K_s to which the streams were equilibrated. This reasoning can be seen by tentatively assuming that equation 3 is equally applicable to both short-term and long-term kinetics. Representing the nutrient addition (ΔC) explicitly in equation 3 yields $V_f = V_{fmax} K_s/(K_s + \Delta C + C)$ or $V_{fmax} K_s/(K_e + C)$, where $K_e = K_s + C$ (see Wright and Hobbie 1965). The assumption implies that we actually estimated K_e, rather than K_s, so that the true K_s ($= K_e - \Delta C$) would be –18 µg/L, which is untenable. Because of longitudinal decreases from the target concentration, the typical effective concentration elevation (ΔC) was ~20 µg/L, but even using this corrected value still yields a negative (–8 µg/L) estimate for K_s. We infer that the short-term K_s (which we could not estimate because we added at only one concentration, cf. Payn et al. 2005), was much higher than the long-term equilibrated K_s, which we estimated from equation 3. The difference is expected theoretically as the result of variable cellular concentrations, or luxury consumption (Droop 1973) by streambed organisms. Rhee (1973) reported that the short term K_s for PO_4^{3-} exceeded long-term K_s by a factor ~10, and Caperon and Meyer (1972) reported similar differentials for NH_4^+ and NO_3^- uptake.

Nitrification

Nitrification could be estimated only in streams with relatively low concentrations of ambient NO_3 (≤175 µg/L), but among these streams, nitrification accounted for an average of 10% of the NH_4^+ uptake, less than the mean of 56% measured in 19 mountain streams in New Hampshire (Bernhardt et al. 2002), and less than the mean of 26% estimated from ^{15}N-labeled NH_4^+ additions to 11 different streams from various biomes (Webster et al. 2003). However, nitrification was not detected during NH_4^+ additions to 11 mountain streams in Wyoming (Hall and Tank 2003), and the factors responsible for these differences remain unclear. The correlation between NO_3^- concentration and nitrification supports a similar finding of Bernhardt et al. (2002), who hypothesized that NO_3^- at high concentrations supplies much of the assimilatory demand for N, leaving more of the NH_4^+ available to nitrifying bacteria. Unfortunately, this

relationship predicts that the highest nitrification rates in our study may have occurred in the high- NO_3^- streams where we could not estimate nitrification.

Spiraling and measures of ecosystem metabolism

The V_fs of all 4 solutes were positively related to ecosystem metabolism (CR_{24} and GPP), although the evidence for this was varied: For NH_4^+ annual means of V_f correlated with the annual means of CR_{24} and GPP, while for PO_4^{3-}, glucose, and arabinose, the within site, year-to-year variation in V_f correlated with the respective variations in CR_{24} and GPP. Only in the case of PO_4^{3-}-V_f and CR_{24} were both between site and within site variations significant. We interpret these results to imply the V_f s were related to ecosystem metabolism, but not strongly enough to be detected consistently by both approaches. Our previous analysis of only the first three years of the study, which involved only ten of the 17 sites (Newbold et al. 2006), found stronger relationships than we found here for the full dataset. We interepret this to mean that these relationships were weaker among the seven sites added in Phase II, than among the ten original sites. In general, the added sites were smaller, higher in nutrient concentration, and in watersheds with more intensive land use than was characteristic of the original sites.

Several other studies have found correlations between NH_4^+-V_f and either CR, GPP, or both (Hall and Tank 2003, Webster et al. 2003, Meyer et al. 2005). Our study appears to be the first that has observed a relationship between PO_4^{3-}-V_f and metabolism and between carbohydrate-V_f and metabolism. No influence of either benthic chlorophyll *a* or BOM on V_fs of any of the nutrients was observed, although these relationships have been reported in other studies (Mulholland et al. 1985, Niyogi et al. 2004, Meyer et al. 2005). The absence of these relationships in our study may be attributable to a relatively limited range of variation in these variables (Bott et al. 2006).

U can, in principle, be predicted from measures of stream metabolism under certain assumptions of stoichiometric coupling (Hall and Tank 2003, Webster et al. 2003). Therefore, we expected CR_{24} and GPP to be correlated with *U*, particularly with PO_4^{3-}-V_f and NH_4^+-V_f. Instead, we found only a relatively weak correlation between CR_{24} and arabinose-U. For NH_4^+, the absence of a strong correlation probably reflected the variable and unknown contributions of NO_3^- and dissolved organic N (DON) to N uptake, and possibly reflected unmeasured nitrification in the high-NO_3^- streams. TDN (i.e., NO_3^- + DON + NH_4^+) was present in all of the streams at far higher concentrations than NH_4-N alone, and as implied by the influence of TDN on NH_4^+ uptake (Fig. 8.2B), dissolved N forms other than NH_4-N evidently accounted for much of the N assimilation. For P, the unmeasured contribution from dissolved organic P (DOP) may have been a factor. However, DOP averaged only 30% of TDP, and it seems unlikely that the influence of DOP could explain the lack of correlation. Rather, we suggest that variable stoichiometry, or luxury consumption, within the algal (Rhee 1973) and microbial (Senior and Dawes 1971, Makino et al. 2003) communities may have prevented a correlation. In our study, ambient TDP concentrations were negatively correlated with GPP (Bott et al. 2006) and CR_{24} (p = 0.09, TLB, unpublished data). If cellular C:P ratios varied inversely with P concentrations, they would have been lowest (and the ratio of P uptake to C metabolism would have been highest) at sites with the lowest metabolic rates. Thus, 2 opposing trends (1 in stoichiometry, the other in metabolism) may have balanced each other, leaving no net relationship between P concentration and *U*.

Spiraling and human impact

Our results generally support the hypothesis that spiraling, as measured by V_f, is a sensitive indicator of human disturbance. V_f s for either PO_4^{3-}, NH_4^+, or both were correlated with measures of human occupation of the landscape (% forest cover , population density, and % agricultural land use), as well as with several measures of water quality that reflected human influences. These water-quality variables included nutrient concentrations, various molecular tracers, and macroinvertebrate-based indices of water quality (although the latter correlations were marginal). Unlike PO_4^{3-} and NH_4^+, the uptake of carbohydrates—glucose and arabinose—showed little or no response to human impact despite their correlation with community respiration. Carbohydrates are consumed only by heterotrophs, whereas P and N are used by autotrophs as well as heterotrophs. Thus, it is tempting to suggest that autotrophs were preferentially impacted by human activities on the landscape. However, Bott et al. (2006) did not observe a greater sensitivity of GPP than CR_{24} to land use in these same streams. Another possibility is that human impacts affected the efficiency of (or otherwise altered) heterotrophic processes to reduce metabolism and nutrient consumption without affecting the demand for DOC from the water column.

The analysis of uptake kinetics, together with the path analyses, pointed to nutrient enrichment as a major causal link between human activity and spiraling. However, the path analysis supported other causal pathways as well. For example, community metabolism (in particular, CR_{24}) had a positive influence on V_fs, but its inverse relation to human activity (e.g., % forest cover, see also Bott et al. 2006) was inconsistent with a nutrient-enrichment effect and evidently reflected other forms of human disturbance. We caution, however, that Bott et al. (2006) observed that human impacts on metabolism were potentially confounded by stream size and canopy cover. The associations with molecular tracers, particularly that of PO_4^{3-}-V_f with toxic PAHs, offer the possibility that nutrient uptake was affected by toxins. The concentrations of toxins observed in the Project (Chapter 4) were not clearly at levels that would impair ecosystem function, but they do demonstrate that the streams were receiving substances related to human activity. For example, the Kisco River, in which uptake velocities for all of the nutrients ranked among the lowest in our study, and toxic PAHs the highest of the 17 sites (Chapter 4), has been reported by an independent study (Phillips et al. 2002, Phillips and Bode 2004) to receive several pesticides and herbicides, particularly during storm flows, at concentrations that may impair aquatic life.

Literature Cited

Arscott, D. B., C. L. Dow, and B. W. Sweeney. 2006. The landscape template of New York City's drinking-water-supply watersheds. Journal of the North American Benthological Society 25:000–000.

Bencala, K. E., and R. A. Walters. 1983. Simulation of solute transport in a mountain pool-and riffle stream: a transient storage model. Water Resources Research 19:718–724.

Bernhardt, E. S., R. O. Hall, and G. E. Likens. 2002. Whole-system estimates of nitrification and nitrate uptake in streams of the Hubbard Brook Experimental Forest. Ecosystems 5:419–430.

Blaine, J. G., B. W. Sweeney, and D. B. Arscott. 2006. Enhanced source-water monitoring for New York City: historical framework, political context, and project design. Journal of the North American Benthological Society 25:851-866.

Borchardt, M. A. 1996. Nutrients. Pages 183-227 *in* R. J. Stevenson, M. L. Bothwell, and R. L. Lowe (editors). Algal ecology. Freshwater benthic ecosystems. Academic Press, San Diego, California.

Borchardt, M. A., J. P. Hoffmann, and P. W. Cook. 1994. Phosphorus uptake kinetics of *Spirogyra fluviatilis* (Charophyceae) in flowing water. Journal of Phycology 30:403–417.

Bothwell, M. L. 1985. Phosphorus limitation of lotic periphyton growth rates: an intersite comparison using continuous-flow troughs (Thompson River system, British Columbia). Limnology and Oceanography 30:527–542.

Bothwell, M. L. 1988. Growth rate responses of lotic periphytic diatoms to experimental phosphorus enrichment: the influence of temperature and light. Canadian Journal of Fisheries and Aquatic Sciences 45:261–270.

Bott, T. L., D. S. Montgomery, J. D. Newbold, D. B. Arscott, C. L. Dow, A. K. Aufdenkampe, and J. K. Jackson. 2006. Ecosystem metabolism in streams of the Catskill Mountains (Delaware and Hudson River watersheds) and Lower Hudson Valley. Journal of the North American Benthological Society 25:1018-1044.

Butturini, A., and F. Sabater. 1998. Ammonium and phosphate retention in a Mediterranean stream: hydrologic versus temperature control. Canadian Journal of Fisheries and Aquatic Sciences 55:1938–1945.

Caperon, J., and J. Meyer. 1972. Nitrogen-limited growth of marine phytoplankton. II. Uptake kinetics and their role in nutrient limited growth of phytoplankton. Deep-Sea Research 19:619–632.

Cheng, X., and L. A. Kaplan. 2001. Improved analysis of dissolved carbohydrates in stream water with HPLC-PAD. Analytical Chemistry 73:458–461.

Davis, J. C., and G. W. Minshall. 1999. Nitrogen and phosphorus uptake in two Idaho (USA) headwater wilderness streams. Oecologia (Berlin) 119:247–255.

Dodds, W. K., A. J. Lopez, W. B. Bowden, S. Gregory, N. B. Grimm, S. K. Hamilton, A. E. Hershey, E. Martí, W. H. McDowell, J. L. Meyer, D. Morrall, P. J. Mulholland, B. J. Peterson, J. L. Tank, H. M. Valett, J. R. Webster, and W. Wollheim. 2002a. N uptake as a function of concentration in streams. Journal of the North American Benthological Society 21:206–220.

Dodds, W. K., V. H. Smith, and K. Lohman. 2002b. Nitrogen and phosphorus relationships to benthic algal biomass in temperate streams. Canadian Journal of Fisheries and Aquatic Sciences 59:865–874.

Dow, C. L., D. B. Arscott, and J. D. Newbold. 2006. Relating major ions and nutrients to watershed conditions across a mixed-use, water-supply watershed. Journal of the North American Benthological Society 25:000–000.

Doyle, M. W., E. H. Stanley, and J. M. Harbor. 2003. Hydrogeomorphic controls on phosphorus retention in streams. Water Resources Research 39. DOI:1029/2003WR002038.

Droop, M. R. 1973. Some thoughts on nutrient limitation in algae. Journal of Phycology 9:264–272.

Frazier, S. W., L. A. Kaplan, and P. G. Hatcher. 2005. Molecular characterization of biodegradable dissolved organic matter using bioreactors and [$^{12}C/^{13}C$] tetramethylammonium hydroxide thermochemolysis GC-MS. Environmental Science and Technology 39:1479–1491.

Grimm, N. B., R. W. Sheibley, C. L. Crenshaw, C. N. Dahm, W. J. Roach, and L. H. Zeglin. 2005. N retention and transformation in urban streams. Journal of the North American Benthological Society 24:626–642.

Gücker, B., and I. G. Boëchat. 2004. Stream morphology controls ammonium retention in tropical headwaters. Ecology 85:2818–2827.

Haggard, B. E., E. H. Stanley, and D. E. Storm. 2005. Nutrient retention in a point-source-enriched stream. Journal of the North American Benthological Society 24:29–47.

Hall, R. O., E. S. Bernhardt, and G. E. Likens. 2002. Relating nutrient uptake with transient storage in forested mountain streams. Limnology and Oceanography 47:255–265.

Hall, R. O., and J. L. Tank. 2003. Ecosystem metabolism controls nitrogen uptake in streams in Grand Teton National Park, Wyoming. Limnology and Oceanography 48:1120–1128.

Hilsenhoff, W. L. 1988. Rapid field assessment of organic pollution with a family-level biotic index. Journal of the North American Benthological Society 7:65–68.

Kaplan, L. K., and J. D. Newbold. 2003. The role of monomers in stream ecosystem metabolism. Pages 97–119 *in* S. E. G. Findlay and R. L. Sinsabaugh (editors). Aquatic ecosystems. Interactvitiy of dissolved organic matter. Academic Press, San Diego, CA.

Kaplan, L. A., J. D. Newbold, and D. J. Van Horn. 2006. Organic matter transport in New York City drinking-water-supply watersheds. Journal of the North American Benthological Society 25:912-927.

Kratzer, E. B., J. K. Jackson, D. B. Arscott, A. K. Aufdenkampe, C. L. Dow, J. D. Newbold, and B. W. Sweeney. 2006. Macroinvertebrate distribution in relation to land use and water chemistry in New York City drinking-water-supply watersheds. Journal of the North American Benthological Society 25:954-976.

Larned, S. T., V. I. Nikora, and B. J. F. Biggs. 2004. Mass-transfer-limited nitrogen and phosphorus uptake by stream periphyton: a conceptual model and experimental evidence. Limnology and Oceanography 49:1992–2000.

Makino, W., J. B. Cotner, R. W. Sterner, and J. J. Elser. 2003. Are bacteria more like plants or animals? Growth rate and resource dependence of bacterial C:N:P stoichiometry. Functional Ecology 17:121–130.

Martí, E., N. B. Grimm, and S. G. Fisher. 1997. Pre- and post-flood retention efficiency of nitrogen in a Sonoran Desert stream. Journal of the North American Benthological Society 16:805-819.

McIntire, D. C., and J. A. Colby. 1978. A hierarchical model of lotic ecosystems. Ecological Monographs 48:167–190.

Meyer, J. L., M. J. Paul, and W. K. Taulbee. 2005. Stream ecosystem function in urbanizing landscapes. Journal of the North American Benthological Society 24:602–612.

Mulholland, P. J., J. D. Newbold, J. W. Elwood, L. A. Ferren, and J. R. Webster. 1985. Phosphorus spiralling in a woodland stream: seasonal variations. Ecology 66:1012–1023.

Mulholland, P. J., A. D. Steinman, and J. W. Elwood. 1990. Measurement of phosphorus uptake length in streams: comparison of radiotracer and stable PO_4 releases. Canadian Journal of Fisheries and Aquatic Sciences 47:2351–2357.

Mulholland, P. J., J. L. Tank, D. M. Sanzone, W. M. Wollheim, B. J. Peterson, J. R. Webster, and J. L. Meyer. 2000. Nitrogen cycling in a forest stream determined by a ^{15}N tracer addition. Ecological Monographs 70:471-493.

Mulholland, P. J., J. L. Tank, J. R. Webster, W. B. Bowden, W. K. Dodds, S. V. Gregory, N. B. Grimm, S. K. Hamilton, S. L. Johnson, E. Martí, W. H. McDowell, J. L. Merriam, J. L. Meyer, B. J. Peterson, H. M. Valett, and W. M. Wollheim. 2002. Can uptake length in streams be determined by nutrient addition experiments? Results from an interbiome comparison study. Journal of the North American Benthological Society 21:544–560.

Newbold, J. D., J. W. Elwood, R. V. O'Neil, and W. Van Winkle. 1981. Measuring nutrient spiraling in streams. Canadian Journal of Fisheries and Aquatic Sciences 38:860–863.

Newbold, J. D., R. V. O'Neill, J. W. Elwood, and W. Van Winkle. 1982. Nutrient spiraling in streams: implications for nutrient limitation and invertebrate activity. American Naturalist 120:628–652.

Newbold, J. D., T. L. Bott, L. A. Kaplan, C. L. Dow, L. A. Martin, D. J. Van Horn, and A. A. de Long. 2006. Uptake of nutrients in streams in New York City drinking-water-supply watersheds. Journal of the North American Benthological Society 25:998-1017.

Niyogi, D. K., K. S. Simon, and C. R. Townsend. 2004. Land use and stream ecosystem functioning: nutrient uptake in streams that contrast in agricultural development. Archiv für Hydrobiologie 160:471–486.

Odum, E. P. 1985. Trends expected in stressed ecosystems. BioScience 35:419–422.

Palmer, M., E. Bernhardt, E. Chornesky, S. Collins, A. Dobson, C. Duke, B. Gold, R. Jacobson, S. Kingsland, R. Kranz, M. Mappin, M. L. Martinez, F. Micheli, J. Morse, M. Pace, M. Pascual, S. Palumbi, O. J. Reichman, A. Simons, A. Townsend, and M. Turner. 2004. Ecology for a crowded planet. Science 304:1251–1252.

Payn, R. A., J. R. Webster, P. J. Mulholland, H. M. Valett, and W. K. Dodds. 2005. Estimation of stream nutrient uptake from nutrient addition experiments. Limnology and Oceanography: Methods 3:174–182.

Peterson, B. J., W. M. Wollheim, P. J. Mulholland, J. R. Webster, J. L. Meyer, J. L. Tank, E. Marti, W. B. Bowden, H. M. Valett, A. E. Hershey, W. H. McDowell, W. K. Dodds, S. K. Hamilton, S.Gregory, and D. D. Morrall. 2001. Control of nitrogen export from watersheds by headwater streams. Science 292:86–90.

Phillips, P. J., and R. W. Bode. 2004. Pesticides in surface water runoff in south-eastern New York State, USA: seasonal and stormflow effects on concentrations. Pest Management Science 60:531–543.

Phillips, P. J., D. A. Eckhardt, D. A. Freehafer, G. R. Wall, and H. H. Ingleston. 2002. Regional patterns of pesticide concentrations in surface waters of New York in 1997. Journal of the American Water Resources Association 38:731–745.

Rhee, G. Y. 1973. A continuous culture study of phosphate uptake, growth rate and polyphosphate in *Scenedesmus* sp. Journal of Phycology 9:495–506.

Rosemond, A. D., C. M. Pringle, A. Ramírez, M. J. Paul, and J. L. Meyer. 2002. Landscape variation in phosphorus concentration and effects on detritus-based tropical streams. Limnology and Oceanography 47:278–289.

Runkel, R. L., D. M. McKnight, and E. D. Andrews. 1998. Analysis of transient storage subject to unsteady flow: diel flow variation in an Antarctic stream. Journal of the North American Benthological Society 17:143–154.

Senior, P. J., and E. A. Dawes. 1971. Poly-beta-hydroxybutyrate biosynthesis and the regulation of glucose metabolism in *Azotobacter beijerinckii*. Biochemical Journal 125:55–66.

Stream Solute Workshop. 1990. Concepts and methods for assessing solute dynamics in stream ecosystems. Journal of the North American Benthological Society 9:95–119.

Sweeney, B. W., T. L. Bott, J. K. Jackson, L. A. Kaplan, J. D. Newbold, L. J. Standley, W. C. Hession, and R. J. Horwitz. 2004. Riparian deforestation, stream narrowing, and loss of stream ecosystem services. Proceedings of the National Academy of Science of the United States of America 101:14132–14137.

Valett, H. M., C. L. Crenshaw, and P. F. Wagner. 2002. Stream nutrient uptake, forest succession, and biogeochemical theory. Ecology 83:2888–2901.

Valett, H. M., J. A. Morrice, C. N. Dahm, and M. E. Campana. 1996. Parent lithology, surface-groundwater exchange, and nitrate retention in headwater streams. Limnology and Oceanography 41:333–345.

Wallace, J. B., J. R. Webster, and W. R. Woodall. 1977. The role of filter feeders in flowing waters. Archiv für Hydrobiologie 79:506–532.

Webster, J. R., P. J. Mulholland, J. L. Tank, H. M. Valett, W. K. Dodds, B. J. Peterson, W. B. Bowden, C. N. Dahm, S. Findlay, S. V. Gregory, N. B. Grimm, S. K. Hamilton, S. L. Johnson, E. Martí, W. H. McDowell, J. L. Meyer, D. D. Morrall, S. A. Thomas, and W. M. Wollheim. 2003. Factors affecting ammonium uptake in streams – an inter-biome perspective. Freshwater Biology 48:1329–1352.

Webster, J. R., and B. C. Patten. 1979. Effects of watershed perturbation on stream potassium and calcium dynamics. Ecological Monographs 49:51–72.

Whitford, L. A., and G. J. Schumacher. 1961. Effect of current on mineral uptake and respiration by a fresh-water alga. Limnology and Oceanography 6:423–425.

Wollheim, W. M., B. J. Peterson, L. A. Deegan, J. E. Hobbie, B. Hooker, W. B. Bowden, K. J. Edwardson, D. B. Arscott, A. E. Hershey, and J. C. Finlay. 2001. Influence of stream size on ammonium and suspended particulate nitrogen processing. Limnology and Oceanography 46:1–13.

Wright, S. 1934. The method of path coefficients. Annals of Mathematics and Statistics 5:161–215.

Wright, R. T., and J. E. Hobbie. 1965. The uptake of organic solutes in lake water. Limnology and Oceanography 10:22–28.

Table 8.1. Channel and flow characteristics measured during nutrient injections at 17 sites in the New York City drinking-water-supply watersheds. See Figs 2.1 and 2.2 and Tables 2.1 and 2.2 in Chapter 2 for site locations. *Q*= stream low, vw=water velocity, w=stream width, d=stream depth, D=longitudinal dispersion, A_s/A = transient storage ratio where *A*=cross sectional area of the stream and A_s = cross-sectional area of the transient storage zone, and v_{hyd} = hydraulic exchange velocity.

	Site	Year	Q (m^3/s)	v_w (m/s)	w (m)	d (m)	D (m^2/s)	A_s/A	v_{hyd} (mm/s)
Bush Kill	11	2000	0.60	0.21	12.9	0.23	3.99	0.08	0.006
		2001	1.35	0.34	12.2	0.33	5.67	0.11	0.023
		2002	2.98	0.55	13.9	0.39	8.13	0.06	0.030
Cross R.	52	2000	0.16	0.12	8.0	0.17	0.56	0.08	0.009
		2001	0.07	0.07	5.0	0.19	0.21	0.24	0.057
		2002	0.08	0.09	5.5	0.16	0.36	0.18	0.030
		2003	0.34	0.21	8.4	0.19	1.51	0.08	0.016
		2004	0.18	0.13	7.2	0.20	0.40	0.08	0.022
		2005	0.09	0.09	5.51	0.18	0.29	0.20	0.056
E. Br. Delaware R.	10	2003	3.81	0.65	14.9	0.39	4.55	0.20	0.079
		2004	3.37	0.46	16.07	0.46	8.72	0.08	0.028
		2005	0.66	0.18	12.60	0.29	0.82	0.13	0.040
Esopus Cr.	23	2000	1.70	0.33	19.1	0.27	6.06	0.04	0.007
		2001	4.37	0.56	22.8	0.34	2.57	0.12	0.099
		2002	3.16	0.53	20.0	0.30	8.71	0.04	0.010
Haviland Hollow Br.	34	2003	0.42	0.27	7.7	0.20	2.25	0.06	0.010
		2004	0.41	0.24	7.28	0.23	1.60	0.01	0.012
		2005	0.15	0.18	7.19	0.11	1.09	0.07	0.011
Kisco R.	55	2000	0.39	0.17	10.1	0.23	1.28	0.13	0.009
		2001	0.17	0.11	9.4	0.17	0.83	0.19	0.021
		2002	0.10	0.07	8.3	0.18	0.41	0.15	0.014
Middle Br. Croton R.	40	2000	0.25	0.16	8.4	0.19	0.74	0.06	0.007
		2001	0.09	0.09	7.8	0.13	0.50	0.14	0.010
		2002	0.09	0.11	7.3	0.11	0.52	0.08	0.005
Muscoot R., Baldwin	46	2000	0.07	0.10	6.8	0.11	0.45	0.17	0.005
		2001	0.10	0.12	7.6	0.11	1.00	0.65	0.012
		2002	0.03	0.05	6.0	0.11	0.33	0.16	0.006
		2003	0.63	0.31	10.1	0.20	1.99	0.07	0.026
		2004	0.08	0.11	6.7	0.11	0.32	0.13	0.015
		2005	0.16	0.15	8.4	0.13	0.59	0.14	0.019
Muscoot R., Whitehall	139	2003	0.27	2.250	0.4	0.06	7.66	0.01	0.000
		2004	0.89	0.35	10.7	0.24	0.83	0.13	0.253
		2005	1.11	0.36	11.10	0.28	2.56	0.03	0.009
Neversink R.	29	2000	1.91	0.30	23.1	0.27	5.11	0.09	0.055
		2001	0.87	0.21	15.7	0.27	2.38	0.14	0.024
		2002	1.11	0.17	17.1	0.39	1.38	0.14	0.049
		2003	7.67	0.54	24.6	0.58	18.65	0.08	0.029
		2004	3.47	0.34	22.21	0.46	2.95	0.23	0.146
		2005	1.11	0.12	21.53	0.43	0.74	0.13	0.028
Rondout Cr.	30	2000	5.91	0.63	21.6	0.44	11.61	0.02	0.000
		2001	0.39	0.14	14.7	0.19	0.86	0.20	0.017
		2002	0.59	0.19	15.4	0.20	0.96	0.10	0.018

Table 8.1. Continued.

	Site	Year	Q (m^3/s)	v_w (m/s)	w (m)	d (m)	D (m^2/s)	A_s/A	v_{hyd} (mm/s)
Schoharie Cr.	18	2000	0.77	0.16	24.3	0.20	2.42	0.17	0.012
		2001	0.43	0.10	23.7	0.18	0.55	0.25	0.029
		2002	0.23	0.08	19.4	0.15	0.57	0.21	0.017
Titicus R.	130	2003	0.10	0.14	6.6	0.11	0.12	0.23	0.063
		2004	0.25	0.20	8.47	0.15	0.58	0.16	0.068
		2005	0.04	0.08	4.24	0.12	0.02	0.43	0.310
Tremper Kill	15	2003	1.92	0.54	12.1	0.29	5.79	0.07	0.029
		2004	0.78	0.25	11.03	0.28	2.57	0.11	0.045
		2005	0.30	0.12	10.46	0.24	0.74	0.16	0.016
Trout Cr.	9	2003	0.39	0.211	8.0	0.23	1.56	0.22	0.053
		2004	0.67	0.26	7.43	0.35	3.03	0.10	0.040
		2005	0.02	0.04	5.63	0.09	0.10	0.47	0.019
W. Br. Delaware Delhi	5	2000	2.21	0.29	21.7	0.35	1.24	0.20	0.053
		2001	0.87	0.18	19.8	0.24	1.03	0.21	0.031
		2002	2.46	0.26	17.2	0.55	2.38	0.21	0.082
W. Br. Delaware So. Kortright	3	2003	0.67	0.240	11.0	0.26	2.07	0.18	0.043
		2004	1.38	0.39	11.54	0.31	1.15	0.31	0.240
		2005	0.24	0.10	9.98	0.24	0.35	0.25	0.040

Table 8.2. Ambient nutrient concentrations measured just prior to solute injections at 17 sites in the New York City drinking-water-supply watersheds. TDN = total dissolved N, SRP = soluble reactive P, TDP = total dissolved P, nd = no data. Dissolved organic C (DOC) and conductivity were measured at baseflow in the same season but on different dates from the additions. Solute concentrations are in µg/L.

Stream	Date	Analytes								
		NH_4^+-N	NO_3^--N	TDN	SRP	TDP	Glu-cose	Arabi-nose	DOC	Cond. (µS/cm)
Bush Kill	13-Jul-00	9*	98	161	10	13	0.56	0.06*	1360	69
	27-Jun-01	11	156	242	7	11	0.71	0.05*	1040	89
	19-Jun-02	12	91	173	7	12	<0.14	<0.12	1500	71
Cross R	25-Aug-00	6*	224	548	6	9*	1.27	<0.12	2750	264
	10-Oct-01	6*	2*	239	5	9*	8.98	<0.12	3850	297
	11-Sep-02	12	105	360	15	17	2.48	<0.12	3930	283
	2-Jul-03	12	212	481	23	21	0.24	<0.12	4530	251
	16-Jun-04	14	357	604	27	30	0.6	<0.12	3080	293
	22-Jun-05	15	365	593	23	29	0.86	<0.12	3460	276
E. Br Delaware R	16-Oct-03	8*	100	250	9	15	1.75	<0.12	2330	86
	6-Oct-04	7*	208	341	11	12	1.08	<0.12	2480	82
	27-Jul-05	13	123	272	18	21	0.8	0.04*	2320	105
Esopus Cr	19-Oct-00	9*	46	88*	5	5*	1.26	0.05*	851	57
	6-Jun-01	8*	183	257	1*	8*	1	<0.12	752	71
	5-Jun-02	14	92	117	5	5*	1.34	<0.12	1040	60
Haviland Hollow Br	26-Jun-03	20	213	385	4	8*	0.41	<0.12	2880	191
	19-May-04	21	262	425	3	10	0.63	<0.12	2440	151
	18-May-05	12	238	326	3	6*	1.4	<0.12	2420	194
Kisco R	28-Sep-00	21	348	643	19	37	1.01	0.02*	4010	401
	17-Oct-01	5*	206	498	15	22	8.67	0.04*	3000	465
	9-Oct-02	8*	367	657	41	38	10.32	0.04*	2860	556
Middle Br Croton R	20-Sep-00	11	94	524	4	10	3.74	<0.12	4460	459
	24-Oct-01	4*	85	471	5	11	3.35	<0.12	3500	526
	28-Aug-02	13	594	1060	32	34	1.12	<0.12	3990	511
Muscoot R, Baldwin	31-Aug-00	9*	1220	1650	42	50	1.43	<0.12	6340	245
	3-Oct-01	10	994	1440	18	23	2.29	<0.12	2920	634
	25-Sep-02	10	1260	1710	36	48	3.13	<0.12	4200	444
	11-Jun-03	41	403	836	27	29	1.05	<0.12	6040	303
	23-Jun-04	10	1410	1710	39	38	0.5	0.02*	3430	622
	8-Jun-05	28	819	1240	36	36	<0.14	<0.12	4320	623
Muscoot R, Whitehall	16-Jul-03	325	1850	2550	5	16	2.04	<0.12	4700	455
	30-Jun-04	277	1480	2080	2*	7*	0.66	0.08*	4720	514
	25-May-05	401	872	1670	4	11	1.98	0.4	4100	500
Neversink R	12-Oct-00	7*	36	53*	2*	2*	0.97	<0.12	1470	26
	15-Aug-01	8*	191	294	2*	3*	0.39	<0.12	918	34
	7-Aug-02	8*	162	183	2*	5*	1.68	<0.12	1250	30
	12-Nov-03	4*	179	224	2*	4*	0.39	<0.12	1450	27
	11-Aug-04	8*	192	598	2*	11	0.81	0.08*	1590	24
	14-Sep-05	1*	177	235	3	4*	0.7	0.53	1260	33

Table 8.2. Continued.

Stream	Date	Analytes								
		NH_4^+-N	NO_3^--N	TDN	SRP	TDP	Glucose	Arabinose	DOC	Cond. (µS/cm)
Rondout Cr	20-Jul-00	6*	178	254	7	5*	0.63	0.26	852	35
	29-Aug-01	5*	256	287	3	4*	1.36	<0.12	827	42
	25-Jul-02	6*	186	218	4	<10	<0.14	<0.12	1030	38
Schoharie Cr	5-Oct-00	6*	180	220	1*	2*	0.46	0.02*	1510	67
	1-Aug-01	12	62	118	1*	3*	1.31	<0.12	1540	108
	21-Aug-02	8*	22	99*	1*	1*	<0.14	0.04*	1580	107
Titicus R	30-Jul-03	16	560	823	32	39	0.49	<0.12	4690	341
	9-Jun-04	23	629	922	24	30	0.34	<0.12	3310	464
	28-Sep-05	4*	338	528	30	31	1.4	0.04*	3620	373
Tremper Kill	1-Oct-03	1*	216	321	7	10	0.6	<0.12	2040	83
	1-Sep-04	9*	264	392	6	8*	0.64	<0.12	2260	36
	20-Jul-05	11	140	253	9	11	0.95	0.05*	891	68
Trout Cr	13-Aug-03	14	294	419	15	15	1.26	<0.12	1360	113
	18-Aug-04	8*	261	380	10	12	1	0.15	1750	99
	10-Aug-05	12	440	509	2*	8*	1.8	0.29	1010	114
W Br Delaware, S Kortright	28-Aug-03	13	1450	1710	19	23	0.89	<0.12	3150	154
	13-Oct-04	7*	1000	1190	13	12	1.46	<0.12	3850	118
	17-Aug-05	15	1640	1810	14	14	0.96	<0.12	2130	212
W Br Delaware, Delhi	26-Oct-00	14	866	988	20	18	0.67	0.07*	2310	126
	18-Jul-01	17	832	1010	11	15	0.89	<0.12	2160	174
	10-Jul-02	14	1020	1200	17	20	1.41	<0.12	2820	106
Mean		15	371	606	17	24	2.25	0.03	3104	286

Table 8.3. Nutrient uptake velocities estimated from nutrient additions at 17 sites in New York City drinking-water supply watersheds. *=V_f not significantly >0 (p>0.05), – = V_f not estimated.

			Uptake velocity, V_f(mm/s)			
Stream	Site	Date	PO_4^{3-}	NH_4^+	Glucose	Arabinose
Bush Kill	11	13-Jul-00	0.014	0.049	0.047	0.024
		27-Jun-01	0.023	0.077	0.092	0.037
		19-Jun-02	0.023	0.073	0.086	0.026
Cross R.	52	25-Aug-00	0.025	0.056	0.064	0.024
		10-Oct-01	0.011	0.071	0.052	0.014
		11-Sep-02	0.008	0.037	0.030	0.010
		2-Jul-03	0.012	0.052	0.070	0.029
		16-Jun-04	0.014	0.048	0.082	0.021
		22-Jun-05	0.013	0.014	0.031	0.010
E. Br. Delaware R.	10	16-Oct-03	0.021	0.096	0.086	0.024
		6-Oct-04	0.023	0.043	0.048	0.012
		27-Jul-05	0.015	0.059	0.064	0.024
Esopus Cr.	23	19-Oct-00	0.017	0.112	0.077	0.031
		6-Jun-01	0.024	0.062	0.087	0.038
		5-Jun-02	0.023	0.080	0.095	0.029
Haviland Hollow Br.	34	26-Jun-03	0.018	0.036	0.067	0.025
		19-May-04	0.030	0.041	0.082	0.032
		18-May-05	0.017	0.024	0.033	0.014
Kisco R.	55	28-Sep-00	0.002*	0.027	0.031	0.011
		17-Oct-01	0.008	0.038	0.061	0.017
		9-Oct-02	0.014	0.026	0.023	0.014
Middle Br. Croton R.	40	24-Oct-01	0.024	0.072	0.176	0.057
		28-Aug-02	0.010	0.041	0.046	0.014
Muscoot R., Baldwin	46	31-Aug-00	0.014	0.035	0.049	0.017
		3-Oct-01	0.006	0.023	0.040	0.016
		25-Sep-02	0.002*	0.035	0.026	0.021
		11-Jun-03	0.015	0.051	0.136	0.049
		23-Jun-04	0.017	0.035	0.055	0.026
		8-Jun-05	0.018	0.068	0.067	0.032
Muscoot R., Whitehall	139	16-Jul-03	0.014	0.034	0.058	0.016
		30-Jun-04	0.017	0.037	0.057	0.017
		25-May-05	0.029	0.009	0.045	0.016
Neversink R.	29	12-Oct-00	0.019	0.049	0.046	0.018
		15-Aug-01	0.024	0.064	0.052	0.020
		7-Aug-02	0.032	0.072	0.050	0.026
		12-Nov-03	0.039	0.065	0.049	0.020
		11-Aug-04	0.045	0.079	0.071	0.023
		14-Sep-05	0.035	0.085	0.067	0.027
Rondout Cr.	30	20-Jul-00	0.021	–	0.039	0.017
		29-Aug-01	0.028	0.075	0.060	0.013
		25-Jul-02	0.037	0.063	0.046	0.024
Schoharie Cr.	18	5-Oct-00	0.031	0.050	0.028	0.011
		1-Aug-01	0.034	0.076	0.043	0.015
		21-Aug-02	0.024	0.029	0.032	0.009

Table 8.3. Continued.

Stream	Site	Date	Uptake velocity, V_f(mm/s)			
			PO_4^{3-}	NH_4^+	Glucose	Arabinose
Titicus R.	130	30-Jul-03	0.015	0.083	0.047	0.022
		9-Jun-04	0.007*	0.038	0.039	0.024
		28-Sep-05	0.009*	0.038*	0.042	0.044
Tremper Kill	15	1-Oct-03	0.019	0.085	0.097	0.032
		1-Sep-04	0.022	0.050	0.055	0.015
		20-Jul-05	0.027	0.056	0.081	0.032
Trout Cr.	9	13-Aug-03	0.013	0.043	0.051	0.017
		18-Aug-04	0.019	0.050	0.063	0.013
		10-Aug-05	0.010	0.015	0.020	0.007
W. Br. Delaware, South. Kortright	3	28-Aug-03	0.012	0.045	0.056	0.022
		13-Oct-04	0.020	0.059	0.075	0.022
		17-Aug-05	0.017	0.041	0.043	0.015
W. Br. Delaware, Delhi	5	26-Oct-00	0.008	0.049	0.037	0.014
		18-Jul-01	0.005	0.038	0.032	0.011
Mean			0.019	0.052	0.058	0.022

Table 8.4. Pearson correlation coefficients between nutrient uptake velocities (V_f) and measured variables at 17 sites in the New York City drinking-water-supply watersheds. The sample size for all correlations was n=17. Bold font indicates $p < 0.05$. $v_w d$ = specific discharge, A_s/A = transient storage ratio, v_{hyd} = hydraulic exchange velocity, PAR = photosynthetically active radiation, SRP = soluble reactive P, TDP = total dissolved P, TDN = total dissolved N, DOC = dissolved organic C, BDOC = biodegradable DOC, CR_{24} = community respiration, GPP = gross primary production, BOM = periphyton-associated organic matter, HBI = Hilsenhoff Biotic Index, PAH = polyaromatic hydrocarbon, FM = fragrance materials.

	Correlation coefficient with:			
	PO_4^{3-}–V_f	NH_4^+–V_f	Glucose	Arabinose
Stream flow	0.47	**0.75**	0.17	0.11
Water depth	0.41	**0.50**	-0.01	-0.17
Water velocity	0.39	**0.59**	0.30	0.18
$v_w d$	0.44	**0.65**	0.22	0.09
Stream width	**0.53**	**0.54**	-0.17	-0.22
v_{hyd}	-0.23	-0.15	-0.25	-0.01
A_s/A	-0.45	-0.29	**-0.52**	-0.34
log(PAR)	0.45	0.35	-0.05	-0.35
Stream water temperature	-0.12	-0.25	-0.13	-0.04
SRP	**-0.79**	-0.31	-0.06	0.19
TDP	**-0.79**	-0.38	-0.03	0.21
NH_4^+	0.01	-0.43	-0.08	-0.19
NH_4^+ (excluding site 139, Muscoot R, Whitehall)	**-0.66**	**-0.63**	-0.23	0.00
NO_3^-	-0.40	**-0.53**	-0.17	-0.17
TDN	-0.42	**-0.58**	-0.10	-0.11
Glucose	-0.45	-0.41	-0.11	-0.19
Arabinose	0.21	-0.24	-0.28	-0.41
DOC	**-0.57**	**-0.63**	0.01	0.10
BDOC	**-0.56**	**-0.56**	-0.20	-0.15
CR_{24}	**0.50**	**0.52**	0.39	0.30
GPP	0.39	**0.53**	0.23	0.06
Chlorophyll *a* per unit streambed area	-0.10	0.32	0.40	0.22
BOM	-0.43	**-0.81**	-0.22	-0.42
HBI	-0.47	-0.28	-0.30	0.00
species richness/100 individuals	0.45	0.48	0.16	-0.12
log(total PAHs)	**-0.62**	-0.30	-0.13	0.07
log(toxic PAHs)	**-0.68**	-0.35	-0.18	0.08
log(caffeine)	-0.17	-0.47	-0.03	-0.07
log(fragrance materials)	-0.24	-0.39	-0.20	-0.22
log(fecal steroids)	**-0.63**	-0.25	-0.23	-0.26
Watershed-scale arcsin(% forest cover)	**0.79**	**0.72**	0.12	0.08
Watershed-scale population density	**-0.50**	**-0.57**	0.01	0.11
Watershed-scale arcsin(% agricultural land use)	**-0.61**	-0.46	-0.28	-0.31

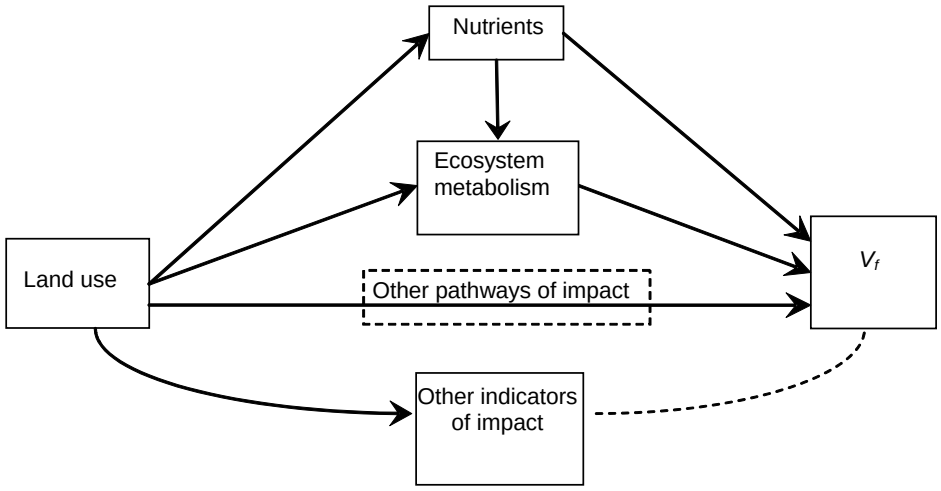

Figure 8.1. Hypothesized links between human activity (land use) and nutrient uptake in the framework of a path analysis.

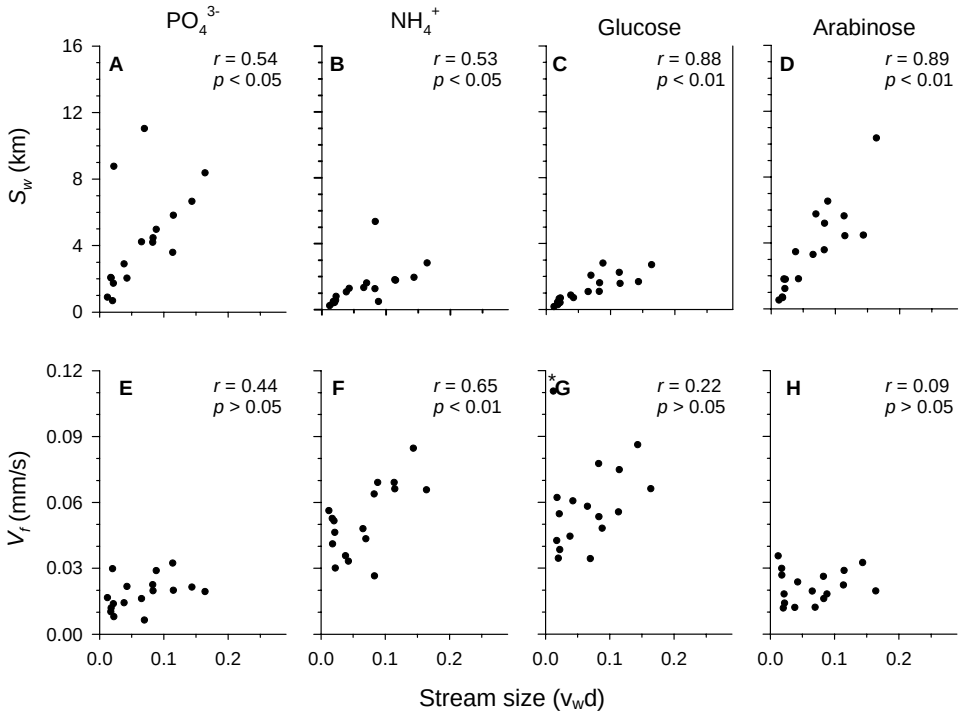

Figure 8.2. Relationships between nutrient uptake lengths (S_w; A–D) and uptake velocities (V_f; E–H) and stream size, expressed as the product of velocity and depth ($v_w d$). The asterisk in panel G indicates a value (0.18 mm/s, 0.012 m^2/s) beyond the range of the vertical axis.

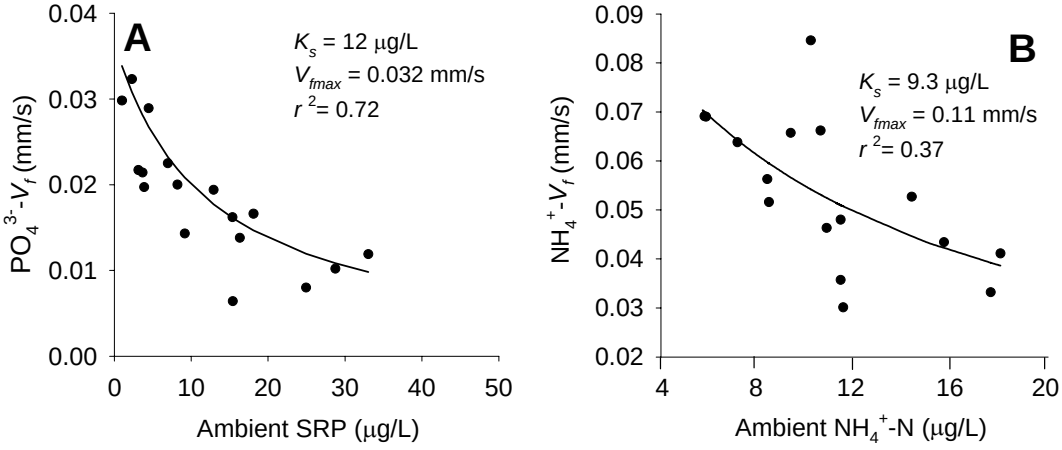

Figure 8.3. PO_4^{3-}-uptake velocity (V_f) as a function of ambient total dissolved P (TDP; A) and NH_4^+-V_f as a function of ambient total dissolved N (TDN; B) concentration. The solid line represents the estimated concentration-specific Michaelis–Menten curve (eq. 3). K_s = half-saturation constant, V_{fmax} = maximum uptake velocity.

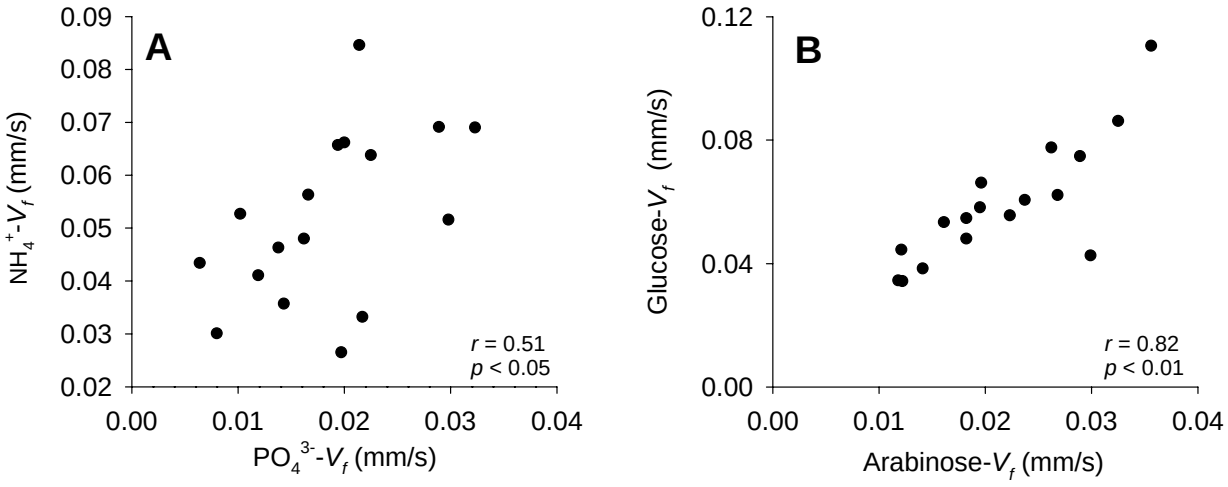

Figure 8.4. Relationships between uptake velocities (V_f) of NH_4^+ and PO_4^{3-} (A) and of glucose and arabinose (B).

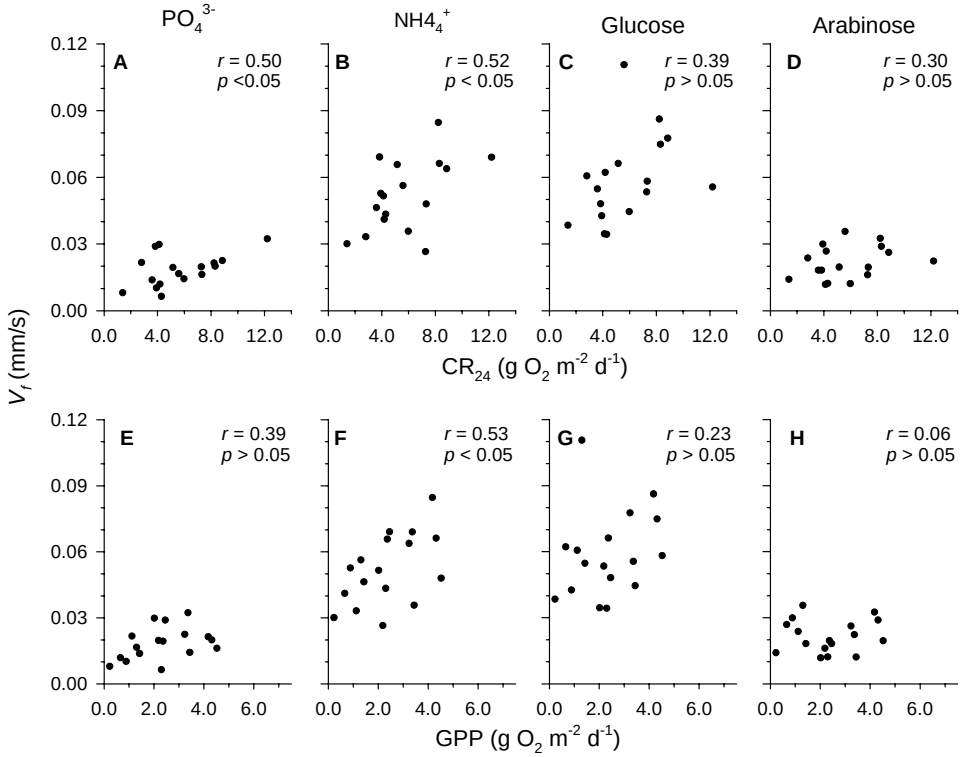

Figure 8.5. Relationships between uptake velocities (V_f) and daily community respiration (CR_{24}; A–D) and gross primary production (GPP; E–H). Correlation coefficients were calculated from individual measurements at each site in each year (n = 26–27).

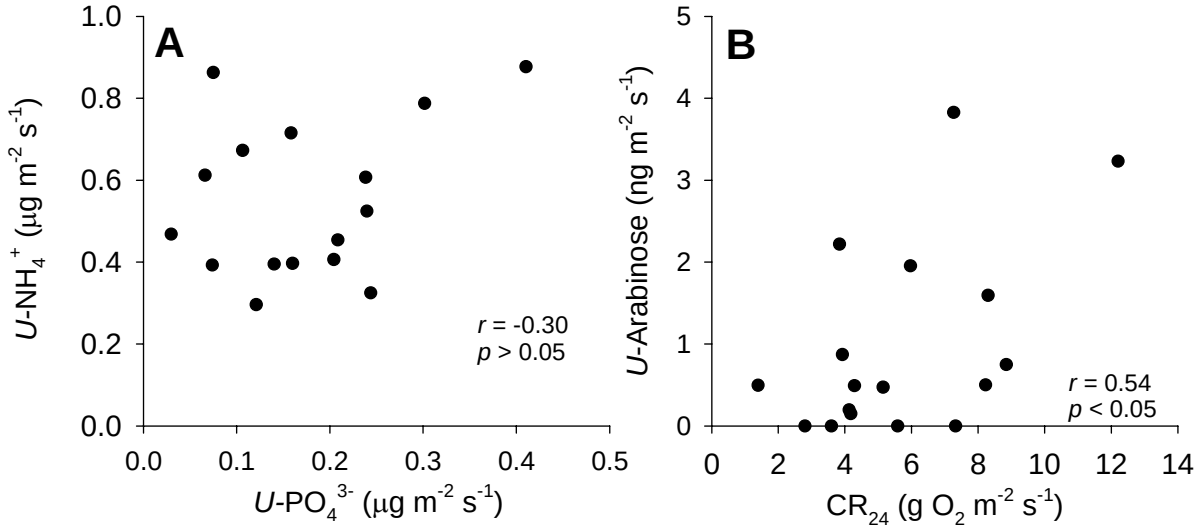

Figure 8.6. Relationships between the uptake fluxes (*U*) of NH_4^+ and PO_4^{3-} (A), and between *U*-Arabinose and community respiration (CR_{24}) (B).

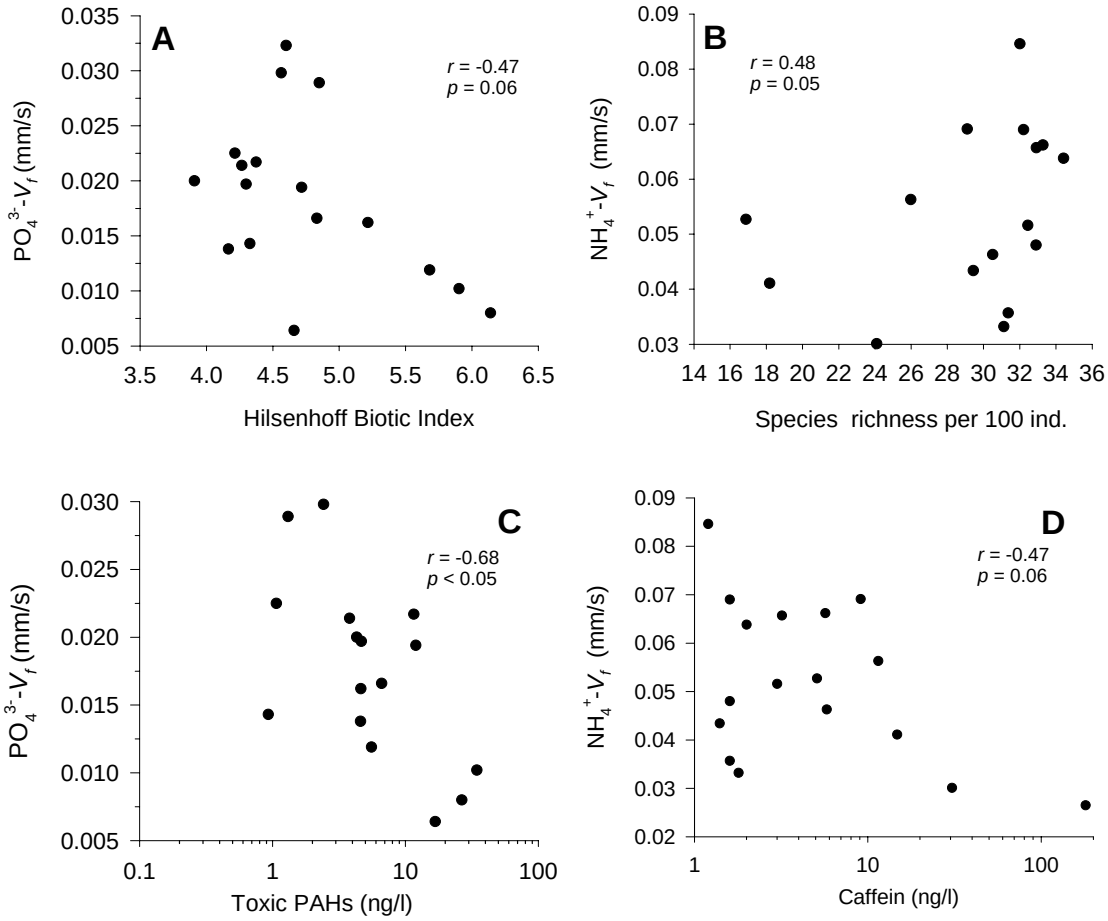

Figure 8.7. Relationships between uptake velocities (V_f) of PO_4^{3-} and NH_4^+ and macroinvertebrate species richness/100 individuals (A, B) and between PO_4^{3-}-V_f and concentrations of toxic polyaromatic hydrocarbons (PAHs) (C), and NH_4^+-V_f and concentrations of caffeine (D). Points represent 3-6 y means. WBRDelaware = West Branch Delaware River, MBRCroton = Main Branch Croton River.

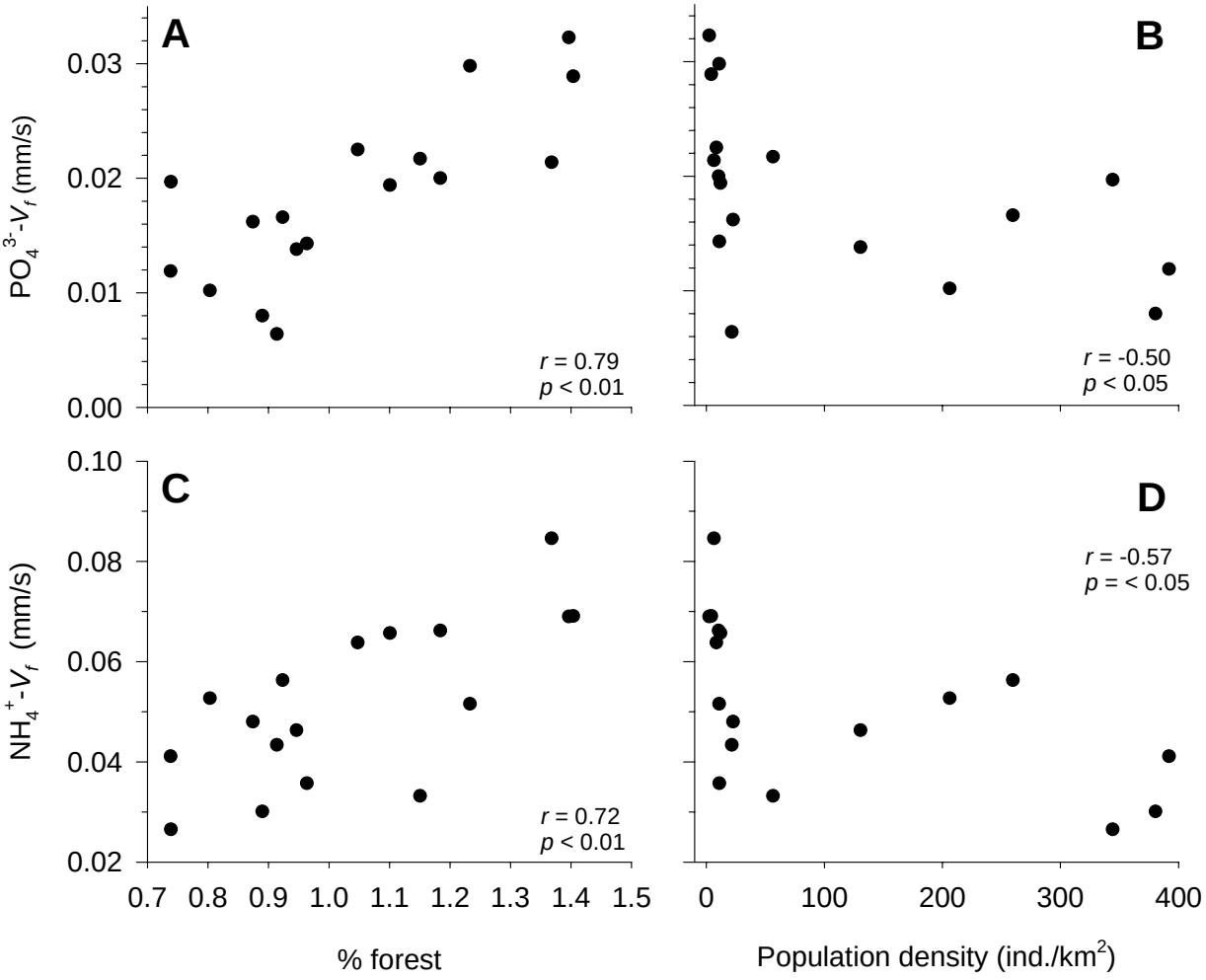

Figure 8.8. Relationships between uptake velocities (V_f) of PO_4^{3-} and watershed-scale % forest cover (A) and population density (B) and NH_4^+-V_f and watershed-scale % forest cover (C) and population density (D). V_fs are 3-y means.

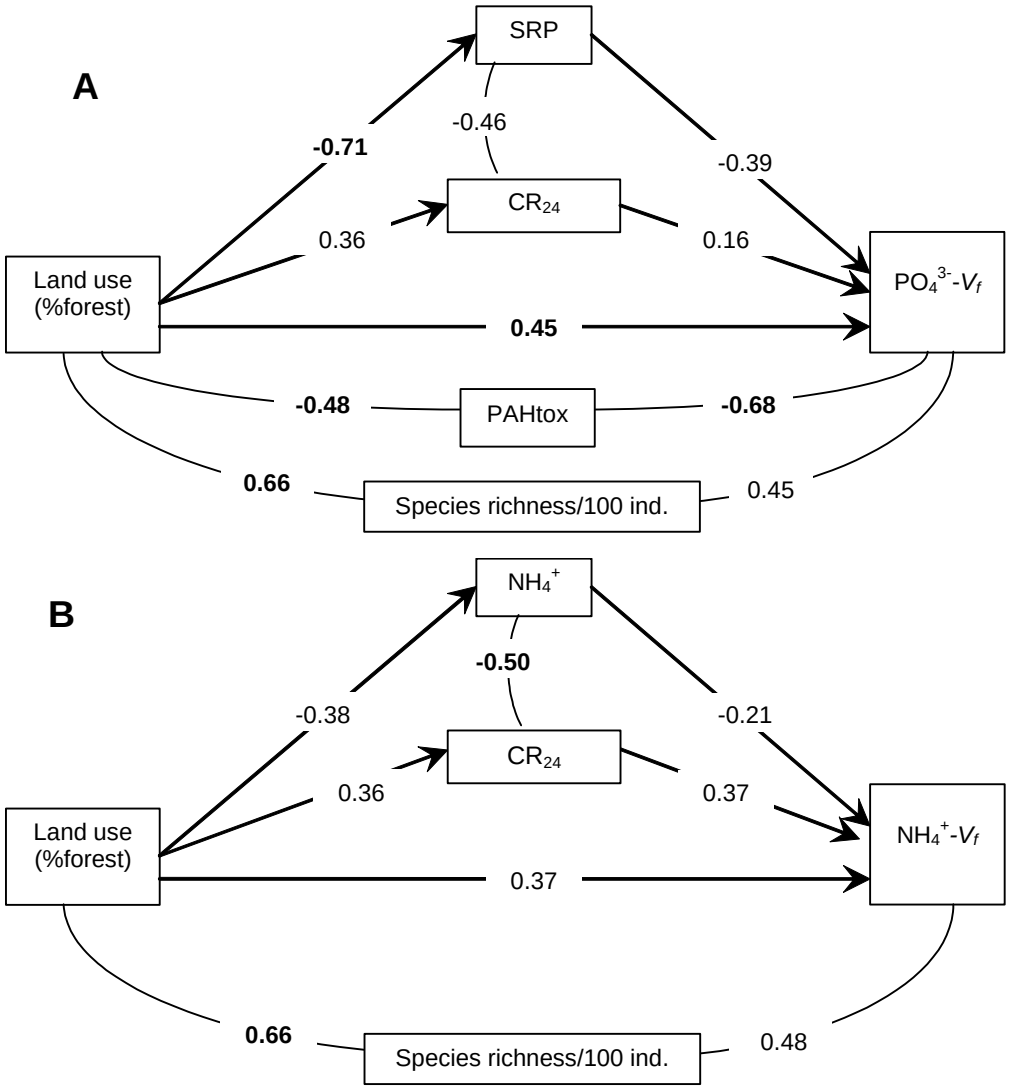

Figure 8.9. Path analysis for effects of land use (represented as % forest cover [%forest]) on PO_4^{3-} uptake velocity (V_f) (A) and on NH_4^+-V_f (B). The path coefficients (associated with solid arrows) represent standardized regression coefficients from the regression of a given (dependent) variable on all of the variables from which an arrow is drawn. Also shown are simple correlation coefficients represented by curves connecting the variables. For simple linear regressions of daily community respiration (CR_{24}) on %forest, and total dissolved P (TDP) or total dissolved N (TDN) on %forest, the path coefficient is the same as the correlation coefficient between the 2 variables. PAHtox = toxic polyaromatic hydrocarbons, HBI = Hilsenhoff Biotic Index.

Chapter 9. Stream Metabolism

Research Task

Ecosystem metabolism was measured at the 17 integrated study sites in order to expand the array of parameters used to assess ecosystem condition. Metabolism measures include the processes of primary productivity and community respiration. Primary productivity is the rate of synthesis of plant biomass and thus indicates the rate of food production occurring within the aquatic ecosystem. Respiration measures the utilization of organic matter and includes the metabolic costs of photosynthesis. These functional measurements complement and augment traditional measures of water quality, e.g., macroinvertebrate community structure and water chemistry. These data aid in the assessment of current status and, since they are the first measures of these functions in these streams, they also provide a baseline against which future measures can be compared. A change in rate of function or in the balance of productivity and respiration over time would suggest a change in stream condition and signal that investigative work on upstream tributaries and the watershed is needed to address causative factors.

Seven streams were studied during Phase I (2000 – 2002) including West Br. Delaware at Delhi (W. Br. Delaware-D), Bush Kill, Schoharie, Esopus, Rondout, Middle Br. Croton and Kisco. During Phase II (2003 – 2005), these were replaced by seven new streams: West Br. Delaware at South Kortright (W. Br. Delaware-SK), Trout Creek, East Br. Delaware, Haviland Hollow, Titicus and Muscoot near Whitehall Corners (Muscoot-WC) (see Chapter 1). Three streams were studied during both phases of work- Cross, Neversink and Muscoot near Baldwin Place (Muscoot-B).

Our specific goals were to rank streams according to the rates of production and respiration occurring in them and to relate those results to the biomasses of organisms involved and environmental correlates such as light, temperature, and nutrients. Benthic algae contributed most plant biomass in these streams, although mosses and macrophytes were found in a few systems. Instream and riparian zone environmental factors were primary controls on metabolism but some of those environmental variables, in turn, are related to watershed land uses and sources of contaminants.

Methods

Field procedures

Metabolism measurements. Ecosystem metabolism was determined using open-system measurements of dissolved O_2 change. Each reach included a top (injection) substation (a point ~ 50 - 175 m upstream of the reach), an upstream sonde substation approximately mid-way through the reach, and a downstream sonde substation, chosen so that conditions affecting reaeration were similar above the upstream and the downstream sondes. YSI model 600XLM sondes with dissolved O_2 probes and internal memory (Yellow Springs Inc., Yellow Springs, OH) were used in years 2 through 5, and YSI model 600XL sondes were coupled with Campbell CR-500 data loggers (Campbell, Logan UT) in year 1. The EPA-approved 600XL and XLM sondes coupled with a rapid pulse dissolved O_2 probe have a manufacturer-certified precision of

0.01 mg/L and an accuracy of ± 0.2 mg/L. Temperature was monitored with a manufacturer-specified precision of 0.01°C and an accuracy of ± 0.15°C.

Five sondes were placed in water-saturated Turkish towels (M. Lizzote, YSI, personal communication) at the field site and calibrated according to the manufacturer's instructions. The sondes then were placed at a single location in the thalweg of the study stream for a 7-12 h comparison prior to deployment for experimental measurements. We compensated for differences between sondes when analyzing data according to the upstream-downstream approach. Two sondes were transferred to the upstream and downstream substations, with pairings based on the similarities of dissolved O_2 concentrations toward the end of the comparison period and probe characteristics (sensor charge and voltage). The fifth was retained for QA/QC (quality assurance/quality control). Dissolved O_2 concentration and water temperature were measured and logged at 15-min. intervals, usually for 3 diel periods. QA/QC checks were made daily by securing that sonde to the stake holding the data sondes and comparing instantaneous readings of dissolved O_2, % saturation, temperature, specific conductance, and sensor charge of the deployed sondes to readings on the QA/QC sonde made with a YSI 650MDS readout meter.

Above-water photosynthetically active radiation (PAR) was measured using two LI 190SA quantum sensors (Li-COR, Lincoln, NE) secured to stakes at both the upstream and downstream substations. PAR was measured every 15 s and 15-min. integrals were logged on a Li-COR 1400 data logger. In 2005, the tree canopy at each study site was photographed at 8 to 12 locations, evenly spaced along each study reach using a digital camera (Nikon Coolpix 995) equipped with a fisheye lens (Nikon FC-E8 28 mm). The camera was positioned 0.67 m above the stream water surface at the center of the stream. Each photograph captured the canopy for a distance of ~25 m.

Reaeration coefficients were determined from a measurement of propane evasion (Marzolf et al. 1994, Young and Huryn 1998, Marzolf et al. 1998) during each 3-d period, performed in conjunction with nutrient spiraling studies. Sampling times for the experiment were set on the day before the experiment by timing the transit of a pulse of rhodamine WT through the study reach. Propane was bubbled into the stream at the injection site through 1.5 m long gas diffuser tubes (Aquatic Eco-Systems, Apopka, FL). A bromide conservative tracer solution was injected simultaneously using a peristaltic pump. The injection site was far enough upstream to ensure mixing of sources and full lateral dispersion at the uppermost sampling substation.

Samples were collected at five substations over the length of the study reach. The entire injection was monitored for bromide at the first substation and at either the fourth or fifth downstream substation, with 5 propane and 5 Br^- samples taken at 2-10-min. intervals when concentrations were at plateau. Propane and Br^- samples were collected at the remaining substations only during the plateau. Field blanks were collected at each substation before start of the injection. A standard curve was prepared by diluting water from the plateau (maximum propane concentration) at the uppermost sampling substation to three lower percentages (50%, 10%, 1%) in site water collected prior to the injection. Br^- samples were collected by filtration through a 0.22µm pore size Millipore Express PES membrane into 125-mL plastic bottles. Propane samples were collected in 73-ml serum bottles that were capped with rubber septa and crimp-sealed in the field. In Year 1, bottles were filled by immersion directly into the stream. In

the remaining years, a bucket was immersed into the stream in an upstream direction and serum bottles were filled by dipping them into the bucket, which minimized turbulence during sampling. Samples were refrigerated during storage.

Open-system metabolism measures include both benthic and water column activity. Water column metabolism was measured separately by filling BOD bottles (6 light and 4 dark) with stream water. Dissolved O_2 concentration, temperature and percent saturation were measured in each bottle using a YSI Model 58 dissolved O_2 meter and probe with stirrer for use with BOD bottles. The bottles were incubated in the stream for 4 - 6 h during which PAR was monitored. After incubation, dissolved O_2 concentration, temperature and % saturation were measured again. Water used for incubation was bubbled with N_2 to lower the percent O_2 saturation to ~ 70 % if values were >85%.

Substratum and plant biomass assessments. Benthic substrata and plant cover types were evaluated together in Year 1 but they were categorized separately thereafter. Twenty transects were set at intervals between the top and bottom sondes. At each transect stream width was measured, and 10 equidistant lateral sampling points were designated. At each point, stream depth was measured and the predominant types of substrata and attached biomass (referred to as "cover type") were assessed using a viewing bucket. Substratum categories followed those of Hynes (1970). Cover types were designated by macroscopic appearance as: filamentous green algae, filamentous diatoms, diatoms (brown velvet appearance), black and green covers (a slime scraped from rocks that appeared either black or green and yielded color when rubbed with a finger), tufts (short filamentous algae, either immature or abraded), and fuzz (silt enmeshed in tufts). Width and depth measurements were also made on additional (8-15) transects between the top sonde and the injection point for use in the computer modeling of solute transport.

Replicate samples (2 – 5) for periphyton chlorophyll *a* and organic matter were collected for cover types constituting ≥10% of encounters during the mapping effort. Soft substrata were sampled by inserting a plastic tube (11.25 cm id) into the streambed and suctioning the enclosed surface sediments with a meat baster. Samples of periphyton on rocks were scraped, brushed and washed into a jar. The planar surface area of the rock was traced onto a piece of paper for quantification using image analysis techniques. Samples were held on ice until return to the laboratory. That evening, samples were centrifuged and recovered pellets were frozen. If supernatant fluids of silt samples remained turbid, the fines were collected on GF/F filters that were subsequently frozen. Nearly all samples were analyzed for chlorophyll *a* within 3 – 4 wk.

Laboratory analyses

Bromide was analyzed by ion chromatography (Model DX-500. Dionex, Sunnyvale, CA; Newbold et al. 2006). For propane analyses, two syringe needles were inserted through the rubber septum and 10 ml of water were displaced by injecting air through into the serum bottle to produce a head space. Bottles were placed on their sides and shaken for 3 h at room temperature to equilibrate propane between the water and head-space. Propane content was determined on 50-µl samples of head-space gas using capillary gas chromatography with flame ionization detection and helium carrier gas (Bott et al. 2006b). Standard curves displayed excellent linearity (R^2 values of 0.96 – 0.99) and tight replication (CV of replicates averaged 7.5% over all concentrations and streams). Propane concentrations at the most downstream substation ranged

between <10 % and ~60% of the first substation values. Absolute concentrations were not critical to assessing reaeration; proportional loss over distance was used to compute the coefficient.

The frozen chlorophyll-containing pellets were thawed and extracted overnight at –20°C in acetone (made basic with $MgCO_3$ or NH_4OH added to the reagent bottle). Following centrifugation (10 - 20 min, ~9,500 x *g*, 4°C) absorbances of the supernatant fluids were determined spectrophotometrically at 665 nm and 750 nm (for turbidity) before and after acidification with 2 drops of 1 N HCl. Extractions were repeated on samples until chlorophyll *a* absorbance was either 10 % of the value for the first extraction or <0.1 absorbance units at 665 nm. Samples were iced and handled under low light during analyses. Chloroplyll concentrations (with correction for pheophytin) were determined using the equation of Lorenzen (1967).

Following extraction, the pellets were dried at 60 °C, weighed, ashed (450°C for 6 h), cooled, and reweighed for an analysis of organic matter content (ash free dry matter, AFDM). The spectrophotometer and Mettler balance were recalibrated at the beginning of the field season.

Rock outlines were digitized and planar surface area was determined using the public domain NIH Image software (developed by the U.S. National Institutes of Health and available on the Internet at hhtp://rsbweb.nih.gov).

Tree canopy photos were processed using Image-Pro Plus 5.0 software. Color photos were segmented to black and white images of (1) sky and (2) tree canopy. The proportion of total area accounted for by the tree category was determined using Image J 1.34 software (public domain available at http://rsb.info.nih.gov/ij/). The canopy values from the 8 –12 photos were averaged to generate a mean % canopy cover for each stream.

Data analyses

Reach chlorophyll estimates. Chlorophyll concentrations were measured for the most important algal cover types. In 2000 these accrued to 89 – 90% of the encounters in all streams but Muscoot-B, Neversink and Cross (65 – 80%). In 2001, chlorophyll data were obtained for >87% of algal encounters in all rivers but the Kisco (> 80%). In 2002, these totaled >91% of the encounters in Esopus, Neversink, Rondout, and Cross rivers; >81% in the Bush Kill, Schoharie, and Muscoot-B; >74% W. Br. Delaware-D and the Kisco rivers; 65% for the Middle Br. Croton. In 2003, chlorophyll concentrations were obtained for 87 – 99% of cover types in Haviland Hollow, Cross, Muscoot-WC, Neversink, Trout and Tremper Kill, but only 74-81% of cover types in Muscoot-B, Titicus, E. Br. Delaware and W. Br. Delaware-SK. In 2004, chlorophyll data were obtained for 89 - 100% of the cover types in all streams. In 2005, the data covered 91 – 99.5 % of cover types for all streams but Cross (82%).

Chlorophyll concentrations were matched with the percentage of total reach area of that cover type to generate a weighted periphyton chlorophyll concentration/m^2. Total chlorophyll values were generated by adding macrophyte (W. Br. Delaware-D) and moss (Rondout, Neversink, Middle Br. Croton, Haviland Hollow, Muscoot-WC, E. Br. Delaware and W. Br. Delaware-SK) chlorophyll to periphyton chlorophyll. The 2002 estimate of macrophyte chlorophyll in the W. Br. Delaware-D was based on chlorophyll concentrations obtained for

macrophytes in 2001 applied to occurrence data collected in 2002. Organic matter data were treated similarly to generate a weighted estimated for each stream reach.

Metabolism estimates. The loss of propane with downstream distance was determined by non-linear regression of the [propane/Br^-] ratio against downstream distance (SAS/STAT, version 9, SAS Institute, Cary, NC) using an exponential model (Wanninkhof et al. 1990). The dilution corrected proportion of propane lost/m was multiplied by water velocity, 1.39 (to correct for molecular size, Rathbun et al. 1978) and 60 (s/min) to generate a K_{O2} (1/min). Water velocity through the reach and mean depth of the reach were derived from the computer modeling of Br^- concentrations using the OTIS-P model (Runkel 1998) as described by Newbold et al. (2006). Reaeration was also computed from geomorphic variables entered into a surface renewal model (SRM; Owens 1974) and an energy dissipation model (Tsivoglou and Neal 1976, APHA et al. 1992), although the latter was not used in further analyses.

Oxygen data usually were analyzed using the 2-station (upstream - downstream) approach (after Owens 1974, Bott 2006) using SAS software. Reaeration coefficients were corrected to streamwater temperature based on Elmore and West (1961). The hourly rate of change of dissolved O_2 concentration (Odum 1956) corrected for reaeration was computed for each 15-min interval over a 24 h diel period. The average hourly rate of community respiration during darkness (defined as PAR <2µmol quanta.m^{-2}.s^{-1}) was extrapolated to 24 h (CR_{24}). Gross Primary Productivity (GPP) was computed by adding respiration during the photoperiod to net oxygen change during the photoperiod. Net daily metabolism was computed as the difference between GPP and CR_{24} (NDM = GPP - CR_{24}) and the P/R ratio as (GPP/CR_{24}). Reaeration coefficients from propane evasion were used for all analyses except that coefficients based on the SRM approach were used for the Esopus, Neversink and W. Br. Delaware-D in 2000. These substitutions presumably introduced little error because GPP data obtained with reaeration estimates from the SRM at other sites that year agreed closely with data obtained with reaeration estimates based on propane evasion (propane/SRM = 0.97 ± 0.66, x ± SD, *n*=16), as did respiration data (propane/SRM = 1.07 ± 0.59, x ± SD, n=14). In 3 instances (Kisco 2000 and 2002, Rondout 2000 and 1 day in 2002 for the Middle Br. Croton), single station analysis was applied to downstream data because the upstream probe failed or exhibited drift in readings.

Water column GPP was computed by adding mean dissolved O_2 change in dark bottles to net O_2 change in each light bottle. The average GPP was compared to whole system metabolism for the corresponding time period, determined by integration of the area under the diel rate of change curve using the overnight respiration rate extrapolated through the daylight hours for a baseline.

Streams were studied between early-June and mid-October with the exception of the Neversink in 2003 when measures were conducted in mid-November because storms interrupted work on numerous streams earlier in the season, causing delays and repeated visits. Neversink 2003 data are shown in figures but were excluded from computations of means and subsequent analyses because of low temperatures (average 5°C). Data for Rondout in 2000 and Kisco in 2002 were handled similarly for the following reasons. Rondout Creek had been severely scoured approximately 1 week prior to the field studies. Approximately 12 h after measurements began, the Kisco experienced an anomalous increase in conductivity of over 80 µS/cm (from ~490 to 570 µS/cm) that lasted for approximately 36 h, followed by a drop of 50 µS/cm to 520

μS/cm, which may have been due to a time-variable unknown discharge upstream of the sampling.

Photosynthesis – irradiation relationships. A photosynthesis-irradiation (PI) curve was prepared for each stream each year by regressing change in dissolved O_2 (photosynthesis, PS) against average PAR (instantaneous light intensity, I) every 15 min as PAR intensity increased from sunrise to mid-day. A hyperbolic tangent function (Jassby and Platt 1976) was fit to the data:

$$PS = \beta' + PS_{max} \times \tanh([\alpha \times PAR]/PS_{max})$$

where α is a constant (initial slope of the regression), β' is analogous to community respiration (used to position the curve correctly in each analysis), and PS_{max} is the maximum rate of photosynthesis in the absence of photoinhibition. In a few instances when photoinhibition was clearly apparent in the data, the data were analyzed using an exponential model with a photoinhibition term (Platt et al. 1980):

$$PS = \beta' + PS_{max} \times (1 - \exp[-\alpha \times PAR/PS_{max}]) \times \exp(-\phi \times PAR/PS_{max})$$

where ϕ is a term describing photoinhibition. Values for PS_{max}, α, and saturation intensity (I_S) were determined. Usually data from all days were combined in a single regression for the year but, in some instances (Rondout 2000; Kisco and Schoharie in 2001; Cross in 2001, 2002 and 2005; Muscoot-B in 2002; Trout in 2003; E. Br. Delaware in 2003 and 2005; Haviland Hollow in 2004; Titicus in 2004; Neversink in 2005; Tremper Kill in 2005) values were obtained from individual daily curves and then averaged, either because the range of intensities varied substantially between days or because different models were used on different days. In addition to data from Rondout (2000) and Kisco (2002) and Neversink (2003), data from the Neversink (2000) and E. Br. Delaware (2004) were excluded from the PI analyses because PAR values at Neversink were extremely low in 2000 and no curve could be fit to the data for E. Br. Delaware in 2004.

GPP was normalized for total daily PAR adjusted for saturation by substituting I_S for each stream and year (from the P-I analyses) for PAR intensities that exceeded I_S, and daily PAR was recomputed ($PAR_{sat\ adj}$). In essence, this procedure excluded surplus radiation above the I_S. Streams were then ranked according to both GPP/PAR and GPP/$PAR_{sat\ adj}$.

Statistical analyses were done using $\log_{10}(x)$-transformed or arcsine$\sqrt{(x)}$-transformed (for %) 3-6 y means with a constant added before transformation when needed. Differences between streams were determined from analyses of variance (ANOVAs) followed by Tukey's tests when ANOVAs were significant ($p \leq 0.05$). Multiple linear regression analyses (MLR) were used to assess the combinations of variables that explained most variance in metabolism variables and biomass. The stepwise forward selection procedure was used (Stat View version 4.02; Abacus Concepts, Berkeley, California) to model biomass or metabolism as a function of instream or riparian (considered local) environmental variables, chlorophyll *a* and biomass (for metabolism regressions), and nutrient-uptake metabolic variables (all specified in Tables 9.3 and 9.7). Measurements of stream metabolism were made concurrently with nutrient-spiraling

experiments, and concentrations of analytes used in data analyses are those reported in Chapter 8, except for total alkalinity and specific conductance (reported in Chapter 3) and biodegradable DOC (BDOC; reported in Chapter 6). Data concerning molecular tracer compounds are reported in Chapter 4. Residuals from each regression were examined for correlations with watershed landscape variables (reported in Chapter 2), selected macroinvertebrate indices of water quality, and selected molecular tracers (again specified in Tables 9.3 and 9.7).

Data preparation for Co-inertia analyses. Data from the 17 sites were averaged over the length of the study (Neversink 2003, Rondout 2000, and Kisco 2002 data were eliminated). Fourteen metabolism-related variables were included in the analysis and included uptake variables (flux and V_f) for glucose, NH_4, and PO_4, GPP, CR_{24}, NDM, chlorophyll *a* (Chl a) and organic matter standing stocks (periphyton and total), and the P/R ratio. Metabolism data were transformed by either log x or [log x + max x] (where max x for CR_{24} or NDM was 1 + maximum value). P/R ratio was not transformed.

Twenty nine environmental variables were selected from a database containing >150 chemical, physical, land use, and invertebrate variables generated by the project. Selection was made using best professional judgment to remove highly correlated, interrelated (hierarchal) variables and greatly reduce the total number of independent variables to a group that was directly relevant to metabolism data. The resulting 29 variables belonged to 3 groups: (1) in-stream or "site" variables (n = 9; % canopy, PAR, mean of mean daily temperatures, flow, water velocity, ΣClaySiltSand, ΣCobbleBoulder, HBI, EPT richness), (2) chemical variables (n = 9; sum of concentrations of the 5 most toxic PAHs, fecal steroids, caffeine, DOC, SRP, TP, glucose, NH_4-N, TN), and (3) land use/cover (n=10; SPDES discharge limits normalized by watershed area, watershed-scale population density, area, road density, % agriculture, % forest, % urban area, and reach-scale road density, % urban, and % agriculture.

Co-Intertia analyses. Three separate Co-inertia analyses (CoI) were conducted, corresponding to the different groupings of the environmental variables (metabolism versus local, chemical, or land use variables). Co-inertia analysis requires that separate PCA computations occur for the metabolism data table and each environmental variable table (local, chemical, and land use). Co-inertia is the statistical process of extracting the covariance between the metabolism PCA and each of the environmental PCA (i.e., 3 separate CoI computations) and projecting that covariance on common axes. Comparing results across CoI is not straight forward, as the analysis does not produce an adjusted R^2 statistic. However, by constraining the number of environmental variables included in each group to be similar and using only the primary factor (Factor 1) the site rankings across the F1 axis for each gradient (i.e., local, chemical, and land use) can be compared to provide statistical insight into possible causal relationships.

Results and Discussion

Habitat characteristics

Physical characteristics of the stream reaches at the time of our studies are presented in Table 9.1. WOH streams were larger than most EOH streams. Trout Creek was the smallest of the WOH streams and Muscoot-WC the largest of EOH streams. Reach lengths varied with

discharge and were longer in wet years than in dry years. For example, reach lengths for all WOH streams in 2005 (a dry year) were half or less of those needed in 2004 (a very wet year), which also was the case for 2 of the EOH streams. WOH streams had more open tree canopies. Canopy density ranged from 45% - 68% at the WOH sites and from 84 – 93% at EOH sites, with the exception of Cross (73%). Thus, PAR intensities were greater in WOH streams than in EOH streams, with the exception of a few high values at the two most open EOH streams, Cross and Muscoot-WC. Most measurements were conducted between early-June and mid-October. Water temperature during 47 of the 60 measurement periods averaged between 13° and 23°C.

Reaeration coefficients (k_t) from propane evasion were in an approximately 10-fold range from average values of 6/d at W. Br. Delaware-D to 60/d (Titicus). Reaeration estimates from propane evasion were unavailable for the Esopus and Neversink in 2000 because of experimental difficulties. While reaeration coefficients (whether at streamwater temperature, k_t, or normalized to 20°C, k_{20}) did not display strong regional bias, the average k_t of EOH sites (38.8 ± 17.3, n= 28) was greater than for WOH sites (22.6 ± 12.1, n=26). Reaeration coefficients were significantly positively correlated with both stream slope ($r = 0.370$, $p = 0.01$) and barometric pressure ($r = 0.741$, $p < 0.001$). Stream slopes were often greater in EOH streams. Given the higher elevations of WOH sites, barometric pressures were lower there (usually 720-730 mm Hg) than at EOH sites (750-760 mm Hg). Reaeration coefficients were all <100/d. McCutchan et al. (1998) noted that metabolism estimates are precise when k_t values are <100/d; k_t values >100/d require high respiration rates in order for data to be reliable.

Five categories of streambed substrata accounted for 95% or more of the substrata encountered in study streams (Fig. 9.1). Cobble made up 50% or more of substrata in WOH streams. The gravel-pebble category was <8% in four WOH streams (Neversink, Rondout, Esopus and Bush Kill) and from 16-23% in the remaining, except for Trout Creek (32%). EOH streams had 11-21% gravel-pebble, except for Middle Br. Croton with 7%. Fine sediments (clay-silt and sand) usually were greater in EOH streams (peaking at 25% and 39% in Kisco and Cross, respectively), and highest percentage WOH was in Trout Creek (16.2%). The boulder-bedrock category was usually greater in EOH streams (20 – 27%, except for Cross with 11%) than in WOH streams (1 - 19% in eight streams, with Esopus and Schoharie the exceptions at 21 and 27%, respectively).

Chlorophyll a, periphyton cover types, macrophyte occurrences and organic mass

Mean periphyton chlorophyll *a* concentrations ranged from 25.5 mg/m^2 (Muscoot-WC) to 98.6 mg/m^2 (W. Br. Delaware-SK) (Fig. 9.2). The greatest concentration EOH occurred at Muscoot-B, with the Middle Br. Croton only slightly lower. Neversink had the lowest concentration among WOH sites, although Trout Creek did not differ appreciably from it. Including macrophyte and moss in the estimates generated total chlorophyll *a* concentrations (numbers in Fig. 9.2) of 145 mg/m^2 for the W. Br. Delaware-D, a 92% increase, and increased concentrations by 76% for Haviland Hollow and 69% for Neversink. Elsewhere, increases ranged only from 1% to 28%. Periphyton chlorophyll *a* differed significantly between streams in an ANOVA ($p = 0.03$), but not in the Tukey test. With mosses and macrophytes included, W. Br. Delaware-D was significantly greater than Kisco (ANOVA, p=0.03 and Tukey test, $p < 0.05$). Macrophytes were most common in W. Br. Delaware, which drained a watershed heavily impacted by agriculture.

Chlorophyll concentrations reflect numerous environmental conditions, the most important of which are discharge, light and nutrient availability, and grazing. Most (61%) streams were sampled 7 or more days after any significant stormflow, and 33% after an extended period (> 14 d) at baseflow. Of the samples collected within 7 d following a storm, the average change in discharge was only 3.3-fold, which usually does not cause significant scour of the streambed. Thus most of our biomass estimates were not seriously compromised by high discharge. The most notable exception was the extremely low concentration for Rondout in 2000; samples were collected approximately 7 d following a 100-y flood. Algae can adapt to low PAR intensity by increasing their chlorophyll content and concentrations in EOH streams, especially Muscoot-B and Middle Br. Croton, were high, possibly for this reason. Titicus and Kisco also had low light intensities but chlorophyll was low in them, perhaps a result of toxic contamination, as is discussed below. Haviland Hollow also had relatively low chlorophyll, even though it had a relatively high macroinvertebrate-based Water Quality Score (WQS). Perhaps macroinvertebrate grazing kept biomass low, but Haviland Hollow also ranked fourth among all streams in concentration of the 5 most toxic PAHs. Muscoot-WC, which is enriched in N from wastewater discharge, did not have greater chlorophyll standing stock among EOH streams. Toxic substances or low concentrations of other nutrients (e.g., phosphorus, silica) may have masked the effect of nitrogen enrichment. Phase II chlorophyll concentrations were relatively similar among EOH streams, but the data for 2001 and 2002, both low-flow years, elevated the mean values for Cross and Muscoot-B (both studied for 6 years). Even though the Neversink also was studied all 6 years, chlorophyll concentrations there did not show the elevation noted in Muscoot-B and Cross during 2001 and 2002, perhaps because it is located WOH.

Algal cover types in each stream are shown in Fig. 9.3. Diatoms predominated (as distinct gold-brown, velvet-like mats or brown filaments) in most WOH streams, contributing an average of 48.8% of cover in W. Br. Delaware-SK, W. Br. Delaware-D, E. Br. Delaware, Bush Kill, Tremper Kill, Schoharie, and Esopus. Diatom cover in Trout, Neversink and Rondout was considerably lower, averaging only 8.5%. Silt occurred to a greater extent in those streams. Silt was included as a cover type because it coated other surfaces and contained diatoms, occasional unicellular chlorophytes, and Cyanobacteria, and thus had measurable chlorophyll. Highest silt cover in EOH streams occurred in Kisco, with only slightly lower occurrence in some other EOH streams. Filamentous algae were more common in W. Br. Delaware-SK, Trout, Neversink and Rondout than in the other WOH streams and infrequent in EOH streams. Moss was most prevalent in Haviland Hollow, Middle Br. Croton and Muscoot-WC, all located EOH. Cyanobacteria were found to an appreciable extent only in Trout, Tremper Kill, Neversink and Haviland Hollow. Trout and Tremper Kill both were agriculturally impacted, and had the highest percentages of cropland and farmsteads in 30 m buffers for a distance 1k upstream of the study reach.

Taxa observed in microscopic examinations of periphyton samples included *Spirogyra* sp. (Schoharie, 2000, 2001), *Ulothrix* sp. (Neversink, 2001), *Cladophora* sp. (Bush Kill, all years, Muscoot-WC, 2005, Titicus 2005) *Cladophora* and *Rhizoclonium* (Rondout, 2001), *Oscillatoria* sp. mats (Neversink, 2002), *Phormidium* sp. (Haviland Hollow 2004, Muscoot-WC 2005), and the diatoms *Rhoicosphenia* sp., *Synedra* sp., and *Nitzschia palea* (Muscoot-WC, 2005). Macrophyte taxa observed included *Callitriche* sp. (Rondout, 2002), *Ranunculus* sp.

(Neversink), *Podostemum* sp., *Ranunculus* sp., and *Potamogeton* sp. (probably *praelongus*) (W. Br. Delaware-D, 2001 and 2002), and *Anacharis* sp. (W. Br. Delaware-D, 2000). Leaf packs were noted in Muscoot, Cross, Neversink, and Kisco when they were studied late in the field season.

Mean organic matter (OM) associated with periphyton in EOH streams ranged from 16.5 g/m^2 to 29.23 g/m^2 except for Titicus (9.03 g/m^2) (Fig. 9.4). EOH streams tended to have greater OM standing crops than WOH streams, where most values were less than 13.6 g/m^2, with Rondout and Trout Creek the exceptions. Differences between streams were non-significant statistically. When OM associated with macrophytes and mosses was included, values increased substantially for Haviland Hollow and W. Br. Delaware-D, but to a lesser extent for the other streams with moss and macrophyte components. Between-stream differences were significant in an ANOVA, p=0.04, but not in a Tukey test.

A [chlorophyll/OM] ratio was computed for each stream with the results shown in Fig. 9.5. WOH streams except for Rondout, Neversink and Trout had higher mean ratios than EOH streams. The ranking of WOH streams suggested that algae dominated periphyton communities in Tremper Kill, Esopus, Schoharie and Neversink to a greater extent than the chlorophyll content alone suggested. This was the case for Titicus as well, but the Kisco had proportionally less algal biomass.

Chlorophyll and organic matter concentrations were examined for individual correlations with environmental and land use variables, molecular tracers, and macroinvertebrate water quality indices. Periphyton chlorophyll *a* standing stock correlated significantly only with % urban land use at the reach scale (Table 9.2). Total chlorophyll concentration was positively correlated with glucose, population density and road density at the watershed scale, and concentrations of the sum of fecal steroids and cholesterol, indicative of positive associations with human influences and wastewater enrichment, and negatively correlated with discharge and watershed area, reflecting the higher concentrations in EOH streams. Total chlorophyll also correlated positively with proportion of fine substrata. Periphyton organic matter showed a positive correlation with glucose and proportion fine substrata, and total organic matter with β-coprostanol (β-COP), a fecal sterol tracer associated with human sewage.

MLR analysis generated a model that explained only ~23% of the variance in periphyton chlorophyll *a* standing stock on the basis of $GPP/PAR_{sat\ adj}$ (Table 9.3) and no equation could be generated for total chlorophyll *a*. The model for periphyton OM standing stock explained 38% of the variance in the data using glucose concentration, and the model for total OM accounted for ~52% of variance using arabinose and $GPP/PAR_{sat.adj}$. Residuals from this model were correlated with β-coprostanol (β-COP). These models were less robust than those generated for Phase I study sites alone (Bott et al. 2006a).

There is no established classification scheme for stream trophic status (eutrophic, mesotrophic or oligotropohic) based on chlorophyll *a* concentrations analogous to the one used for lakes. Dodds et al. (1998) proposed that concentrations of 20 and 70 mg/m^2 might be useful boundaries between oligotrophic-mesotrophic and mesotrophic-eutrophic conditions, respectively. Those concentrations were arrived at by assigning one-third of the values in a large

data set to each category. Accordingly, W. Br. Delaware-SK, Rondout, E. Br. Delaware, and W. Br. Delaware-D would be considered eutrophic, while Bush Kill, Tremper Kill and Muscoot-B lie at the eutrophic-mesotrophic boundary (Fig. 9.2). Note that three other streams were eutrophic during one of the study years. None of the streams would be considered oligotrophic based on mean chlorophyll concentrations, although a few streams had chlorophyll <20 mg/m^2 during one of the study years.

Periphyton chlorophyll *a* standing stocks of 100–150 mg/m^2 were considered indicative of nuisance algal growths by Horner et al. (1983) and Welch et al. (1988). In British Columbia (Nordin 1985) and New Zealand (Zuur 1992), periphyton chlorophyll *a* standing stocks of 50 mg/m^2 were considered protective of recreational uses of streams and standing stocks of 100 mg/m^2 were considered protective of other forms of aquatic life. Biggs (1996) also argued that concentrations > 100 mg/m^2 were at nuisance levels. Using a cut-off of 100 mg/m^2, none of our study streams had a mean chlorophyll concentration at a nuisance level. However, in one or more individual years, the measured chlorophyll standing stock would indicate a nuisance growth in W. Br. Delaware-SK, Rondout, E. Br. Delaware, and Muscoot-B.

Stream Ecosystem metabolism

Mean gross primary productivity (GPP) in WOH streams ranged from 2.015 g $O_2 \cdot m^{-2} \cdot d^{-1}$ (Schoharie) to 4.522 g $O_2 \cdot m^{-2} \cdot d^{-1}$ (W. Br. Delaware-SK, Fig. 9.6). In EOH streams the range was only from 0.227 g $O_2 \cdot m^{-2} \cdot d^{-1}$ (Kisco) to 2.262 g $O_2 \cdot m^{-2} \cdot d^{-1}$ (Muscoot-WC). Mean GPP in WOH streams was significantly greater than in EOH streams (ANOVA, $p<0.001$, df = 16). Presumably, this was largely a response to greater light intensities in WOH streams. GPP in W. Br. Delaware-SK and Neversink was significantly greater than in Titicus, Muscoot-B and Kisco; Bush Kill, Rondout, Trout Creek, Tremper Kill, Esopus, and W. Br. Delaware-D had greater GPP than Muscoot-B and Kisco, and Muscoot-WC, Schoharie, E. Br. Delaware and Cross had significantly more than Kisco (Tukey test, $p=0.05$, df=55).

Water-column metabolism accounted for only a minor percentage (at most 5.9%, with two-thirds of streams <1%) of total ecosystem GPP (Table 9.4). Streams with mean values >2% were Muscoot-WC, Middle Br. Croton, Cross, Kisco (all EOH) and Bush Kill and W. Br. Delaware-D (WOH), but the only stream with water column metabolism >5% during more than one year was W. Br. Delaware-D (7.8% in 2001 and 9.8% in 2002). Thus, ecosystem metabolism is attributed primarily to periphyton activity. Although macrophytes were most common in W. Br. Delaware-D, GPP there was similar to rates in several other streams, at least at the times of our studies. Other studies conducted in the Fort River, MA (Fisher and Carpenter 1976), and the Jackson River, VA (TLB, unpublished data) also indicate that macrophytes contribute less to ecosystem primary productivity than benthic algae.

GPP was significantly negatively correlated with several water-chemistry variables including SKN, TKN, TDP, TP, total alkalinity, specific conductance, DOC, glucose and DON and with the proportion small-sized substrata (Table 9.5). These correlations are consistent with (1) the greater dissolved organic matter and ionic strength in EOH streams (Dow et al. 2006, Chapter 3) and (2) the potential for high rates of photosynthesis to reduce nutrient concentrations. GPP was positively correlated with PAR (and negatively with % canopy) and several indicators of stream size, reflecting the higher rates in WOH streams. GPP correlated positively with other metabolic

variables including community respiration (CR_{24}) and the velocity of P utilization (V_f-P), and negatively with periphyton organic matter (which tended to be greater in EOH streams). GPP was negatively correlated with watershed landscape variables indicative of urbanization, which of course was greater in EOH watersheds (e.g., 2000 population density, % urban land use). While GPP was positively correlated with % forested land use in the watershed, which was greater WOH (Arscott et al. 2006), it was negatively correlated with % forested land use in the riparian buffer for a distance of 1 km upstream of the study reach. This is consistent with the negative correlation with % tree canopy and indicates that algal growth can be reduced by riparian zone management that includes tree planting to increase shade. GPP showed no significant correlations with molecular tracers, but was positively correlated with macroinvertebrate indices of good water quality.

Parameter estimates from photosynthesis-irradiation (P-I) analyses are summarized in Table 9.6. The average maximum rate of photosynthesis (PS_{max}) was significantly greater in WOH than EOH streams (*t*-test, p=0.006, df=15). The initial slope of the P-I curve (α) was greater in EOH streams, although not to a statistically significant extent (*t*-test, p=0.46) and average β' values (analogous to respiration) did not differ between regions (*t*-test, p = 0.25). However photosynthesis saturation intensities were significantly lower in EOH sites than WOH sites (*t*-test, p = 0.01). The greater α values, lower PS_{max} values and lower saturation intensities for periphyton in EOH streams suggest that algae there are adapted to lower PAR intensities resulting from greater shade.

GPP data were normalized for total daily PAR (Fig. 9.7A) and for PAR following adjustment for saturation intensity ($PAR_{sat.adj}$, Fig. 9.7B). Following these adjustments, EOH and WOH streams intermixed when ranked according to either parameter and differences between streams were not statistically significant (ANOVA, p>0.05). Even after adjusting for light, Kisco had the lowest productivity among EOH streams and Titicus ranked highest. Trout shifted to that rank among the WOH streams when normalized for $PAR_{sat.adj}$.

Average daily community respiration (CR_{24}) ranged from 1.39 g $O_2 \cdot m^{-2} \cdot d^{-1}$ (Kisco) to 9.85 g $O_2 \cdot m^{-2} \cdot d^{-1}$ (Neversink, excluding the high value of 24 g $O_2 \cdot m^{-2} \cdot d^{-1}$ for 2003; Fig. 9.8). Respiration rates tended to be higher in WOH streams although two EOH streams ranked among the WOH streams. One was Muscoot-WC, which, as noted above, was impacted by WWTP effluent. The other was Middle Br. Croton, which was studied twice in October. Leaf packs were present at those times and respiration rates were elevated presumably by their decomposition. Although others have shown that hyporheic respiration can contribute substantially to community respiration, the transient storage volume, a measure of the extent of the hyporheic zone, in Middle Br. Croton was not especially large (Newbold et al. 2006). Thus, it is unlikely that hyporheic respiration made a significant contribution to total system respiration there. Respiration rates in WOH streams were significantly greater than in EOH streams (ANOVA, p=0.02, df=16). CR_{24} in Neversink was significantly greater than in Muscoot-B, Cross, Haviland Hollow, and Kisco; CR_{24} in Tremper Kill, Bush Kill, Esopus, Muscoot-WC and W. Br. Delaware-SK was greater than in Kisco (Tukeys test, p=0.05, df=55).

CR_{24} did not correlate with temperature, presumably because most work was done at similar water temperatures. CR_{24} was positively correlated with discharge, depth, and PAR, consistent

with higher rates in WOH streams (Table 9.5), and with V_f-P. CR_{24} was negatively correlated with glucose and total alkalinity, and periphyton and total organic matter, all of which were greater in EOH streams. Although CR_{24} was elevated by nutrients, it correlated negatively with some other indicators of human impact, such as population density and road density, which were greater EOH. It was surprising that CR_{24} was not higher in EOH streams, given that baseflow concentrations of glucose and BDOC tended to be higher there. Like GPP, CR_{24} may have been impaired by toxic pollution in some of the EOH streams.

All systems were on balance, heterotrophic, i.e., mean NDM values were negative and P/R ratios were <1 (Fig. 9.9A and 9B). NDM was positive (and P/R ratios >1) only twice (Rondout in 2001 and Trout Creek in 2005). In Rondout this possibly reflected the clearing of accumulated particulate organic matter from the streambed by the storm scour of 2000, resulting in lower respiration rates. By 2002 metabolism in Rondout was again dominated by respiration, presumably reflecting a build up of detritus in the streambed. Trout Creek was dominated by respiration in 2003 and 2004, but 2005 was a low-flow year and the stream was dammed by farmers into a series of pools. In this instance the greater P/R ratio seems to be the result of lower respiration, because GPP was similar among those years. There were significant differences in NDM between streams (ANOVA, $p = 0.01$), with NDM for the Neversink being significantly more negative than in either Rondout or Cross (Tukeys test, $p = 0.05$).

Even though all systems were heterotrophic, P/R (GPP/CR_{24}) ratios in WOH streams were significantly higher than in EOH streams (ANOVA, $p<0.001$). The highest mean GPP/CR_{24} ratio occurred in Rondout (0.92), and the remaining WOH streams (except for Neversink) had ratios between 0.7 and 0.45. In contrast, the highest ratio for EOH streams was 0.45 and three of them had ratios < 0.2. The P/R ratio for Rondout was significantly greater than the ratio for Titicus, Kisco, Middle Br. Croton and Muscoot-B; Trout Creek and W. Br. Delaware-SK both had ratios significantly greater than the ratios for Middle Br. Croton and Muscoot-B; and ratios for the W. Br. Delaware-D, Bush Kill, and Schoharie were greater than Muscoot-B. The only stream on which we had more than one station was the W. Br. Delaware. NDM at S. Kortright was slightly more negative than at Delhi, perhaps a response to the slightly greater tree canopy density and lower average PAR at S. Kortright (Table 9.1). Overall, energy budgets for these streams were dependent on inputs of allochthonous organic matter, a result that is consistent with data for numerous other streams. However, a heterotrophic status does not mean that algae are unimportant in the food web because macroinvertebrates may preferentially ingest algae over more abundant detrital foods (e.g., Bunn et al. 1999, Finlay et al. 2002, McCutchan and Lewis 2002).

NDM showed no statistically significant individual correlations with environmental, biomass, land cover and population variables or molecular tracers, but GPP/CR_{24} was positively correlated with PAR (negatively with % canopy, Table 9.5). The P/R ratio showed many of the same correlations with chemical and watershed landscape variables, and water quality indices that were shown by GPP (Table 9.5).

Results of MLR analyses of metabolic parameters are shown in Table 9.7. MLR generated a model that explained 93% of the variance in GPP using PAR, V_f-NH_4, background concentration of NO_3-N and V_f-P . Variance in the absolute value of respiration was ~ 95% accounted for on

the basis of PAR, V_f-arabinose, streamwater concentrations of TDN and arabinose, V_f-P and % canopy. The inclusion of PAR in the model (and the significant correlation of CR_{24} with PAR noted above) most likely results from the link between plant (and associated microbial) biomass and PAR which tended to be greater in WOH streams. MLR generated a model that explained ~84% of the variance in NDM on the basis of the uptake flux of arabinose, V_f-glucose, V_f-P, and streamwater concentrations of DON and particulate P. The uptake flux (concentration of solute removed per m^2 streambed per unit time) of arabinose was substituted for the uptake velocity of arabinose because no model was generated when V_f-arabinose was used. A model explaining 88% of the variance in GPP/CR_{24} was generated that included PAR and streamwater concentrations of DON, total N and arabinose. Residuals from the NDM and P/R models were significantly correlated with road density in buffer 1 km upstream of the study reach and % urban in the buffer 1km, respectively (Table 9.7). P/R was the only metabolism-related variable with residual variance that correlated with a molecular tracer, specifically benz[a]anthracene, a compound with chronic toxicity to aquatic life.

As for chlorophyll, there are no criteria for placing streams into trophic categories (eutrophic, oligotrophic, mesotrophic) according to algal productivity, in contrast to the well-established criteria available for lakes. Thus, we developed the following approach to evaluate stream ecosystem conditionon the basis of primary productivity. Metabolism measurements were made on paired meadow and forested reaches in 13 southeastern PA streams with methods identical to those used here in another research program (Bott et al. 2006b). Six of those streams had discharges that were in the range of the streams studied here (albeit at the lower end) and macroinvertebrate community analyses indicated that all of them were in good condition. Reaches differed only in riparian zone management. We determined the coefficient of variation (CV) for GPP, CR_{24}, and P/R data collected between mid-April and October for the forested and meadow reaches of those six streams The CVs for the forested reaches were applied to mean metabolism values of 2 EOH streams in best condition based on macroinvertebrate multimetric index scores (WQS > 8), i.e., Haviland Hollow and Cross. The CVs for meadow reaches were applied to the means of data from four WOH streams with WQS > 8, Trout Cr., E. Br. Delaware, Bush Kill, Tremper Kill. This produced potential ranges for GPP, CR_{24}, and P/R data for streams in good condition in each region. Those ranges are shown as shaded areas in Figs. 9.6, 9.8 and 9.9. GPP in WOH streams fell into the range expected for streams in good condition except for Schoharie, and the E. Branch Delaware was at the low end of the range. Muscoot-WC exceeded the upper bound for EOH streams in good condition, while Muscoot-B and Kisco were lower than that range, and Titicus was borderline (Fig 9.6). Mean values for CR_{24} in WOH streams fell within the range for healthy streams, but Muscoot-WC, Muscoot-B, and Middle Br. Croton exceeded the range for the EOH region and Kisco fell below the range for healthy EOH streams (Fig. 9.8). P/R ratios of all WOH streams fell within the range predicted for healthy streams except for Rondout and Neversink, which exceeded and fell below the range, respectively. EOH streams not falling within the P/R range predicted for healthy streams included the Kisco, Middle Br. Croton and Muscoot-B (Fig. 9.9B).

Of the 17 integrative study sites only 2 had macroinvertebrate multimetric index scores indicative of streams with "moderate" impact (Kisco, Titicus), and most had scores in the ranges indicative of "slight" or "no" impact (Kratzer et al. 2006; Chapter 7). Thus metabolism was not measured in poorest quality streams in the total array of 110. However, based on GPP,

respiration, and the P/R ratio and the range finding approach described above, these functional measures indicated that the Kisco, Middle Br. Croton, Muscoot-B and Muscoot-WC, and perhaps Titicus and Schoharie are streams where further investigation of sources of nutrients and/or toxicity are warranted. Muscoot-B had the highest chlorophyll *a* standing stock among the EOH streams and had high concentrations of most nutrients, but GPP was low. Since GPP/PAR was relatively high in Muscoot-B (Fig. 9.7), its low GPP was attributable in part to low light intensities. Kisco had the 2nd highest concentrations of many nutrients (NO_3-N, SRP, TDP) but ranked lowest in GPP, even after normalization for both PAR and chlorophyll *a* standing stock in 2001, suggesting impairment of metabolic function for other reasons. Titicus is of interest because it ranked highest in GPP/PAR (owing to its low light levels) but also had high concentration of the 5 most toxic PAH (benzo(a)pyrene (BAP), benzo(b)fluoranthene (BBF), benzo(k)fluoranthene (BKF), benzo(a)anthracene (BAA), and chrysene (CHR)).

Impaired function in the Kisco River is probably accounted for by contamination from toxic compounds. Baseflow concentrations of the 5 most toxic PAHs in 2002 were the highest concentrations measured anywhere in the Project (>0.1 µg/L; Aufdenkampe et al. 2006), with the concentration of BAA exceeding the chronic toxicity guidance value (0.03 µg/L) and approaching the acute toxicity value (0.23 µg/L) set by New York State (NYS DEC 1998). Although PAH concentrations there and elsewhere were below those shown to impact algae in laboratory experiments, only a few studies have been conducted, and they were with compounds tested individually (Warshawsky et al. 1995, Halling-Sorensen et al. 1996, Dijkman et al. 1997, Marwood et al. 1999). In our study sites there was the possibility of synergistic effects among these compounds as well as interactions with other potentially toxic substances.

Molecular tracers indicative of sewage contamination (i.e., caffeine, fragrances, and fecal steroids) were high in Kisco (Aufdenkampe et al. 2006) and also in Muscoot-WC, which was downstream of Hallocks Mill tributary, where a failing sewage treatment plant was located. Fecal steroids were also elevated in Muscoot-B and Middle Br. Croton (especially in 2000 and 2002). These tracers are likely to be proxies for unmeasured compounds (e.g., metals, pesticides, herbicides, personal care products, pharmaceuticals) with known toxicity (Kolpin et al. 2002, Glassmeyer et al. 2005). Phillips and Bode (2004) found that concentrations of 4 insecticides (diazinon, carbaryl, malathion, and chlorpyrifos) and the herbicide 2,4-D exceeded guidelines for protection of aquatic life in some Kisco samples, although none violated standards for human health. Highest concentrations (and most exceedences) occurred in stormflow samples (Phillips and Bode 2004). During the limited time when we were actually making measurements in Kisco, we twice observed evidence of significant point-source pulses: 1st with the specific conductance step (490 to 570 µS/cm) during our 2002 metabolism experiment and 2nd during a storm on 8-9 September 2004 (see Fig. 3.7 in chapter 3). Insecticides, herbicides, and fungicides also have been detected in Middle Branch Croton (Phillips and Bode 2002, 2004, Phillips et al. 2002). In other studies, Triclosan (an antimicrobial), Tergitol NP 10 (surfactant), and Ciprofloxacin (antiobiotic) did not alter exponential growth rates of algal communities but did lower final biomass yield and affect community structure in laboratory bioassays at concentrations in the ranges of 0.012-1.2, 0.005 – 0.50, and 0.015 – 1.5 µg/L, respectively (Wilson et al. 2003). Caffeine (at 10 µg/L) increased algal (non significantly) and bacterial (significantly) biomasses in river biofilms (presumably through C and N enrichment), while suppressing (significantly) Cyanobacterial biomass (Lawrence et al. 2005). Furosemide (a diuretic) had a similar effect,

while both ibuprofen (anti-inflammatory) and carbamazepine (anti-convulsant, anti-epileptic) reduced bacterial and Cyanobacterial biomasses and had little or slight increasing effects on green algae in the same study.

Molecular tracer sampling did not coincide with metabolism studies and data suggests that water-column concentrations of potential toxics in Kisco were highly variable in time, but most toxic compounds have high partitioning coefficients (log K_{OW}) and bioaccumulation factors (e.g., log K_{OW} = 6.44 for BAP, BBF, and BKF and log K_{OW} = 5.84 for fluoranthene and CHR; DelVento and Dachs 2002). A contaminant with log K_{OW} between 5 and 7 poses greater risk of bioconcentration or biomagnification than a compound with log K_{OW} <5 (Baird et al. 2001). Thus, these compounds were likely to be at higher and more constant concentrations in the benthos, where their potential effects on stream metabolism would be greatest. Measured concentrations of toxics were not high enough to depress metabolism conclusively, but the sum of stresses imposed by measured compounds and unmeasured toxics, including photodegradation products (Warshawsky et al. 1995, Huang et al. 1997, Marwood et al. 1999) interacting with other environmental variables, certainly could have depressed metabolism.

Among WOH streams, Neversink had fairly low GPP/$PAR_{sat\ adj}$, consistent with its low chlorophyll *a* standing stocks, and Rondout and Bush Kill had higher GPP/$PAR_{sat\ adj}$ values, consistent with relatively high chlorophyll *a* standing stocks. However, W. Br. Delaware-D was anomalous, with high chlorophyll *a* standing stocks but low GPP/$PAR_{sat.adj}$, perhaps because of chemical impacts. Concentrations of the 5 most toxic PAHs were higher in W. Br. Delaware-D than in other WOH streams, and these contaminants may have depressed metabolism. Additionally, concentrations of fecal steroids, which may be proxies for other contaminants, were nearly tenfold higher there than at other WOH sites. Herbicide (atrazine, metolachlor) concentrations in reservoirs receiving drainage from the W. Br. Delaware, E. Br. Delaware (which includes Bush Kill), and Schoharie watersheds where % agricultural land uses were greatest among the study watersheds were higher than in other WOH reservoirs (Phillips et al. 2000). Atrazine was shown to be toxic to algae in laboratory bioassays (Fairchild et al. 1998), although grazing (Muñoz et al. 2001) and light history (Guasch and Sabater 1998) also influenced periphyton susceptibility. Laursen and Carlton (1999) reported depression of microbial respiration, denitrification, and nitrification in stream sediments by exposure to atrazine. While a consideration, the effective atrazine concentrations in these studies were orders of magnitude greater than concentrations reported in New York field sites, and available data are for receiving reservoirs rather than the tributary streams studied here.

Co-Inertia analyses. Initial PCA loadings for each analysis are shown in Table 9.8. The first two factors of the metabolism PCA accounted for 52.8 percent of the among site variability of the 14 metabolism variables and Factors 1 and 2 of each of the environmental PCA's accounted for ~70% of the site variability in 9 or 10 environmental variables. Co-inertia computes a covariance matrix for each pairwise data table comparison (i.e., metabolism versus each of the environmental tables). This covariance matrix is projected on CoI axes and eigenvalues are computed that represent the proportion of the covariance projected on each axis. Table 9.9 presents the covariance projected on either the F1 or F2 axis for each CoI analysis. Note that all CoI analyses resulted in a large amount of the covariance expressed on F1 (71- 85%).

Other statistics define the strength of relationships between PCA Factors generated for metabolism and environment data tables (Table 9.10). For the metabolism versus Site data table the F1 axes were strongly correlated ($r = 0.88$) and a high proportion of the variance loading on each PCA F1 (INER1 and INER2) was re-projected on the F1 Co-inertia axis (Varian1 and Varian2). This strong correlation of PCA F1 axes and high proportion of variance included on the F1 of the CoI axis was similar for all the CoI analysis (i.e., vs. chemical and land use data tables). However, the correlations and variance loadings on the F2 axis was low for the metabolism versus Site Co-inertia analysis compared to the other Co-inertia analyses.

Ultimately it is the arrangement in the 2-dimensional space (typically F1 and F2 axis scores) of sites based on metabolism variables versus sites based on environmental variables that we are interested in interpreting. The Metabolism – Site CoI showed clear separation of EOH and WOH sites (Fig. 9.10). Within the EOH region (left side of figure) the streams also arrayed from the most impaired (Kisco) at the far left to the two best condition sites in the EOH (Haviland Hollow and Cross) located toward the lower right of all EOH sites, and the most enriched EOH site (Muscoot-WC) toward the upper right of all EOH sites. The WOH streams all clustered toward the right of the figure and were arrayed from most forested (top) to agriculturally dominated and otherwise disturbed streams (bottom). In general, environmental and metabolism variables loading near the origin of their respective axes (e.g., V_fP, tot Chl *a*) indicate lesser influence on the overall definition of that axis (i.e., small eigenvectors for those variables). Therefore, the location of sites along each axis should be interpreted in relation to factors loading near the positive and negative ends of each axis. Contributing to the separation on the F1 axes in the Metabolism – Site CoI were HBI value and proportion of fine substrates (clay, silt, sand) as well as shade and discharge, and on the F2 axis - water velocity and temperature. Metabolic variables contributing to stream separation were GPP and CR_{24} (higher WOH), and NH_4 -Upflux and V_f-glucose.

An east-west separation was also apparent in the Metabolism – Chemistry CoI (Fig. 9. 11) and again the more impaired streams arrayed to the left of the better water quality streams in each region, although there was some overlap of EOH good quality streams with WOH poorer quality streams. Toxic PAHs, glucose and DOC concentrations all contributed to this separation, as did GPP, the P/R ratio, and V_f-P. Muscoot-WC separated from the other streams on the F2 axis, presumably because of its high N concentration and caffeine signal (indicative of human contamination).

Lastly, there was distinct east-west separation of sites in the Metabolism – Land Use CoI (Fig. 9.12) with the arrangement within each region similar to that for the Metabolism – Site CoI. Urbanized EOH sites were to the left of the figure, forested sites in the upper right and agriculturally impacted sites (defined based on both the watershed snd the 1 km upstream buffer-scales) in the lower right and the poorer quality sites were arrayed to the left in each group, especially the EOH streams. Separation of sites on the F2 axis was primarily on the basis of chlorophyll *a* concentrations.

Factor loadings from the F1 axis of each CoI analysis (metabolism vs. site, chemistry or land use variables) were combined into one plot in Fig. 9.13. The interpretation of the arrangement in 2-dimensional space of streams based on metabolism variables vs. streams based on

environmental variables and the similarity of position resulting from each CoI analysis are of greatest interest. The average (±1SD; n=3) metabolism CoI score for each site (17 sites) derived from each metabolism versus environment CoI analysis is plotted on the x-axis, along with individual scores. The loadings for metabolism variables for each CoI are expressed on the x-axis above the figure. The lines connect the location of each metabolism variable loading from each separate CoI. The locations of the metabolism loadings along the F1 axis were remarkably consistent among the CoI analyses. The average (±1 SD; n=3) environment CoI score for each site is plotted on the y-axis and the environmental loadings are illustrated on the right-hand side of the figure. The tight linear relationship ($r^2 = 0.80$) between average metabolism scores and environment scores is a consequence of high metabolism-environment correlations in covariance structure of each CoI. Note that EOH sites are located toward the negative end of both X and Y axes where GPP and CR_{24} were lowest and both periphyton organic matter and uptake flux of nutrients were highest. Kisco appears to be an outlier as the most negative site along both the X and Y axes due to high organic matter standing stock and low rates of metabolism. In fact, when the Kisco was removed from the data sest and the analyis was rerun the correlation between average metabolism scores and average environment scores increased to r = 0.912.

Environmental variables associated with the negative y-axis were elevated concentrations of nutrients, toxic PAHs, caffeine, fecal steroids, high % urban, population density, high %fine substrate (ΣCSS – clay, silt, sand), high HBI (Hilsenhoff biotic index of organic pollution), and high % canopy. Reference EOH streams (Haviland Hollow and Cross) were located toward the center of the plot higher on the Y axis than the remaining EOH sites which were perturbed to a greater extent by urban infrastructure. WOH sites had higher GPP, P/R ratio, and CR_{24} and were associated with higher % forest and agriculture, larger catchment areas, high PAR, higher EPT richness, and lower concentrations of nutrients and other chemical variables. WOH sites were distributed from the upper right of the diagram towards the origin and site order along that gradient was related to catchment size, % agriculture in the catchment and in the buffer, and road density in the buffer. Streams with greater % agriculture in the watershed and in the 1-km buffer clustered toward the lower end of WOH streams (West Br. Delaware-SK, West Br. Delaware-D, Trout Creek, E. Br. Delaware, and Tremper Kill, respectively) and those in more heavily forested watersheds at the upper right (Esopus and Neversink, respectively).

Literature Cited

American Public Health Association (APHA). 1992. Standard methods for the examination of water and wastewater. American Public Health Association, Washington.

Arscott, D. B., C. L. Dow and B. W. Sweeney. 2006. Landscape template of New York City's drinking-water-supply watersheds. Journal of the North American Benthological Society 25: 867-886.

Aufdenkampe, A. K., D. B. Arscott, C. L. Dow and L. J. Standley. 2006. Molecular tracers of soot and sewage contamination in streams supplying New York City drinking water. Journal of the North American Benthological Society 25: 928-953.

Baird, D. J., T. C. M. Brock, P. C. deRuit4r, A. B. A. Boxall, J. M. Culp, R. Eldridge, U. Hommen, R. G. Jak, K. A. Kidd, and T. DeWitt. 2001. The food web approach in the environmental management of toxic substances. Pg. 83-122 in D. J. Baird and G. A. Burton (eds). Ecological variability: Separating natural from anthropogenic causes of ecosystem impairment. Society of Environmental toxicology and Chemistry, Pensacola, FL.

Biggs, B. J. F. 1996. Patterns in benthic algae of streams, pp. 31-56. In: R. J. Stevenson, M. L. Bothwell and R. L. Lowe, eds. Algal Ecology, Freshwater Benthic Ecosystems. Academic Press, San Diego.

Bott, T. L. 2006. Primary productivity and community respiration, pp. 663-690. In: F. R. Hauer and G. A. Lamberti, eds. Methods in Stream Ecology, 2nd ed. Elsevier, New York.

Bott, T. L., D. S. Montgomery, D. B. Arscott, J. D. Newbold and C. L. Dow. 2006a. Ecosystem metabolism in streams of the Catskill Mountains (Delaware and Hudson River watersheds) and Lower Hudson Valley. Journal of the North American Benthological Society 25:1018-1044.

Bott, T. L., J. D. Newbold and D. Arscott. 2006b. Ecosystem metabolism in Piedmont streams: Reach geomorphology modulates the influence of riparian vegetation. Ecosystems 9: 398-401.

Bunn S. E., P. M. Davies and T. D. Mosisch. 1999. Ecosystem measures of river health and their response to riparian and catchment degradation. Freshwater Biology 41: 333 - 345.

DelVento, S. and J. Dachs. 2002. Prediction of uptake dynamics of persistent organic pollutants by bacteria and phytoplankton. Environmental Contamination and Toxicology 21: 2099-2107.

Dijkman, N. A., P. L. A. vanVlaardingen and W. A. Admiraal. 1997. Biological variation in sensitivity to n-heterocyclic PAHs; effects of acridine on seven species of micro-algae. Environmental Pollution 1: 121-126.

Dodds, W. K., J. R. Jones, and E. B. Welch. 1998. Suggested classification of stream trophic state: Distributions of temperate stream types by chlorophyll, total nitrogen, and phosphorus. Water Research 32: 1455-1462.

Dow, C. L., D. B. Arscott and J. D. Newbold. 2006. Relating major ions and nutrients to watershed conditions across a mixed-use, water-supply watershed. Journal of the North American Benthological Society 25:887-911.

Elmore H. L. and W. F. West. 1961. Effect of water temperature on stream reaeration. Journal of the Sanitary Engineering Division ASCE 87: 59-71.

Fairchild, J. F., D. S. Ruessler, and A. R. Carlson. 1998. Comparative sensitivity of five species of macrophytes and six species of algae to atrazine, metribuzin, alachlor, and metolachlor. Environmental Toxicology and Chemistry 17: 1830-1834.

Finlay, J. C., S. Khandwala and M. E. Power. 2002. Spatial scales of carbon flow in a river food web. Ecology 83: 1845-1859.

Fisher, S. G. and S. R. Carpenter. 1976. Ecosystem and macrophyte primary production of the Fort River, Massachusetts. Hydrobiologia 47: 175-187.

Glassmeyer, S. T., E. T. Furlong, D. W. Kolpin, J. D. Cahill, S. D. Zaugg, S. L. Werner and M. T. Meyer. 2005. Transport of chemical and microbial compounds from known wastewater discharges: Potential for use as indicators of human fecal contamination. Environmental Science and Technology 39: 5157-5169.

Guash, H. and S. Sabater. 1998. Light history influences the sensitivity to atrazine in periphytic algae. Journal of Phycology 34: 233-241.

Halling-Sorensen, B., N. Nyholm and A. Baun. 1996. Algal toxicity tests with volatile and hazardous compounds in air-tight test flasks with CO_2 enriched headspace. Chemosphere 32: 1513-1526.

Horner, R. R., E. B. Welch and R. B. Veenstra. 1983. Development of nuisance periphytic algae in laboratory streams in relation to enrichment and velocity, pp. 121-134. In R. G. Wetzel, ed. Periphyton of Freshwater Ecosystems. Dr. W. Junk, The Hague.

Huang, X-D., B. J. McConkey, T. S. Babu, and B. M. Greenberg. 1997. Mechanisms of photoinduced toxicity of photomodified anthracene to plants; Inhibition of photosynthesis in the aquatic higher plant *Lemna gibba* (duckweed). Environmental Toxicology and Chemistry 16: 1707-1715.

Hynes, H. B. N. 1970. The ecology of running waters. University of Toronto Press, Toronto.

Jassby AD, and T. Platt. 1976. Mathematical formulation of the relationship between photosynthesis and light for phytoplankton. Limnology and Oceanography 21: 540-547.

Kolpin, D. W., E. T. Furlong, M. T. Meyer, E. M. Thurman, S. D. Zaugg, L. B. Barber and H. T. Buxton. 2002. Pharmaceuticals, hormones and other organic wastewater contaminants in U.S. Streams, 1999-2000. A national reconnaissance. Environmental Science and Technology 36: 1202-1211.

Kratzer, E. B., J. K. Jackson, D. B. Arscott, A. K. Aufdenkampe, C. L. Dow, L. A. Kaplan, J. D. Newbold, and B. W. Sweeney. 2006. Macroinvertebrate distribution in relation to land use and water chemistry in New York City drinking-water-supply watersheds. Journal of the North American Benthological Society 25: 954-976.

Laursen, A. E. and R. G. Carlton. 1999. Responses to atrazine of respiration, nitrification and denitrification in stream sediments measured with oxygen and nitrate microelectrodes. FEMS Microbiology Ecology 29: 229 – 240.

Lawrence, J. R., G. D. W. Swerhone, L. I. Wassenaar and T. R. Neu. 2005. Effects of selected pharmaceuticals on riverine biofilm communities. Canadian Journal of Microbiology 51: 655-669.

Lorenzen, C. J. 1967. Determination of chlorophyll and pheo-pigments: Spectrophotometric equations. Limnology and Oceanography 12: 343-346.

Marwood, C. A., R. E. H. Smith, K. R. Solomon, M. N. Charlton and B. M. Greenberg. 1999. Intact and photomodified polycyclic aromatic hydrocarbons inhibit photosynthesis in natural assemblages of Lake Erie phytoplankton exposed to solar radiation. Ecotoxicology and Environmental Safety 44: 322-327.

Marzolf, E. R., P. J. Mulholland and A. D. Steinman. 1994. Improvements to the diurnal upstream-downstream dissolved oxygen change technique for determining whole-stream metabolism in small streams. Canadian Journal of Fisheries and Aquatic Science 51: 1591-1599.

Marzolf, E. R., P. J. Mulholland and A. D. Steinman. 1998. Reply: Improvements to the diurnal upstream-downstream dissolved oxygen change technique for determining whole-stream metabolism in small streams. Canadian Journal of Fisheries and Aquatic Science. 55: 1786-1787.

McCutchan, J. H., W. M. Lewis, Jr. and E. D. Andrews. 1998. Uncertainty in the estimation of stream metabolism from open-channel oxygen concentrations. Journal of the North American Benthological Society 17:165-178.

McCutchan, J. H. and W. M. Lewis, Jr. 2002. Relative importance of carbon sources for macroinvertebrates in a Rocky Mountain stream. Limnology and Oceanography 47: 742-752.

Muñoz, I., M. Real, H. Gausch, E. Navarro and S. Sabater. 2001. Effects of atrazine on periphyton under grazing pressure. Aquatic Toxicology 55: 239-249.

Newbold, J. D., T. L. Bott and L. A. Kaplan. 2006. Uptake of nutrients and organic C in streams in the New York City drinking-water-supply watersheds. Journal of the North American Benthological Society 25:998-1017.

Nordin, R. N. 1985. Waer quality criteria for nutrients and alage (Technical Appendix.). Water Quality Unit, Resource Quality Section, Water Management Branch British Columbia Ministry for the Environment, Victoria.

NYC DEC (New York State Department of Environmental Conservation). 1998. Ambient water quality standards and guidance values and groundwater effluent limitations. Division of Water Technical and Operational Guidance Series 1.1.1. New York State department of Environmental Conservation, Albany.

Odum, H. T. 1956. Primary production in flowing waters. Limnology and Oceanography 1: 102-117.

Owens, M. 1974. Measurements on non-isolated natural communities in running waters, pp. 111 - 119. In: R.A. Vollenweider (ed). A manual on methods for measuring primary production in aquatic environments. IBP Handbook No. 12, Blackwell Scientific, Oxford.

Phillips, P. J. and R. W. Bode. 2002. Concentrations of pesticides and pesticide degradates in the Croton River Watershed in southeastern New York, July-September 2000. U. S. Geological Survey Water-Resources Investigations Report 02-4063, 20 pp.

Phillips, P. J. and R. W. Bode. 2004. Pesticides in surface water runoff in south-eastern New York State, USA: seasonal and stormflow effects on concentrations. Pest Management Science 60:531-543.

Phillips, P. J., D. A. Eckhardt, D. A. Freehafer, G. R. Wall and H. H. Ingleston. 2002. Regional patterns of pesticide concentrations in surface waters of New York in 1997. Journal of the American Water Works Association 38: 731-745.

Phillips, P. J., D. A. Eckhardt, M. A. Smith and L. Rosemann. 2000. Pesticides and their metabolites in selected surface-water public supplies in New York State, 1999. U. S. Geological Survey Water-Resources Investigations Report 00-44119, 16 pp.

Platt, T., C. L. Gallegos and W. G. Harrison. 1980. Photoinhibition of photosynthesis in natural assemblages of marine phytoplankton. Journal of Marine Research 38: 687-701.

Rathbun, R. E., D. W. Stephens, D. J. Shultz, and D. Y. Tai. 1978. Laboratory studies of gas tracers of reaeration. Journal of Environmental Engineering American Society of Civil Engineers 104: 215-229.

Runkel RL. 1998. One-dimensional transport with inflow and storage (OTIS): A solute transport model for streams and rivers. U. S. Geological Survey Water Resources Investigations Report 98-4018.

Tsivoglou, H.C. and L. A. Neal. 1976. Tracer measurement of reaeration: III. Predicting the reaeration capacity of inland streams. Journal of the Water Pollution Control Federation 489: 2669-2689.

Wanninkhof, R., P. J. Mulholland and J. W. Elwood. 1990. Gas exchange rates for a first-order stream determined with deliberate and natural tracers. Water Resources Research 26: 1621-1630.

Warshawsky, D., T. Cody, M. Radike, R. Reilman, B. Schumann, K. LaDow and J. Schneider. 1995. Biotransformation of benzo[a]pyrene and other polycyclic aromatic hydrocarbon heterocyclic analogs by several green algae and other algal species under gold and white light. Chemico-Biological Interactions 97:131-148.

Welch, E. B., J. M. Jacoby, R. R. Horner and M. R. Seeley. 1988. Nuisance levels of periphytic algae in streams. Hydrobiologia 157: 161 –168.

Wilson, B. A., V. H. Smith, F. Denoyelles, Jr., and C. K. Larive. 2003. Effects of three pharmaceutical and personal care products on natural freshwater algal assemblages. Environmental Science and Technology 37: 1713-1719.

Young, R. G. and A. D. Huryn. 1998. Comment: Improvements to the diurnal upstream-downstream dissolved oxygen change technique for determining whole-stream metabolism in small streams. Canadian Journal of Fisheries and Aquatic Sciences 55: 1784-1785.

Zuur, B. ed. 1992. Water Quality Guidelines No. 1: Guidelines for the control of undesirable biological growths in water. New Zealand Ministry for the Environment, Wellington.

Table 9.1. Pertinent physical characteristics at study streams at times measurements were made.

Stream	Year	Measurement dates	Discharge (m3/s)	Reach Length (Between-sonde distance) (m)	Width (m)	Depth (m)	Velocity (m/s)	Water travel time through reach (min)	Tree canopy closure (%)	Mean daily PAR (mol quanta $m^{-2} d^{-1}$)	Mean Temperature (°C)	Slope (m/km)	Barometric Pressure (mm Hg)	k_{20} (1/d)
W. Br. Delaware-SK	2003	26-28 Aug	0.67	745	10.96	0.26	0.240	51.7	57.12	21.33	17.9	3.4	725.8	22.03
	2004	12-14 Oct	1.38	1,446	11.54	0.31	0.391	61.7		11.94	10.1	3.6	715.1	25.79
	2005	16-18 Aug	0.24	610	9.98	0.24	0.100	103.4		24.04	19.0	3.6	727.8	13.40
W. Br. Delaware-D	2000	26-27 Oct	2.21	1,913	21.71	0.35	0.290	109.9	46.11	17.86	11.7	3.1	.	.
	2001	17-19 Jul	0.87	806	19.76	0.24	0.183	73.6		33.38	21.0	2.2	.	4.44
	2002	9-11 Jul	2.46	1,950	17.22	0.55	0.262	124.2		38.66	20.2	2.2	731.4	7.77
Trout Creek	2003	12-14 Aug	0.39	385	7.97	0.23	0.211	30.4	45.51	21.50	19.8	3.8	733.7	16.27
	2004	17-19 Aug	0.67	865	7.43	0.35	0.256	56.3		27.78	16.8	2.9	735.3	17.74
	2005	9-11 Aug	0.02	184	5.63	0.09	0.039	78.8		35.93	21.6	2.9	738.7	11.39
E. Br. Delaware	2003	14-16 Oct	3.81	1,175	14.92	0.39	0.647	30.3	65.97	8.99	10.4	3.3	725.6	9.78
	2004	5-7 Oct	3.37	1,445	16.07	0.36	0.578	41.6		18.07	10.4	3.3	736.5	13.21
	2005	26-28 Jul	0.66	548	12.60	0.29	0.180	50.7		26.09	22.8	3.3	731.3	16.14
Bush Kill	2000	13-15 Jul	0.60	2,040	12.85	0.23	0.205	165.9	68.35	27.69	16.8	3.4	.	13.24
	2001	26-28 Jun	1.35	2,220	12.20	0.33	0.335	110.3		29.45	17.7	3.8	733.8	30.98
	2002	18-20 Jun	2.98	2,214	13.92	0.39	0.546	67.6		29.41	14.2	4.3	736.2	22.90
Tremper Kill	2003	30Sep-2Oct	1.92	1,202	12.06	0.29	0.540	37.1	61.47	10.20	10.6	5.8	729.5	45.45
	2004	31 Aug-2 Sep	0.78	885	11.03	0.22	0.321	45.9		20.42	17.4	8.0	751.2	24.43
	2005	19-21 Jul	0.30	473	10.46	0.24	0.119	66.1		34.84	21.9	8.0	733.4	21.64
Schoharie	2000	5-6 Oct	0.77	1,275	24.31	0.20	0.155	137.1	49.05	3.12	11.7	3.9	.	36.61
	2001	31 Jul - 2 Aug	0.43	421	23.73	0.18	0.100	69.9		40.33	23.6	5.6	733.0	11.12
	2002	20-22 Aug	0.23	191	19.37	0.15	0.079	40.4		23.13	22.4	6.4	732.5	24.01
Esopus	2000	19-20 Oct	1.70	1,333	19.13	0.27	0.330	67.3	51.46	8.01	9.7	9.8	.	.
	2001	5-7 Jun	4.37	1,438	22.80	0.34	0.562	42.6		38.20	12.9	8.8	737.0	60.92
	2002	4-6 Jun	3.16	1,502	20.02	0.30	0.534	46.9		21.20	13.3	7.4	738.4	57.79
Neversink	2000	12-13 Oct	1.91	1,839	23.14	0.27	0.300	102.17	53.53	20.48	8.6	5.4	.	.
	2001	15-16 Aug	0.87	741	15.69	0.27	0.208	59.5		26.40	17.7	5.2	723.0	25.50
	2002	6-8 Aug	1.11	730	17.10	0.39	0.168	72.6		35.91	17.3	6.6	727.5	22.95
	2003	11-13 Nov	7.67	1,754	24.58	0.58	0.541	54.0		6.08	5.5	6.3	712.9	57.81
	2004	10-11 Aug	3.47	1,591	22.21	0.34	0.463	57.3		20.64	15.5	6.0	721.8	46.15
	2005	13-15 Sep	1.11	847	21.53	0.43	0.119	119.0		27.06	17.5	6.0	728.4	22.45
Rondout	2000	20-21 Jul	5.91	1,457	21.56	0.44	0.630	38.5	65.85	36.68	13.2	4.8	750.0	28.79
	2001	28-30 Aug	0.39	378	14.65	0.19	0.142	44.3		11.23	16.3	5.6	743.6	32.47
	2002	23-25 Jul	0.59	374	15.36	0.20	0.195	32.0		23.67	17.1	7.3	746.9	39.83
Haviland Hollow	2003	24-26 Jun	0.42	610	7.66	0.20	0.271	37.6	89.21	4.81	20.0	10.3	754.7	48.62
	2004	18-20 May	0.41	610	7.28	0.23	0.242	42.0		6.61	17.1	11.0	755.6	61.73
	2005	17-19 May	0.15	606	7.19	0.11	0.182	55.5		14.37	14.3	11.0	753.3	49.96
Middle Br. Croton	2000	21-22 Sep	0.25	500	8.35	0.19	0.160	52.1	89.9	4.98	19.3	10.0	759.0	60.09
	2001	23-24 Oct	0.09	153	7.81	0.13	0.090	28.3		6.74	14.9	11.6	743.5	39.16
	2002	27-29 Aug	0.09	277	7.35	0.11	0.115	40.3		1.63	20.3	8.3	753.8	58.25
Muscoot-B	2000	31Aug-1Sep	0.07	150	6.75	0.11	0.095	26.3	92.58	1.50	20.3	13.3	756.0	38.05
	2001	2-4 Oct	0.10	255	7.59	0.11	0.121	35.0		0.91	13.9	9.5	752.6	27.65
	2002	24-26 Sep	0.03	150	5.95	0.11	0.053	47.5		1.19	15.8	9.5	757.7	22.54
	2003	10-12 Jun	0.63	708	10.06	0.20	0.309	38.2		1.78	18.0	12.3	753.5	63.16
	2004	22-24 Jun	0.08	214	6.74	0.11	0.107	33.4		5.88	18.8	12.3	754.6	41.81
	2005	7-9 Jun	0.16	336	8.40	0.13	0.150	37.2		6.89	21.3	12.3	752.8	41.93
Cross	2000	23-25 Aug	0.16	1,337	7.96	0.17	0.120	185.7	73.36	9.05	17.5	9.0	763.0	25.07
	2001	9-11 Oct	0.07	253	5.04	0.19	0.071	59.1		14.14	9.6	7.8	764.6	16.53
	2002	10-12 Sep	0.08	255	5.53	0.16	0.090	47.0		19.17	17.9	5.6	752.4	18.36
	2003	1-3 Jul	0.34	673	8.39	0.19	0.209	53.6		7.48	20.2	9.9	758.1	37.59
	2004	15-17 Jun	0.18	492	7.18	0.20	0.127	64.5		16.88	20.6	9.2	756.6	33.91
	2005	21-23 Jun	0.09	249	5.51	0.18	0.089	46.8		24.57	18.2	9.2	758.3	20.68
Kisco	2000	28-29 Sep	0.39	398	10.08	0.23	0.169	39.3	93.07	1.55	12.2	2.5	.	23.28
	2001	16-18 Oct	0.17	376	9.38	0.17	0.107	58.4		4.39	11.8	6.2	762.3	14.96
	2002	8-10 Oct	0.10	366	8.25	0.18	0.067	91.0		2.16	12.8	4.5	767.1	11.83
Titicus	2003	29-31 Jul	0.10	327	6.60	0.11	0.136	40.2	94.36	1.84	20.1	8.2	757.9	66.17
	2004	8-10 Jun	0.25	350	8.47	0.15	0.202	28.8		3.10	19.7	13.2	753.7	78.12
	2005	27-28 Sep	0.04	160	4.24	0.12	0.077	34.4		1.02	15.5	13.2	754.8	38.24
Muscoot -WC	2003	15-17 Jul	0.69	1,529	10.23	0.22	0.306	83.3	84.27	18.18	14.2	17.6	758.6	45.78
	2004	29Jun-1Jul	0.89	1,046	10.66	0.24	0.347	50.2		19.37	14.5	7.0	760.7	53.15
	2005	24-26 May	1.11	1,046	11.10	0.28	0.360	48.4		5.60	12.0	7.0	753.4	44.58

Table 9.2. Individual correlations of biomass variables with environmental, population and land cover variables, molecular tracers and macroinvertebrate indicators of water quality. w=watershed scale, 1k= 30m buffer for a 1 km distance upstream of the study reach (i.e. reach scale).

Metabolic Parameter	Environmental Variables	*r*	*p*	Population and Land Cover Variables	*r*	*p*	Molecular tracers and Macroinvertebrate Water Quality Variables	*r*	*p*
Periphyton Chl *a*				% Urban (1k)	0.511	0.035			
Total Chl *a*	Glucose	0.647	0.004	Area (w)	-0.499	0.04	Cholesterol	0.561	0.018
	Discharge	-0.569	0.016	2000 Pop. Density (w)	0.501	0.039	Fecal sterols	0.533	0.026
	Σ clay, silt, sand	0.617	0.007	% Road Density (w)	0.541	0.024			
	Σ cobble, boulder	-0.546	0.022						
Periphyton OM	Glucose	0.503	0.039						
	Σ clay, silt, sand	0.512	0.034						
Total OM							β coprostanol	0.516	0.033

Table 9.3. Multiple linear regression models for weighted periphyton chlorophyll (chl) *a* (mg/m^2) (p=0.03) and organic matter content (OM, g/m2) (p = 0.005), and total OM (g/m2) (p = 0.002), as functions of environmental and metabolic variables. Correlations of residual variances from the MLR analyses ($p < 0.05$) with watershed landscape variables and molecular tracers are shown. β = standardized partial regression coefficient, $GPP/PAR_{sat.adj.}$ = gross primary productivity normalized for total daily photosynthetically active radiation adjusted for saturation intensity, Vf = uptake velocity.

Dependent variable	Coeff.	Independent variable	β	Cumulative adjusted R^2	Correlations of residuals: Parameter	*r*	*p*
log_{10}(periphyton chl *a*)	0.581 1.905	$log_{10}(GPP/PAR_{sat.adj.})$	0.526	0.228			
log_{10}(periphyton OM)	0.449 0.609	log_{10}(glucose)	0.666	0.380			
					β		
log_{10}(total OM)	-0.814	$log_{10}(GPP/PAR_{sat.adj.})$	-0.751	0.247	Coprostanol	0.64	0.005
	-0.116	log_{10}(arabinose)	-0.573	0.519			
	0.862						

log_{10} transformed independent variables used in chlorophyll equations: PAR, temperature, NH_3-N, NO_3-N, TKN, TN, SRP, TDP, TP, total alkalinity, discharge, stream width, water depth, V_f-NH_4, V_f-P, seston particulate P, seston particulate N, $GPP/PAR_{sat.adj.}$, % Canopy, % [Σ Clay, silt, sand], % [Σ Cobble & Boulder].

log_{10} transformed independent variables used in organic matter equations in addition to those used in the chlorophyll equations: DOC, BDOC, glucose, arabinose, DON, V_f-arabinose, V_f-glucose.

Residuals from regressions were tested for correlations with the following parameters (log_{10} or arc sine-sq. root transformed): % agriculture, % forest, % urban, % water, % wetland, population density, population density, road density, and area at the watershed, riparian, and reach scales, as well as wastewater treatment plant (WTP) annual discharge, total no. WTP.

Residuals from regressions were tested for correlations with the geometric means of the following molecular tracers and log_{10} transformed macroinvertebrate indices of water quality: total PAHs, volatile PAHs, soot PAHs, benzo-[a]-pyrene, caffeine, 5B-cholestan-3B-ol (bCOP), fragrances, fecal steroids, benz-[a]-anthracene, benzo-[b]-fluoranthene, benzo-[k]-fluoranthene, chrysene, anthracene, 1-methyl phenol, 2-methyl phenol, cholesterol, and 5 toxic PAHs, 1-methyl phenol, 2-methyl phenol, cholesterol, and 5 toxic PAHs, Water Quality Score, Hillsenhof Biologic Index, EPT richness, total richness.

Table 9.4. Water column metabolism as a fraction of total ecosystem metabolism in study streams.

		Water Column GPP ($g\ O_2 \cdot m^{-2} \cdot h^{-1}$)		Whole Stream GPP ($g\ O_2 \cdot m^{-2} \cdot h^{-1}$)		Water Column GPP / Whole Stream GPP (%)	
Stream	n Years	Mean	SD	Mean	SD	Mean	SD
W. Br. Delaware - SK	3	0.0051	0.0080	0.4748	0.0607	1.08	1.81
W. Br. Delaware - D	3	0.0233	0.0280	0.2820	0.2444	5.91	5.06
Trout Creek	3	0.0002	0.0024	0.3398	0.0622	0.13	0.80
East Br. Delaware	3	0.0034	0.0098	0.1530	0.2123	-3.80	6.54
Bush Kill	3	0.0032	0.0081	0.3923	0.3024	3.49	6.75
Tremper Kill	3	-0.0002	0.0008	0.4011	0.0646	-0.03	0.20
Schoharie	3	0.0004	0.0004	0.2206	0.0921	0.18	0.12
Esopus	3	-0.0023	0.0017	0.4094	0.2404	-0.49	0.21
Neversink	6	0.0009	0.0013	0.3644	0.2186	0.99	2.00
Rondout	2	-0.0004	0.0014	0.3652	0.0723	-0.08	0.37
Haviland Hollow	2	-0.0014	0.0008	0.0878	0.0212	-1.72	1.46
Middle Br. Croton	3	0.0033	0.0033	0.1627	0.1113	3.04	3.11
Muscoot - B	6	0.0001	0.0006	0.0705	0.0237	0.28	1.01
Cross	6	0.0040	0.0094	0.1532	0.0845	4.69	11.34
Kisco	2	0.0004	0.0008	0.0270	0.0268	5.39	8.34
Titicus	2	-0.0002	0.0009	0.0979	0.0694	0.24	1.10
Muscoot - WC	3	0.0041	0.0070	0.2547	0.0726	2.32	3.92

Table 9.5. Correlations of metabolic parameters with environmental, biomass and other metabolic, and population and land cover variables, molecular tracers and macroinvertebrate indices of water quality. Analyses performed on log or arc sine (square root) transformed variables. Periphyton = Peri, Organic matter = OM, watershed scale = w, Riparian scale= b, Reach scale = 1k, Total = Tot., Water quality score = WQS, Hilsenhof Biological Index = HBI.

Metabolic Parameter	Environmental Variables			Biomass and other Metabolic Variables			Population and Land Cover Variables			Molecular tracers and Macroinvertebrate Water Quality Variables		
		r	*p*		*r*	*p*		*r*	*p*		*r*	*p*
GPP	PAR	0.873	<0.001	Peri. OM	-0.54	0.024	Area (w)	0.642	0.004	WQS	0.636	0.005
	% Canopy	-0.820	<0.001	CR_{24}	0.818	<0.001	2000 Pop. Density (w)	-0.795	<0.001	HBI	-0.622	0.006
	Discharge	0.678	0.002	V_f-P	0.52	0.031	% Forest (w)	0.49	0.045	EPT richness	0.66	0.003
	Width	0.52	0.031				% Urban (w)	-0.711	<0.001	Tot. richness	0.606	0.009
	Depth	0.652	0.004				% Road Density (w)	-0.774	<0.001			
	Clay, silt, sand	-0.554	0.02				% Wetland (w)	-0.744	<0.001			
	Soluble Kjeldahl N	-0.559	0.018				Area (b)	0.522	0.03			
	Total Kjeldahl N	-0.547	0.022				2000 Pop. Density (b)	-0.75	<0.001			
	Total dissolved P	-0.524	0.03				% Road Density (b)	-0.546	0.022			
	Total P	-0.512	0.034				% Wetland (b)	-0.762	<0.001			
	Total alkalinity	-0.725	<0.001				% Forest (1k)	-0.491	0.044			
	Sp. Conductivity	-0.731	<0.001									
	DOC	-0.658	0.003									
	Glucose	-0.601	0.009									
	DON	-0.601	0.009									
ER_{24}	PAR	0.602	0.009	Tot. OM	-0.529	0.028	2000 Pop. Density (w)	-0.519	0.032	HBI	-0.539	0.024
	% Canopy	-0.546	0.022	Peri. OM	-0.609	0.008	% Road Density (w)	-0.483	0.049			
	Discharge	0.574	0.014	V_f-P	0.512	0.035	% Wetland (b)	-0.478	0.051			
	Depth	0.504	0.038									
	TA	-0.487	0.046									
	Glucose	-0.497	0.041									
GPP/PAR	Depth	-0.534	0.026							WQS	-0.557	0.019
										Tot. richness	-0.496	0.042
$GPP/PAR_{sat.adj.}$	Glucose	-0.581	0.013	Peri. Chlor. *a*	0.526	0.029	% Urban (1k)	0.553	0.02			
				Tot. OM	-0.542	0.023						
				Peri. OM	-0.546	0.022						
				V_f-NH_4	0.496	0.042						
				Uptake $flux_{Gluc}$	-0.531	0.027						
P/R ratio	PAR	0.801	<0.001				Area (w)	0.565	0.017	WQS	0.603	0.009
	% Canopy	-0.766	<0.001				2000 Pop. Density (w)	-0.729	<0.001	HBI	-0.483	0.049
	Discharge	0.5	0.04				% Forest (w)	0.513	0.034	EPT richness	0.613	0.008
	Depth	0.519	0.031				% Ur(b)an (w)	-0.74	<0.001	Tot. richness	0.651	0.004
	Soluble Kjeldahl N	-0.723	<0.001				Road Density (w)	-0.727	<0.001			
	Total Kjeldahl N	-0.646	0.004				% Wetland (w)	-0.726	<0.001			
	Total dissolved P	-0.549	0.021				% Water (w)	-0.558	0.018			
	Total P	-0.518	0.032				2000 Pop. Density (b)	-0.701	0.001			
	Total alkalinity	-0.633	0.005				% Ur(b)an (b)	-0.586	0.012			
	Sp. Conductivity	-0.668	0.003				Road Density (b)	-0.621	0.007			
	DOC	-0.666	0.003				% Wetland (b)	-0.73	<0.001			
	DON	-0.753	<0.001				% Forest (1k)	-0.547	0.022			

Table 9.6. Parameters derived from analysis of photosynthesis-irradiation relationships. Net oxygen change was analyzed using the hyperbolic tangent model [a] for all stream/year combinations but Cross (2000, 2001, 11Sep2002, 2004), Middle Br. Croton (2002), and Schoharie (2002) for which the exponential model with a photoinhibition term [b] was used.

	n	PS_{max} ($\mu g\ O_2 \cdot m^{-2} \cdot s^{-1}$)		α (g O_2/mol quanta PAR)		β' ($\mu g\ O_2 \cdot m^{-2} \cdot s^{-1}$)		I_S (μmol quanta$\cdot m^{-2} \cdot s^{-1}$)	
Stream	years	Mean	SD	Mean	SD	Mean	SD	Mean	SD
WOH Region									
W. Br. Delaware - SK	3	111.04	11.88	0.704	0.231	-52.89	32.55	171	49
W. Br. Delaware - D	3	67.74	33.78	0.310	0.109	-35.93	10.80	251	164
Trout Creek	3	95.96	13.59	0.252	0.122	-65.69	17.78	467	263
E. Br. Delaware	2	69.39	11.39	0.456	0.126	-48.73	33.85	188	91
Bush Kill	3	73.85	33.87	0.473	0.108	-53.11	22.72	170	105
Tremper Kill	3	79.22	1.06	0.444	0.111	-90.93	50.75	187	62
Schoharie	3	42.88	29.48	0.581	0.381	-29.99	22.91	74	14
Esopus	3	74.33	47.57	0.415	0.271	-57.61	33.18	267	205
Neversink	4	74.42	29.76	0.344	0.152	-97.72	39.81	304	68
Rondout	2	84.72	15.32	0.629	0.177	-23.61	16.58	144	65
EOH Region									
Haviland Hollow	3	22.04	5.87	0.407	0.170	-23.22	11.91	86	49
Middle Br. Croton	3	66.15	27.72	0.661	0.345	-67.89	20.73	106	42
Muscoot - B	6	29.48	17.42	0.794	0.614	-49.07	36.90	55	51
Muscoot - WC	3	85.70	13.17	0.444	0.193	-85.30	4.58	270	228
Cross	6	40.07	22.23	0.595	0.757	-30.97	12.06	151	117
Kisco	2	8.08	5.85	0.153	0.059	-7.92	6.72	49	20
Titicus	3	35.59	10.51	1.370	0.841	-43.78	5.97	30	9
WOH Region Average		**77.36**	**17.99**	**0.46**	**0.14**	**-55.62**	**24.16**	**222.33**	**108.11**
EOH Region Average		**41.02**	**26.57**	**0.63**	**0.38**	**-44.02**	**26.48**	**106.69**	**82.62**

[a] Equation for the hyperbolic tangent model: $PS = \beta + PS_{max} \cdot \tanh[(\alpha \cdot PAR)/PS_{max}]$.

[b] Equation for the exponential model with photoinhibition: $PS = \beta + PS_{max} \cdot [1-\exp(-\alpha \cdot PAR/PS_{max})] \cdot \exp(-\phi \cdot PAR/PS_{max})$ where ϕ is a parameter describing photoinhibition and PSmax is the maximum rate of photosynthesis in the absence of photoinhibition.

Table 9.7. Multiple linear regression models for GPP (p <0.0001), CR_{24} (p = 0. 0005), NDM (p <0.0001), all expressed as g $O_2 \cdot m^{-2} \cdot d^{-1}$, and the GPP/$CR_{24}$ ratio (p <0.0001) as functions of environmental, biological and periphyton biomass variables. Coefficients are given for significant (p<0.05) correlations among residual variances from the MLR analyses and watershed landscape variables and concentrations of molecular tracers. β = standardized partial regression coefficient, PAR = photosynthetically active radiation, V_f = uptake velocity, Peri. OM = weighted organic matter associated with periphyton, DON = dissolved organic N, TN = total N, WTP = wastewater treatment plant, Upflux = uptake flux within stream reach, 1k = reach scale (30m buffer for a distance 1km upstream).

					Correlations of residuals		
Dependent variable	Coeff.	Independent variable	β	Cumulative adjusted R^2	Parameter	*r*	*p*
$\log_{10}$(GPP)	0.755	$\log_{10}$(PAR)	0.826	0.747			
	0.841	$\log_{10}$(V_f -NH_4)	0.359	0.810			
	0.356	$\log_{10}$(NO_3-N)	0.387	0.879			
	0.402	$\log_{10}$(V_f -P)	0.264	0.934			
	1.434	Intercept					
$\log_{10}$([CR_{24}])	0.205	$\log_{10}$(PAR)	0.370	0.362			
	0.957	$\log_{10}$(V_f -arabinose)	0.639	0.620			
	0.315	$\log_{10}$(TDN)	0.518	0.691			
	0.957	$\log_{10}$(arabinose)	0.358	0.774			
	0.430	$\log_{10}$(V_f -P)	0.467	0.887			
	-0.817	$\log_{10}$(% canopy)	-0.433	0.946			
	4.512	Intercept					
$\log_{10}$(NDM + 8)	-0.088	$\log_{10}$(Up flux-arabinose)	-0.463	0.169	Road density (1k)	0.557	0.02
	-0.794	$\log_{10}$(V_f -glucose)	-0.518	0.409			
	-0.331	$\log_{10}$(V_f -P)	-0.441	0.537			
	-0.446	$\log_{10}$(DON)	-0.916	0.736			
	0.225	$\log_{10}$(particulate P)	0.655	0.836			
	-0.991	Intercept					
$\log_{10}$(GPP/CR_{24})	0.321	$\log_{10}$(PAR)	0.566	0.618	% Urban (1k)	0.500	0.04
	-0.501	$\log_{10}$(DON)	-0.817	0.715	Benz[a]anthracene	0.519	0.03
	0.319	$\log_{10}$(TN)	0.499	0.830			
	-0.055	$\log_{10}$(arabinose)	-0.233	0.881			
	-1.163	Intercept					

$\log_{10}$ transformed independent variables used in GPP equations: PAR, % canopy, temperature, NH_3-N, NO_3-N, SKN, TKN, SRP, TDP, TP, total alkalinity, total dissolved N, DON, discharge, stream width, water depth, V_f-NH_3, V_f-P, periphyton chlorophyll *a*, total chlorophyll *a*, periphyton organic matter, total organic matter, seston particulate P, seston particulate N, Σ [clay,silt,sand], Σ [cobble, boulder].

$\log_{10}$ transformed independent variables used in CR_{24} equation: Same as for GPP plus DOC, BDOC, glucose, arabinose, V_f - glucose and V_f-arabinose.

$\log_{10}$ transformed independent variables used in NDM and P/R equations: PAR, % canopy, temperature, NH_3-N, NO_3-N, SKN, TKN, TN, SRP, TDP, TP, total alkalinity, glucose, BDOC, DOC, arabinose, DON, water velocity, discharge, stream width, water depth, Vf NH3, Vf SRP, Vf glucose, Vf arabinose, periphyton chlorophyll a, total chlorophyll a, periphyton organic matter, total organic matter, seston particulate P, seston particulate N, S [clay,silt,sand], S [cobble, boulder].

Residuals from regressions were tested for correlations with the following watershed parameters ($\log_{10}$ or arc sine[square root] transformed as appropriate): % agriculture, % forest, % urban, population density and road density at the watershed, riparian, and reach scales, watershed area, conductivity, wastewater treatment plant (WTP) annual discharge, no. WTP in watershed, water quality score, total and EPT richness.

Residuals from regressions were tested for correlations with geometric means of the following tracers: total PAHs, volatile PAHs, soot PAHs, benzo-[a]-pyrene, caffeine, 5B-cholestan-3B-ol (bCOP), fragrances, fecal steroids, benz[a]anthracene, benzo[b]fluoranthene, benzo[k]fluoranthene, chrysene, cholesterol, Σ [5 toxic PAHs], HHCB and AHTN, 1-methyl phenanthrene, 2-methyl phenanthrene.

Table 9.8. Inertia loading on Principal Components Analysis Factors 1 and 2 and cumulative (F1+2) for metabolism, site, chemistry, and land use datasets.

PCA	F1	F2	F1-F2 Cumulative
Metabolism	34.01	18.79	52.8
Site	51.11	21.63	72.74
Chemistry	49.29	21.51	70.8
Land use	44.68	26.3	70.98

Table 9.9. Proportion of covariance projected on F1 and F2 and Cumulative F1+F2 for each Co-inertia analysis

Co-Inertia Analysis	F1	F2	Cumulative F1+2
Metabolism-Site	85.33	6.21	91.54
Metabolism-Chemistry	71.04	17.27	88.31
Metabolism-Land Use	78.89	12.16	91.05

Table 9.10. Co-inertia (CoI) statistics for each analysis (3 analyses). CoI axis is either axis 1 or 2 for each CoI analysis. Covariance is covariance between PCAs expressed on that CoI axis. Varian1 is the new (CoI) variance from site, chemistry, or land use PCA expressed on that CoI axis. Varian2 is the new (CoI) variance from metabolism PCA expressed on that CoI axis. Correlation is the correlation coefficient between new CoI scores for sites based on metabolism and site scores based on site, chemistry, or land use variables. INER1 is the original eigenvalue/inertia from site, chemistry, or land use PCA. INER2 is the original eigenvalue/inertia from metabolism PCA.

Co-Inertia Analysis	Co-Inertia axis	Covariance	Varian1	Varian2	Correlation	INER 1	INER 2
Metabolism-Site	1	3.884	4.515	4.353	0.876	4.599	4.764
	2	1.048	1.675	1.665	0.628	1.947	2.631
Metabolism-Chemistry	1	3.558	4.306	3.913	0.867	4.436	4.764
	2	1.754	1.924	2.042	0.885	1.937	2.631
Metabolism-Land Use	1	3.736	4.372	4.219	0.870	4.468	4.764
	2	1.467	2.082	1.946	0.729	2.63	2.631

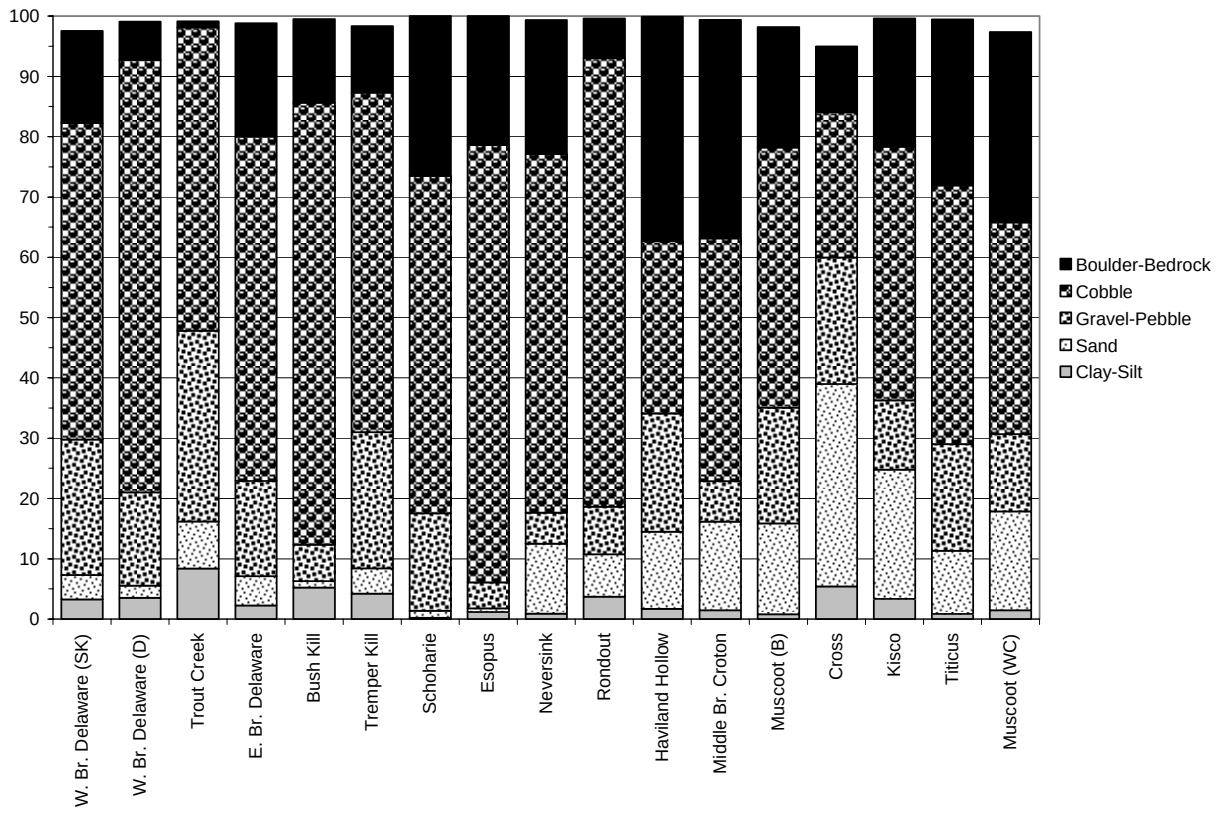

Figure 9.1. Occurrence of substrata in study streams. Data shown are means of 2 or 5 years of measurement.

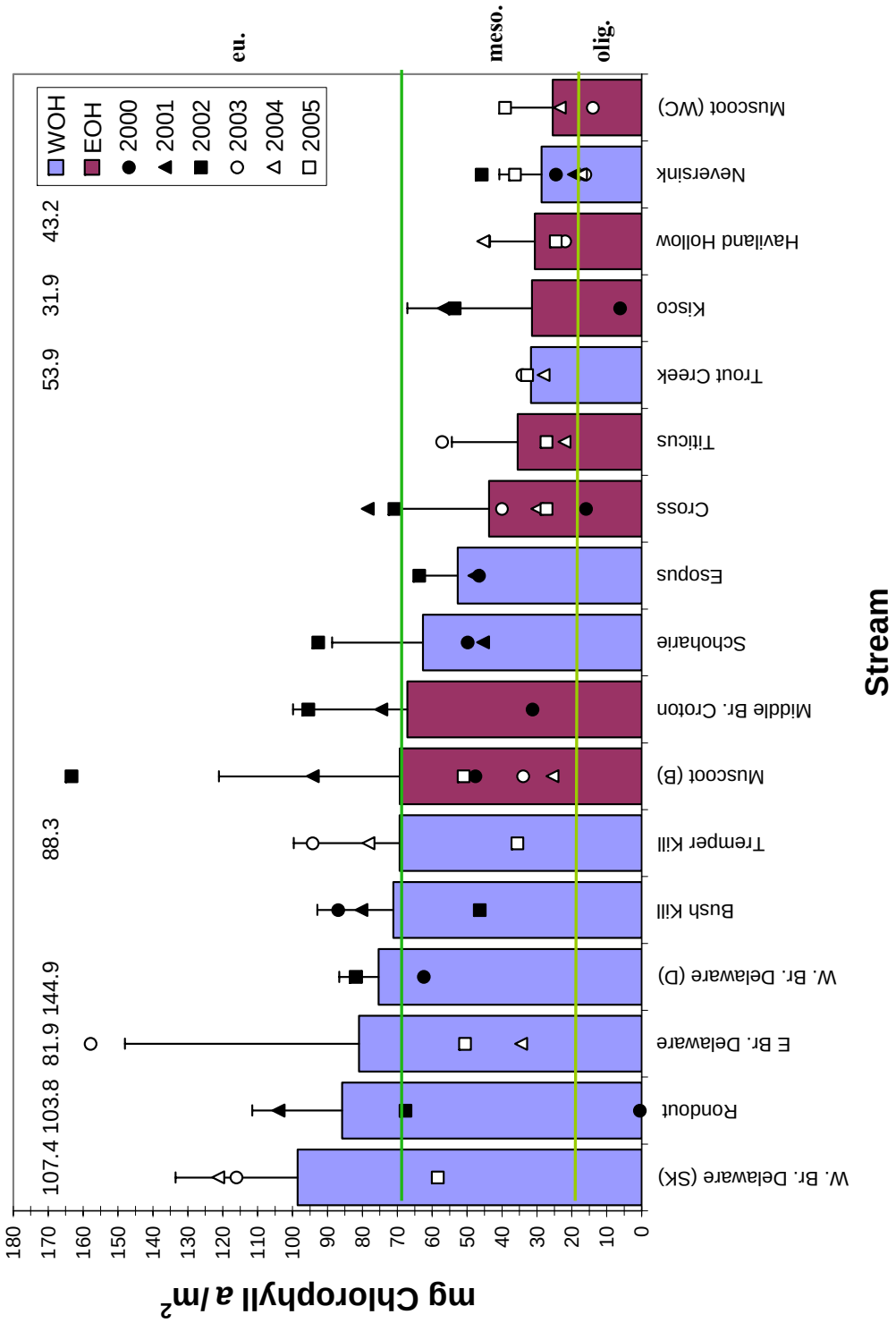

Figure 9.2. Periphyton chlorophyll *a* concentrations in study streams. Histograms depict the 3- or 6-year mean (+1 SD). Data for individual years shown by symbol. Numbers indicate total chlorophyll concentrations (incluing macrophyte and moss contributions). Lines depict proposed concentrations for designating stream trophic condition as oligo-, meso-, or eu- trophic (see text).

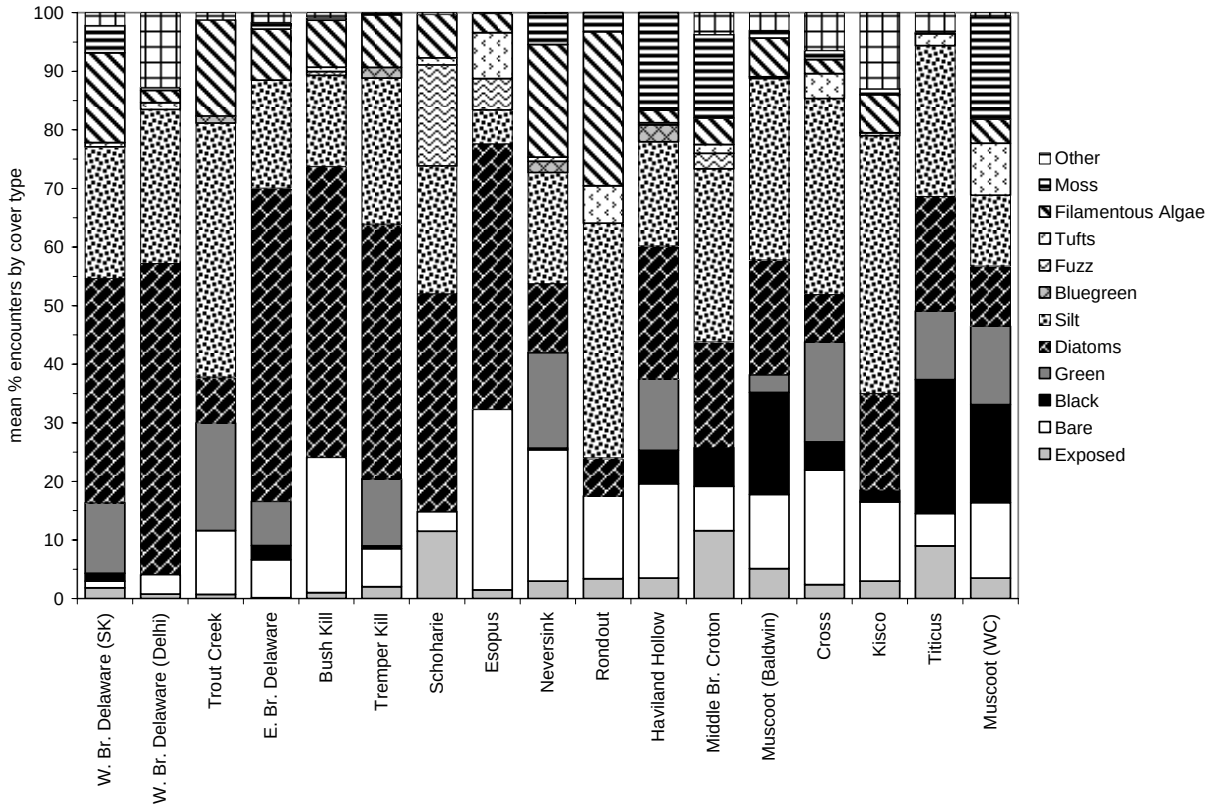

Figure 9.3. Algal cover types in study streams. Data shown are means of 2 or 5 years of study.

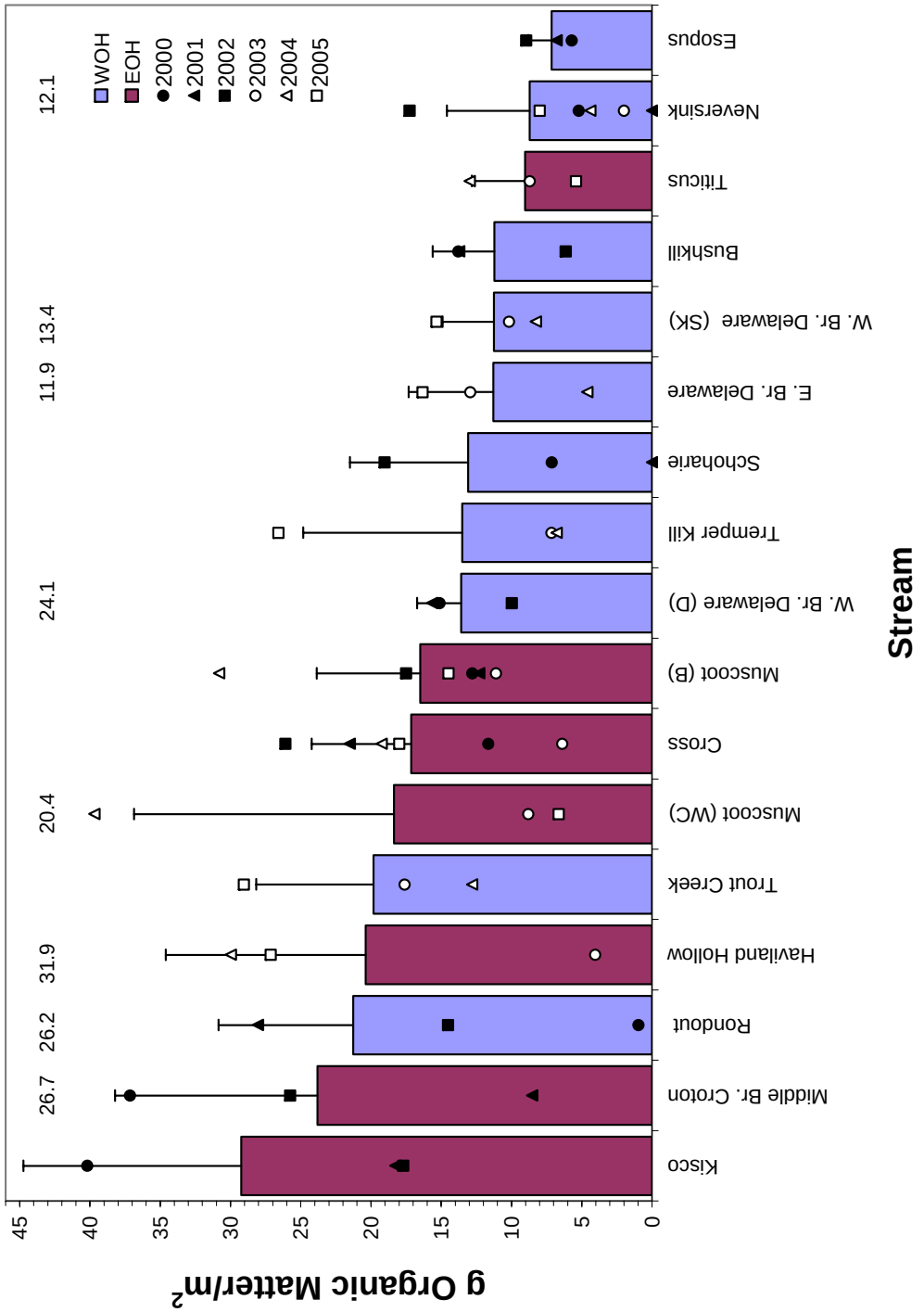

Figure 9.4. Periphyton organic matter concentrations in study streams. Histograms depict the 3- or 6-yr mean (±1 SD). Data for individual years shown by symbol. Numbers indicate total concentrations (including macrophyte and moss contributions).

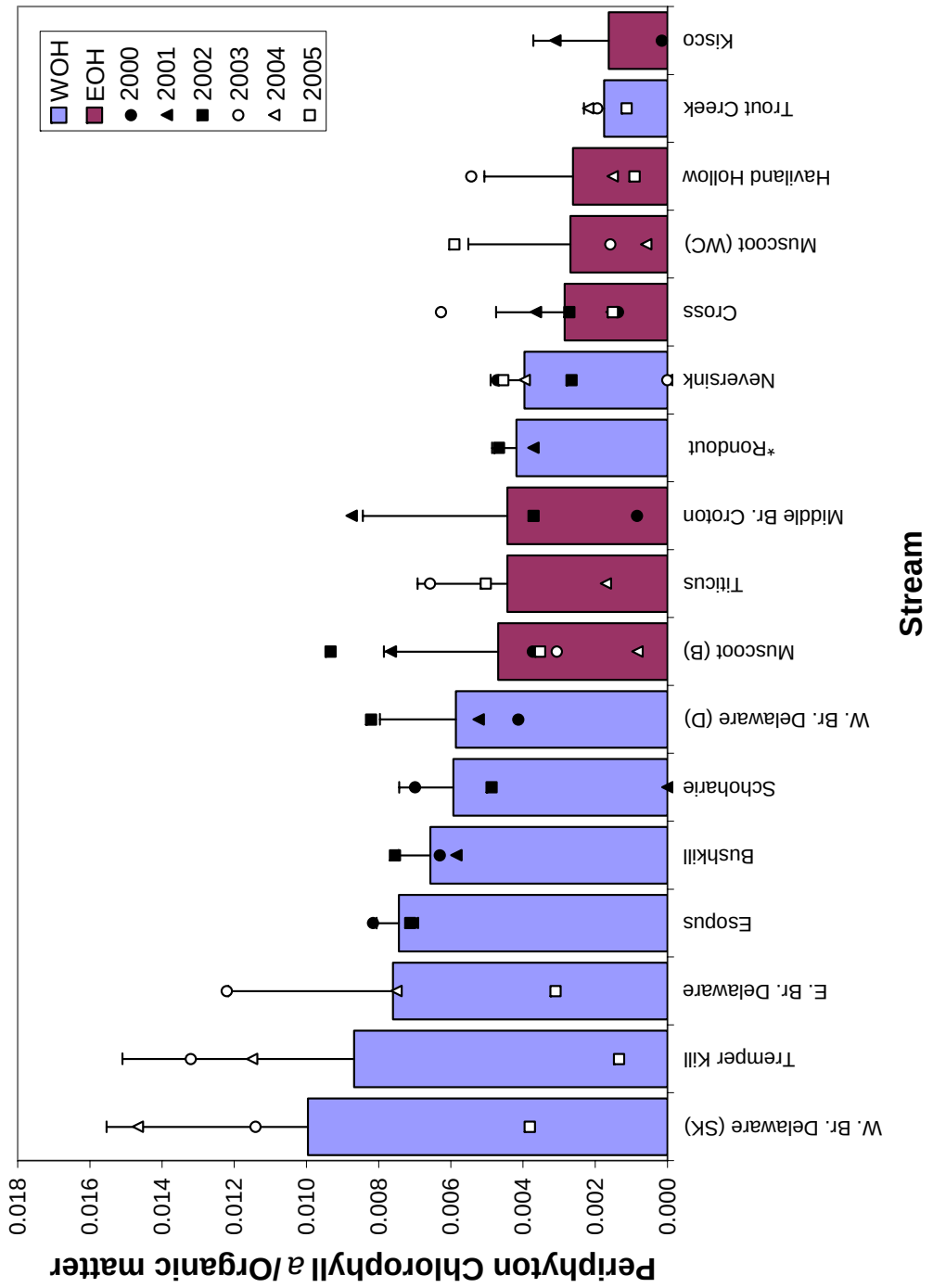

Figure 9.5. Periphyton chlorophyll a /organic matter ratios in study streams. Histograms depict the 3- or 6-year mean (±1 SD). Data for individual years shown by symbol.

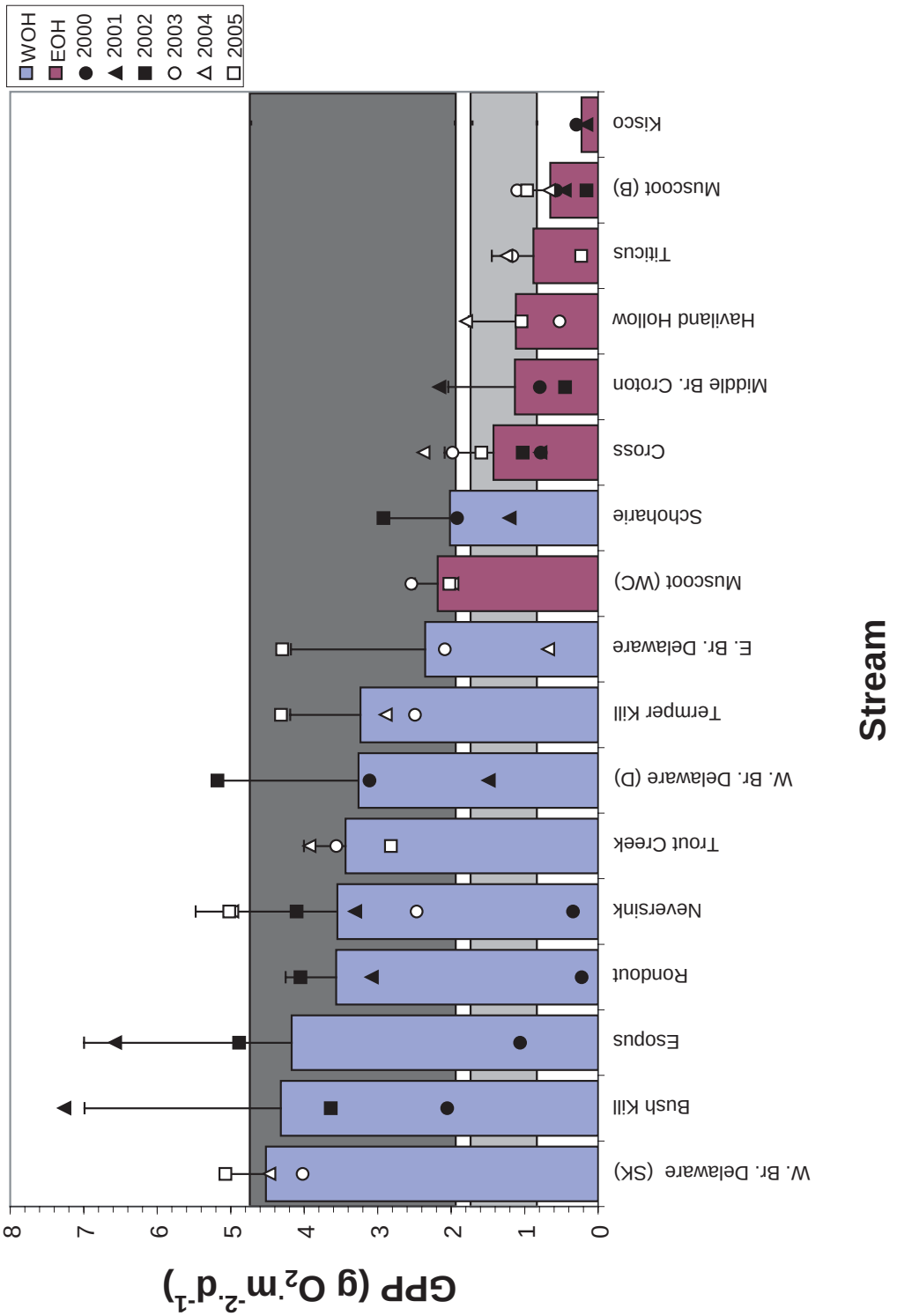

Figure 9.6.Gross primary productivity (GPP) in study streams. Histograms depict 3- or 6-year means (±1 SD). Data for individual years shown by symbol. For explanations of shaded areas, see text; upper shaded area = meadow CV applied; lower shaded area = forested CV applied.

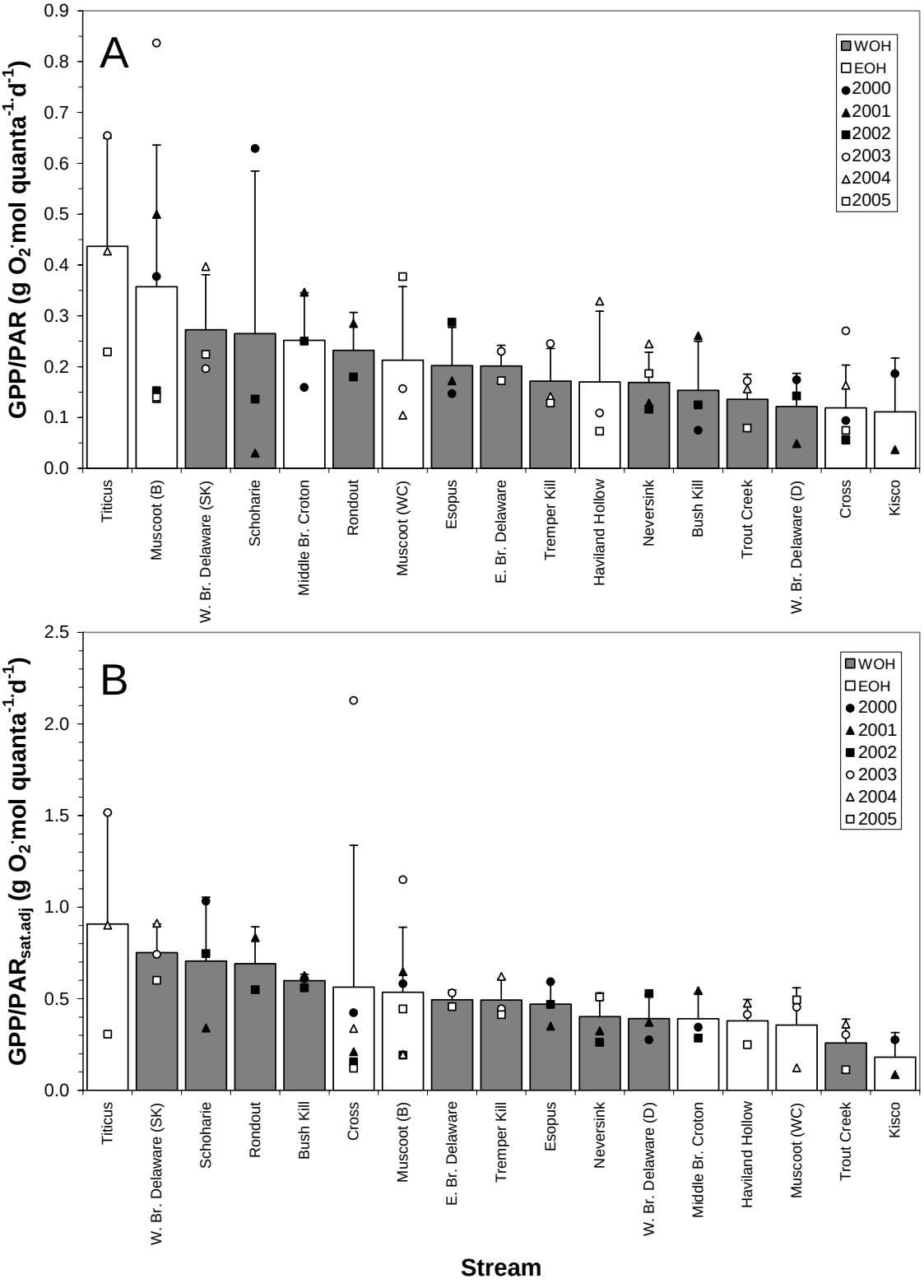

Figure 9.7. Ranking of streams according to GPP normalized for PAR (A) and for PAR following adjustment for saturation intensity (B).

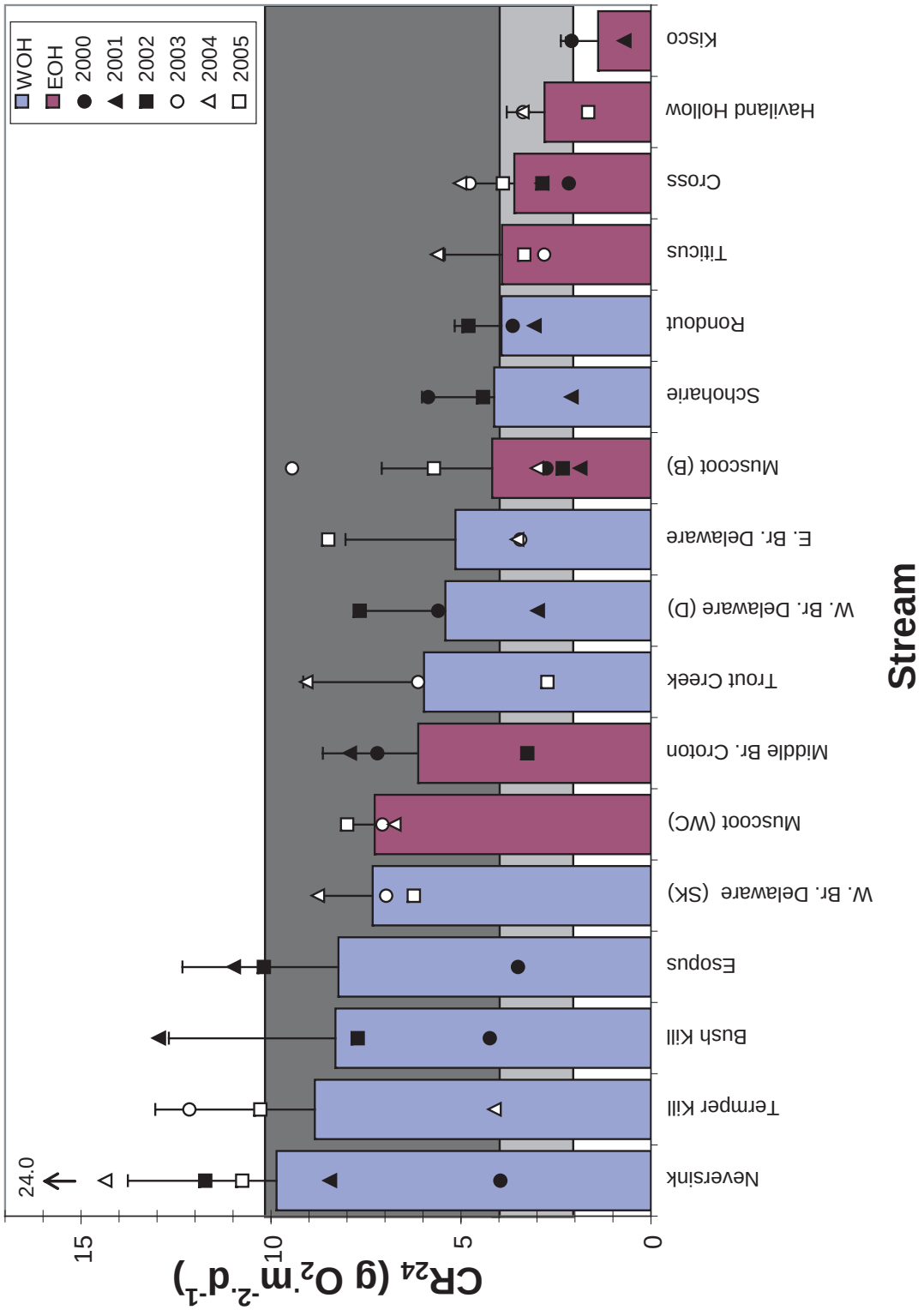

Figure 9.8. Community respiration (CR_{24}) in study streams. Historgrams depict 3- or 6-year means (±1 SD). Data for individual years shown by symbol. For explanations of shaded areas, see text; upper shaded area = meadow CV applied; lower shaded area = forested CV applied.

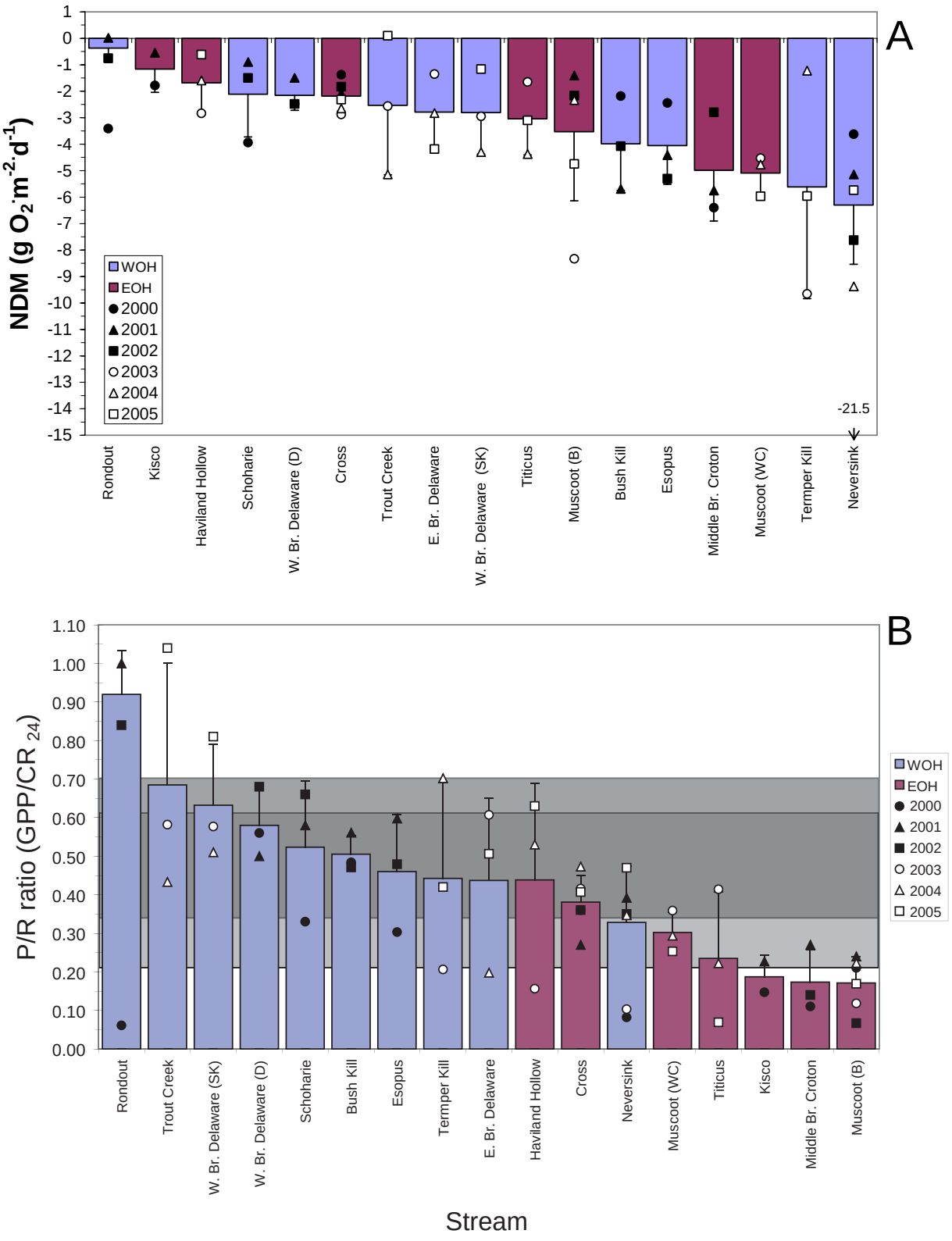

Figure 9.9. Balance of GPP and CR_{24} in study streams shown as Net Daily Metabolism (NDM, A) and P/R ratio (B) in study streams. Histograms depict 3- or 6-year means (±1 SD). Data for individual years shown by symbol. See text for explanation of shaded areas in B.

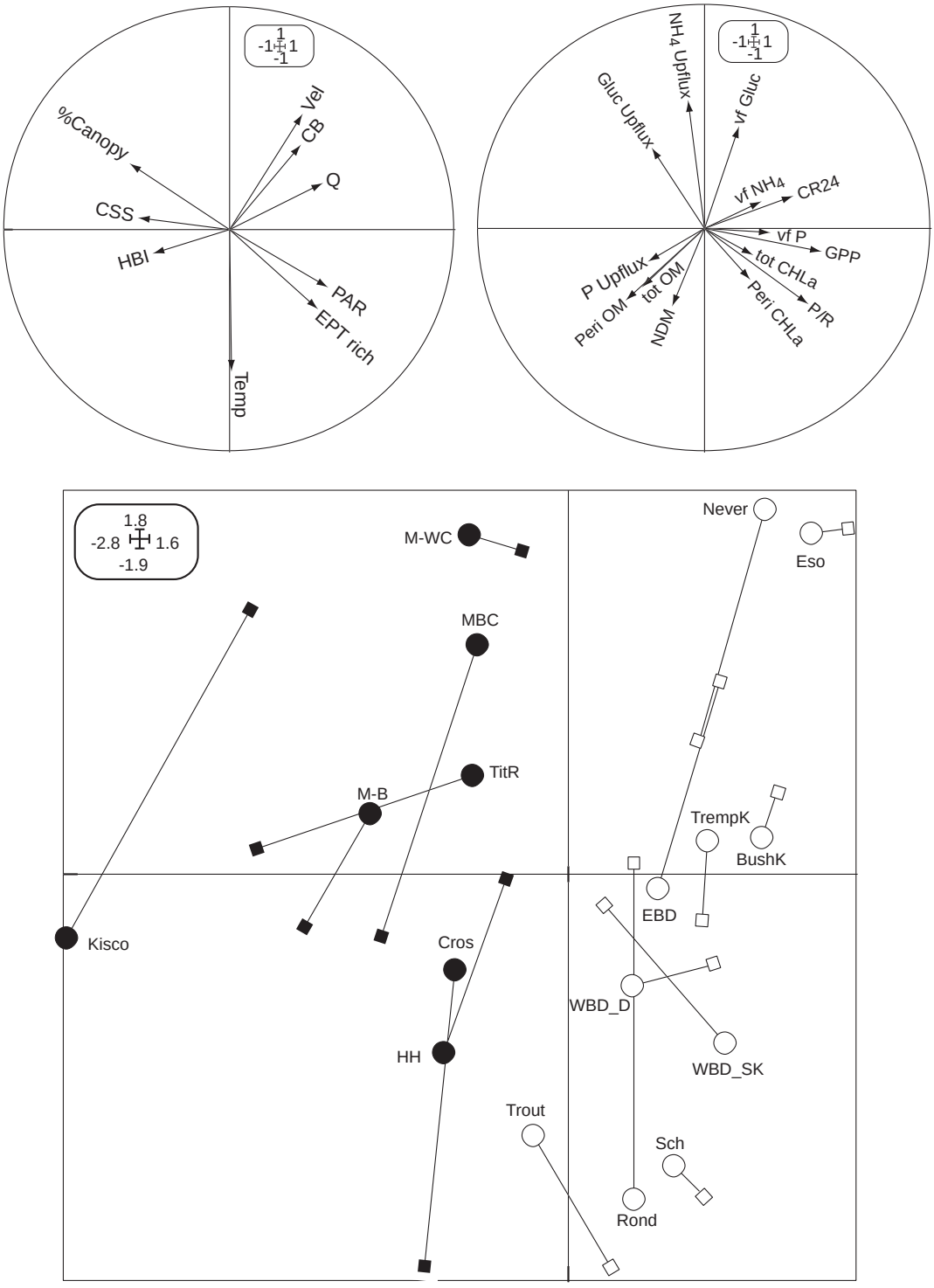

Figure 9.10. Results of CoInertia analysis showing ordination of site variables (top left) and biological variables (top right). The analysis maximizes covariance between these variables and relates sites to the covariance (bottom). Each site is plotted twice, once on the basis of site scores (circles) and once on the basis of metabolism scores (squares) with the symbols linked by lines. Open symbols designate WOH sites; closed designate EOH sites.

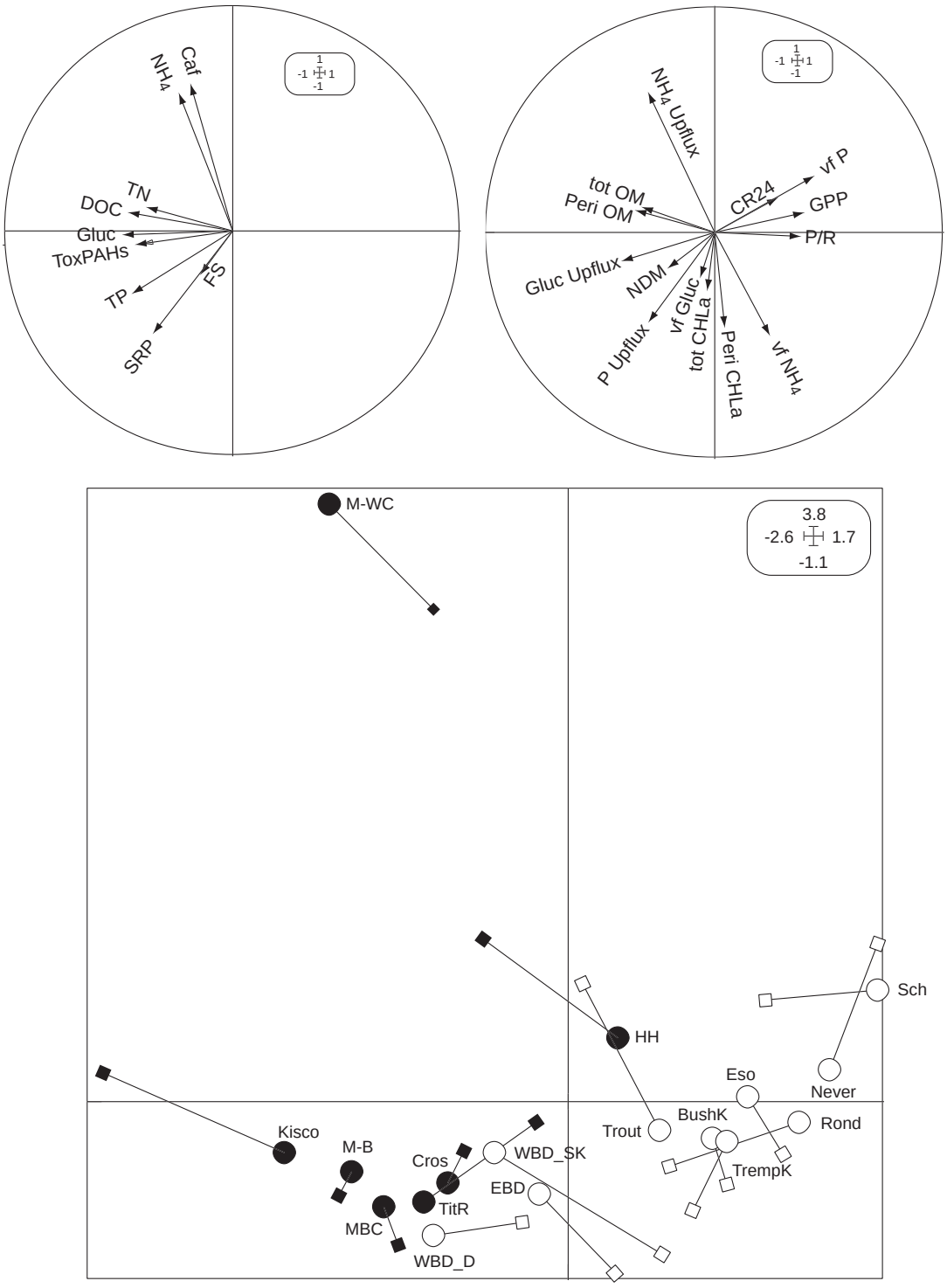

Figure 9.11. Results of CoInertia analysis showing ordination of chemical variables (top left) and biological variables (top right). The analysis maximizes covariance between these variables and relates sites to the covariance (bottom). Each site is plotted twice, once on the basis of chemical scores (circles) and once on the basis of metabolism scores (squares) with the symbols linked by lines. Open symbols designate WOH sites; closed designate EOH sites.

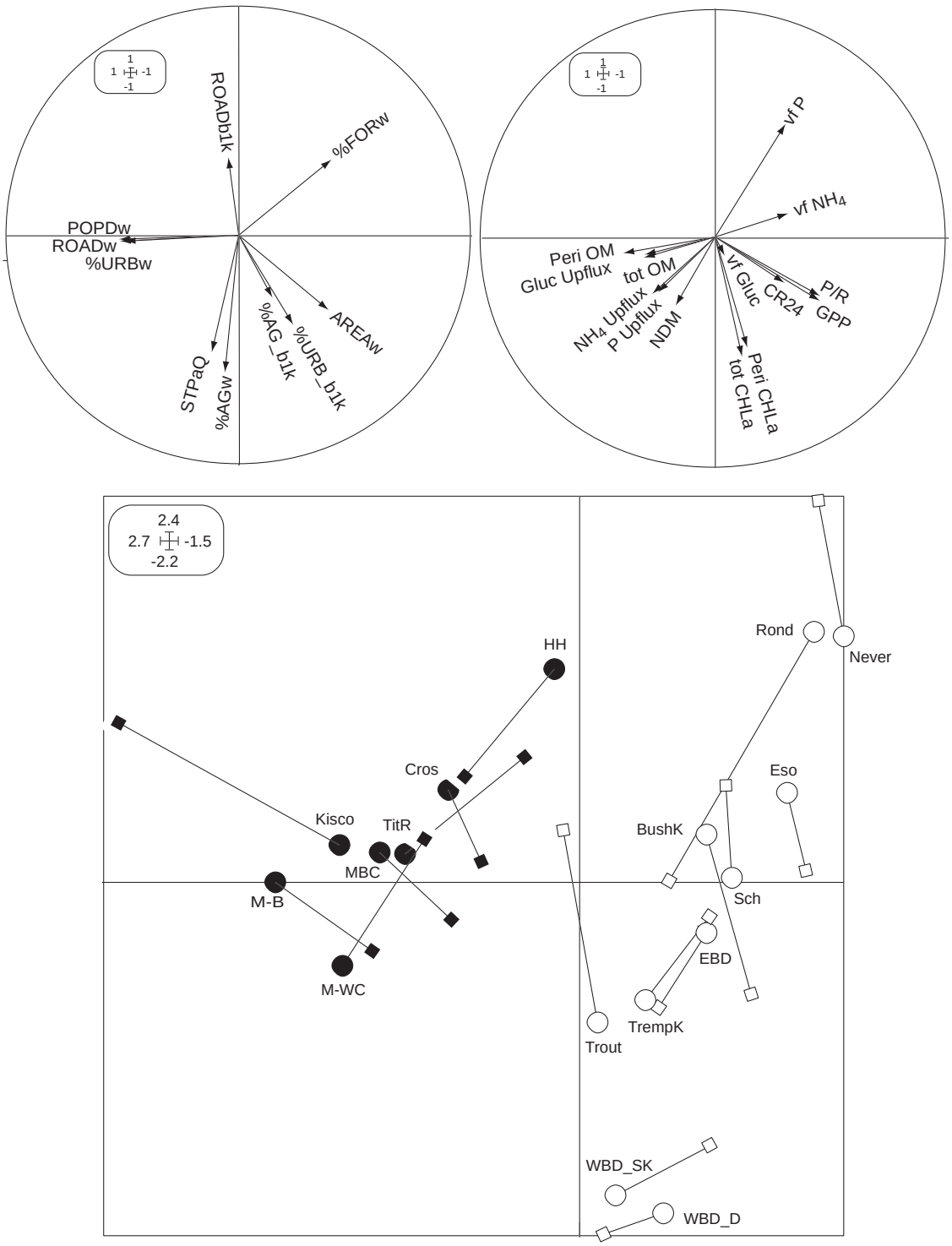

Figure 9.12. Results of CoInertia analysis showing ordination of land-use variables (top left) and biological variables (top right). The analysis maximizes covariance between these variables and relates sites to the covariance (bottom). Each site is plotted twice, once on the basis of land-use scores (circles) and once on the basis of metabolism scores (squares) with the symbols linked by lines. Open symbols designate WOH sites; closed designate EOH sites.

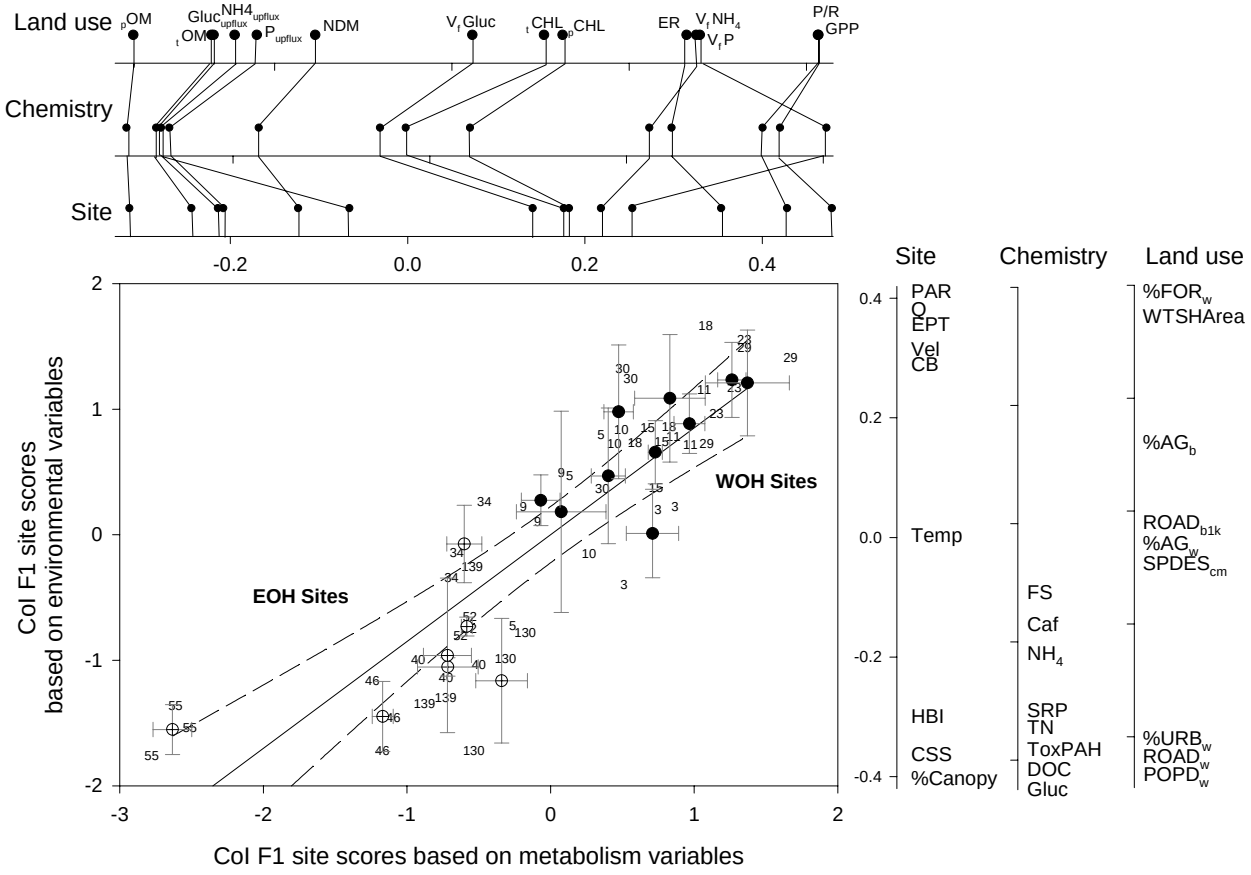

Figure 9.13. Summary diagram illustrating results from 3 separate co-inertia analyses. See Tables 8 - 10 for variance explained and correlations between Factors derived from multivariate analysis of metabolism variables versus environmental variables (grouped into "site", "chemistry", and "land use" categories). The site scores (n = 17) derived from multivariate analyses of metabolism variables averaged (± 1 SD) from 3 separate CoI's are plotted on the x-axis. The metabolism variable loadings from Factor 1 for each of the CoI (metabolism versus site, chemical, and land use) are plotted above the x-axis and lines connect identical metabolism variables across analysis to aid interpretation. The site scores (n = 17) derived from multivariate analyses of environmental variables averaged (± 1 SD) from 3 separate CoI's are plotted on the y-axis. Scores from the land use CoI were multiplied by -1 to flip the F1 axis so that WOH sites were positive and EOH sites were negative. Environmental variable loadings from Factor 1 for each of the CoI (metabolism versus site, chemical, and land use) are plotted to the right of the y-axis to aid interpretation. A regression line (± 95% CI bands) is plotted through the average x and y site scores ($r^2 = 0.80$).

----------Intentionally Blank----------

Chapter 10. Reservoir Productivity

Research Task

The six largest reservoirs of the NYC drinking water supply lie west of the Hudson River (WOH) in the Catskill Mountains and 13 reservoirs and 3 controlled lakes are located east of the Hudson River (EOH) in the Croton watershed. The WOH reservoirs make up ~90% of the supply, although drought conditions can affect this percentage. Catskill water is delivered to NYC by two routes: (1) from the Schoharie reservoir (WOH) to the Ashokan (WOH) via Esopus Creek, and then to the Kensico reservoir (EOH) via the Catskill aqueduct, and (2) from the Pepacton, Neversink, and occasionally the Cannonsville, reservoirs to Rondout (all WOH), then to the West Branch reservoir via the Delaware aqueduct, and ultimately the Kensico (both EOH) (National Research Council 2000). Water collected in the EOH reservoirs studied here (Cross River, Titicus, Amawalk) is transferred to the Muscoot reservoir, which overflows to the New Croton.

The Catskill supply is presently unfiltered. Watershed-scale remediation efforts are underway to maintain a low level of suspended particulate matter in the reservoirs. Phytoplankton productivity could be a significant source of particles generated within each reservoir, at least seasonally, reflecting, in part, the input of nutrients from the watershed. In addition to affecting suspended particulate loads, algae can affect drinking water quality in other ways. For example, some Cyanobacteria and diatoms produce unpleasant tastes and odors, algae excrete dissolved organic C compounds and thus increase the potential for production of disinfection by-products, and some Cyanobacteria produce toxins. Algal blooms increase hypolimnetic O_2 demand when they decay, and when severe, this can result in anoxic conditions. However, apart from physical and chemical data for the Cannonsville reservoir (Auer and Forrer 1998, Effler and Bader, 1998) and studies of particles in several reservoirs (Peng et al. 2004) there is little published data concerning the biology or ecosystem processes occurring in NYC drinking water reservoirs.

We measured primary productivity and algal biomass in 12 reservoirs. During Phase I of the study (2000 - 2002) we studied Cannonsville, Pepacton, Neversink, Rondout, Schoharie, and the west basin of the Ashokan (all WOH) and New Croton and Kensico (both EOH). During the second phase of work (2003 - 2005) we studied the Amawalk, Cross River, Titicus, and Muscoot reservoirs (all EOH), and continued work on the Neversink, Cannonsville, and Pepacton. Our goal was to assess reservoir condition on the basis of phytoplankton biomass and primary productivity. In addition, we hypothesized that if the major tributary to a reservoir were the principal source of nutrients, gradients of productivity and algal biomass would occur within the reservoir. Finally, these data form a baseline for comparison with data collected in the future.

Methods

Study sites

Three locations (substations [SS]) were established on most reservoirs (Fig. 10.1 and Fig. 10.2), with 5 substations on the Cannonsville (SSs 1, 2, and 3 in the W. Br. Delaware main stem during Phase I; SSs 4 and 5 in the Trout Creek arm and SS 3 in the main stem during Phase II),

and 6 in the Pepacton (SSs 1, 2, and 3 during Phase I, and SSs 1, 3, 4, 5, 6, 7 during Phase II). The location of each SS was fixed using GPS during the 2nd y of work and those coordinates are given in Table 1. Reservoirs included in this study with the largest storage capacities were the Cannonsville and Pepacton, and those with the smallest capacities were the Schoharie and New Croton (National Research Council 2000). Water residence time was short in the Kensico (a storage and mixing reservoir) and long in the Cannonsville, Neversink, and Pepacton (National Research Council 2000; Table 10.2).

Field procedures

Phytoplankton productivity in each reservoir was measured on 1 day each summer. One day before measuring productivity, photosynthetically active radiation (PAR) was measured at successive 0.5-m increments through the water column, coupled with simultaneous measurements made above water, to establish the depth of the photic zone (1% of surface PAR) at each SS. A spherical underwater quantum sensor and a quantum sensor for use in air were used with a LI-Model 1400 light meter (LI-COR, Lincoln, Nebraska) for these measurements, which were made as close to midday as possible. Dissolved O_2 and temperature profiles at each SS also were determined using a YSI model 5739 probe and model 58 meter (Yellow Springs Instruments, Yellow Springs, Ohio) each year between 2001 and 2005.

The next day, primary productivity was measured using dissolved O_2 changes in light and dark bottles. Except for 2000, measurements were made only on bright days when objects cast distinct shadows, which was also the condition for all but Rondout and Kensico in 2000. Incubations were conducted during the 4.5 to 6 h period around solar noon. Water was collected using Van Dorn samplers from just beneath the water surface and at the depths where PAR was 50%, 25%, 10% and 1% of incident light. Water (12–15 L) from a given depth was pooled and bubbled with N_2 for ~6 min to reduce the dissolved O_2 saturation (often >95%) to between 70 and 80% (a step usually not required for water from the 1% intensity depth). It was assumed that the concentration of dissolved CO_2 was not affected by this step because pH did not change measurably. Biological oxygen demand (BOD) bottles (2 light and 1 dark) used for incubations were rinsed 3 times with water from depth, immersed in that water to bring the bottle to temperature at depth, flushed 3 times, filled without introducing bubbles, stoppered, and transferred to a holding bath in a shaded location on the boat. Water temperature, dissolved O_2 concentration, and O_2 % saturation were measured in each bottle using a YSI model 58 meter and model 5905 probe with stirrer. Each bottle was topped off with 0.5 to 1 mL of reserved pooled water, resealed, and replaced in a holding bath. The process was repeated with water collected from each depth. After bottles from all depths were prepared, they were placed horizontally (label to the side) in Plexiglas holders (Wetzel and Likens 1991) and suspended in the reservoir at the appropriate depth. The entire process was repeated at each substation. After incubation, dissolved O_2 concentration, O_2 % saturation, and water temperature were measured again in each bottle. During the incubation period, above-water PAR was measured from the boat deck. Between reservoirs, BOD bottles were filled with a 30% bleach solution for 15 min, rinsed, and air-dried to kill any microbial biofilm.

A 2-L sample of water from each depth was collected for analysis of phytoplankton chlorophyll *a*. Samples were iced immediately, vacuum-filtered (at 0.5 atmosphere) onto GF/F filters within 24 h, and filters were frozen until extraction. Other samples of surface water were

filtered through precombusted Gelman GF/F filters (250 mL for inorganic nutrient analyses and 40 mL for dissolved organic C (DOC). Samples for inorganic nutrient analyses were placed on ice until they could be frozen in the laboratory; DOC samples were fixed with 0.27 mM azide and refrigerated. Additional water was collected directly into 125-mL bottles (leaving no head space), iced, and later refrigerated for total alkalinity determinations.

Laboratory analyses

During Phase I work, chlorophyll *a* was analyzed spectrophotometrically with correction for pheophytin according to Lorenzen (1967). The frozen filters were macerated in 4 ml of 90% acetone/10% saturated $MgCO_3$ solution (Method 10200H; APHA 1998) at 4°C. Additional acetone solution was added and samples were extracted in a freezer for 16 to 24 h in darkness, and centrifuged (8000 x *g*, 20 min, 4°C). All manipulations were done on ice and in subdued light to prevent photobleaching of pigments. To insure complete extraction, samples were re-extracted until the OD_{665} before acidification either was ≤0.1 absorbance units or ≤10% of the absorbance in the initial extraction. Lab control standards of pure chlorophyll a (Sigma, St. Louis, MO) at a concentration of 10 µg/ml were assayed with each set of samples.

During Phase II, chlorophyll concentrations were determined fluorometrically (Arar and Collins 1997). Filters were macerated as described, and the volume was brought to 9 ml with additional acetone solution. After extraction in 90% acetone at -20°C, the filters were compressed using a Teflon pestle and the supernatant fluid was transferred to a centrifuge tube. The samples were centrifuged (8,000 x *g*, 20 min, 4°C). The supernatant fluid was then transferred to a test tube in an ice bath and covered with aluminum foil; the pelletized filter was held in the freezer for re-extraction if necessary, with manipulations performed in subdued light. An aliquot of the supernatant fluid (4 ml) was analyzed fluorometrically by making an appropriate dilution (between 1:2 and 1:32) in a 9 ml cuvette and measuring fluorescence intensity before and after acidification in a Model 10-AU fluorometer (Turner Design, Sunnyvale, CA). Samples were re-extracted to insure complete extraction of each sample. Throughout the field season, laboratory control standards were prepared at a concentration of ~ 40 µg of chlorophyll *a*/sample (Sigma, St. Louis, MO). A solid standard calibrated against a fluorometrically-determined chlorophyll standard (Turner Design) was used for fluorometric assays on a daily basis. During the first year of Phase II, fluorometric and spectrophotometric analyses were compared on each chlorophyll sample. The mean [flourometric/spectrophotometric] concentration ratio of 136 samples was 1.38 ± 0.43 (x ± SD). Thus, estimated concentrations were slightly higher from the fluorometric analyses. However, because the standard deviation was considerable, we decided not to convert concentrations from one method to the other because that might introduce considerable error and data are reported as analyzed concentration. Fluorescence readings for the Pepacton, Titicus and Cross River reservoirs were higher after acidification in 2004, therefore chlorophyll concentrations for all reservoirs in 2004 were computed based on initial fluorescence values. The 2004 data for most reservoirs were close to 2003 data, suggesting that the pheophytin contribution was small. Water-chemistry analyses were done using procedures documented in chapters 6 and 8.

Data analyses

Estimates of gross primary productivity (GPP) were obtained by summing dissolved O_2 change in each light bottle with the change in the dark bottle at that depth. The mean value for each depth was integrated to the midpoint between incubation depths and summed to generate an estimate of area-specific productivity over the photic zone at each substation. SS data were averaged for each reservoir. Chlorophyll *a* concentrations were integrated similarly. Each reported light extinction coefficient is the mean of two estimates, both using PAR intensity measured just under the water surface, but one using PAR measured at the 10% intensity depth and the other PAR at the 1% depth.

Reservoir trophic status was assessed by comparison with published criteria using chlorophyll *a* concentrations and algal productivity (Lampert and Sommer 1997). Total daily productivity was estimated by multiplying hourly volume-normalized production rates by 5 h (although some incubations lasted close to 6 h) and then by 1.11 (a factor based on conservative extrapolation of PAR reaching the water surface during the incubation period to total daily PAR). Carlson's Trophic State Indices based on chlorophyll concentration, Secchi Disc depths and total P concentrations were computed using published equations (Carlson 1977, Wetzel 2001). Secchi Disc depths measured at each SS between 2001 and 2005 were used to compute that Tropic State Index (TSI) and the mean value for each substation was averaged to generate a reservoir mean. A mean value of TP in reservoir water during 2000 and 2001 was computed from data reported by NYC DEP (2002) to compute the TSI from TP. If the mean for those 2 years differed by more than 1.5 µg/L from the 5-y mean (1997-2001) reported by NYC DEP, the 5 y mean was used in the computation (Muscoot, Titicus, New Croton, Ashokan, Schoharie) as being more representative of reservoir condition.

Statistical tests were done on $\log_{10}(x)$-transformed or arcsine-square-root(x)-transformed (for percentages) data. Differences in chlorophyll *a* and light-normalized GPP (GPP/PAR) among reservoirs were determined using ANOVA and Tukey's test and data from each year (SAS/STAT version 9.0; SAS Institute, Cary, North Carolina). Stepwise multiple linear regression (MLR) using reservoir means was used to identify the influence of local physicochemical variables (e.g., PAR, depth of the photic zone, nutrients, total alkalinity) on chlorophyll *a* and GPP/m^2 using reservoir mean data (Stat-View version 4.02; Abacus Concepts, Berkeley, California). Pearson correlations were used to evaluate relationships among reservoir characteristics and watershed-scale land use variables (Chapter 2). Data for the Kensico in 2000 were excluded from the 3-y mean because of extremely low PAR. Data for Kensico also were deleted from correlation and regression analyses because its water was predominantly of WOH origin with high turnover, so local land use/cover was expected to exert little influence on reservoir characteristics.

Co-inertia Analysis (CIA; Thioulouse et al. 1997), an unconstrained, direct gradient multivariate analysis, was used to summarize relationships between watershed-scale land use and in-reservoir productivity, vertical photic and thermal properties, and water chemistry. CIA enables the joint analysis of tables having few or different numbers of environmental variables, species, and/or samples (Dolédec and Chessel 1994). All in-reservoir variables (GPP/PAR, GPP/m^2, chlorophyll *a*, photic-zone temperature, photic depth, total dissolved P [TDP], DOC, NH_4-N, and NO_3-N) were log transformed and land-use variables were either arcsine-square-root

transformed (percentages) or log transformed before analysis. Alkalinity was eliminated from the analyses because it was correlated strongly with DOC. Land-use variables were summarized at the watershed level (Chatper 2), and means were calculated for SS-specific biological, chemical, and physical data in each reservoir. Thus, data from each SS within a reservoir were matched with identical land-use variables.

Results and Discussion

NH_4^+ concentrations were higher in Ashokan, Cannonsville, and Schoharie than other WOH reservoirs, presumably reflecting the agricultural activity in Schoharie and Cannonsville watersheds and the transfer of Schoharie water to the Ashokan (Table 10.2). NH_4^+ in the Muscoot was much higher than in other EOH reservoirs, perhaps a response to sewage effluent discharged to a tributary of the Muscoot River, which drained to the reservoir. NO_3 concentrations were high in all WOH reservoirs but Pepacton and the Trout Creek arm of Cannonsville. The NO_3 concentration in the Kensico mirrored the high concentration in the Ashokan, but except for the Muscoot and New Croton, NO_3 concentrations were low in other EOH reservoirs. Total dissolved P (TDP) and soluble reactive P (SRP) concentrations were higher in the Ashokan than in the other reservoirs, and TDP was only slightly lower in the Titicus and Muscoot reservoirs (both EOH). Total alkalinity was higher in the EOH reservoirs, reflecting the differing geology between EOH and WOH regions (Dow et al. 2006). The Kensico also is located EOH but receives most of its water from WOH reservoirs and, thus, had a total alkalinity similar to WOH reservoirs. DOC concentrations were greater in the EOH reservoirs, reflecting a similar difference in DOC concentrations in WOH and EOH streams (see Chapter 6). The only differences in water chemistry that were significant statistically between reservoirs were for total alkalinity and DOC, both of which were higher EOH than WOH (ANOVA and Tukeys tests, $p < 0.05$). The difference in DOC was distinctly EOH vs. [WOH + Kensico]. However, Neversink differed in total alkalinity from all other reservoirs, Rondout and Pepacton differed from Titicus, New Croton, Muscoot and Amawalk; Ashokan, Kensico and Cannonsville differed from Titicus, New Croton, and Muscoot; and Schoharie differed from Titicus.

Temperature, O_2, and light penetration

Surface water temperatures at the time of our studies ranged from 20 to 25°C in WOH reservoirs and up to nearly 30°C in EOH reservoirs and graded to bottom temperatures between 5 and 13°C with a few exceptions (Fig. 10.3). The surface water temperatures in Muscoot and Titicus were lower in October 2003 and bottom temperatures were higher in the Kensico in 2000 (18° C) and 2002 (16° C) and at SS1 of New Croton in 2002 (18° C).

Temperature profiles for each reservoir displayed expected seasonal patterns, with a deeper epilimnion later in the season and less-pronounced thermocline on earlier dates of study. The depth of the epilimnion in WOH reservoirs ranged from 1 to 2 m in late June-early July and increased to between 3 and 9 m in late July to mid-September (Fig. 3). The thermocline was less apparent in the Ashokan in mid-September than when studied between late June and early August. Reservoirs with shorter residence times, e.g., Rondout and Schoharie, also tended to have a less well-developed thermocline (Table 10.2). The Ashokan and Rondout are transfer reservoirs with large water inputs and withdrawals, although the Schoharie is not. In EOH reservoirs, the depth of the epilimnion ranged from 1 to 4 m in late June-early July and increased

to between 3 and 6 m later in the summer. The epilimnion in the Titicus was 8 m in late October. The thermocline was poorly developed in the Kensico in late August-early September and Muscoot (the shallowest reservoir), the two EOH reservoirs with the shortest residence times (Fig. 10.3, Table 10.2).

In addition to seasonal variation, variability in tributary stream inflows also may have affected the development of the thermocline and epilimnion depth. For example, Pepacton SSs 1,4,3 displayed a pronounced thermocline in 2005 when inputs from the E. Br. Delaware and Tremper Kill were 0.283 m^3/s and 0.043 m^3/s, respectively (Fig. 10.3). In contrast, inputs from those tributaries were 19.8 and 1.98 m^3/s, respectively in 2003, and 3.68 and 0.51 m^3/s in 2004, years in which temperature profiles were characterized by a gradual decrease in temperature to the bottom of the reservoir.

Dissolved O_2 profiles were clinograde (i.e., hypolimnetic O_2 values approached 0) in the Cannonsville (2001) and surprisingly, even at Pepacton SSs 1, 4, 3 in 2005 (Fig. 10.4). A clinograde profile occurred in every EOH reservoir but Kensico during at least one year of study, e.g., New Croton during August 2002 and at SSs 2 & 3 even in early July 2001 (Fig. 10.4). The reservoir average profile was clinograde for the Amawalk and Muscoot every year, the Cross River in September 2004 (but not when studied in July of 2003 and 2005), and Titicus in October 2003 and September 2004 (but not in June 2005). Profiles were orthograde (nearly constant O_2 concentration with depth) in the Neversink, Rondout, Schoharie (2002), and Kensico (2001) (Fig. 4). The profiles at some SSs were either positive or negative heterograde (dissolved O_2 concentration elevated or depressed, respectively, at an intermediate depth, usually the thermocline). Positive heterograde profiles occurred in the Pepacton (pronounced at SS2 and SS3 in 2002), Rondout (2002), Neversink (2002) and Cross River (all SSs in 2003). Negative heterograde profiles occurred in the Schoharie (SS1 in 2001), Kensico (2002), Pepacton (SS1 in 2001), Neversink SS2 (2005), and Cannonsville SS3 (2004) and SS4 (2004, 2005). Surface O_2 % saturation was ≥100% except for Cannonsville (August 2005), Muscoot (October 2003) and Titicus (October 2003), where the water was only approximately 80% saturated. It is possible that phytoplankton densities were declining at those times that the reservoirs were impacted negatively by watershed inputs, or both. A low chlorophyll concentration and GPP/PAR in the Cannonsville in 2005 supports the former explanation, but this was not the situation in the EOH reservoirs.

The WOH reservoirs were deeper (reservoir mean depth 16.6 – 18.9 m) than those located EOH (mean depth 7 – 16.6 m), although some EOH reservoirs had SSs ~20 m. Water depths at SSs near tributaries were shallower than at other SSs on the same reservoir (Table 10.3). SS1 on the Ashokan and Cannonsville were nearest the influent tributaries, Esopus Creek and West Branch Delaware River, respectively. SS1 on the Amawalk, Cross River, and Titicus reservoirs also were located toward influent tributaries, the Muscoot River, Cross River and Titicus Creek, respectively. SS3 on the New Croton was near the mouth of the Kisco River. The Muscoot reservoir was uniformly shallow.

The mean depth of the photic zone (to 1% of surface light intensity) ranged from low values of 4.8 (Muscoot), 5.9 (Titicus), and 6.4 m (New Croton) to highs of 9.3 (Pepacton) and 9.9 – 10.3 m (Neversink, Kensico, and Rondout) (Table 3). Photic-zone depth increased >2 m in the

Ashokan between SS1 and SS3, and 2.3 m from the near-mouth of the Tremper Kill (Pepacton SS4) to down-reservoir stations, and ~1 m or more on some of the other reservoirs (Cannonsville, Rondout, Kensico, Amawalk and New Croton) between the most up-reservoir and most down-reservoir SSs. The depth of the photic zone was uniformly shallow on the Muscoot, but improved on water passage through the New Croton, the next reservoir in the chain. As expected, Secchi disc depths mirrored these photic zone depths with greatest Secchi disc readings in Neversink and Rondout (Table 10.3). However, Amawalk and Titicus had shallower Secchi depths than the Muscoot, and the large difference in photic zone depth between Kensico and Cross River reservoirs was not seen in the Secchi Disc data.

The reservoir mean light extinction coefficient (η) was extraordinarily high in the Muscoot ($\eta = 1.003$). Elsewhere the mean coefficient ranged from 0.813 – 0.712 in the Titicus, Cannonsville (SSs 1 – 3 in the W. Br. Delaware mainstem), New Croton and Amawalk; from 0.647 – 0.582 the Cross River, Schoharie, Cannonsville (Trout Creek arm), and Ashokan; 0.512 in the Pepacton and only 0.467 – 0.439 in the Kensico, Neversink and Rondout (Table 10.3). Many of the smaller primary reservoirs located EOH had high coefficients. In contrast, WOH primary reservoirs (Neversink, Rondout and Pepacton) had low coefficients. The coefficient decreased in the series Schoharie > Ashokan > Kensico, and between Neversink and Rondout, and Pepacton and Rondout. The Kensico – the terminus of numerous water transfers - had a low coefficient, in the range of WOH reservoirs, presumably reflecting the settling of particles that occurred in prior basins as well as the large component of WOH water. In the EOH reservoirs the coefficients increased between Cross River, Amawalk, Titicus and Muscoot, but then decreased between Muscoot and New Croton. The coefficient for the Muscoot was significantly greater than the coefficients for the Neversink, Kensico and Pepacton (ANOVA and Tukey's test, $p < 0.05$).

Chlorophyll a

Reservoirs were studied between June 26 (Ashokan 2002) and October 24 (Titicus 2003), with most measures performed by September 26 (Table 10.2). While maximum chlorophyll concentrations tended to occur in mid- to late-summer when data from all years were combined, differences in weather patterns between years also could influence the trend.

Three- or six-year mean photic-zone chlorophyll *a* concentrations ranged from 16 to 77 mg/m^2 with data for individual years ranging from <10 (Schoharie 2001) to 141 mg/m^2 (Cannonsville 2003) (Fig. 10.5). Mean photic zone $chlorophyll/m^2$ was highest in Cannonsville, followed by all the EOH reservoirs, and then the remaining WOH reservoirs. The concentration in the Schoharie was significantly lower than in the Cannonsville and all EOH reservoirs and chlorophyll in the Neversink was lower than in the Cannonsville (ANOVA and Tukey test: $p \leq 0.05$). Chlorophyll concentrations tended to increase between Schoharie and Ashokan and Kensico (one path to NYC). Concentrations in Rondout were also greater than in tributary reservoirs (Neversink and Pepacton) (the other path to NYC). This contrasts with the decreasing pattern observed for light extinction coefficients and suggests that although particle deposition occurs within each each reservoir, particle generation during the growing season can increase through the chain of reservoirs.

MLR analysis of chlorophyll *a* concentrations generated an equation that explained 93% of variance in the data with the inclusion of only GPP/m^2 and PAR (Table 10.4). Except for the inclusion of the PAR term, this equation is similar to one generated for the reservoirs studied during Phase I of work (Bott et al. 2006).

Water transparency in many reservoirs was quite good (Table 10.3). Between-year variation in the extinction coefficient for some SSs could be related to numerous factors, including differences in days of measurement and the time of day measures were made, changes in reservoir volume related to drawdown and drought, storms that affected turbidity of reservoir water and influent river water, and phytoplankton development. Field observations provided examples of several of these factors. For examples: 1) Cannonsville: In 2000, sampling occurred during a bloom of *Microcystis* sp. that was especially pronounced at SS1 near the mouth of the West Branch Delaware River. In 2001, sampling followed an algal bloom observed a few weeks earlier by the field team, and detritus from decay of that bloom might have restricted light penetration. In 2002, the water had a green tint and suspended material was visible at SS1 and SS2. In 2005 suspended and floating fine green particles were abundant at SS3. There was considerable suspended fine material in the Trout Creek arm, sometimes clumped together into larger particles. 2) Ashokan: The photic zone at SS1, closest to Esopus Creek, was shallower than at the other 2 mid-reservoir SSs. In 2000, Esopus Creek carried considerable turbidity that apparently influenced the depth of the photic zone at all SSs. In 2001, a brown floc was apparent in some incubation bottles, reflecting a turbidity gradient that was apparent from mid-reservoir to the mouth of Esopus Creek. 3) New Croton: In 2002, fine suspended material was noted at all SSs, and floating surface material occurred at SS3. 4) Pepacton: In 2002, suspended floc occurred at all SSs, and green floating clumps were noted on the surface at SS1. Between 2003 and 2005 fine green suspended matter was abundant at SS1 at the mouth of the East Br. Delaware river, and SS4 at the mouth of the Tremper Kill, but densities were lower at the other SSs. 5) Rondout (2002) and Neversink (most years): Fine, light green suspended material was observed, even though water clarity was excellent. 6) Kensico: In 2002, all SSs appeared faintly green and visible suspended material was present at SS1. 7) Muscoot: Floating and suspended green clumps were abundant at SS1, and less so at the other substations. *Lemna* (duckweed) and floating scums were observed at SS2 in 2005. Beds of submerged macrophytes were noted near SS2, but not in its immediate vicinity. 8) Amawalk: Suspended and sometimes floating fine green particles were noted, giving a slight green tint to the water, with densities decreasing between SS1 and SS3. 9) Cross River: Fine suspended material occurred in light to moderately heavy densities, and diatoms and ciliates were observed microscopically. 10) Titicus: Fine suspended green material was common at most SSs with heaviest densities at SS1. Especially heavy densities in 2004 imparted a brownish-green tint to the water at SS1 (where floating material also occurred) and SS2.

GPP and GPP/PAR

Hourly mean PAR during measurements varied from 0.89 to 5.89 mol quanta·m^{2}·h^{-1} with 87% of the values between 3.00 and 5.89 mol quanta·m^{2}·h^{-1}. Differences between reservoirs were not statistically significant (ANOVA, $p = 0.50$). Temperatures were ≥19°C at the time photosynthesis measures were made with two exceptions, Muscoot 2003 (16.0° C) and Titicus 2003 (11.7 °C), reflected in the lower 3-y mean for Titicus (Table 10.1). The impact of this lower temperature on productivity was apparently small, however, because GPP/PAR in 2003 was

similar to the rate in 2005 when chlorophyll was similar but the temperature was ~21°C (Fig. 10.6). Overall, temperature at the times measurements were made was not different statistically between reservoirs (ANOVA, $p = 0.11$).

Three-y or 6-y means for GPP normalized by surface PAR ranged from 0.03 to 0.18 mg O_2/mol quanta (Fig. 10.6). GPP/PAR was greater in EOH reservoirs than in WOH reservoirs with the exception of the Cannonsville. As found for chlorophyll, GPP/PAR in the Kensico was in the range of WOH reservoirs because it contains largely WOH water even though it is located EOH. Differences between reservoirs were significant (ANOVA, $p = 0.0005$). GPP/PAR in Muscoot, Titicus and Cannonsville was significantly greater than in the Schoharie and Neversink; and GPP/PAR in New Croton and Amawalk was greater than that in Schoharie (Tukey's MRT, $p < 0.05$). With the addition of Phase II reservoirs, evidence that GPP/PAR peaked later in the summer was weaker than with Phase I data alone (when GPP/PAR increased ~2- to 3- fold later in the season in the Kensico, New Croton, Ashokan and Pepacton reservoirs). The only reservoir where increases of that magnitude occurred during Phase II was the Neversink. Elsewhere rates of productivity either remained relatively constant or decreased throughout in the season. The correlation of GPP/PAR with Julian Day was non-significant ($r = 0.270$, $p = 0.10$).

Mean areal rates of GPP ranged from 0.14 to 0.54 g $O_2 \cdot m^{-2} \cdot h^{-1}$. The pattern was similar to GPP/PAR with higher rates occurring in EOH reservoirs although there were slight shifts in rank (Fig. 10.7). MLR regression analyses produced an equation that explained 95% of the variance in GPP/m^2 using chlorophyll *a*, temperature, and total alkalinity (Table 10.4). GPP was significantly positively correlated with total % agriculture (sum of farmstead, cropland, and grass land use categories; $r = 0.740$, $p = 0.007$), total % urban (sum of residential, industrial, commercial and other urban land use categories; $r = 0.699$, $p = 0.014$) and negatively correlated with total % forest (sum of coniferous, deciduous, and mixed coniferous and deciduous categories; $r = –0.791$, $p = 0.002$). GPP/PAR was significantly negatively correlated with total % forest ($r = –0.717$, $p = 0.011$) and positively with total % urban ($r = 0.633$, $p = 0.035$) land uses, but non-significantly with total % agriculture ($r = 0.561$, $p = 0.073$).

Similar to chlorophyll, average GPP/m^2 tended to increase as water was transferred from Schoharie and Ashokan, but in contrast, showed no further increase with transfer to the Kensico. Productivity in Rondout exceeded that in Neversink, but not that in Pepacton. Water transfers may have stimulated productivity in the Rondout, but inputs from Rondout Creek (which ranked moderately high in GPP/PAR among streams) or recycling of nutrients also may have elevated productivity there. Peng et al. (2004) noted that suspended particles decreased as water passed through the sequence of reservoirs for both the Catskill (Schoharie, Ashokan) and Delaware (Pepacton, Neversink, Rondout) chains, whereas silica-containing particles (diatom frustules) were greatest in Rondout. Our chlorophyll and productivity estimates are consistent with that observation. In the Croton System, GPP was lower in both the Cross River and Titicus reservoirs than in the Muscoot. GPP in the Muscoot was less than in the Amawalk, but GPP increased dramatically in New Croton.

Phytoplankton community respiration was slightly greater in EOH reservoirs than in WOH reservoirs (data not shown), but differences between reservoirs were not significant statistically

whether expressed per m^2 or per unit volume (ANOVAs, p = 0.82, p=0.61, respectively).

Gradients within reservoirs

GPP/PAR at each SS within a reservoir was expressed as a proportion of the GPP/PAR at the SS farthest from the major incoming tributary to that reservoir. An up- to down-reservoir gradient was observed each year in the mainstem of the Cannonsville during Phase I, with maximum rates occurring at SS1 near the West Branch Delaware River (Fig. 10.8A). In contrast measures in the Trout Creek Arm during Phase II were less than at SS 3, again the furthest SS from the Trout Creek. (Note that the down-reservoir SS was the same in both phases but different distances from the tributary being studied). An up- to down-reservoir gradient was observed in the New Croton in 2000 and 2002 but not during 2001 (when measurements were done 1–2 mo earlier than in the other years) (Fig. 10.8B). A strong up- to down-reservoir gradient was observed in 2000 in the Pepacton, with maximum rates occurring at SS1 near the East Branch Delaware River. This gradient was not observed in 2002, and data for SS2 were suspect in 2001 (Fig. 10.8C). During Phase II, gradients were weak except for an increasing trend in 2003 (a rainy year). Up- to down-reservoir gradients were weak in the Ashokan (except for a peak at SS2 in 2000; Fig. 10.8D). Weak decreasing trends occurred in Amawalk in 2003 and 2005 but a strong increasing trend occurred in 2004, when studied approximately 2 months earlier (Fig. 10.8E). Similar weak decreasing patterns occurred in the Cross River in 2003 and 2005, when studied in July, but GPP/PAR increased slightly at SS2 in 2004, when the reservoir was studied in October (Fig. 8 F). A decreasing pattern occurred in the Titicus only in 2005 (Fig. 10.8G).

Up- to down-reservoir gradients of chlorophyll *a* concentrations were observed in the Cannonsville during 2000 and 2002, with maximum concentrations at SS1 (Fig. 10.9A). As for GPP/PAR, the gradient in the Trout Creek arm of the reservoir was strong only in 2004. In New Croton, maximum chlorophyll *a* occurred at SS3 near the mouth of the Kisco River in 2002 (Fig. 10.9B). The maximum occurred at SS2 (farther down-reservoir) in 2000 and 2001, but never at the most down-reservoir station. In the Pepacton, maximum chlorophyll *a* occurred at either SS1 (closest to the East Branch Delaware River) in 2000 or at SS2 in 2002, but during Phase II of work gradients in chlorophyll were not strong any year (only 2003 shown) (Fig. 10.9C). In the Ashokan, chlorophyll *a* concentrations typically increased along the up- to down-reservoir gradient but decreased on 2 August 2000 and showed little change on 25 July 2001 (Fig. 10.9D). Chlorophyll in the Amawalk showed a decreasing trend only in 2003 (Fig. 10.9E). Titicus and Cross River reservoirs showed decreasing trends in 2003 and 2004 but an increasing trend in the Cross River and a peak at SS2 in the Titicus in 2005 (Fig. 10.9F and G).

Clear gradients in GPP/PAR or chlorophyll *a* did not occur at other times or in the other reservoirs. Thus, we conclude that in some, but not all, reservoirs the primary tributary has greatest influence on reservoir condition. In some of the smaller EOH reservoirs, the influence is less pronounced.

Co-inertia analysis

Co-inertia between the land-use PCA (14 variables) and the in-reservoir PCA (9 variables) expressed ~ 95% of the original F1 and F2 axes on the first two co-inertia axes. Concordance

between watershed-scale land-use and in-reservoir data matrices was highly significant (Monte Carlo permutation test [10,000 times], $p \leq 0.001$). Factor 1 (F1) accounted for 51.1% and 46.3% of the variability in the landuse or in-reservoir data matrices, respectively, and these axes were highly correlated with each other ($r = 0.85$). Factor 2 (F2) accounted for 28.3% and 13.9% of the variability in the landuse and in-reservoir matrices, respectively. However, landuse and in-reservoir variables loading on F2 were less well-correlated ($r = 0.67$).

In-reservoir productivity and water-chemistry variables contributing to the definition of the F1 axis (Fig. 10.10A) were DOC (24.5% of F1 definition), chlorophyll *a* (21%), GPP/m^2 (17%), photic zone depth (14%), and GPP/PAR (12%). Only photic-zone temperature (44%), DOC (26%), and GPP/m2 (19%) contributed substantially to the definition of F2. Landuse variables contributing to the definition of F1 (Fig. 10.10B) included % coniferous forest (15%), % other urban (13%), population density (11%), % residential (10%), watershed-area-normalized point-source discharges (10%), and % wetland (9.5%). Land use variables contributing to the definition of F2 included: watershed area (26%), % farmstead (16%), % wetland (13%), watershed-area-normalized point-source discharges (11%), and % cropland (9.5%).

Three primary patterns emerged from the plot of SSs on F1 and F2 (Fig. 10.10C). First, Cannonsville and all EOH (but Kensico) SSs were located along the negative F1 axis, and these SSs had highest PAR-normalized primary productivity, chlorophyll *a*, and shallowest photic zone depths. Primary land uses in these watersheds were urban (EOH) or agricultural and rural/urban (Cannonsville). The difference between Cannonsville and EOH reservoirs along the F2 axis was driven primarily by DOC (higher in EOH reservoirs and probably related to higher population densities and a naturally higher proportion of wetlands EOH), and the greater agriculture in the Cannonsville watershed. EOH reservoir SSs aligned along F2 with Titicus and Cross River SSs on the positive F2 end, Amawalk and Muscoot SSs near the origin, and New Croton SSs on the negative F2 end. It is also interesting that Cannonsville SS3 appears to be more eutrophic during Phase II, especially since P loadings to the reservoir have been reduced and it is now in compliance with TMDL requirements. Neversink and Schoharie SSs with low primary productivity and chlorophyll grouped to the right along F1. Second, Kenisco SSs clustered with SSs from WOH reservoirs. Kensico is an EOH reservoir that receives water transfers from WOH reservoirs. Third, SSs closest to contributing streams (e.g., SS1 in the Cannonsville and most EOH reservoirs, and SS3 in the New Croton) had the highest primary productivity and chlorophyll *a* and these SSs tended to have scores closer to the negative end of F1 than other SSs within a reservoir (i.e., SS scores on F1 decreased in a down-reservoir manner). Pepacton 4 and 7, draining the Tremper Kill and Coles Clove, along with P1, near the East Br. Delaware were the stations furthest to the left on the F1 axis for that reservoir.

Reservoir trophic condition

The Muscoot and Cannonsville ranked highest in µg chlorophyll/L and the Schoharie and Neversink lowest (Fig. 10.11). Concentrations in Neversink and Schoharie were significantly lower than the Cannonsville and EOH reservoirs with the exception of Cross and Kensico (ANOVA and Tukeys test, $p < 0.05$). Cannonsville chlorophyll was also greater than in the Pepacton. Chlorophyll concentration expressed on volumetric basis allows comparison of our data to trophic categories established for lakes. Lakes with chlorophyll *a* concentrations ≤3 µg/L are classified oligotrophic, and those with concentrations >10 µg L are classified eutrophic, with

a mesotrophic category between (Lampert and Sommer 1997). Accordingly, the Muscoot, Cannonsville, and Titicus would be considered eutrophic and the Amawalk and New Croton (where the standard deviation for chlorophyll *a* encompassed 10 µg/L) were close to the eutrophic–mesotrophic boundary (Fig. 10.11). In contrast, the Schoharie and Neversink were classified oligotrophic (although chlorophyll *a* standard deviations in the Neversink and Schoharie overlapped with the boundary for mesotrophic status). The remaining reservoirs were mesotrophic, with data for individual years for the Pepacton, Ashokan and Rondout spanning the oligotrophic-mesotrophic boundary. Thus, if categorization were based on data for individual years a reservoir might be categorized differently than when evaluated using multiple data points.

Although sampling date can influence results when sampling is limited, the 3-y mean chlorophyll *a* concentrations in the Muscoot and Cross River reservoirs agreed with those reported by NYC Department of Environmental Protection (DEP) for the entire growing season (May–October 1988–1996; National Research Council 2000). Concentrations in Cannonsville, Amawalk, New Croton, Ashokan and Rondout were within 10% of those means, while concentrations in Pepacton and Neversink were within 30% of the NYC DEP growing-season means. Concentrations in the Titicus and Schoharie were slightly <50% different from the NYC DEP growing-season means. Thus, our data provide reasonable estimates for this important reservoir variable in many reservoirs.

GPP per m^2 was extrapolated to a daily value to enable its use as another means of categorizing reservoir trophic status. Oligotrophic and eutrophic lakes are typified by daily primary productivity values <300 and >1000 mg C m^{-2} d^{-1}, respectively (Lampert and Sommer 1997). These values are approximately equivalent to 0.96 and 3.2 g O_2 m^{-2} d^{-1}, respectively, assuming a photosynthetic quotient of 1.2. Extrapolation of our hourly productivity measurements from the 4- to 6-h measurement period used in our study to total daily primary productivity probably yielded underestimates. Total daily rates ranged from 1.6–3.0 g $O_2 \cdot m^{-2} \cdot d^{-1}$ and from 0.75 – 1.6 g $O_2 \cdot m^{-2} \cdot d^{-1}$ in EOH and WOH reservoirs, respectively, except for Cannonsville and Kensico, with values of 2.9 and 1.1 g $O_2 \cdot m^{-2} \cdot d^{-1}$, respectively (Fig. 10.12). None of the reservoir means fell into the eutrophic category although data for individual years did for the New Croton, Cannonsville and Titicus. The means for the Schoharie and Neversink were in the oligotrophic category, but some data crossed the oligotrophic-mesotrophic boundary. Rondout, Ashokan and Kensico were close to the mesotrophic–oligotrophic boundary, but if the data for 2000 (obtained on a fairly overcast day) were excluded from the Rondout data, Rondout would have ranked closer to the Titicus. These results were generally consistent with classification according to chlorophyll *a* concentrations.

Dissolved O_2 profiles support these categorizations. A clinograde profile for one or more measurement dates (usually late in the season) for the Cannonsville and all of the EOH reservoirs suggest high rates of photosynthesis in the epilimnion and degradation of accumulated organic matter in the hypolimnion. This is the pattern characteristic of a eutrophic condition (Lampert and Sommer 1997). In addition, hypolimnetic dissolved O_2 saturation approached 50% at one or more SSs in the Ashokan, Pepacton, and Schoharie in one of the years of study. Negative heterograde patterns at some SSs in the Pepacton, Ashokan, and New Croton suggest that fine particulate organic matter may have accumulated at the thermocline where it underwent

decomposition. Positive heterograde profiles at a few SSs in the Rondout, Pepacton, Ashokan, and Neversink suggest phytoplankton accumulation at the thermocline and elevated primary productivity at that depth. Orthograde (or nearly so) profiles in the other reservoirs suggest a relatively low trophic status.

Chlorophyll *a* concentrations were entered into the Carlson's equation for TSI. Our TSI values agreed within 6% of the median values reported by NYC DEP (2002) for 1991 to 2000 for all reservoirs but the Kensico (12%), Muscoot (9%) and Titicus (10%) (Table 10.5). Thus, even with our limited sampling in each reservoir, our data present a reliable "snapshot" of reservoir condition. A TSI(CHL) >50 suggests an eutrophic condition, and a value <40 an oligotrophic condition, although Wetzel (2001) used a lower cut-off of 30 to differentiate between oligotrophy and mesotrophy. Most of the reservoirs had a TSI(CHL) value indicative of either a eutrophic (Cannonsville and all EOH but Kensico) or mesotrophic (3 WOH reservoirs) condition, although Schoharie and Neversink were oligotrophic. Note that the Cross River is at the mesotrophic – eutrophic boundary.

TSIs computed based on total P (TP) and Sechi Disc (SD) depth are reported in Table 10.5 as well. Comparison of TSIs can provide some indication of primary factors controlling trophic state of a water body. A chlorophyll-based TSI greater than a TP-based TSI is indicative of P limitation. The Schoharie was a clear exception to this, and similar but less strong exceptions were seen in Amawalk and Titicus, and perhaps the Muscoot. TSI(CHL) exceeded TSI(SD) for most reservoirs. Where TSI(CHL) > TSI(SD), and in the Neversink, where TSI(CHL) = TSI(SD), algae are presumed to dominate light attenuation but suspended material was predominately larger particles which allowed for greater water clarity than expected based on chlorophyll. In the Schoharie and Ashokan, the TSI(SD) exceeded TSI(CHL), suggesting that non-algal particles played a greater role in light attenuation.

A plot of [TSI(CHL) – TSI(SD)] vs. [TSI(CHL) – TSI(TP)] (after Carslon 1992, Wetzel 2001) helps to illustrate deviations from expected TSIs based on chlorophyll (Fig. 10.13). The position of a reservoir on the y-axis indicates the relative importance of P limitation on algal biomass. Position on the x-axis provides information concerning particle size, the occurrence of zooplankton grazing, and small inorganic particle turbidity, with a location toward the right of the figure indicative of greater water clarity than would be predicted from chlorophyll concentration and a location to the left indicating light attenuation from non-algal particles as well. Most reservoirs were located in the upper right quadrat, suggesting they were P limited but that many had greater water clarity than would be expected from chlorophyll concentrations (Fig. 10.13). P limitation appeared to exert greater control in many WOH reservoirs (and the Kensico) than in EOH reservoirs, especially Titicus, Amawalk and Muscoot. The Cannonsville was closer to the Cross River and New Croton in this analysis than it was to the other WOH reservoirs. The Schoharie had the greatest non-algal turbidity, and algal growth there is perhaps the most susceptible to limitation from a factor other than phosphorus. This conclusion supports the findings of Peng et al. (2004), who reported greater turbidity from a high particle load in the Schoharie and our own field observations of silt at several substations in Schoharie. Along with Schoharie, the Titicus, Amawalk Muscoot and Ashokan were lower on the y-axis than the other reservoirs, which suggests greater potential for limitation by something other than phosphorus.

In summary, despite limited sampling, rankings based on chlorophyll *a* and primary productivity indicated a range of reservoir conditions from eutrophic to oligotrophic. In general, trophic-state rankings based on several different parameters were in agreement. Linkages between reservoir and influent streams were evidenced by gradients of productivity or chlorophyll *a* in some reservoirs, and as might be expected were most pronounced on larger systems. Co-inertia analysis showed that GPP per area and GPP normalized for PAR were positively related to agricultural land use in and chlorophyll concentrations to urban land use, and negatively related to percent forested land use. Correlation analyses corroborated these findings. Thus, ongoing watershed management programs (Blaine et al. 2006) that enhance riparian forest cover and minimize nutrient loading from nonforested landscapes are ways to reduce reservoir productivity and algal biomass. The differences in patterns of K_d and chlorophyll *a* concentrations as water moves through the series of reservoirs, and the pattern of differences in TSIs based on chlorophyll, phosphorus and Secchi Disc depths suggests that while water clarity improves, the potential for a build-up of algae remains, and that the generally good water clarity in most reservoirs is related to a larger size of algal particles and/or removal of algae by zooplankton grazing.

Literature Cited

APHA (American Public Health Association). 1998. Standard methods for the evaluation of water and wastewater. 20th edition. American Public Health Association, American Water Works Association, and Water Environment Federation, Washington, DC.

Arscott, D. B., C. L. Dow, and B. W. Sweeney. 2006. Landscape template of New York City's drinking-water-supply watersheds. Journal of the North American Benthological Society 25:000–000.

Auer, M. T., and B. E. Forrer. 1998. Development and parameterization of a kinetic framework for modeling light- and phosphorus-limited phytoplankton growth in Cannonsville Reservoir. Lake and Reservoir Management 14:290–300.

Blaine, J. G., B. W. Sweeney, and D. B. Arscott. 2006. Enhanced source-water monitoring for New York City: historical framework, political context, and project design. Journal of the North American Benthological Society 25:000–000.

Bott, T. L., D. M. Montgomery, J. D. Newbold, C. L. Dow, and D. B. Arscott. 2006. Ecosystem metabolism in streams of the Catskill Mountains (Delaware and Hudson River watersheds) and Lower Hudson Valley. Journal of the North American Benthological Society 25:000–000.

Carlson, R. E. 1977. A trophic state index for lakes. Limnology and Oceanography 22:361–369.

Carlson, R. E. 1992. Expanding the trophic state concept to identify non-nutrient limited lakes and reservoirs, pp. 59-71. In: Proceedings of a National Conference on Enhancing the States' Lake Management Programs. Monitoring and Lake Impact Assessment, Chicago.

Dolédec, S., and D. Chessel. 1994. Co-inertia analysis: an alternative method for studying species-environment relationships. Freshwater Biology 31:277–294.

Dow, C. L., D. B. Arscott, and J. D. Newbold. 2006. Relating major ions and nutrients to watershed conditions across a mixed-use, water-supply watershed. Journal of the North American Benthological Society 25:000–000.

Effler, S. W., and A. P. Bader. 1998. A limnological analysis of Cannonsville Reservoir, NY. Lake and Reservoir Management 14:125–139.

Effler, S. W., and D. A. Matthews. 2004. Sediment resuspension and drawdown in a water supply reservoir. Journal of the American Water Resources Association 40:251–264.

Kaplan, L. A., J. D. Newbold, and D. J. Van Horn. 2006. Organic matter transport in New York City drinking-water-supply watersheds. Journal of the North American Benthological Society 25:000–000.

Lampert, W., and U. Sommer. 1997. Limnoecology: the ecology of lakes and streams. Oxford University Press, New York.

Lorenzen, C. J. 1967. Determination of chlorophyll and pheo-pigments: spectrophotometric equations. Limnology and Oceanography 12:343–346.

National Research Council. 2000. Watershed management for potable water supply: assessing the New York City strategy. National Academy Press, Washington, DC.

Newbold, J. D., T. L. Bott, L. A. Kaplan, C. L. Dow, L. A. Martin, D. J. Van Horn, and A. A. de Long. 2006. Uptake of nutrients and organic C in streams in New York City drinking-water-supply watersheds. Journal of the North American Benthological Society 25:000–000.

NYC DEP (New York City Department of Environmental Protection). 2002. 2001 watershed water quality annual report. Division of Drinking Water Quality Control, New York City Department of Environmental Protection, New York. (Available from: http://www.ci.nyc.ny.us/html/dep/html/wsstate.html)

Peng, F., D. L. Johnson, and S. W. Effler. 2004. Characterization of inorganic particles in selected reservoirs and tributaries of the New York City water supply. Journal of the American Water Resources Association 40:663–676.

SWRC (Stroud Water Research Center). 2003. Water quality monitoring in the source water areas for New York City: an integrative approach. A report on the first phase of monitoring. Stroud Water Research Center, Avondale, Pennsylvania. (Available from: http://www.stroudcenter.org/research/nyproject.htm)

Thioulouse, J., D. Chessel, S. Dolédec, and J.-M. Olivier. 1997. ADE-4: a multivariate analysis and graphical display software. Statistics and Computing 7:75–83.

Wetzel, R. G. 2001. Limnology: Lake and River Ecosystems, 3rd edition. Academic Press, San Diego.

Wetzel, R. G., and G. E. Likens. 1991. Limnological analyses. 2nd edition. Springer, New York.

Table 10.1. GPS coordinates for sampling substations on reservoirs.

Reservoir	Substation Number	Latitude	Longitude	Maximum Position Dilution of Precision	Horizontal Precision (95% CI) m
		decimal degrees			
Kensico	1	41.110546276	-73.748599160	1.9	0.4
	2	41.093226190	-73.748125420	3.0	0.5
	3	41.088159781	-73.757836225	2.4	0.7
New Croton	1	41.232320183	-73.837969887	3.9	0.5
	2	41.232426089	-73.787510401	2.0	0.4
	3	41.240035883	-73.753733103	2.6	0.5
Ashokan	1	41.975325085	-74.256829980	2.2	0.4
	2	41.967465317	-74.251666610	3.3	0.5
	3	41.948185175	-74.224774362	3.0	0.4
Rondout	1	41.821500909	-74.462172577	2.8	0.4
	2	41.832797499	-74.481426862	4.7	0.6
	3	41.820963789	-74.475321682	2.8	0.5
Neversink	1	41.836900881	-74.650095294	2.0	0.4
	2	41.833466986	-74.663798499	2.4	0.4
	3	41.845261905	74.668146539	3.1	0.5
Pepacton	1	42.087044780	-74.801450249	2.6	0.4
	2	42.095078110	-74.837208565	4.7	0.7
	3	42.081926771	-74.874659985	2.5	0.5
	4	42.101354864	-74.827558108	2.8	0.3
	5	42.074321967	-74.837316006	2.2	0.3
	6	42.075005506	-74.887725400	2.4	0.3
	7	42.102170222	-74.901478472	2.2	0.3
Cannonsville	1	42.093092755	-75.260166084	4.5	0.4
	2	42.109542329	-75.266740278	1.9	0.4
	3	42.102088545	-75.297650117	3.1	0.4
	4	42.097968653	-75.318630711	2.2	0.4
	5	42.123510722	-75.309177431	4.3	0.3
Schoharie	1	42.385318850	-74.438261862	2.0	0.4
	2	42.368707917	-74.441444496	2.6	0.4
	3	42.355735199	-74.442608665	2.7	0.4
Muscoot	1	41.278224725	-73.691015831	2.0	0.4
	2	41.268159975	-73.691927569	3.1	0.7
	3	41.271916797	-73.713454261	2.7	0.5
Amawalk	1	41.317636400	-73.742120483	3.0	0.5
	2	41.312593142	-73.739958317	4.8	0.8
	3	41.296617947	-73.747771122	6.0	0.9
Titicus	1	41.331221803	-73.613175497	4.8	0.8
	2	41.331538817	-73.627928011	3.6	0.6
	3	41.327679661	-73.642325836	3.9	0.6
Cross River	1	41.252777778	-73.621666667	2.4	0.3
	2	41.253888889	-73.631944444	4.1	0.9
	3	41.262500000	-73.654722222	4.3	0.5

Table 10.2. Physical and chemical characteristics of 12 reservoirs in the New York City source-water watersheds west of Hudson River (WOH) and east of Hudson River (EOH). Historical data for reservoir storage capacity and water residence time were obtained from the National Research Council (2000) except as indicated. Water chemistry, light, and temperature data are means of data collected on 3 -6 measurement dates during the summers between 2000 and 2005. TDP = total dissolved P, SRP = soluble reactive P, TA = total alkalinity, PAR = photosynthetically active radiation, Ashokan = west basin of the Ashokan Reservoir.

Reservoir	Storage capacity (10^6 m^3)	Water residence time (mo.)	NH_4-N	NO_3-N	TDP	SRP	DOC	TA	hourly mean PAR during measurements (mol quanta)	mean °C	Measurement date (Julian Day) 2000	2001	2002	2003	2004	2005
					(mg/L)											
WOH																
Ashokan-W	178.7[a]	2.4[a]	0.017	0.096	0.006	0.005	2.17	10.47	3.13	21.09	19-Sep (262)	28-Aug (240)	26-Jun (177)			
Cannonsville[c]	366.1[a]	5.2[a]	0.015	0.083	0.004	0.002	2.83	16.2	4.69	24.33	9-Aug (221)	23-Aug (235)	17-Jul (198)			
Cannonsville[d]			0.012	0.039	0.004	0.002	2.29	13.8	3.82	23.29				21_Aug (233)	26-Aug (238)	24-Aug (236)
Neversink	134.2[a]	5.0[a]	0.006	0.099	0.003	0.001	1.95	2.41	4.42	21.93	13-Sep (256)	12-Jul (193)	1-Aug (213)	7-Aug (219)	4-Aug (216)	3-Aug (215)
Pepacton[e]	543.9[a]	8.5[a]	0.004	0.012	0.003	0.002	1.97	10.97	4.04	22.08	17-Aug (229)	9-Aug (221)	2-Jul (183)	25-26-Sep (268-269)	15-16-Sep (258-259)	21-22-Sep (264-265)
Pepacton[f]			0.003	0.007	0.002	0.002	1.99	10.28	3.14	20.69				25-26-Sep (268-269)	15-16-Sep (258-259)	21-22-Sep (264-265)
Rondout	189.4[a]	1.7[a]	0.008	0.105	0.004	0.002	2.11	8.91	3.66	21.2	26-Jul (207)	10-Jul (191)	30-Jul (211)			
Schoharie	74.2[a]	1.2[a]	0.011	0.062	0.003	0.001	2.17	17	5.43	21.92	6-Sep (249)	31-Jul (212)	20-Jun (171)			
EOH																
Amawalk	22.7[b]	7.2[b]	0.006	0.005	0.004	0.001	4.82	42.77	4.49	23.01				11-Sep (254)	8-Jul (189)	8-Sep (251)
Cross River	34.1[b]	15[b]	0.009	0.008	0.003	0.002	4.23	33.75	30.8	21.14				10-Jul (191)	1-Oct (274)	7-Jul (188)
Kensico	115.8[a]	0.7[a]	0.005	0.075	0.003	0.001	2.00	12.5	3.74	20.79	23-Aug (235)	20-Jun (171)	5-Sep (248)			
Muscoot	18.9[b]	0.6[b]	0.023	0.127	0.005	0.002	4.11	55.33	2.87	21.24				9-Oct (282)	21-Aug (233)	13-Jul (194)
New Croton	71.9[a]	2.4[a]	0.007	0.043	0.004	0.002	4.33	51.28	4.73	24.94	30-Aug (242)	3-Jul (184)	14-Aug (226)			
Titicus	26.5[b]	11.3[b]	0.009	0.007	0.005	0.002	4.26	82.41	2.41	18.13				24-Oct (297)	22-Sep (265)	29-Jun (180)

[a] from NAS (2000)

[b] from Westchester County (2002) Comprehensive Mosquito-Borne Disease Surveillance and Control Plan, Generic Environmental Impact Statement, February, 2002.

[c] Cannonsville- W. Br. Delaware main stem

[d] Cannonsville- Trout Creek arm

[e] Pepacton- 3 stations for six years

[f] Pepcton- 3 new stations for 3 years

Table 10.3. Water column, photic zone, Secchi disc depths and light extinction coefficient (mean of values computed for 1% and 10% intensities) for each substation within each reservoir (3- or 6-y means).

Reservoir	Sub-station	Years n	Water depth (m) mean	Water depth (m) SD	Photic zone depth (m) mean	Photic zone depth (m) SD	Mean Light Extinction coefficient (η)	Secchi Disc depth (m) mean	Secchi Disc depth (m) SD
WOH									
Ashokan-W	1	3	10.8	1.4	6.0	2.2	0.639	1.93	0.95
	2	3	20.0	1.7	7.4	1.2	0.572	2.33	0.81
	3	3	20.0	3.4	8.6	1.7	0.534	2.58	0.46
reservoir mean			**17.0**		**7.3**		**0.582**	**2.28**	
Cannonsville	1	3	12.1	3.7	5.9	1.6	0.856	1.68	0.60
	2	3	14.6	2.8	6.8	2.2	0.770	2.55	1.48
	3	6	22.0[a]	3.8	7.5	1.7	0.647	3.02	1.56
	4	3	24.5	5.2	8.6	1.9	0.571	3.42	1.84
	5	3	15.3	5.0	8.0	2.4	0.629	3.50	2.17
reservoir mean			**16.6**		**7.4**		**0.695**	**2.83**	
Neversink	1	6	18.1	1.5	10.2	2.3	0.466	4.75	1.29
	2	6	19.0	3.3	10.1	2.2	0.442	4.60	1.1
	3	6	18.8	3.2	9.5	2.1	0.456	4.10	0.98
reservoir mean			**18.6**		**9.9**		**0.455**	**4.48**	
Pepacton	1	6	18.7	3.2	8.9	2.1	0.541	2.95	0.86
	2	3	16.9	0.1	10.1	2.3	0.447	3.88	1.59
	3	6	20.0	5.6	10.1	1.5	0.461	3.80	0.54
	4	3	17.7	5.0	7.7	1.8	0.636	2.92	0.58
	5	3	18.0	5.0	8.9	0.9	0.523	3.35	0.38
	6	3	21.4	6.5	10.0	0.5	0.466	4.17	0.52
	7	3	19.1	6.0	9.3	0.3	0.504	3.50	0.25
reservoir mean			**18.8**		**9.3**		**0.511**	**3.51**	
Rondout[b]	1	3	22.0	1.7	9.9	1.6	0.460	3.63	0.53
	2	3	16.3	0.5	10.5	0.4	0.430	4.00	0.35
	3	3	18.4	0.6	10.6	0.9	0.427	4.25	0.71
reservoir mean			**18.9**		**10.3**		**0.439**	**3.96**	
Schoharie	1	3	23.0	1.7	7.7	1.8	0.646	2.63	0.53
	2	3	17.3	2.3	8.3	1.5	0.578	3.13	1.24
	3	3	14.7	2.9	7.6	0.8	0.616	3.00	1.06
reservoir mean			**18.3**		**7.9**		**0.613**	**2.92**	
EOH									
Amawalk	1	3	7.9	0.8	6.3	0.7	0.747	2.15	0.41
	2	3	12.2	0.9	6.6	0.6	0.721	2.33	0.52
	3	3	19.6	1.3	7.5	1.0	0.625	2.43	0.12
reservoir mean			**13.3**		**6.8**		**0.697**	**2.30**	
Cross River	1	3	12.7	0.1	6.7	0.5	0.659	3.00	0.43
	2	3	16.8	0.3	7.0	0.9	0.606	3.42	0.38
	3	3	20.4	1.2	7.2	1.1	0.624	3.50	0.75
reservoir mean			**16.6**		**6.9**		**0.629**	**3.31**	
Kensico	1	3	12.9	0.1	9.4	1.5	0.493	3.38	0.18
	2	3	14.9	1.6	10.5	0.7	0.468	3.63	0.18
	3	3	19.7	0.5	10.4	0.3	0.439	3.40	0.14
reservoir mean			**15.8**		**10.1**		**0.467**	**3.47**	
Muscoot	1	3	9.0	0.1	4.8	0.9	0.943	2.92	1.01
	2	3	5.7	0.6	4.6	0.5	0.958	2.43	0.81
	3	3	6.1	0.2	4.9	0.4	0.900	2.70	1.27
reservoir mean			**7.0**		**4.8**		**0.934**	**2.68**	
New Croton	1	3	20.0	1.7	7.0	0.9	0.706	2.88	0.18
	2	3	11.7	0.5	6.3	0.4	0.730	2.88	0.53
	3	3	10.3	0.5	5.8	0.4	0.788	2.75	0.71
reservoir mean			**14.0**		**6.4**		**0.741**	**2.84**	
Titicus	1	3	6.6	0.2	5.1	1.0	0.940	2.33	1.04
	2	3	17.0	0.1	6.5	2.2	0.759	2.58	1.04
	3	3	10.8	1.8	6.2	1.1	0.757	2.58	1.04
reservoir mean			**11.4**		**5.9**		**0.819**	**2.50**	

a - Depth for 2004 excluded, substation moved into shallower water for anchoring.

b - Data for 2000 excluded for all but mean water depths due to high turbidity from scouring rains a few weeks earlier. Photic zone depth of 5 m at all substations and and average η = 0.941 in 2000.

Table 10.4. Multiple linear regression equations for chlorophyll *a* and primary productivity (Kensico excluded) in 11 reservoirs in the New York City source-water watersheds. GPP = gross primary productivity $m^{-2} h^{-1}$, CR= community respiration $m^{-2} h^{-1}$ PAR = photosynthetically active radiation, temp = temperature, chl*a* = chlorophyll *a*, SRP= soluble reactive P, TDP = total dissolved P, TA = total alkalinity, K_d= light extinction coefficient, β = standardized partial regression coefficients (given in order of variables in equation).

Dependent variable	Equation	Variables included in analysis	Adjusted R^2	*p*
$\log_{10}$(chl*a*)	= 0.915 $\log_{10}$(GPP) - 0.451 $\log_{10}$(PAR) + 2.355 β = 0.903, -0.234	Temp, PAR, depth of photic zone, GPP, CR, NH_4-N, NO_3-N, SRP, TDP, TA, K_d	0.93	<0.0001
$\log_{10}$(GPP)	= 0.784 $\log_{10}$(chl*a*) + 1.383 $\log_{10}$(temp) + 0.087 $\log_{10}$(TA) – 3.756 β = 0.794, 0.261, 0.201	Temp, PAR, depth of photic zone, chl*a*, NH_4-N, NO_3-N, SRP, TDP, TA, K_d	0.95	0.0001

Table 10.5. Carlson's Trophic State Indices (TSI) computed using chlorophyll *a*, Secchi disc depth, and total P, TSI(CHL), TSI(SD), and TSI(TP), respectively. An index <40, 40-50, and >50 indicates oligotrophic , mesotrophic, and eutrophic conditions, respectively.

Reservoir	TSI(CHL)	TSI(SD)	TSI(TP)*	TSI ranking
Muscoot	53.9	46.7	53.5	C=TP>SD
Cannonsville	52.2	46.7	46.0	C>SD>TP
Amawalk	52.1	48.1	52.8	TP>C>SD
Titicus	51.6	47.6	55.1	TP>C>SD
New Croton	51.5	45.1	47.2	C>TP>SD
Cross	50.1	42.9	44.1	C>TP>SD
Kensico	46.2	42.1	35.5	C>SD>TP
Rondout	45.2	40.3	35.7	C>SD>TP
Pepacton	44.2	42.3	34.8	C>SD>TP
Ashokan	43.5	48.8	41.8	SD>C>TP
Neversink	38.7	38.8	28.7	C=SD>TP
Schoharie	35.5	45.0	48.5	TP>SD>C

*TSI(TP) calculated from total P values reported by NYC DEP (2002). The mean of values from 2000 and 2001 was used (all data as µg/L) for Cannonsville (18.3), Amawalk (29.2), Cross River (16.0), Kensico (8.8), Rondout (8.9), Pepacton (8.4), and Neversink (5.5). When the mean 2000-2001 mean differed from the 1997-2001 mean by more than 1.5 µg/L, the 5y mean was used instead as follows: Muscoot (30.7), Titicus (34.4), New Croton (19.9), and Ashokan (13.6).

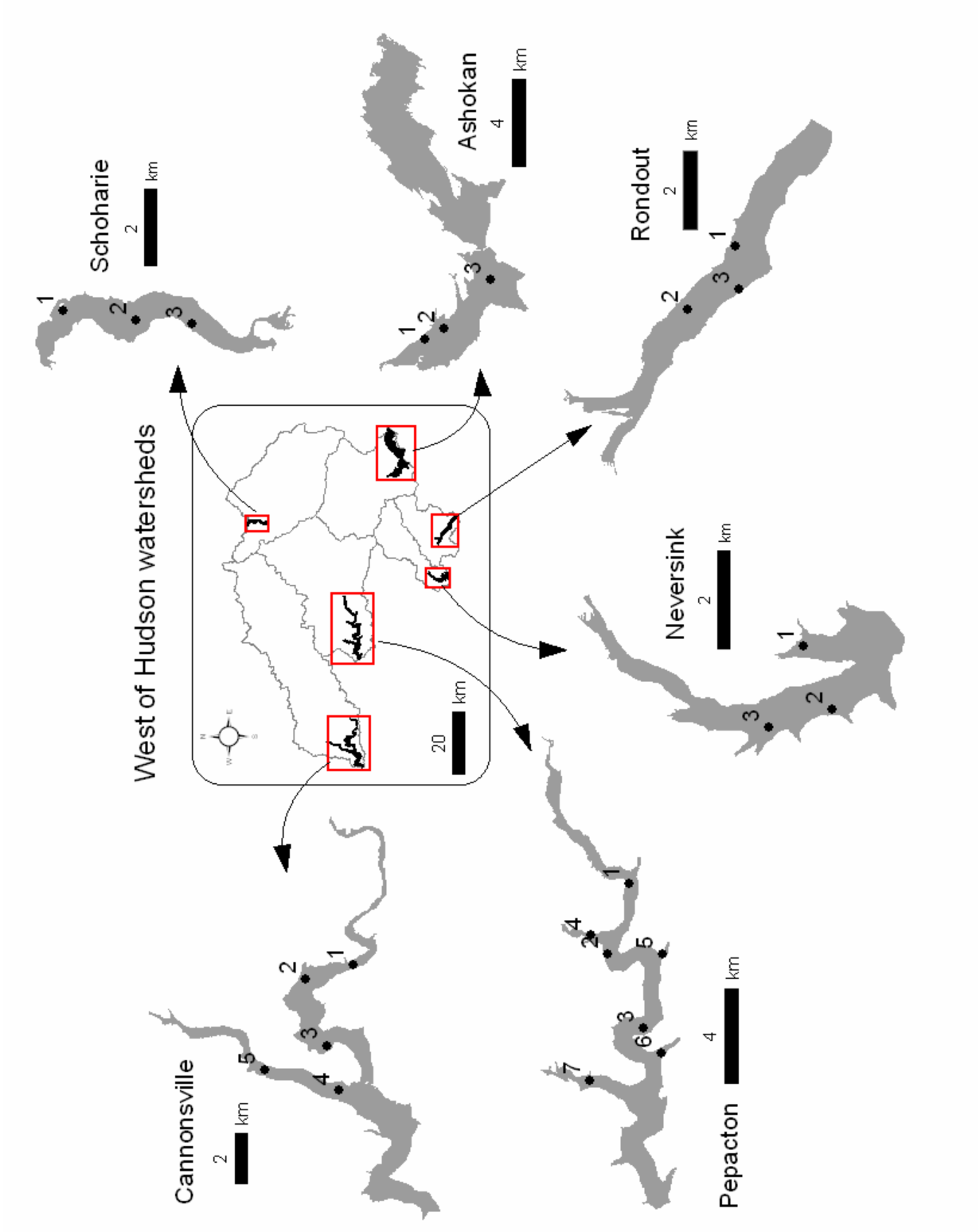

Figure 10.1. Reservoirs in West of Hudson (WOH) watersheds and substation locations in each reservoir.

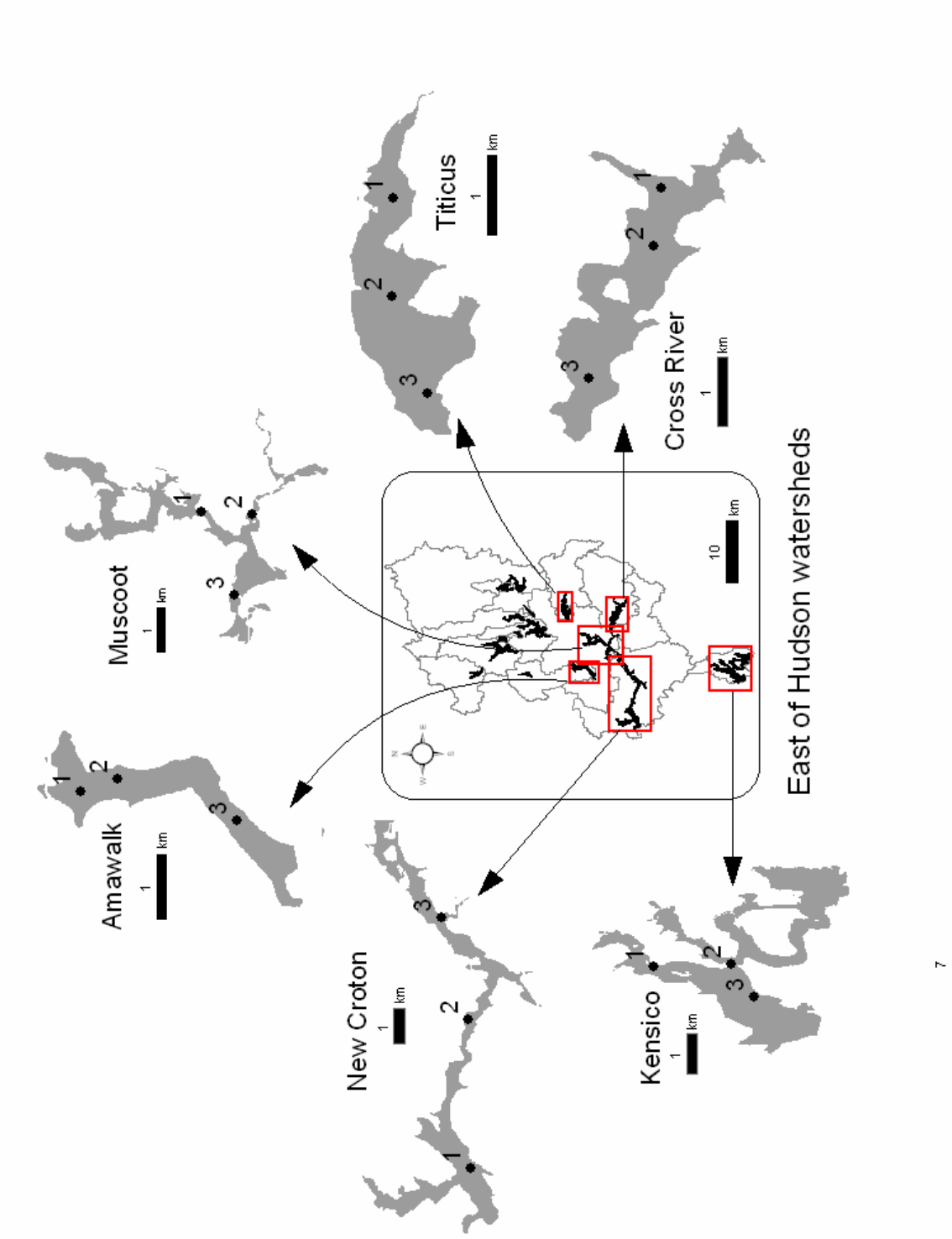

Figure 10.2. Reservoirs in East of Hudson (EOH) watersheds and substation locations in each reservoir.

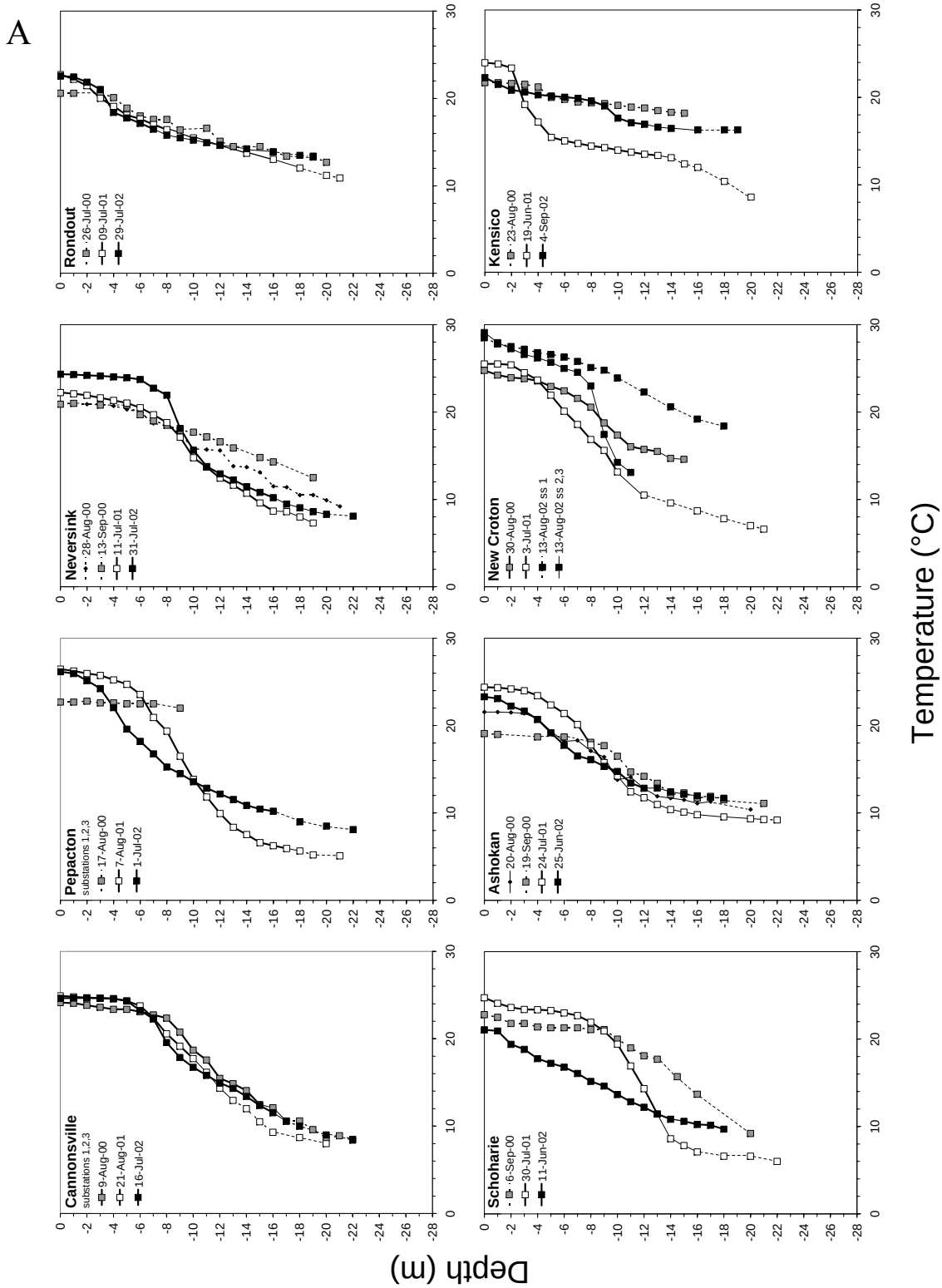

Figure 10.3. Temperature profiles in Phase I (A) and Phase II (B) reservoirs. Data are shown as means of 3 substations [SS] except where data from shallow water SSs no longer apply and n=1 or 2 (dashed lines). No data taken below 9 m in the Pepacton in 2000.

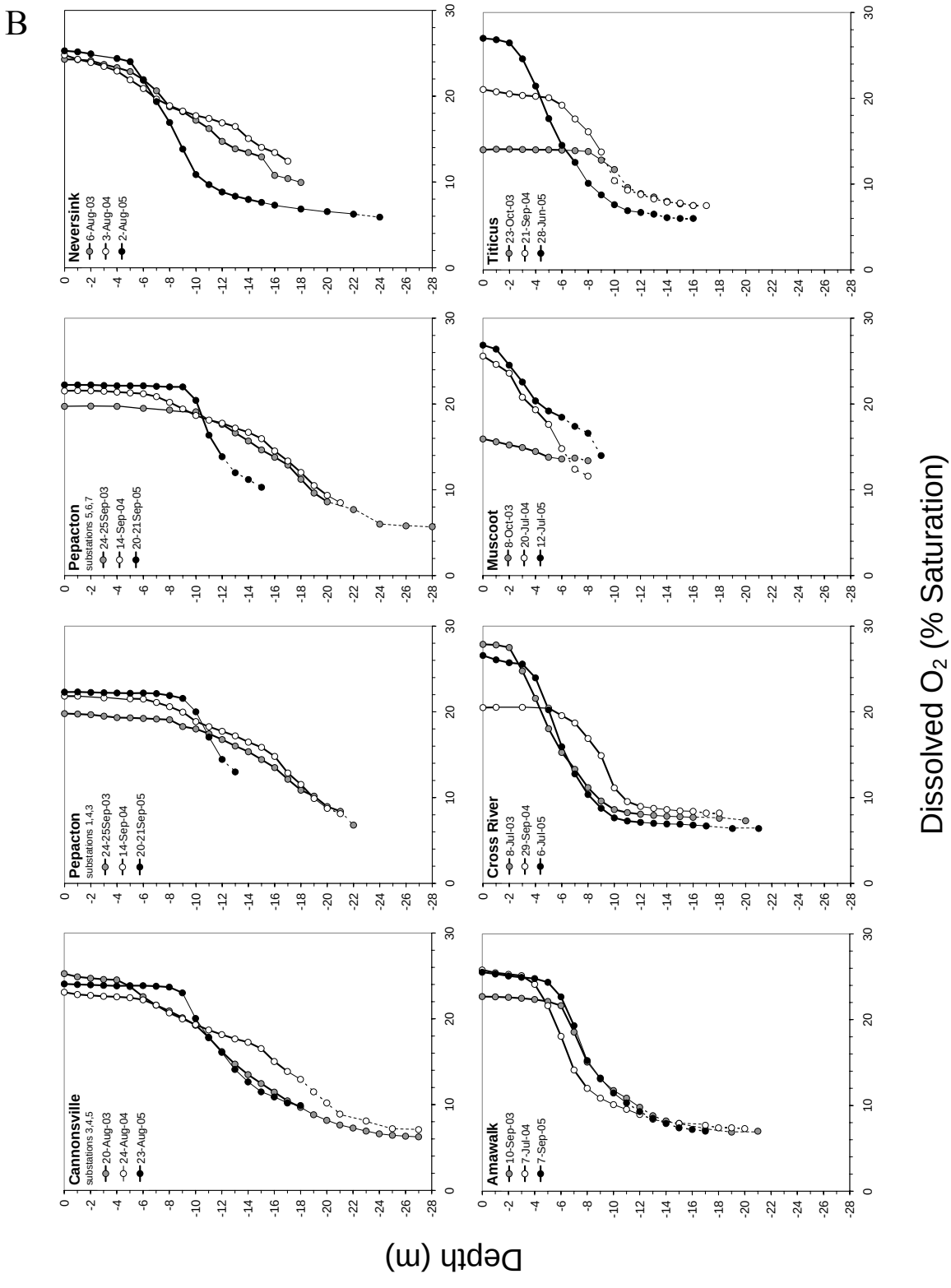

Figure 10.3. (Continued)

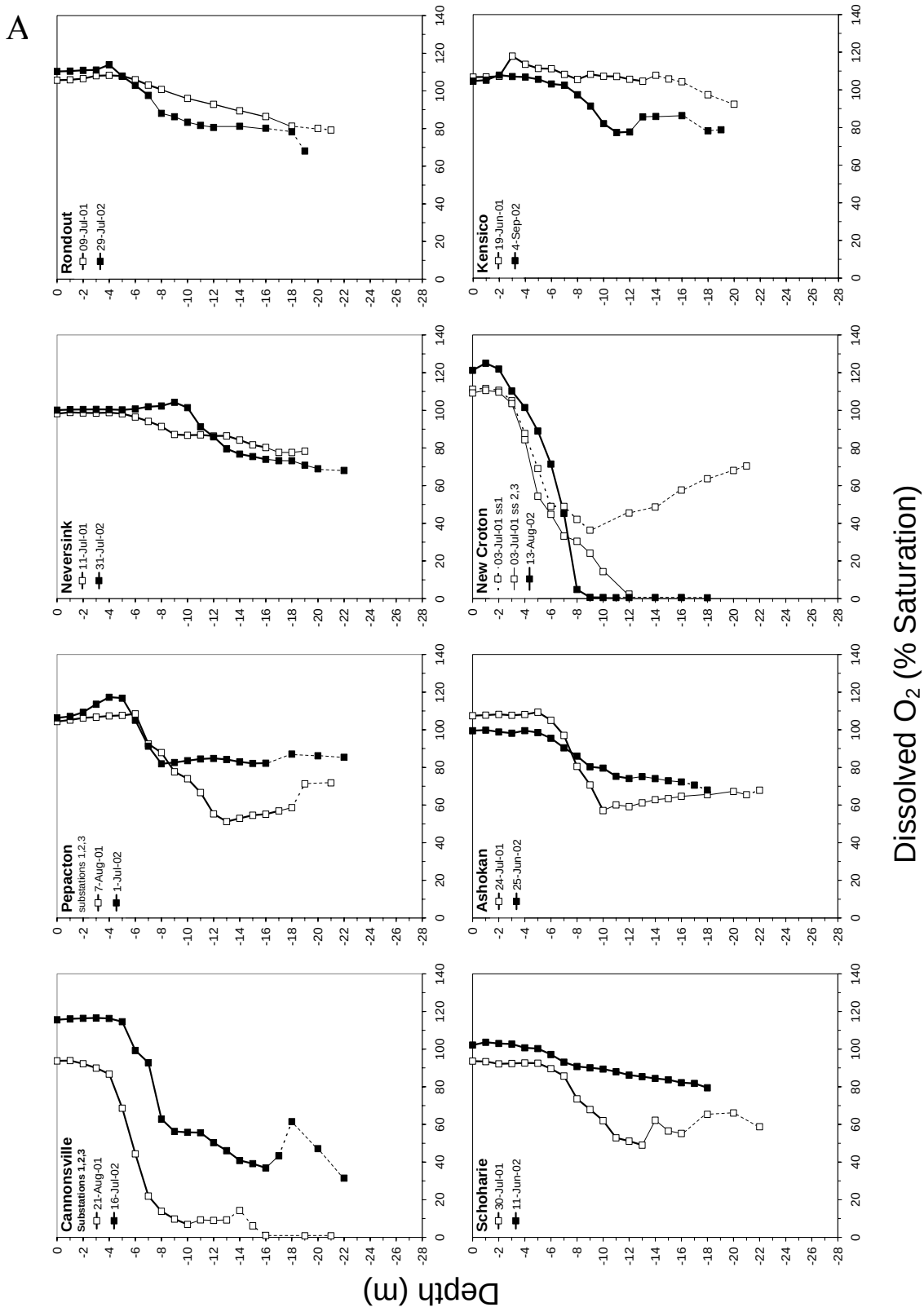

Figure 10.4. Dissolved O_2 profiles (% saturation) for Phase I reservoirs (A, 2001 & 2002) and Phase II (2003-2005) reservoirs (B). Data are the mean of 3 substations [SS], except where data from shallow-water SSs no longer apply and n=1 or 2 (dashed lines).

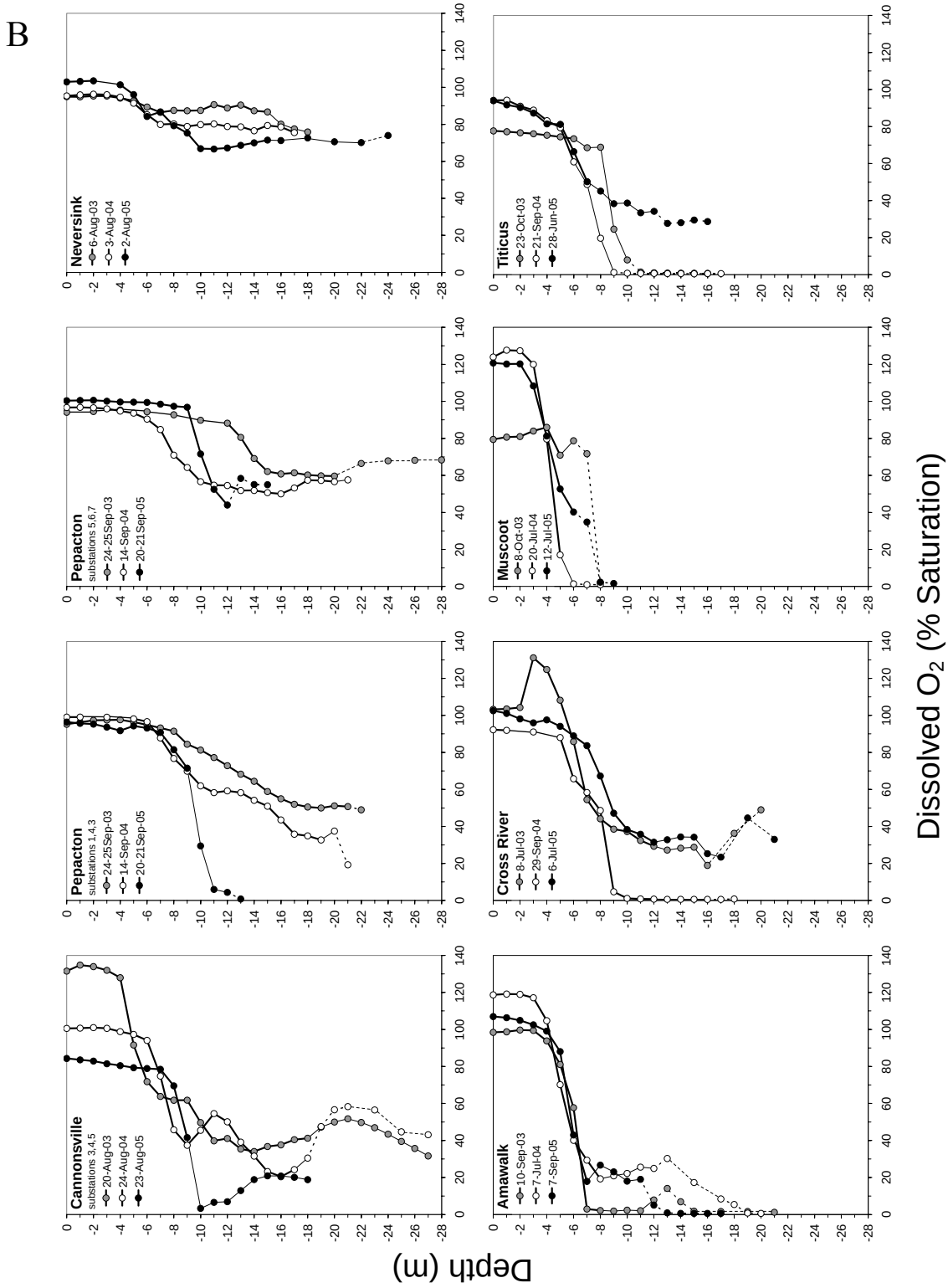

Figure 10.4. (Continued)

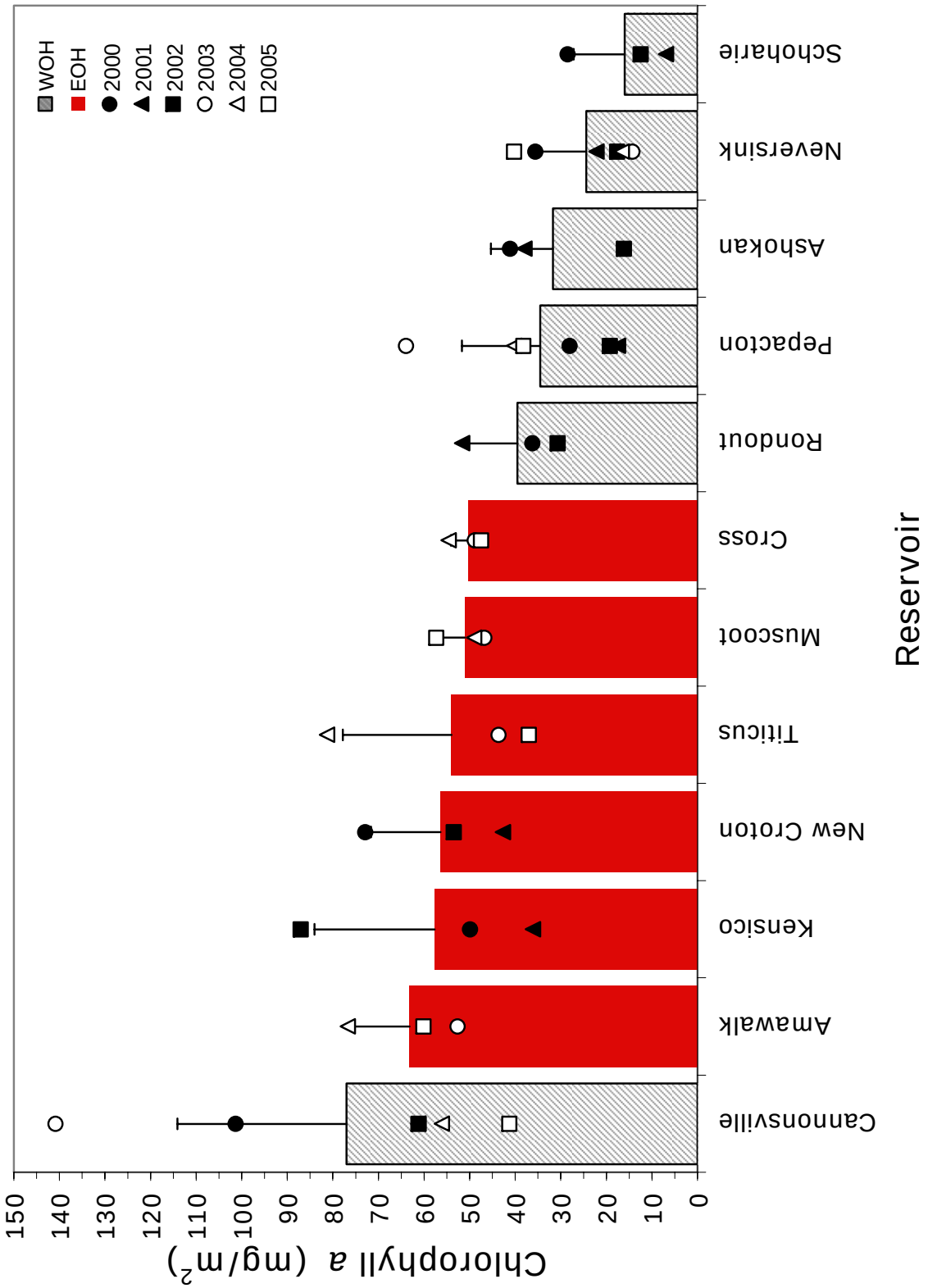

Figure 10.5. Ranking of reservoirs based on 3- or 6-y mean (+ 1SD) chlorophyll *a* concentrations with data for individual years shown by symbols.

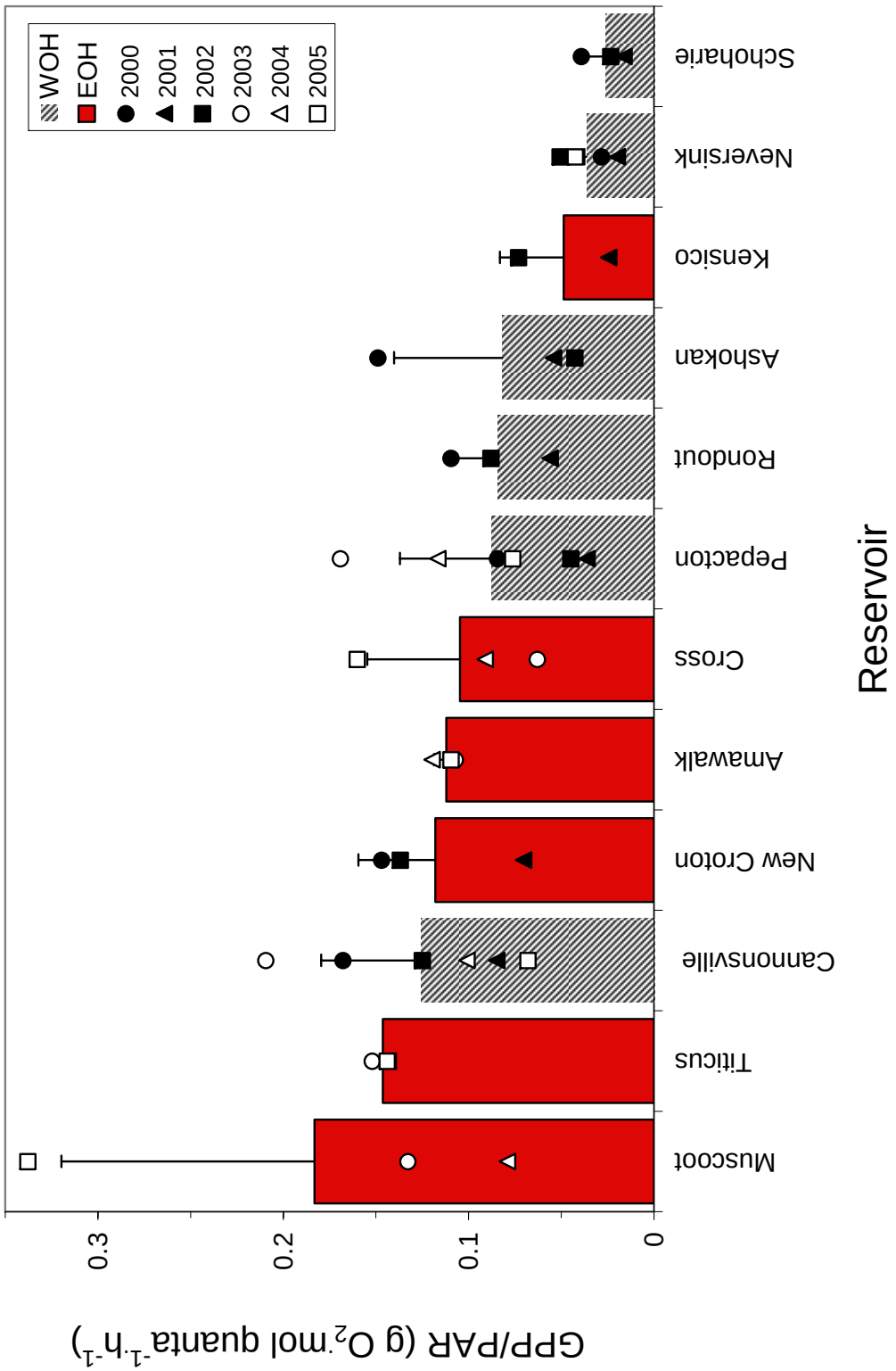

Figure 10.6. Ranking of reservoirs based on 3- or 6-y mean (+ 1SD) light normalized gross primary productivity (GPP/PAR) with data for individual years shown by symbols. Data for Kensico in 2000 and Neversink in 2003 deleted because of low PAR and lost PAR data, respectively.

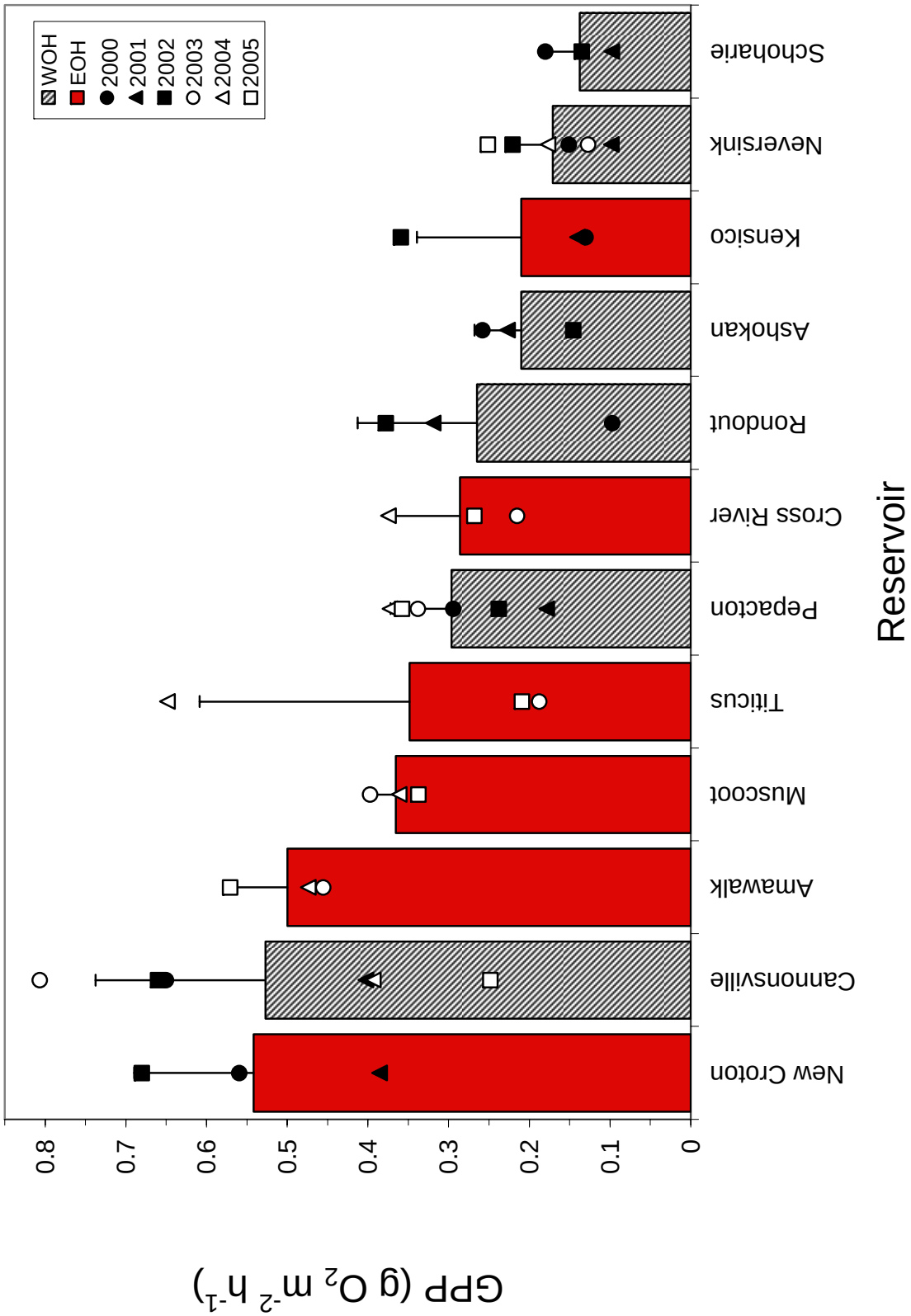

Figure 10.7. Ranking of reservoirs based on 3- or 6-y mean values of gross primary productivity (GPP) with data for individual years shown by symbols.

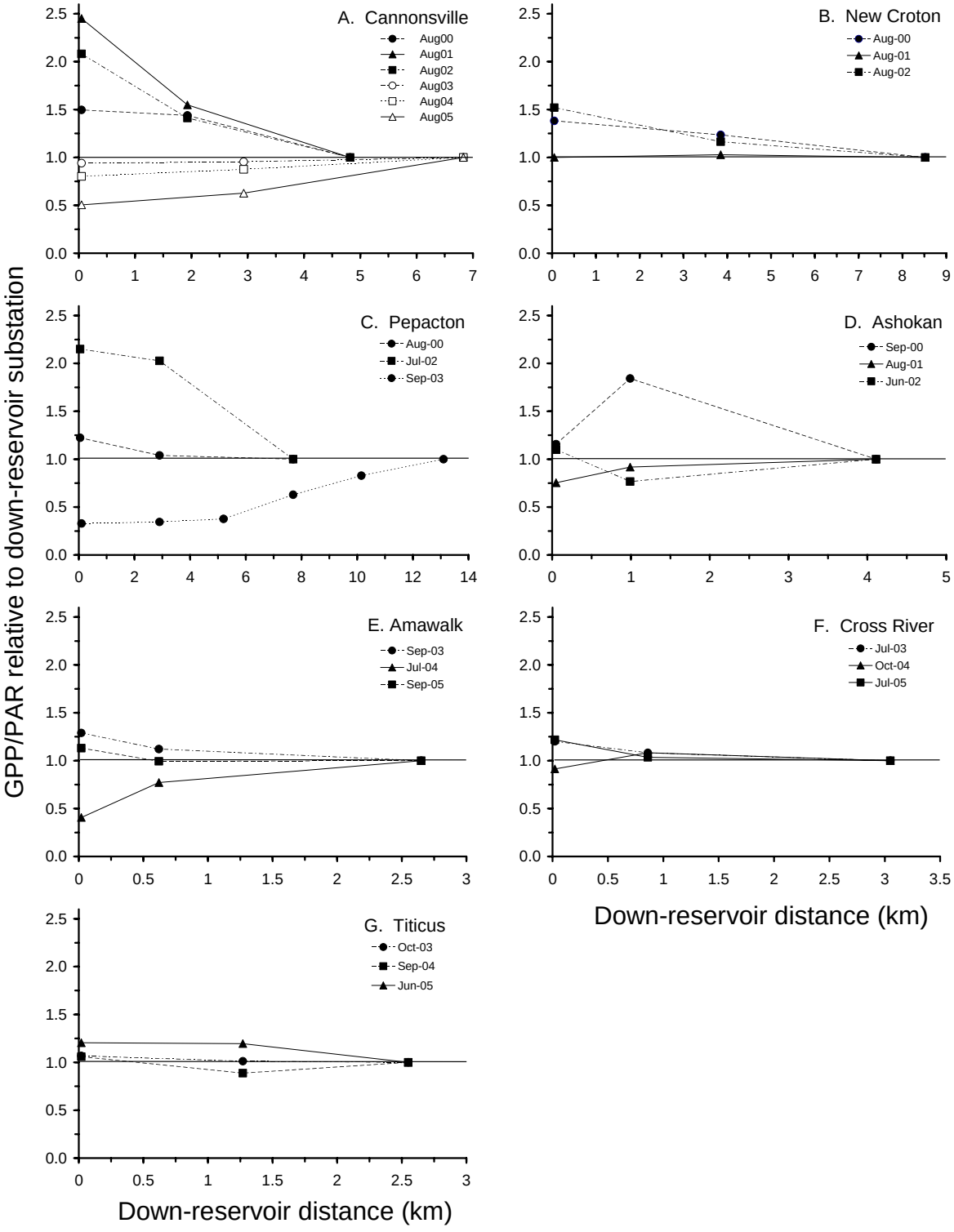

Figure 10.8. Longitudinal trends in light-normalized gross primary productivity (GPP/PAR) when data are expressed relative to the respective value at the farthest down-reservoir substation (SS).

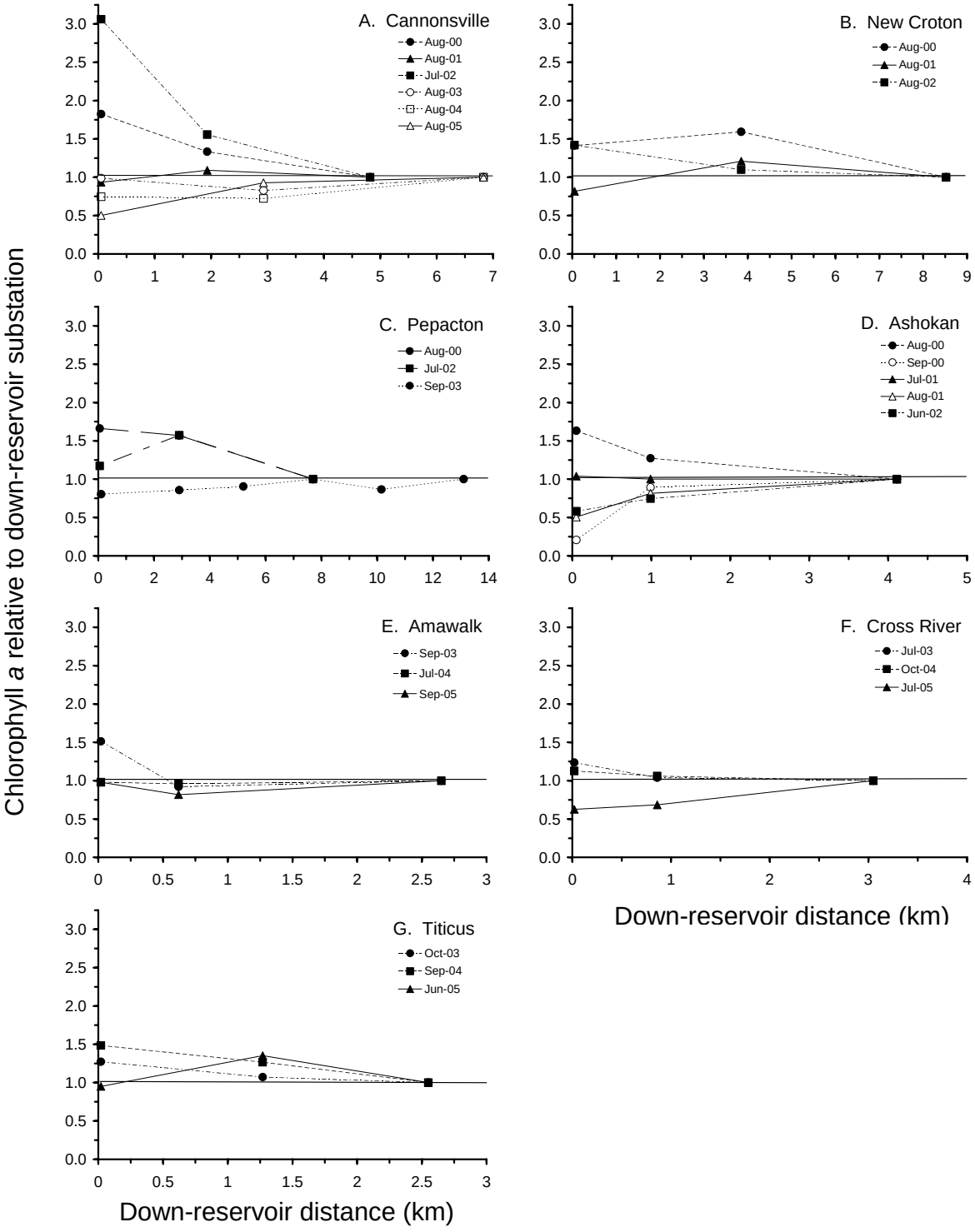

Figure 10.9. Longitudinal trends in phytoplankton chlorophyll *a* when data are expressed relative to the respective value at the farthest down-reservoir substation (SS).

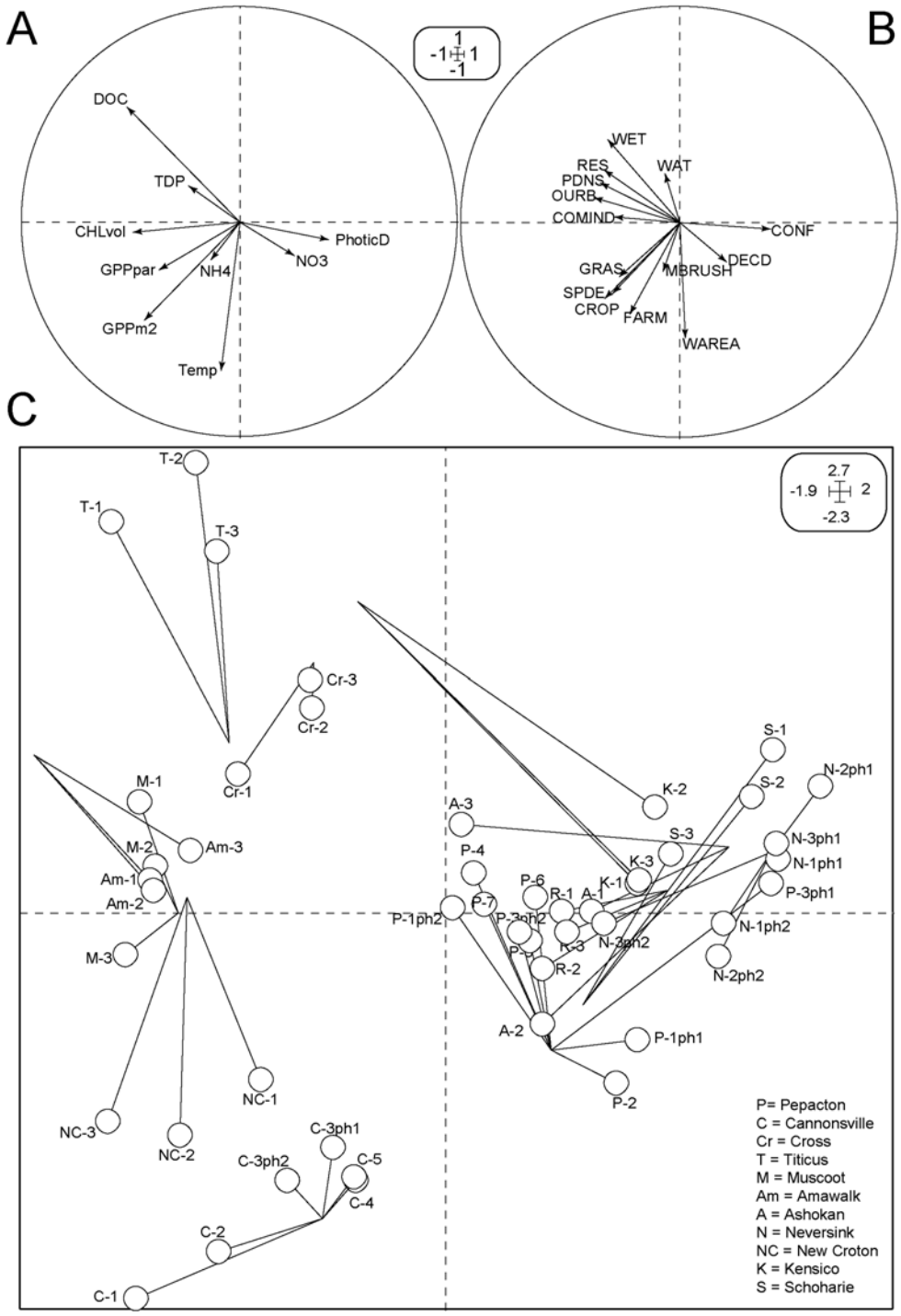

Figure 10.10. Co-Inertia analysis showing ordination of in-reservoir productivity, chemistry, and physical variables (A), watershed-scale land-use variables (B), and substations (SS 1-7 with phase of study where applicable within each reservoir). SSs were plotted based on scores for in-reservoir variables (circles) and reservoirs were plotted based on scores for watershed-scale land-use variables (nodes). The length of the lines connecting SSs and resesvoirs indicate concordance between the two data matrices. Insets show axis lengths. Data points labeled according to reservoir, substation, and phase (if applicable).

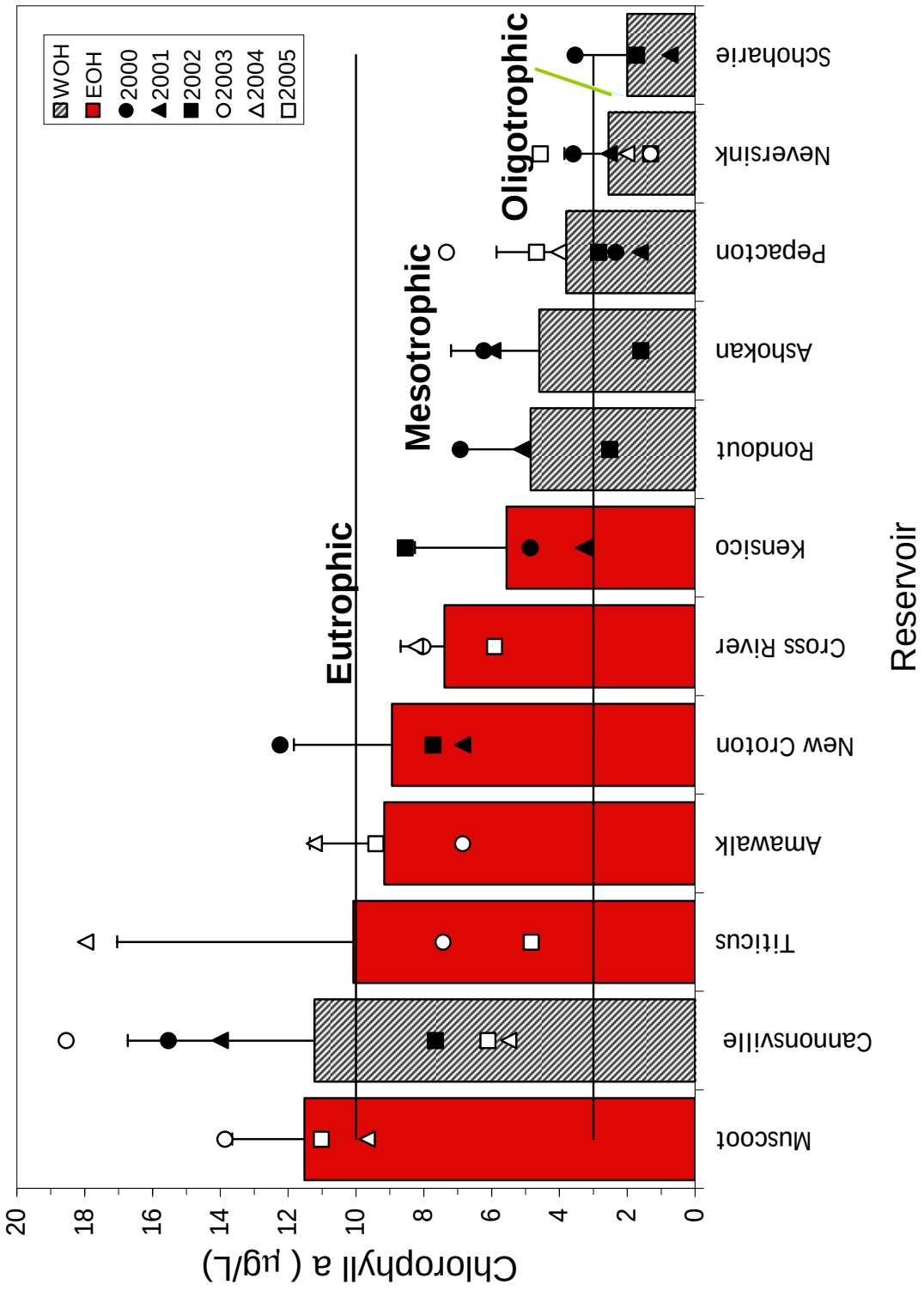

Figure 10.11. Classification of reservoir trophic condition according to chlorophyll *a* concentration.

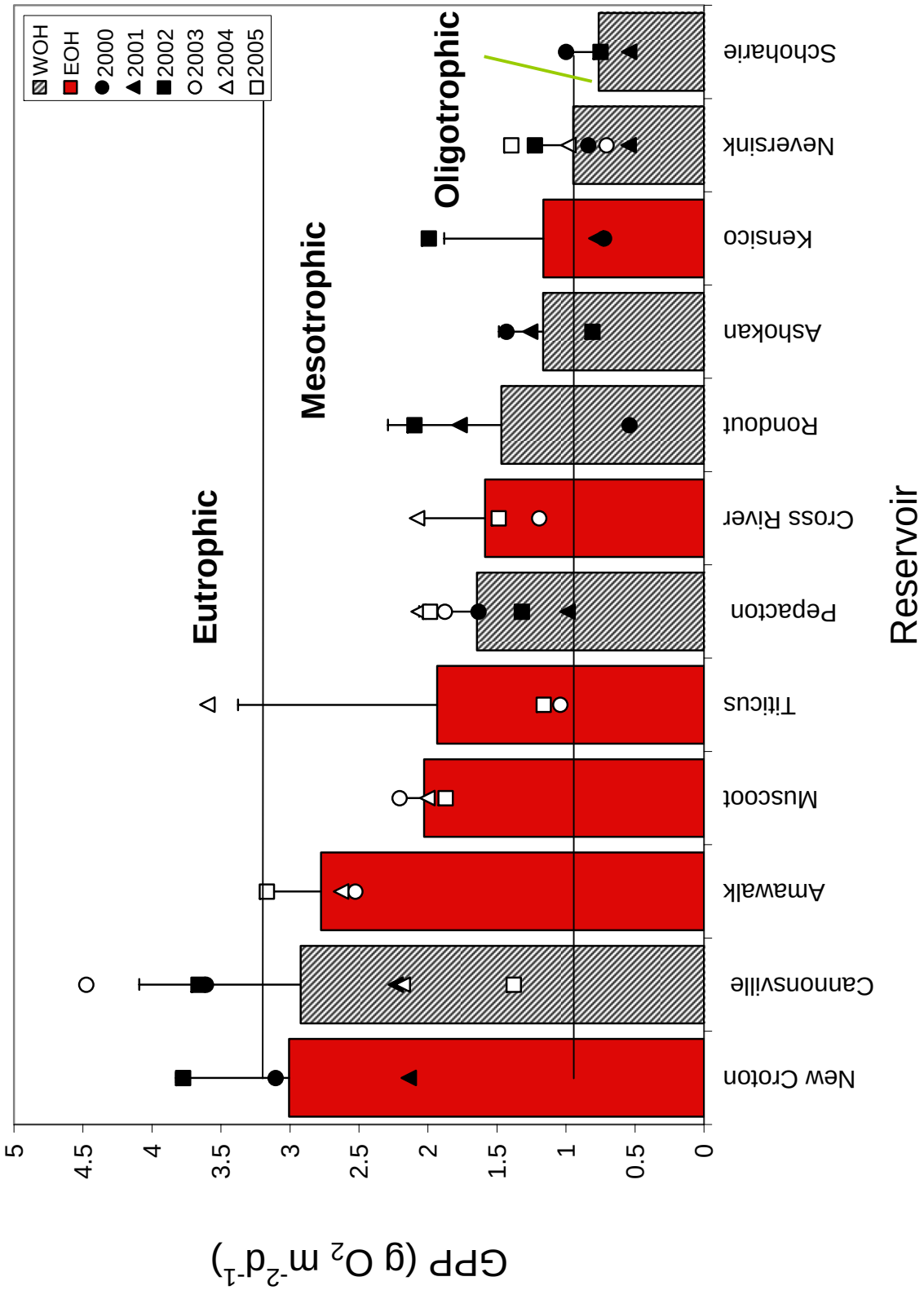

Figure 10.12. Classification of reservoir trophic condition according to daily primary productivity.

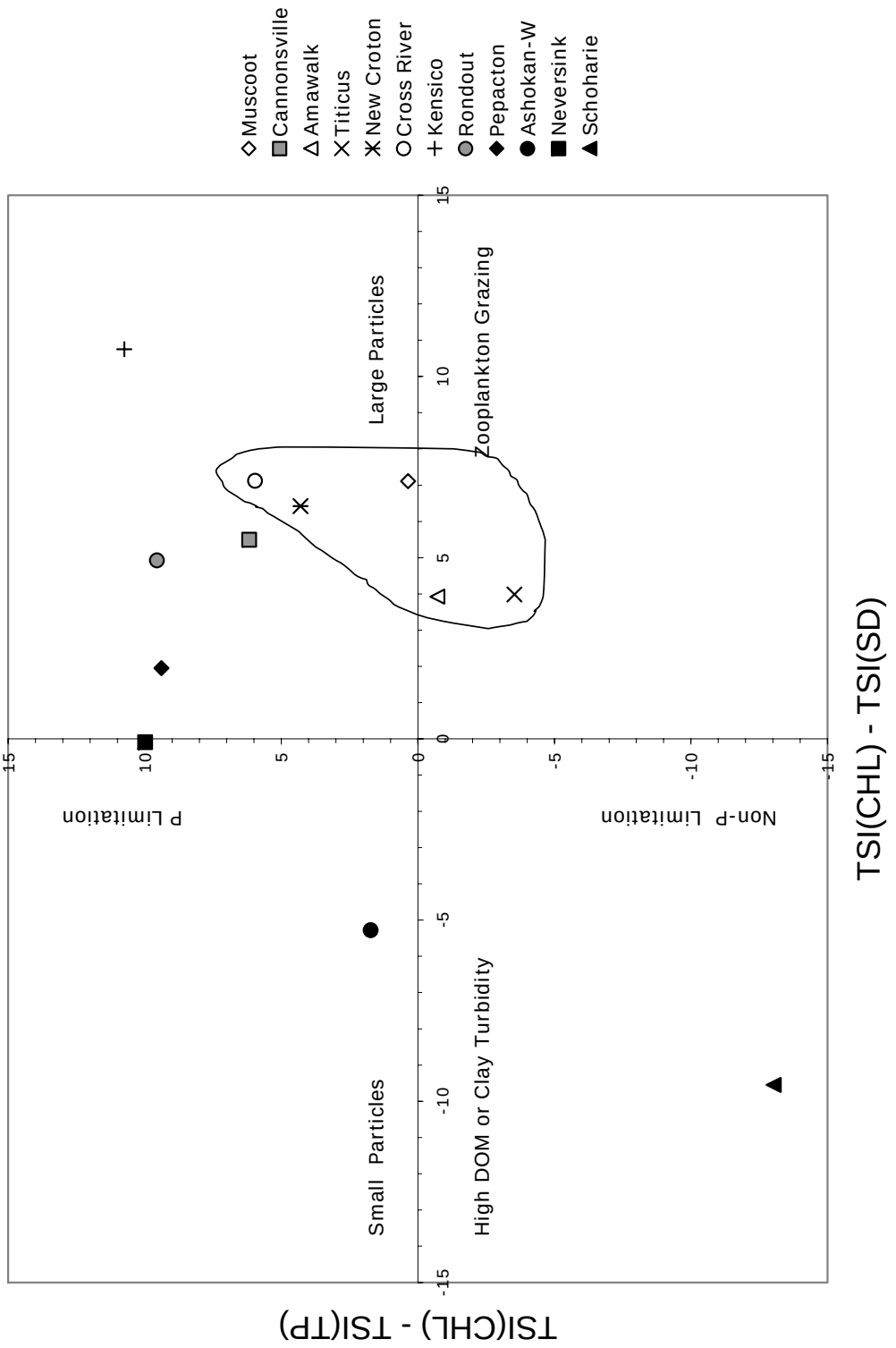

Figure 10.13. Potential causes of deviations of the chlorophyll-based trophic state index.